





# For Reference

Not to be stored in the room

# THE CARNEGIE ATLAS OF GALAXIES



# THE CARNEGIE ATLAS OF GALAXIES

Volume II



by

**ALLAN SANDAGE**

The Observatories of the Carnegie Institution of Washington

and

**JOHN BEDKE**

Computer Sciences Corporation at Space Telescope Science Institute

and formerly of the

Carnegie Institution of Washington

CARNEGIE INSTITUTION of WASHINGTON

with

THE FLINTRIDGE FOUNDATION

WASHINGTON, D.C.

1994

(1996 REPRINTING)

523.112

521ca

v. 2

CARNEGIE INSTITUTION OF WASHINGTON PUBLICATION 63 8

Library of Congress Catalog Card Number: 93-71702

ISBN 0-87279-667-1

3 00-Line-Screen Plates and Printing by Allen Press, Inc., Lawrence, Kansas

Binding by BindTech, Binding Technology, Inc., Nashville, Tennessee

Composition by AlphaTechnologies, Mechanicsville, Maryland

Design by FTM Design Studio, Bethesda, Maryland

Printed on S. D. Warren 100# Lustro Dull

**OX**

Copyright © 1994, Carnegie Institution of Washington

# CONTENTS

VOLUME I		Page
PREFACE		vii
CHAPTER I. CLASSIFICATION IN SCIENCE		1
CHAPTER II. GALAXY CLASSIFICATION		5
CHAPTER III. SUMMARY OF THE CLASSIFICATION		11
E GALAXIES (PANEL S1)		11
E/SO, SO/E GALAXIES; SO GALAXIES; SO/a, SO/Sa (PANEL S2)		14
Sa GALAXIES; <b>Sab</b> GALAXIES (PANEL S3)		18
<b>Sb</b> GALAXIES (PANEL S4)		22
Sbc GALAXIES; Sc GALAXIES (PANEL S5)		24
<b>Scd</b> GALAXIES; Sd, SBd, Sm, SBm, AND Im (PANEL S6)		28
SBO GALAXIES (PANEL S7); SBO/a, SBO/SBa GALAXIES		32
BARRED SPIRAL SEQUENCE: SBa, SBab, SBb, SBbc, SBc		35
BARRED SPIRALS OF THE (S) SUBTYPE (PANEL S8)		38
BARRED SPIRALS OF THE (r) SUBTYPE (PANEL S9)		40
INCREASING STAR-FORMATION RATE IN Sbc(s) (PANEL S10)		42
VARIATION OF BULGE SIZE ALONG THE SEQUENCE (PANEL S11)		44
PROGRESSIVE CHANGE OF THE MAS PATTERN (PANELS S12, S13)		46
ARMS DEFINED PRIMARILY BY DUST (PANEL S14)		50
AMORPHOUS GALAXIES		52
CHAPTER IV. THE MEANING OF THE CLASSIFICATION		53
CHAPTER V. THE ATLAS		Panel
THE E CLASSIFICATION SECTION		1
THE E/SO CLASSIFICATION SECTION		25
THE SO CLASSIFICATION SECTION		30
THE SBO CLASSIFICATION SECTION		54
THE Sa CLASSIFICATION SECTION		61
THE SBO/SBa CLASSIFICATION SECTION		89
THE SBa CLASSIFICATION SECTION		91
THE Sab CLASSIFICATION SECTION		108
THE SBab CLASSIFICATION SECTION		120
THE Sb CLASSIFICATION SECTION		124

VOLUME II		Panel
CHAPTER V. THE ATLAS (continued)		
The SBb CLASSIFICATION SECTION		L54
The Sbc CLASSIFICATION SECTION		171
The <b>SBbc</b> CLASSIFICATION SECTION		199
The Sc CLASSIFICATION SECTION		213
THE SCI SUBCLASS		213
THE ScII SUBCLASS		235
THE SCII-III SUBCLASS		259
THE SaiI SUBCLASS		272
THE SBC CLASSIFICATION SECTION		293
THE Scd/SBcd CLASSIFICATION SECTION		314
THE Sd/SBd CLASSIFICATION SECTION		321
THE Sm/SBm/Im CLASSIFICATION SECTION		325
THE AMORPHOUS SECTION		333
REFERENCES		Page 725
INDEX		731

*Codes used in the short tables accompanying the illustrations throughout the atlas are summarized on pages 8—9. Notations employed in the classifications of galaxy type are treated in chapter 3 (e.g., pp. 14, 18).*

*The endpapers depict the several telescopes where most of the images printed in this atlas were obtained. At the front of Volume I are views of the 100-inch Hooker Telescope, Mount Wilson Observatory, California. At the back of Volume I are scenes showing the 60-inch telescope at Mount Wilson. (The solar tower telescopes are also seen in the outdoors print.) Shown at the front of Volume II is the 200-inch Hale Telescope at the Palomar Observatory, California. At the back of Volume II are scenes at the Carnegie Institution's Las Campanas Observatory: close views are provided of the 2.5-meter du Pont Telescope and the 1.0-meter Sivope Telescope.*

*The galaxy shown on the cover of Volume I is **NQC** 5746. Depicted on the cover of Volume II is NGC 2997.*

*This second (1996) printing of the atlas is identical to the first printing except for a small number of incidental corrections.*

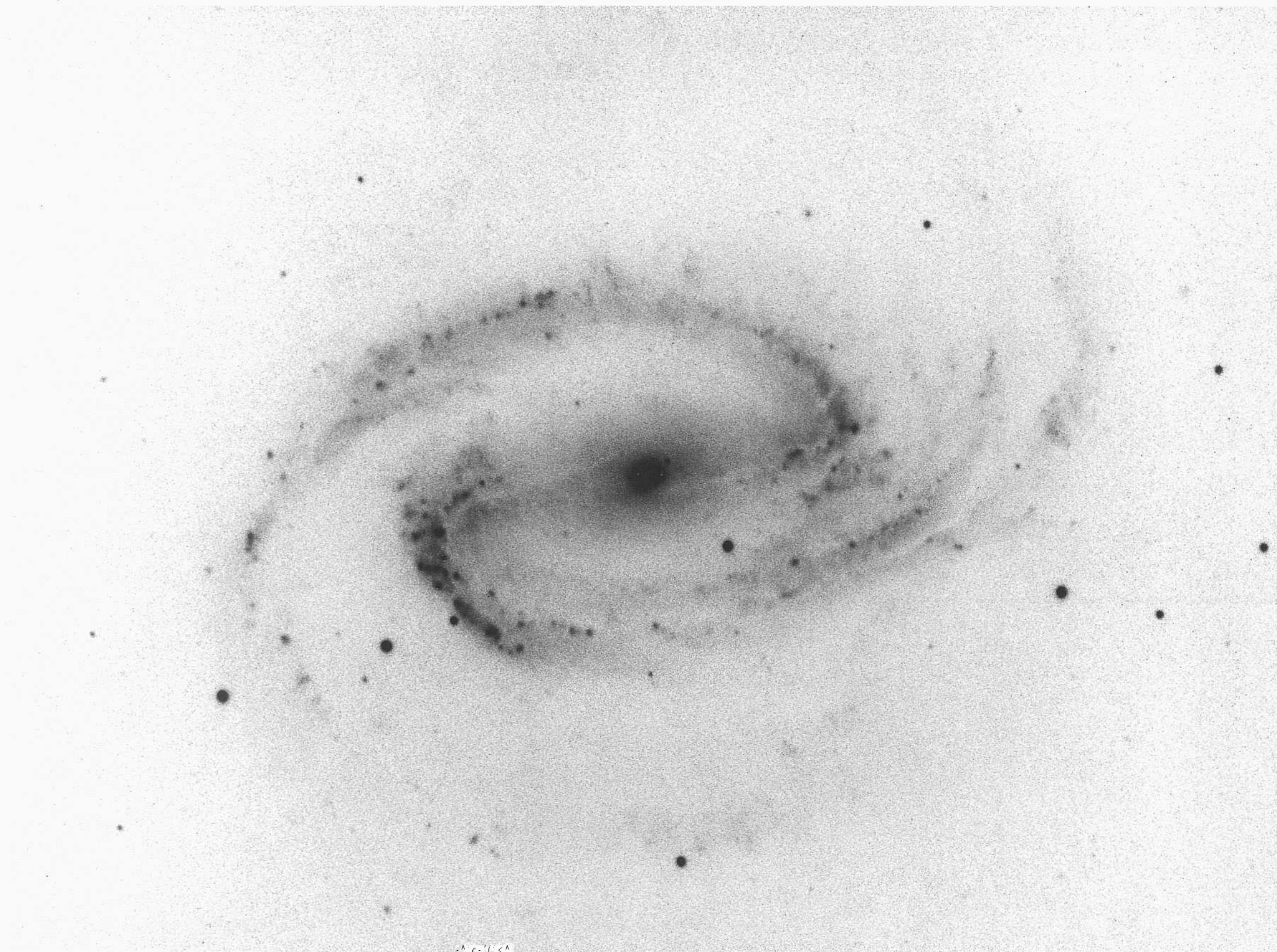




## THE ATLAS

---

PANEL  
154



^ c - ( < ^

## The SBb Classification Section

NGC 1300      SBb(s)L2      HA, p. 45  
PH-75-H      panel S8  
Oct 14/15, 1950  
103aO  
30 min

NGC 1300 is the prototype for the spiral pattern where the arms spring from the ends of the bar. Most galaxies of this spiral-arm subclass (s) have **grand** design arms rather than a **filamentary**, multiple-armed MAS pattern where the arms generally begin tangent to an almost-complete ring (which defines the (r) subclass). The arms in NGC 1300 are tightly wound **but** not as tightly as in NGC 3185 (Sa; panel 99) where they nearly overlap after each arm unwinds by half a revolution to form an almost-complete inner ring.

SBb(s) galaxies like NGC 1300 have several distinctive features characteristic of the class. (1) The bar is well formed and prominent. (2) In most SBb(s) types two *straight* dust lanes exist within the bar, each on the outside of the otherwise smooth bar; the lanes **are** on symmetrically opposite sides of the central amorphous center. In every case, the dust lanes *are on the sides of the bar that lead the rotation*, the direction of the **rotation** being judged from the sense of the spiral pattern. (3) Recent star formation is generally most robust in the arms near the ends of the bar. The increased star-formation **rate** near these two points is clearly evident in the arms and outer tips of the bar in NGC 1300, shown by the many bright knots that are **probably** small III regions. None of the **candidate** **Mil** regions resolve at the 2" level. The redshift of NGC 1300 is  $v_o = 1526 \text{ km s}^{-1}$ .

These several characteristic features have been reproduced in a series of theoretical **studies** concerned with the **hydrodynamic** response of the gas in the disk to the presence of the rotating bar. Following pioneering work by Prendergast (1962), detailed **hydrodynamical** models of the velocity field and the presence of shocks in the gas in the neighborhood of the bar have been made. The early papers that predict the velocity **field** in **detail** are by Huntley (1978), Huntley, Sanders, and Roberts (1978), Roberts, Huntley, and van Albada (1979), Peterson and Huntley (1980), and Huntley (1980). A review up to 1983 is given by Prendergast (1983).

The comparison of the calculated models with the observed features in NGC 1300 is generally so close that it can be said that the straight dust lanes in SBb(s) types and the **enhanced star-formation rate** at the ends of the **bar** **are** both understood. The **features** are **related** to the shock **properties** of the gas at these points.

In **viewing** the SBb galaxies in this section and in the SBc section later, it is useful to keep in mind the three conclusions of Prendergast (1983):

(1) *Weak bars give open spiral patterns which extend throughout the gas; stronger bars give spirals which emerge at sharp angles to the bar. [added here: as in NGC 1300]*

(2) *The gas response leads the bar, by an angle which is greater the weaker the bar.*

(3) *Strong bars favor the appearance of strong shocks within the bar. When they occur, they lie near the leading edge, which is just where they should be if the identification of shocks and dust lanes is correct.*

The four galaxies on this panel are of luminosity class I; the spiral pattern is very well defined, i.e., the geometrical entropy is very low. In every case the arms start near the ends of the bar, as in NGC 1300, rather than tangent to an almost-complete internal ring, although close inspection is required in NGC 3992 (lower right) to avoid an incorrect first impression that the form here is more (r)-like than (s)-like.

NGC 2935      SBb(s)I.2  
 CD-815-S  
 Feb 26/27, 1979  
 103aO + GG385  
 15 min

The bar in NGC 2935 is weaker than in NGC 1300, being a central oval rather than a strong straight bar. Consistent with Prendergast's second point quoted on the preceding page, the spiral pattern of the outer arms is more open than in NGC 1300.

Two principal dust lanes exist in the inner oval, each curved into a tight spiral pattern. The underlying luminosity distribution in the oval is smooth; no large current star-formation rate exists there.

Robust star formation is occurring in each of the outer arms along their entire length. The largest HII regions resolve into disks at the 1.5" level. The redshift is  $v_o = 2003 \text{ km s}^{-1}$ .

NGC 2633      SBb(s)I.3  
 PH-7705-S  
 Feb 11/12, 1980  
 103aO  
 12 min

The bar in NGC 2633 is an oval within which the current star-formation rate is high. The luminosity distribution is neither amorphous, as in the bar of NGC 1300, nor smooth over most of the oval, as in NGC 2935, above. The pattern is similar to that in NGC 210 (Sb; panel 124), which itself could be classed an SBb if its central disk were an oval rather than an inclined circular disk.

NGC 6951      Sb/SBb(rs)L.3      HA, p. 46  
 PH-5374-S  
 Sep 11/12, 1969  
 103aO + GG13  
 25 min

The relative straightness of the two opposite dust lanes within the central disk of NGC 6951 identifies the central region as an oval rather than simply an inclined circular disk. However, the bar (the oval) is weak; the spiral pattern is open, and there is no enhanced star formation at the ends of the bar.

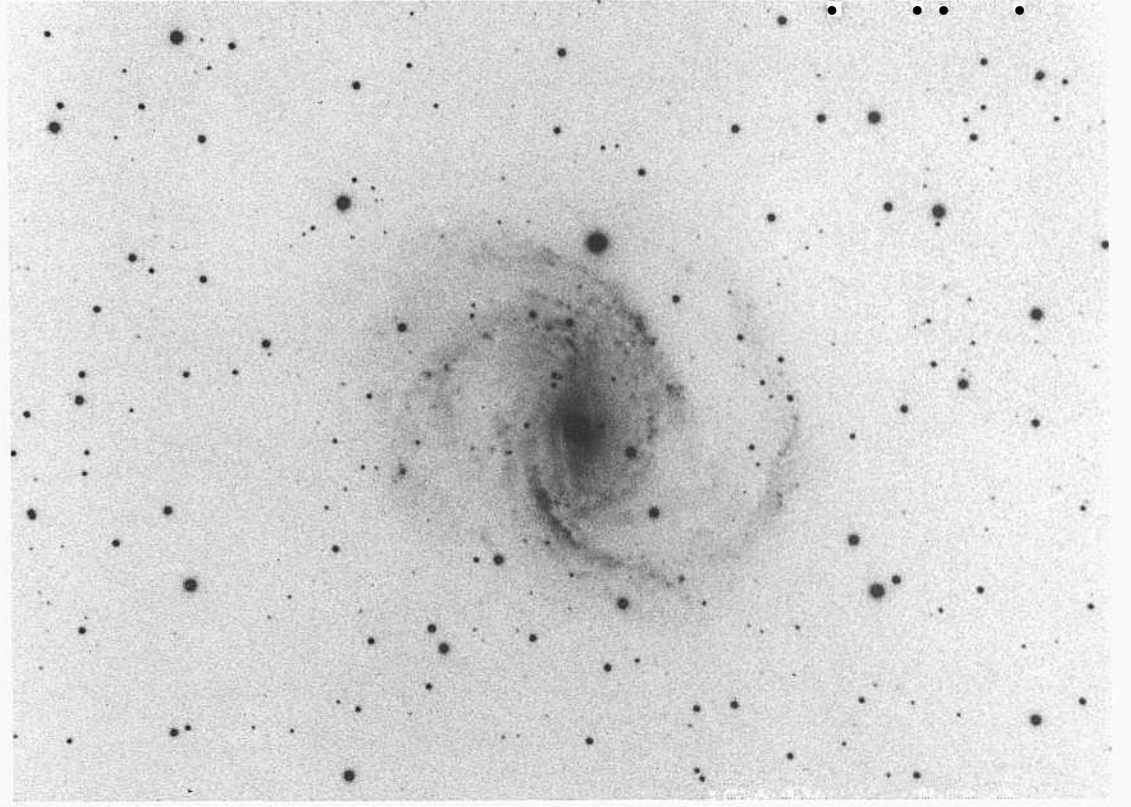
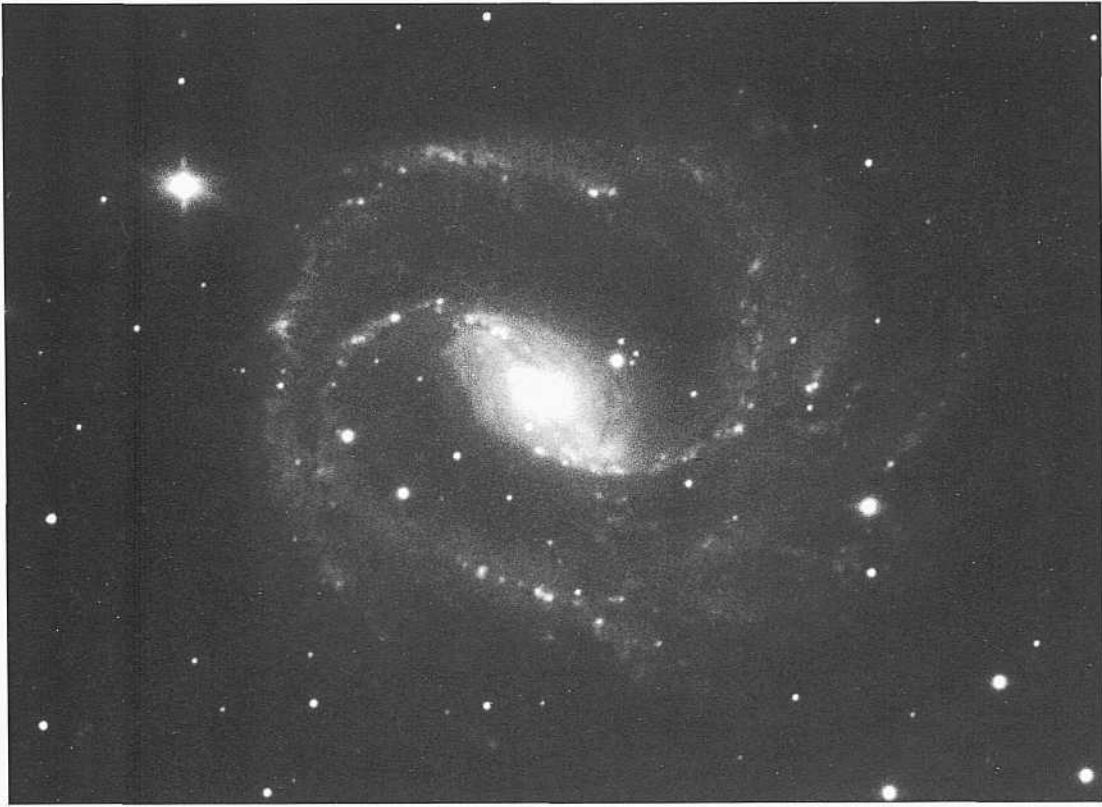
The HII regions in the arms are unresolved at the 1" level. The redshift of NGC 6951 is  $v_o = 1710 \text{ km s}^{-1}$ .

NGC 3992      SBb(rs)I      Racine wedge  
 PH-8027-S  
 Feb 3/4, 1981  
 103aO  
 12 min

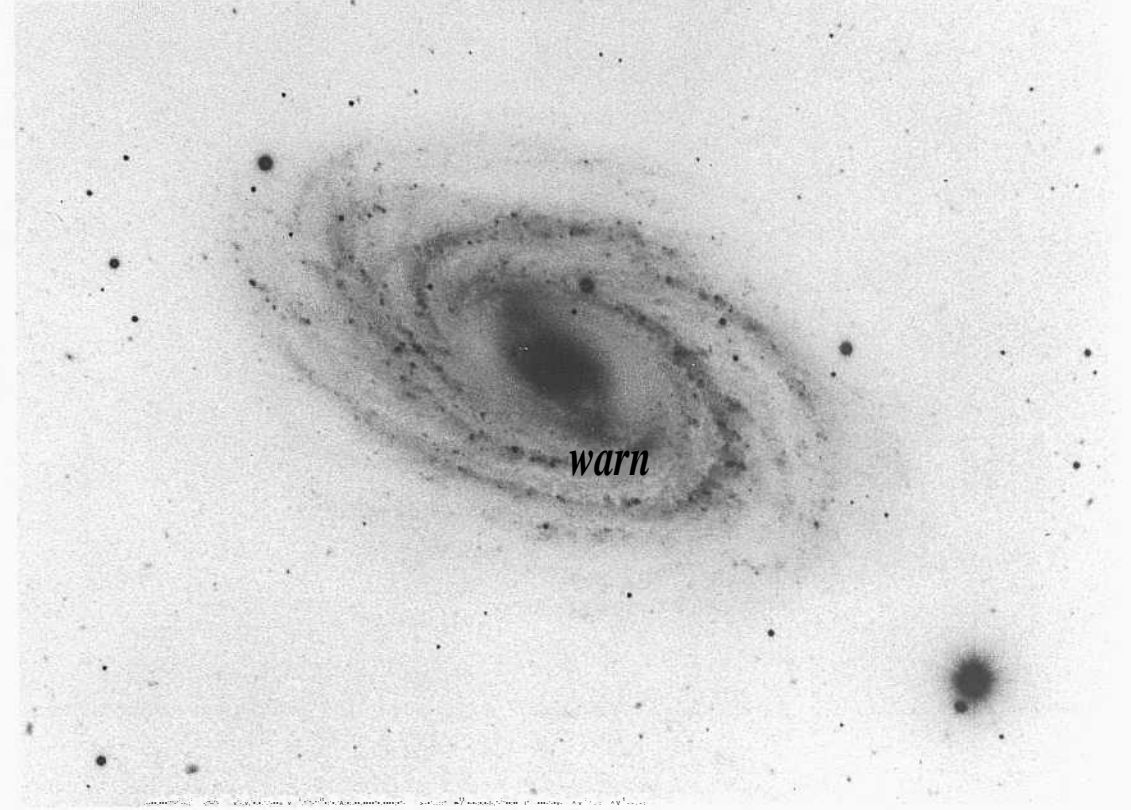
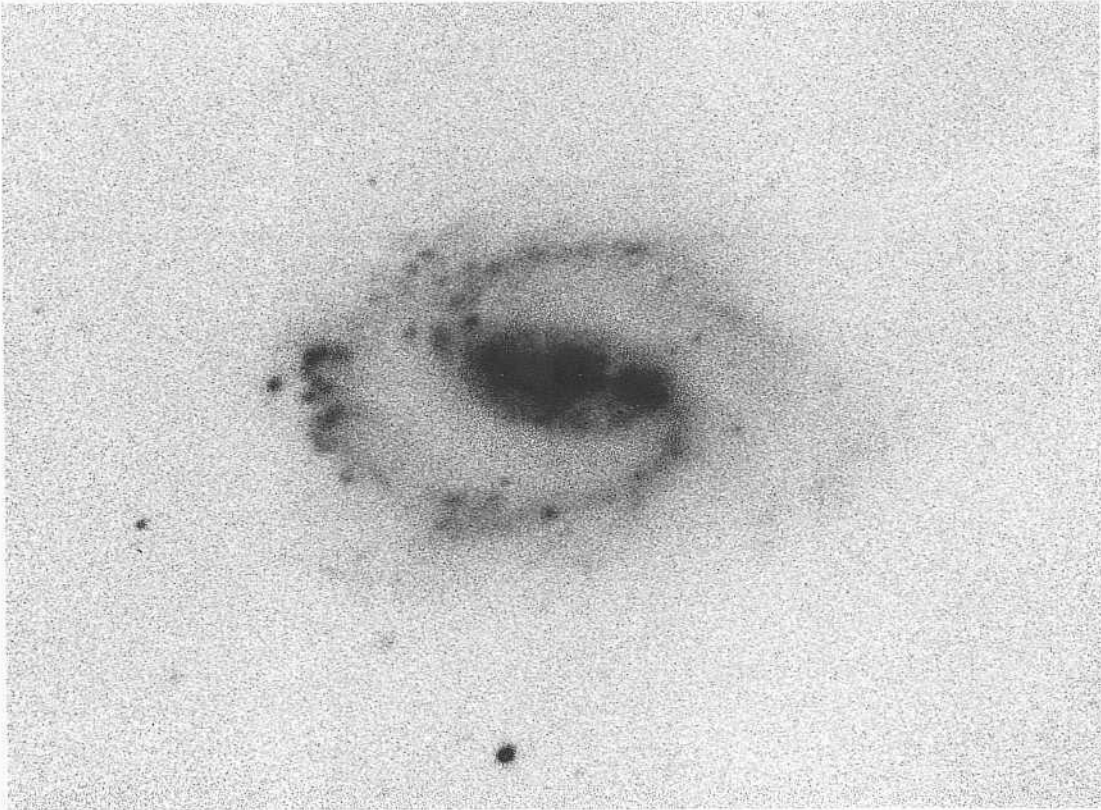
The spiral pattern in NGC 3992 is among the most regular known in the sky. Before it fragments, one of the two principal arms can be traced for nearly a complete revolution from its start near the end of the bar. The opposite arm fragments into three segments after unwinding for only about 90°.

The arms do not begin at the tips of the bar but rather at a position about 10° upstream from these ends, i.e., in a direction opposite the direction of rotation (inferred from the sense of the spiral pattern). One of the several calculated hydrodynamical models of Huntley (1980, Fig. 4) reproduces the pattern.

The largest of the many HII regions in the arms resolve into disks at the 1" level. The redshift is  $v_o = 1134 \text{ km s}^{-1}$ .

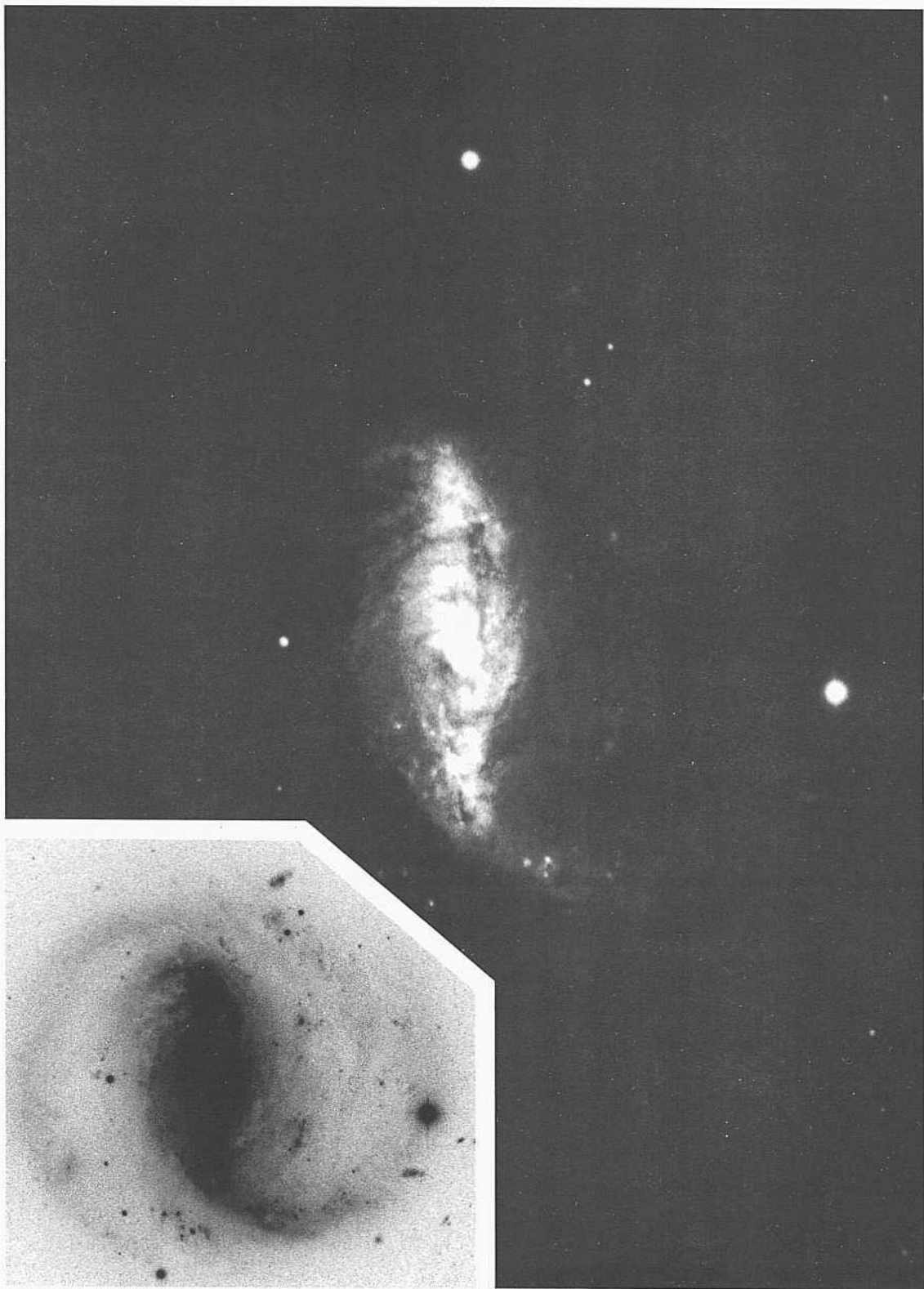


PANEL  
155



*warn*

PANEL  
156



NGC 7552      SBb(8)I-H

**CD-1587-S/Br**

**Aug 11/12, 1980**

**103aO + GG385**

**15 min**

The same **original** plate was used to make the two prints of **different** contrast of NGC 7552 offered **here**. The low-contrast **print shows the detail of the intricate dust pattern in the oval, which is the weak bar. The high-contrast print shows the generally low-surface-brightness spiral pattern of the (s) type, where the arms begin at the end of tin<sup>1</sup> bar (the oval here).**

The **two straight** dust lanes **characteristic** of SBb types **are** best seen in **the low-contrast print**, which shows the center well. These lanes, as in NGC 1300, start from opposite sides of **the nucleus** and are straight almost to the end of the oval. They are not as well defined as in [NGC 1300 but are obviously present. It is well **understood that** these lanes are due to hydrodynamic shocks in the gas in response to the gravitational **perturbation** of the rotating bar. The stronger the bar, the stronger are the shocks, according to the calculated models (see Prendergast 1983 **for** a review).

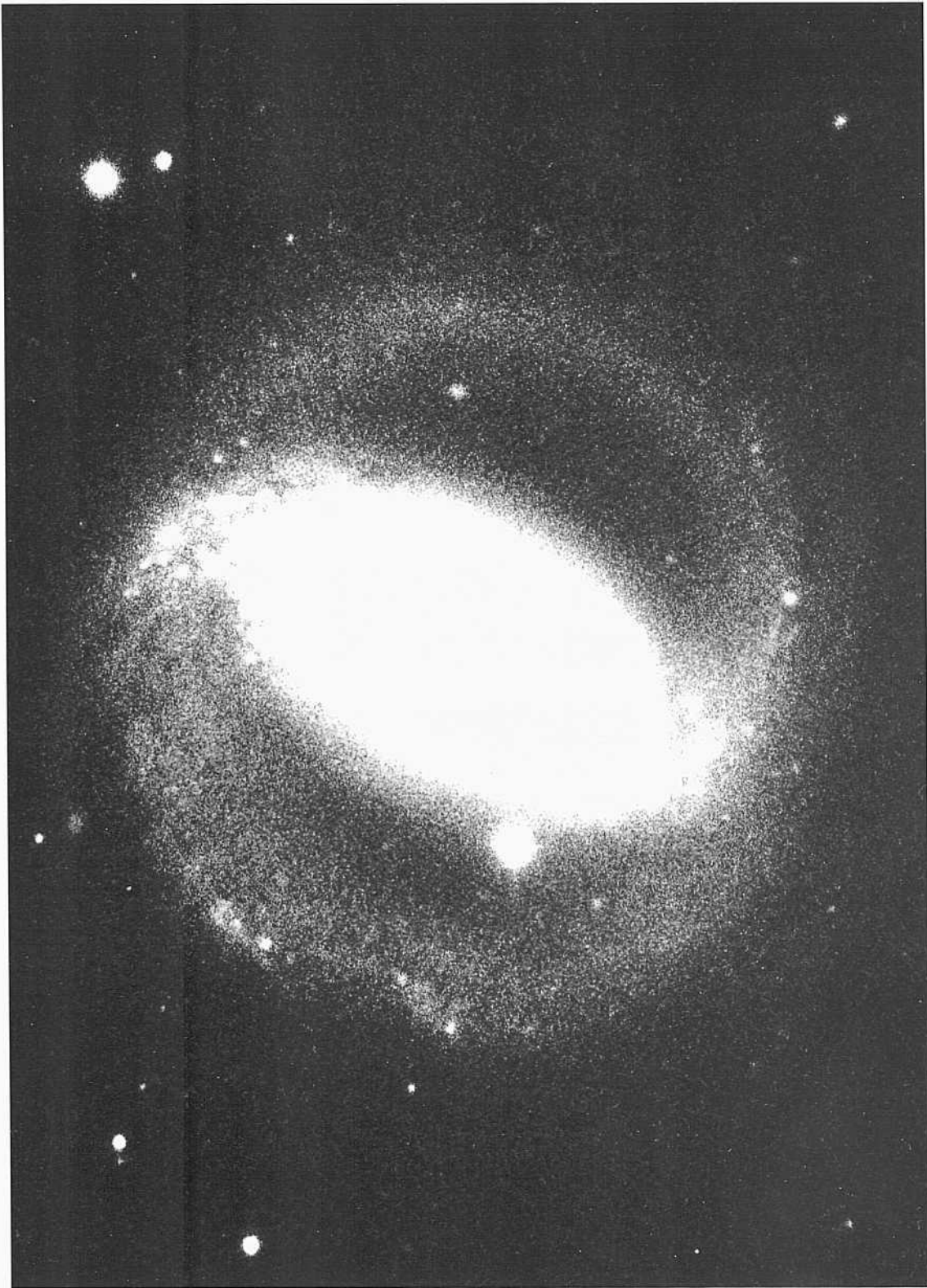
Dust lanes, **curved** into spiral fragments, exist in the central oval starting from the two straight lanes on opposite sides of the oval.

The outer luminous arms shown in the high-contrast print start **from** the ends of the oval. On one side the principal arm branches into three fragments, the inner of which nearly overlaps the other principal arm, which starts from the opposite side of the oval. This arm remains single for the half-revolution over which it can be traced.

Only a few IIII regions exist in the arms, the largest of which resolve at about the 2" level. **The redshift** is  $v_D = 1565 \text{ km s}^{-1}$ .







PANEL  
157

PANEL  
158



**T**he general features of the two galaxies shown on this panel are similar to the SBb galaxies on preceding panels, but the spiral patterns are more complex.

NGC 986 SB(rs)I-II panels 169, 170  
 CD-2007-Bedke/Gregory  
 Oct 23/24, 1981  
 103aO + GG385  
 15 min

In NGC 986 in the top row, the short-exposure print shows that the bar is strong, it is narrow in its central, high-luminosity part, along which, on either side, the two characteristic, straight, well-defined dust lanes exist. Two sets of arms emerge from the ends of the bar. The inner set spring from the bar at a sharp angle, similar to the pattern in NGC 1300. These nearly overlap after half a revolution, forming an almost-complete inner ring, seen best in the middle print.

The two grand design outer arms also begin at the ends of the bar at the same place as the inner arms. They emerge from the bar at a shallower angle than the inner arms. They are brightest for about one-eighth of a turn from their beginning, after which the surface brightness becomes much fainter. The highest star-formation rate occurs near the ends of the bar and in the parts of the outer arms nearest the bar. The pattern is well reproduced in many of the model calculations described on panel 154 in the commentary on NGC 1300.

NGC 1433 SBh(s)I-II panels 169, 170  
 CD-153-S  
 Feb 3/4, 1978  
 103aO + GG385  
 45 min

The short-exposure print of NGC 1433 shows the strong bar and the two "shock-produced" dust lanes on each of the two leading edges of the bar (i.e., leading in the sense that we

know the direction of rotation from the sense of the spiral pattern). Two bright grand design, lightly wound, inner spiral arms begin at the ends of the bar, similar to the pattern in NGC 1300. The star-formation rate is high in the two inner arms where they nearly overlap at the ends of the bar. This overlapping seems, on first inspection of the middle print, to form an inner ring, but the pattern is simply one of overlapping, tightly wound spiral arms.

After slightly more than half a revolution, these inner arms branch into two sets of lower-surface-brightness outer arms. Note the high degree of symmetry of the four outer arms. The set closer to the broken ring are only two fragments which unwind for only about 30° before they can no longer be traced.

The small IIII regions in the inner arms do not resolve at the L' level. The redshift of NGC 1433 is  $v_r = 923 \text{ km s}^{-1}$ .

**G**alaxies on the preceding five panels are of the (s) subtype, have very ordered spiral structures (all are of high-luminosity class), and have spiral arms of the grand design type. Grand design arms almost always occur in the (s) subtype.

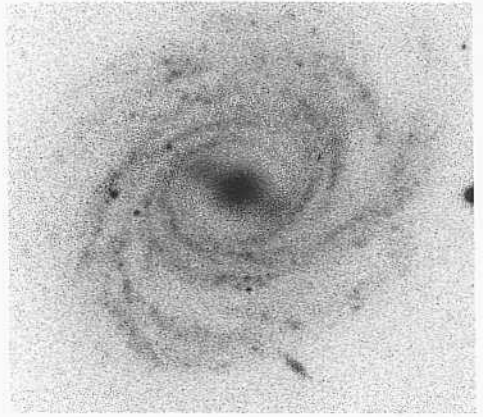
The galaxies on the next five panels are of the (r) subtype. The spiral pattern is invariably of the fragmented, multiple-armed-spiral (MAS) type.

SBb(r) galaxies of luminosity class I are illustrated on the next three panels. Less-regular galaxies (which by definition have a lower luminosity class) are shown on the panels following them.

NGC 4999      SBb(rs)I      panel S9  
CD-1835-HB  
April 1/2, 1981  
103aO + GG385  
45 min

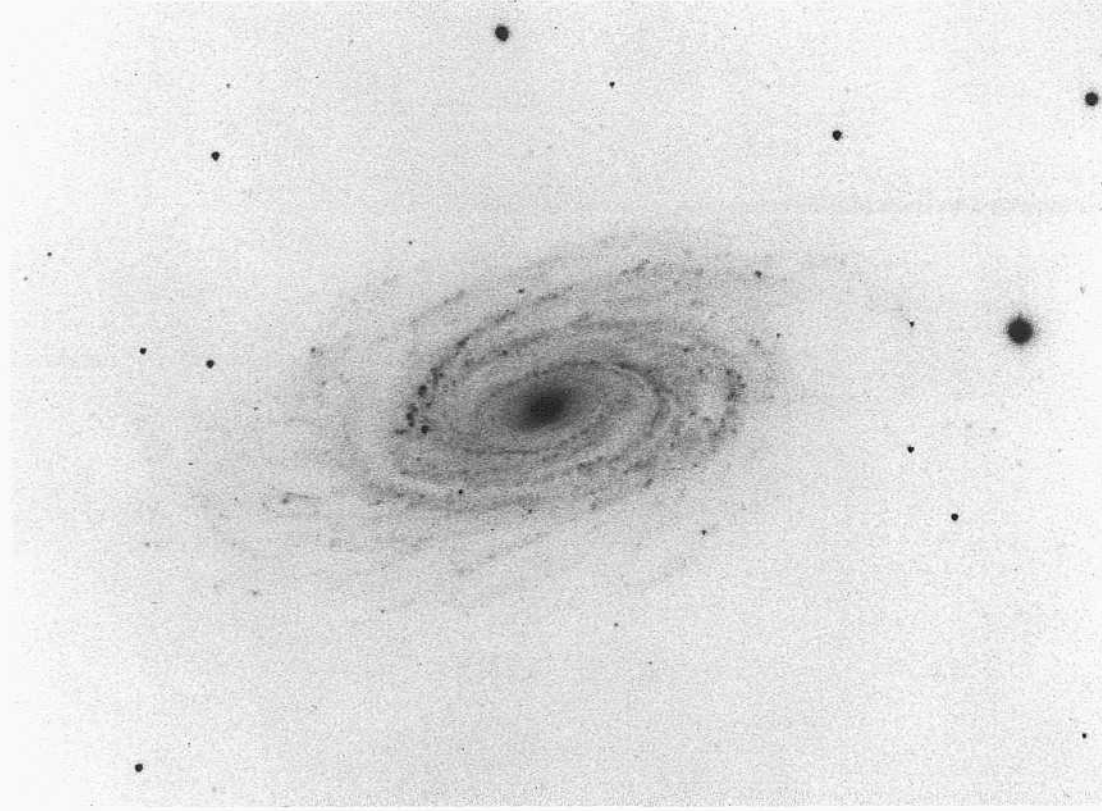
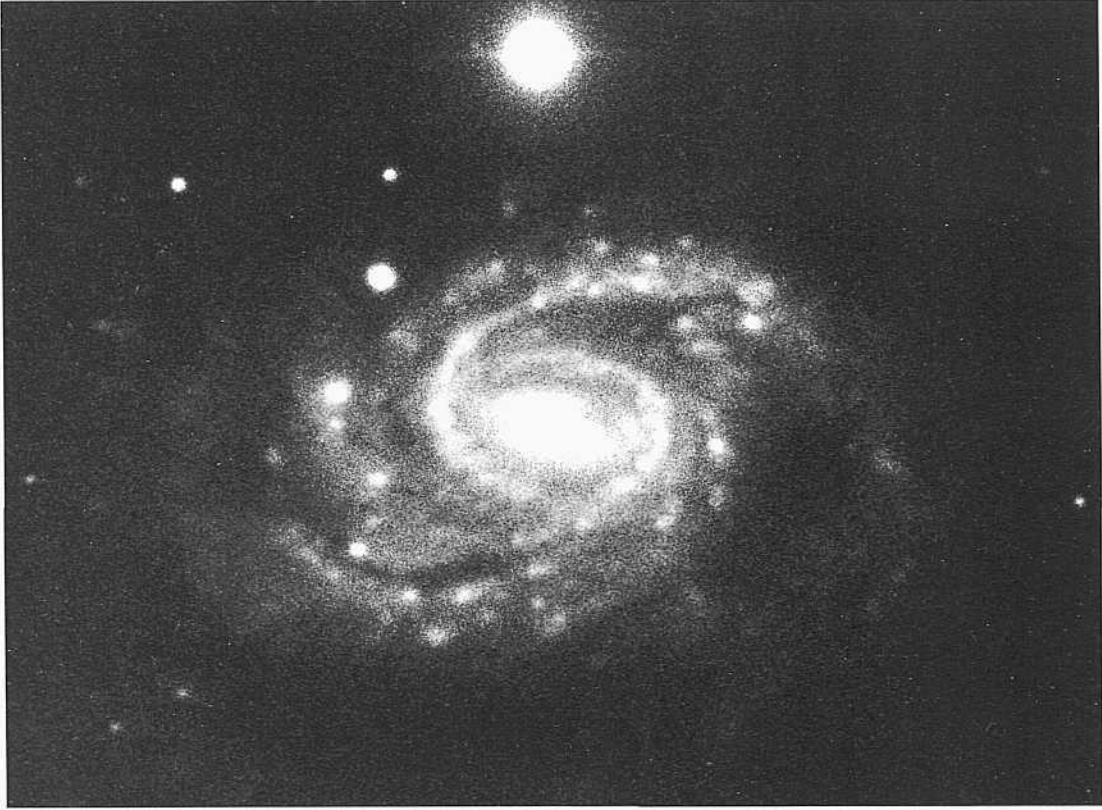
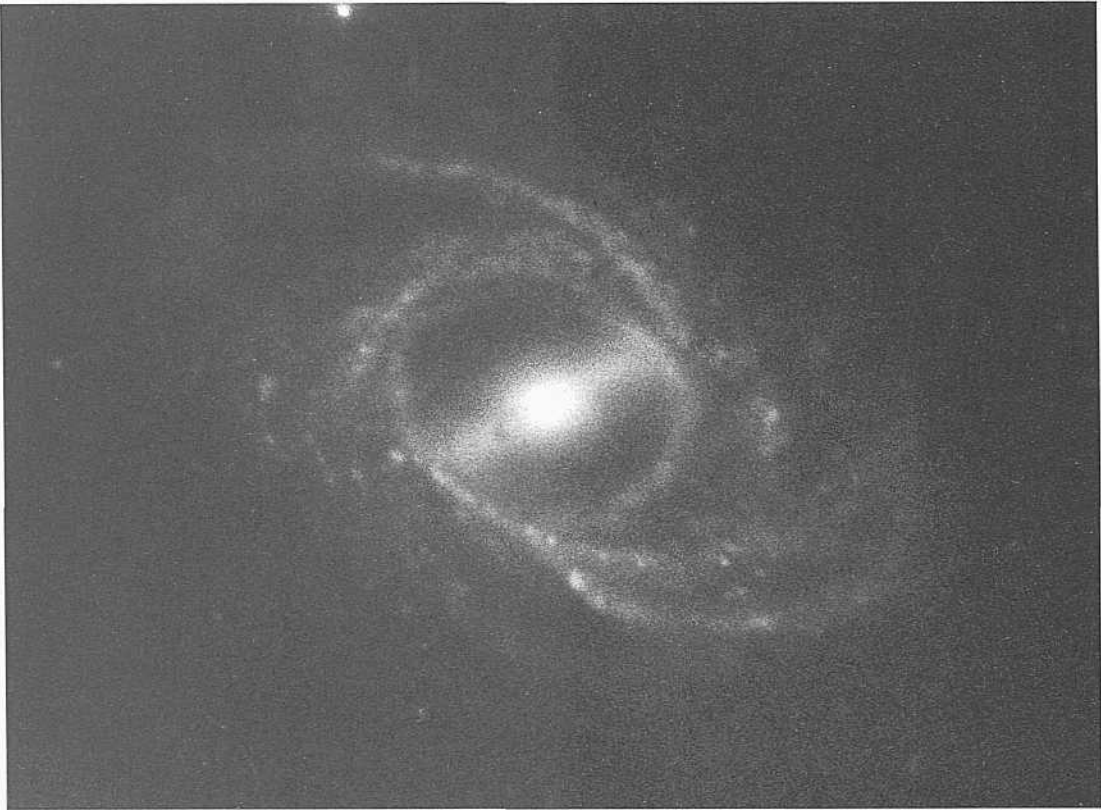
NGC 4999 is **the** prototype of the very regular (**high-luminosity** class) multiple-armed-spiral (MAS) type where the arms begin tangent **to** an almost-complete internal ring. Again, to **emphasize** what is often described in these notes, this ring represents the near overlapping of separate arms springing from opposite ends of the bar and approaching one another after each has unwound by half a revolution. The pattern is well seen in NGC 4999, although the near-ring is very nearly complete because the first wrap of the arms is so tight: the separate arms nearly intersect after each has unwound **by** half a revolution.

The bar is strong. The arm pattern is multiple and fragmented. The arms are thin; the **geometrical** entropy is **low**.



*PANEL  
159*

PANEL  
160



Three of the four galaxies on this pane] have so regular an arm pattern that they are classed as luminosity class 1. All but NGC 5985 have prominent bars. All have multiple spiral arms, beginning from an almost-complete internal ring. This pattern defines the (r) spiral subtype.

NGC 2523            SBb(r)I  
 PH-850-S  
 Nov 2/3, 1954  
 103aO  
 30 min

The arms in NGC 2523 are narrow. One of the two main arms that would form a grand design pattern branches into two narrow arms starting at about  $30^\circ$  around the ring from the termination of the bar on the ring. The other main arm begins near, but not on, the ring at the place where the bar terminates on the ring. This arm can be traced in its bright part for only about one-fourth turn from its origin at the end of the bar.

The HII regions are unresolved. The redshift of NGC 2523 is  $v_o = 3638 \text{ km s}^{-1}$ .

NGC 5406            SBb(r)I  
 PH-8100-S  
 Feb 6/7, 1981  
 103aO  
 12 min

NGC 5406 is a MAS type although the arms are quite well defined. The bar is strong. The central lens containing the bar is smooth, indicating an old stellar population.

The many evident HII regions do not resolve at the 1" level. The redshift of NGC 5406 is high for a Shapley-Ames galaxy, at  $v_o = 5241 \text{ km s}^{-1}$ .

NGC 1832            SBb(r)I  
 PH-70-II  
 Oct 13/14, 1950  
 103aO  
 30 min

NGC 1832 is nearly a grand design spiral except that the second principal arm (at the top in the print here) does not exist as a separate arm but consists of fragments starting at progressive places on the nearly complete bright internal ring.

The spiral-arm fragments are all narrow. They are well defined, explaining the bright luminosity class. Each arm is studded with HII regions, the largest of which resolves at the 2" level. The redshift of NGC 1832 is  $v_o = 1855 \text{ km s}^{-1}$ . At this redshift (in the absence of noise in the Hubble flow), the angular size of the largest HII region corresponds to a linear size of 3.60 ppc ( $// = 50$ ), which agrees well with the calibration of Sandage and Tammann (1974a).

NGC 5985            SB1,(r)I  
 PH-7273-S  
 July 22/23, 1976  
 103aO + GG13  
 25 min

The multiple-arm pattern is especially evident in NGC 5985. The arms are thin and well defined, requiring the highest luminosity classification. A few large HII regions exist in parts of the image. They do not resolve at the 1" level. The redshift of NGC 5985 is  $v_o = 2694 \text{ km s}^{-1}$ .



**T**he (our galaxies on this panel continue luminosity class I because the spiral arms are so well defined and are thin, and the inter-arm regions are relatively clear.

NGC 3347      SBb(r)I  
 CD-191-S  
 Feb 7/8, 1978  
 103aO + GG385  
 -15 min

NGC 3347 is a two-armed spiral of the grand design type despite the fact that the spiral subclass is (r) because of what appears, at this high inclination angle, to be an internal ring.

The two principal arms have high surface brightness. They are studded with small, generally unresolved HII regions. The redshift of NGC 3347 is  $v_r = 1201 \text{ km s}^{-1}$ .

NGC 5792      SBh(rs)I.3  
 CD-1436-S/Br  
 March 26/27, 1980  
 103aO + GG385  
 45 min

NGC 5792 is a highly inclined, well-formed barred spiral with an evident almost-complete inner ring from which the grand design two-armed spiral pattern emerges. The redshift is  $v_o = 1889 \text{ km s}^{-1}$ .

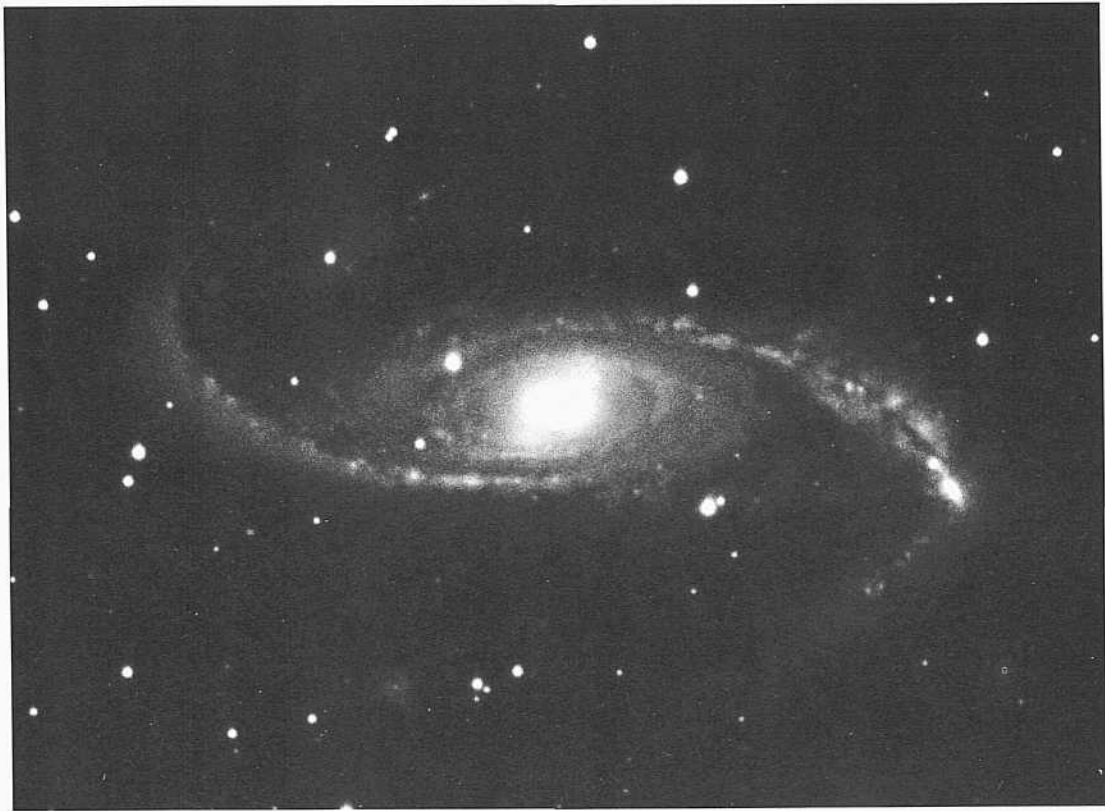
NGC 1512      SBb(rs)I pec      pair  
 CD-184-S  
 Feb 7/8, 1978  
 103aO + GG385  
 45 min

NGC 1512 is an almost-normal SBb(r) where interaction with NGC 1510 distorts the outer thin arm pattern. Description of the features of this encounter are given by Kinman (1978), and by Sandage and Brucato (1979).

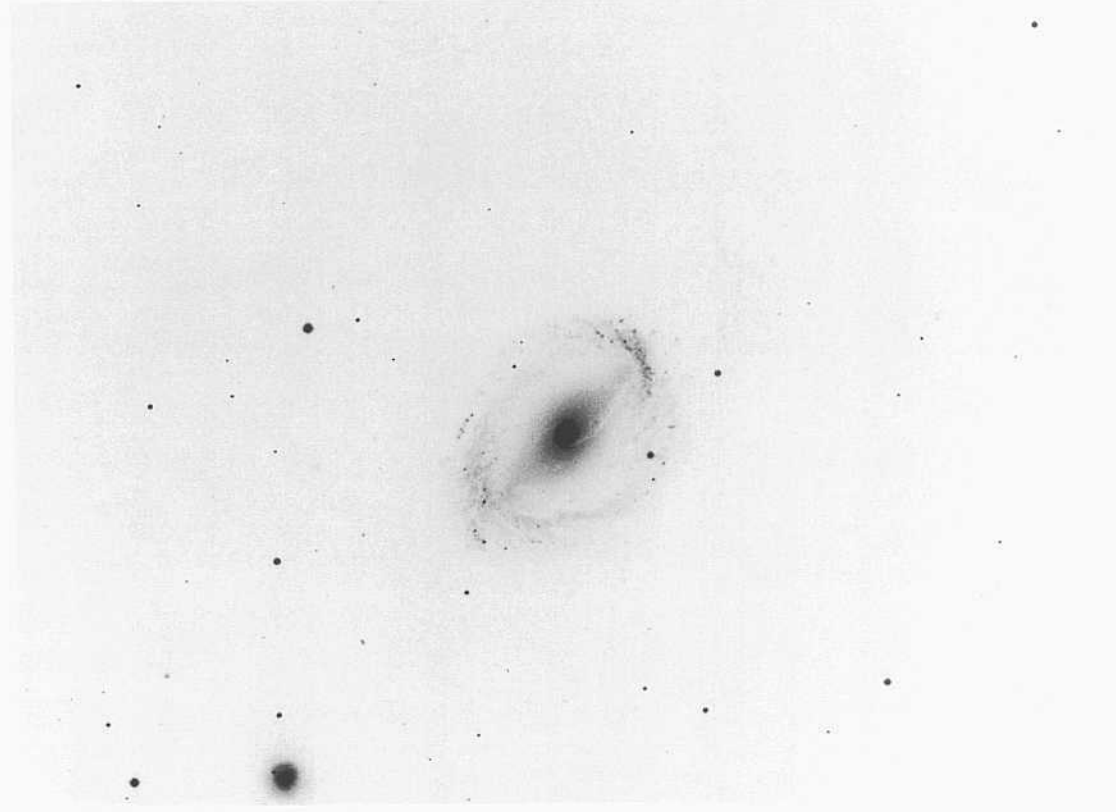
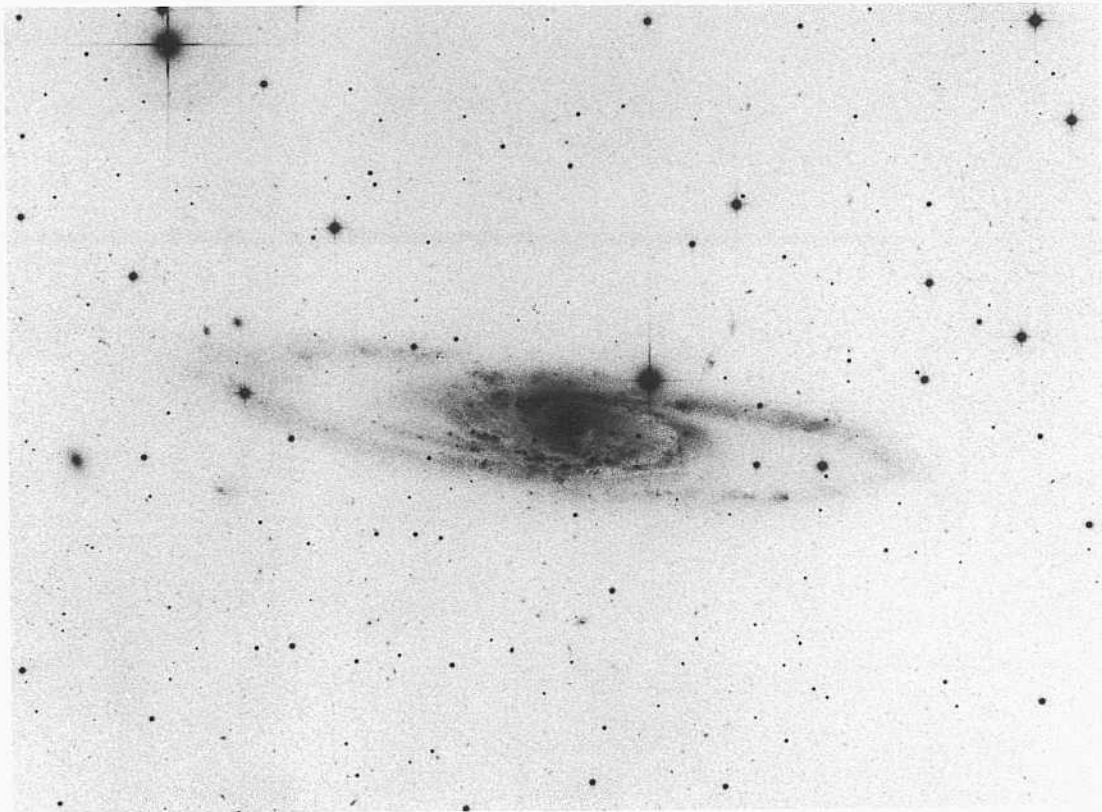
The nearly complete inner ring in NGC 1512 is composed of two closely overlapping bright, tightly wound spiral-arm segments, which begin at the ends of the bar. This near-ring is of very high surface brightness. Star formation, evidenced by the many HII regions, is most robust in one of the spiral fragments at one end of the bar, seen well in the low-contrast print at the bottom right. The smooth nature of the bar and the single straight dust lane are seen best on the side of the bar where the HH-region density is highest in the associated arm that starts there.

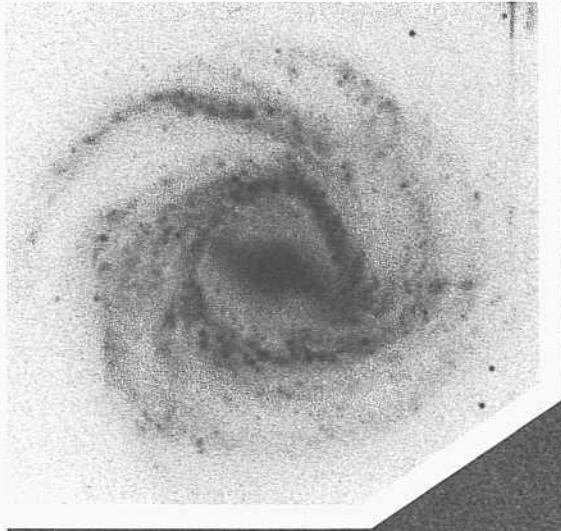
Very faint outer arm fragments exist, associated both with the inner arm structure of NGC 1512 and the perturbing companion, NGC 1510. Parts of these arm fragments are seen in the high-contrast print at the top right but are seen better in the photograph by Kinman (1978), where the pair is also described.

The separation of the pair is 4.9'. The redshift of NGC 1512 is low, at  $v_o = 760 \text{ km s}^{-1}$ . At the redshift distance of 15 Mpc the projected linear separation of NGC 1512 and NGC 1510 is small at 2.1 kpc, supporting the suggestion that a close encounter is in progress.

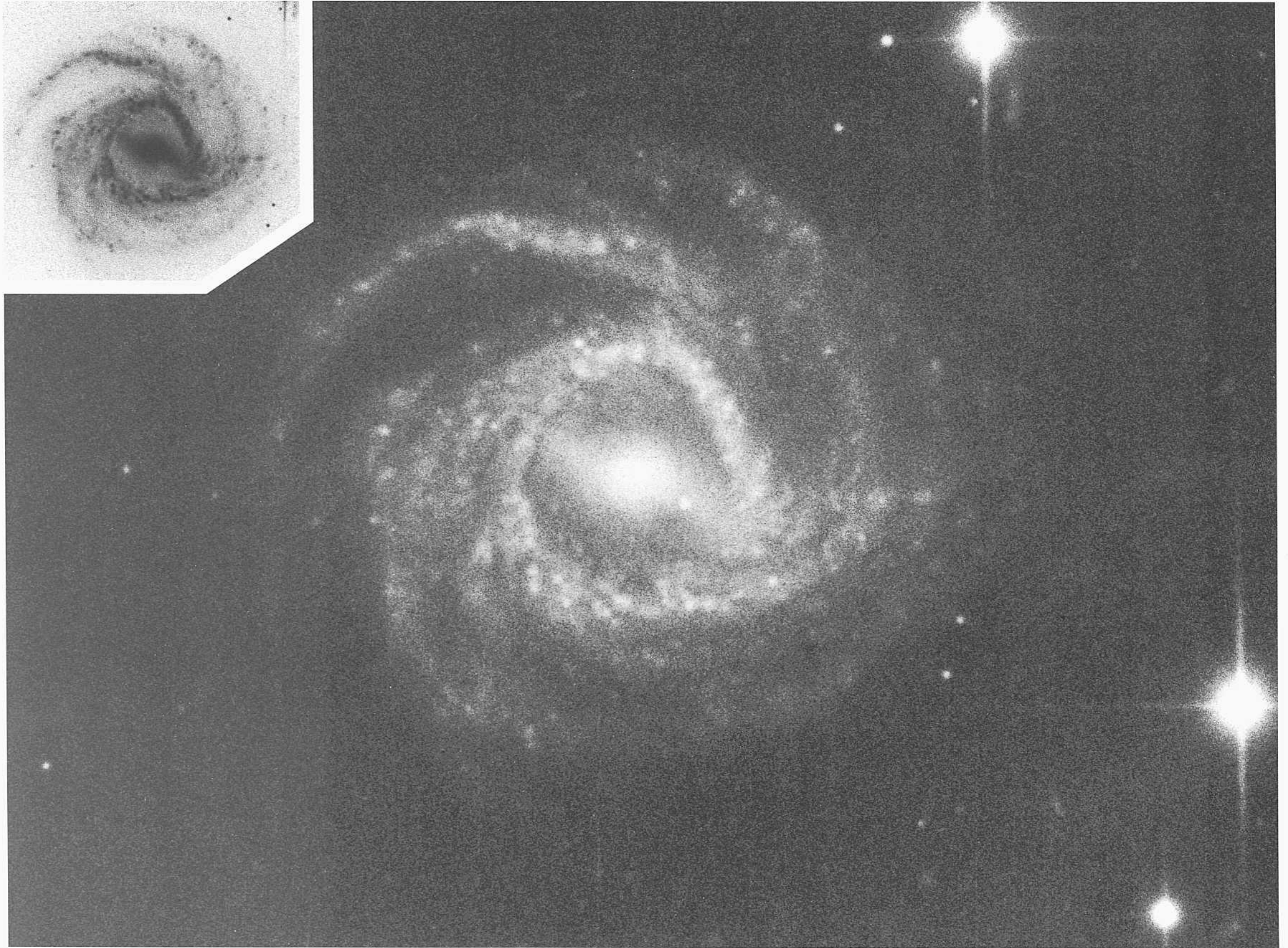



PANEL  
161





PANEL  
162




 OIBb galaxies of luminosity class **I-II** (along with a few of class **II**) are shown on this and **the next** four panels. Although the spiral arms are well defined, **the** arms are **thicker** in these galaxies than in luminosity class I galaxies and, as a consequence, the inter-arm regions are more cluttered with spiral-arm-like matter.

NGC 4902      **S151(rs)I-II**      **group**  
**CD-1842-HB**  
 April 2/3, 1981  
**103aO**  
 75 min

The apparent internal ring in NGC 4902 is the overlapping of two very bright arms of the NGC 1300 type which begin at opposite ends of the bar. Sets of other outer arms also exist, the brightest of which is semi-detached from the bright main inner arm (at the bottom of the print on the facing panel).

Many IIII regions exist in the bright parts of the several arms and the arm fragments.

NGC 4902 is kinematically associated with a loose group that includes NGC 4899 (Se; panel 232), 34' to the north, NGC 4891 (SBbc; panel 205), 64' to the north, and several other probable members listed in the RC2. The redshifts are  $z_o(4891) = 2418 \text{ km s}^{-1}$ ,  $z_o(4899) = 2437 \text{ km s}^{-1}$  and  $z_o(4902) = 2426 \text{ km s}^{-1}$ . At a mean redshift distance of 48 Mpc ( $z = 50$ ) the projected linear separations from NGC 4902 are 480 kpc and 903 kpc for NGC 4899 and NGC 4891, respectively. This aggregate, then, has a size nearly the same as the Local Group.

The four galaxies on this panel continue the illustration of SBbl-II barred spirals of the (r) and (rs) subset. The arms are generally multiple (MAS type), although NGC 5850 also has features of a grand design spiral.

NGC 7329 SB(r)I-II

CD-1586-S/Br

Aug 11/12, 1980

103aO + GG385

45 min

The almost-complete inner ring in NGC 7329 is very tight, and the overlapping spiral arms that compose it can be traced. The arms composing the ring do not begin at the end of the bar, as in NGC 1300, but rather about 15° downstream (relative to the direction of rotation) from these ends. The pattern is reproduced in some of the calculated models of Huntley (1978, 1980).

Multiple fragments of arms exist outside the inner ring.

The redshift is  $v_r = 3043 \text{ km s}^{-1}$ .

NGC 5850 SB(sr)I-II

CD-1417-S/Br

March 24/25, 1980

103aO + GG385

45 min

The pattern of an almost-complete inner ring in NGC 5850 is similar to that in NGC 7329, above. One of the overlapping inner arms that forms the ring begins about 15° downstream from one end of the bar. The star-formation rate is high there. Again, this pattern is reproduced in some of the models calculated by Huntley (1978, 1980) and others cited in the description to NGC 1300 (panel 154).

The fragmented outer arms are extensions of the two tightly wound inner arms, which form the ring after they nearly meet after half a revolution. HH-region candidates indicate a moderate current star-formation rate, especially in the inner arms.

A faint straight dust lane along the outside edge (in the direction leading the rotation, as inferred from the sense of the spiral pattern) is present along one side of the smooth straight bar.

The redshift is  $v_r = 2130 \text{ km s}^{-1}$ .

NGC 2642 SB(rs)I-II

CD-1325-S/Br

March 13/14, 1980

103aO + GG385

45 min

The bar in NGC 2642 is strong, and the inner arms spring from its ends, as in NGC 1300. The arms branch into multiple fragments soon thereafter.

Two weak, straight dust lanes exist along the outside of the smooth bar, as usual in the direction that leads the rotation.

The arms are filled with bright HII regions, the largest of which resolve at the 1.5" level. The redshift of NGC 2642 is  $v_r = 4262 \text{ km s}^{-1}$ .

NGC 7723 SB(rs)I-II

pair

PH-78-H

Oct 15/16, 1950

103aO

30 min

NGC 7723 forms a pair with NGC 7727 (See panel 83) that is about 40' northwest. The redshifts are  $v_r(7723) = 1976 \text{ km s}^{-1}$  and  $v_r(7727) = 1973 \text{ km s}^{-1}$ . The projected linear separation of the pair is 460 kpc using a redshift distance of 39 Mpc ( $H_0 = 50$ ).

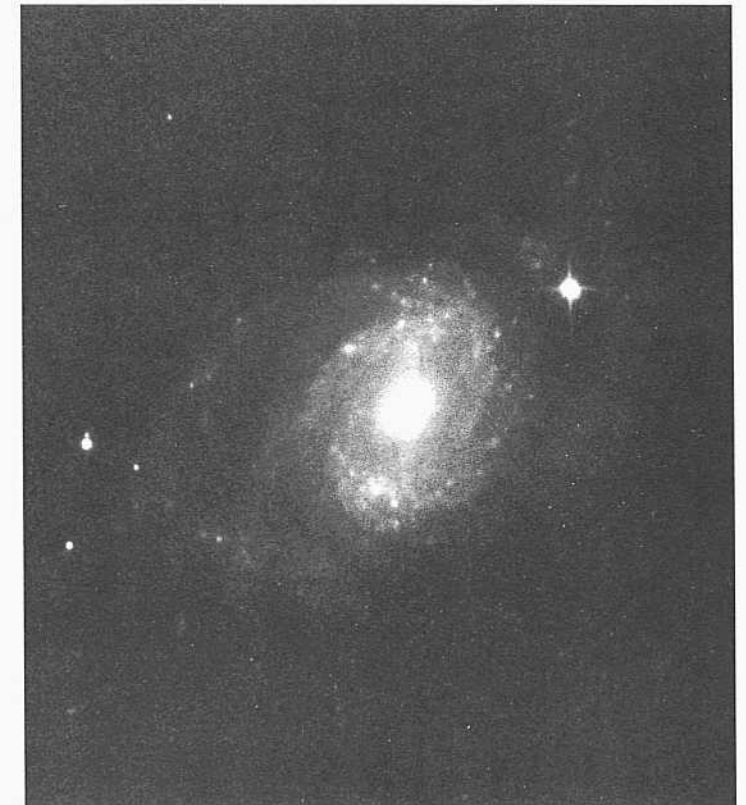
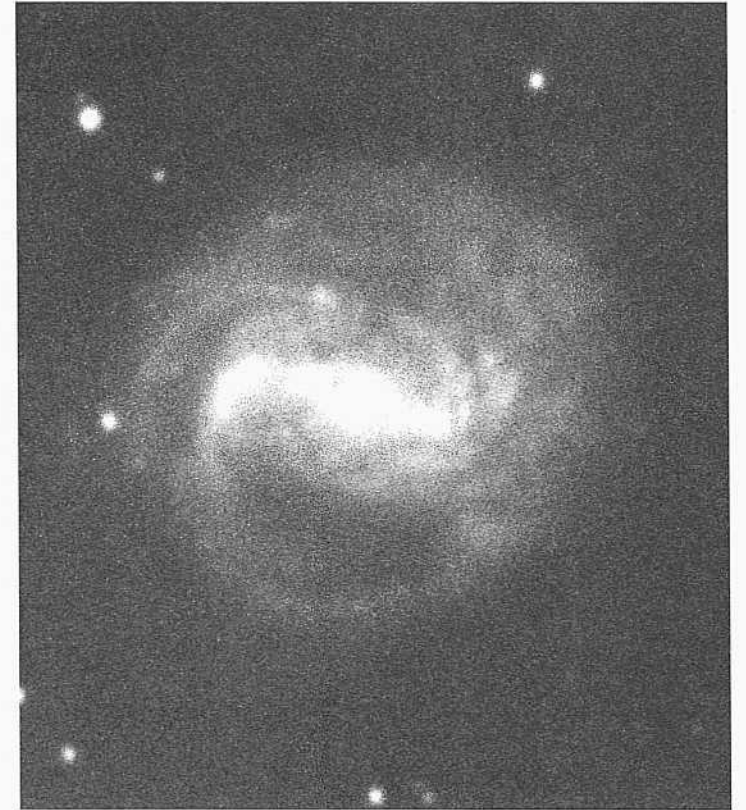
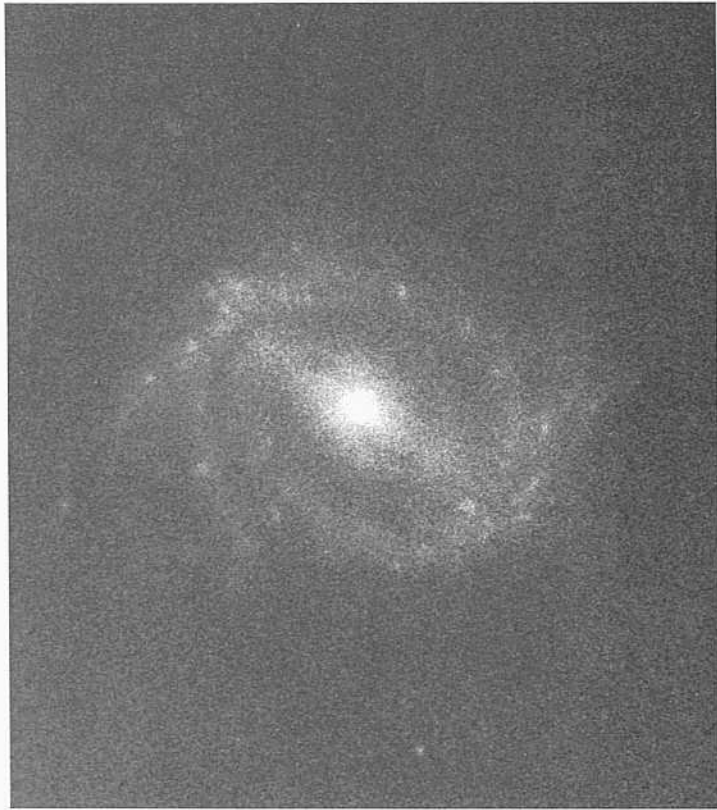
The characteristic straight dust lanes exist on the outside of the smooth bar in the direction leading the rotation. The lane on one side is smooth; on the other it is slightly broken. The internal ring from which the MAS spiral pattern begins is almost complete.



PANEL  
163



PANEL  
164



The six galaxies on this panel continue the illustration of SBb galaxies of high (I-T) to moderate (II) luminosity class; the well-formed arms show minimum disorder in the spiral pattern.

NGC 5347 SBb(s)I-II  
PH-8097-S  
Feb 6/7, 1981  
103aO  
12 min

The bar in NGC 5347 is straight, similar to the bar in NGC 1300, but it is not as luminous. The two characteristic straight dust lanes exist in the bar, but they are weak.

The arm pattern is of the NGC 1300 type, where two grand design arms spring from the ends of the bar. They are tightly wound in NGC 5347, giving the incorrect impression at first glance of a complete inner ring. The type is unmistakably SBb(s), but this case shows the need for high spatial resolution when classifying galaxies of small angular size.

The redshift is  $z_0 = 2394 \text{ km s}^{-1}$ .

NGC 3681 SBb(r)I-II  
CD-1841-HB  
April 2/3, 1981  
103aO  
75 min

The bar in NGC 3681 is a central oval, not a well-defined feature as in NGC 1300. The classification in the RC2 is that of a transition type between barred and ordinary spiral, denoted SABbc(r).

The arm type is multiple (MAS) and fragmented. A set of high-surface-brightness inner arms exists, together with a set of low-surface-brightness outer arms.

HII regions occur in both arm sets. They are unresolved at the 1" level. The redshift of NGC 3681 is  $z_0 = 1135 \text{ km s}^{-1}$ .

NGC 5156 SBb(rs)I-II  
CD-2141-S  
March 22/23, 1982  
103aO + GG385  
30 min

The bar in NGC 5156 is well formed and ends on the rim of one of the best-defined almost-complete rings in the RSA. The arms do not start exactly from the ends of the bar as in NGC 1300, but instead begin from about  $50^\circ$  downstream from each bar tip. This large downstream position (see previous descriptions of this phenomenon in this section) cause different arm segments to nearly overlap, creating the impression of a complete inner ring. The pattern is reproduced in some of the models of Huntley (1980) by changing the fraction of the total mass that is in gas.

NGC 782 SBb(r)I-II  
CD-1999-Bedke/Gregoiy  
Oct 22/23, 1981  
103aO + GG385  
46 min

The pattern of the almost-complete inner ring in NGC 782 is nearly identical to that in NGC 5156, above; the same description applies.

A set of three faint outer arms exists, starting at different points on the almost-complete inner near-ring.

NGC 5757 SHh(rs)II  
CD-I 171-Hr  
Aug 23/24, 1979  
103aO + GG385  
45 min

The spiral arms in NGC 5757 are not well defined. They are thick and somewhat chaotic. They primarily spring from the ends of a bar in the general style of NGC 13011, but are less well defined.

The several IIII-region candidates are unresolved at the 1" level. The redshift of NGC 5757 is  $z_0 = 2598 \text{ km s}^{-1}$ .

NGC 4639 SB1(;)II VCC 1943  
CD-818-S  
Feb 26/27, 1979  
103aO + Vr2c  
45 min

NGC 4639, a member of the Virgo Cluster, has a redshift of  $z_0 = 860 \text{ km s}^{-1}$ . Many of its IIII regions are concentrated in the spiral arms, where they begin at the ends of the bar. The largest of these regions resolves into disks at the 3" diameter level.



Three of the four galaxies on this panel combine features of (s) and (r) subtypes of spiral arms. All are of high-luminosity class I-II because of the regularity of the spiral pattern.

NGC 2712 SBh(s)I-II  
PH-7955-S  
Nov 8/9, 1980  
103aO  
12 min

The bar in NGC 2712 is moderately weak and is partially curved. The spiral pattern has three principal arms, two of which spring from the ends of the bar. The third begins at the middle of the bar and winds outward in fragments traceable for a total unwind of about  $300^\circ$ , overlapping the inner arm that begins at the opposite end of the bar for much of its final path. The largest HII region in the arms resolves at the 3" level. The redshift of NGC 2712 is  $v_o = 1892$  km s<sup>-1</sup>.

NGC 4593 SBb(rs)I-II HA, p. 48  
CD-1400-S/Br  
March 22/23, 1980  
103aO  
75 min

NGC 4593 has a strong straight bar with a characteristic straight dust lane along one of the leading edges (leading the rotation, whose sense is inferred from the sense of the spiral pattern).

A nearly complete inner ring is formed by the arms. One arm begins at the same distance from the center as where the bar terminates but at a position downstream by about  $15^\circ$ . The other principal arm begins at the end of the bar, as in NGC 1300.

The redshift is  $u_o = 2505$  km s<sup>-1</sup>. The galaxy is in the southern extension of the Virgo Cluster at a declination of  $-5^\circ$ , near the ridge of the supergalactic plane.

NGC 5135 SBbpec  
CD-2179-S  
March 28/29, 1982  
103aO + GG385  
15 min

The dust lanes in the bar of NGC 5135 are themselves curved into a spiral pattern similar to, but not as extreme as, the famous case of NGC 4314 (SBa; Hubble Atlas, p. 44; panels 95, 106 here). The faint spiral arms begin in an (s)-type NGC 1300 pattern from the ends of the bar. The brightest HII region candidates occur in one of the arms close to its beginning near the end of the bar. The largest of these resolves into a disk at about the 1" level. The redshift of NGC 5135 is  $v_o = 3906$  km s<sup>-1</sup>.

The absolute magnitude of the galaxy is bright, at  $M_B = -22.5$  ( $M = 50$ ).

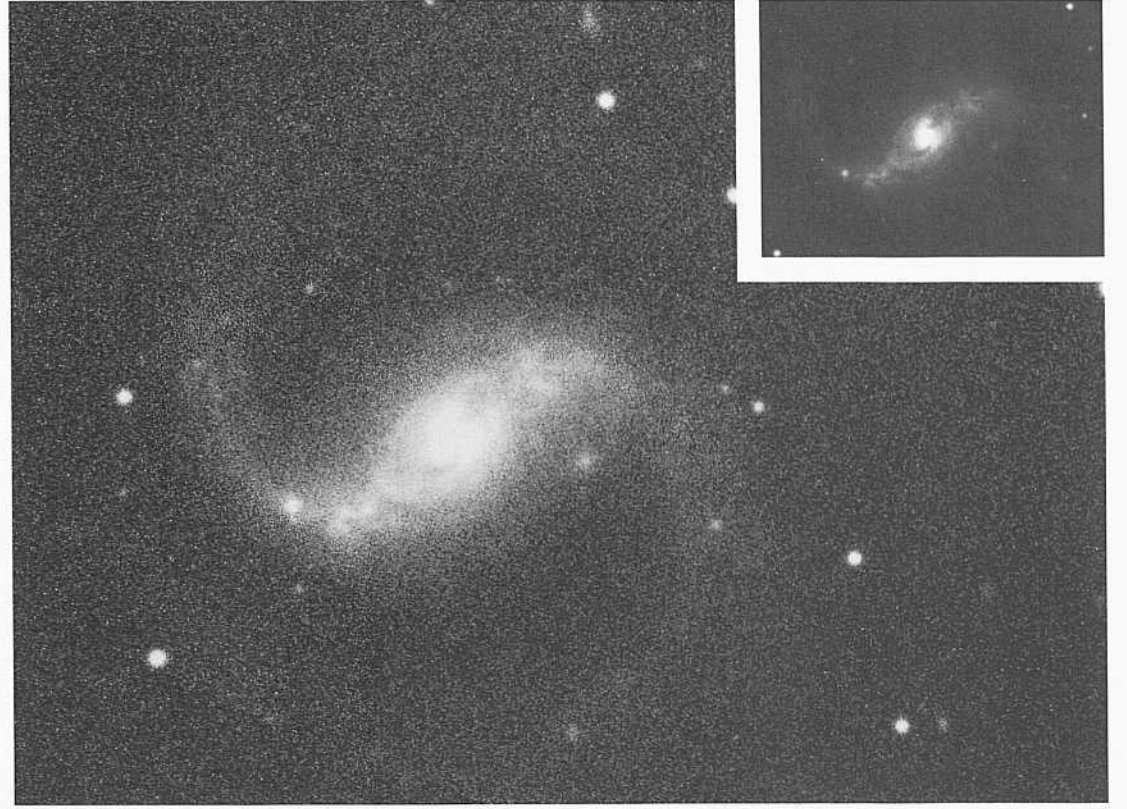
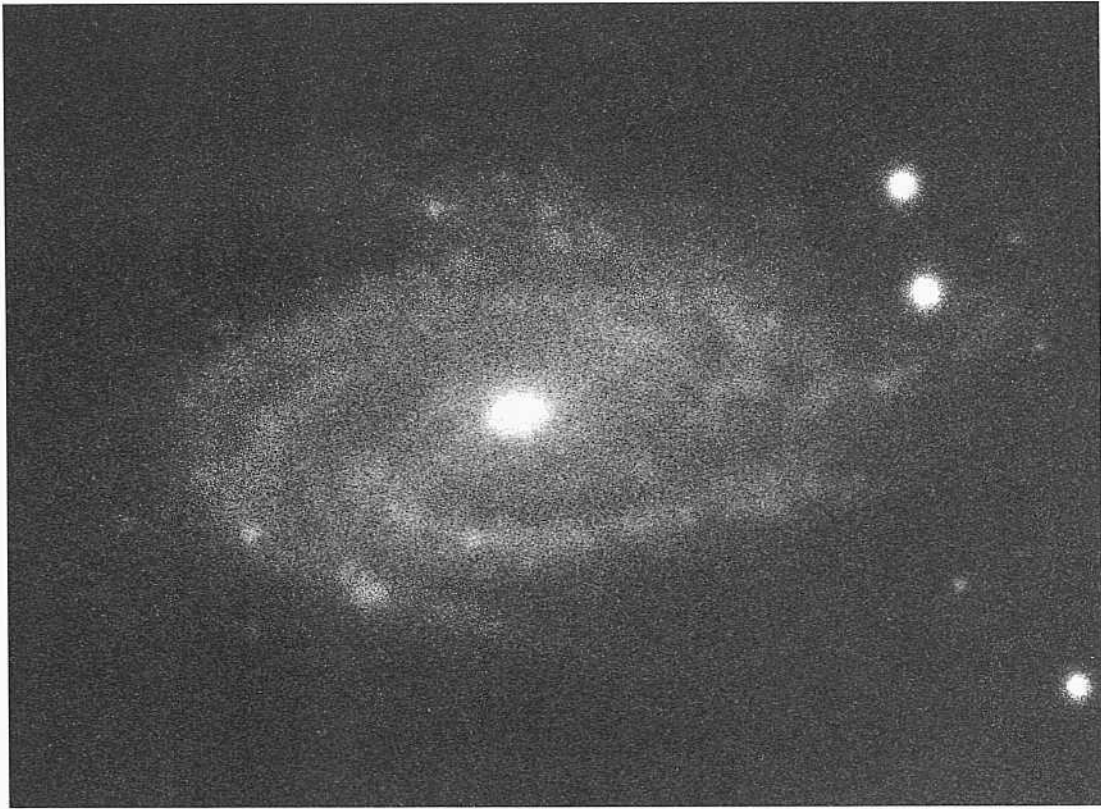
NGC 4394 SBb(sr)I-II VCC 857  
PH-425-MH HA, p. 47  
April 16/17, 1952  
103aO  
30 min

The bar in NGC 4394 is strong, but absent are the straight dust lanes along the leading edges seen in other SBb galaxies having strong bars. Instead there is a series of dust lanes close to one of the leading edges of the bar. (The leading edge on the other side may be on the far side of the image: a symmetrical pattern in the dust that may exist is undoubtedly hidden behind the bulge, similar to the pattern in other galaxies.)

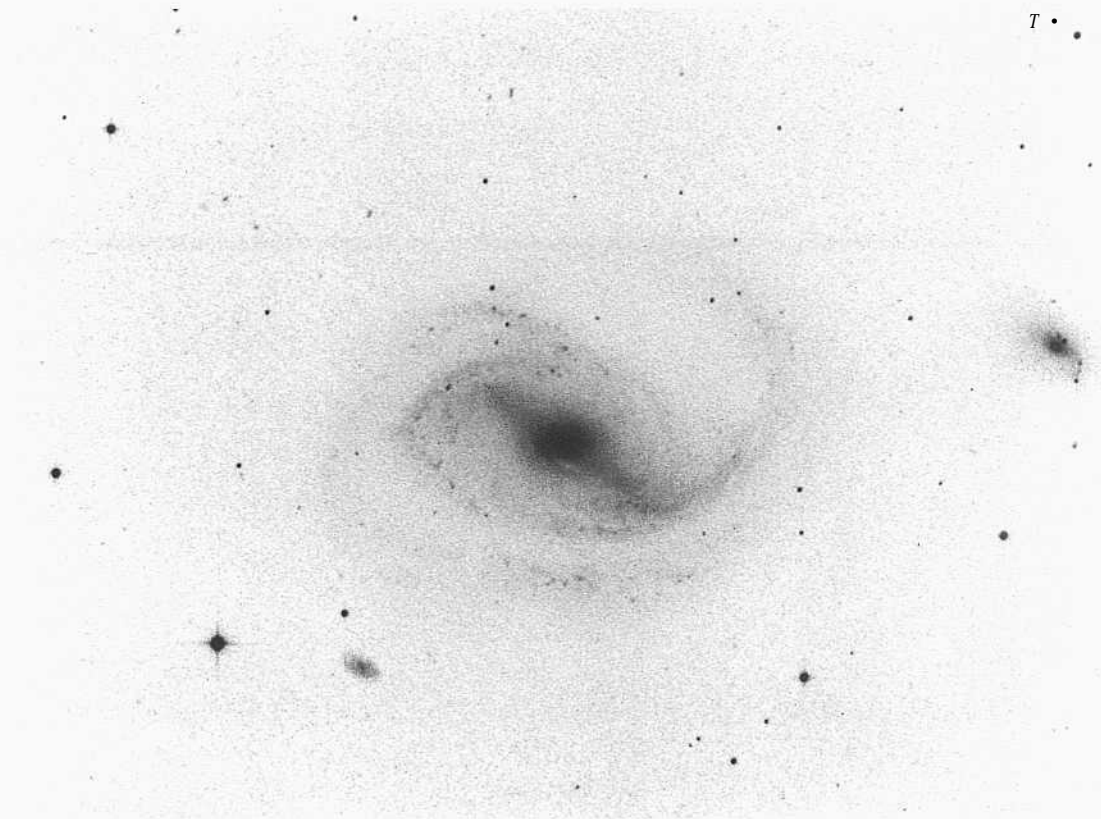
The dust lanes near the bar on the assumed near side have a pitch angle to their spiral pattern quite different from the pitch angle of the outer Luminous spiral arms. This pattern in the dust may outline the vectors of the velocity field near the bar that is determined by the hydrodynamic response of the gas to the rotating bar. The pattern seen here closely resembles the velocity maps near the bar that have been calculated in some of the models cited in the description of NGC 1300 (panel 154).

The spiral pattern of the luminous arms in NGC 4394 is intermediate between the (s) and the (r) subtypes, noted here by the mixed designation of (rs).

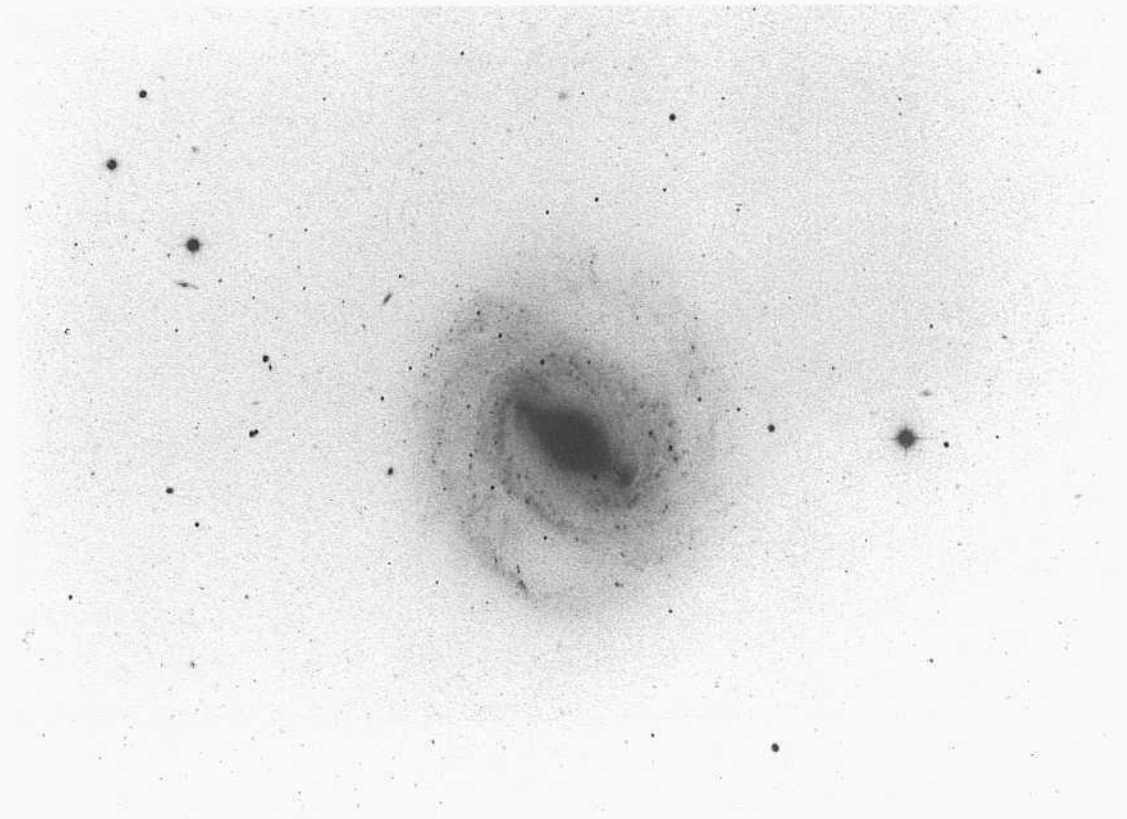
NGC 4394 is in the region of the Virgo Cluster north of the center of subcluster A around NGC 4486. Its redshift is  $u_o = 853$  km s<sup>-1</sup>.



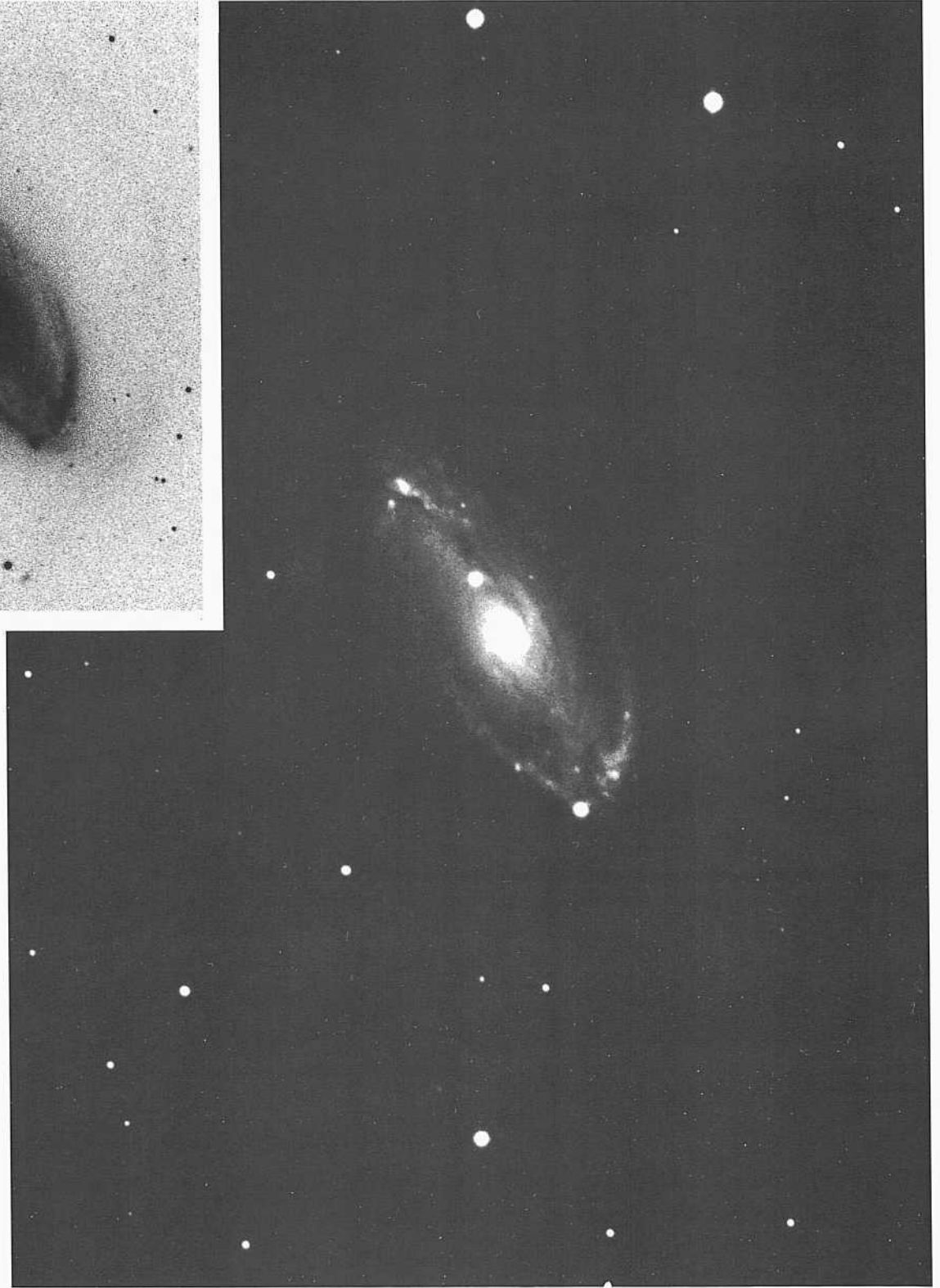
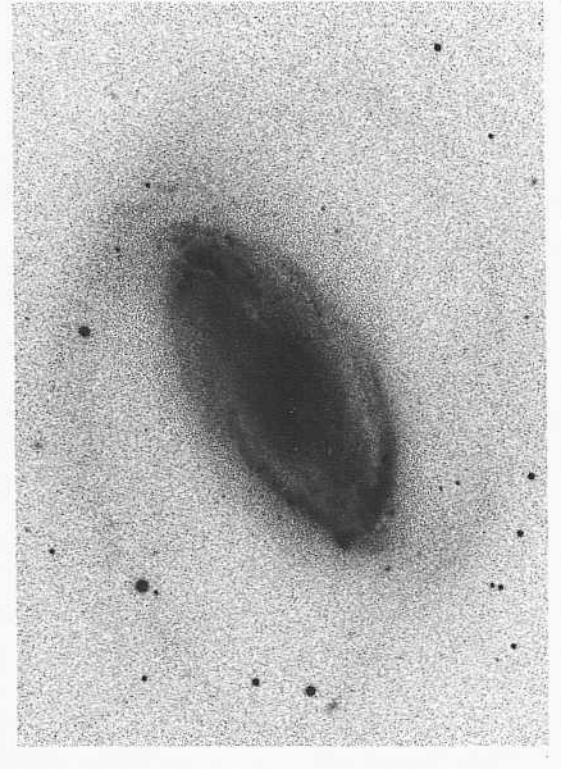
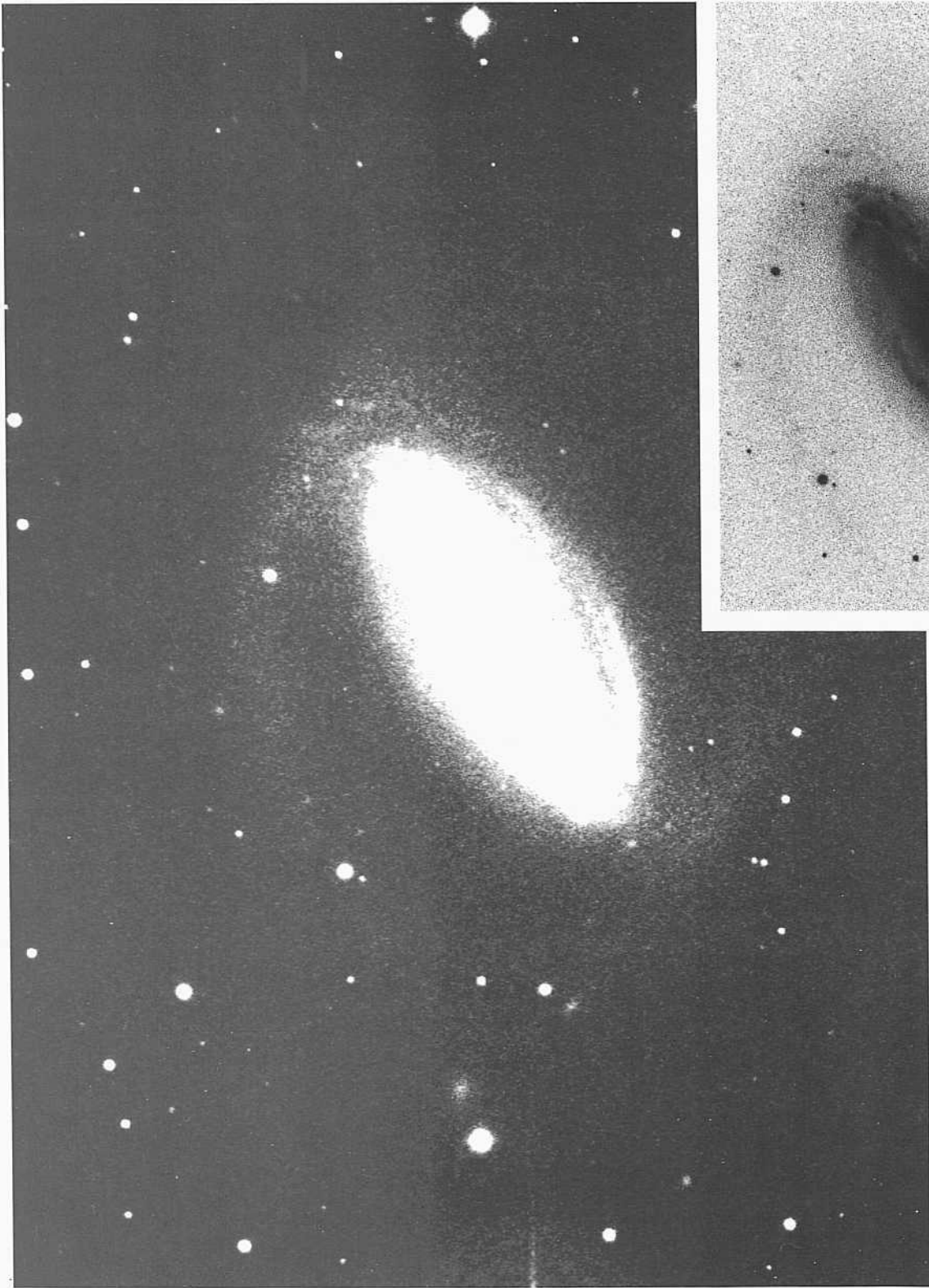
PANEL  
165



T •



PANEL  
166



*SBb Classification Section (continued)*

NGC 5728            sm><s)ll  
CD-226-S  
IV) 13/14, 1978  
103aO + GG385  
15 miii

The bar in NGC 5728 is weak, is a light oval, and has considerable internal structure in dust.

Two sets of spiral arms exist. The very-high-surface-brightness inner set spring from the ends of the bar, as in NGC 1300, and arc (er) Light!) wound, nearly overlapping out\* another after half a revolution. The impression of near-overlap is enhanced here because of the high inclination angle to the line of sight.

Two straight dust lanes exist on each of the leading edges of the bar. One lane is more visible than the other, presumably because of the usual different projection effects (it is normal asymmetry of dust patterns) on the near and the far sides. Besides the straight dust lanes on the leading bar edges, spiral dust lanes exist within the bar oval, as seen on the near side in the low-contrast print.

III regions are present in the inner arms near their beginnings at the end of the bar.

A set of very-low-surface-brightness regular outer arms exist, also beginning at the ends of the bar, seen only in the high-contrast print.

The redshift is  $v_D = 2001 \text{ km s}^{-1}$ . The absolute magnitude of the galaxy is bright at  $M_V = -22.5$ .

*SBb Classification Section (continued)*

NGC 613            SBb(rs)II

CD-443-Rose

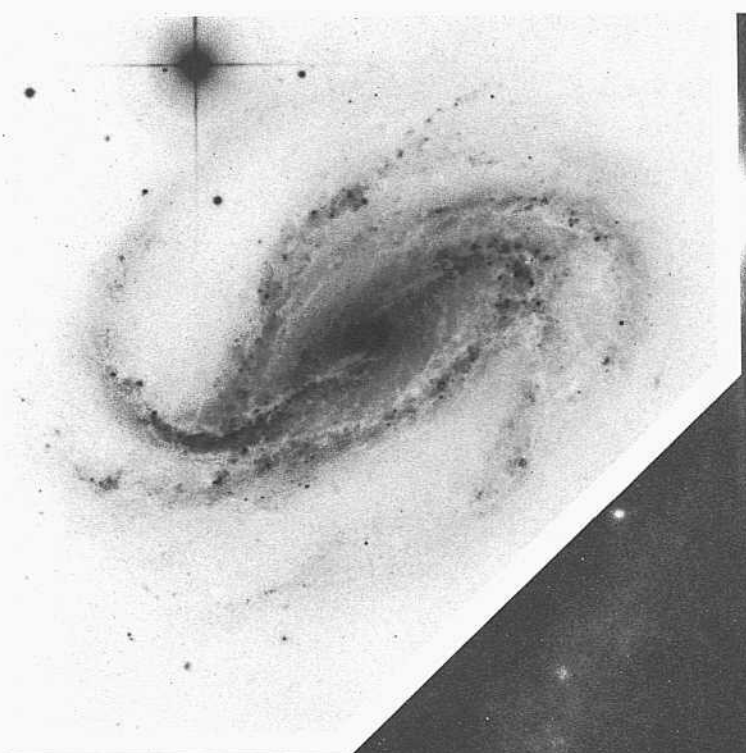
Aug 9/10, 1978

**103a0** + \Yr2c

**90min**

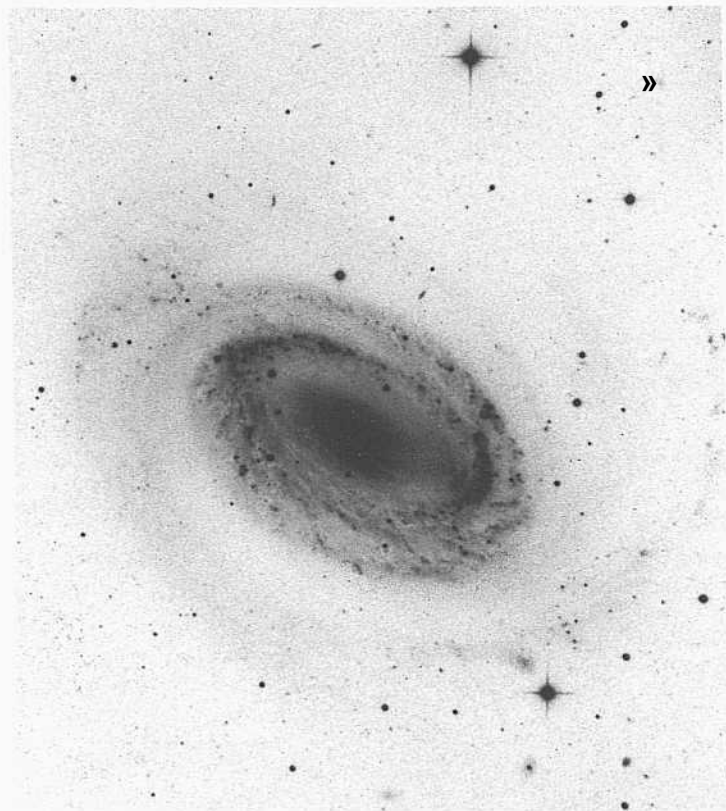
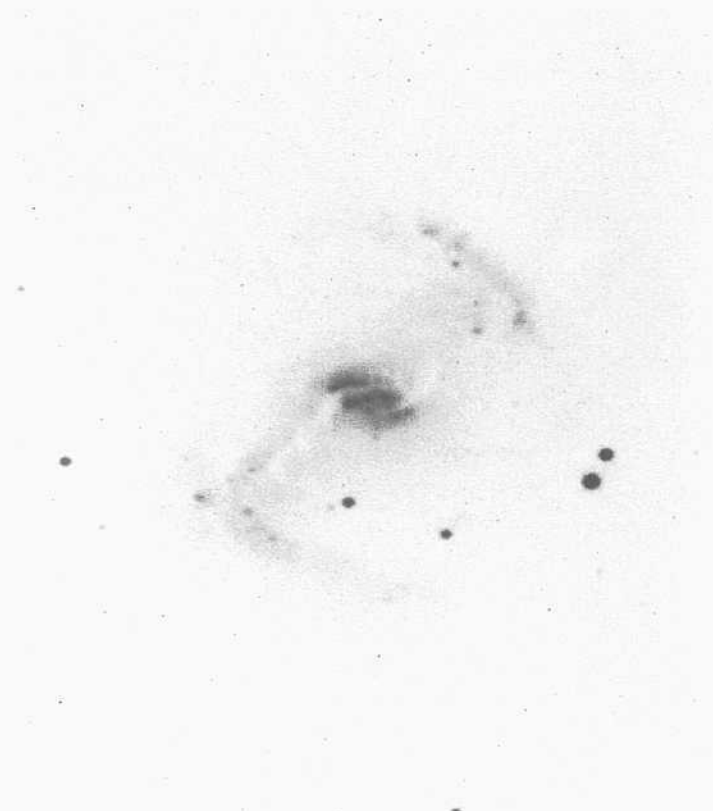
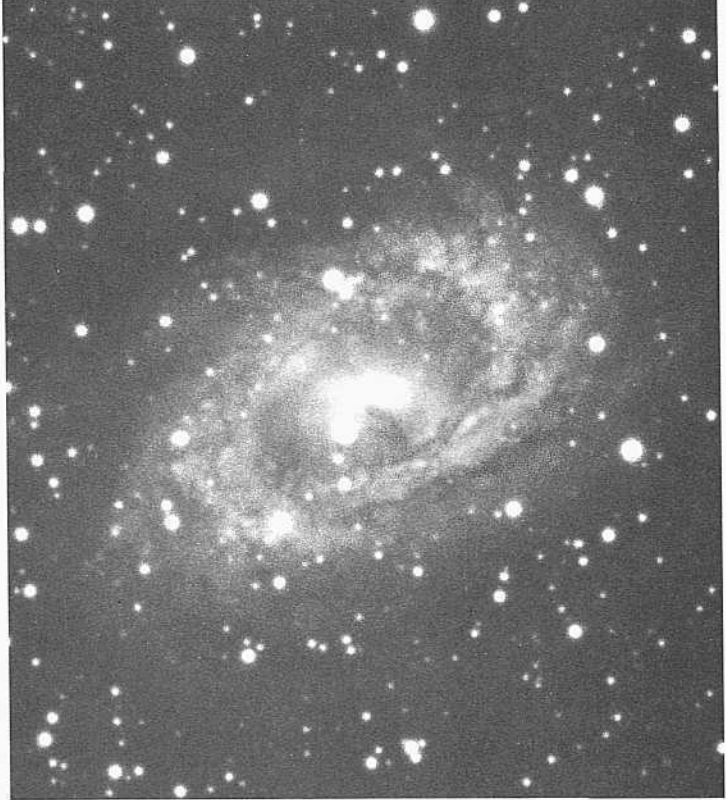
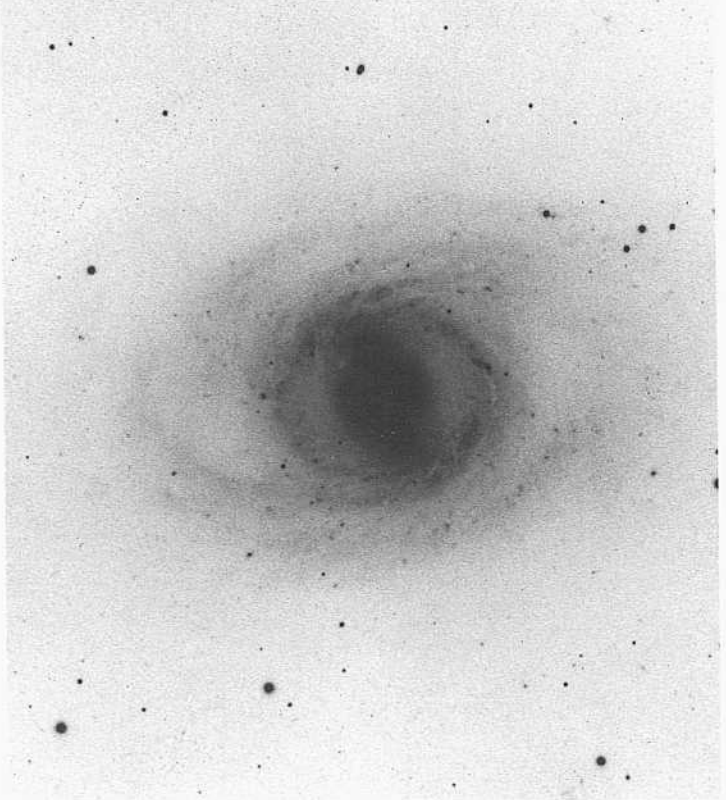
The bar in NGC 613 is a strong (high-surface-brightness) oval. The characteristic two straight dust lanes on opposite sides of the oval are evident. Each lane is on the leading edge of [the oval as judged from the direction of rotation determined by the sense of the spiral pattern. Other dust lanes at the outer boundary of the oval are curved into spiral patterns at sharp pitch angles which differ from the pitch angles of the outer spiral arms. The various patterns of inner luminous arms and inner dust lanes have a striking resemblance to maps of velocity fields based on calculations of the hydrodynamic response of gas to the rotating bar (or oval) gravitational potential, as cited in the description of NGC 1310 (compare **Huntley** 1980 with earlier references).

The high surface brightness of the arms and the many IIII-region candidates show a moderate-to-large current star-formation rate. The largest IIII regions resolve at the 3" level. The redshift of NGC 613 is  $v_r = 1534 \text{ km s}^{-1}$ . The absolute magnitude is bright, at  $M_B = -22.2$  ( $H = 50$ ).



PANEL  
167

PANEL  
168



**T**  
 1 be five galaxies on this panel arc of later luminosity class than most of the previous galaxies in this section. The arm pattern is generally less well defined, the arms are thicker, and the inter-arm region is more heavily filled with spiral-arm material.

NGC 5383      SBh(s)II      HA, p. 46  
**PH-8099-S**  
 Feb 6/7, 1981  
 103aO  
 12 min

High- and low-contrast prints of NGC 5383 shown here and below, are made from different original plates, one with the Palomar Hale 200-inch and the other with the Mount Wilson 60-inch telescopes.

The most prominent feature of NGC 5383 is the characteristic two-lane dust pattern along the bar. One of the lanes is very straight; the other has curves in its passage from the center to the end of the bar.

The arms that begin in an (s)-type NGC 1300-like pattern are brightest near their junction with the ends of the bar. Low-surface-brightness fragments of arms exist as branches (twigs?) inside (i.e., closer to the bar) the positions of the two major arms.

The redshift is  $v_r = 2322 \text{ km s}^{-1}$ .

NGC 5383      SBb(s)II      HA, p. 46  
 S-195-Pease  
 April 3/4, 1913  
 probably blue  
 180 min

The Mount Wilson plate used here was taken by the legendary astronomer Francis Pease, engineer extraordinary, who designed the Mount Wilson 60-inch and 100-inch reflectors and did much of the early design of the Palomar 200-inch telescope.

The nature of the dust pattern in the center of NGC 5383 is well seen in the low-contrast print here of the central regions. One lane passes in front of the nucleus, the other behind it. This form may be present in all SBb galaxies having straight dust lanes, but is seldom seen with the clarity that is provided by the particular viewing aspect given us with NGC 5383. The detail is also well seen in the Hubble Atlas print, made from the same Mount Wilson 60-inch plate used here.

NGC 3351      SBb(r)II      HA, p. 48  
**PH-315-S**      panel 170  
 Jan 8/9, 1953  
**103aD + GG11**  
 30 min

NGC 3351 is seen almost face on. The details of the nearly complete inner ring are well shown at this viewing angle. The two main inner arms spring from the end of a very strong bar. They nearly meet after each has turned by  $180^\circ$ , giving the impression of a true ring, yet the structure is clearly broken, being composed of two separate spiral segments.

The outer arms, of low surface brightness, are multiple and are branched into separate fragments, none of which can be separately traced for more than about one-quarter revolution.

Star formation is only moderate in these outer arms. The III regions are few and are small. The redshift of NGC 3351 is small,  $v_r = 641 \text{ km s}^{-1}$ , yet the stellar content is not well resolved.

The high-surface-brightness inner arms forming the usual near-ring pattern are well seen in the Hubble Atlas print where, however, the extensive low-surface-brightness outer arm pattern is largely invisible, it is well seen in the print here.

NGC 4725      Sb/SBb(r)II      HA, p. 21  
**H-2156-H**  
 Jan 2/3, 1941  
 Cr-Hi-Sp-Sp  
 80 min

The bar is not well defined in NGC 4725. It is a region of enhanced luminosity but still of low surface brightness, elongated across the central lens. (See the print in the Hubble Atlas for good detail of this region.)

The inner, high-surface-brightness spiral pattern forms one of the most complete near-rings of any galaxy in the RSA. Star formation is high in this near-ring. Many bright III regions exist, as well as a number of faint small ones. A few of these in the outer faint-surface-brightness arms resolve into disks at the 3" level. The redshift of NGC 4725 is  $v_r = 1167 \text{ km s}^{-1}$ .

Very-faint-surface-brightness outer arms are branched. The principal one of these arms is an extension of a bright inner arm that forms part of the nearly complete inner ring. This arm branches into two, which then travel together for another  $200^\circ$  of unwind.

NGC 6300      SHh(s)II pec  
 CD-1479-S/Rr  
 May 1 1/12, 1980  
 103aO + GG385  
 15 min

NGC 6300 is in low galactic latitude ( $b = -14^\circ$ ), and may have Galactic dust silhouetted against its face.

The original plate from which the print here is made was obtained in poor seeing, clearly seen from the size of the stellar images.

The bar is ill defined but evidently is straight. The arms spring from opposite sides of outer regions, far from the nucleus and, evidently, from the ends of a bar.

Dust is evident, but, again, some of what is seen may lie of superposed Galactic origin. The arms are branched, one after about half a revolution from its origin on the bar. The other arm branches twice, once after about  $15^\circ$  of unwind and again after about a one-quarter additional turn. Outer, low-surface-brightness fragmented multiple arms are extensions of the bright inner arms.

NGC 5691      S(B)b pec III:  
 CD-1391-S/Br  
 March 21/22, 1980  
**L03aO**  
 75 min

The classification of NGC 5691 is uncertain. There is a suggestion of a bar in a region of enhanced luminosity buried in the disk: hence the S(B) tentative classification is given. A weak spiral pattern exists together with dust patches and knots which are presumed to be III regions. The chaos is high; hence the low luminosity class, by definition, is assigned. However, the absolute magnitude is still moderately bright at  $M_B = -20.3$ . The redshift is  $v_r = 176 \text{ km s}^{-1}$ .



SUMMARY OF THE SBb CLASSIFICATION SECTION (PROTOTYPE EXAMPLES)

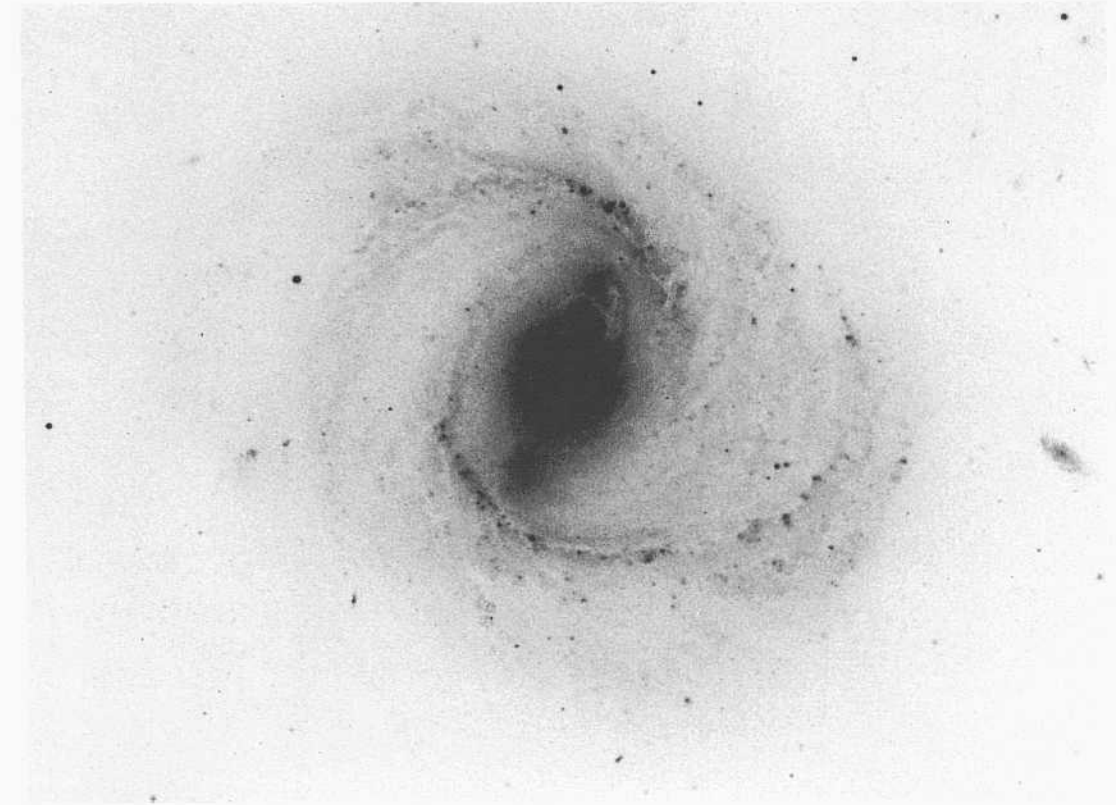
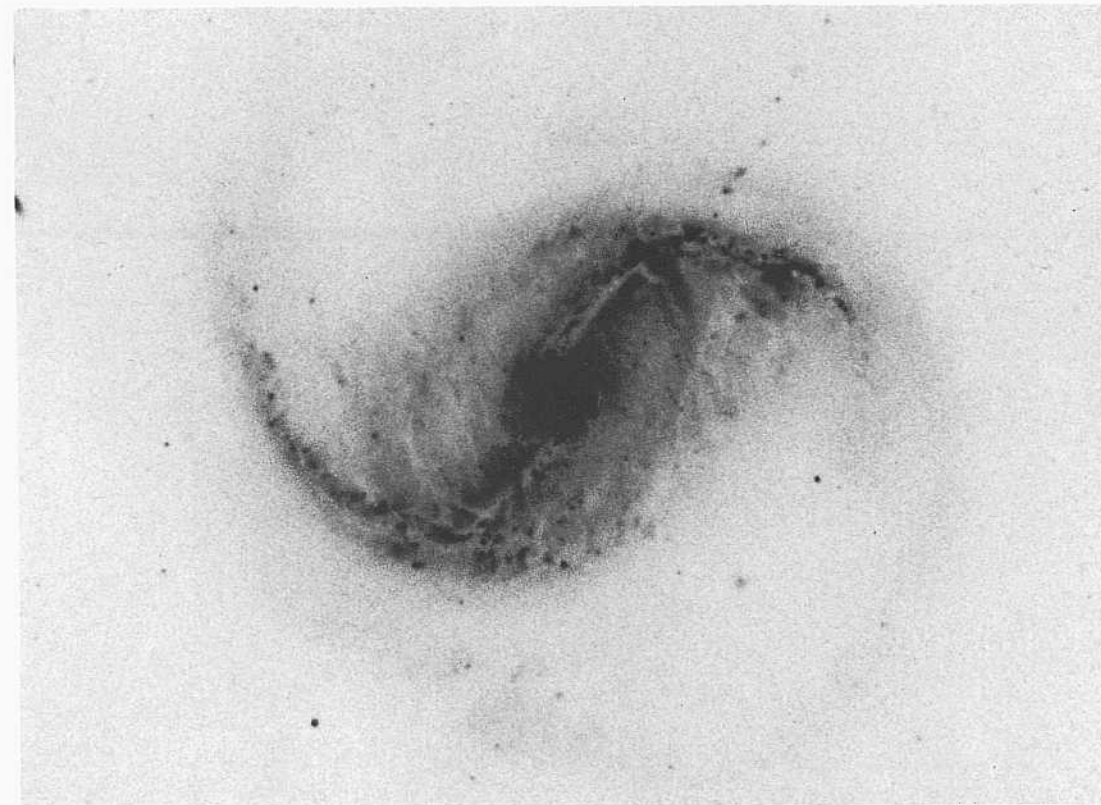
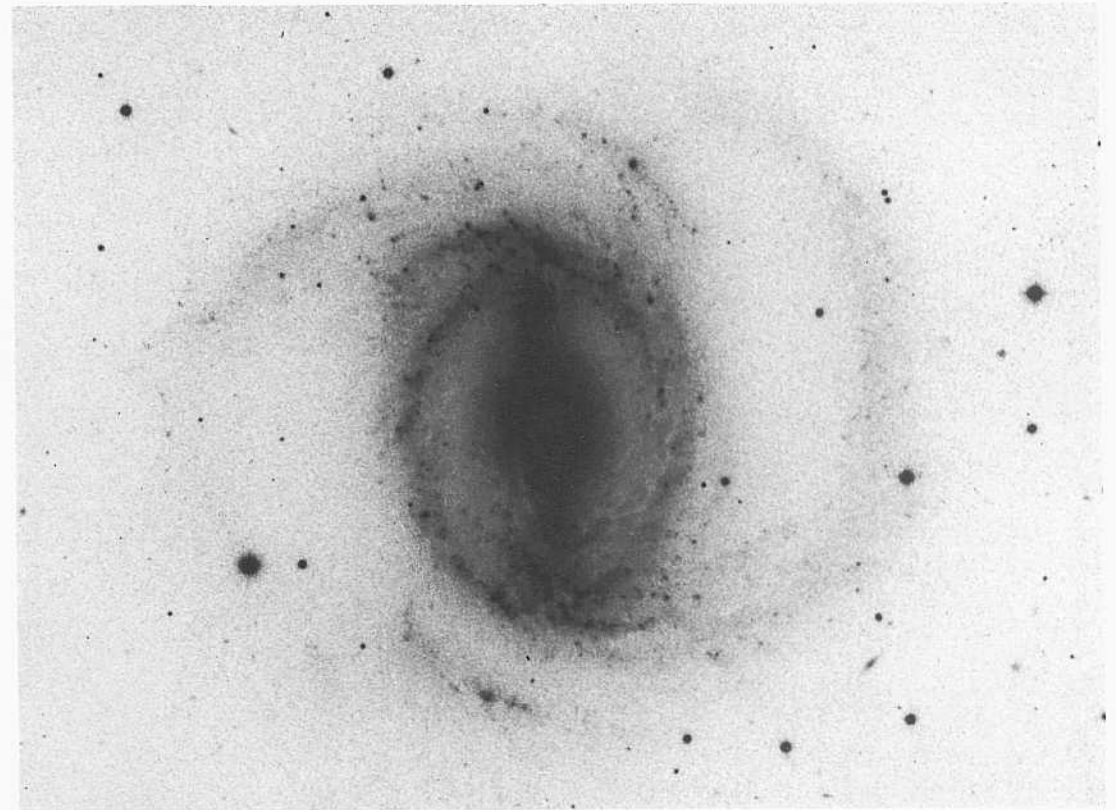
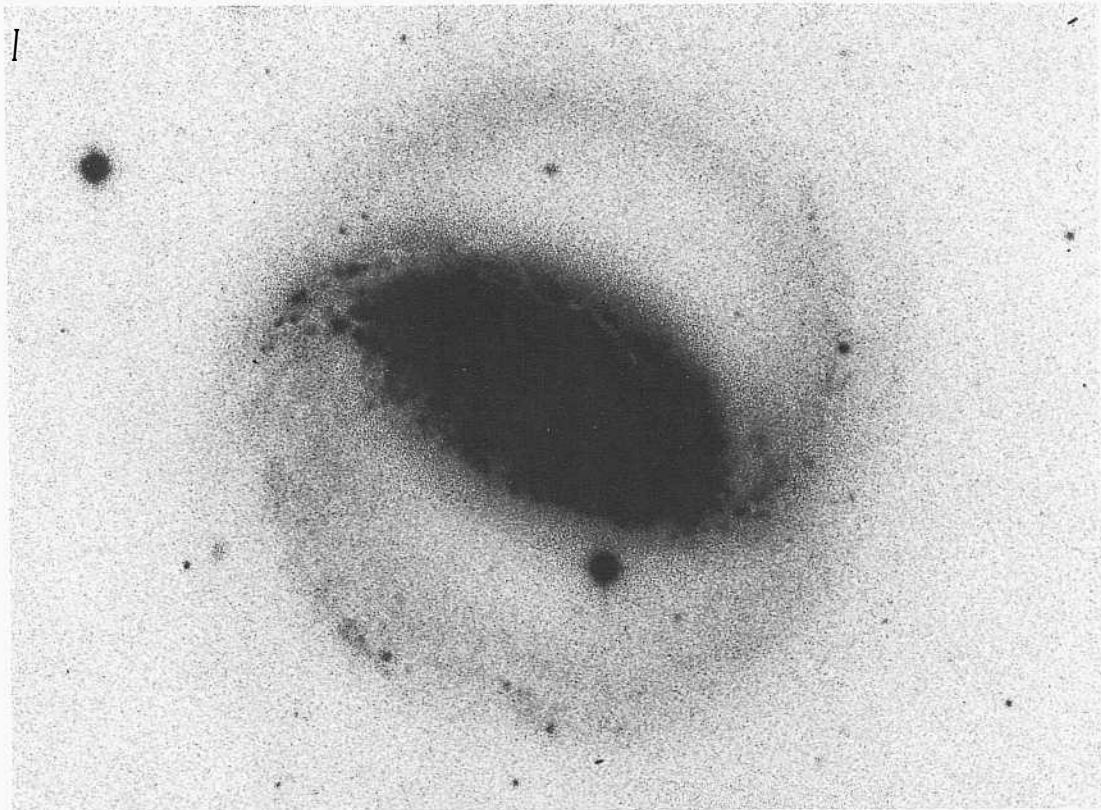
**T**he galaxies on this and the following panel are **illustrated** as summaries of **similarities** in the basic **forms of** outer arm structure (this page) and characteristics of strong bars (next panel). Four of the five galaxies shown on these two panels have been illustrated in previous panels of this SBb section.

The images of all four galaxies on this page have been overprinted to show the structure of the faint-surface-brightness grand design outer arms; the central barred regions are mostly burned out but are shown on the next panel.

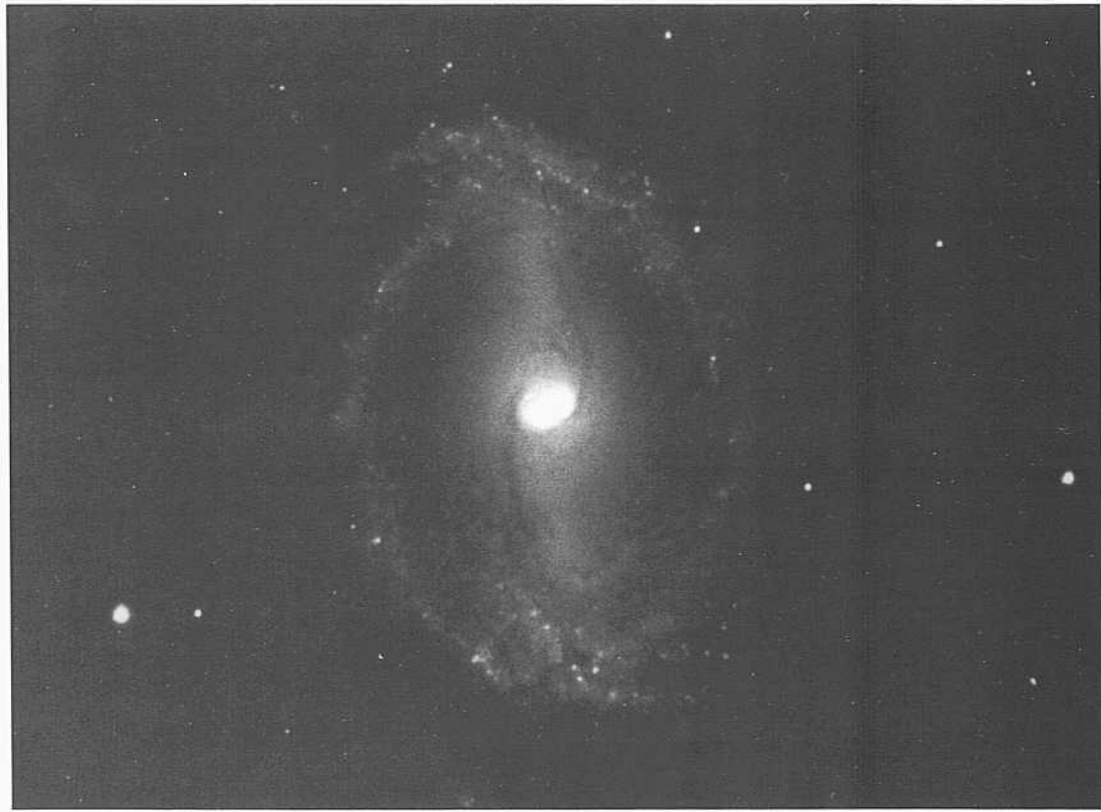
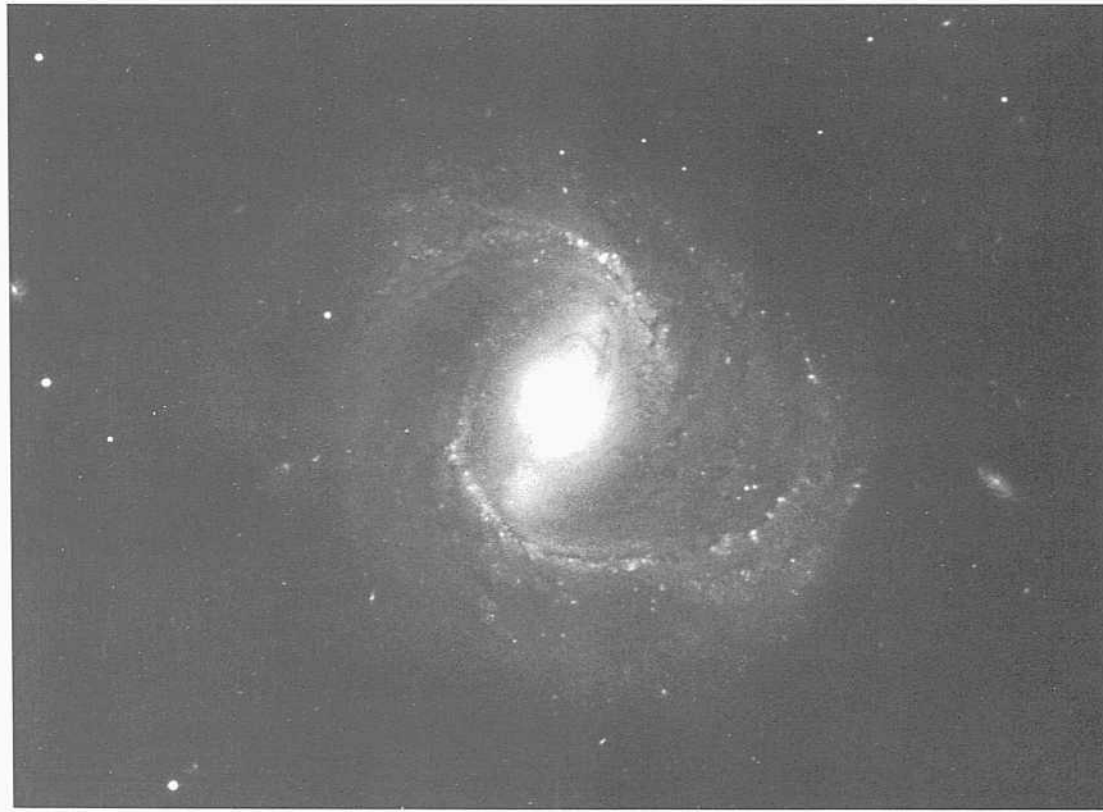
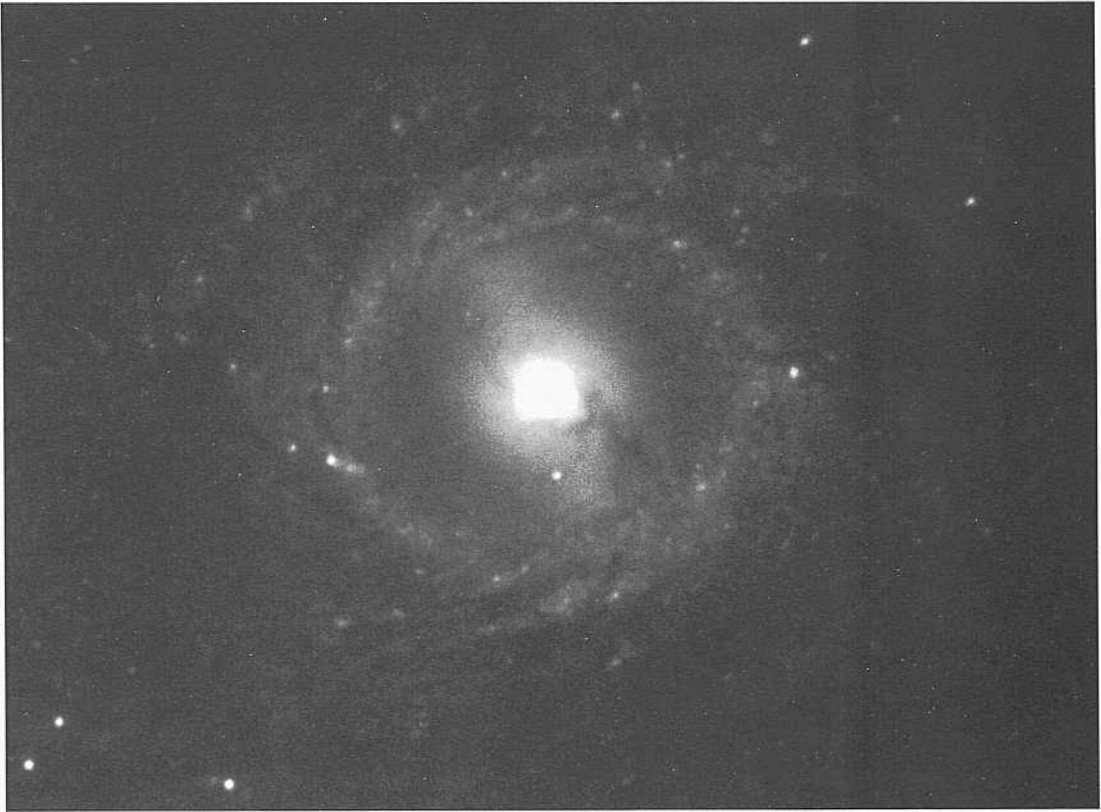
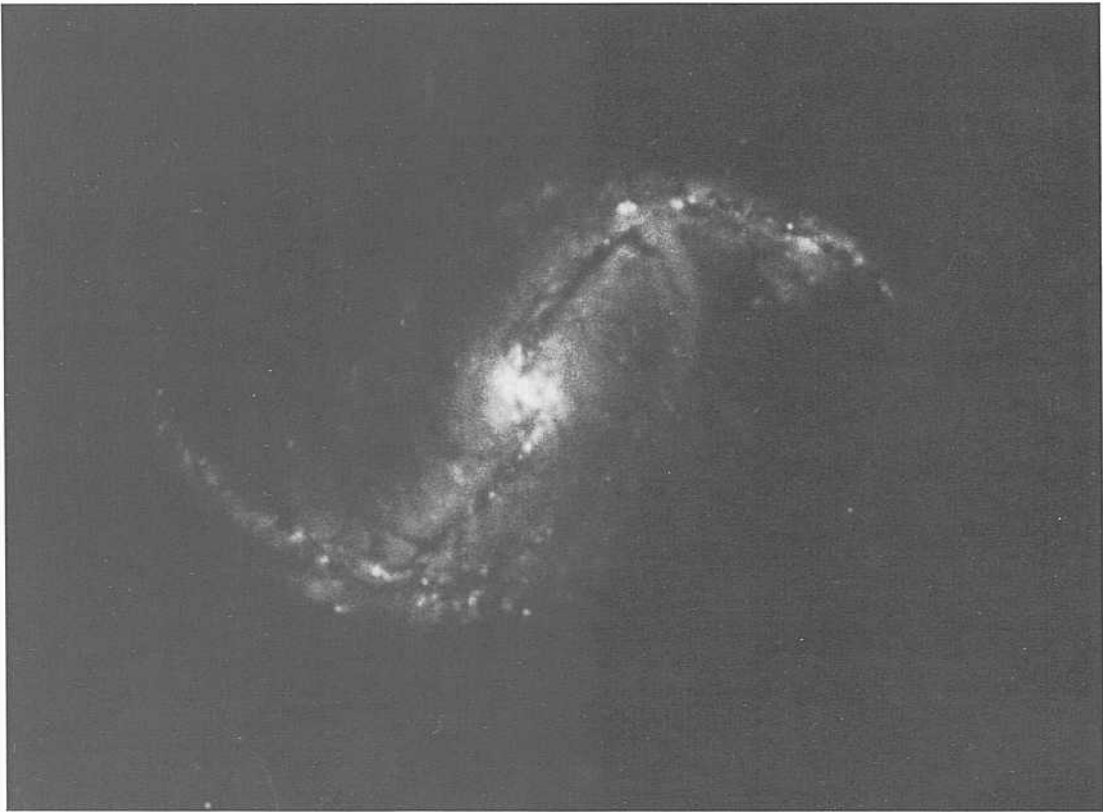
The outer arm pattern in all four cases here is highly symmetric on reflection of any part of the pattern through the center.

The two main outer arms can each be traced for about a half revolution, at which point they come close to, but are slightly outside, the point on the bar where the opposite arm begins, forming an almost-complete outer ring. The closest to a completed outer ring occurs in NGC 3504, at the upper left.

NGC 3504	Sb(s)/SBb(s)I-n	HA, p. 46	NGC 1433	SBb(s)I-H	panels 158, 170
<b>PH-1169-S</b>		panel 157	CD-177-S		
Dec 14/15, 1955			Feb 6/7, 1978		
103aO			103aO + GG385		
30 miii			45 niin		
NGC 986	SBI(:s)I-II	panels 158, 170	NGC 4548	SBb(is)I-II	VCC 1615
CD-2007-Bedke/Gregory			CD-756-S		HA, p. 48
Oct 23/24, 1981			Feb 4/5, 1979		panel 170
103aO + GG385			103aO + Wr2c		
45 mill			50min		



PANEL  
170



**E**ach of the four galaxies on this last panel of the SBb section have strong bars **from** whose ends the outer spiral pattern begins. There are no true complete inner rings in any of these four galaxies, although the near-overlapping of the first set of high-surface-brightness inner arms in NGC 3351 and NGC 1433 in the right-hand column gives such a first impression. Yet close inspection shows that each set of inner arms begins from the ends of the bar in the manner of NGC 1300 (panels 154, S8).

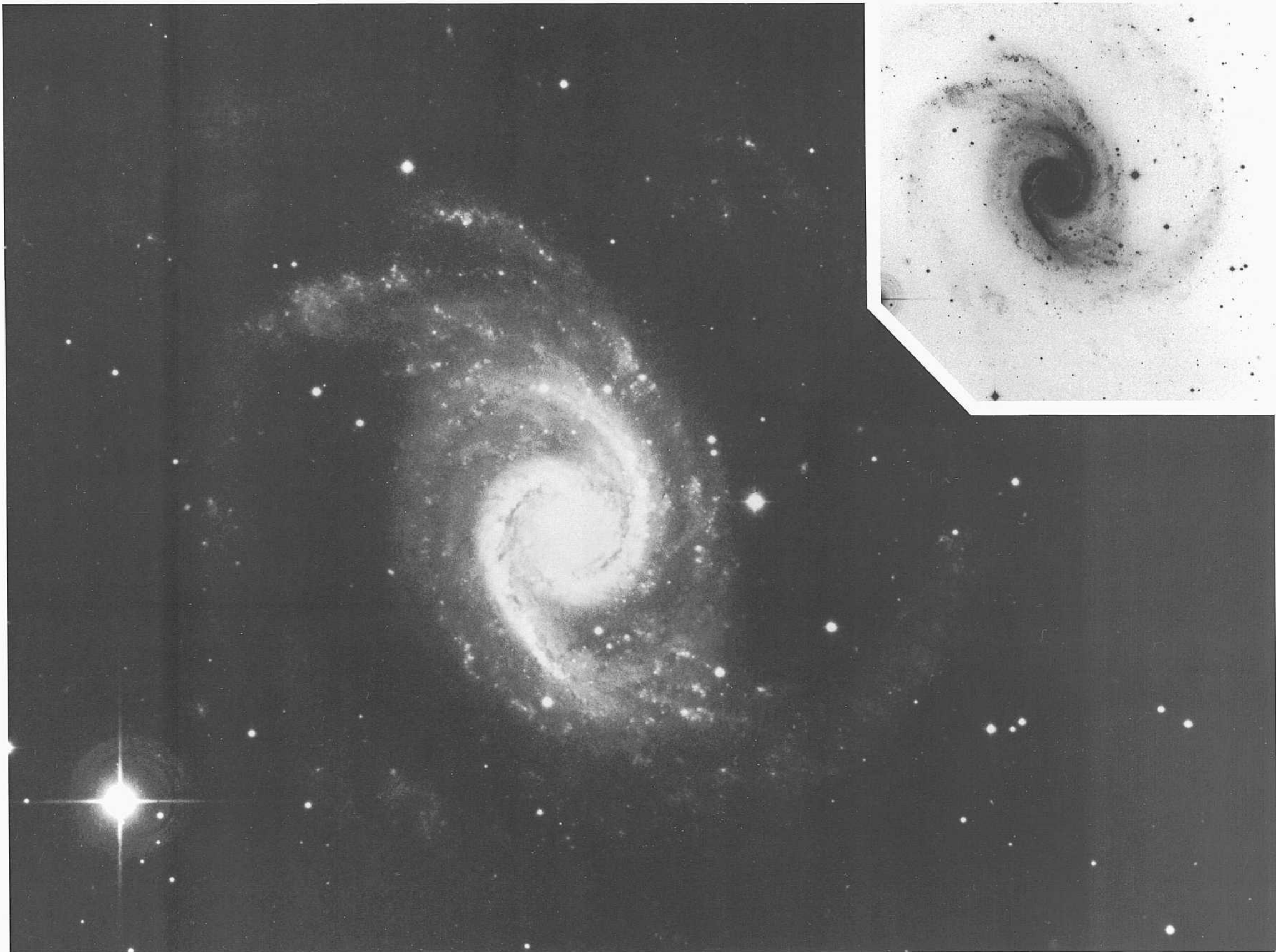
The characteristic straight dust lanes at the two leading edges (relative to the direction of the rotation determined

by the sense of the spiral **pattern**) of **the** bar are well seen in NGC 986, at the **upper** left. Similar, **1>ll** less **pronounced** and less straight lanes exist in NGC 4548 (lower left) and NGC 1433 (lower right). Only one such lane exists in NGC 3351 (**upper** right), and it is less regular than in the other galaxies here.

Calculated models of **the hydrodynamical** response of the gas to a rotating bar, cited in **the description** of NGC 1300 (panel 154), **reproduce** well **with the patterns** of **the dust** lanes, the central oval **around** the bar, and the outer spiral arms.

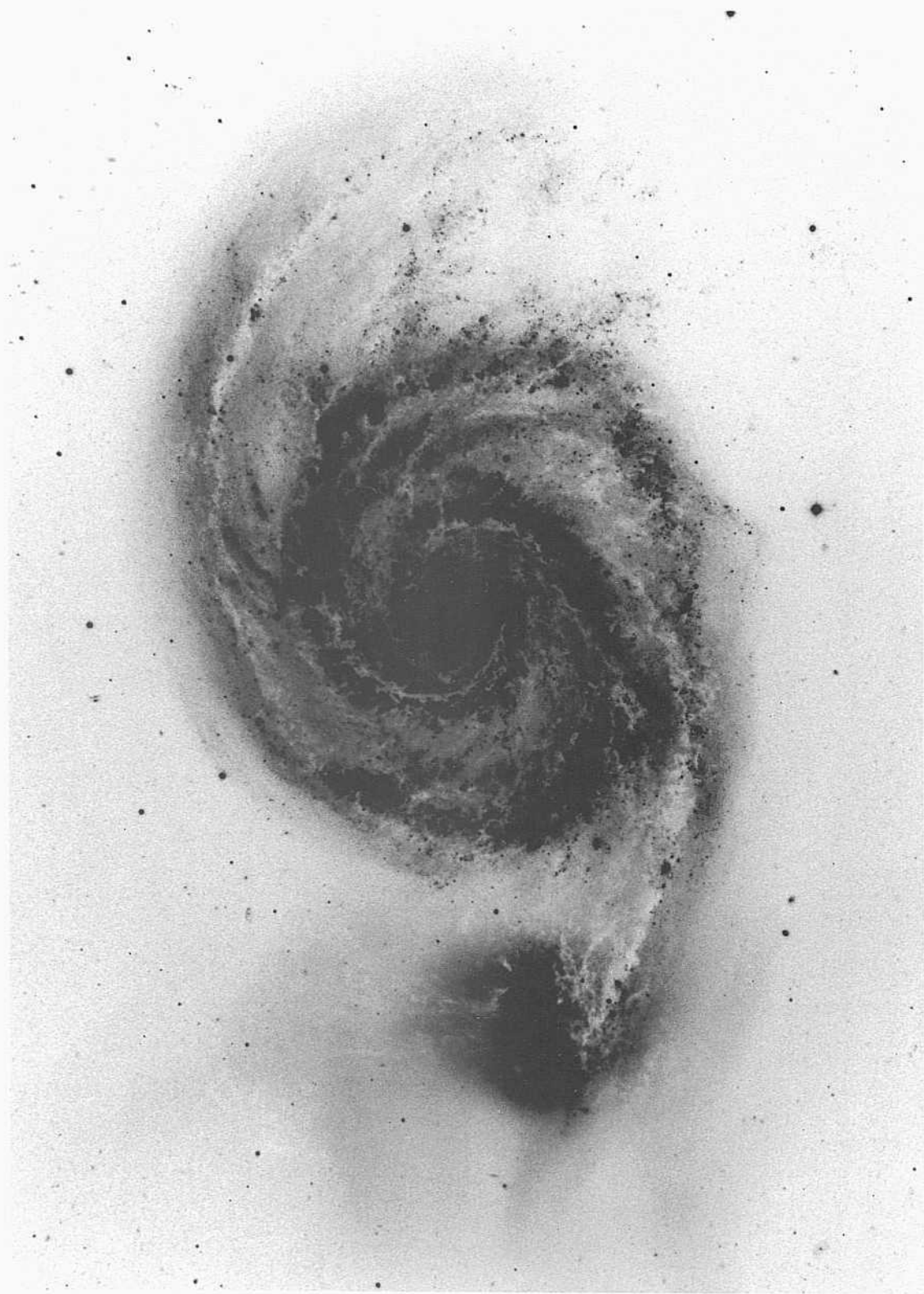
NGC 986	SBI(is)WI	panels 158, 169	NGC 3351	SBb(r)II	HA, p. <i>Hi</i>
CD-2007-Be<lke/Gregory			PH-314-S		panel 168
Oet23/24, 1981			Jan 8/9, 1953		
103aO + GG385			103aO + WG2		
<b>45 mill</b>			<b>15 mill</b>		
NGC 4548	SBh(is)I-II	VCC 1615	NGC 1433	SBb(s)I-D	panels 158, 169
CD-756-S		HA, p. 48	CD-177-S		
Feb4/5, 1979		panel 169	Fcl)6/7, 1978		
103aO + Wr2c			103aO + GG385		
<b>50 mill</b>			45 min		





PANEL  
171

PANEL  
172



*Sbc Classification Section (continued)*

NGC 519-1/5195 **Sbc(s)I-II** **HA, pp. 26, HI**  
**PH-201-MH** **SBOi pec** **M51**  
May **14/15, 1950** **panels 55, 177**  
**103aO**  
**20 min**

NGC 5194 (MS1) is similar **Lo** NGC 1566 **on the preceding** panel. **The surface brightness of the two principal grand design arms is high**, seen best in **the print on the right**. **This lighter print shows the intricate but well-organized dust lanes inside the two major inner arms**. Dust is also present in **the inter-arm region**, well **silhouetted against the background** disk **lijihl at the rim of the bright central bulge where the short dust lanes emerge almost radially from the bulge before breaking into the general spiral** pattern.

The heavy **print on the Left** shows the smooth luminosity that envelops the **companion** whose **classification is outside the classification** system, although it has variously **been** classified as SBO pec and Amorphous. The dust lanes from one of the branched arms of M5 1 are silhouetted against the **companion**, which obviously is **behind** the arm that sweeps across its image.

The strength of the spiral pattern is well shown in the composite **photographs** given by Zwicky (1955), where the dust pattern is also **particularly** well seen. The prevalent dust lanes in the central bulge close **to the nucleus** are shown in a greatly **enlarged** image **of the center** on page 31 of the Hubble Atlas.

The distance **to** M5 1 is considerably **smaller** than the distance **to the** Virgo **Cluster**, as judged by the ease of resolution **into** brightest stars and **HII** regions. The redshift of M51 is  $v_0 = 541 \text{ km s}^{-1}$ . This value is consistent with **the** distance modulus **of**  $m - M = 30$ , estimated from the ease **of resolution into** stars.

**This** agreement shows that any **random (non-cosmological)** velocity is near zero within **the** distance of 10 Mpc from the Local Group. This conclusion follows because **the velocity-distance** ratio (i.e., **the** local value **of the Hubble** constant) for M5 1 **itself is**  $54 \text{ km s}^{-1} \text{ Mpc}^{-1}$  using **the** M51 distance modulus **of**  $m - M = 30$  ( $D = 10$  Mpc), and noting that this **local** ratio is the **same** as **the global** value **of the** Hubble constant (Sandage and Tammann 1990).



*Sbc Classification Section (continued)*

NGC 3338      **Sbc(s)I-II**

**CD-1711-S**

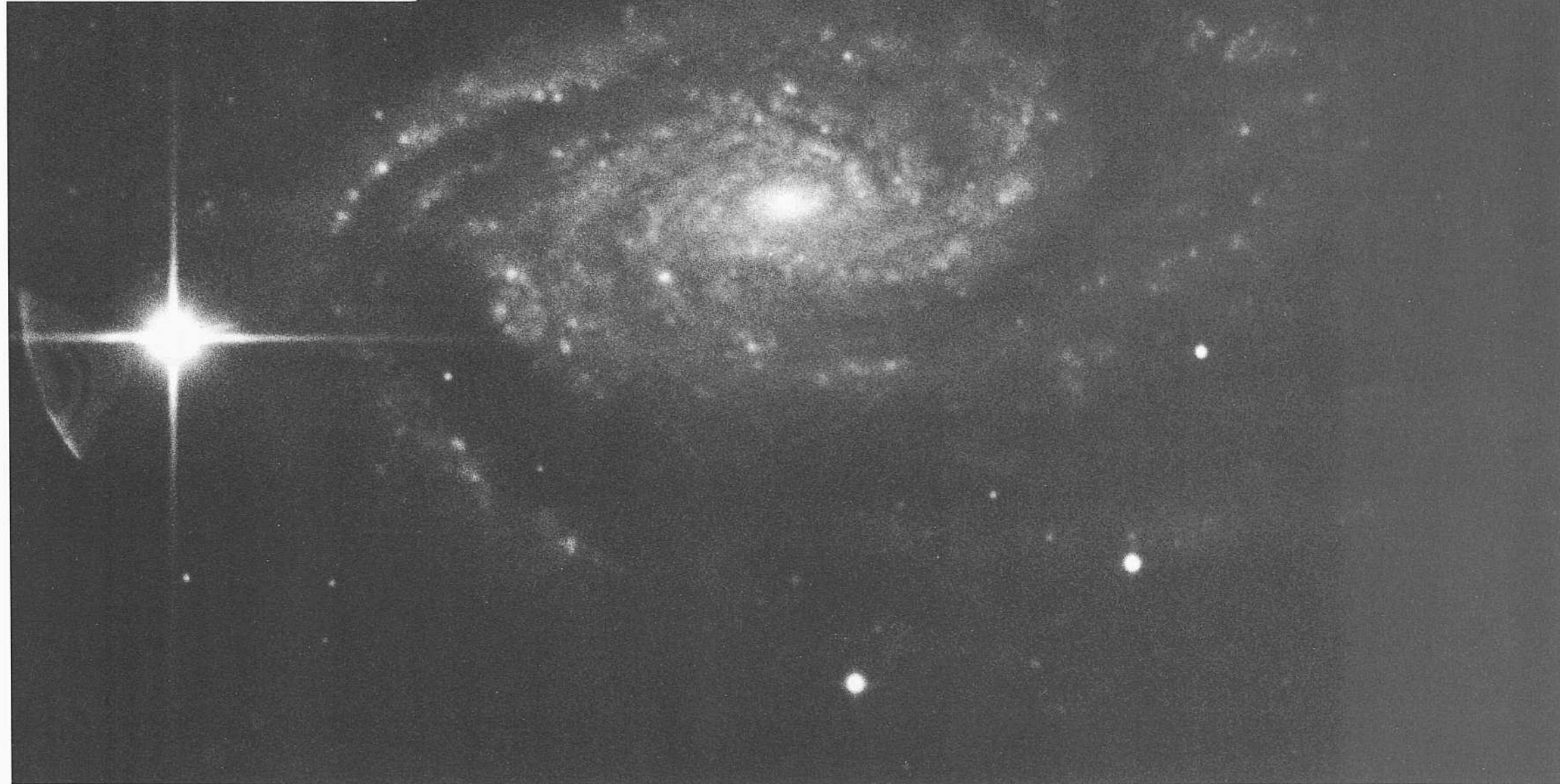
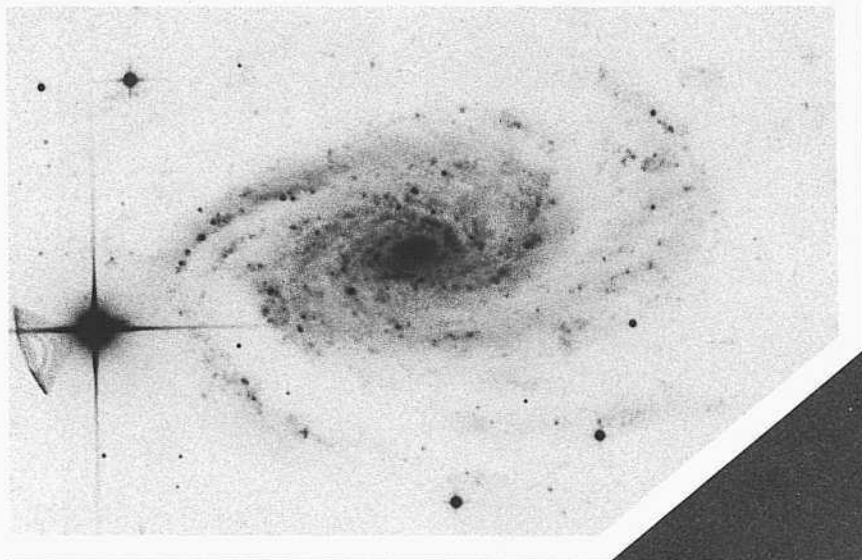
**Jan 6/7, 1981**

**103aO**

75 min

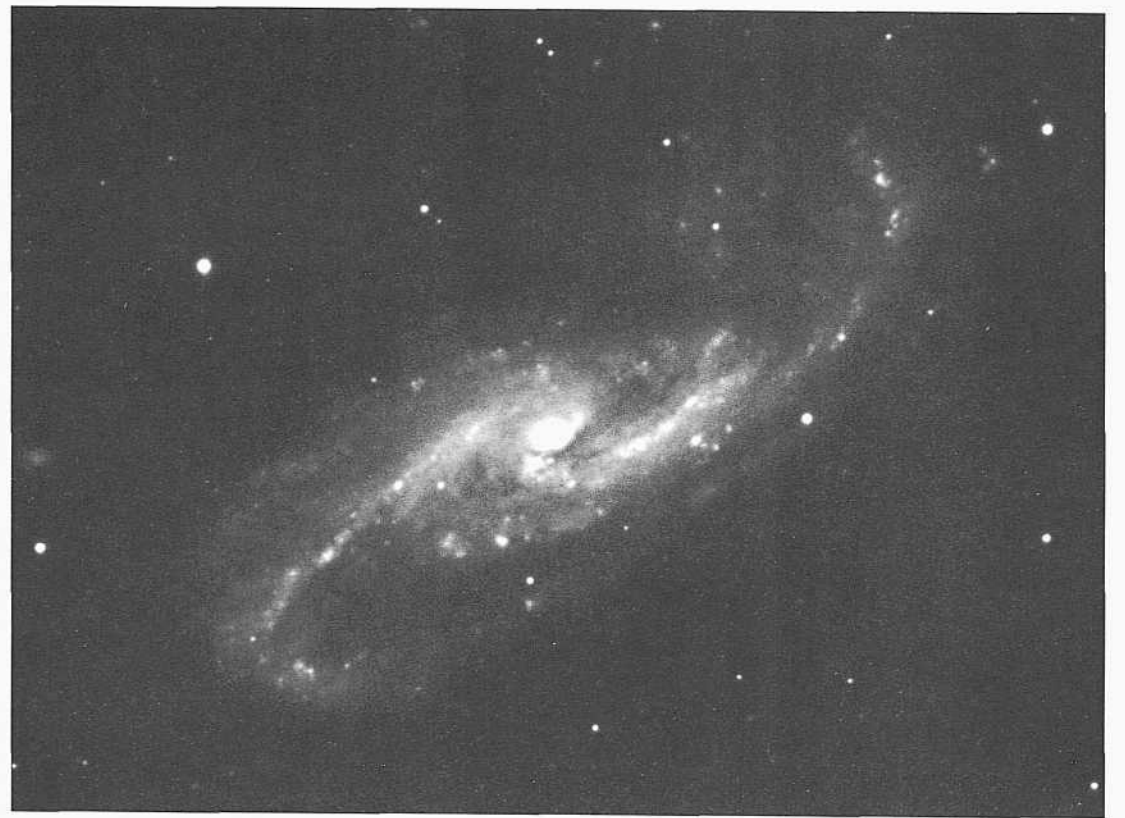
The spiral pattern of NGC 3338 is intermediate between **that** of a grand design and **filamentary** (MAS) type. The galaxy is shown **here** in the grand design section because of its similarity to NGC 1566 (panel 17 1) **and** M51 (**preceding** panel). When viewed more face on (by tipping **the print** along **the** minor axis and viewing the page almost edge **on**) the similarity becomes apparent. **There are two** major arms, which specify the grand design, but as in M51 **the** inter-arm regions also contain spiral **fragments**.

**The** arms in NGC 3338 are thin and well ordered: hence **the** early luminosity class is indicated. The largest of the many HII regions **resolve** at the 2" level. The redshift of NGC 3338 is  $v_{\theta} = 1171 \text{ km s}^{-1}$ .



PANEL  
173

PANEL  
174



The spiral patterns of the four galaxies on this panel are of the grand design type; each has two major spiral arms that can be well traced for an unwind of more than a half revolution.

NGC 2713      Sl>c(s)I  
 CD-1292-S/Br  
 March 10/11, 1980  
 103aO + GG385  
 45 min

The two outer arms in NGC 2713 are very thin, regular, and are not branched into fragments. They can be traced into the center in a tightly wound pattern. A few bright, unresolved HII regions exist in each of the outer arms. The redshift of NGC 2713 is  $v_0 = 3690 \text{ km s}^{-1}$ .

NGC 5248      Sbc(s)I-II      HA, p. 33  
 PH-209-MH  
 May 15/16, 1950  
 103aO  
 30 min

The two major spiral arms dominating the inner disk of NGC 5248 have high surface brightness, similar to the pattern in NGC 1566 (panel 171) and M51 (panel 172). The spiral pattern breaks into three fragments of very low surface brightness beyond the rim of the inner disk. The two main spiral fragments of this outer pattern are well defined and can be traced outward for another half revolution.

Resolution into individual stars occurs at apparent magnitude of about  $B = 22$ , which is about 1 mag above the plate limit. The largest of the numerous HII regions resolve at the 3" level. The redshift of NGC 5248 is  $v_0 = 1049 \text{ km s}^{-1}$ .

NGC 4536      Sbc(s)I-U      VCC 1562  
 CD-2139-S  
 March 22/23, 1982  
 103aO  
 50 min

NGC 4536 is one of the largest spirals in the Virgo Cluster region. It is located about  $6^\circ$  south of the center of Virgo subcluster H around NGC 4472, and is near the beginning of what was once called the southern extension of the Virgo Cluster, now known as the Virgo Cluster envelope along the supergalactic plane. The redshift of NGC 4536 is  $v_0 = 1646 \text{ km s}^{-1}$ .

The spiral pattern is dominated by the two principal spiral arms, clearly of the grand design type. Many HII regions exist in the arms, the largest of which are resolved into disks with core diameters of about 3".

NGC 7124      Sbc(rs)I-U  
 CD-1554-S/Br  
 Aug 8/9, 1980  
 103aO + GG385  
 45 min

NGC 7124 is one of the most distant galaxies in the Shapley-Ames Catalog, having a redshift of  $v_0 = 4957 \text{ km s}^{-1}$ . The spiral pattern is highly organized into the grand design type; there are two principal spiral arms that can each be well traced for slightly more than a half revolution. The HII knots in the arms are unresolved at the 1" level.

*Sbc Classification Section (continued)*

NGC 7038      **Sbc(s)I.8**      **Indus Gr**  
**CD-1157-Br**  
Aug 22/23, 1979  
103aO + GG385  
45 niin

Based on the redshift of  $v_o = 4785 \text{ km s}^{-1}$ , NGC 7038 is placed as a member of the NGC 7014 Indus Group, whose mean redshift is  $\langle v_o \rangle = 4934 \text{ km s}^{-1}$  (Sandage 1975b); the galaxy is one of the more distant in the RSA.

NGC 7038 is illustrated here in the grand design section because the number of arms is small compared with the many fragments present in galaxies of the filamentary (MAS) type, shown later in this section (panels 184-192).

The arms are narrow and are well formed, with only sparse arm material in the inter-arm region explaining the early luminosity class. Much recent star formation is evident in the arms. The numerous HII regions are unresolved at the 1" level, consistent with the large redshift distance of 96 Mpc ( $z = 50$ ).

NGC 5592      **Sbc(s)I-II**  
**CD-1470-S/Br**  
May 10/11, 1980  
103aO + GG385  
45 niin

NGC 5592 has one prominent, thin, high-surface-brightness arm and the beginning of a symmetrical opposite arm that fragments into a series of low-surface-brightness arm fragments of the filamentary type soon after its beginning near the center.

The redshift is  $v_o = 4190 \text{ km s}^{-1}$ . The several brightest HII regions in the bright arm are unresolved at the 1" level.

NGC 6814      Sbc(rs)I-II      **HA**, p. 20  
**PH-236-B**  
Sep 11/12, 1950  
103aO + GG11  
30 niin

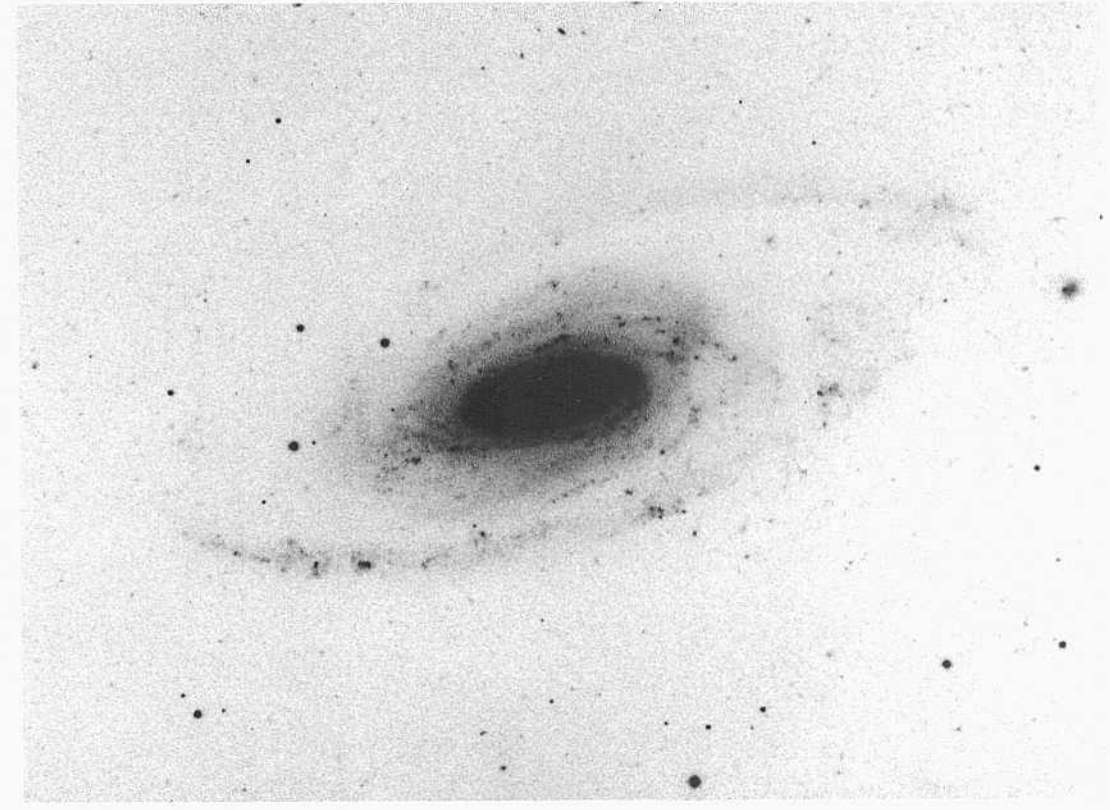
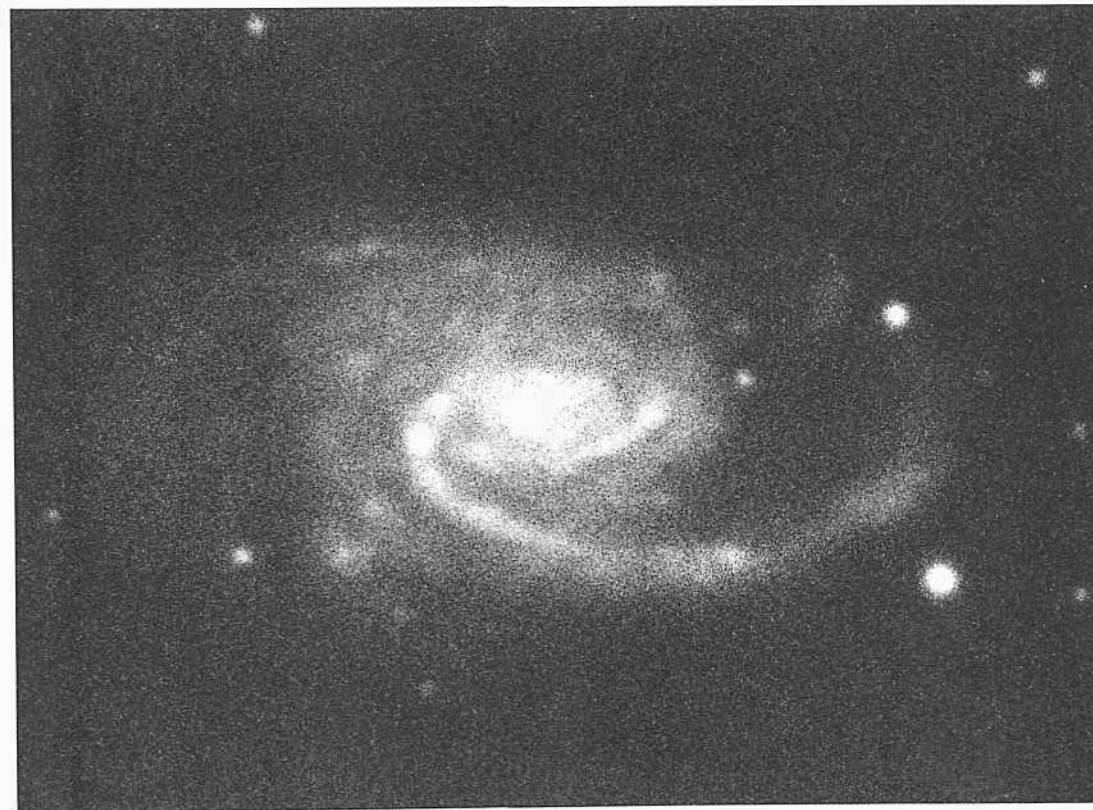
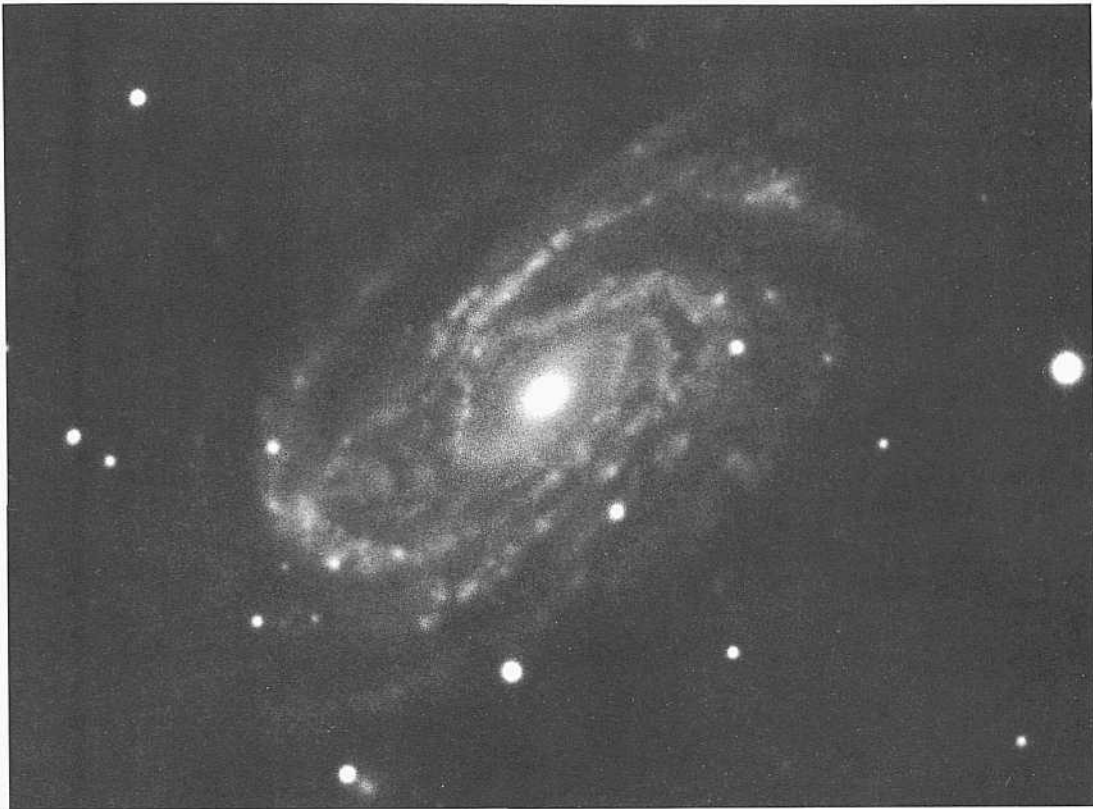
The spiral pattern in NGC 6814 has features of both grand design and multiple-armed (MAS) types. However, the arms are quite well defined as separate entities unlike the arms in pure MAS galaxies, such as NGC 2841 (panels 142, S4, S12). Here, the main arms can each be traced for about half a revolution before they branch and become multiple.

The redshift is  $v_o = 1643 \text{ km s}^{-1}$ ,

NGC 7531      **Sbc(r)I-II**  
CD-550-S  
Oct 2/3, 1978  
103aO + GG385  
45 mill

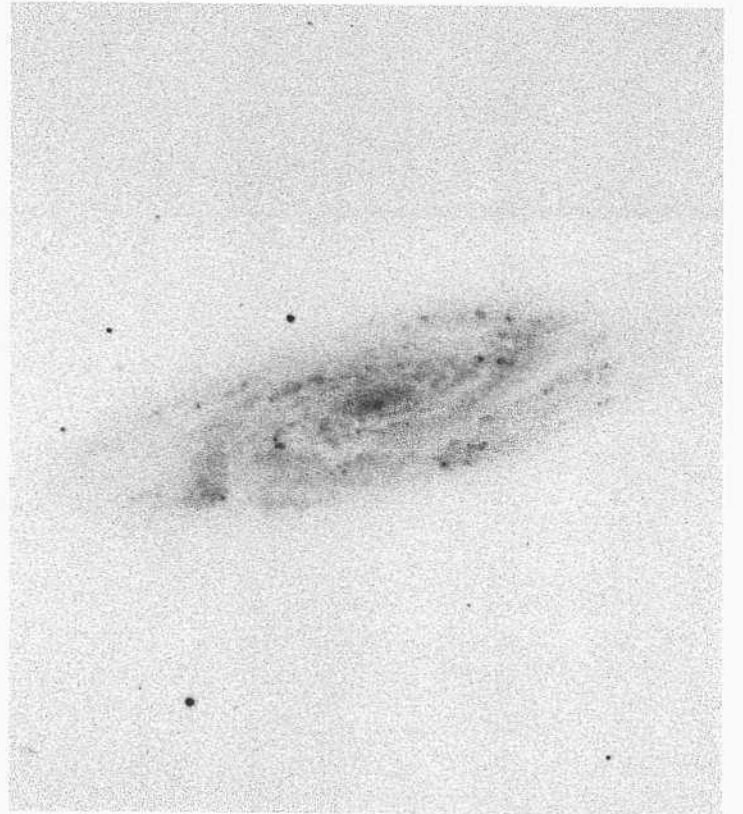
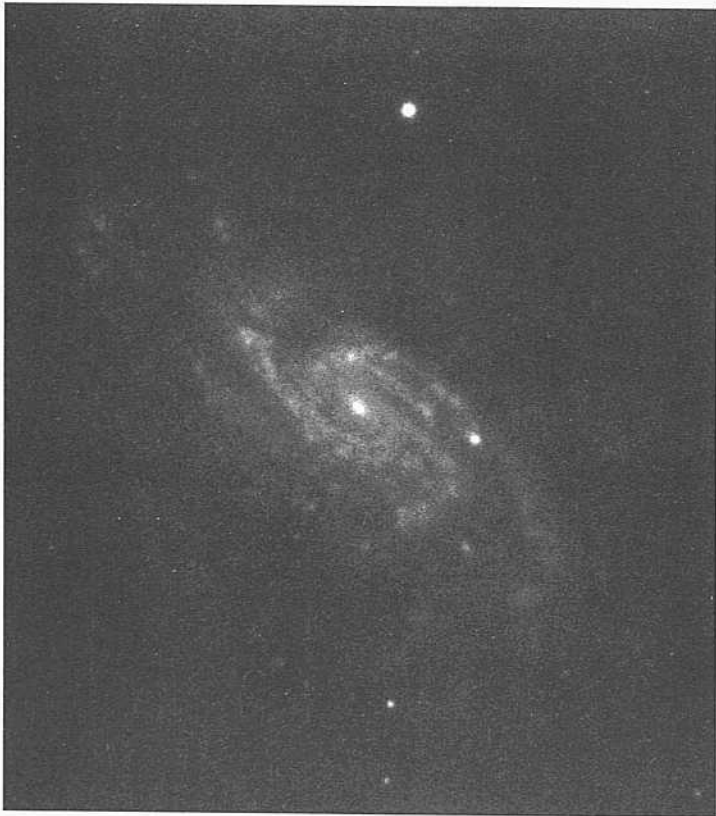
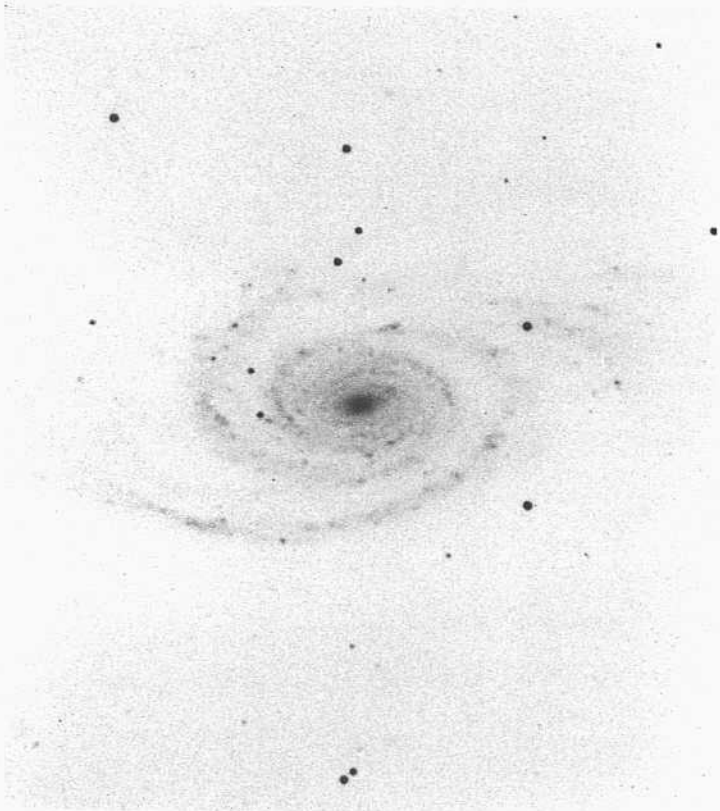
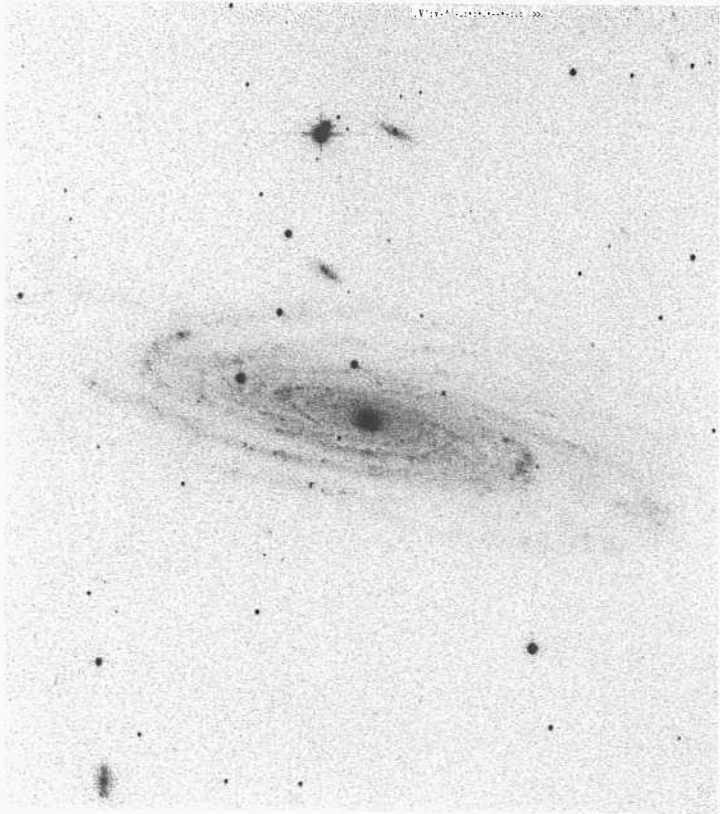
Two main outer arms are each attached to the rim of a high-surface-brightness inner disk, within which a tightly wound luminous spiral pattern also exists. Numerous HII regions are present in the disk arms and in the outer arms as well. The largest of the HII regions resolve at the 2" level. The redshift of NGC 7531 is  $v_o = 1607 \text{ km s}^{-1}$ .

If seen more face on, NGC 7531 would resemble NGC 3031 (**M81**; panels 129, 332), but it is of slightly later type because the central bulge in NGC 7531 is smaller.



PANEL  
775

PANEL  
176



Most of the galaxies on this panel are classed as grand design types despite giving a first-glance impression of a multiple pattern. On second inspection, each of the six galaxies here has two principal arms, which can be traced for at least half a revolution (from their beginning in the central region) before they branch into well-defined fragments continuing outward. That the branched outer arms are progeny of the two inner grand design

arms is definite. The ability here to identify the parenthood of the outer-arm fragments differs from the case in a pure MAS pattern, such as that of NGC 284 1 (panels 142, S4, S12) and INCC 488 (panels I 15, 1 1 6, S3, SI 2), where the arms fragment so completely that their parenthood close to the center cannot be determined,

NGC 3200      Sbc(r)I  
CD-810-S  
Feb 25/26, 1979  
103aO + GG385  
45 min

The spiral arms in NGC 3200 are very thin and well defined. The pattern is similar to that in NGC 3031 (panels 129, 332) except that the central bulge and smooth inner disk in NGC 3200 are smaller; the galaxy is later in the classification sequence.

The very early luminosity class is due to the great regularity of the spiral pattern. The redshift of NGC 3200 is  $v_o = 3313 \text{ km s}^{-1}$ . The absolute magnitude, based on the redshift distance of 66 Mpc ( $H = 50$ ), is  $M_B = -23.0$ , which is among the brightest galaxies in the Shapley-Ames Catalog (see Fig. 5 of the RSA).

NGC 4939      Sbc(rs)I  
H-1812-H  
May 3/4, 1937  
Imp. Eel.  
40 min

The two principal outer arms in NGC 4939 are remarkably thin. They can each be traced inward in a nearly continuous way for about 1 1/4 revolutions, which is unusually large. The arms are very regular and are well formed, requiring, by definition, the very early luminosity class.

The redshift is  $v_o = 2903 \text{ km s}^{-1}$ , giving a redshift distance of 58 Mpc. The apparent magnitude, corrected for absorption, is  $B_p = 11.0$ , which gives the bright absolute magnitude of  $M_B = -22.8$ , similar to that of NGC 3200 above.

The pitch angle of the arms is close to  $0^\circ$ : i.e., if NGC 4939 were viewed face on the spiral pattern would appear nearly circular, as in NGC 488 (panels 115, 116, S3, S12).

NGC 4603      Sbc(s)I-H    Centaurus Cluster  
CD-2168-S  
March 27/28, 1982  
103aO + GG385  
45 min

Two principal arms can be traced in NGC 4603 starting as Luminous segments at the rim of the inner disk. These can also be traced farther inward as dust lanes.

Branching occurs as the luminous arms are traced outward; the outer spiral pattern appears mildly multiple. Particularly interesting is the "third" principal outer arm, which begins as two branches connected to nothing in the intermediate disk on the left side of the major axis here, meeting as they wind outward into a single outer fragment.

The redshift is  $v_o = 2073 \text{ km s}^{-1}$ . The galaxy is on the western edge of the rich Centaurus Cluster. It is listed as entry 120 in the master catalog of Dickens, Currie, and Lucey (1986).

NGC 3430      Sbc(rs)I-II  
PH-7996-S  
Feb 2/3, 1981  
103aO  
12 min

The spiral pattern in NGC 3430 is intermediate between the grand design and the MAS types. The arms are thin. The high-surface-brightness segments can each be well traced for at least half a revolution.

The redshift is  $u_o = 1555 \text{ km s}^{-1}$ .

NGC 7171      Sbc(r)I-H  
CD-1585-S/Br  
Aug 11/12, 1980  
103aO + GG385  
45 min

The two principal arms of relatively high surface brightness begin at the rim of the inner disk in NGC 7171. They can be traced for about half a revolution before disappearing. Multiple arm fragments of lower surface brightness exist between the two principal arms.

The HII regions here generally unresolved. The redshift of NGC 7171 is  $v_o = 2765 \text{ km s}^{-1}$ .

NGC 7721      Sbc(s)II.2  
PII-7691-S  
Sep 26/27, 1979  
103aO  
10 min

NGC 7721 is of later luminosity class than the other galaxies on this panel; the arms are thicker and less well defined. The pattern is of the grand design type.

The many bright HII regions in the principal arm are unresolved at about the 1.5" level. The redshift of NGC 7721 is  $v_o = 2191 \text{ km s}^{-1}$ .



*Sbc Classification Section (continued)*

NGC 5194/5195 Sbc(s)I-II HA, pp. 26, 31  
 PH-3922-S SBO| pec M51  
 March 30/31, 1962 panels 55, 172  
 103aE + Ha interference  
 120 iiiin

The H $\alpha$  interference filter image of NGC 5194/5195 on the facing page illustrates why the spiral pattern of this galaxy is of the grand design, despite the superficial appearance of multiple arms in the deep prints on panel 172. The numerous H $\alpha$  regions outline the two principal arms, which can each be traced for nearly a whole revolution.

The most unusual feature of the pattern concerns the arm that begins near but not on the rim of the inner disk on the right-hand side of the image here (the opposite side of the major axis from NGC 5195). This principal arm is detached from the rim, in contrast to its opposite mate, which can be traced continuously inward until it meets the rim.

The largest HII regions have cores that resolve at the 10" level. This is consistent with the calibration of HII "lineal" core sizes in luminosity class I-II late-type spirals (Sandage and Tammann 1974a), putting M51 at a distance of 10 Mpc. as described earlier (panel 172).

NGC 3433 Sbc(r)1.3  
 CD-2109-S  
 March 19/20, 1982  
 103aO + GG385  
 45 min

The two principal arms in NGC 3433 are of the grand design type. They have relatively high surface brightness compared with the outer arms that branch from them. The HII region knots are few, faint, and unresolved. The redshift of NGC 3433 is  $v_r = 2566 \text{ km s}^{-1}$ .

NGC 3344 Sbc(rs)1.2  
 PH-7959-S  
 Nov 8/9, 1980  
 103aO  
 12 min

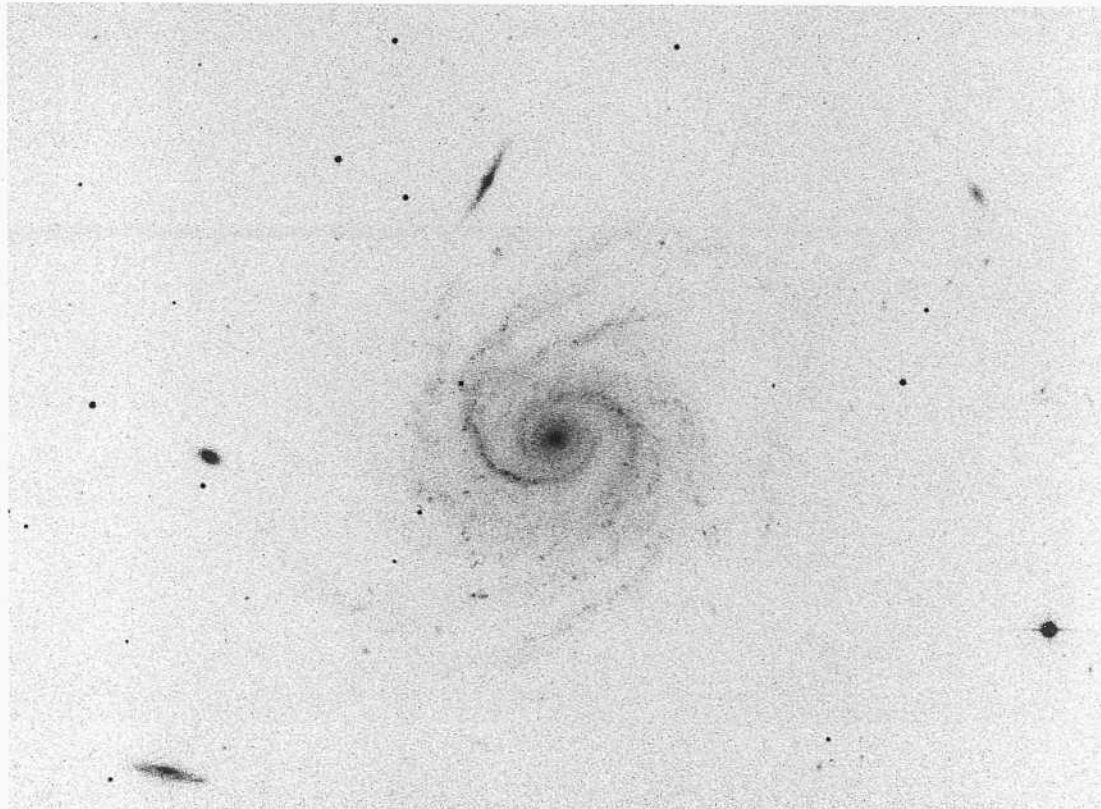
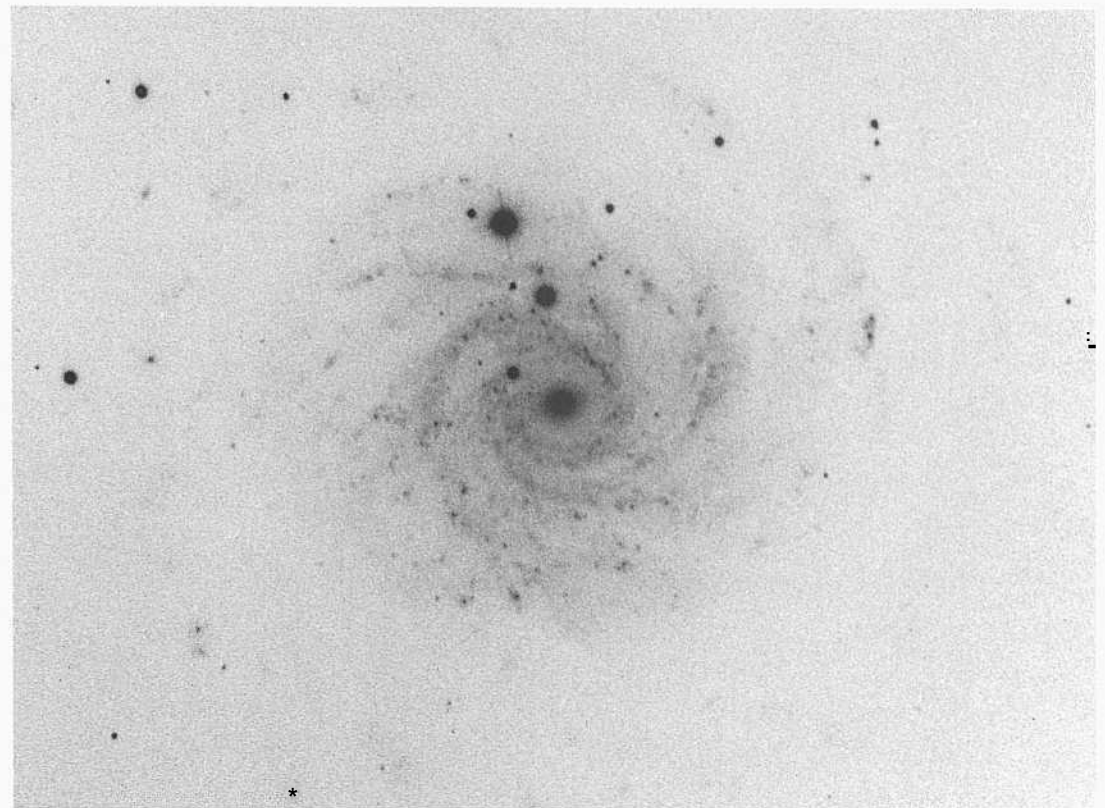
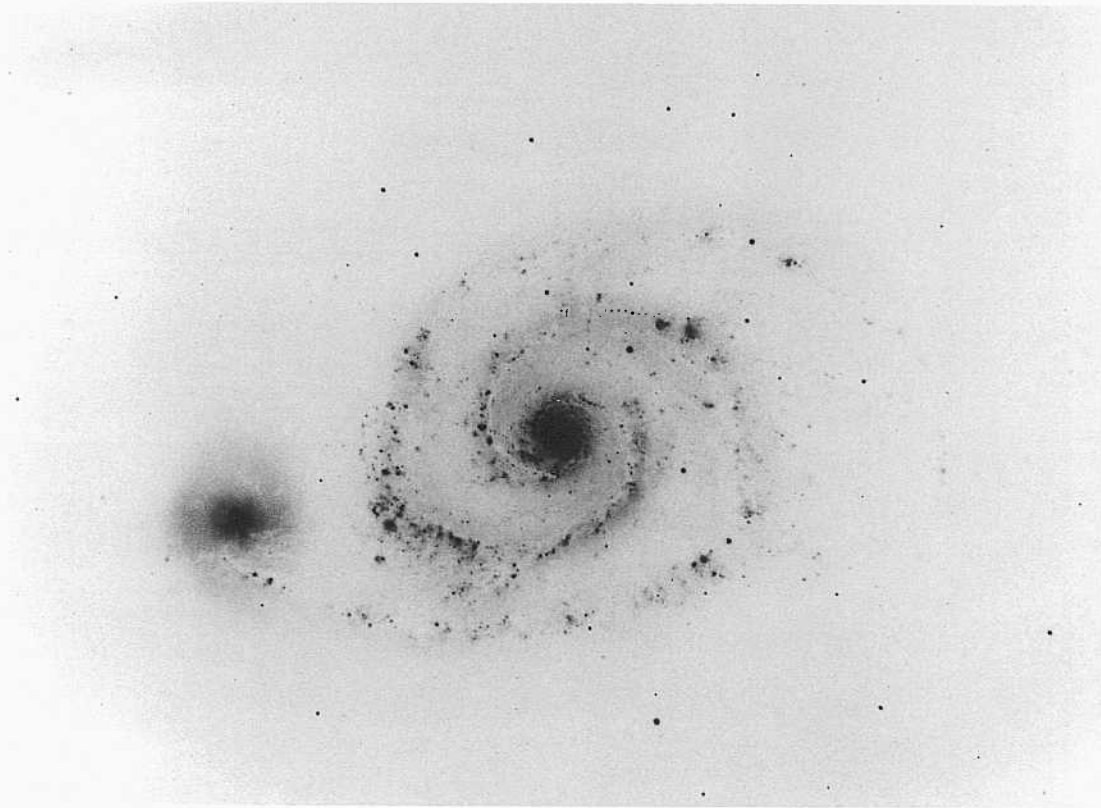
The two principal arms in NGC 3344 from which other arms branch begin as an almost-complete inner ring which, however, as usual, is the overlapping of tightly wound opposite spirals connected by dust lanes to the central region.

The redshift of NGC 3344 is small,  $v_o = 627 \text{ km s}^{-1}$ , yet the HII regions do not resolve into large-core disks, as in M51, which has a smaller redshift of  $v_o = 541 \text{ km s}^{-1}$ . The data are, however, consistent with the fainter absolute magnitude of NGC 3344,  $M_B = -20.3$ , compared with  $M_B = -21.6$  for M51, calibrated elsewhere (Sandage and Tammann 1974a).

NGC 6780 Sbc(rs)I-II  
 CD-924-HB  
 May 3/4, 1979  
 103aO + GG385  
 45 min

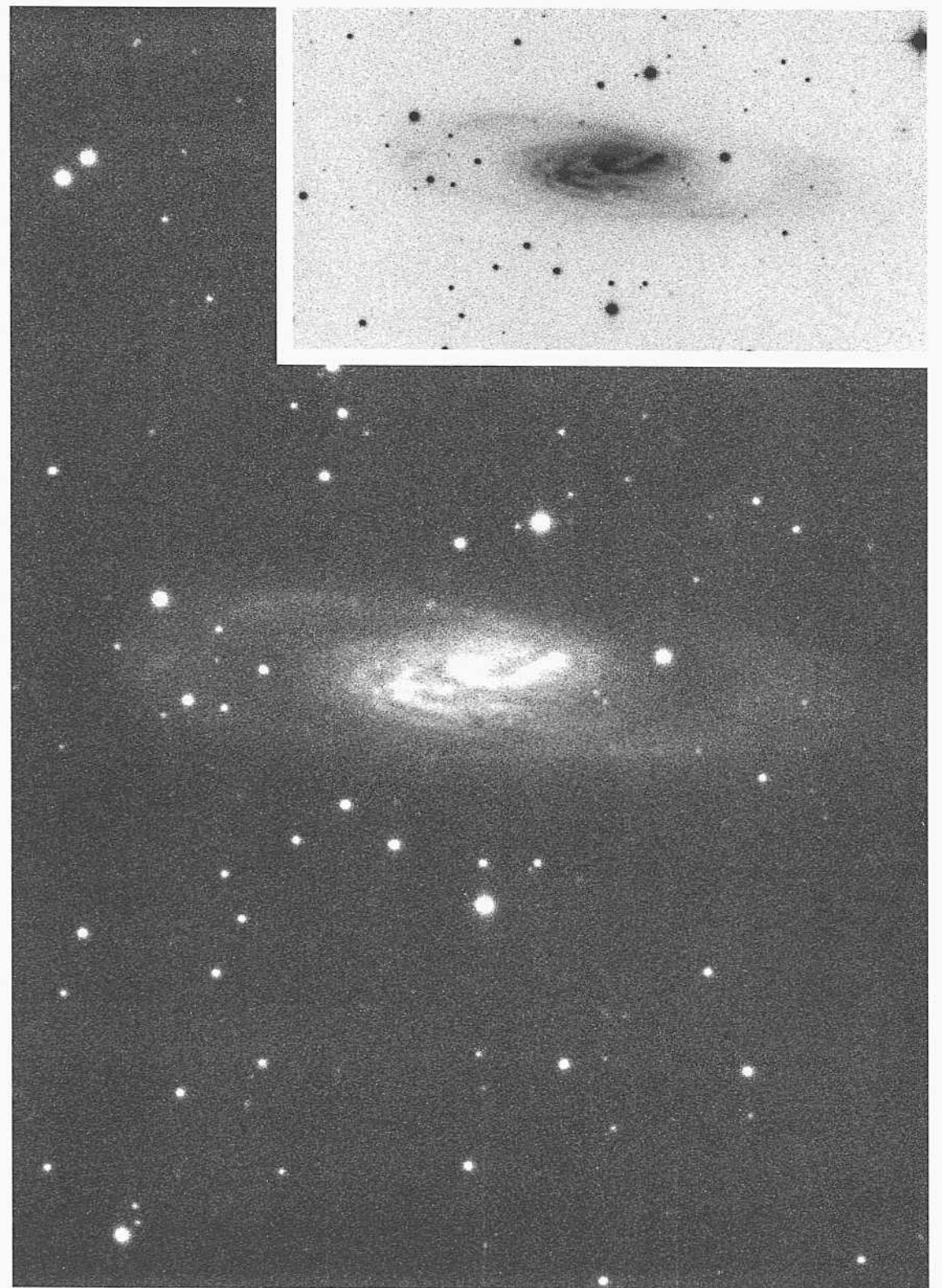
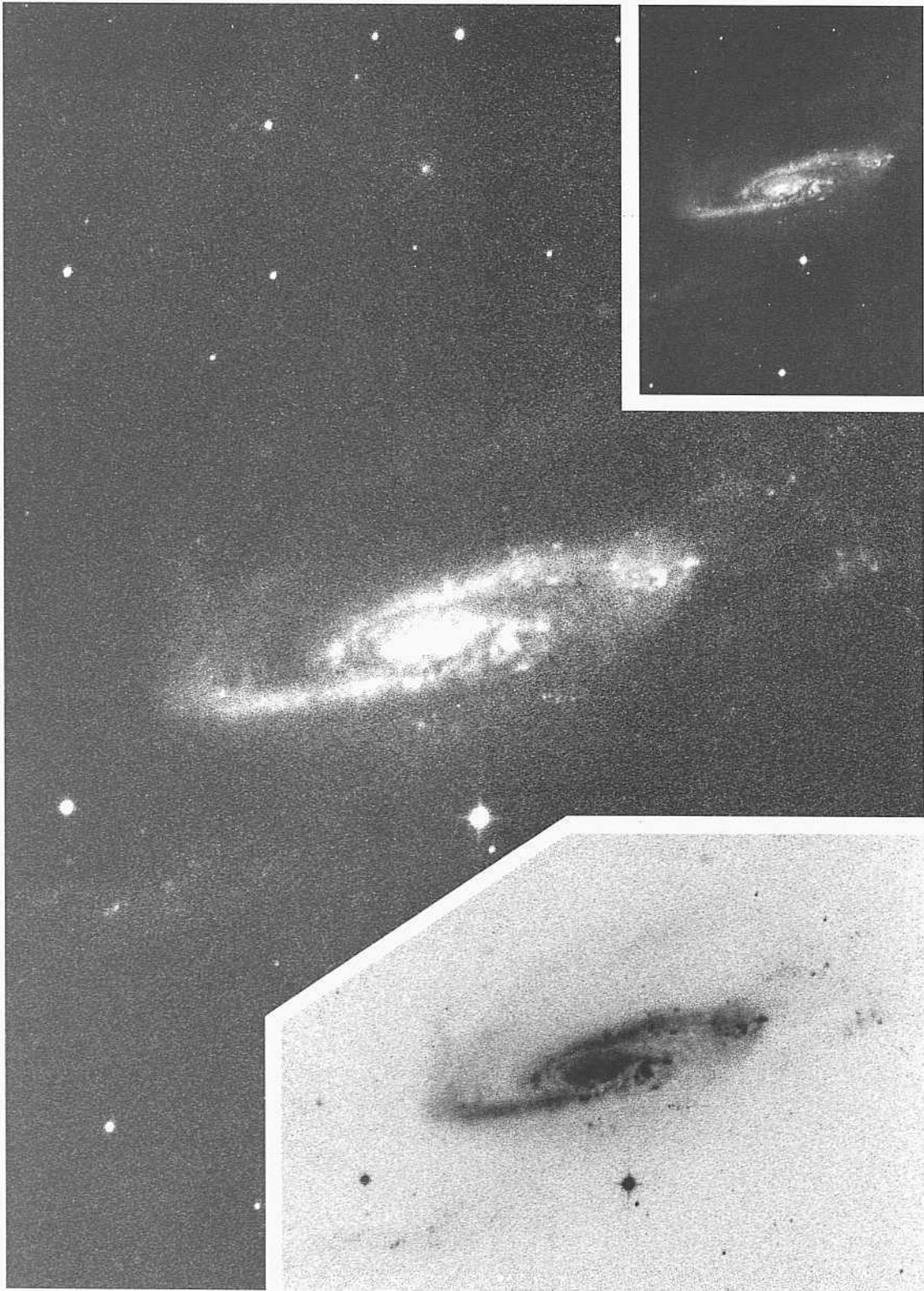
NGC 6780 may be an outlying member of the NGC 6769 Group (Sandage 1975a), whose mean redshift is  $\langle v_o \rangle = 3953 \text{ km s}^{-1}$ ; the redshift of NGC 6780 is  $v_o = 3381 \text{ km s}^{-1}$ . The grand design spiral pattern of the two principal arms is similar to that of M51 at the upper left.

Note that both principal arms begin at detached positions relative to the central bulge, similar to the situation in barred spirals. But if a luminous bar is present in NGC 6780 it is weak to the point of invisibility here.



PANEL  
177

PANEL  
178



NGC 3981      Sbc(s)I-II(tides?)  
CD-1672-S  
Dec 31/Jan 1, 1980/1981  
103aO  
60 min

The two **well-defined** principal arms of the grand design type in NGC 3981 have high surface brightness. They can be traced for about **Haifa revolution** outward from their origin **near** the center until they **abruptly decrease in surface** brightness, become more open, and **exhibit** a smooth appearance. It is **the plume-like** appearance of the very **faint outer "arms"** that gives the notation (tides?) in **the** classification, although no companion is present. The designation simply describes the morphology not the cause, which probably is not interaction via an encounter but rather is endemic to the galaxy.

The heavy main print shows faint IIII regions in the outer extensions of the inner arms and in a separate outer arm not connected with the two main inner arms. This third faint outer arm can be faintly seen as a straight segment along the major axis (at the top of the facing print) **which then** sweeps at a large **pitch** angle to the right in the orientation of **the** image here.

The redshift is  $v_r = 1554 \text{ km s}^{-1}$ .

NGC 2369      Sbc(s)I pec  
CIM36-S  
Jan 31/Feb 1, 1978  
103aO + GG385  
15 min

NGC 2369 is **similar to NGC 3981 at the left except** that the bright inner arms are not as well **defined** and **their outer extensions** as smooth arms have a **higher surface** brightness. The pattern is **clearly of the grand** design.

The redshift of NGC 2369 is  $v_r = 1016 \text{ km s}^{-1}$ .

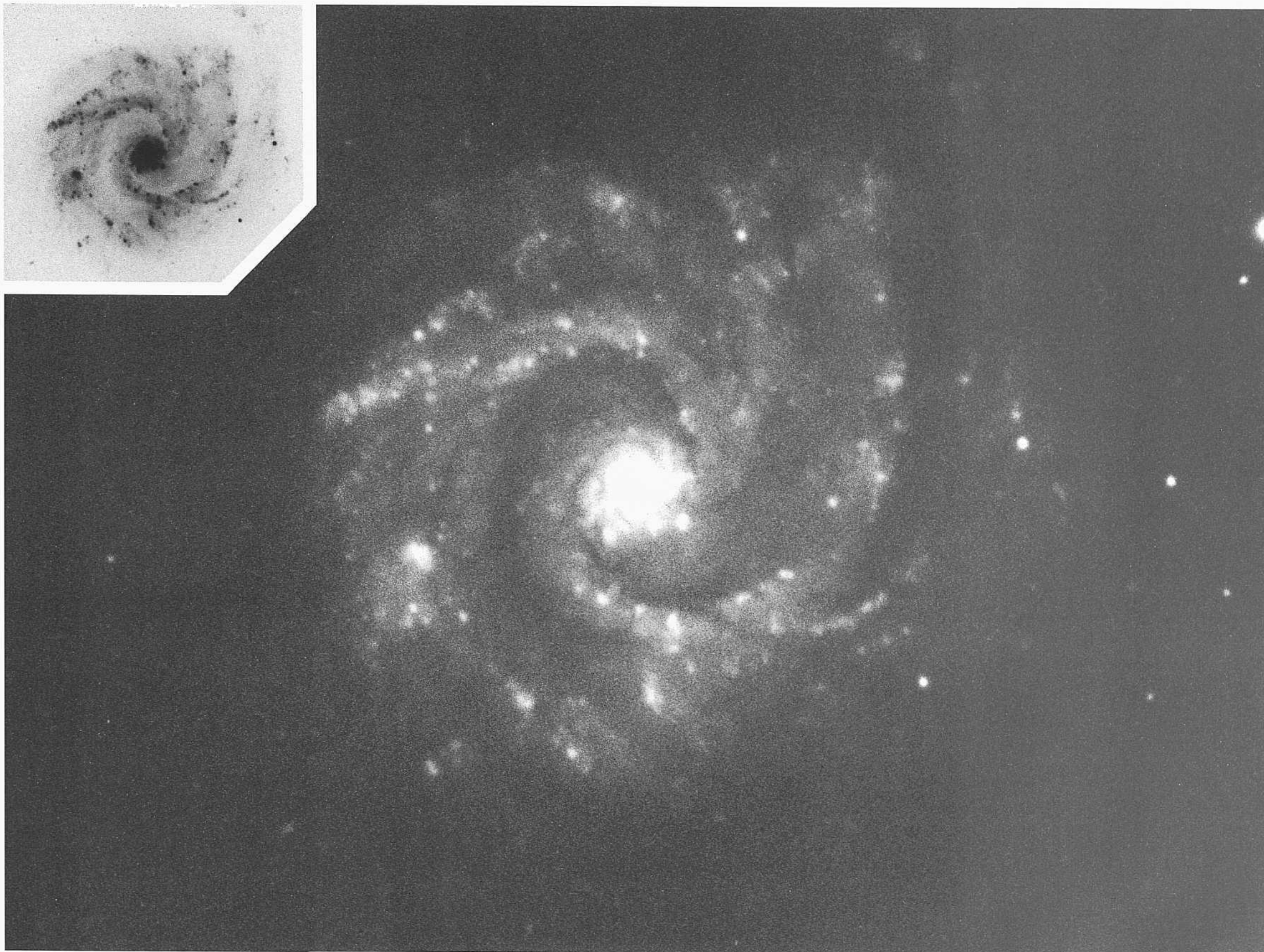
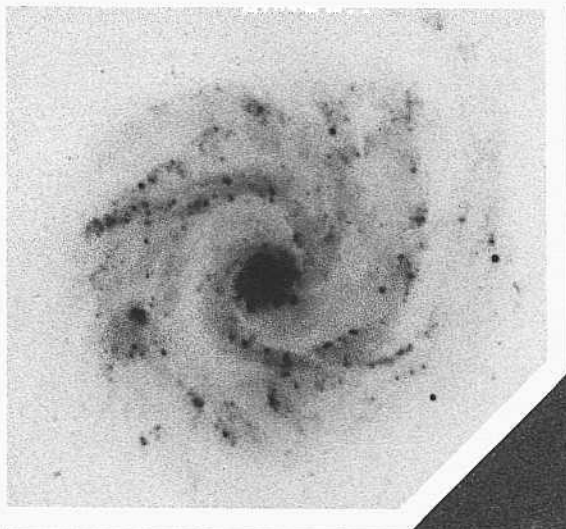
*Sbc Classification Section (continued)*

NGC3631      Sbc(s)II  
PH-8052-S  
Feb4/5, 1981  
103aO  
12 min

The grand design nature of the arms in **this** striking spiral is evident, as is the larger disorder (higher geometrical entropy) of the pattern compared with previous Sbc galaxies of earlier luminosity classes on the **preceding** eight panels. NGC 3631 is the **prototype** of this later SbcII luminosity class.

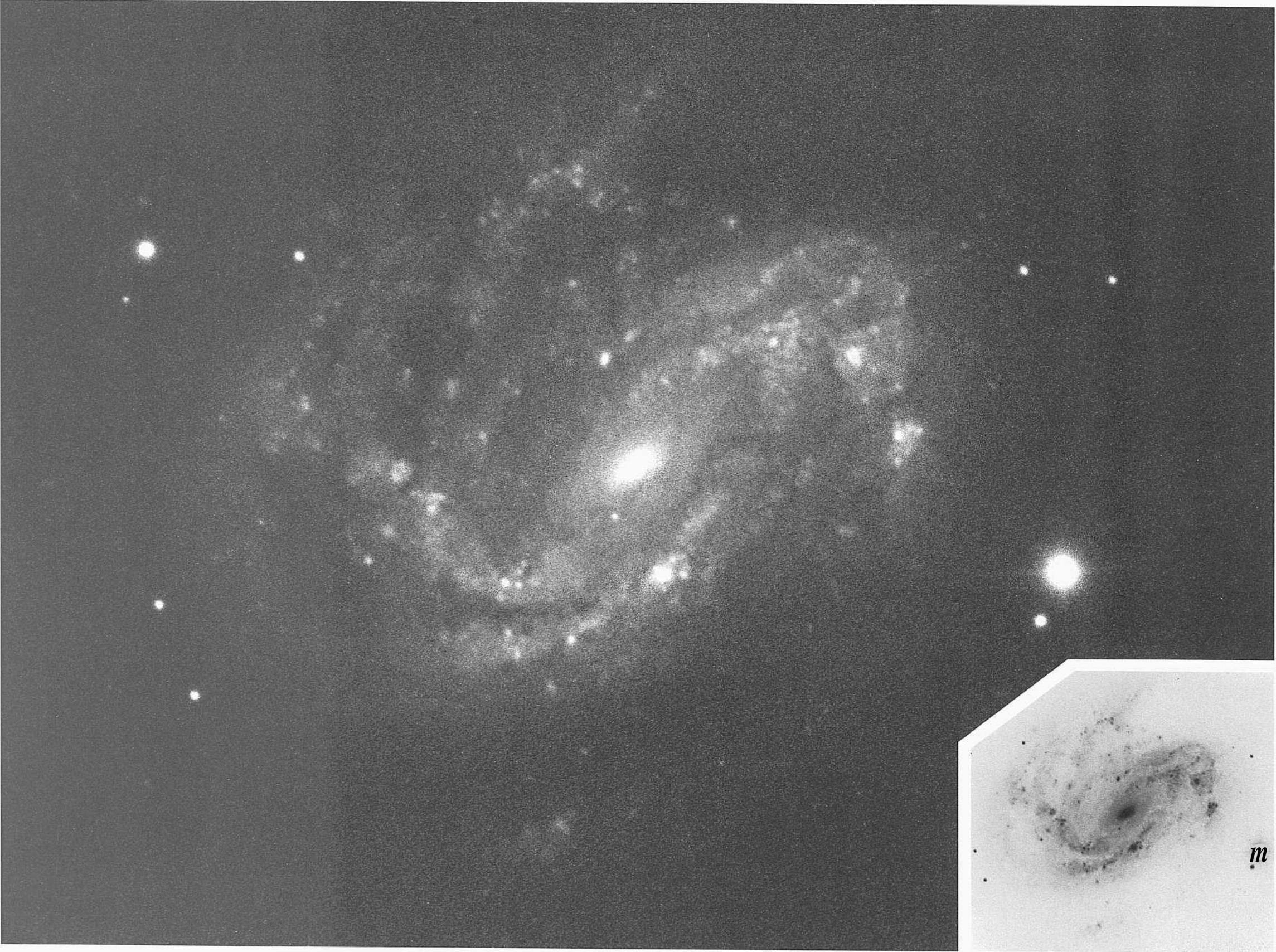
The two principal spiral arms begin near **the** center and become evident as luminous structures at the rim of the central, **high-surface-brightness** disk. Secondary arms of lower surface **brightness** branch outward from these two principal inner arms.

Bright **III** regions are present in all the arms: the rate of recent star formation is moderate-to-high. The largest **HII** regions coalesce at this angular resolution and have a combined core diameter at the 3" level. The redshift of NGC 3631 is  $v_r = 1238 \text{ km s}^{-1}$ .



1'ANHL  
179

PANEL  
180



*m*

*Sbc Classification Section (continued)*

NGC 4051      Sbc(r)II      Racine wedge  
PH-8056-S  
Feb4/5, 1981  
L03aO  
12 min

NGC 4051 is one of the original six emission-line galaxies used by Seyfert (1943) in his discussion of M101 Wilson spectra and direct plates of a class of galaxies known initially in Hubble, to Minkowski, and to Hubble to have star like (unresolved) nuclei and very broad emission lines in their spectra.

The beginning of the modern work on Seyfert galaxies and related objects, now called active galactic nuclei (AGN), was made in a seminal paper by Woltjer (1959). Seyfert galaxies and quasars are the most prominent examples of this class. Quasars are maxi-Seyferts.

Short-exposure plates of NGC 4051 and direct visual inspection at a large telescope show an intense starlike (unresolved) nucleus which is a mini-quasar at the center<sup>1</sup> of the galaxy.

The outer spiral structure is nearly of the grand design type, having only several major arms rather than a series of fragments as in the MAS type.

The largest of the many HII regions in the several arms resolve (core plus halo) at about the 4" level. The redshift of NGC 4051 is  $v_0 = 746$  km s<sup>-1</sup>.

Secondary Racine wedge images are below and slightly to the left of the brightest stars in the frame and also of the center of NGC 4051. The Racine wedge image of this starlike center is seen here below and slightly to the left of the center of the central region. NGC 4051 clearly has an AGN (a mini-quasar) nucleus.



*Sbc Classification Section (continued)*

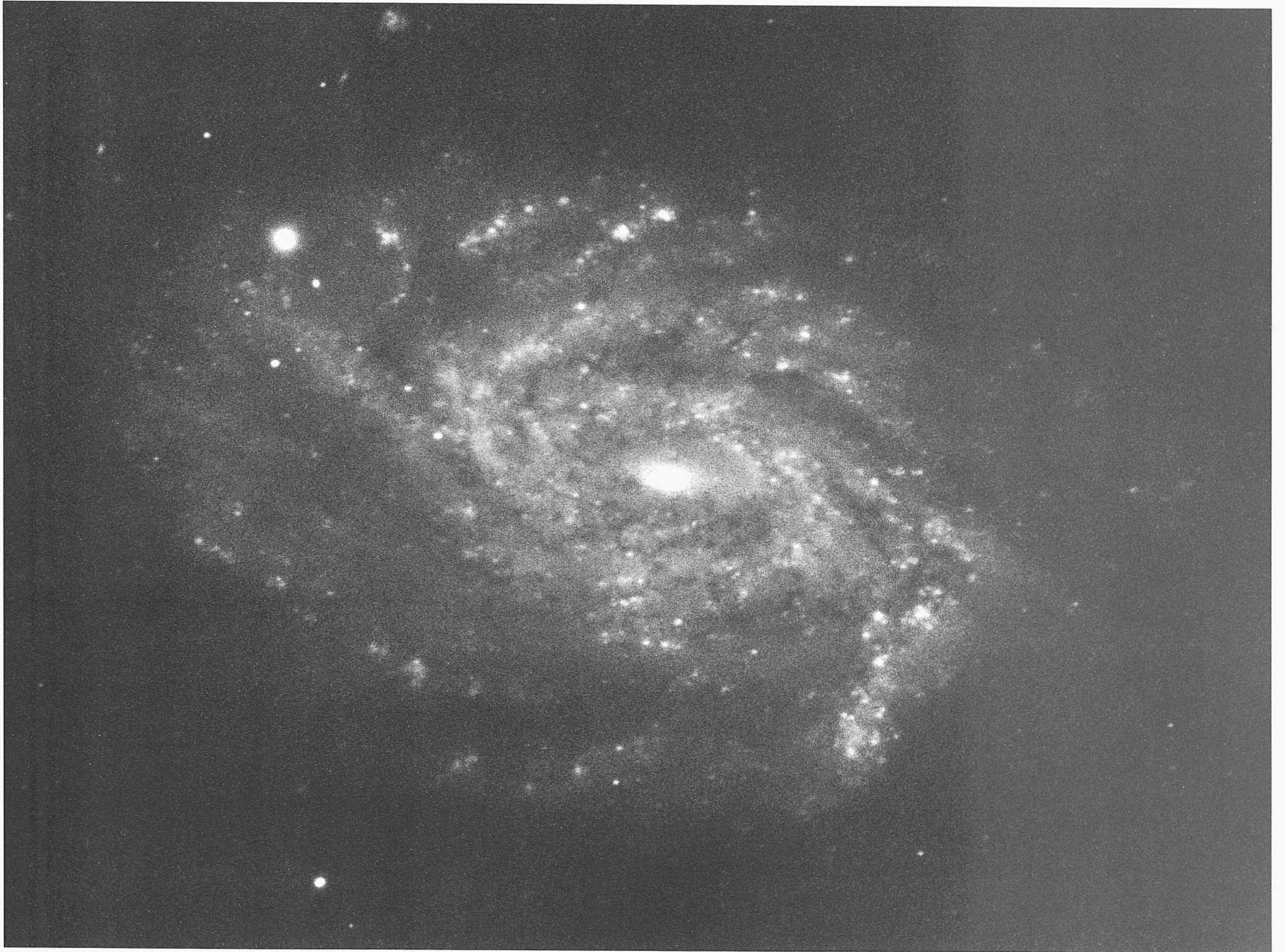
NGC 3726      **Sbc(rs)H**      **triplet?**  
**PH-8024-S**      Racine wedge  
Feb 3/4, 1981  
103aO  
12 min

NGC 3726, with a redshift of  $v_r = 909 \text{ km s}^{-1}$ , may be kinematically related to the much smaller nearby galaxies NGC 3769 (**SbcII; panel 311**) with  $v_r = 791 \text{ km s}^{-1}$  and NGC 3782 (**SBcdIIh panel 328**) with  $v_r = 785 \text{ km s}^{-1}$ . The angular distances of these two galaxies from NGC 3726 are 68' and 69', respectively. With a mean redshift distance of 17 Mpc ( $H = 50$ ), the projected linear separations of these nearby galaxies from NGC 3726 are 336 kpc and 341 kpc—about half the diameter of the Local Group.

The spiral pattern in NGC 3726 is more disordered than in the Sbc I and I-II galaxies of earlier luminosity class shown on preceding panels. The arms are thick, although each are well-enough defined to be traced as continuous segments for about half a revolution despite the branching from the main arms into outer fragments. The luminosity class is late II.

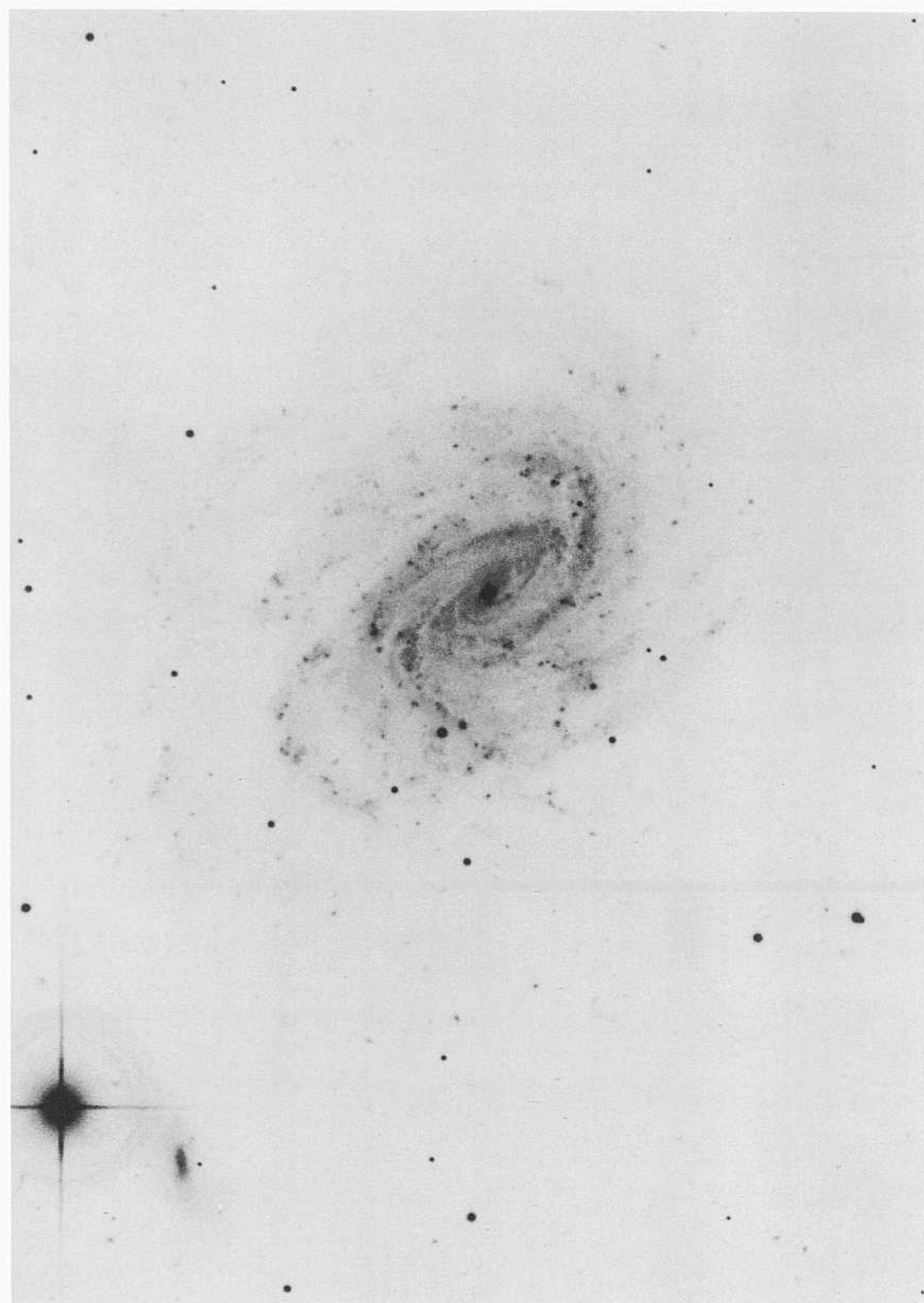
The largest of the numerous bright **HII** regions resolve into core plus halo diameters of about 4". At a redshift distance of 17 Mpc, this size corresponds to a linear diameter of 330 psc, consistent with the calibration of linear HII sizes as a function of luminosity class given elsewhere (Sandage and Tammann 1974a).

Secondary images from the Racine wedge are below and slightly to the right of the two **brightest** stars in the frame.



PANEL  
181

PANEL  
182



*Sbc Classification Section (continued)*

NGC 1187                      Sbc(s)II

CD-1548-S/Br

Aug 7/8, 1980

103aO + (s);i«s

15 min

The light print on the rigil shows that Ili\* inner-arm pattern is composed of three high-surface-brightness grand design spirals. Each begins near the small central nucleus, which itself is of very high surface brightness and which has a starlike inner core at the center at 0.8" resolution of the available plate material. The two principal arms of the inner triad pattern are traced for about three-quarters of a revolution outward before they abruptly decrease in surface brightness; beyond that point, lower-surface-brightness arm fragments exist, shown best at the left.

This pattern—bright, well-defined inner arms, abrupt surface-brightness change, and fragments beyond the point of change—is common, and has been seen earlier in this section. The examples are NGC 1566 (panel 171), NGC 5248 (panel 174), NGC 7171, NGC 4603, and NGC 3430 (panel 176), NGC 3433 (panel 177), NGC 2369 and NGC 398] (panel 178), and NGC 3726 (panel 181).

The largest of the numerous III regions everywhere in the arms resolve at the 2" level. The redshift of NGC 1187 is  $u_n = 1424 \text{ km s}^{-1}$ .

*Sbc Classification Section (continued)*

NGC 4995            Sbc(s)II            pair  
 CD-1860-HB  
 April 6/7, 1981  
 103aO  
 75 min

NGC 4995 at redshift  $v_o = 1\,645 \text{ km s}^{-1}$  may form a kinematic pair with NGC 4981 (SBbcII; panel 2 10) at  $u_o = 1\,492 \text{ km s}^{-1}$  at an angular separation of  $65^\circ$ . At a mean redshift distance of 3.1 Mpc ( $H = 50$ ) the projected linear separation of the pair is 5.86 kpc, similar to the separation of our Galaxy and M3 1.

The luminous spiral pattern of NGC 4995 is intermediate between the grand design type and the MAS filamentary-arm type, although the grand design is more evident. Three high-surface-brightness principal arms define the pattern. The inter-arm regions are bright, providing a good background against which the spiral dust lanes are silhouetted throughout the underlying disk.

NGC 6984            Sbc(r)1.8  
 CD-1595-S/Br  
 Aug 12/13, 1980  
 103aO + GG385  
 45 min

The two principal arms in NGC 6984 begin on the rim of an almost-complete internal ring which, as usual, is itself the near-overlapping of the tightly wound spirals near the center.

One of the two principal outer arms is thick near its beginning, although it is detached at this point from the inner near-ring much like one of the principal arms in M5 1 (panel 177).

The redshift of NGC 6984 is one of the larger in the RSA at  $v_o = 443.5 \text{ km s}^{-1}$ . Nevertheless, the two largest fill regions in the thick arm resolve at the 1" level, consistent with core plus halo diameters of 450 kpc in luminous galaxies (Sandage and Tammann 1974a).

NGC 3583            Sbc            Racine wedge  
 PH-8075-S  
 Feb 5/6, 1981  
 103aO  
 12 min

The inner arms of very high surface brightness change abruptly in luminosity after only about a half revolution as they develop into the outer arm pattern. This characteristic is the same as has been discussed for other galaxies in this section (compare NGC 1187 on the preceding panel).

The redshift of NGC 3583 is  $v_n = 2\,184 \text{ km s}^{-1}$ .

NGC 3596            Sbc(r)II.2  
 CD-2101-S  
 March 18/19, 1982  
 103aO + GG385  
 52 min

Two principal arms emerge from the rim of the inner disk. Their spiral patterns can be well traced, each for half a revolution of unwind. After this point one of the principal arms breaks into a broad pattern that continues to wind outward, nearly overlapping the opposite inner arm after nearly a whole revolution.

The several bright HII regions are unresolved at the 1.5" level despite the small redshift,  $v_n = 10\,72 \text{ km s}^{-1}$ .

NGC 2608            Sbc(s)II  
 PII-7990-S  
 Feb 2/3, 1981  
 103aO  
 12 min

The arm pattern is clearly of the grand design type. Two principal arms that start at the center dominate the pattern.

The redshift is  $v_o = 2\,112 \text{ km s}^{-1}$ .

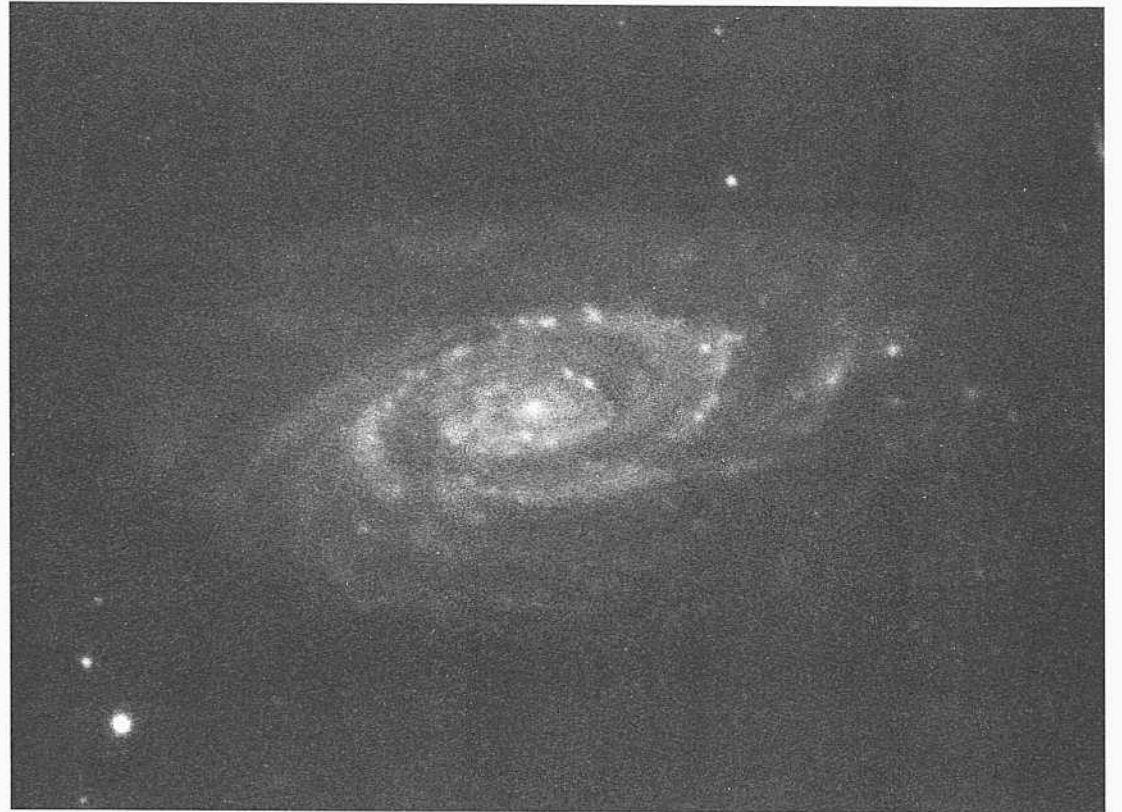
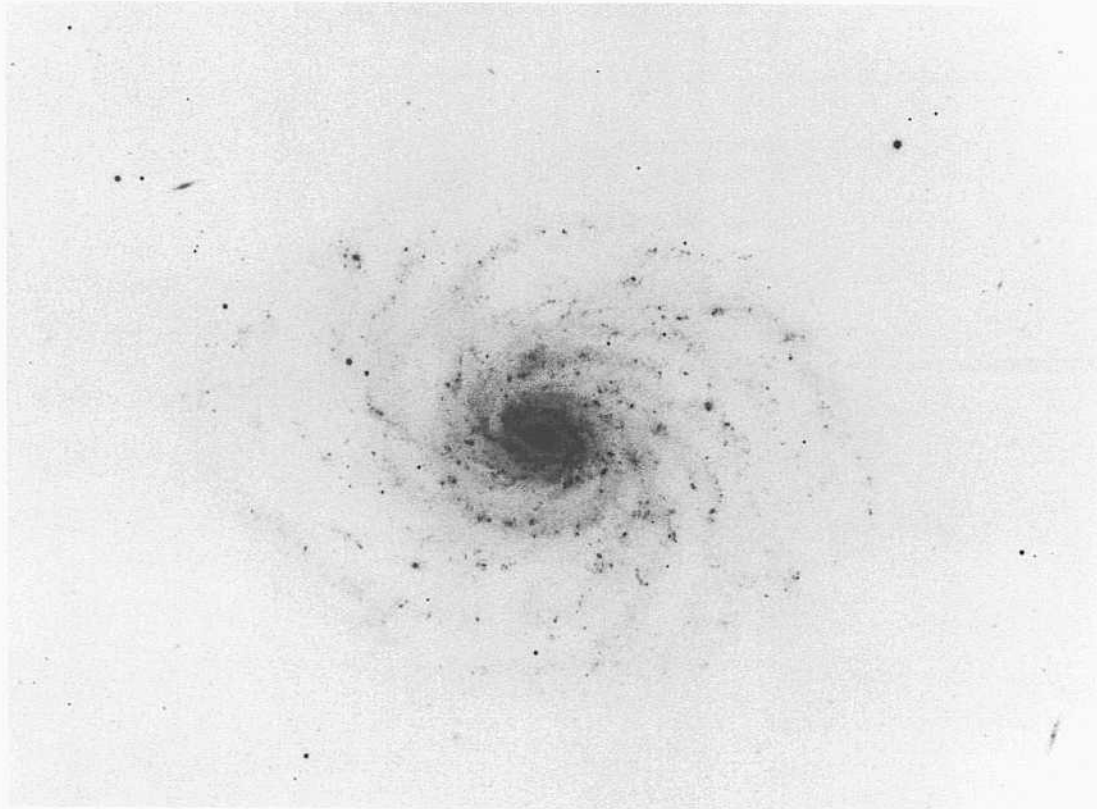
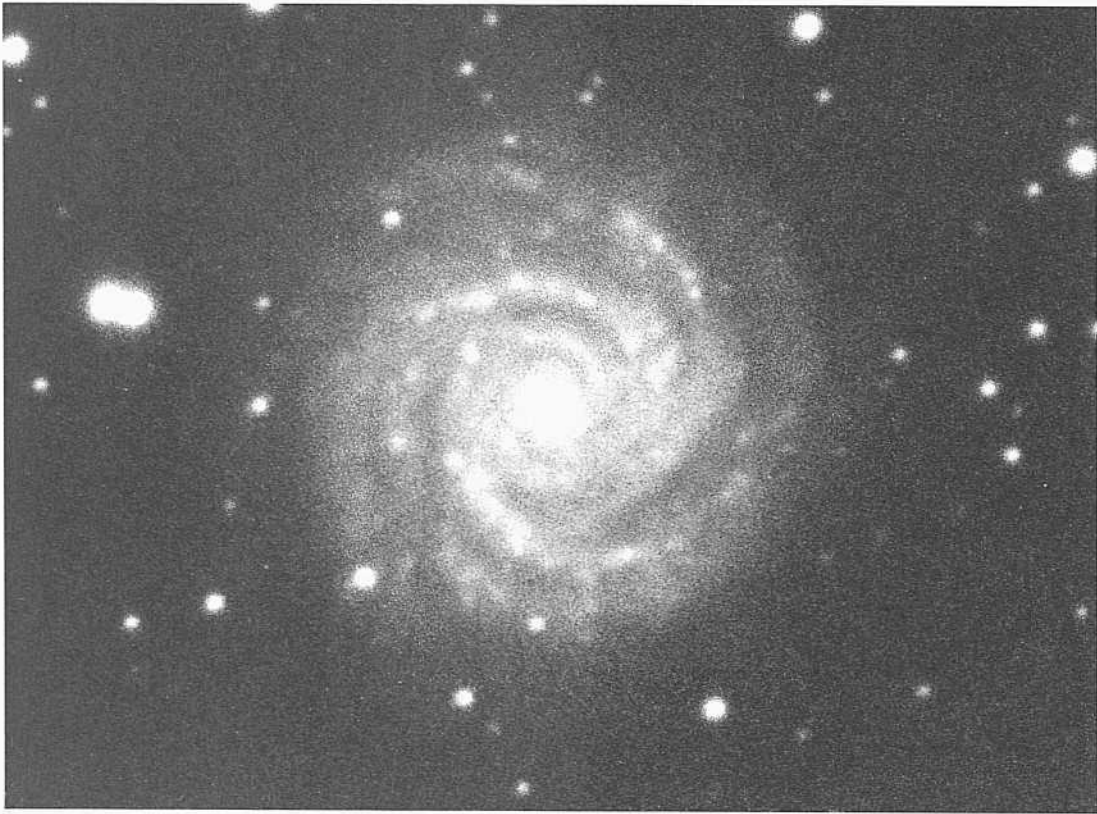
NGC 3162            Sbc(s)1.8  
 H-572-S  
 Feb 5/6, 1956  
 103aO + GG13  
 20 min

The inner arm pattern in NGC 3162 has a high surface brightness that abruptly decreases after slightly more than half a rotation, forming at that point the very faint outer arm pattern.

The redshift is  $v_n = 12\,23 \text{ km s}^{-1}$ .



PANEL  
184



Three of the (Our galaxies on this panel have mixed characteristics of both the grand design and the multiple-armed-spiral (MAS) types. They would define an intermediate position in the 12-step arm classification system of Elmegreen and Elmegreen (1982, 1987) that spans the range from grand design, to filamentary, to chaotic. The arm systems in three of these galaxies are highly multiple, not of the classic morphology with two principal arms of a pure grand design pattern.

The arms in all four galaxies are highly regular, requiring an early luminosity classification.

NGC 6699      **Sbc(s)1.2**  
 CD-1540-S/Br  
 Aug 7/8, 1980  
 103aO + GG385  
 45 min

Four principal arms can be traced in NGC 6699, found by counting the number of arm crossings in a cut across the major axis of the image. The numerous III regions in each arm are like heads on a string, similar to the two-arm pattern in M51 (panels 172, 177).

The redshift is  $v_r = 3357 \text{ km s}^{-1}$ .

NGC 3486      **Sbc(r)1.2**      panel S13  
 PH-8022-S  
 Feb 3/4, 1981  
 103aO  
 12 min

Many of the spiral fragments in NGC 3486 can be traced for only short distances before their surface brightness becomes so low that the outer features are lost. In these outer regions, the tilt region content that defines the path of the spiral substantially decreases.

The overall spiral pattern is very regular. The pattern starts at the rim of a high-surface-brightness inner ring. The nucleus is exceedingly bright, appearing nearly starlike by visual inspection at a large telescope.

The several largest III regions resolve at the 4" level for the core plus halo diameter. The redshift is low,  $v_r = 636 \text{ km s}^{-1}$ .

NGC 4947      **Sbc(s)I-II pec**  
 CD-915-III5  
 April 30/May 1, 1979  
 103aO + GG385  
 -10 min

The arm pattern in NGC 4947 is of the grand design type. Two principal arms exist, beginning at the center as dust lanes and becoming luminous at the edge of the inner disk. The HH regions are numerous.

The redshift is  $v_r = 2222 \text{ km s}^{-1}$ .

NGC 5351      **Sbc(rs)1.2**  
 PH-8096-S  
 Feb 6/7, 1981  
 103aO  
 12 min

The inner arms are of high surface brightness. The faint outer arms branch from them and form a multiple-arm pattern. The redshift of NGC 5351 is  $v_r = 3663 \text{ km s}^{-1}$ .



The six galaxies on this page, having very **regular** spiral patterns, consequently are assigned to the earliest luminosity classes I or **I-II**. All six are of the multiple-arm variety.

NGC 214            **Sbc(r)I-II**

**PH-7819-S**

Sep 2/3, 1980

**103aO**

12 mill

The **two** brightest arm fragments in NGC 214 start from the edge of a high-surface-brightness disk close to the center. Some of the **faint** outer multiple arms branch from these **two** main inner arms, but others exist throughout the moderately high surface brightness intermediate disk, similar to the **earlier pattern** in NGC 2841 (panels 142, S4, S12).

The III regions are unresolved at the 1" level. The redshift of NGC 214 is  $v_r = 4757 \text{ km s}^{-1}$ .

NGC 6925            **Sbc(r)I-II**

**CD-2020-Bedke/Gregory**

Oct 26/27, 1981

**103aO + GG385**

**15 min**

The MAS **pattern** in NGC 6925 is similar to but later than the prototype multiple-armed pattern in NGC 488 (panels 11a, 11b, S3, S12) and in NGC 2841 (panels 142, S4, S12). Also, the luminous arms are somewhat better defined here **than** in NGC 2841.

The diameters of the III regions are smaller than 1". The redshift of NGC 6925 is  $v_r = 2780 \text{ km s}^{-1}$ .

NGC 5324            **Sbc(r)1.3**

**H-2388-H**

Feb 21/22, 1947

**103aO**

**30 min**

The MAS spiral pattern in NGC 5324 is a later version of the Sab prototype NGC 488 and an earlier version of the prototype ScI MAS galaxy NGC 1232 (panels 216, S13). The redshift of NGC 5324 is  $v_r = 2853 \text{ km s}^{-1}$ .

NGC 3963            **Sbc(r)1.2      Racine wedge**

**PH-8112-S**

Feb 7/8, 1981

**103aO**

**12 min**

The plate used here for NGC 3963 was taken through clouds and gives a false impression of the true surface brightness of the galaxy; the sky was thick, decreasing the surface-brightness contrast between the galaxy and the night sky glow.

The plate was taken with a Racine wedge. The secondary images are faintly visible for (1) the brightest star in the field, superposed on one of the arms below and to the right of center, and (2) the nucleus, which is almost starlike upon visual inspection at the telescope, evidenced here also by the secondary image made by the wedge.

The spiral pattern is of the grand design rather than of the multiple-armed type. Only two principal arms exist; one, highly regular, can be traced for almost a whole revolution, while the other branches into **two** after half a revolution.

The redshift is  $v_r = 3295 \text{ km s}^{-1}$ .

NGC 3720            **Sbc(s)            pair**

**CD-1426-S/Br**

March 25/26, 1980

**103aD + GG495**

**31 min**

NGC 3720 forms a close pair with NGC 3719 (She) at an angular separation of 2.2'. The near equality of the redshifts, at  $v_r(3720) = 5804 \text{ km s}^{-1}$  and  $v_r(3719) = 5723 \text{ km s}^{-1}$ , assures a physical association. At the mean redshift distance of 115 Mpc ( $H = 50$ ) the projected linear separation is small, at 74 kpc.

The nucleus is small and bright. The multiple arms are smooth at the resolution of the present plate material. The galaxy is clearly a spiral. The classification as EO by van den Bergh, based on 48-inch Schmidt paper prints, is inappropriate.

NGC 3259            **Sbc(r)I**

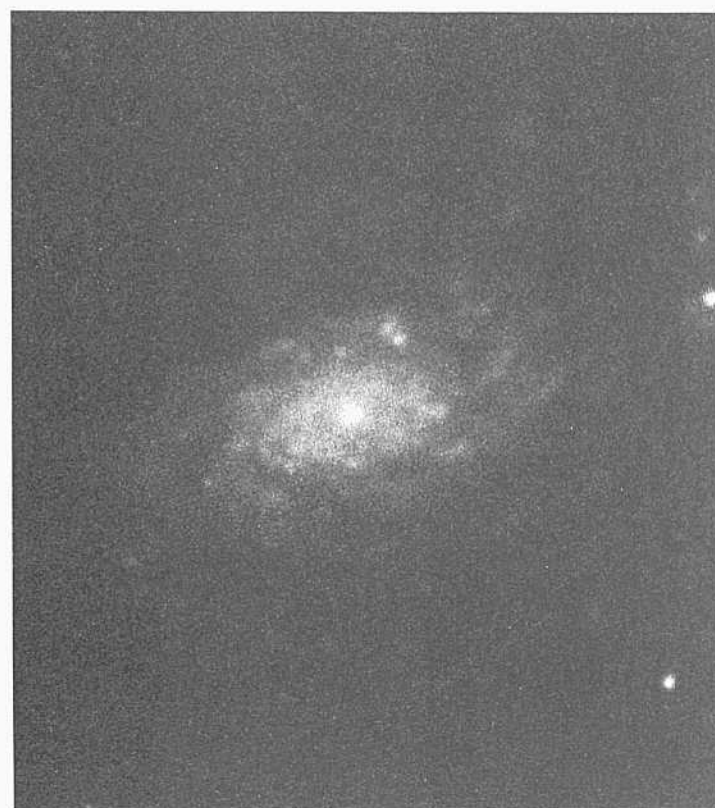
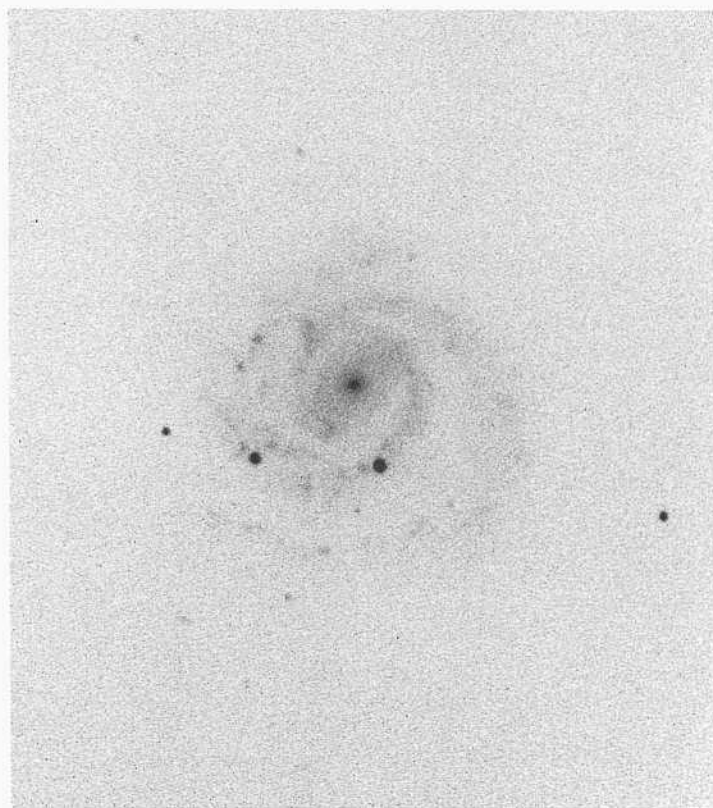
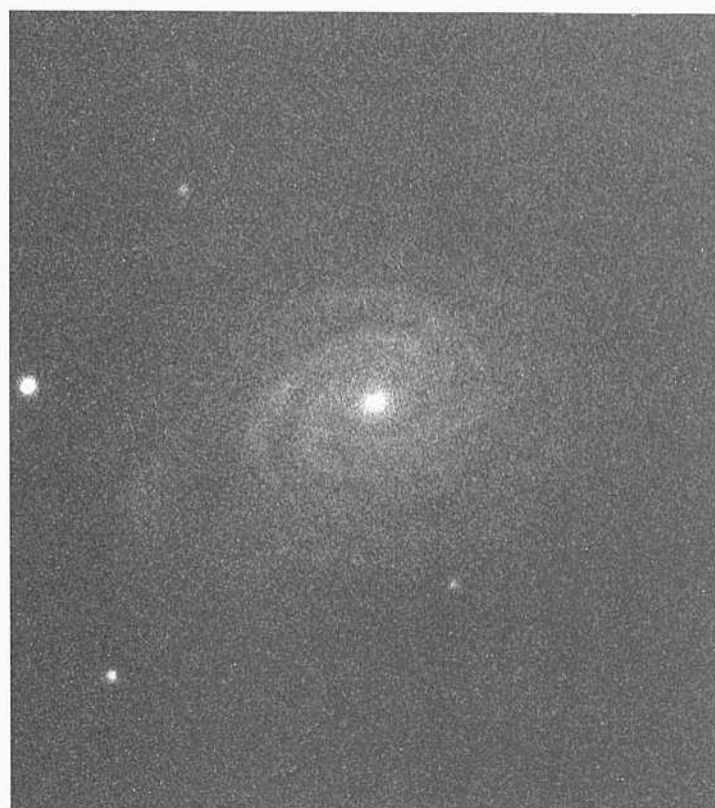
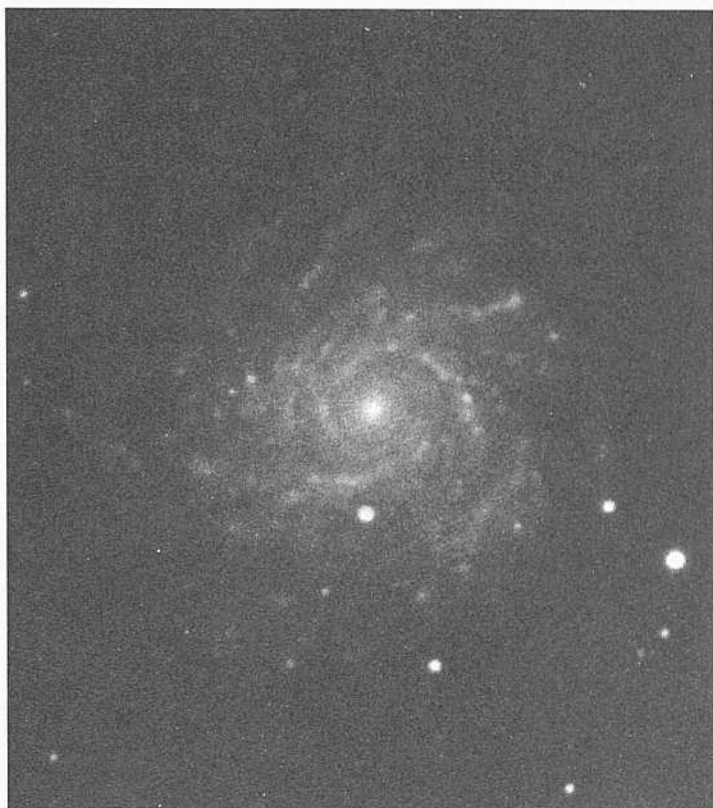
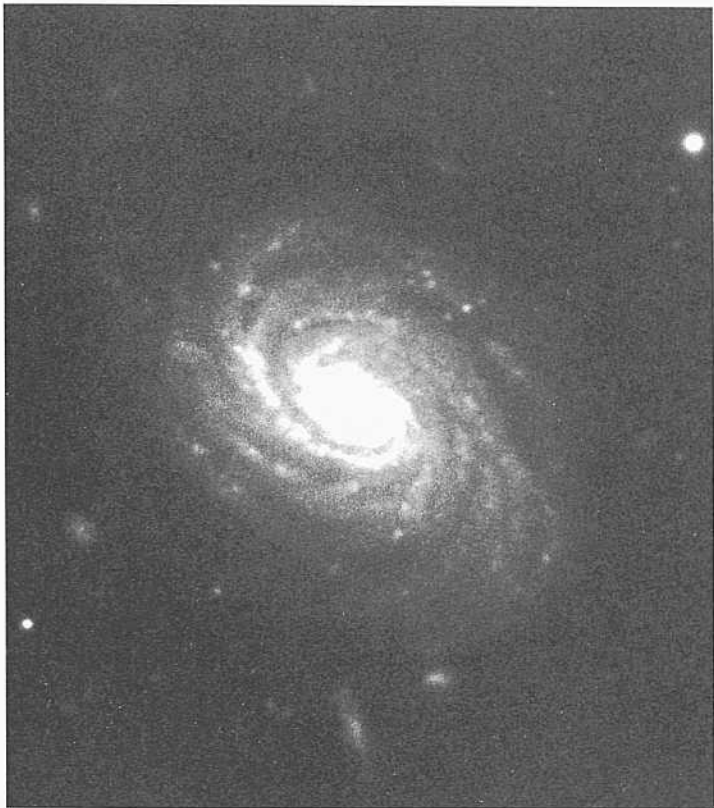
**PH-8072-S**

Feb 5/6, 1981

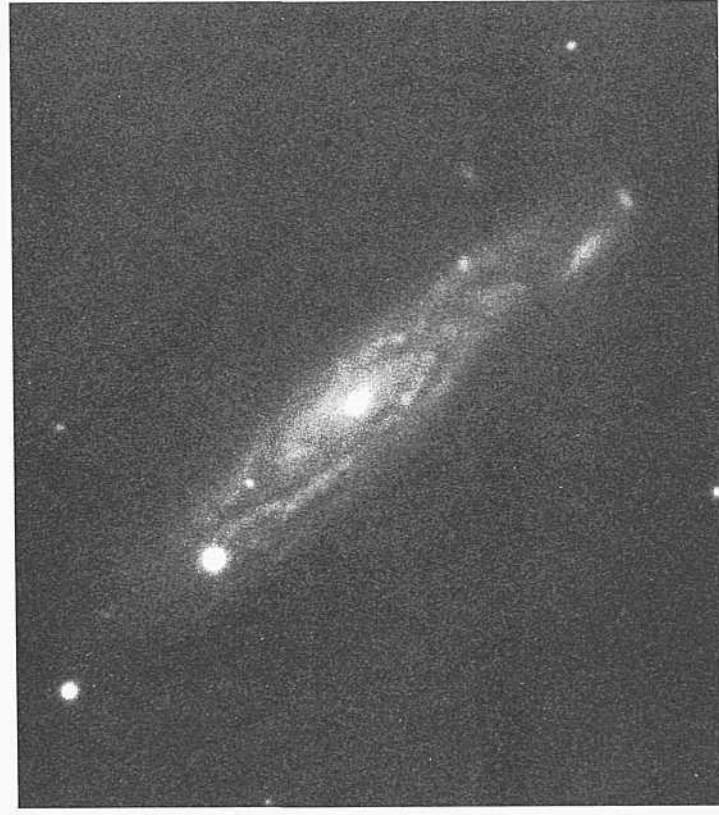
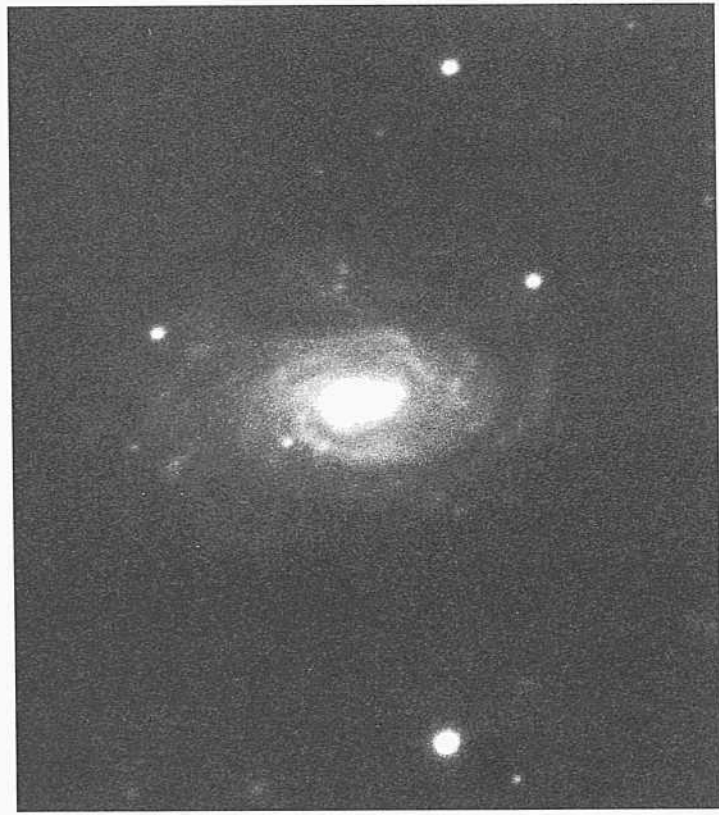
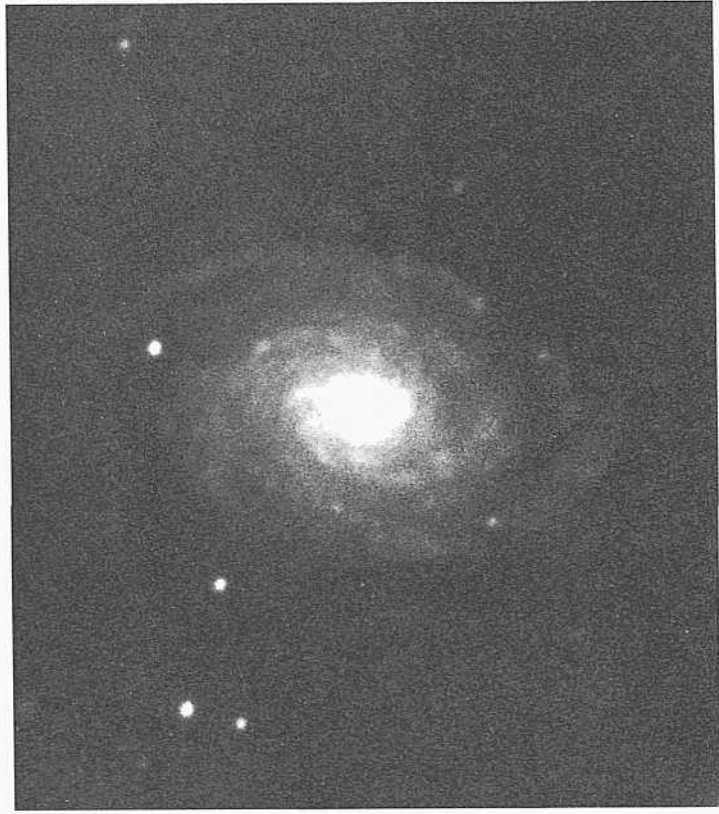
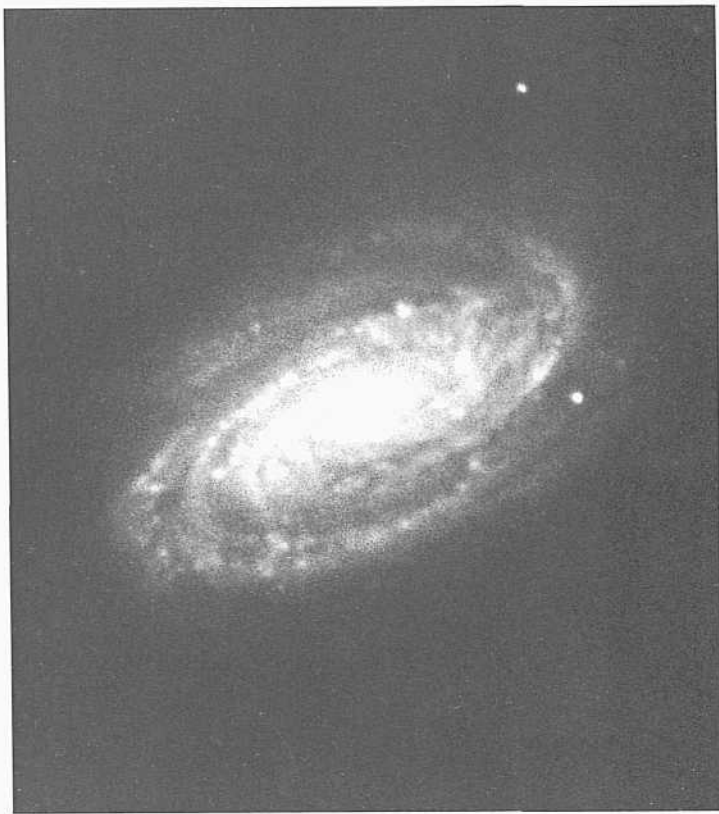
**103aO**

**12 min**

NGC 3259 is a multiple-armed spiral with a bright nucleus and a small **angular** diameter. Its redshift is  $v_r = 2005 \text{ km s}^{-1}$ .



PANEL  
186



**T**hese six galaxies on this panel continue the illustration of Sbc forms having spiral patterns of the multiple-armed type. All are of luminosity class [-II].

NGC 7392      Sbc(s)I-H      HA, p. 20  
 CD-1127-Br  
 Aug 20/21, 1979  
 103aO + GG385  
 4.5 min

The main arms in NGC 7392 are narrow, and each can be traced as separate fragments for more than half a revolution outward. The largest HII region resolves at the 1.5" level; the others are unresolved. The redshift of NGC 7392 is  $v_0 = 3035 \text{ km s}^{-1}$ .

NGC 3506      Sbc(s)I-II  
 CD-1853-HB  
 April 4/5, 1981  
 103aO + GG385  
 4.5 min

Two principal high-surface-brightness arms begin near the bright center and wind outward for half a revolution, at which point they decrease in brightness. On one side, the arm fragments into four pieces of spiral arc with steeper pitch angles.

The HII regions are unresolved at the 1" level. The redshift is  $v_0 = 6348 \text{ km s}^{-1}$ , which is one of the largest in the RSA (RSA, Fig. 2).

NGC 976      Sbc(r)I-II  
 PH-7548-S  
 Nov 6/7, 1978  
 103aO  
 12 min

The thin, regular, multiple arms begin on the rim of a bright internal ring which is largely burned out on this print. Very few Mil regions exist in the arms. The few faint candidates are unresolved at the 1" level. The redshift of NGC 976 is large for RSA galaxies, at  $v_0 = 4550 \text{ km s}^{-1}$ .

NGC 2347      Sbc(r)I-II  
 PH-7897-S  
 Nov 6/7, 1980  
 103aO  
 12 min

NGC 2347 has the small angular diameter of 1.5' and a large redshift of  $v_0 = 4592 \text{ km s}^{-1}$ . The spiral pattern is similar to that of NGC 976, above: the thin, easily traced arms begin on the rim of a bright internal ring.

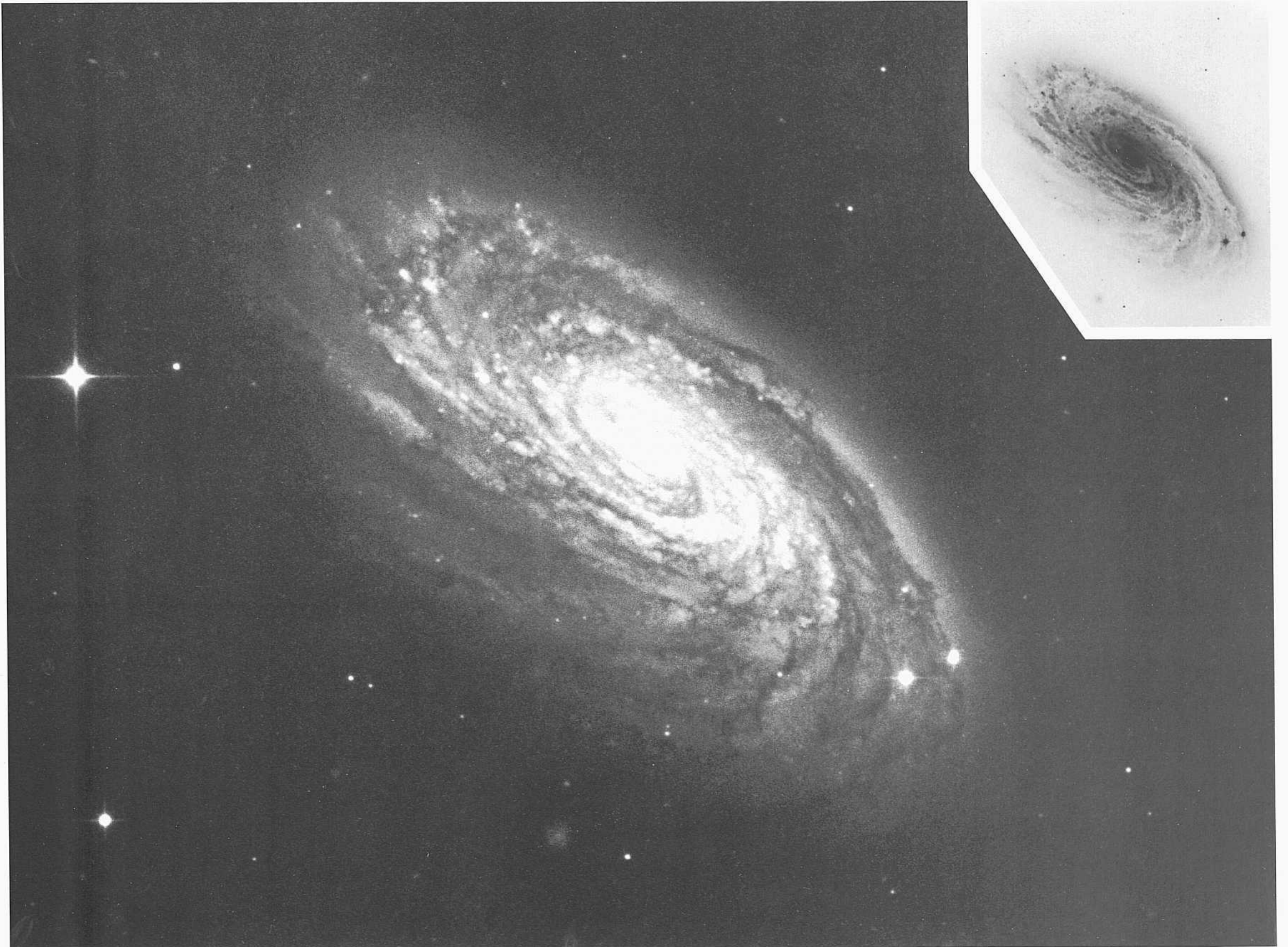
IC 1788      Sbc(s)I-II  
 CD-1599-S/Br  
 Aug 12/13, 1980  
 103aO + GG385  
 1.5 min

The arm pattern in IC 1788 is similar to (but later in the classification sequence than) how NGC 488 would appear if viewed nearly edge on. The redshift of IC 1788 is  $v_0 = 3306 \text{ km s}^{-1}$ ; the HII regions are unresolved.

NGC 1625      Sbc(s)I-H      small group?  
 PH-7921-S  
 Nov 7/8, 1980  
 103aO  
 12 min

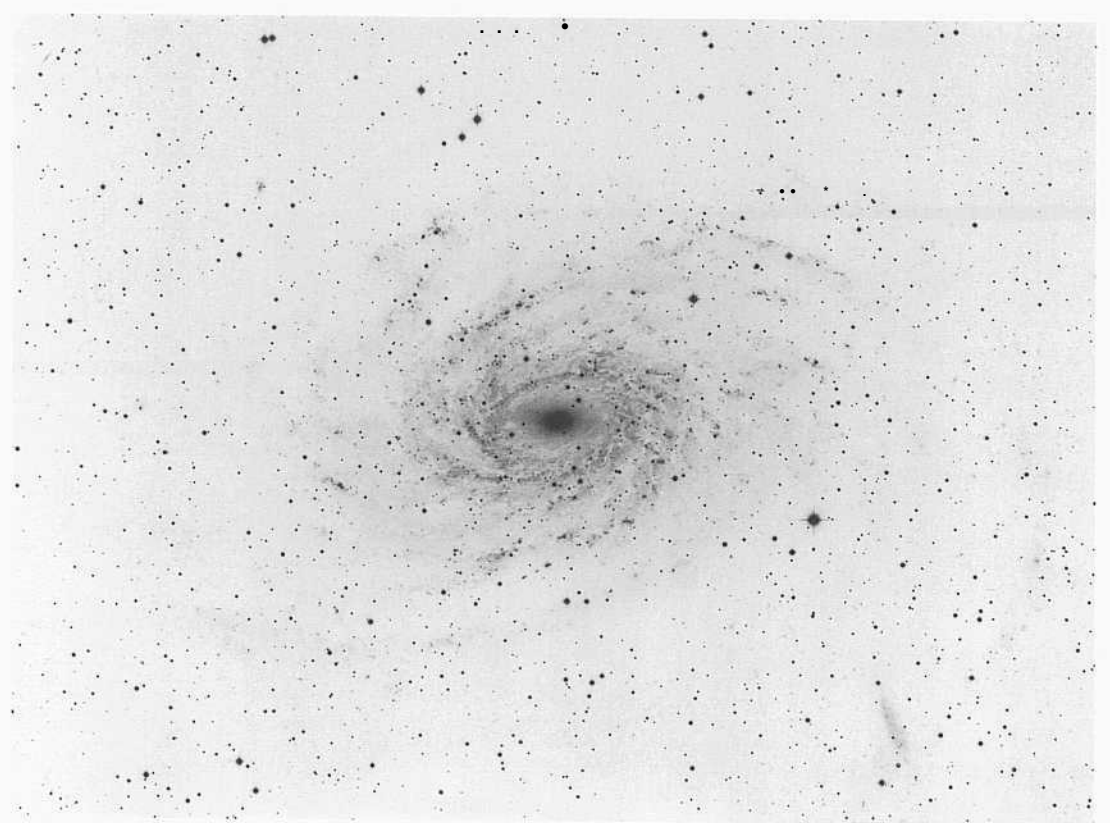
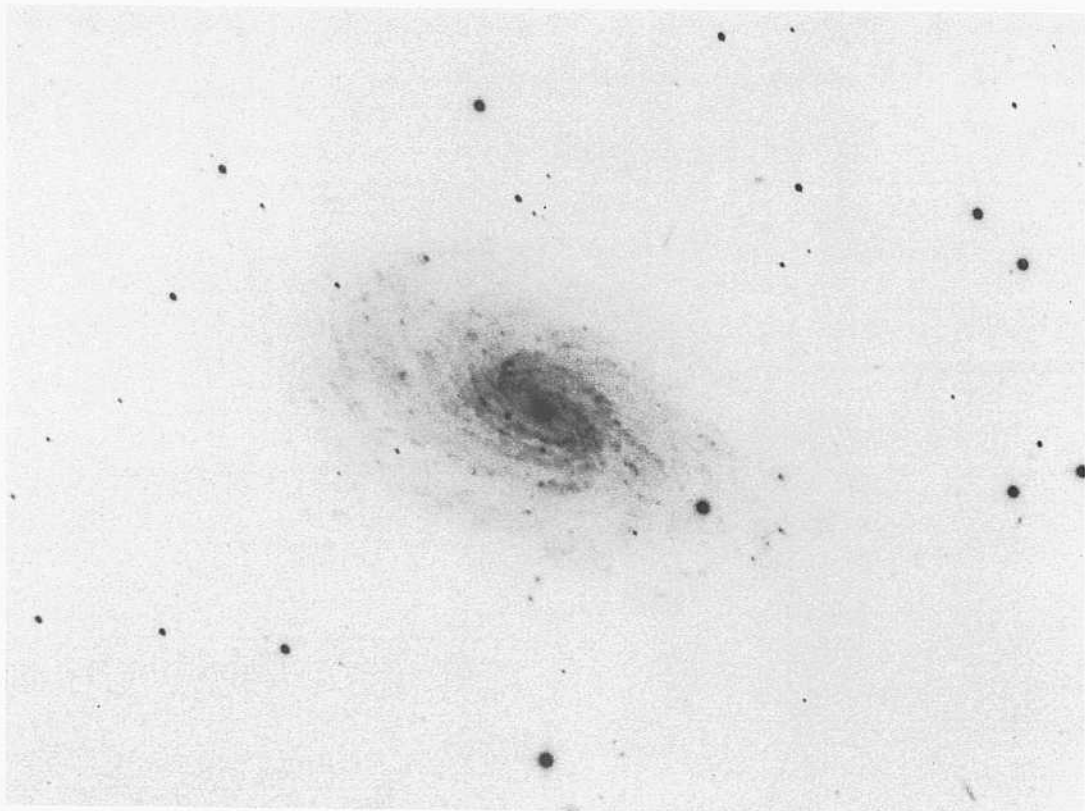
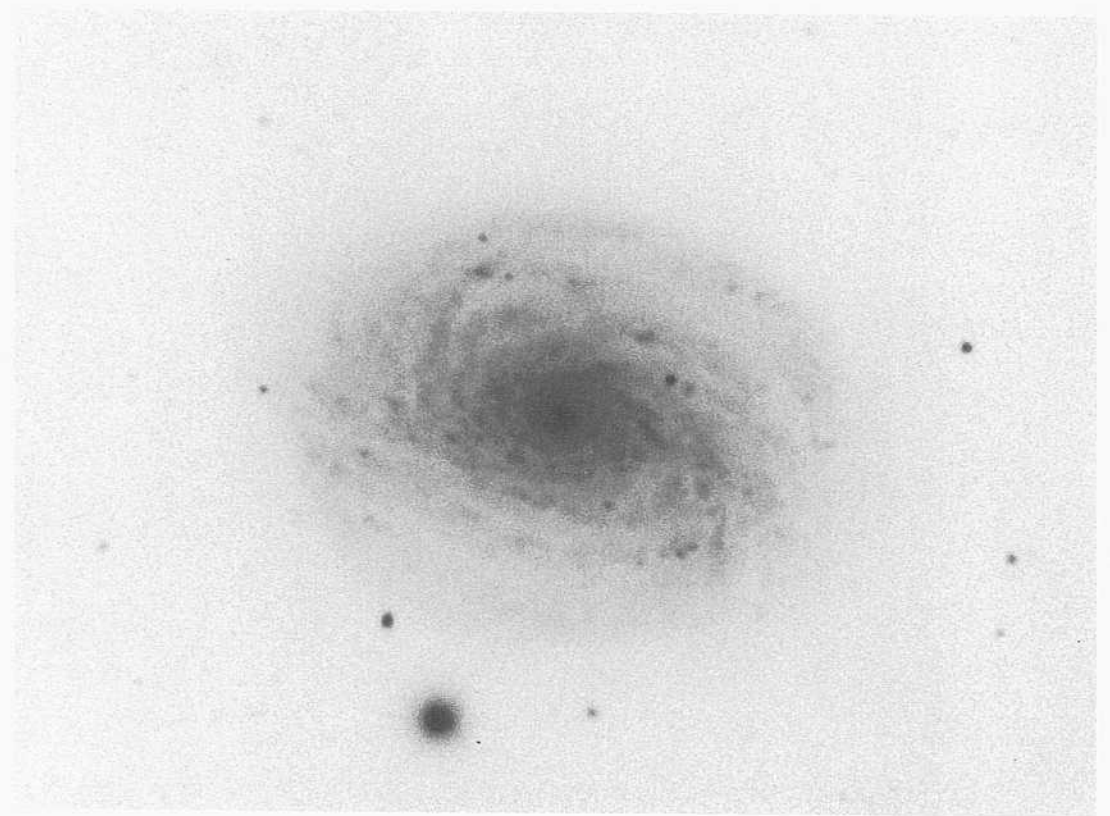
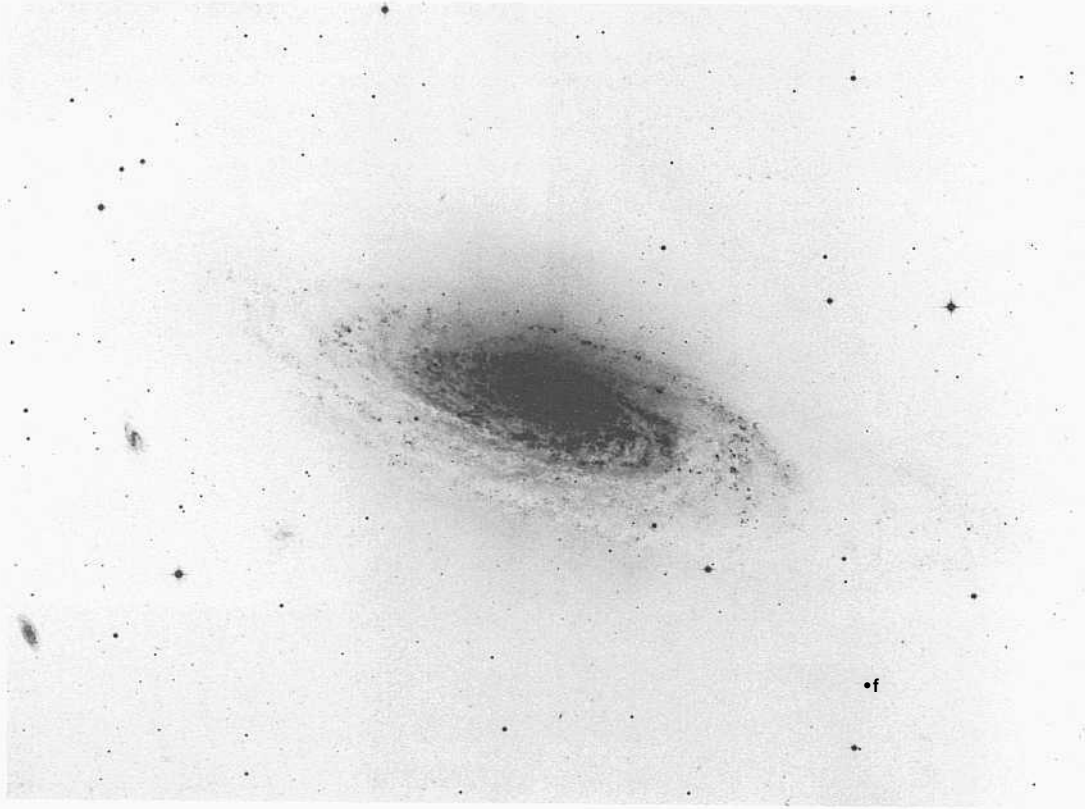
NGC 1625 may form a physical group with NGC 1622 (Sa with exquisite narrow arms) and NGC 1618 (SBa?) at separations of 10.2' and 17.6', respectively, but both are of unknown redshift. If the redshifts are the same as that of NGC 1625,  $v_0 = 3033 \text{ km s}^{-1}$ , their projected lineal separations from NGC 1625 are 180 kpc and 310 kpc, respectively.





PANEL  
187

PANEL  
188



The four galaxies on this panel are good prototype examples of the Sbc morphology, having extreme filamentary spiral patterns at the intermediate luminosity class II or even as late as II-III. Three of the four galaxies have very low redshifts and, as a consequence, have well-resolved stellar contents.

NGC 3521      Sbc(s)II      HA, p. 15  
 CD-1748-S  
 Jan 12/13, 1981  
 103aO + GG385  
 45 min

The central 1' (diameter) region of NGC 3521 is a high-surface-brightness disk having spiral dust lanes but no luminous arms. Luminous arm fragments begin at the edge of this inner disk. They are interspersed with associated dust lanes and define the outer MAS pattern, which is of the NGC 2841-NGC 488 type.

The moderately short exposure print in the Hubble Atlas, made from an original Mount Wilson 100-inch plate, shows the bright central disk and a hint of a luminosity distribution above the plane, centered on this central region. In the Hubble Atlas print this appears as an overlay of luminosity in silhouette against the far side of the disk. In the print here from a deeper Las Campanas plate, this "cylinder" of light perpendicular to the plane, concentric with the center, is more evident. It can be traced in height until it appears even beyond the image of the disk on the far side, showing that the distribution is, in fact, perpendicular to the plane.

The disk is resolved into individual stars. The largest HII regions have core-plus-halo diameters of 4", which, with a redshift distance of 12.5 Mpc based on the redshift of  $v_o = 627 \text{ km s}^{-1}$ , is a linear diameter of 240 psc, consistent with the calibration elsewhere (Sandage and Tammann 1974a).

NGC 2268      Sbc(s)II  
 PH-7550-S  
 Nov 5/6, 1978  
 103aO  
 12 min

The spiral pattern consists of an inner set of very-high-surface-brightness arms (partly burned out here) and an outer set of multiple-fragment arms of lower surface brightness. The redshift of NGC 2268 is  $v_o = 2458 \text{ km s}^{-1}$ . No resolution occurs of the HII regions or of individual stars.

NGC 4-800      Sb(rs)II-III      HA, p. 76  
 PII-8032-S  
 Feb 3/4, 1981  
 103aO  
 12 min

NGC 1800 is classed Sb here, in the RSA, and in the Hubble Atlas. It is shown in the section here which illustrates that the differences between Sb and Sbc classes are subtle and arbitrary; nevertheless it is clear from this print and the one in the Hubble Atlas that NGC 4800 is slightly earlier than NGC 3521 at the left. It has a larger and brighter central region, and its arms are less well resolved into stars and HII regions.

The redshift of NGC 4800 is  $u_o = 808 \text{ km s}^{-1}$ .

NGC 6744      Sbc(r)II/SBI>c(r)II  
 CD-1473-S/Br  
 May 10/11, 1980  
 103aO + GG385  
 45 min

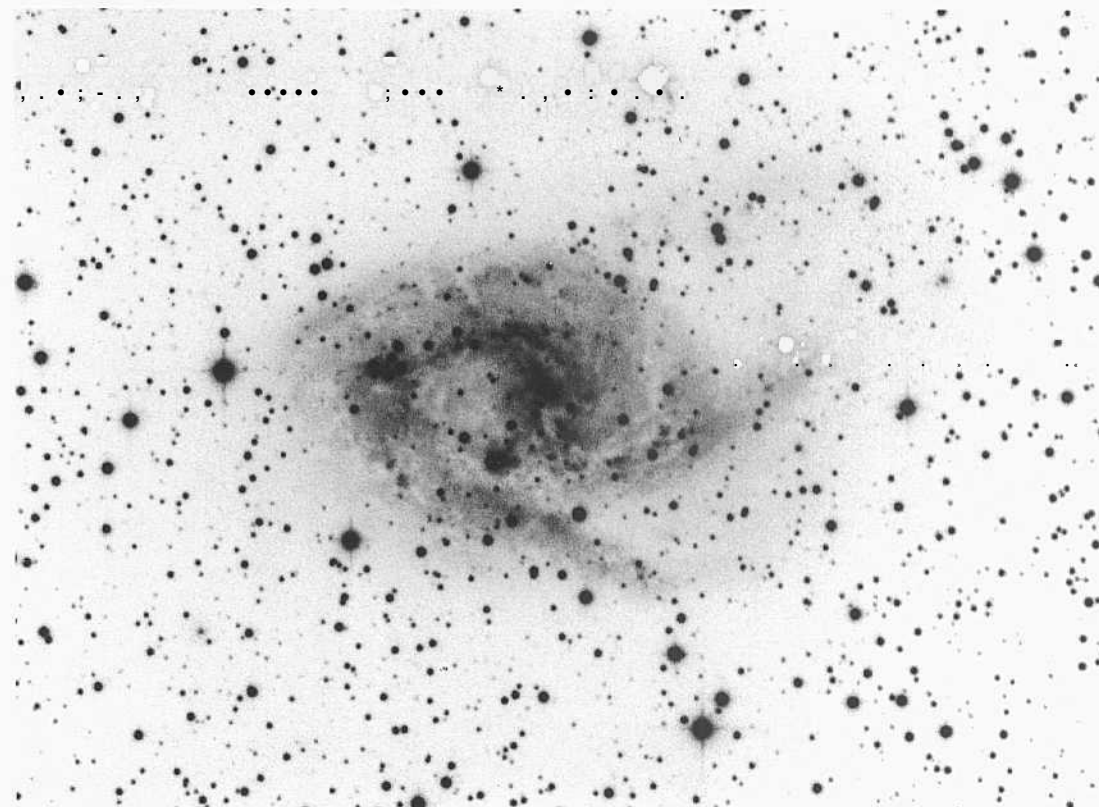
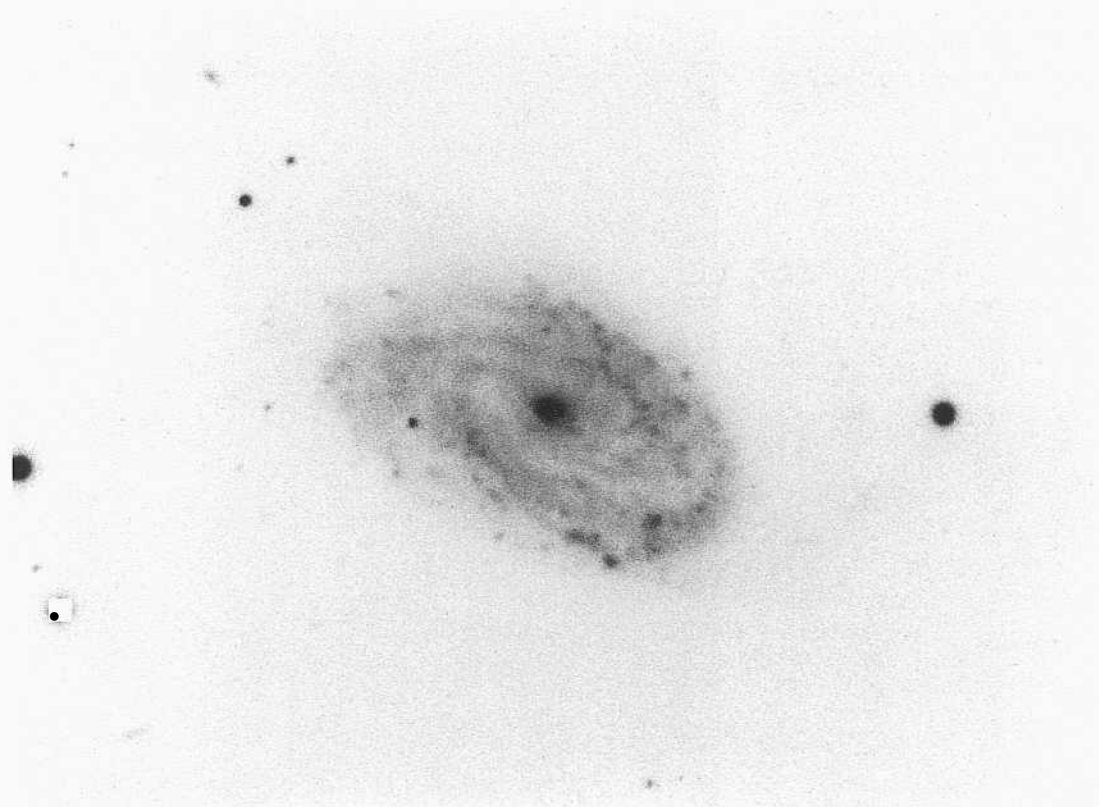
This very large (the angular diameter measured from the outermost arms is 18'), nearby spiral is at low galactic latitude ( $l = -26^\circ$ ), making foreground field contamination by Galactic stars apparent and the identification of any particular individual resolved star's in the arms uncertain.

But the resolved HII regions are more easily identified. The largest of these have core-plus-halo diameters of about 6". At the redshift distance of 13 Mpc, based on the redshift of  $v_D = 663 \text{ km s}^{-1}$ , this corresponds to a linear diameter of 385 psc, consistent with a calibration given elsewhere (Sandage and Tammann 1974a).

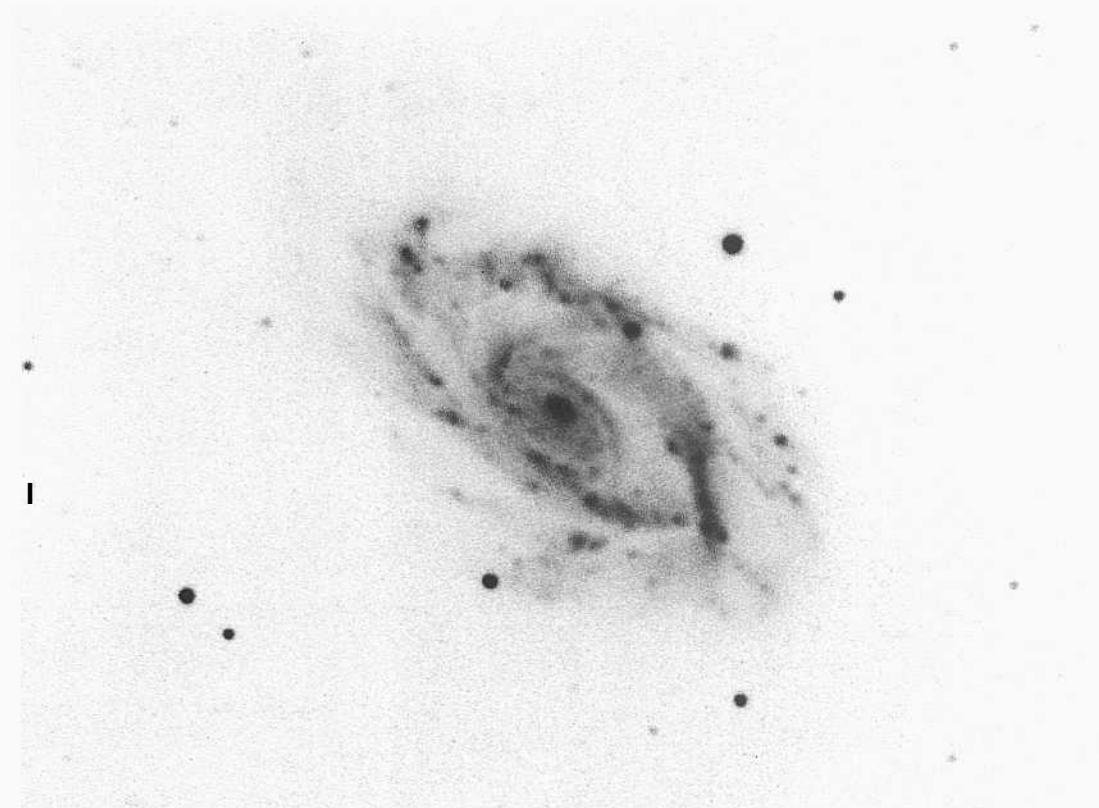
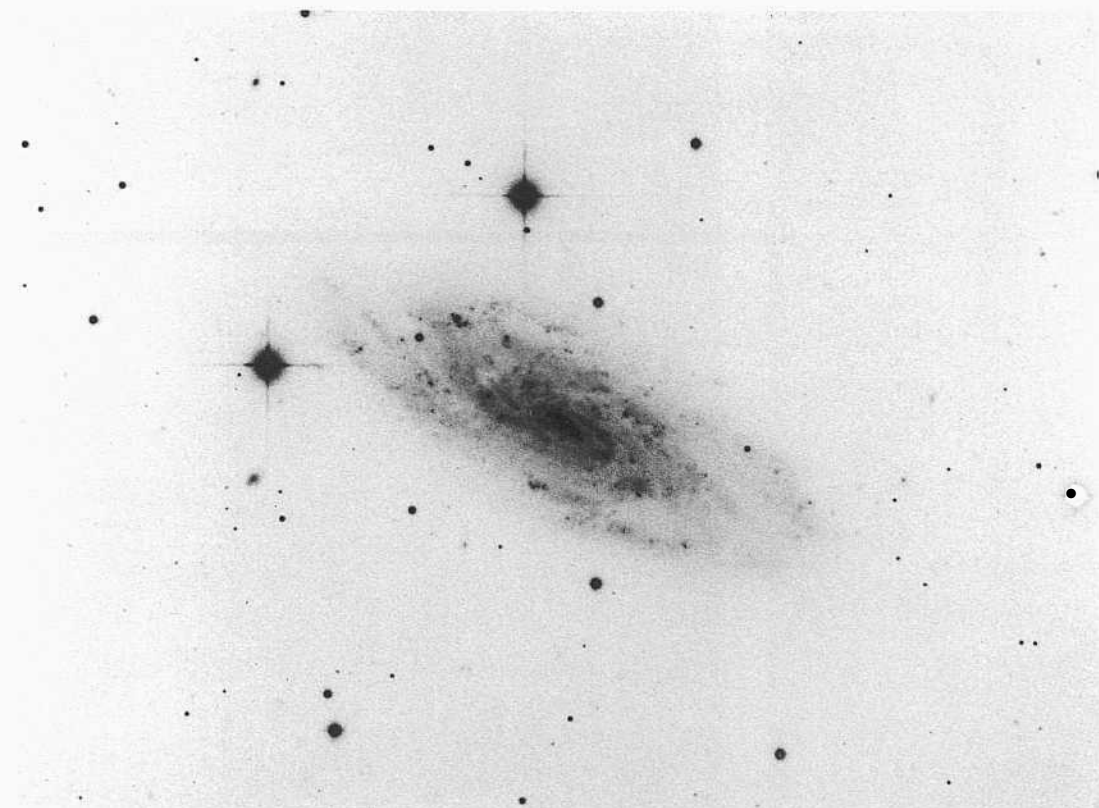
The arm pattern is clearly multiple. The outermost arm, out of the frame of this print, overlaps the spindle Iml galaxy at the lower-right corner. This companion is highly resolved. Its separation from NGC 6744 is 10.1' northwest (the orientation of the print here is north at the right, west at the bottom), corresponding to a small projected linear separation of 3.9 kpc.



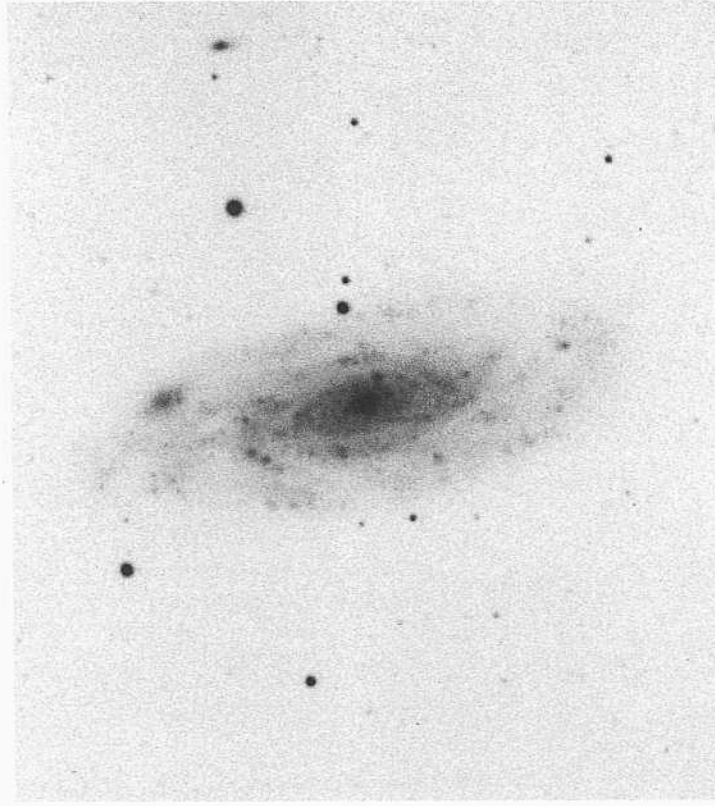
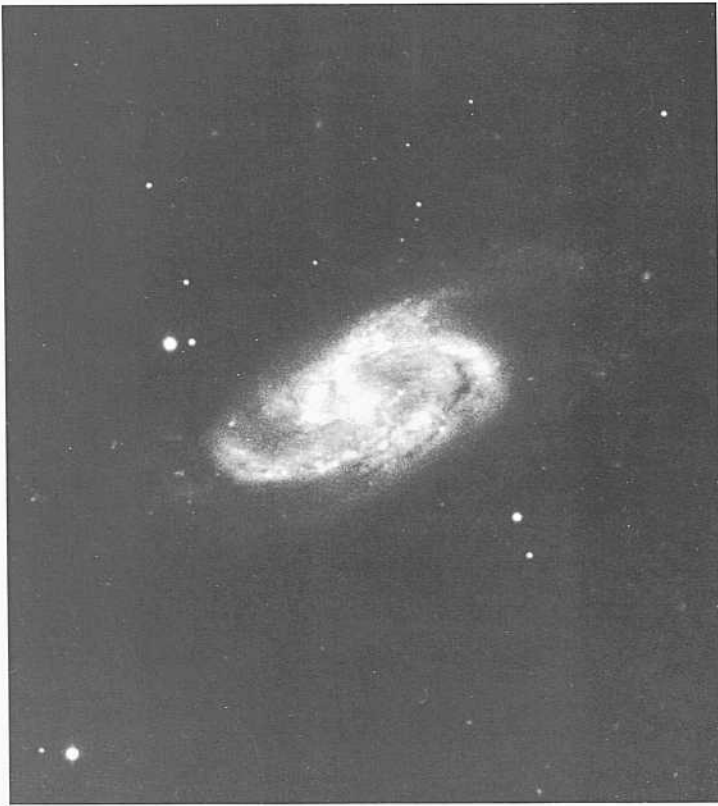




PANEL  
189



PANEL  
190



**THE** six galaxies on this panel are of **intermediate-to-late** luminosity class **II** or **11-111**. Most have **filamentary** arm structure, although each has two dominant principal **arms inside** the filamentary fragments **that are in the outer arm pattern**.

NGC 150            Sl)c(s)H pec  
 CD-1588-S  
 Aug 11/12, 1980  
 103aO + GG385  
 45 min

The spiral pattern in NGC 150 is of the grand design type although there are three high-surface-brightness arms rather than only two in the reflection symmetry of grand design patterns. Two bright inner arms start from the center. After half a revolution one of these (called here the first) nearly overlaps the second which, however, can only be traced for less than half a revolution; consequently it does not overlap the first. The third arm crosses the first (out of the fundamental plane?) after the first has made only a quarter revolution outward. The third then decreases in surface brightness and continues outward as a very-low-luminosity arm which can be traced for another half revolution. A prominent dust lane threads the middle of the first arm. Such a three-armed pattern is unusual but not unknown.

The redshift is  $v_0 = 1620 \text{ km s}^{-1}$ .

NGC 4219            Sbc(s)II-III  
 CD-1877-HB  
 April 11/12, 1981  
 103aD + GG495  
 45 min

NGC 4219 has a small central bulge (nucleus). Two main, moderately ill-defined luminous arms with associated dust lanes begin at the center and can be traced as bright fragments of a grand design pattern for about half a revolution. The disk inside the edges of these arms has moderately high surface brightness from the center outward (i.e., the inter-arm region is filled with disk light).

The redshift is  $v_n = 1684 \text{ km s}^{-1}$ .

NGC 7162            Sbc(rs)II            pair  
 CD-1584-S/Br  
 Aug 11/12, 1980  
 103aO + GG385  
 45 min

The spiral pattern in NGC 7162 is multi-armed in thick fragments that begin at the center.

NGC 7162 forms a physical pair with NGC 7166 (SO; panel 34) at an angular separation of  $11'$ . The redshifts are  $v_0(7162) = 2169 \text{ km s}^{-1}$  and  $v_0(7166) = 2376 \text{ km s}^{-1}$ . At the mean redshift distance of 45 Mpc ( $H = 50$ ) the projected linear separation is 145 kpc.

NGC 5376            Sbc(s)II  
 PH-7644-S  
 April 27/28, 1979  
 103aO  
 12 min

The disk of NGC 5376 is filled with moderately thin arm fragments and associated dust lanes.

The redshift is  $v_n = 2210 \text{ km s}^{-1}$ .

IC 1783            Sbc(rs)II  
 CD-542-S  
 Oct 1/2, 1978  
 103aO + GG385  
 45 min

Two principal bright inner arms form an almost complete inner ring. Lower-surface-brightness, outer (fossil?) arms are relatively thin and well defined.

The redshift is  $v_0 = 1272 \text{ km s}^{-1}$ .

NGC 1353            Sbc(r)II  
 CD-I 183-Br  
 Aug 23/24, 1979  
 103aO + GG385  
 45 min

The spiral pattern of NGC 1353 is nearly identical with those in NCC 7162, NGC 5376, and IC 1783 on this panel. Two bright, tightly wound inner arms have the grand design pattern. Fainter outer arms, with many fragments, spread throughout the outer disk, giving the appearance that the disk is filled with arm segments similar to in NGC 2841. NGC 1353 is later in the classification sequence.

The redshift is  $v_n = 1521 \text{ km s}^{-1}$ .

*Sbc Classification Section (continued)*

NGC 5055      Sbc(s)II-III      HA, p. 15  
S-59-Ritchey                              panel S5  
March 9/10, 1910  
Seed 23 (blue)  
300 min

NGC 5055 insert  
H-93-Duncan  
May 14/15, 1926  
E33  
180 **min**

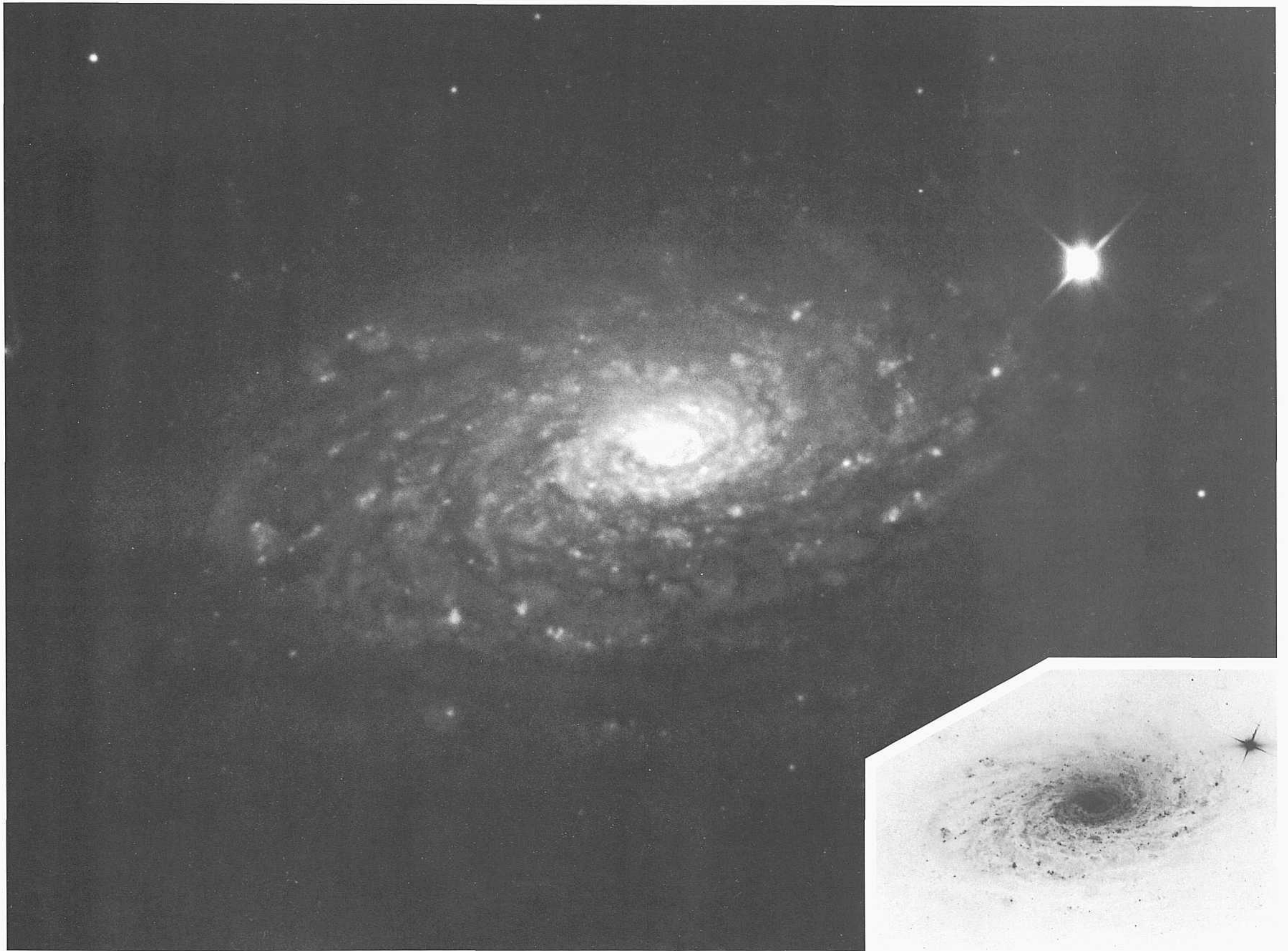
The original plate used here as the main print was taken by Ritchey in 1910 with the newly completed Mount Wilson 60-inch reflector, which many astronomers believe was the most productive telescope of all time. The insert negative print is made from the plate used for the reproduction in the Hubble Atlas, taken by John Duncan **with** the Mount Wilson 100-inch reflector in 1926.

The quality of the images shows the superior nature of both the 60-inch and the 100-inch telescope optics in their ability to resolve to the seeing limit of the Mount Wilson site (better than 0.4" under the best conditions).

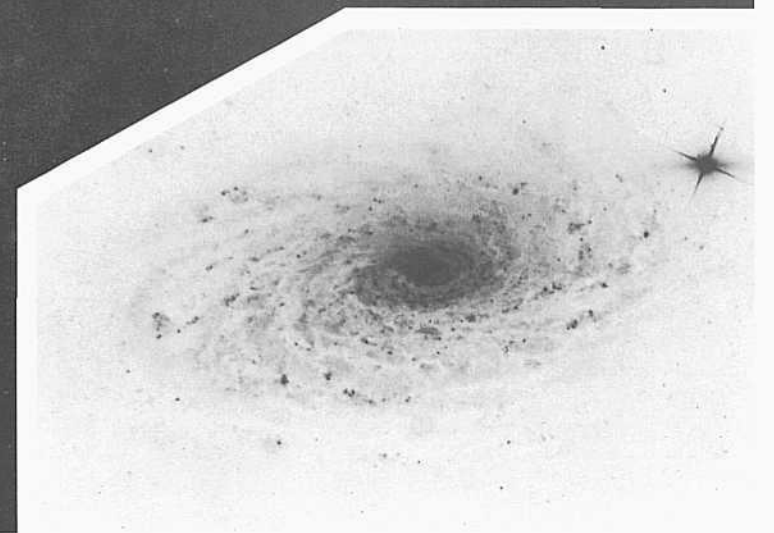
The spiral pattern of NGC 5055 is similar to those in four of the six galaxies on the preceding panel. The inner region has very-high-surface-brightness arms which thread throughout the disk. These filamentary arms can be traced as fragments almost to the center of the galaxy.

The surface brightness of the multiple-armed pattern decreases abruptly at radius 5.0" (2.7 kpc) from the center. The outer, lower-surface-brightness multiple arm fragments, together with their associated dust lanes, wind outward and cover the extended disk, similar to the pattern in the earlier Sb prototype NGC 2841 (panels 142, S4, S12).

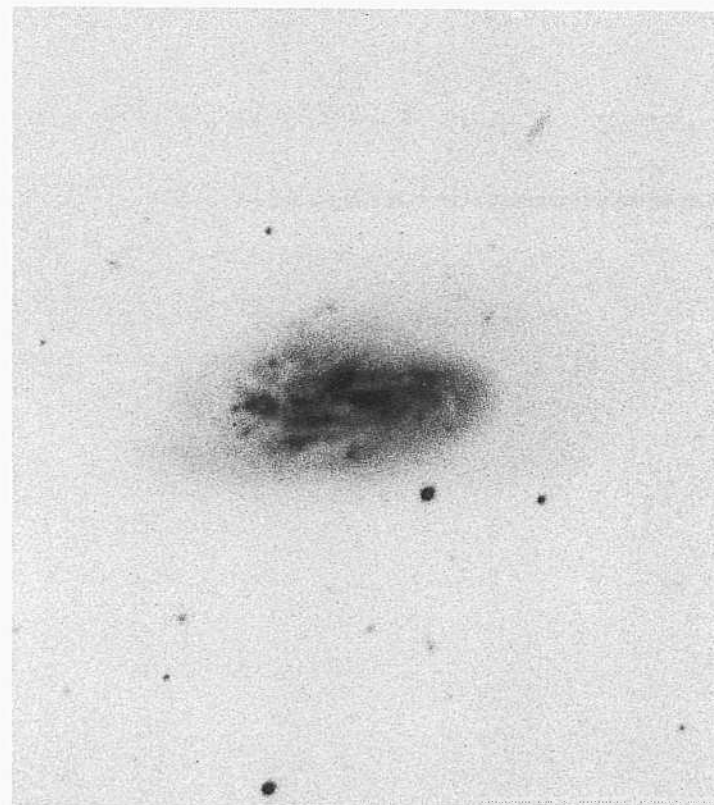
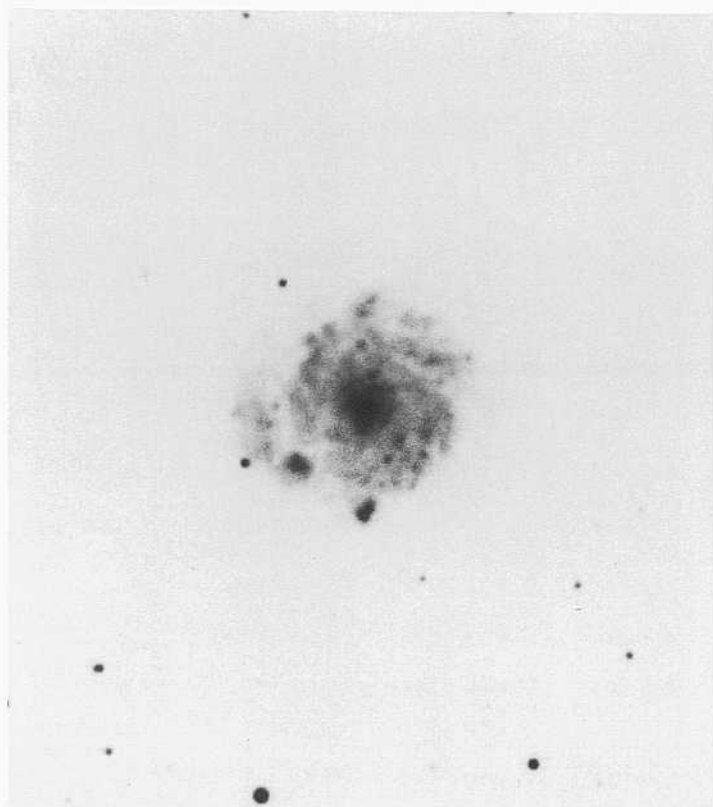
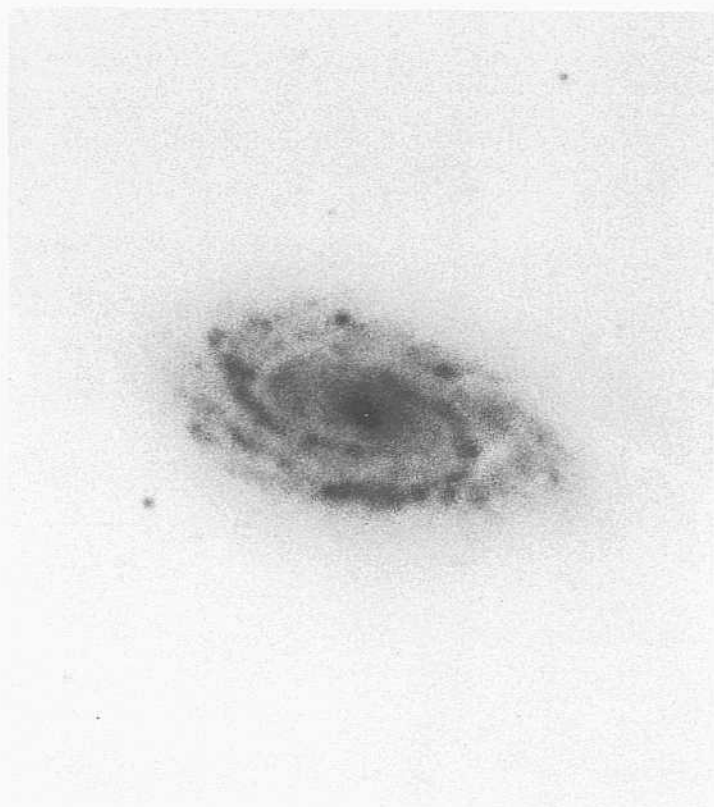
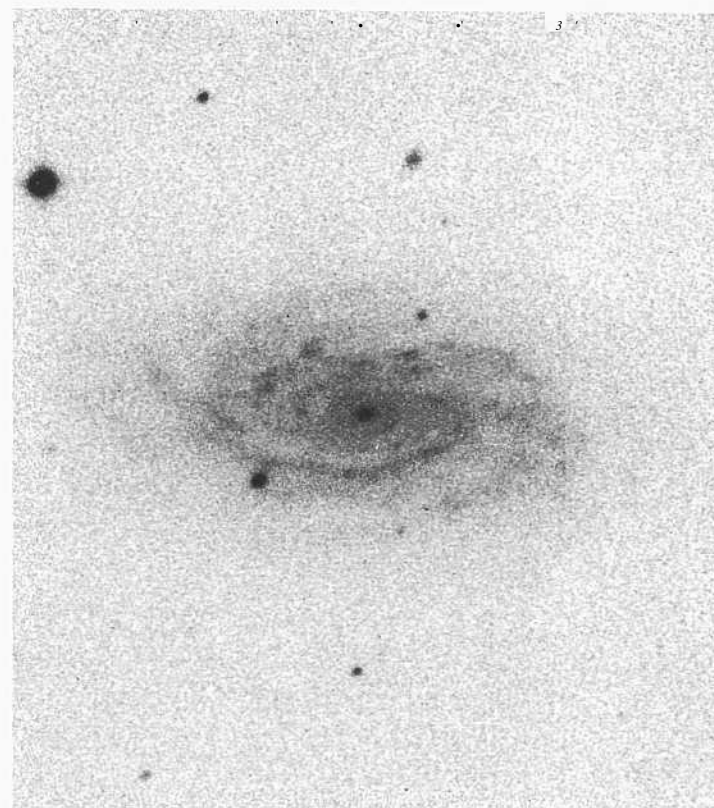
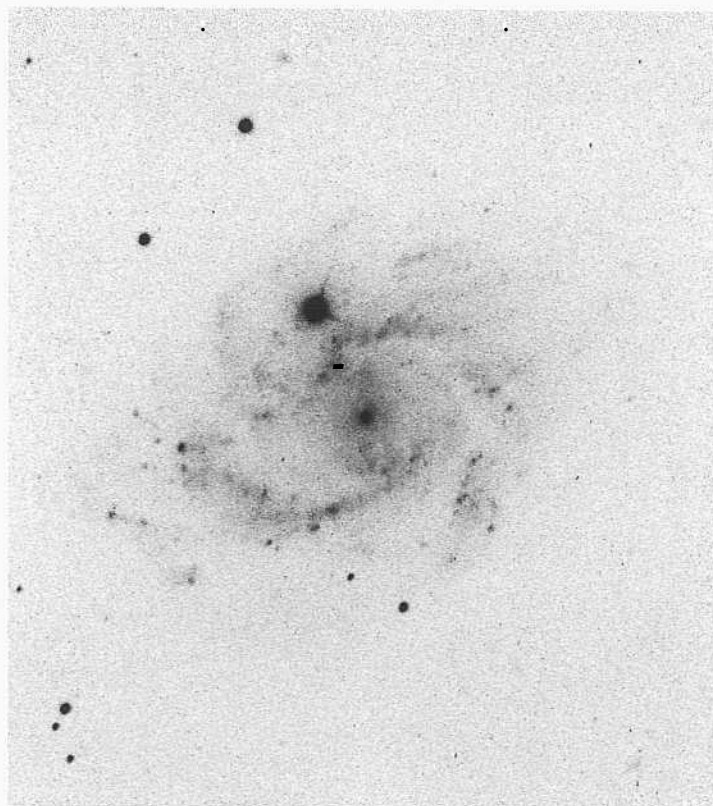
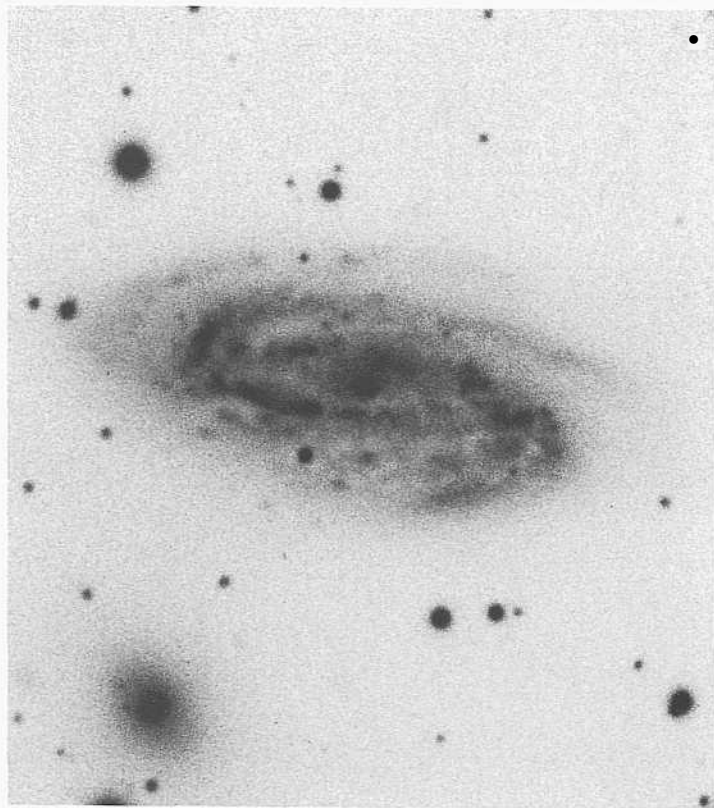
Many small, generally unresolved III regions exist, the largest of which are less than 1.5" in diameter. The redshift of NGC 5055 is small at  $v_0 = 550 \text{ km s}^{-1}$ .



PANEL  
191



PANEL  
192



NGC 6754      Sbc(s)IMII      pair  
 CD-528-S/Br  
 Sep30/Oct 1, 1978  
 103aO + GG385  
 45 niin

NGC 6754 forms an apparent pair with an anonymous SBO galaxy of unknown redshift at an angular separation of 1.1/.

The spiral pattern is not multiple, as in NGC 5055 on the preceding panel, nor is it as regular as in grand design spirals of earlier luminosity classes. One principal bright arm is easily traced, but the other, which begins on the far side of the center, is more difficult to follow; it breaks into fragments as it comes to the near side on the outside of the first principal arm. The asymmetry of the luminosity distribution of the dust silhouetted against the disk identifies the near and far sides.

No individual HII regions are easily identified. The redshift is  $v_0 = 3207 \text{ km s}^{-1}$ .

NGC 5313      Sbc(s)II  
 PH-8094-S  
 Feb6/7, 1981  
 103aO  
 12 niin

NGC 5313 forms an apparent pair with NGC 5311 (Sa, very early), of similar angular diameter but of unknown redshift at a separation of 9.4'. If the redshift of NGC 5311 is similar to that of NGC 5313,  $v_0 = 2588 \text{ km s}^{-1}$  the projected linear separation of the pair would be 140 kpc.

The spiral pattern of NGC 5313 is of the grand design type. The luminosity class is II. There are only two principal arms, both of high surface brightness and tight pitch angles so that they nearly overlap in their outer regions after each has unwound by about half a revolution. A prominent dust lane exists on one side of the spiral pattern, silhouetted against the background disk.

Visual inspection at the telescope shows the disk to be of very high surface brightness. There is an unresolved (starlike) nucleus.

NGC 864      Sbc(r)n-III/SBbe(r)II-III  
 H-1438-H  
 Nov 21/22, 1932  
 Imp. Eel.  
 45 niin

The central oval forms a weak bar. The two principal arms spring from the ends of the bar's major axis. Fainter outer arm fragments exist.

The two largest of the many III regions resolve at about the 2" level; the others are unresolved. The redshift of NGC 864 is  $v_0 = 1707 \text{ km s}^{-1}$ .

NGC 278      Sbc(s)II.2  
 PH-12-S  
 Sep 25/26, 1951  
 103aO  
 5 miii

The surface brightness of the multiple-armed spiral pattern in NGC 278 is exceedingly high, although not as high as those of the two principal inner arms of the Seyfert galaxy NGC 1068 (Sb; panel 138), which are among the brightest arms in the RSA. Multiple exposures at short-exposure times also show a very bright nucleus in NGC 278, which, however, is still diffuse at the 2" level rather than unresolved (starlike) as in many Seyfert galaxies. The print here is from a short-exposure, early 200-inch Palomar plate, underexposed to show the multiple-armed pattern that begins at the center.

The redshift of NGC 278 is  $u_0 = 932 \text{ km s}^{-1}$ . The two diffuse knots may be HII complexes; the largest has an angular diameter of about 5", corresponding to a linear diameter of 450 pc.

Faint luminosity exists outside the edge of the bright disk. A spiral pattern exists in dust that is silhouetted against the envelope luminosity.

NGC 4682      Sbc(rs)II  
 CD-1883-HB  
 April 11/12, 1981  
 L03aO  
 60 min

The principal arms in [NGC 4682 are narrow and are well traced for almost a whole revolution from their beginning near the center. They branch and have a fainter surface brightness in the outer regions.

The redshift is  $v_0 = 2099 \text{ km s}^{-1}$ .

NGC 3547      Sbr(s)II-III pec  
 CD-1852-HB  
 April 4/5, 1981  
 103aO + GG385  
 45 min

Spiral structure is present as segments rather than in a regular pattern. The surface brightness of the arms and the underlying disk is high. The redshift is  $v_0 = 1411 \text{ km s}^{-1}$ .



*Sbc Classification Section (continued)*

**NGC1808**      Sbc pec

**CD-706-S**

**Jan 30/31, 1979**

**I03aO + GG385**

45 min

The central region of NGC 1808 **provides what** appears to be direct evidence of a galactic fountain **composed** of narrow dust lanes **perpendicular to the plane**. The shallow print on the right shows a series of dust lanes cutting across **the far edge of the disk, perpendicular to the major axis**. A short-exposure Mount Wilson 100-inch plate (not shown here) shows the far side of the disk to be heavily **obscured** within a  $15^\circ$  cone centered on the minor axis. The optical depth of the dust in the cone is about unity.

The cone originates in the plane at the center of the galaxy **where** at least six **very-high-surface-brightness (unresolved)** knots exist, evidently connected with the origin of the fountain. Weaker dust lanes, also perpendicular to the plane, are silhouetted along about half the length of the far-side image of the disk.

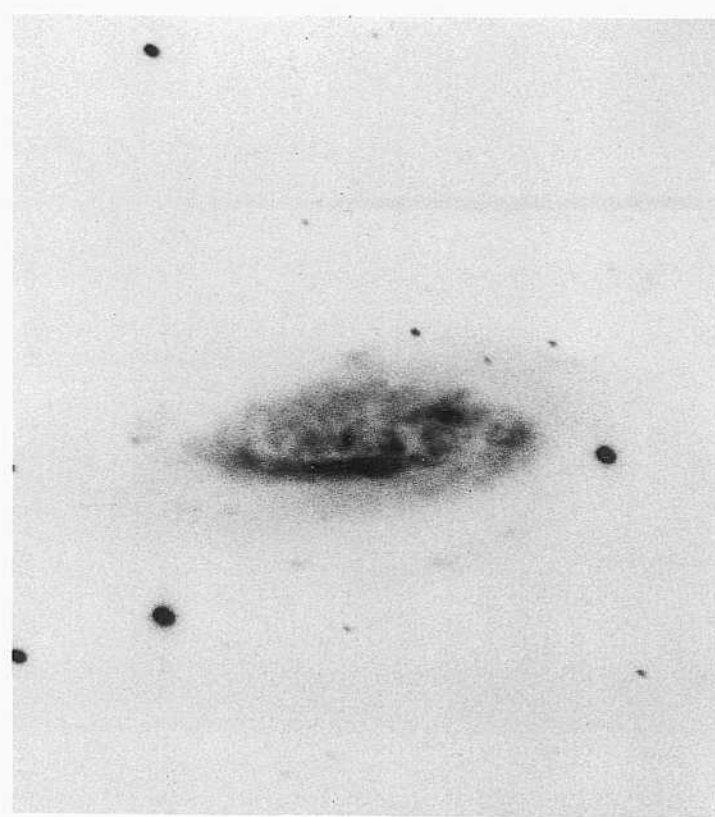
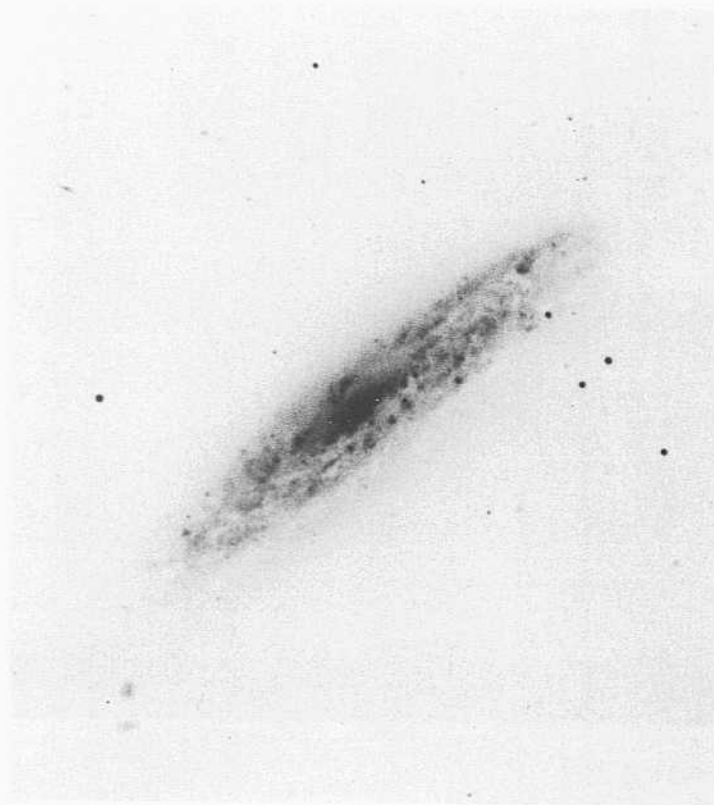
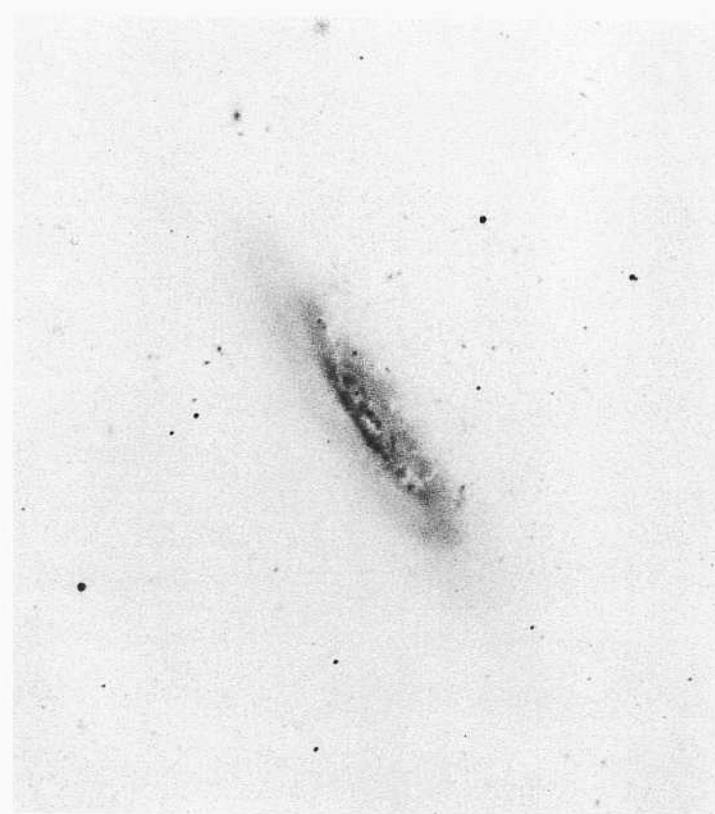
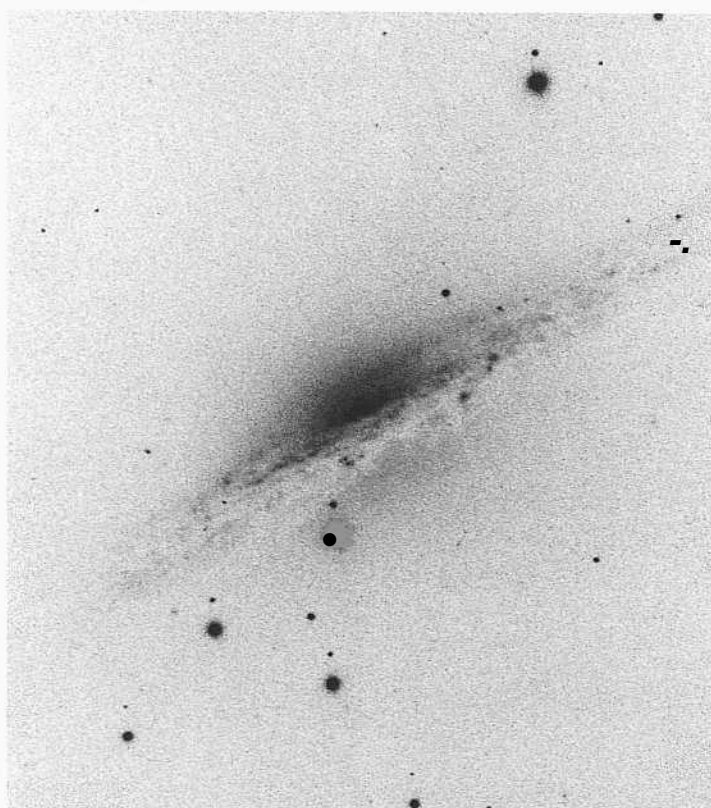
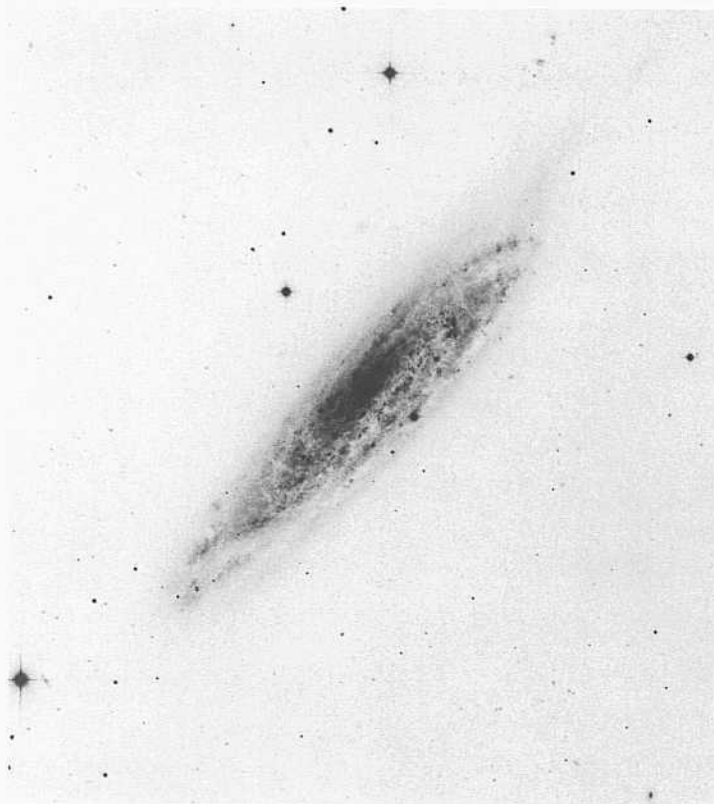
Heavy dust lanes in the disk are evident in silhouette on the near side, most easily seen in the thin right-hand print.

Two oppositely symmetrical, very-low-surface-brightness outer arms emerge from opposite ends of the major axis. Each can be traced for half a revolution before they overlap to form what at first glance would appear as a complete outer ring.

No HII-region candidates are obvious. The redshift of NGC 1808 is low,  $v_o = 820 \text{ km s}^{-1}$ .



PANEL  
194



**G**alaxies on this and the following panel are seen nearly edge on. Their classification as Sbc is, of course, uncertain because the spiral structure is at best difficult to trace. The classification criteria used here are (1) the size of the central bulge (smaller than in SI) types shown on panels 149—154 and larger than in Sc's) and (2) good dust lanes and, where visible, a moderate rate of recent star formation, as judged by the number of HII-region candidates and other signs of recent star formation.

NGC 134            Sbc(s)II-III  
 CD-448-Rose  
 Aug 10/11, 1978  
 103aO + Wr2c  
 90 min

The innermost part of the disk is smooth over the first 50" (**diameter**) region. The multiple dust lanes that outline the arm fragments then begin at the rim of the disk.

Dust-lane asymmetry between the near and far sides is **particularly** strong in this galaxy. As the sense of the opening of the spiral pattern is also unambiguous in the image here, NGC 134 is another excellent case for determining the sense of the rotation relative to the opening of the spiral arms (Hubble 1943; de Vaucouleurs 1958).

The redshift is  $v_0 = 1594 \text{ km s}^{-1}$ .

NGC 4666            SbcII.3            triplet  
 CD-1411-S/Br  
 March 23/24, 1980  
 103aO  
 75 min

NGC 4666 is in the busy area of the southern extension of the Virgo Cluster, at RA =  $12^{\text{h}} 42^{\text{m}}$ , Dec =  $-00^{\circ} 11'$ . It forms an apparent pair with NGC 4668 (**Sbc**; panel 313), at a separation of 7.8'. The redshifts are  $u_0(4668) = 1530 \text{ km s}^{-1}$  and  $w_0(4666) = 1474 \text{ km s}^{-1}$ . NGC 4632 (Sc; panel 288), with a redshift of  $v_0 = 1557 \text{ km s}^{-1}$ , is 46' distant from NGC 4666. At a mean redshift distance of 30 Mpc for the apparent triplet, the **projected** linear separations of NGC 4668 and NGC 4632 from NGC 4666 are 68 kpc and 400 kpc, respectively.

NGC 1055            Sbc(s)II  
 PH-7700-S  
 Sep 26/27, 1979  
 103aO  
 12 min

The **direction of opening of the spiral arms** (clockwise going from the inside outward) and the identification of the near side is unambiguous in this galaxy. Note that the light from the moderate-sized central bulge can be seen above and below the near side of the disk.

The redshift is  $v_0 = 1098 \text{ km s}^{-1}$ .

NGC 4013            Sbc:  
 H-1997-H  
 May 25/26, 1938  
 Agfa Blue  
 60 min

The size of the bulge is the only classification criterion for NGC 4013; the galaxy is nearly edge on.

NGC 4522            SWSb:            VCC 1516  
 CD-1352-S/ISr            panel 291  
 March 15/16, 1980  
 103aO  
 75 min

NGC 4522 here and NGC 4433, below, have almost **identical morphologies** outside the ridge-line of the **classification** system. (They are not down the middle »I the morphological box but exhibit a **classification dispersion** perpendicular to that **ridge-line**.) A **single, high-surface-brightness arm fragment** is visible on one side of the **major** axis. If a symmetrical arm exists on the other side it is hidden by dust. But the pattern of extreme asymmetry may indeed be in fact, not merely in appearance.

The **redshift** of NGC 4522 is  $v_0 = 2186 \text{ km s}^{-1}$ . The galaxy is listed as a **cluster** member in the Virgo Cluster Catalog (Binggeli, Sandage, and Tammann 1985).

NGC 4433            SbcIII            pair  
 PH-1171-S            HA, p. 23  
 Dec 14/15, 1955  
 103aO  
 30 min

NGC 4433 forms a **physical pair** with NGC 4428 (Sc; panel 265), with angular separation of 7.2'. The redshifts are  $v_0(4428) = 2828 \text{ km s}^{-1}$  and  $u_0(4433) = 2771 \text{ km s}^{-1}$ . At a mean redshift distance of 56 Mpc, the projected linear **separation** is 117 kpc.

The **morphology** of NGC 4433 is similar in that of NGC 4522, above.

*Sbc Classification Section (continued)*

**IC 750**                    **S(b)**    Karachentsev **313**  
**CD-1544-S/Br**  
**Aug 7/8, 1980**  
**103aO + GG385**  
4.5 niii

IC 750 forms a close pair with IC 749 (Sbc; panel 306) at a separation of 3.3'. The **redshifts** are closely the same,  $u_o(749) = 827 \text{ km s}^{-1}$  and  $u_o(750) = 742 \text{ km s}^{-1}$ . At the mean redshift distance of 16 Mpc, the projected linear separation is small, at **15 kpc**.

The **morphology** of IC 750 is similar to that of both NGC 4522 and NGC 4433 on the preceding panel. The surface brightness of the central parts of IC 750 is very high, but the resolution into individual HII regions is not nearly as great as it is in the companion. The normal morphology of IC 749 shows no evidence of tidal perturbation, but, like the morphology of NGC 4522 and NGC 4433, the form of IC 750 is outside the ridge-line of the classification sequence (i.e., it is **outside** the middle line through the morphological box).

**NGC 2764** Amorphous or Sb pec    panel **145**  
**PH-7602-S**  
**April 3/4, 1979**  
**IIIaJ + GG385**  
30 min

NGC 2764 has been discussed on panel 145, in the Sb section. It is shown here to contrast the sizes of the central bulge in Sb, Sbc, and Sc galaxies.

The redshift of NGC 2764 is  $v_r = 2636 \text{ km s}^{-1}$ .

**NGC 7090**                    **Amorphous or Sbc:(on edge)**  
**CD-1544-S/Br**  
**Aug 7/8, 1980**  
103aO + GG385  
45 min

NGC 7090 is a large-angular-diameter, late-type galaxy, seen nearly on edge. The main body, shown well in the heavily printed image at the top middle, is 6' in diameter. At the redshift distance of 15 Mpc from the redshift of  $v_o = 754 \text{ km s}^{-1}$ , the corresponding linear diameter is large, at 26 kpc.

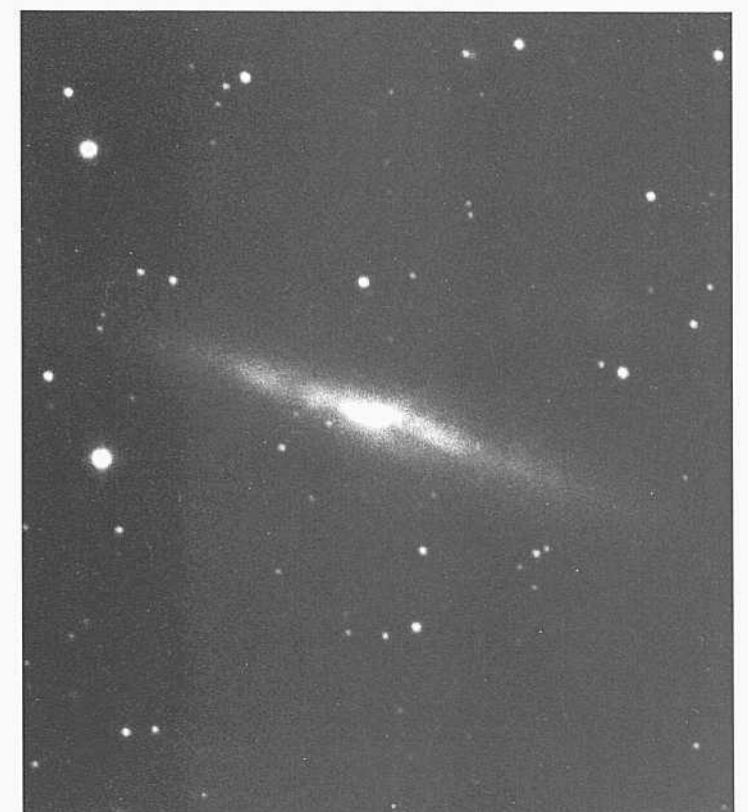
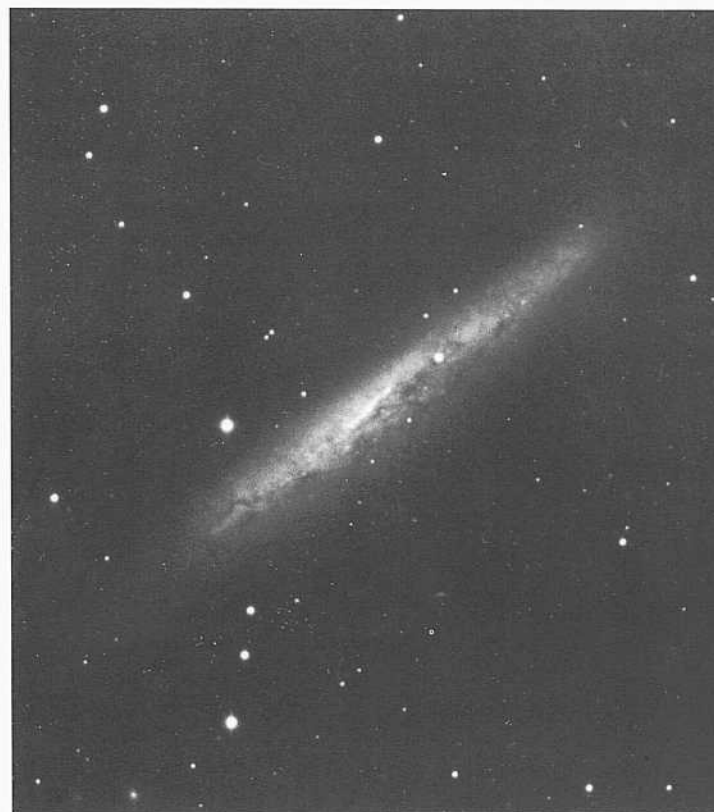
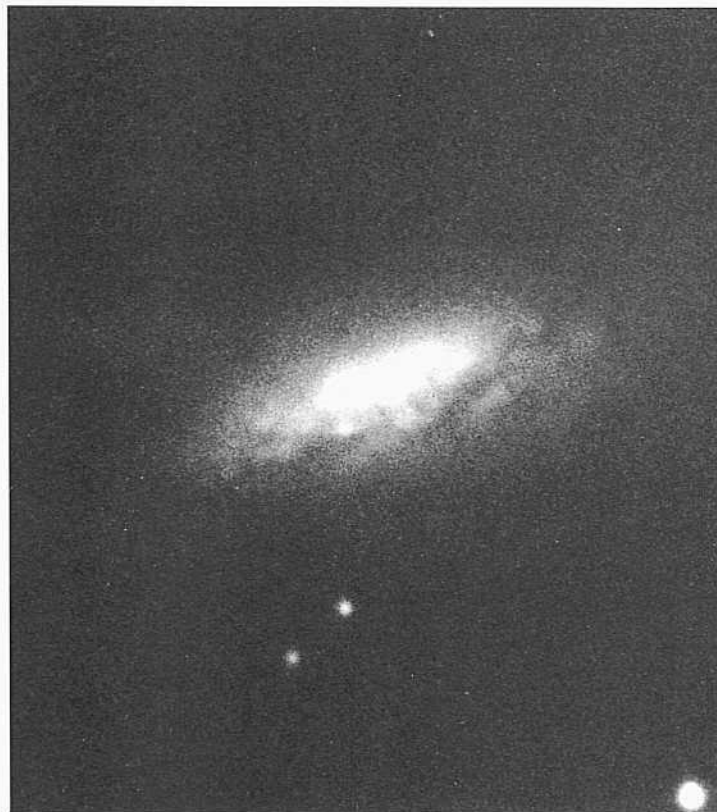
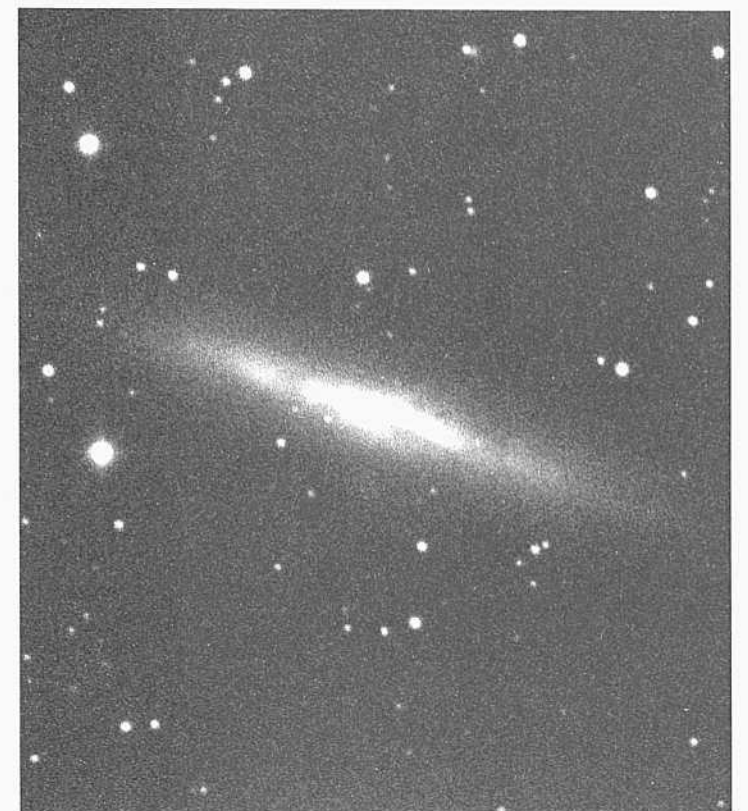
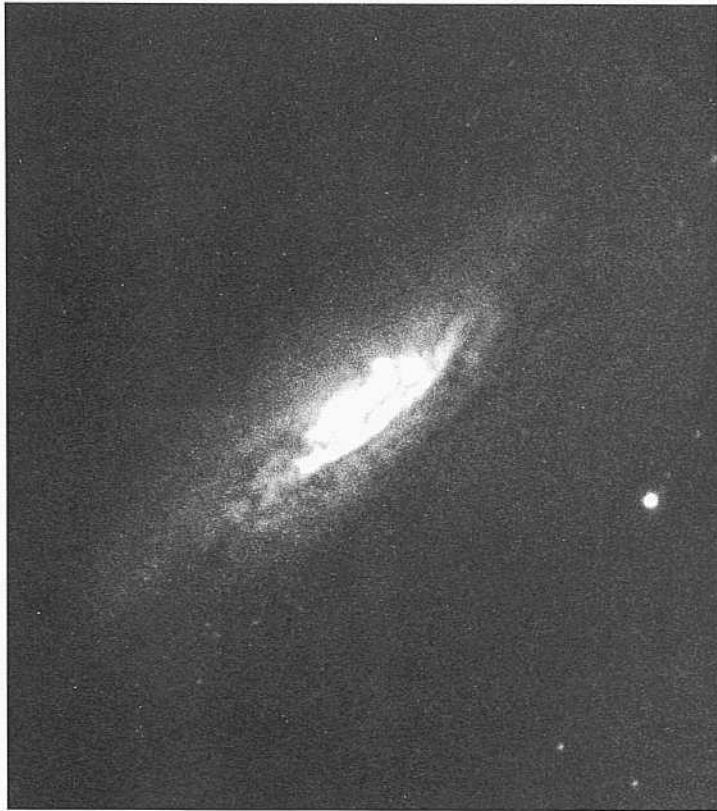
The central bulge is small or nonexistent. There is no visible halo or bulge above the plane. The asymmetry of the luminosity distribution in the disk is the reason for the barred subtype. Based on these criteria, the (uncertain) classification here is Sbc.

NGC 6835                    Amorphous?  
CD-911-HB  
April 29/30, 1979  
103aO + GG385  
**40 min**

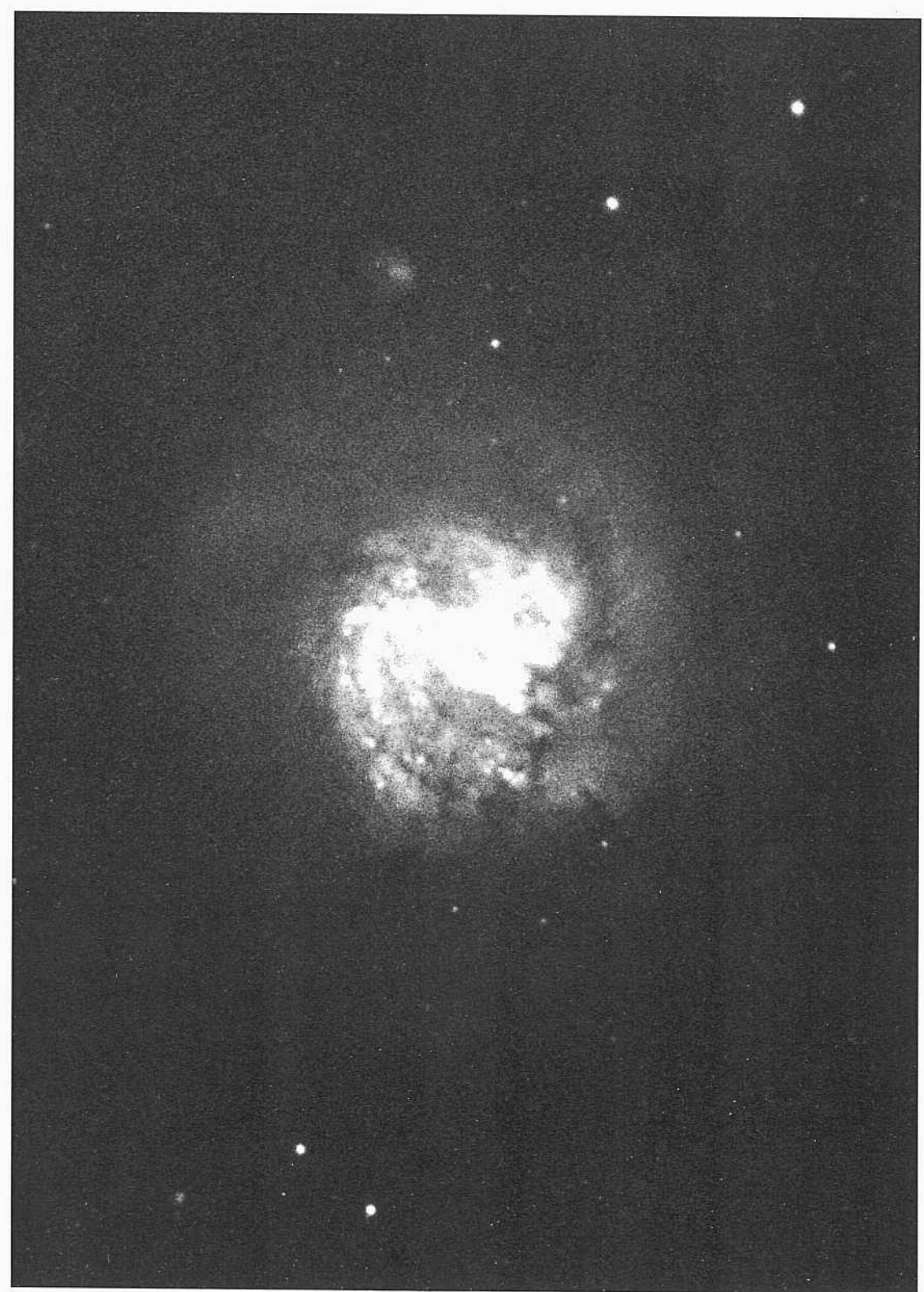
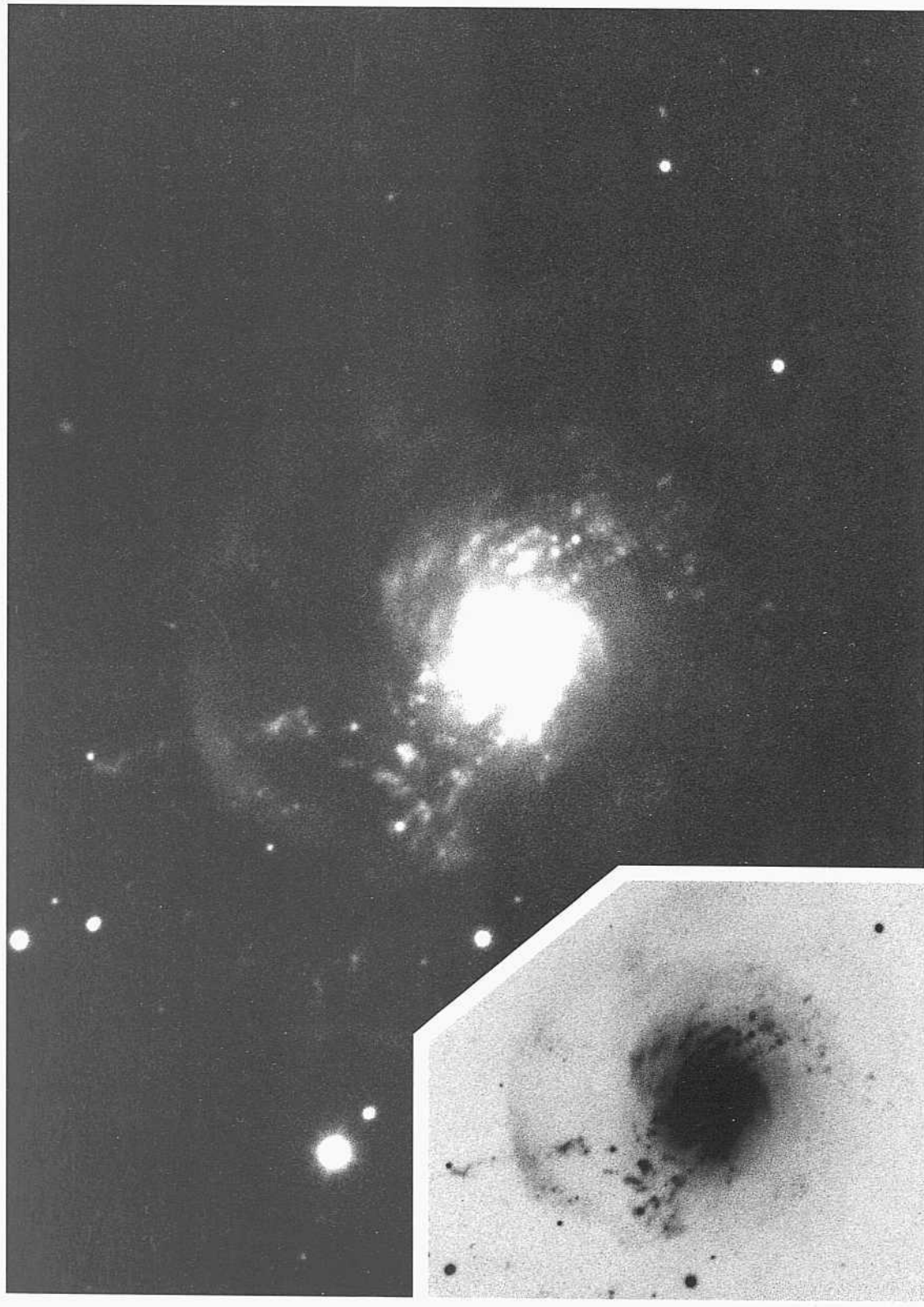
The classification of NGC 6835 is uncertain. From the asymmetry in the pattern seen in the short-exposure image at the top right, one guesses the presence of spiral structure, similar to the case in the very early galaxies NGC 4425 (SBO or SBa; panels 57, 60) or NGC 4429 (SO/Sa; panels 60, S2) if that galaxy could be viewed more edge on. On the other hand, the asymmetry in NGC 6835 may simply be due to dust patches.

No resolution into components of the stellar content is seen. The heavy print at the upper right shows high-surface-brightness luminosity of the face; hence the Amorphous? classification is suggested.

The redshift is  $v_r = 1711 \text{ km s}^{-1}$ .



PANEL  
196



NGC 3310      Sbc(r)(merger)      Racine wedge  
 PH-7982-S  
 Feb 1/2, 1981  
 103aO  
 12 min

NGC 3310 is unusual **because** of the smooth outer **plume** that **surrounds half the** image. It is similar to plumes in NGC 7252 (panel 340), NGC 4038/4039 (panel 280), and others mentioned earlier in this section. **Interpretation** of these plumes and of the polar rings as merger events, by **Toomre** and Toomre (1972), **Toomre** (1977), **Schweizer** (1980, 1982, 1983, 1986), **Quinn** (1984), Schweizer, Whitmore, and Rubin (1983), Schweizer and Seitzer (1988), and others, may apply here as well.

That the feature may be a merger rather than a **tidal** plume **due to** encounter is suggested by two circumstances. (1) NGC 3310 is isolated; there are no candidates in the nearby field for tidal companions. (2) Very short **exposures** on a plate taken with the Mount Wilson 60-inch **reflector** show *two nuclei* buried in the high-surface-brightness image, separated by 2". Each nucleus is sharp, and each is surrounded by galaxy material belonging separately to each.

The chaotic nature of the spiral fragments, with their many knots and their high rate of current star formation, may have been induced by the event.

The redshift of NGC 3310 is  $v_0 = 1073 \text{ km s}^{-1}$ .

NGC 5713      Sbc(a) pec      group  
 CD-1391-S/Br  
 March 21/22, 1980  
 103aO  
 75 min

[NGC 5713 is the center of a group of late-type spirals that includes NGC 569 1 [S(B)b pec; panel 168,  $v_0 = 1768 \text{ km s}^{-1}$ ], NGC 5705 (Slid. not in the RSA;  $v_0 = 1660 \text{ km s}^{-1}$ ), NGC 5713 here ( $v_0 = 1777 \text{ km s}^{-1}$ ), and NGC 5719 (Sab?, not in the KSA;  $v_0 = 1628 \text{ km s}^{-1}$ ). The mean redshift distance of the group is 34 Mpc. The angular and the projected linear separations of the galaxies from NGC 5713 are 34.9' and 345 kpc for NGC 569 1, 25.8' and 255 kpc for NGC 5705, and 11.4' and 113 kpc for NGC 5719. The group defined by these four members is evidently smaller than the Local Group.

The inner arms of NGC 5713 are chaotic and are of the MAS type rather than the grand design. They are of high surface brightness for half a revolution from the center, beyond which a single smooth, low-surface-brightness arm continues in a spiral pattern outward. Star formation is evident in the inner arm fragments, as judged from the knots that are HH-region candidates.



*Sbc Classification Section (continued)*

NGC 1531/1532            Amorphous    group  
CD-2025-Bedke/Gregory    Sbc(s)(tides?)  
**Oct 27/28, 1981**                            panel 337  
103aD + **GG495**

**120 min**

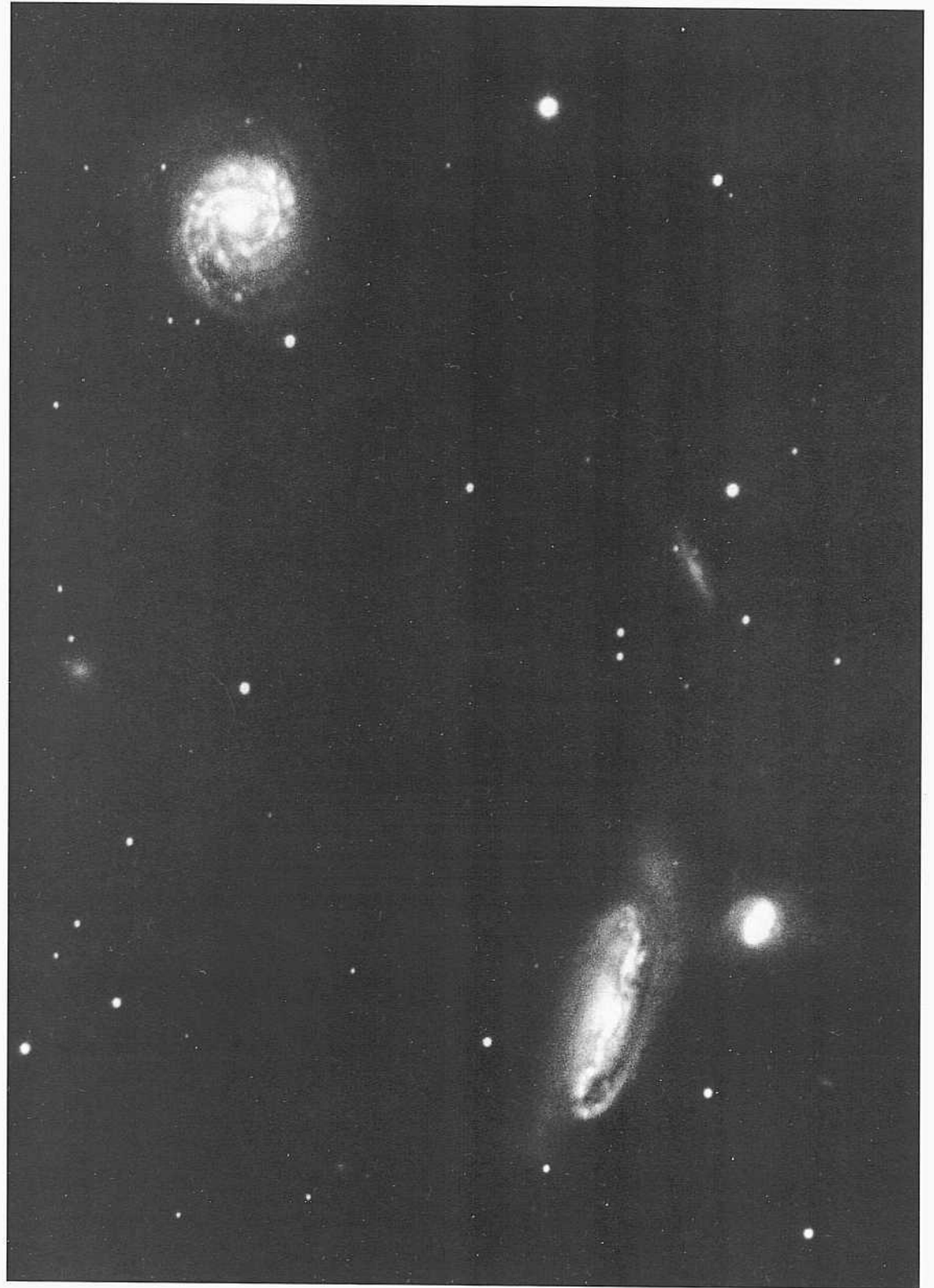
The unusual plumes in NGC 1532 suggest a tidal **distortion** due to an encounter. The evident candidate responsible for the **perturbation** is the amorphous companion NGC 1531, whose morphology is **of the** same class as M82. The two galaxies form a physical pair; the redshifts are  $u_o(1531) = 1053 \text{ km s}^{-1}$  and  $u_o(1532) = 1105 \text{ km s}^{-1}$ .

Three **dwarf** candidate companions form a wider physical group centered on the bright pair. The most interesting of the **companions** is at RA (1950) =  $4^{\text{h}} 10^{\text{m}} 56^{\text{s}}$ , Dec (1950) =  $-33^{\circ} 07' 36''$ . It **appears** as a dwarf **S0(8),N** on a yellow plate but as an Im with **condensations** on a blue plate, similar to the transitional (im-dE.N) case of NGC 4286 (panel 20) (Sandage and Hoffman 1991). The low ratio of the hydrogen mass to total mass also suggests that the dwarf is in transition between Im and dE.N dwarf types (Sandage and **Fomalont** 1993).

The other two dwarf candidate companions are a **high-surface-brightness** SBO ( $M = -19$ ) at **RA (1950) =  $4^{\text{h}} 10^{\text{m}} 39^{\text{s}}$** , Dec (1950) =  $-32^{\circ} 56' 33''$ , and a prototype faint dEO.N nucleated dwarf elliptical at RA (1950) =  $4^{\text{h}} 09^{\text{m}} 32^{\text{s}}$ , Dec (1950) =  $-32^{\circ} 59' 09''$ .



PANEL  
198



*She Classification Section (continued)*

NGC 5426/5427 Sbc(rs)1.2 **pair**  
 CD-909-HB Sbc(s)1  
 April 29/30, 1979  
 103aO + GG385

**40 miu**

Both NGC 5426 and NGC 5427 have normal She morphologies. They evidently form a physical pair; the redshifts are  $u_0 = 2455 \text{ km s}^{-1}$  and  $v_0 = 2565 \text{ km s}^{-1}$ , respectively. The angular separation of  $2.1''$  corresponds to a projected linear separation of 34 kpc at the mean redshift distance of 50 Mpc ( $z = 50$ ).

The only evidence for a close tidal encounter are the two thin straight strands of the multiple outer arms of NGC 5426 that overlap the outer thin spiral arms of NGC 5427, where the spiral pattern is of the grand design. Otherwise, each galaxy has beautifully formed arms that are so regular that each is assigned the earliest luminosity class because of the small geometrical entropy. Evidently, close encounters at some phase in their action have had nearly negligible perturbative effects on the visible morphology.

NGC 7769/7770/7771 Sbc(s)(ticlea?) panel 8 1  
 PH-7545-S Sa pec Karnchenlsev 592  
 Nov 6/7, 1978 SBab pec  
 L03aO

**12 min**

The triplet evidently forms a physical group: the redshifts (Maytill, in 11 it mason. Mayall, and Sandage L956) are  $u_0 = 4565 \text{ km s}^{-1}$ ,  $v_0 = 4554 \text{ km s}^{-1}$ , and  $v_0 = 4492 \text{ km s}^{-1}$  for NGC 7769 (She), NGC 7770 (Sa pec), and NGC 7771 (SBab pec), respectively. At the mean redshift distance of 91 Mpc the angular separations of NGC 7771 from NGC 7770 of  $3.15''$  and from NGC 7770 of  $60''$  correspond to the small projected linear separations of 1.1 kpc and 26 kpc, respectively.

The morphologies of NGC 7770 and NGC 7771 suggest tidal interactions due to a close encounter. Both have smooth luminous outer regions, which are either well-defined (tidal?) outer arms as in NGC 7771, or compose an outer envelope that has a broken symmetry, as in NGC 7770.

## The SBbc Classification Section

NGC 1365      SBbc(s)I      FCC 121  
CD-1668-S      panel S8  
Dec 31/Jan 1, 1980/1981  
103a0  
75 min

NGC 1365 is nominally classed as a **member** of the Fornax Cluster on the basis of its position and its **redshift**. It is  $1.2^\circ$  southwest of **the center of the cluster** defined by NGC 1399. The core radius **of the cluster** is  $0.7^\circ$  (Ferguson 1989); hence NGC 1365 is  $1.7$  core **radii** from **the cluster center**. The redshift velocity of NGC 1365 is  $v_0 = 1562 \text{ km s}^{-1}$ , which is close to the mean cluster redshift of  $\langle v_0 \rangle = 1366 \text{ km s}^{-1}$ . The velocity dispersion of the cluster is  $32.5 \text{ km s}^{-1}$ .

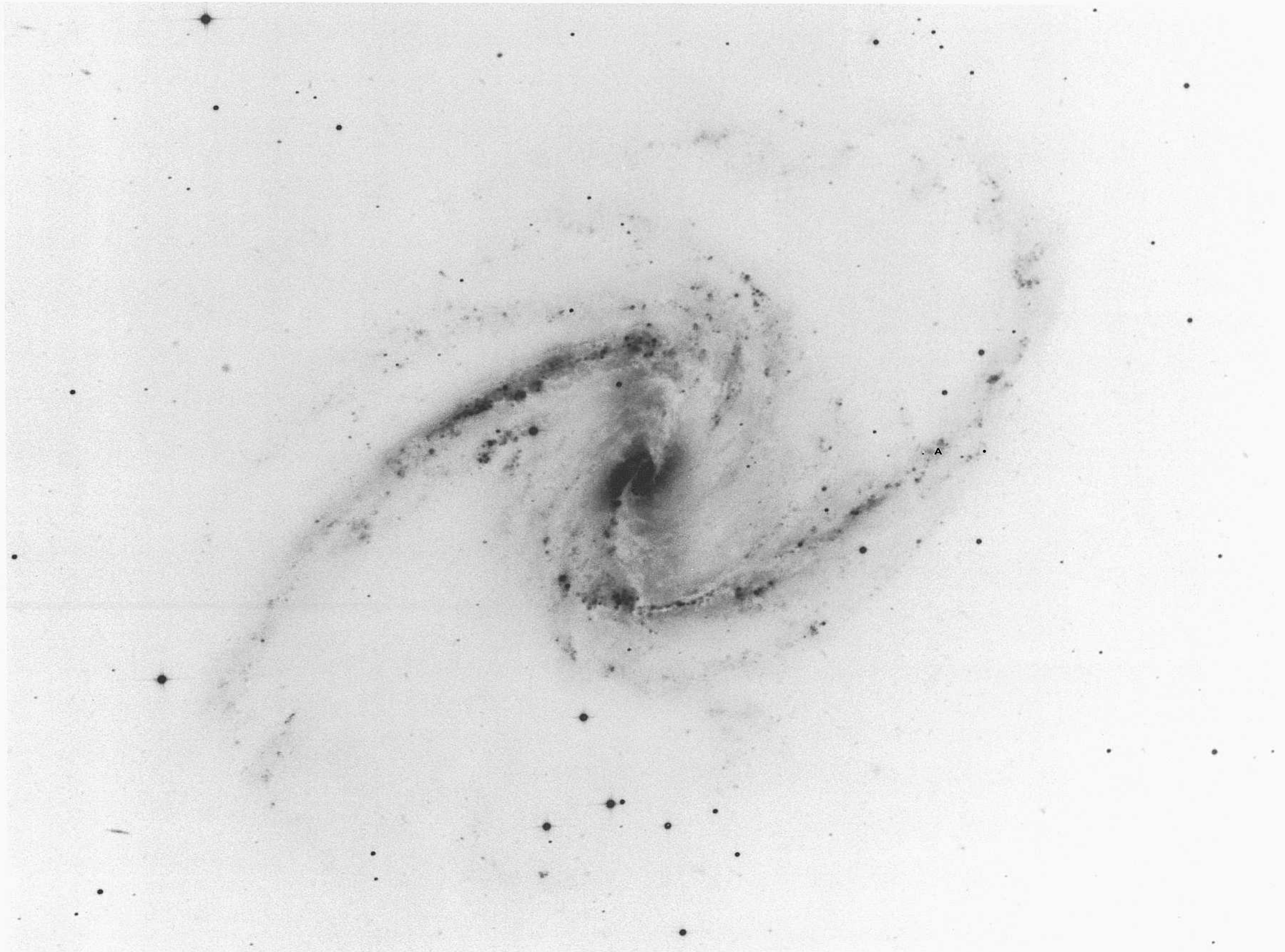
Despite the close agreement of the **position** and redshift of NGC 1365 to the Fornax **Cluster** values, the cluster membership of NGC 1365 is often **questioned** because its angular size,  $D_{95} = 9.8'$ , is so large. Yet **this** angular size is comparable to the  $D_{95}$  angular diameters of the largest spirals in the Virgo Cluster, which is at nearly the same distance. The four largest Virgo spirals and their angular diameters and redshifts  $v_0$  are NGC 4192 ( $9.5'$ ,  $-251 \text{ km s}^{-1}$ ), NGC 4536 ( $7.4'$ ,  $1646 \text{ km s}^{-1}$ ), NGC 4321 ( $6.9\%$   $1464 \text{ km s}^{-1}$ ), and NGC 4501 ( $6.9\%$   $2161 \text{ km s}^{-1}$ ). The negative redshift of NGC 4192 and other large spirals in the Virgo Cluster region assures Virgo Cluster membership; negative redshifts occur in the RSA (**excluding** galaxies in the Local Group) only in the  $6^\circ$  radius centered on the **Virgo Cluster** (Sandage and Tammann 1976a), attributable to the large velocity dispersion in the Virgo Cluster.

The **morphological** type of NGC 1365 is later than NGC 1300 (SBb; panels 154, S8), which **is** the prototype of the (s)-**subtype** barred **spirals**; **the bar** in NGC 1365 is less straight and less smooth, and the arms which spring from the ends of **the bar** are more open. Hence, the type is intermediate between SBb and SBc.

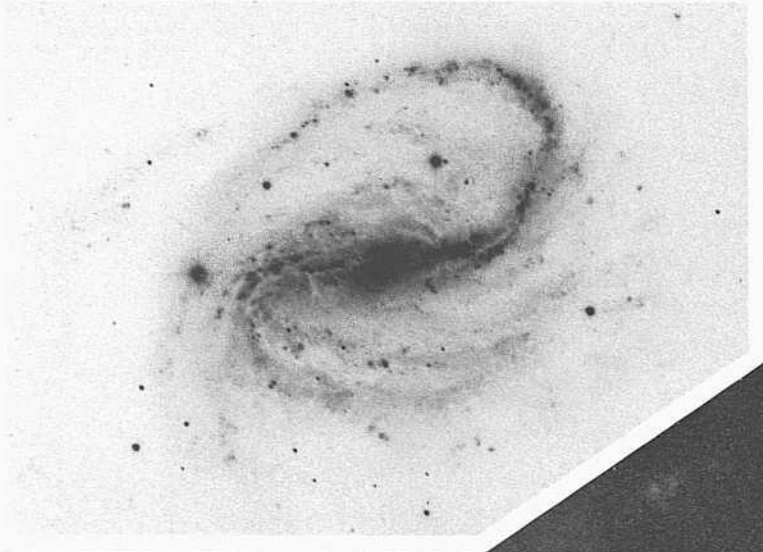
The straight dust lanes are **on** opposite sides of **the bar**. Again (as in the SBb types) these **lanes** are **on the** *leading edges* of the bar relative to the **direction** of rotation. The positions of maximum star **formation** in the thin arms begin at the ends of the bar. The largest **Mil** regions resolve into disks at about the  $2''$  level.

The circulation pattern of the well-ordered but intricate velocity **field** in the vicinity of the bar appears to be well traced **by** the delicate wisps of dust lanes that begin at the two strong shock positions. Note that these delicate lanes are along *the following* edges of the bar and that they are nearly perpendicular to the resulting two nearly **straight** dust shock lanes in the bar.

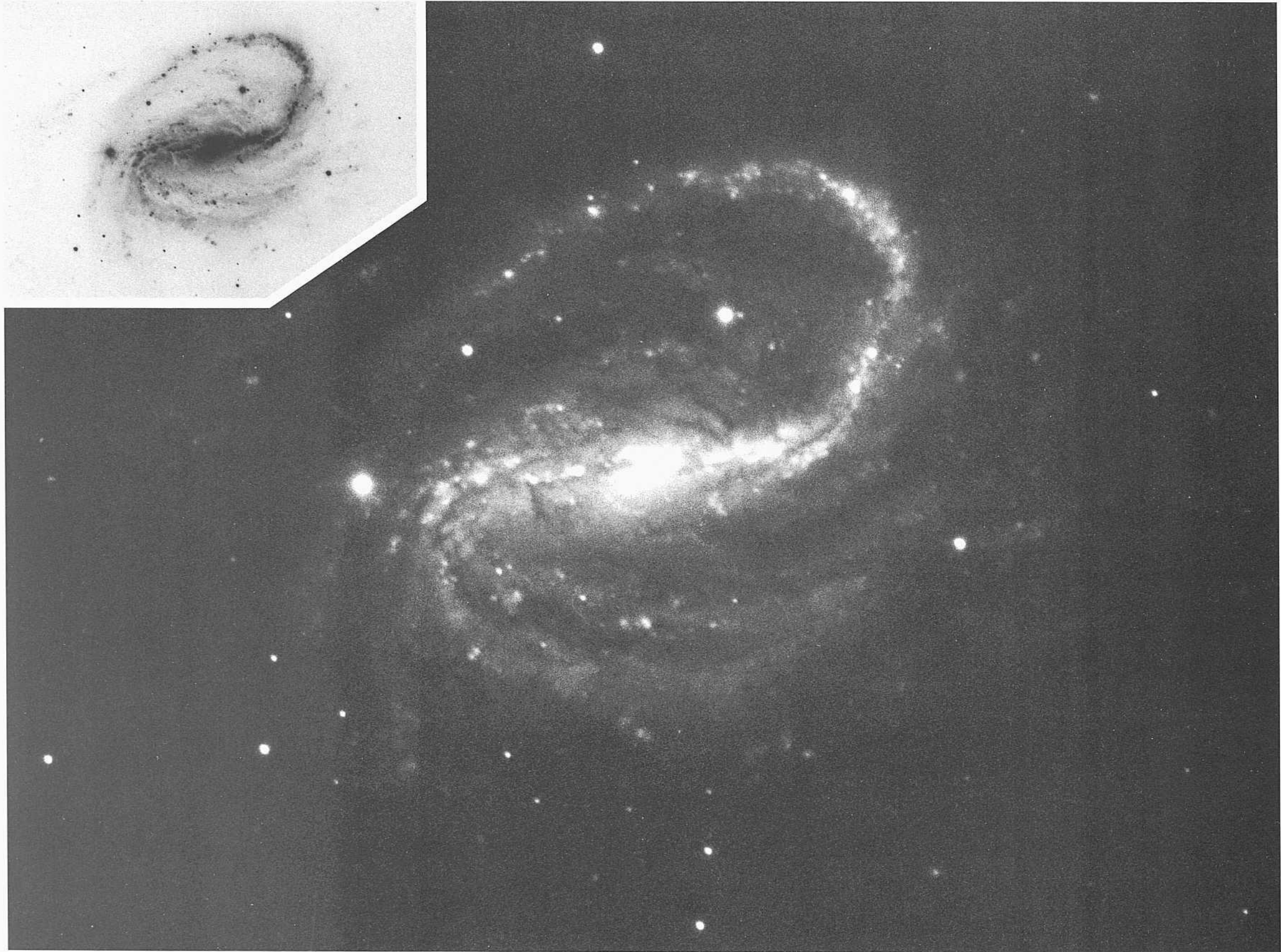
The luminosity class of NGC 1365 is in the highest bin, at I, because of the regularity and thinness of the arms.



PANEL  
199



PANEL  
200



*SBbc Classification Section (continued)*

NCC 7479 SBbc(s)I-II panel S»

PH-152-H

Ocl 14/15, 1952

L03aO

30min

The arms in [NCC TIT<sup>1</sup>] are less regular than in NCC 1365. They are branched into secondary low-surface-brightness fragments on the inside of the two main grand design principal arms that spring from the ends of the bar.

The two characteristic nearly straight (hint lanes in the bar continue into the two high-surface-brightness parts of the principal arms. The lane in what is taken to be the near side (from the asymmetry of the luminosity pattern by the usual argument; Hubble L943) is well silhouetted and is in the middle of that arm. The largest Mil region in the opposite arm resolves at the angular diameter (core plus halo) of 2", which is large (5.10 psc; compare Sandage and Tammann 1974u) at the distance corresponding to the observed redshift of  $v_0 = 2630 \text{ km s}^{-1}$ .



*SBbc Classification Section (continued)*

NGC 1097      RSBbc(s)I-II      HA, p. 46  
 H-2025-B  
 Oct 21/22, 1938  
 Agfa Blue  
 90 min

The reproduction here is from the same original Mount Wilson 100-inch plate that was used for the print in the Hubble Atlas. In the meantime the plate has suffered surface scratches that may not have been completely removed in tile reproduction here.

The central region in NGC 1097 is an oval rather than a well-defined bar as in NGC 1300 (SBb; panels 154, S8). Nevertheless, the two straight dust lanes characteristic of SBb spirals are present, presumably resulting from the shocks caused, as usual, by the response of the gas to the rotation of the oval gravitational field.

A tightly wound high-surface-brightness spiral pattern exists in the nucleus, similar to but not as well defined as in NGC 4314 (SBa; Hubble Atlas, p. 44; panels 95, 106 here). The complex structure is shown by Sersic in *Observatory* (1958) and in the insert print here.

The outer arms are of low surface brightness. The star-formation rate is low. The HII regions do not resolve at the 2" level. The redshift of NGC 1097 is  $v_0 = 1284 \text{ km s}^{-1}$ .

NGC 7678      SBbc(s)I-II  
 PH-6547-S  
 July 25/26, 1973  
 098 + RG2  
 60 min

This distant SBbc spiral of the NGC 1300 type, with redshift  $v_0 = 3756 \text{ km s}^{-1}$ , has massive star formation in one of its principal grand design arms. Note the two dust patches near the ends of the central oval, which is the bar. These patches occur near the beginning of the (s)-type arms.

NGC 4123      SBbc(rs)I.8      Karachentsev 322  
 CD-1847-HB      panel S8  
 April 3/4, 1981  
 103aO  
 75 min

NGC 4123 forms an apparent pair with NGC 4116 (SBc; panel 306) at an angular separation of 14'. The redshifts are  $z_0(4116) = 1140 \text{ km s}^{-1}$  and  $z_0(4123) = 1157 \text{ km s}^{-1}$ . The projected linear separation is 93 kpc using a mean redshift distance of 23 Mpc ( $H = 50$ ). Note that this separation is small, similar to the distance of the Small Magellanic Cloud from the Galaxy.

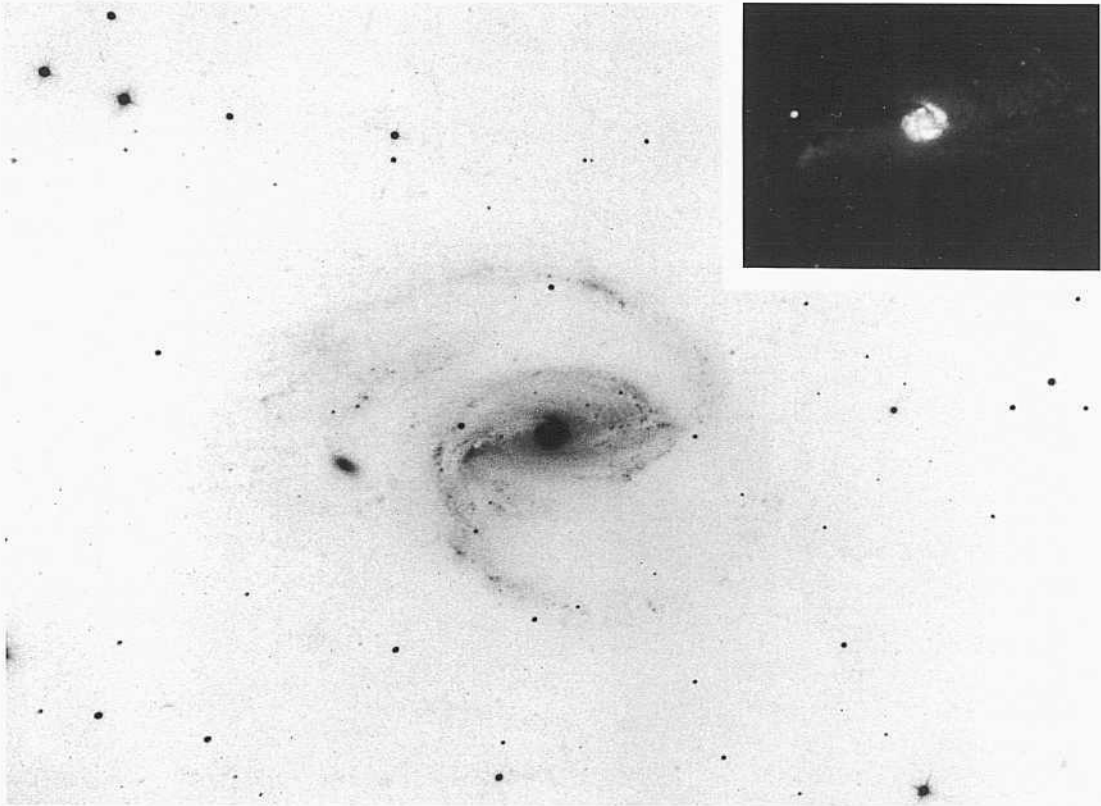
Despite the closeness of the pair there is no evident distortion of the morphology of NGC 4123. The bar is moderately well formed. The characteristic nearly straight dust lanes on the leading edges of the bar are present. Star formation is profuse at the ends of the bar.

The two principal arms are of the grand design type, but a second set of arms, also of high surface brightness, exist. Each starts symmetrically near the start of the principal arms at the strict ends of the bar. The pattern is unusual, leading to four principal arms, three of which are moderately well defined. Because of the outer set of arms that do not start from the ends of the bar, the arm subtype is (rs), although the pattern is unusual.

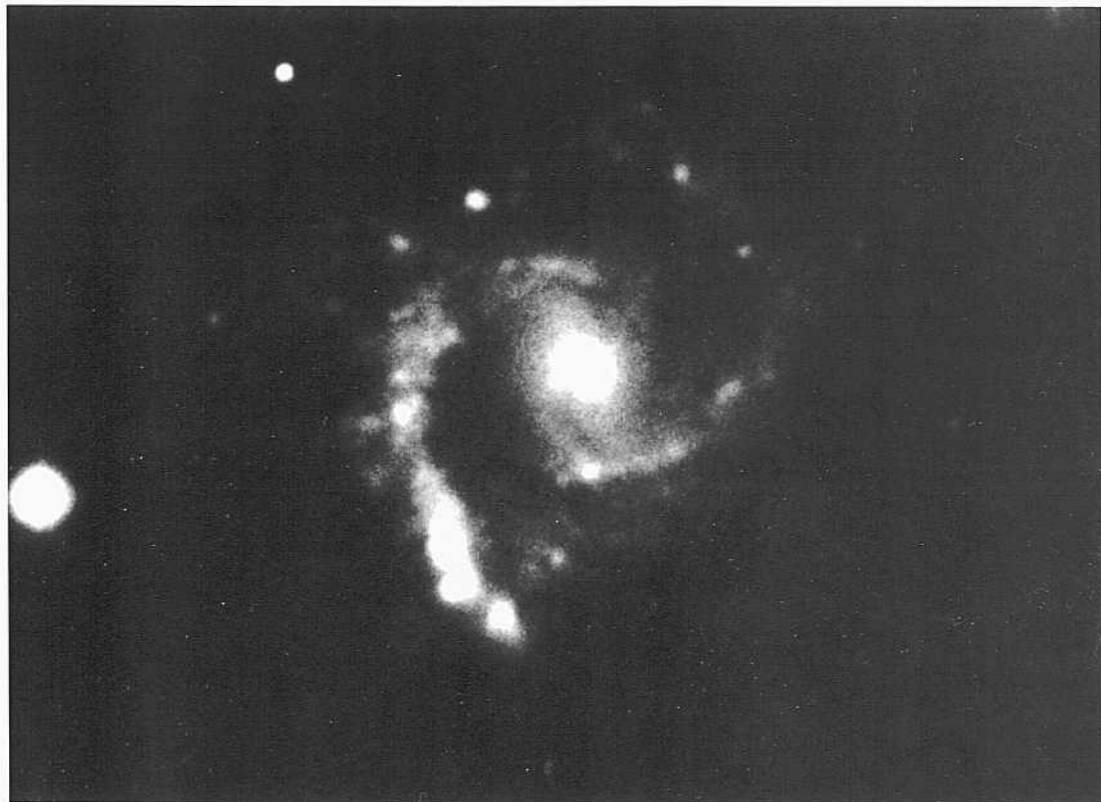
NGC 4412      SBbc(s)I-II pec      VCC 921  
 H-1947-H  
 Feb 23/24, 1938  
 E40  
 50 min

NGC 4412 is listed as a Virgo Cluster member in the Virgo Cluster Catalog. A negative print, enlarged to a common scale with other Virgo Cluster galaxies, is shown in paper IV of the Virgo Cluster series (Sandage, Binggeli, and Tammann 1985a).

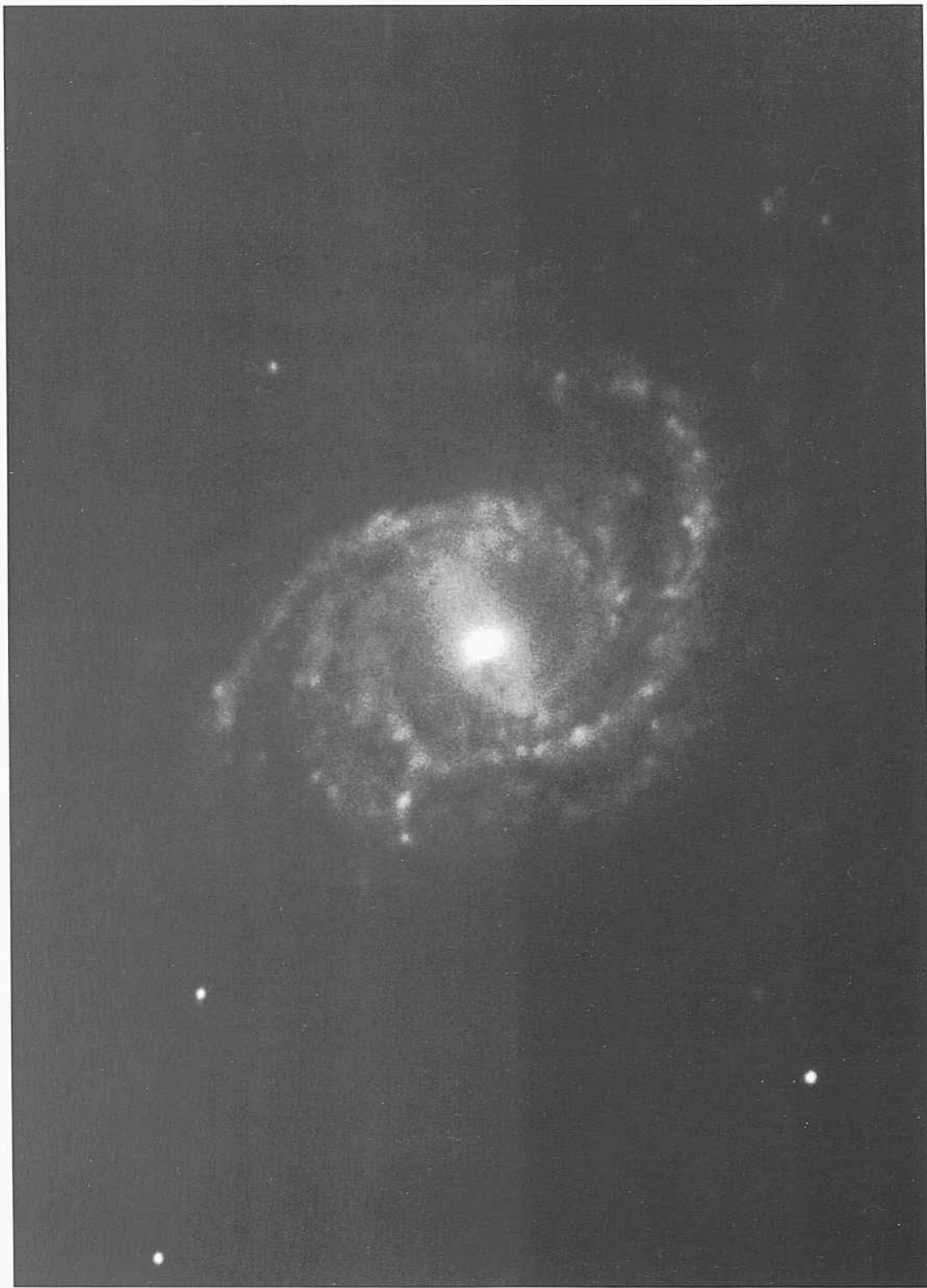
The two principal arms springing from the ends of a bar are of very high surface brightness.



PANEL  
201



PANEL  
202



NGC 5350 SBbc(rs)I-II group  
 PH-7624-S panel 29  
 April 27/28, 1979  
 103aO  
 8 niin

NGC 5350 forms a physical pair with NGC 5353 (S0/E7; panel 29) with a separation of 5.5'. The redshifts are  $u_o(5350) = 2305 \text{ km s}^{-1}$  and  $u_o(5353) = 2224 \text{ km s}^{-1}$ . At a mean redshift distance of 45 Mpc ( $H = 50$ ) the projected linear separation is small at 72 kpc. The pair is in a group with NGC 5354, 5355, 5358, and perhaps 5371, several of which have been shown earlier on panel 29. NGC 5371 (Sh) is shown on panel 126.

The arm pattern in NGC 5350 is intermediate between that of the grand design and MAS types. Two main arms start at the ends of the bar but are so tightly wound that they form an inner near-ring after each has unwound by half a revolution. Fragmentary secondary arms exist on one side of the pattern more strongly than on the other.

NGC 3145 SBbc(rl) HA, p. 21  
 CD-790-S panel S9  
 Feb 23/24, 1979  
 103aO + GG385  
 •15 iuiu

The description in the Hubble Atlas is:

*The thin multiple units of this galaxy are complex. The brightest arms in the northwest quadrant appear to approach the nucleus at right angles (tangent rather than spiraling inward). There is a single faint arm in the southwest quadrant which crosses one of the regular arms nearly at right angles. This is a very rare feature of galaxies and is particularly well shown here. A few dust lanes can be seen near the crossover point.*

The above language describes how the arms approach the nucleus at right angles instead of spiraling inward. It is, of course, an explanation of how arms in barred spirals start. NGC 3145 is obviously a barred spiral not recognized in the Hubble Atlas because of the combination of an unfavorable inclination angle and the position of the line of nodes.

The arms are thin and are very well defined, requiring typing as luminosity class I. The redshift of NGC 3145 is  $v_o = 3416 \text{ km s}^{-1}$ .

The three galaxies on this panel have arms that are intermediate between those of the pure grand design and the MAS types. Also, in all three the arms begin at the edge of either a complete or an almost-complete inner ring.

NGC 7755 SBbc(r)/Sbc(r)I-II  
 CD-1165-Br  
 Aug 22/23, 1979  
 103aO + GG385  
 45 min

The possible bar in NGC 7755 is betrayed, if it exists, by the two thin, nearly straight dust lanes connecting the center with the almost-complete ring composed of the inner spiral arms. These two dust lanes are, as in all more-pronounced barred SBb and SBbc galaxies, on the leading edge of the bar, which here is the central oval.

The numerous HII regions are unresolved at the 1" level. The redshift of NGC 7755 is  $v_o = 2969 \text{ km s}^{-1}$ .

A compact EO, possibly M32-like, candidate companion exists at an angular separation of 100", well visible on this print.

NGC 2545 SBbc(r)I-II  
 PH-7899-S  
 Nov 6/7, 1980  
 103aO  
 12 min

The inner ring in NGC 2545 is of very high surface brightness and appears to be nearly complete. A short-exposure plate shows that the surface brightness varies around the ring. The feature is related to the two positions on the ring where the faint bar terminates.

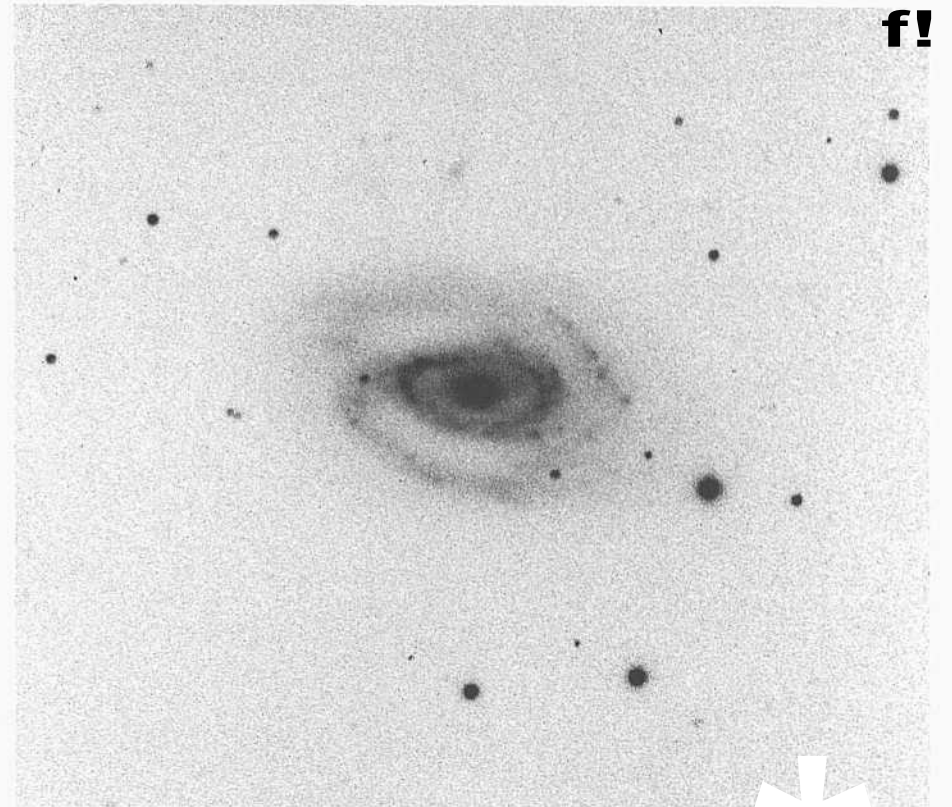
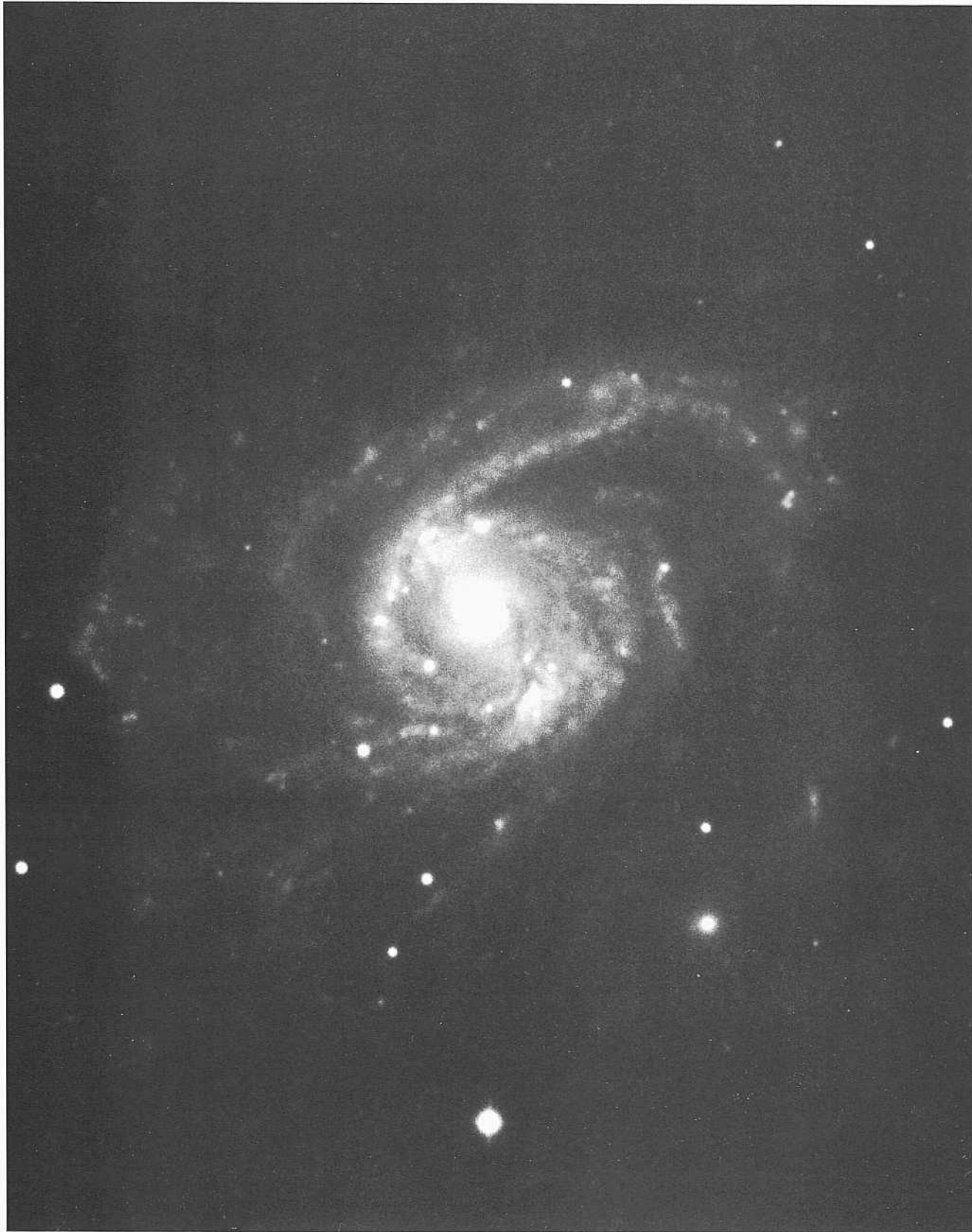
As in other barred SBb and SBbc types, the maximum star-formation rate occurs near the ends of the bar, continuing for about a quarter revolution along the arms. It is this feature that causes the surface-brightness variation around the seeming ring. But, as usual, the form is made by two overlapping, tightly wrapped separate arms. The morphology is similar to that of NGC 3081 (SBa; panels 99, 107), NGC 3185 (SBa; panel 99), NGC 1326 (SBa; panel 100), and NGC 6902 (Sa; panel 69). The most extreme example of a near-perfect ring is NGC 7742 (Sa; panel 66).

The redshift of NGC 2545 is  $v_o = 3312 \text{ km s}^{-1}$ .

NGC 5905 SBbc(rs)I  
 PH-7741-S  
 June 11/12, 1980  
 103aO  
 12 min

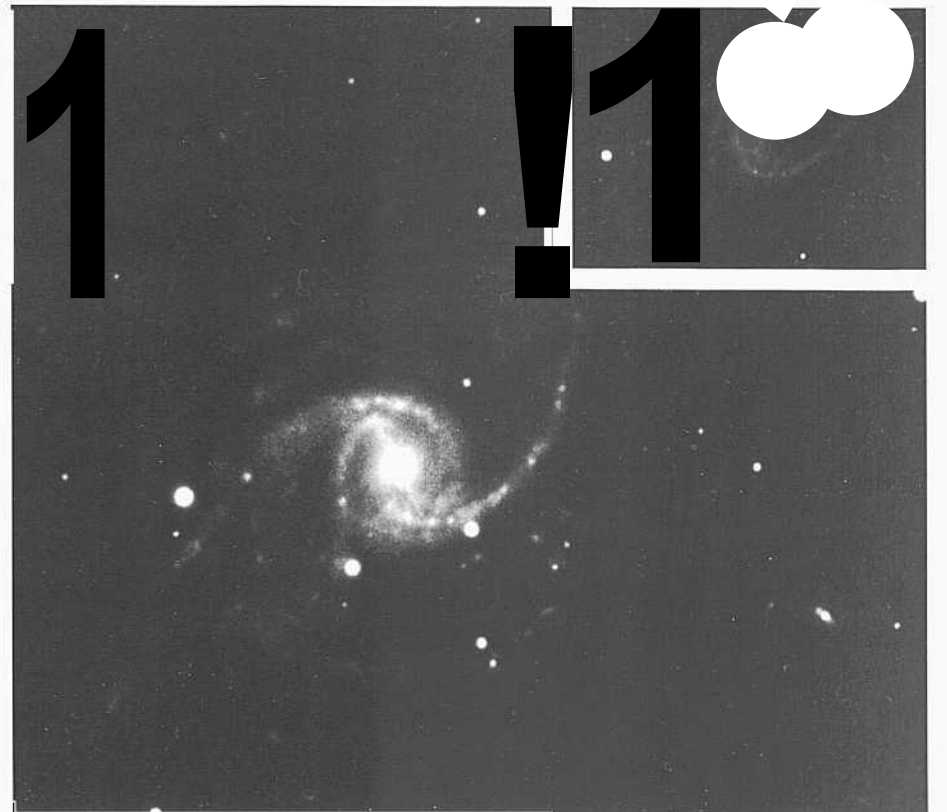
The thin arms in NGC 5905 spring from the ends of the well-defined bar and are so tightly wound as to nearly overlap after each unwinds by half a revolution. Each becomes a thin outer arm of high surface brightness that can be traced for another half revolution outward, beyond which they continue but at much lower surface brightness. Fragmentary secondary arms exist over the outer face.

The redshift is  $v_o = 3544 \text{ km s}^{-1}$ . The numerous HII regions are unresolved at the 1" level.

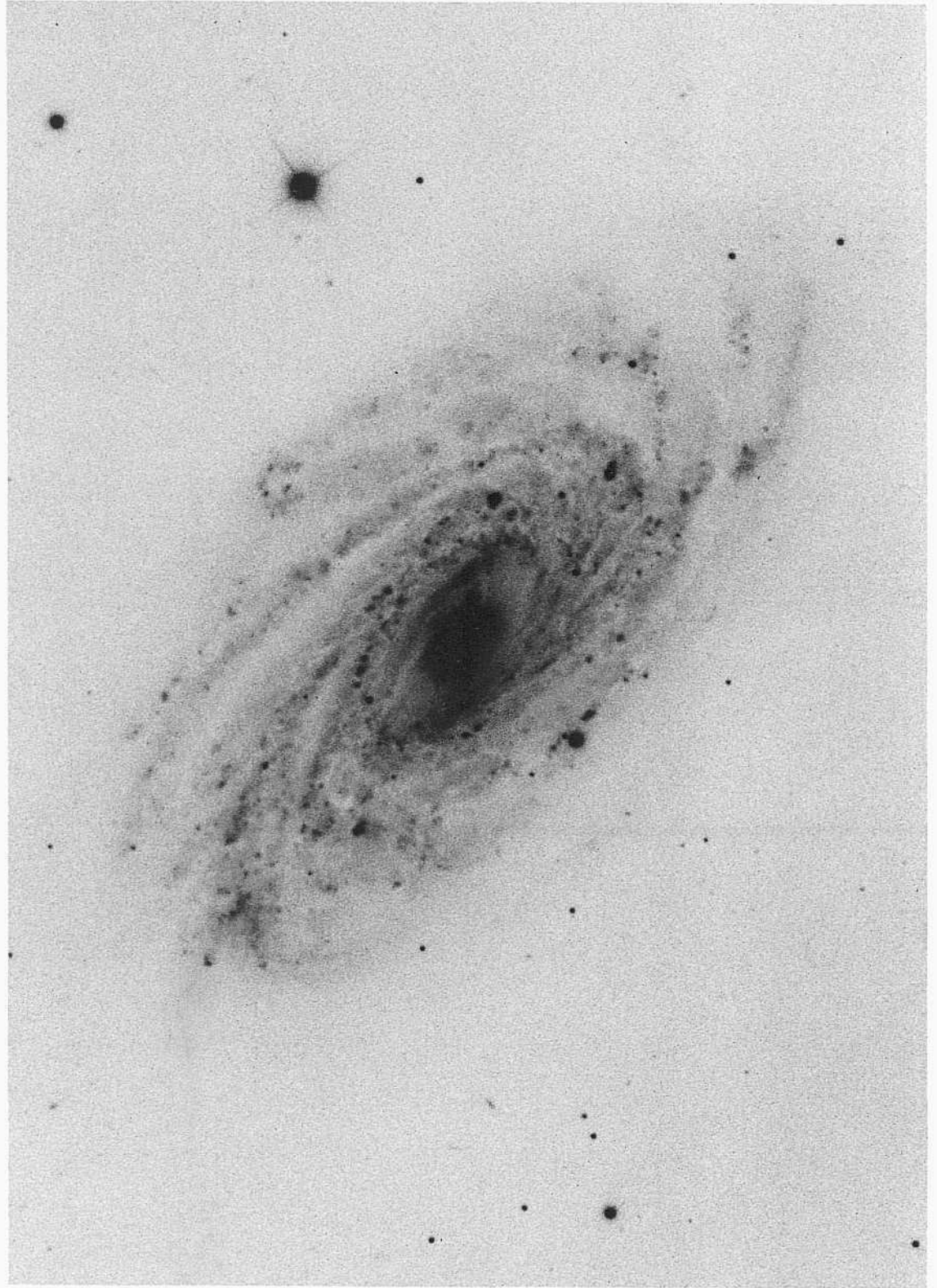
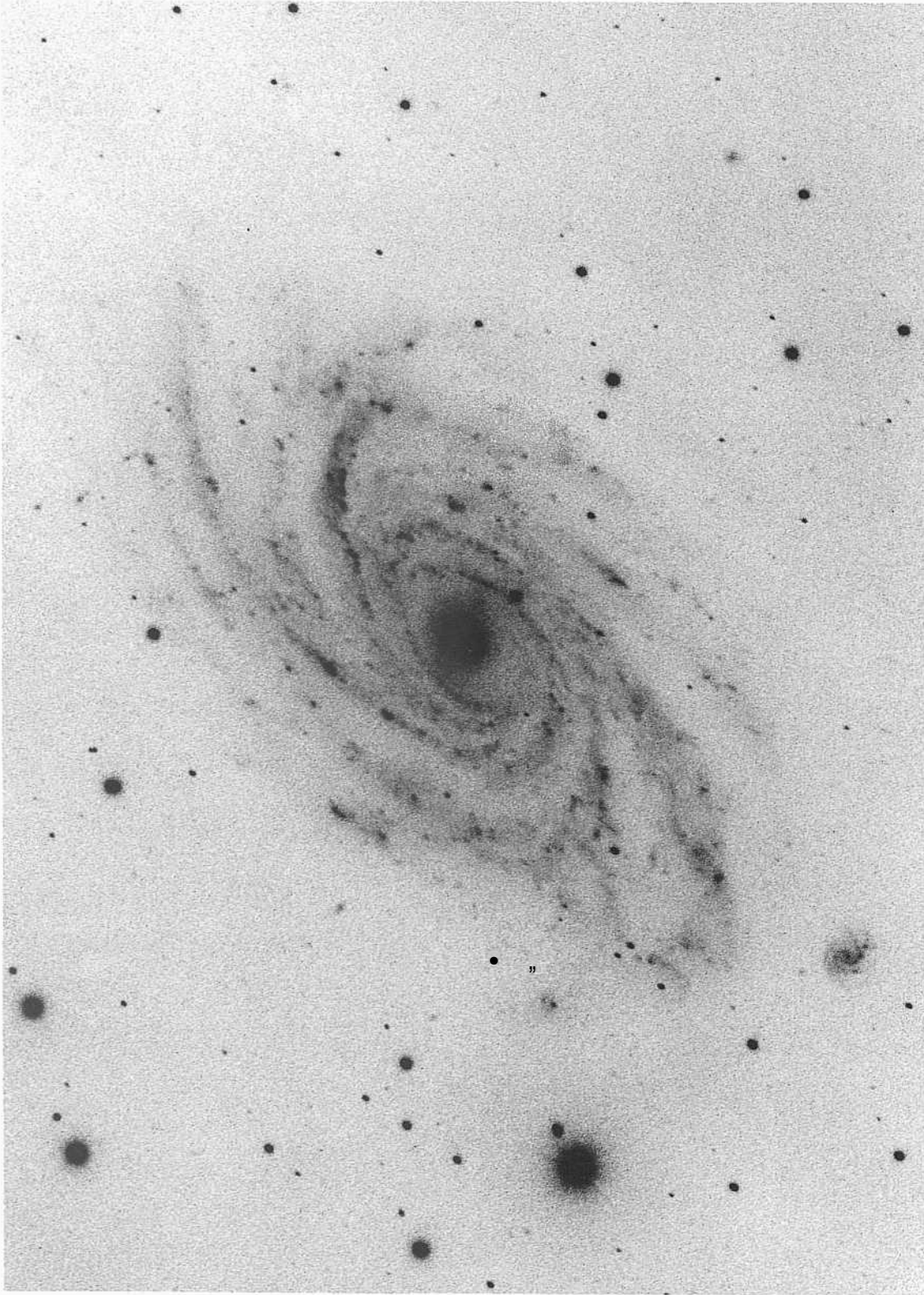


f!

I'AN EL  
203



PANEL  
204



The two galaxies on this panel are of luminosity class I or I-II because the arms are well formed with minimum chaos. Both galaxies are of the filamentary-arm type (MAS), and the arms in both begin on the rim of an inner smooth disk at the radius where the bar terminates in the disk.

NGC 2336      **SIS-(r)I**      panel S13  
 PH-7703-S  
 Feb 11/12, 1980  
 103aO  
 12 mill

At least eight major arm fragments can be identified in NGC 2336, which is the prototype SBbc galaxy of the MAS type at early luminosity class.

The numerous **Mil** regions in NGC 2336 are not resolved at the 1" level. The redshift is  $v_0 = 2424 \text{ km s}^{-1}$ .

NGC 3953      **SBbc(r)MI**  
**PH-7639-S**  
 April 28/29, 1979  
**103aO**  
**12 mill**

The multiple arms in NGC 3953 are thicker than in NGC 2336; they cover more of the disk and have a greater geometrical entropy; hence the luminosity class is later than in NCC 2336.

The central region of NGC 3953 is more of an oval than a bar. The two characteristic thin (shock-induced) dust lanes may be present in the central disk.

The largest **Mil** regions (core plus halo) resolve at about the 3" level. The redshift of NGC 3953 is  $z = 1036 \text{ km s}^{-1}$ .



The four galaxies on this panel continue the examples of the intermediate arm type between the grand design and the filamentary (MAS) spiral patterns. As on the preceding panel, the galaxies here are of the earliest luminosity class. Three of the four galaxies are of the (r) subtype; one is of the (s) subtype.

NGC 3124      SBbc(r)I  
 CD-1665-S  
 Dec 30/31, 1980  
 103aO + GG385  
 40 min

The spiral pattern in NGC 3124 is highly regular. Each of the two principal inner arms begins slightly downstream from an end of the well-defined bar. Each of the tightly wound arms nearly overlaps the other after half a revolution. Subsequently, they spiral outward and branch into the outer fragments, which remain at high surface brightness for another half a revolution.

The HII regions are unresolved at the 1" level. The redshift is  $v_o = 3307 \text{ km s}^{-1}$ .

NGC 2223      SBbc(r)I.3  
 CD-146-S  
 Feb 3/4, 1978  
 103aO + GG385  
 45 min

The multiple arms in NGC 2223 are thicker and slightly less well defined than in NGC 3124, above, but the spiral pattern is similar. The redshift of NGC 2223 is  $v_o = 2529 \text{ km s}^{-1}$ . The HII regions are unresolved.

NGC 3054      SBbe(s)I  
 CD-708-S  
 Jan 30/31, 1979  
 103aO + GG385  
 45 min

The arm pattern in NGC 3054 is primarily of the grand design type but with branched fragments in the outer regions. A feature to be noted are the two thin, very-well-formed dust lanes down the middle of the two principal arms in their first half-turn from the place of origin on the inner disk. The central region is a diffuse bar or an oval.

The arms are symmetrical and well formed, requiring the luminosity class I.

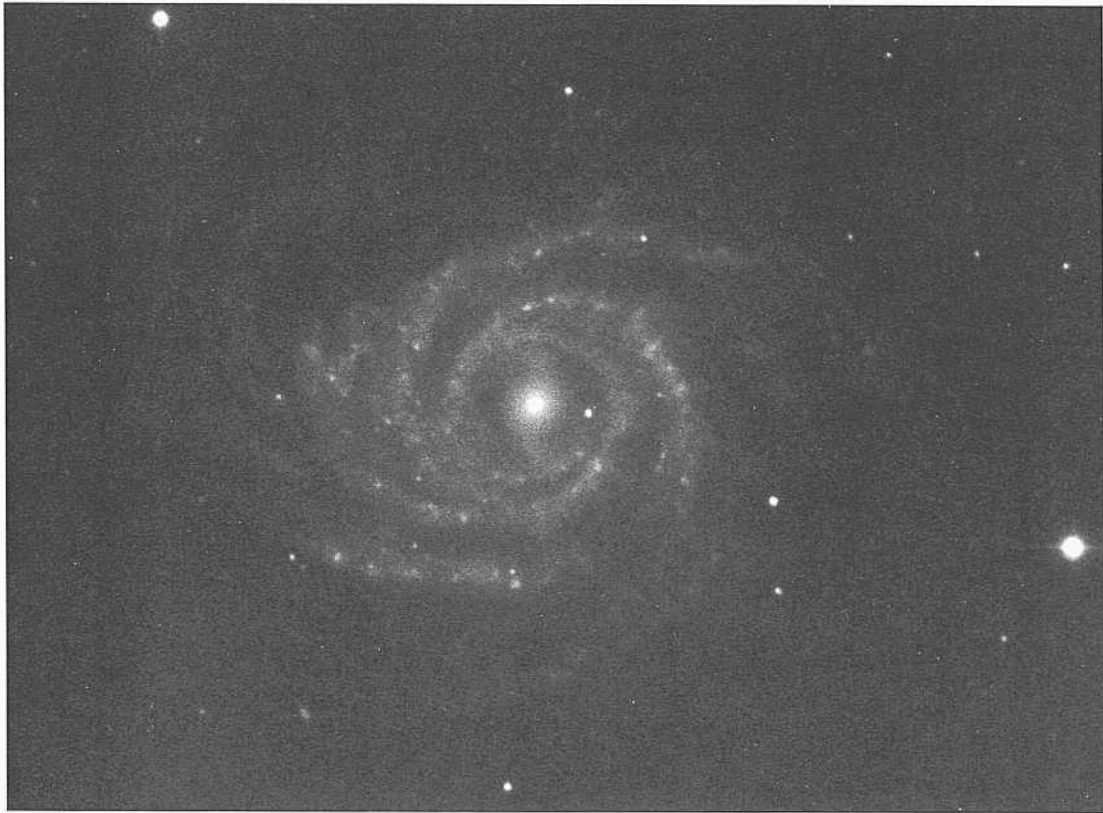
The HII regions are unresolved. The redshift of NGC 3054 is  $v_o = 1923 \text{ km s}^{-1}$ .

NGC 4891      SBbe(r)I-II      group  
 CD-1468-S/Br  
 May 10/11, 1980  
 103aO + GG385  
 45 min

NGC 4891 forms an apparent loose physical group with NGC 4899 (Sc; panel 232) at a separation of 30', and with NGC 4902 (SBb; panel 162) at a separation of 64'. The  $v_o$  redshifts are  $2418 \text{ km s}^{-1}$ ,  $2437 \text{ km s}^{-1}$ , and  $2426 \text{ km s}^{-1}$  for NGC 4891, 4899, and 4902, respectively. At the mean redshift distance of 48 Mpc ( $H = 50$ ) the projected linear separations from NGC 4891 are 420 kpc for NGC 4899 and 895 kpc for NGC 4902. Hence the size of this group is similar to that of the Local Group.

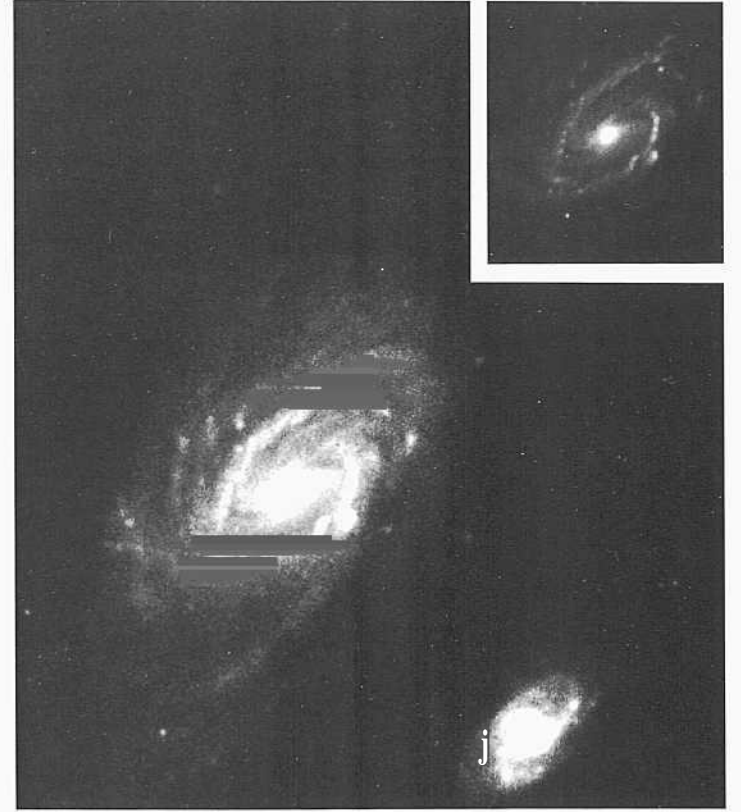
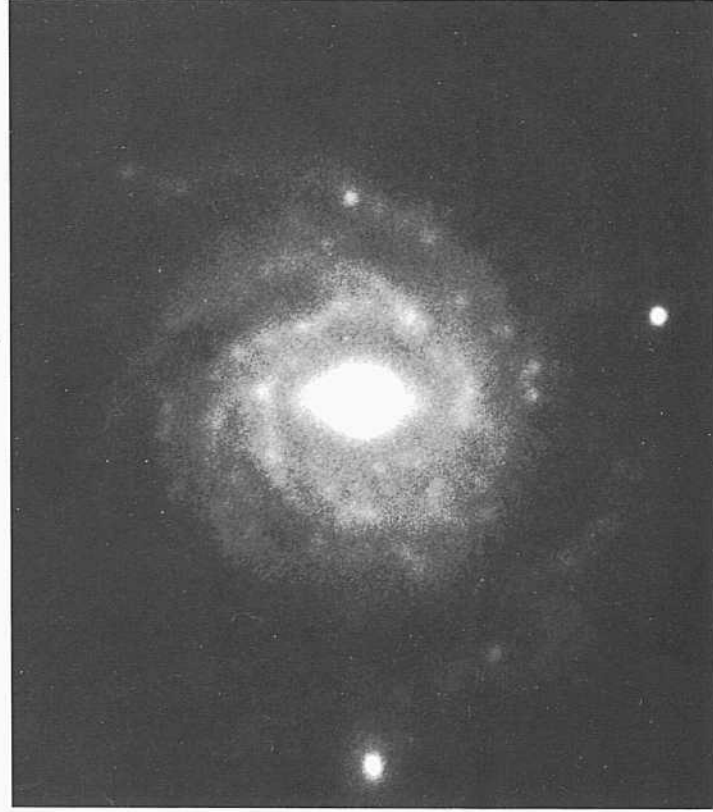
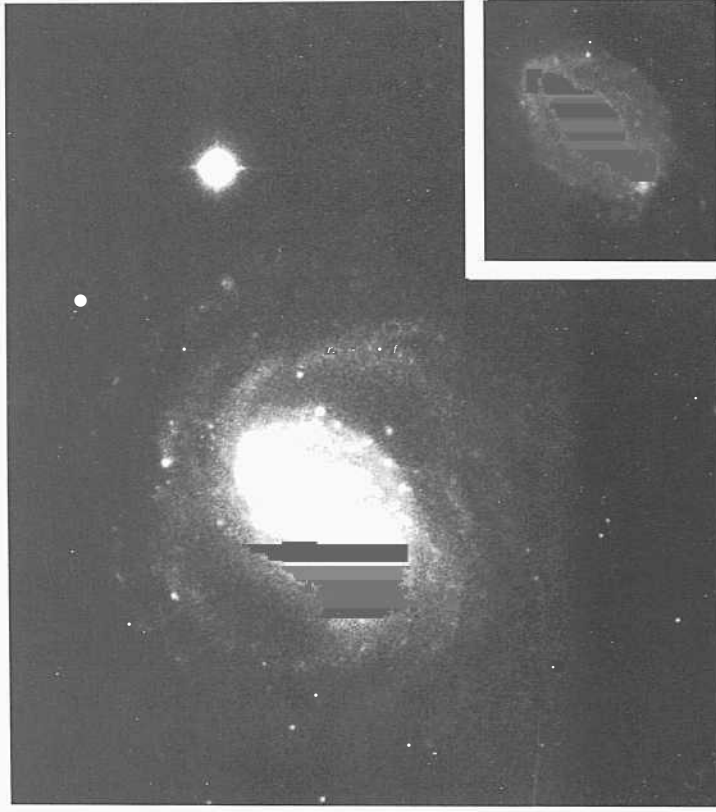
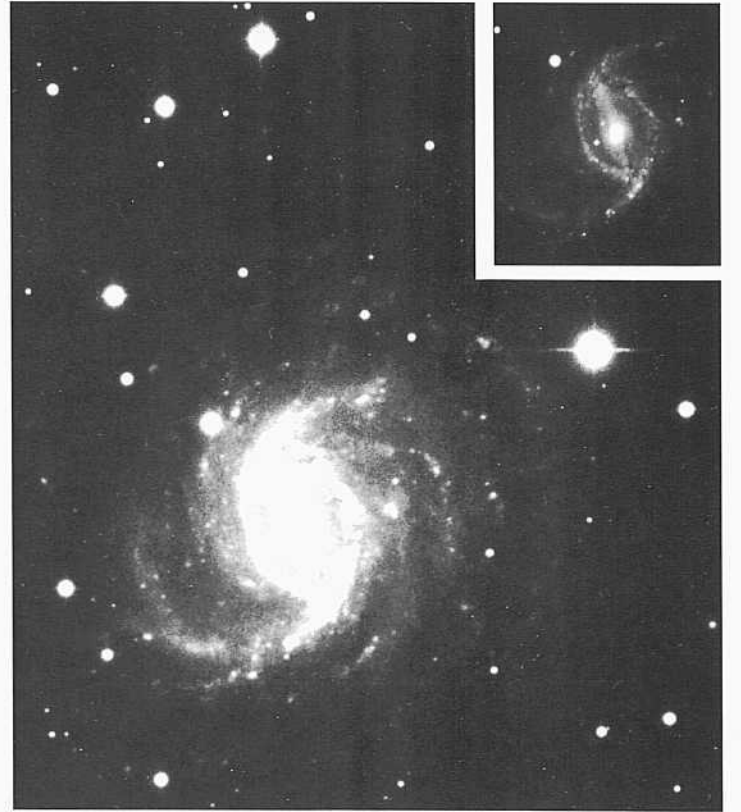
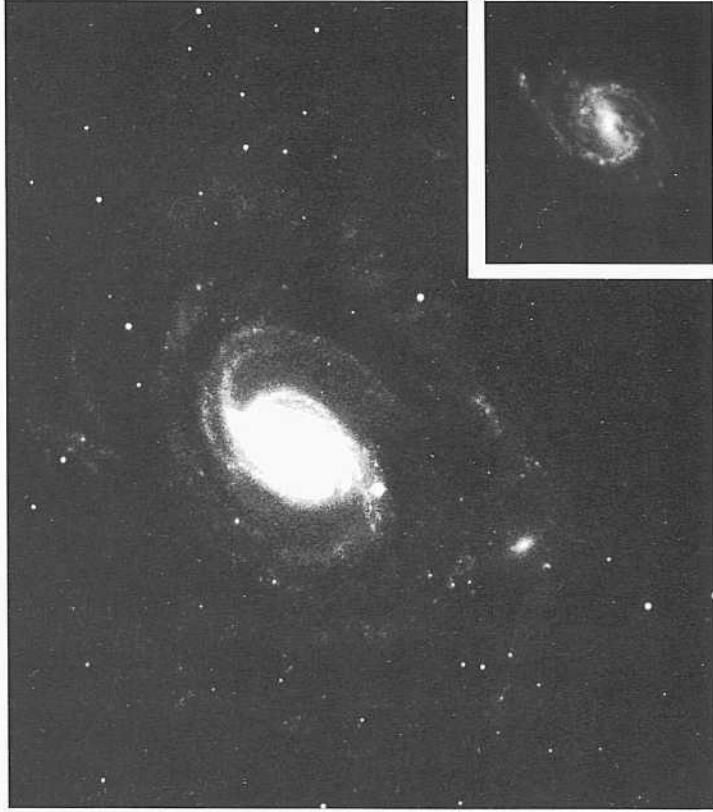
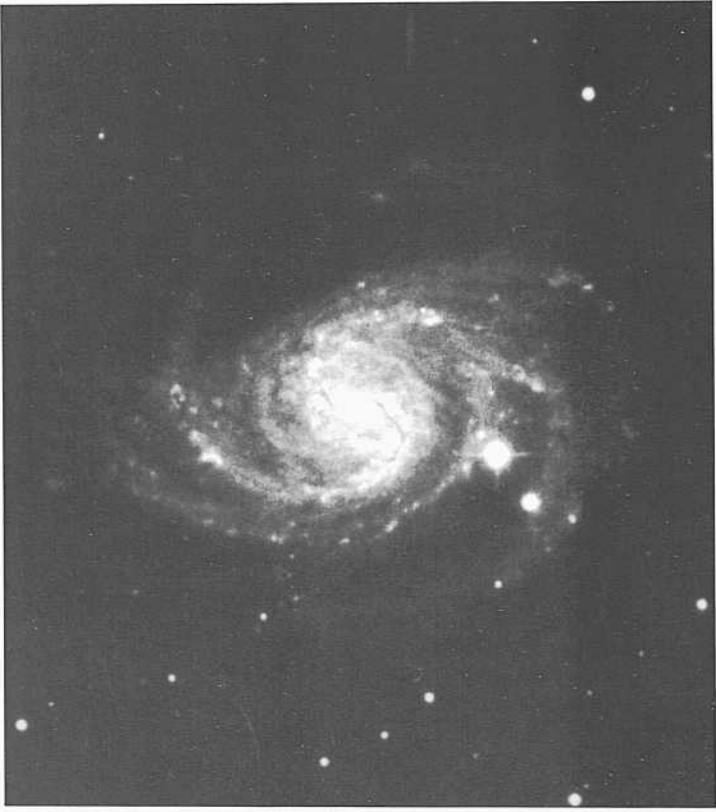
The spiral pattern in NGC 4891 starts with a grand design set of arms tangent to a very-high-surface-brightness internal ring (perhaps burned out in the reproduction here) which in reality, as usual, is an internal set of two tightly wound arms springing from the ends of the bar, as in NGC 1300. The principal outer grand design arms fragment after half a rotation beyond the ring to form a regular exterior multiple-arm pattern.

The largest HII region may resolve at the 1" level.



PANEL  
205

PANEL  
206



**T**his panel of six galaxies completes the early luminosity class I-II. MAS spiral type, SBbc morphological class section.

NGC 3001 SBbc(s)I-II group?  
CD-729-S  
Feb 2/3, 1979  
103aO + Wr2c  
45 min

The arms in NGC 3001 begin at the center as two very thin, nearly straight (at first) dust lanes characteristic of the straight lanes on the leading edges of the bar in SBb and SBbc galaxies. The spiral pattern has features of both the grand design and the MAS types. The bright arms branch into multiple fragments that remain well defined.

The III regions do not resolve at the 1" level. The redshift is  $v_o = 217.1 \text{ km s}^{-1}$ .

Three Im candidate companions exist at angular separations of 10', 12', and 12', which, at the redshift distance of 43 Mpc, are at projected linear separations of 125 kpc and 150 kpc. The candidate companions resolve into stars to the same degree as NGC 3001 itself, suggesting a common distance.

NGC 1640 SBbc(r)I-II  
CD-2010-Bedke/Giegory  
Oct 23/24, 1981  
103aO + GG385  
45 min

The bar in NGC 1640 is smooth and well defined. Two stubby dust lanes exist near both ends of the bar, where luminous tightly wound spiral arms begin; the arms form an almost-complete inner ring when each has unwound by half a revolution. Low-surface-brightness outer arms begin on the rim of this almost-complete inner ring.

The largest III region resolves at about 2". The redshift of NGC 1640 is  $v_o = 1600 \text{ km s}^{-1}$ .

NGC 289 SBbc(rs)I-U  
CD-1578-S/lir  
Aug 10/1 I, 1980  
103aO + GG385  
45 min

The inner spiral pattern of NGC 289 is of the grand design type. Two arms of high surface brightness begin near, but not at, the ends of the bar. As in other cases that are similarly advanced toward the (r) spiral subtype from the pure NGC 1300 (s) type, each inner arm begins about 15° downstream from the ends of the bar, winding outward but missing the opposite arm after half a revolution. The inner arms in NGC 289 are not tightly wound. Consequently, there is no prominent almost-complete inner near-ring, as in earlier examples of the pattern such as NGC 3081 (SBa; panels 99, 107) and NGC 3185 (SBa; panel 99).

The inner arms cover a high-surface-brightness disk, outside of which the delicate, thin, well-formed, very-low-surface-brightness, outer multiple-arm pattern exists.

These arms are fragments that cannot be individually traced for more than about a quarter revolution each.

The brightest knot in one of the inner arms has an angular diameter (core plus halo) of about 4". It may be a complex of several III regions, unresolved at this resolution. The redshift of NGC 289 is  $v_o = 1834 \text{ km s}^{-1}$ .

NGC 3687 SBbc(r)I.2  
PH-7606-S  
April 3/4, 1979  
IIIaJ + GG385  
30 min

The multiple-arm pattern in NGC 3687 begins from an almost-complete inner ring that defines the end of the inner smooth disk. The bright part of the bar terminates just before the inner edge of the internal ring.

The thin, regular spiral arms, which eventually divide into multiple fragments, wind outward for a radius over the outer disk that is about twice the radius of the inner ring. The pattern is regular, requiring an early luminosity class.

The redshift is  $v_o = 2456 \text{ km s}^{-1}$ . The galaxy that is superposed on one of the outermost arms is probably a distant elliptical associated with a cluster that can be seen over the extended field.

NGC 5921 SBbc(a)I-II  
CD-1539-S/Br  
Aug 7/it, 1980  
L03aO + GG385  
15 min

The two inner arms of high surface brightness and of the grand design type, are beautiful examples of the NGC 1300 type, springing from the ends of a well-defined smooth bar within which are the two characteristic straight dust lanes on the leading side of the bar. The arms are very tightly wound, giving the impression of an inner ring.

The largest of the numerous III regions resolve at the 1" level. The redshift of NGC 5921 is  $v_o = 1428 \text{ km s}^{-1}$ .

NGC 1241 SBbc(rs)I.2 pair  
PH-7917-S Racine wedge  
Nov 7/8, 1980  
103aO  
12 min

NGC 1241 forms a close pair with NGC 1242 (She; not in the RSA) at an angular separation of 1.6'. The redshift of NGC 1242 is unknown, but if it is nearly the same as that of NGC 1241,  $v_o = 4072 \text{ km s}^{-1}$ , the redshift distance of the pair is 8.1 Mpc ( $z = 50$ ) giving the small projected linear separation of 38 kpc. However, there is no evidence of morphological distortion in either NGC 1241 or NGC 1242 that would lie evidence of a close encounter; the pair may be optical rather than binary. (Redshifts are needed.)

The two high-surface-brightness inner arms begin at the ends of the central oval; the latter has the properties of a bar, signaled by the two characteristic dust lanes in the oval (bar) of prototype SBb and SBbc types. Multiple arms branch from the two main grand design inner arms.

*SBbc Classification Section (continued)*

NGC 2442          SBIc(is)II          triplet?

CD-149-S

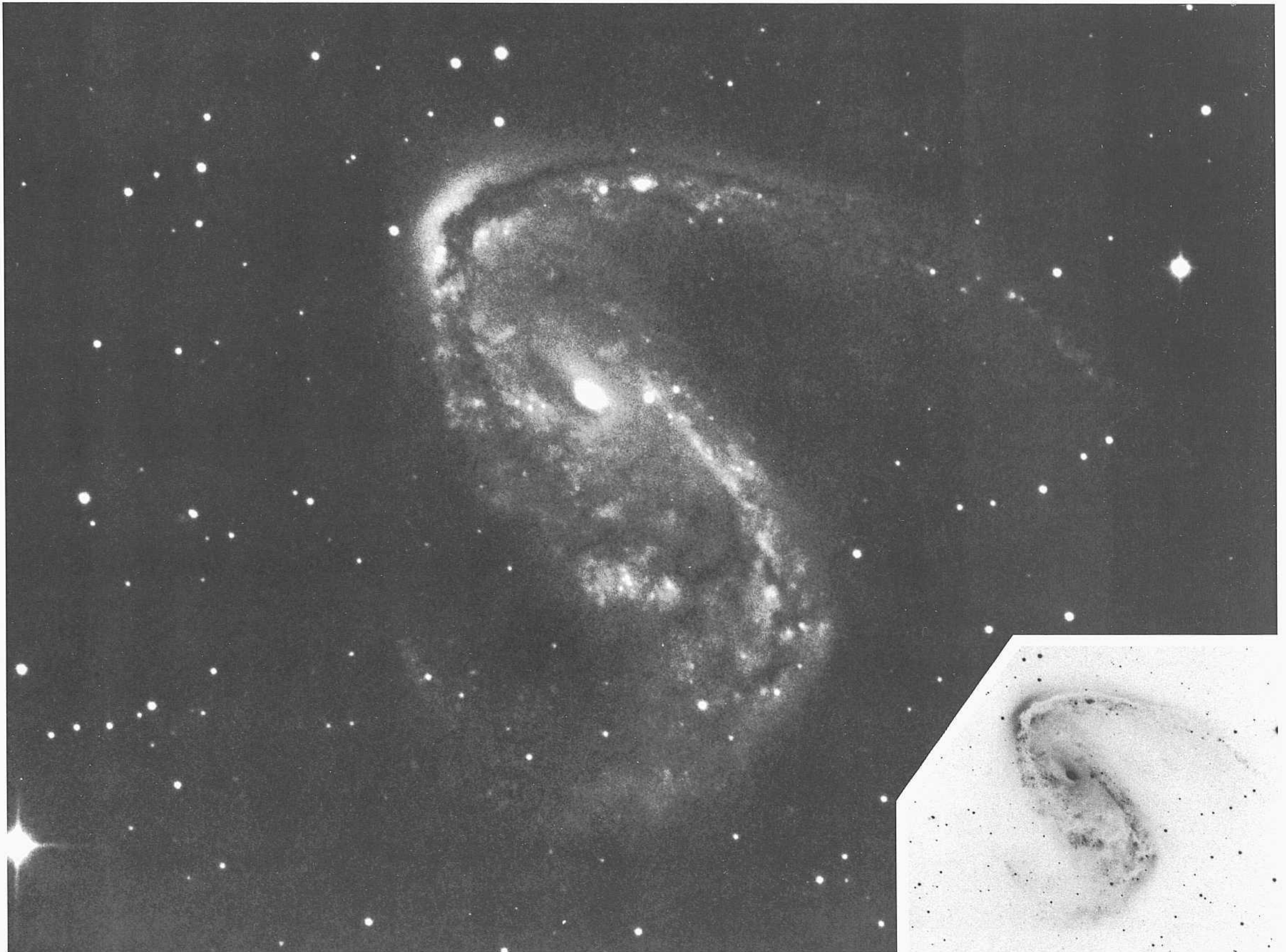
Feb 2/3, 1978

103aO + GG385

45 min

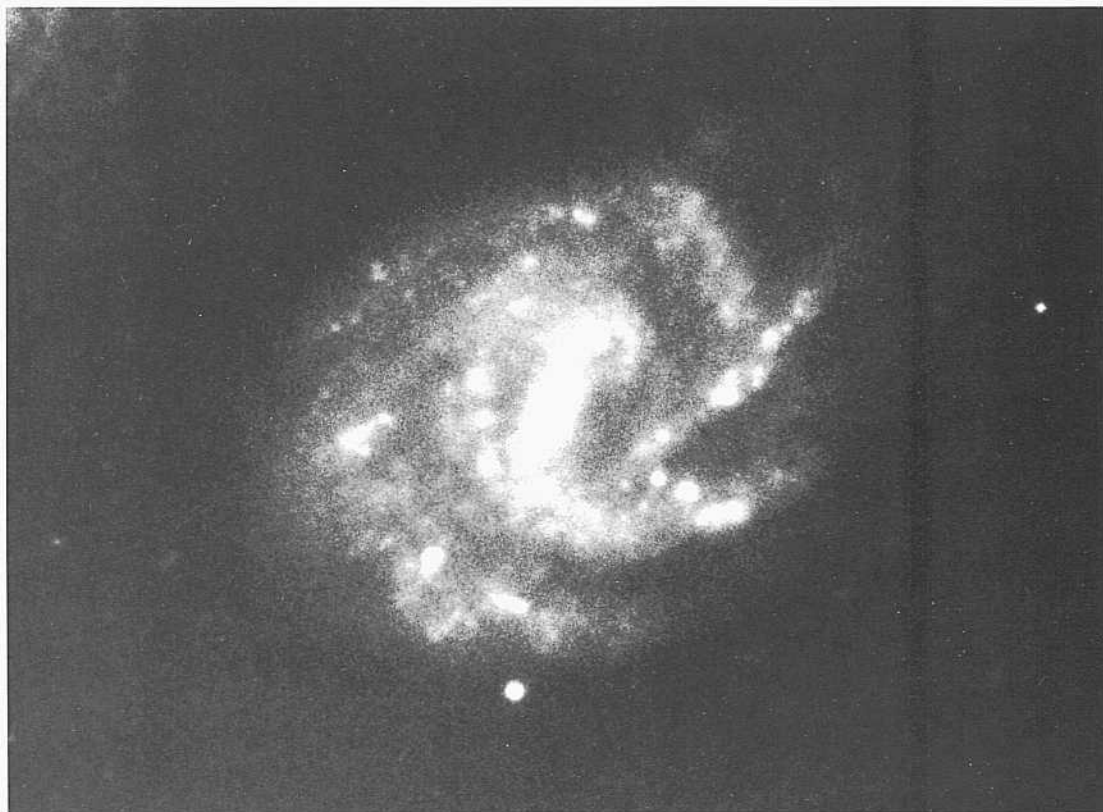
NGC 2442 forms an apparent pair with NGC 2434 (EO; panel I) at a separation of 16.a'. The redshifts are  $u_o(2442) = 1157 \text{ km s}^{-1}$  and  $r_{o,(2434)} = 1111 \text{ km s}^{-1}$ . At the mean redshift distance of 23 Mpc ( $\mu = 50$ ) the projected linear separation is 112 kpc. A possible distant association is with NGC 2397 (Sc; panel 279) at a separation of 85' at a redshift of  $v_o = 1044 \text{ km s}^{-1}$ . The projected linear separation would be 570 kpc if there is a common distance.

The central part of NGC 2442 is an oval rather than a well-defined bar. Heavy dust lanes exist, the strongest of which threads the middle of the best-defined arm of the grand design pattern. The largest IIII region in this arm resolves (core plus halo) at about the 5" level.



PANEL  
207

PANEL  
208



**TH**e SBhc galaxies on this and the following panel arc all of the grand design type but arc of later luminosity class (greater geometrical entropy) than the galaxies on preceding panels.

NGC 4304            **SBbc(s)n**  
**CD-225-S**  
 Feb **12/13**, 1978  
 103aO + GG385  
**45 niii**

The two principal arms in NGC 4304 spring from the ends of the bar, which is relatively smooth but is less well defined than in NGC 1300. Dust exists in the bar, but the lanes are less regular than the two straight lanes that are characteristic of the strong shock lanes in SBb and SBhc galaxies of luminosity class I. Nevertheless, the dust-lane pattern is believed to trace the velocity field (the streamlines) near the bar (e.g., Huntley 1978, 1980). Note that the dust lanes are nearly perpendicular to the bar on one side and arc along the bar on the other.

Copious star formation occurs in both of the main arms. The Mil regions have high surface brightness. They are individually unresolved at the 1" level, but a complex of them in one of the arms has a halo diameter of about 5". The redshift of NGC 4304 is  $v_0 = 2327 \text{ km s}^{-1}$ .

Low-surface-brightness spiral fragments of arms branching from the two main arms exist on the outside of the main pattern. Such sets of outer low-surface-brightness, often called fossil, arms, are common features of spirals of all types.

NGC 6907            **SBbc(s)II**  
 CD-553-S  
 Oct 4/5, 1978  
 103aO + GG385  
 45 min

The spiral pattern in NGC 6907 is remarkably similar to that in NGC 4304, above. The bar is slightly less well defined. It is a highly flattened oval rather than a strong bar, but its dust pattern is the same as in NGC 4304. One heavy, nearly straight dust lane exits at one of the leading edges of the oval. The dust lanes on the other side are nearly perpendicular to the major axis of the oval.

The individual III regions are generally unresolved. The largest Mil complex, composed of several overlapping III regions, has a halo diameter of about 4". The redshift of NGC 6907 is  $v_0 = 3192 \text{ km s}^{-1}$ .

IC 1953            **SBbc(ra)II**  
 CD-2001-Bedke/Gregory  
 Oct 22/23, 1981  
 L03aO + GG385  
 45 min

The arms spring from the ends of the ill-defined bar in IC 1953 and overlap on one side to form a partial internal ring that is incomplete in one quadrant. The arm on the opposite side from that with the light pitch angle (and therefore the overlap) has a straight section causing it to miss the opposite arm, creating a partial rather than a complete internal ring.

Many bright MM regions exist throughout the arm pattern. The largest may resolve at about the 1.5" level. The redshift of IC 1953 is  $v_a = 1856 \text{ km s}^{-1}$ .

An apparent companion (anonymous; type Sc or SBc) of unknown redshift is at a separation of 2.6'. If it is at a common distance the projected linear separation would be small at 27 kpc. A second apparent companion (a blue compact dwarf, i.e., type BCD; see Sandage and Binggeli 1984) at a separation of 6.1' would be at a projected linear separation of 64 kpc.

NGC 6923            **SBbc(s)H**  
**CD-1518-S/Br**  
 Aug 5/6, 1980  
**103aO + GG385**  
**45 mill**

The seeming bar in NGC 6923 is a small, very-high-surface-brightness internal ring. The two grand design main outer arms emerge from the ends of the major axis of the ring. The fact that the arms begin at the ends of the major axis of the projected image in this obviously inclined galaxy, suggests that the internal ring is a true oval rather than a circle seen in projection.

The Mil regions in the arms are unresolved. The redshift of NGC 6923 is  $u_0 = 2858 \text{ km s}^{-1}$ .



The four galaxies on this panel continue the SBbc spirals of the (s)-arm subtype of the grand design. The luminosity classes are II and II-III.

NGC 5430 SBbc(s)I.8 Racine wedge  
PH-7829-S  
Sep 3/4, 1980  
103aO  
12 min

The central region of NGC 5430 is an oval rather than a well-formed bar. The arm pattern is not symmetrical. Threads of multiple arms exist on one side of the oval. A single low-surface-brightness, well-defined arm exists on the other side. The early luminosity class is based on the lack of chaos in the arm pattern, despite its lack of good symmetry.

The few HII regions are unresolved. The redshift of NGC 5430 is  $v_0 = 3016 \text{ km s}^{-1}$ .

NGC 6217 RSBbc(s)II  
PH-6601-S  
Aug 23/24, 1973  
103aE + RG2  
30 min

The reproduction on the facing panel is from a red plate: the HII regions are emphasized because the Balmer-a line is in the band-pass of the plate.

The bar is very much better defined in the red here than on blue plates which emphasize the young stars. Clearly, such stars do not dominate the bar.

The (s)-type spiral arms originate from the ends of this smooth red bar. There is also a semblance of a straight dust lane in one of the legs of the bar, characteristic of SBb and SBbc systems.

The unusual feature of the spiral pattern is the third arm coming from the center as a double bar on one side of the image. On blue plates this arm begins at the center, as in normal Sbc or Sc non-barred galaxies, rather than at the end of the bar.

The redshift is  $v_0 = 1598 \text{ km s}^{-1}$ . The largest HII regions resolve at about the 2" level.

NGC 3887 SBbc(s)II-III  
CD-1685-S  
Jaii 2/3, 1981  
103aO + GG385  
45 min

The central region of [VGC 3887 is an oval rather than a well-defined bar. The principal reason for classification as a barred spiral is the presence of two thin dust lanes starting on opposite sides of the center, as is usual in prototype SBb and SBbc bars (e.g. NGC 5383: SBb; Hubble Atlas, p. 46: panel 168 here). These remain straight throughout the oval but bend at the end where they begin to accompany the luminous arms.

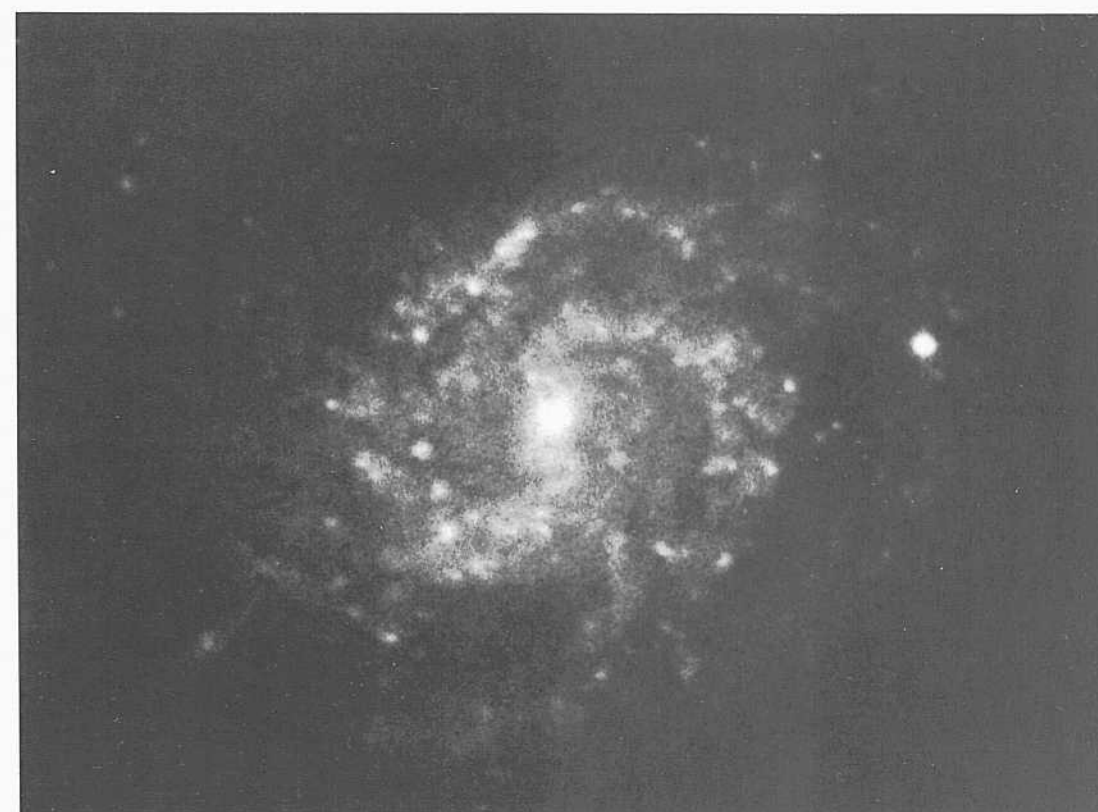
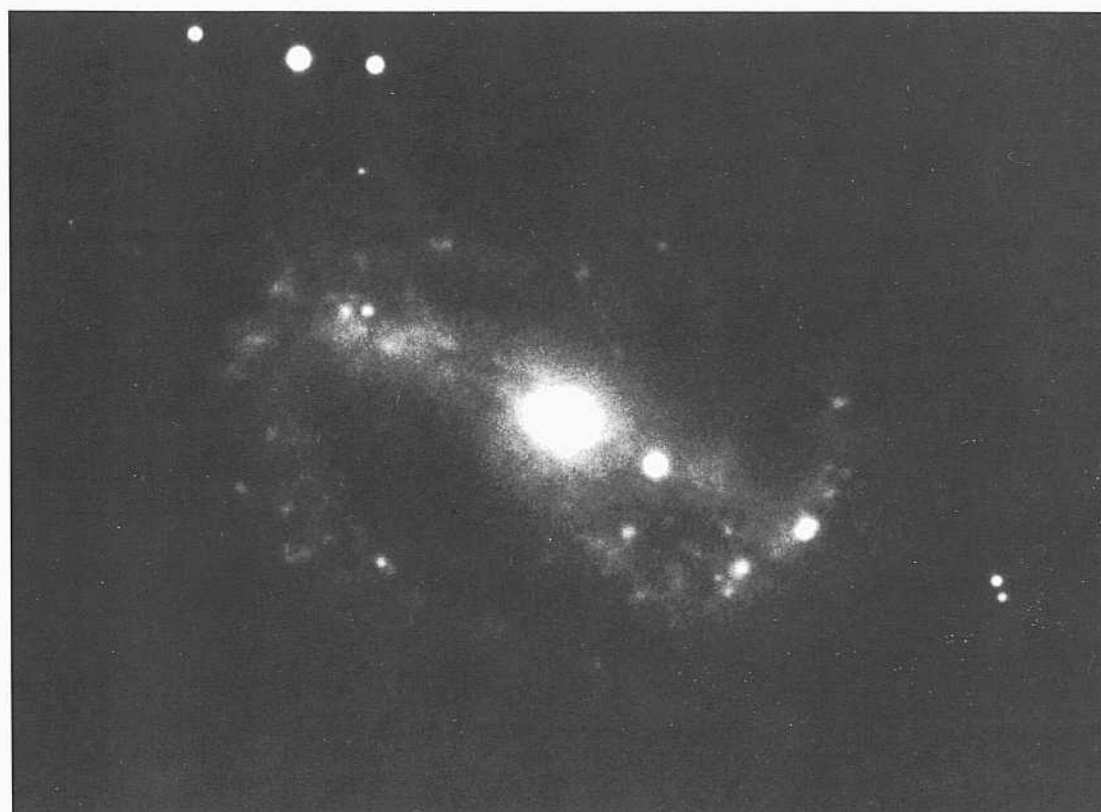
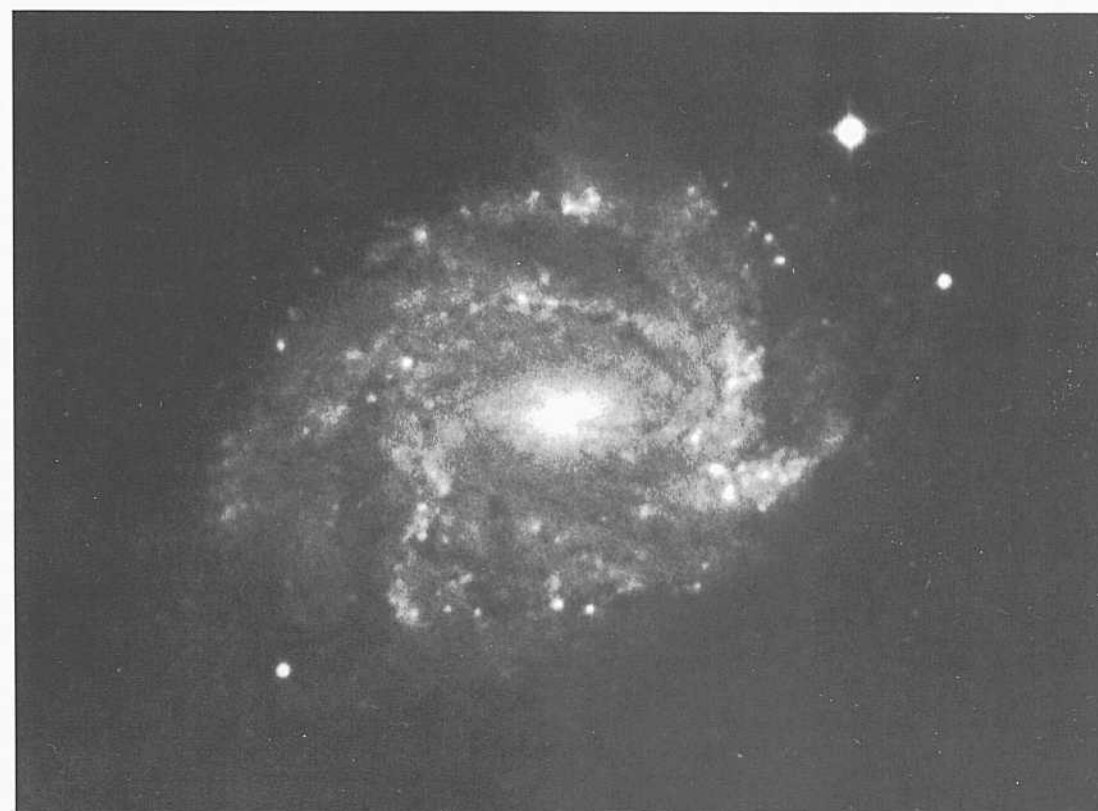
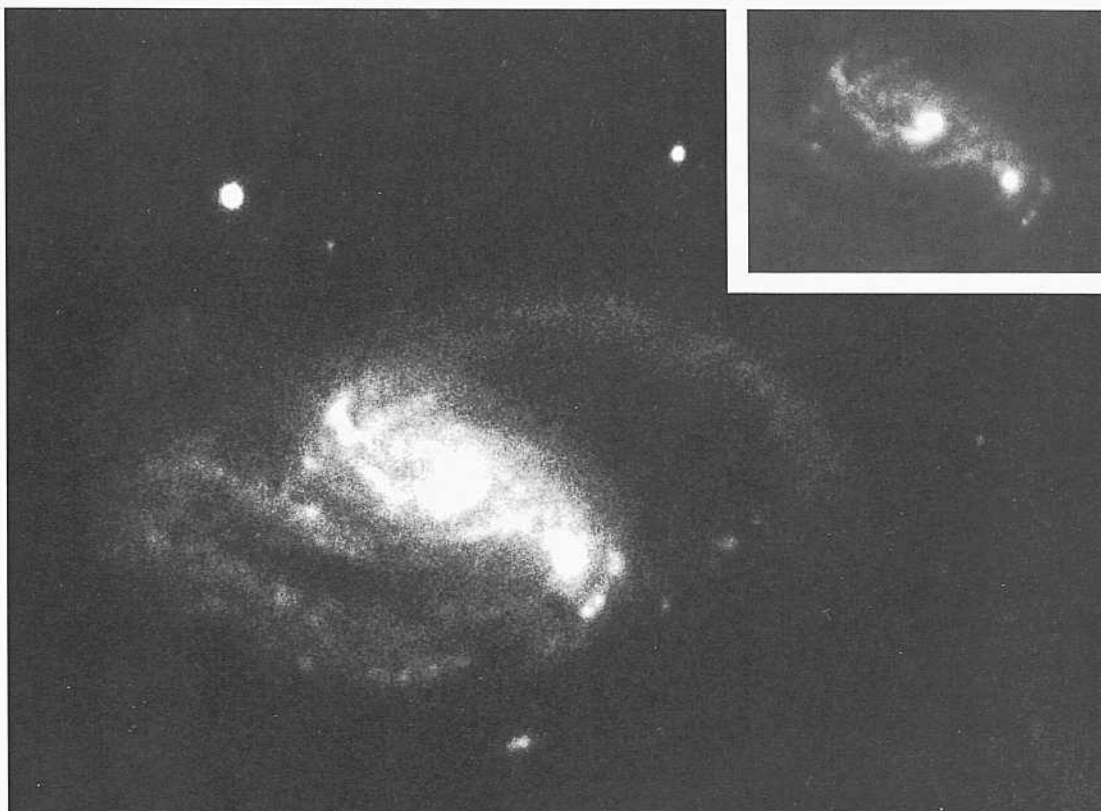
The largest of the many HII regions resolve (core plus halo) at the 2" level. The redshift of NGC 3887 is  $v_0 = 915 \text{ km s}^{-1}$ .

NGC 3686 SBbc(s)II group  
CD-1841-HB  
April 2/3, 1981  
103aO  
75 min

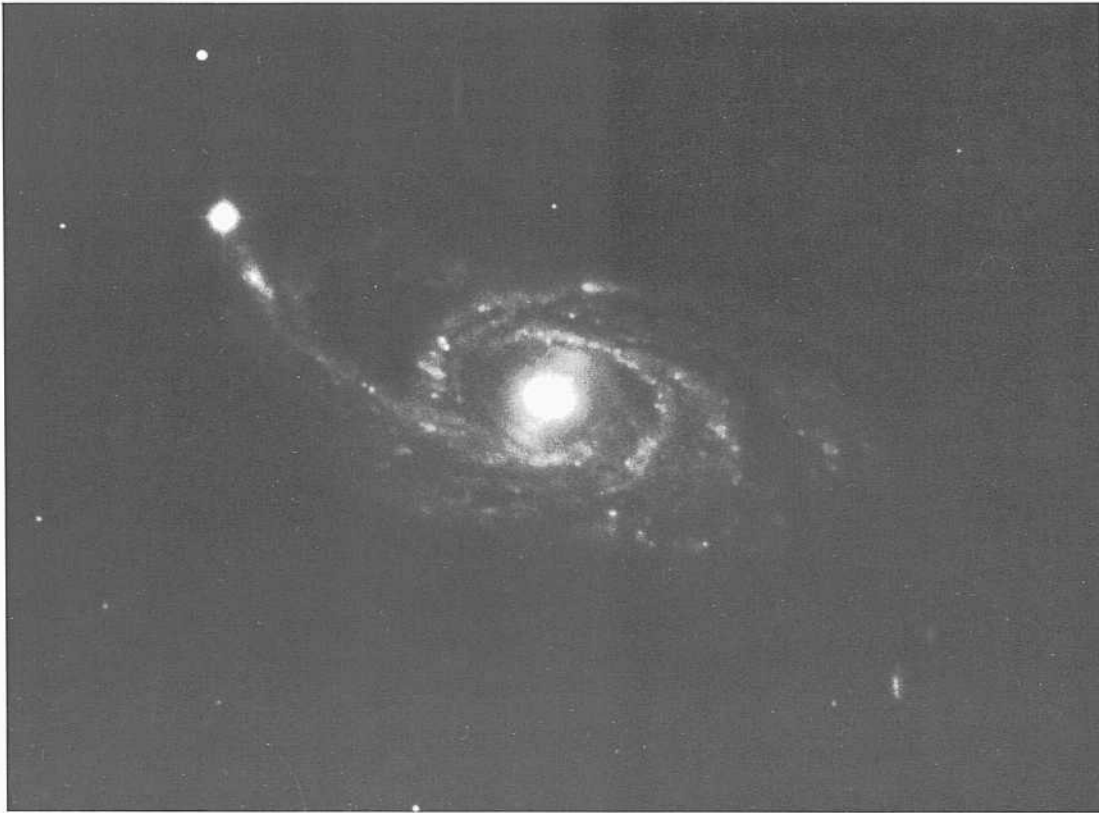
NGC 3686 is the brightest member of a small group of at least seven galaxies that have closely the same redshift and that are within about 1° radius from NGC 3684, which is the central member of the group. The brightest four group members are in the RSA: NGC 3681 (SBb: 1135 km s<sup>-1</sup>; panel 164), NGC 3684 (Sc: 1065 km s<sup>-1</sup>; panel 256), and NGC 3691 (Scd: 947 km s<sup>-1</sup>; panel 317). The redshift of NGC 3686 is  $v_0 = 1034 \text{ km s}^{-1}$ .

Three anonymous members for which redshifts and other data are available (Hoffman *et al.* 1987) are A1127 + 1642 (ImIII-IV,  $v_0 = 957 \text{ km s}^{-1}$ ), A1122 + 1709 ( $v_0 = 909 \text{ km s}^{-1}$ ), and A1122 + 1721 (ImIV:  $v_0 = 1209 \text{ km s}^{-1}$ ). There are also several candidates for dE dwarf ellipticals in the group. The mean redshift of the seven known group members is  $\langle v_0 \rangle = 1021 \text{ km s}^{-1}$ . At the redshift distance of 20 Mpc the linear radius corresponding to an angular radius of 1° is 360 kpc, similar to the radius of the Local Group.

The arm pattern in NGC 3686 is slightly better defined than in NGC 3887, above. The luminosity class is II here and II-III above.



PANEL  
210



NGC 151 SBbc(rs)n

PH-1076-S

Aug 25/26, 1955

103aO

30 min

The **beautifully symmetrical grand design** in the pattern of NGC 151 contains a **smooth** central bar **which** terminates **at the place where** two inner arms begin. The arms do not **spring** from the ends of the bar but start from **two** symmetrically placed points about  $15^\circ$  **downstream** from the termination of the bar—a common-enough feature, noted before on previous panels.

The two principal arms that **start** at these places relative to the bar, **fragment** as they move outward and form the multiple-arm pattern in which at least four arm segments can **be** traced on each side of the galaxy.

None of the many **III!** regions resolve at the 1" level.

NGC 4981 SBbc(sr)II pair

CD-1860-HB

Aug 6/7, 1981

103aO

75 min

NGC 4981 may form a wide physical pair with NGC 4995 (See panel 183) which has a redshift of  $v_o = 1645 \text{ km s}^{-1}$  at an angular separation of  $65'$ . The redshift of NGC 4981 is  $v_o = 1492 \text{ km s}^{-1}$ . If the pair is at the same redshift distance of 31 Mpc ( $z = 5.0$ ), the projected linear separation is 593 kpc.

The arms in NGC 4981 begin at the **rim** of the inner disk where the oval **central** region ends. The numerous **III!** regions may **resolve** at about the 1" level.

NGC 7121 SBbc(ra)II-III

CD-1080-Hr

Aug 17/18, 1979

103aO + GG385

45 min

One of the two principal arms that can be **traced** begins about a quarter turn downstream from one of the ends of the bar. The **opposite** arm seems to **begin** at the end of the **other** side of the bar.

**These arms fragment almost immediately** into a **semi-chaotic** filamentary arm structure; hence **the late luminosity classification is required**.

The redshift is  $v_o = 1838 \text{ km s}^{-1}$ . The largest III! region may resolve at the 2" level.

NGC 1781 SBbc(r)II

CD-1677-S

Jan 1/2, 1981

103aO + GG385

45 min

The bar in NGC 1781 is well **developed**. Dust lanes and patches exist in the bar: their description would be similar to the paragraphs on NGC 4304 and NGC 6907 two panels back.

The two, very tightly wound inner arms spring from the ends of the well-defined bar and overlap, **forming a nearly complete inner** ring. The **continuation** of these arms **results** in an outer pattern of **low-surface-brightness** spiral fragments that cannot be individually traced over more than about a **quarter** revolution each.

The **redshift** is  $v_o = 2254 \text{ km s}^{-1}$ . The III! regions are **unresolved**.

**T**he nine galaxies on this panel complete the illustrations of normal SBbc systems in the RSA. All are of luminosity class II or II-III, and all are of the multiple-armed (MAS) type.

ISGC 5970 SBbc(r)II  
S-530-H  
June 4/5, 1926  
E40  
45 min

The print of NGC 5970 here is from a Mount Wilson 60-inch plate.

The arms begin from the ends of the bar that terminate at the edge of an inner smooth disk. The pattern is a prototype (r) configuration where the outer arms are an extension of the apparent inner ring at the edge of the disk.

The numerous HII regions in the disk are unresolved at the 1" level. The redshift of NGC 5970 is  $v_0 = 2047 \text{ km s}^{-1}$ .

NGC 5483 SBbc(s)II-III  
CD-1526-S/Br  
Aug 6/7, 1980  
103aO + GG385  
45 min

The two principal grand design arms are of the prototype (s) configuration, yet the entire disk is filled with spiral arcs, many of which are dust lanes. These arcs are not branch fragments from the principal arms. Rather they originate in the disk independently, like the arms in the MAS prototype galaxy NGC 2841.

One large HII complex appears to be multiple, having a combined halo diameter of about 4". The redshift of NGC 5483 is  $v_n = 1517 \text{ km s}^{-1}$ .

NGC 3318 SBbc(rs)II.2  
CD-1481-S/Br  
May 12/13, 1980  
103aO + GG385  
35 min

NGC 3318 is in the complicated region of the Hydra-Centaurus Supercluster, about  $6.5^\circ$  south of the core of the embedded Antlia Group (Ferguson and Sandage 1990). A map of the region containing the neighborhood of NGC 3818 is given by Hopp and Materne (1985).

The redshift  $v_n = 2306 \text{ km s}^{-1}$  for NGC 3318 is among the lowest in the region. Hopp and Materne have identified six redshift groups with  $\langle v_o \rangle$  values ranging from 2700 to  $4500 \text{ km s}^{-1}$ . The adopted mean redshift of the Antlia Cluster is  $\langle v_o \rangle = 2503 \text{ km s}^{-1}$  (Ferguson and Sandage 1990).

NGC 4961 SBbc(s)II  
PH-8091-S  
Feb 6/7, 1981  
103aO  
12 min

The ill-defined bar in NGC 4961 terminates where the spiral pattern begins. The arm pattern is not well defined. Several bright HII regions are evident. Each is unresolved at the 1" level. The redshift of NGC 4961 is  $v_o = 2508 \text{ km s}^{-1}$ .

NGC 4763 SBbc(r)II  
CD-1458-S/Br  
May 7/8, 1980  
103aO + GG385  
45 min

The spiral pattern in NGC 4763 is of the classic (r) barred subtype: the multiple outer arms begin tangent to an almost-complete inner ring which begins at the end of a smooth, well-defined bar. As usual, the near-ring is composed of two coils of tightly wound principal spiral arms which spring from the ends of the bar.

The redshift is  $v_o = 3961 \text{ km s}^{-1}$ .

NGC 3485 SBbc(s)II  
CD-2128-S  
March 21/22, 1982  
103aO + GG385  
45 min

The arm pattern in NGC 3485 is a particularly good example of the NGC 1300 (s)-type arm beginning at the ends of the bar but with almost-complete overlap after each arm has unwound by half a revolution to form an almost-complete inner ring. The ring, however, is broken, and the outer arms branch outward from the extension of these tightly wound inner arms.

The redshift is  $v_n = 1395 \text{ km s}^{-1}$ .

NGC 4385 SBbc(s)H  
CD-698-Br  
Jan 28/29, 1979  
103aO  
45 min

The bar in NGC 4385 is not well defined except by the non-symmetrical luminosity distribution of spiral-like fragments; there is no smooth, definite bar as in NGC 1300.

The redshift is  $v_o = 1969 \text{ km s}^{-1}$ .

NGC 491 SBbc(r)II  
CD-2006-Bedke/Gregory  
Oct 23/24, 1981  
103aO + GG385  
45 min

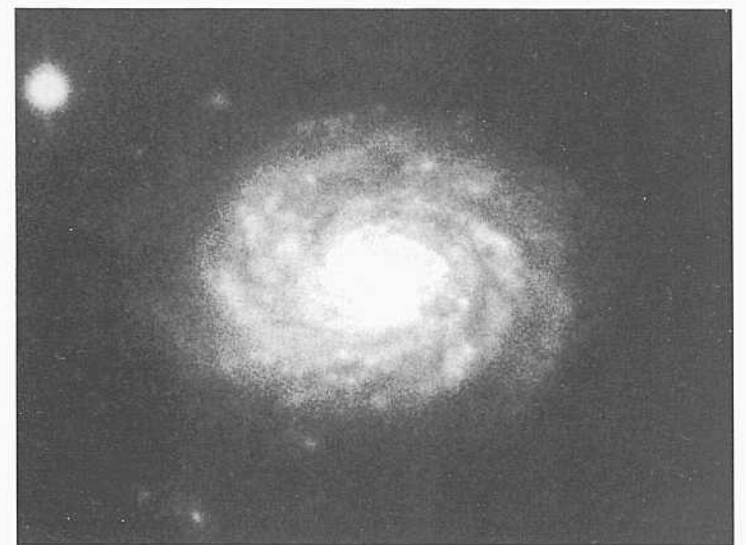
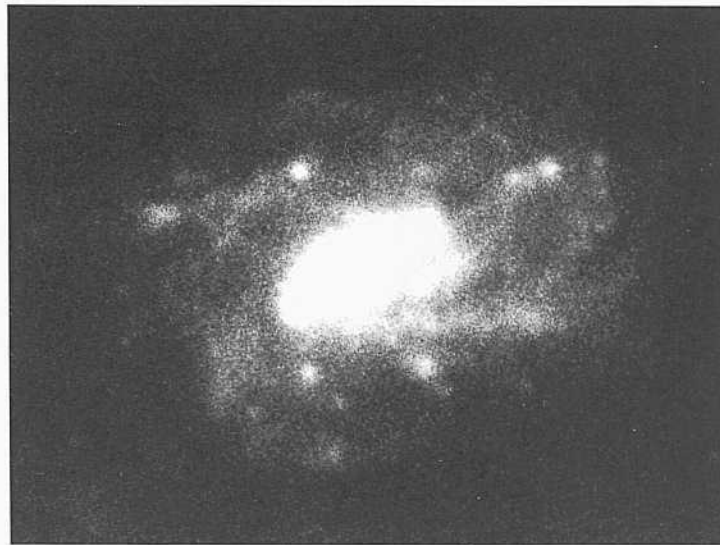
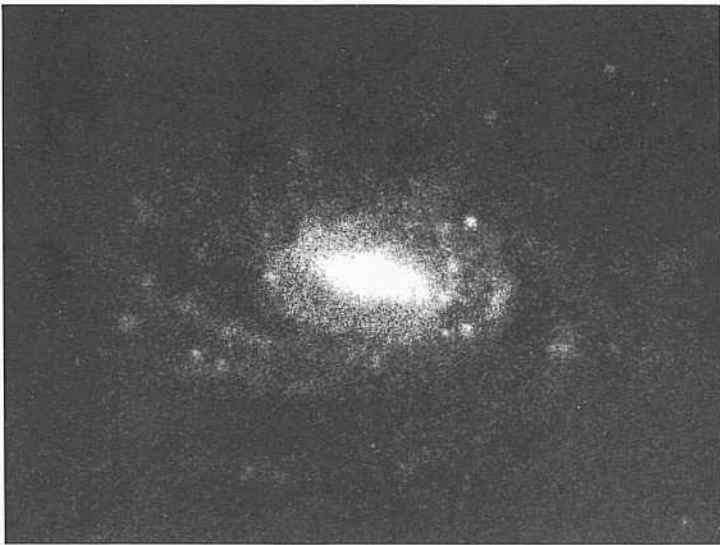
The spiral pattern is multiple in NGC 491, starting from an internal ring upon which the bar terminates. The galaxy is remote compared with most others in the RSA: the spatial resolution is about a factor of four less than in the average RSA galaxy.

The redshift is  $v_o = 3890 \text{ km s}^{-1}$ .

NGC 5188 SBbc(s)II-III pec  
CD-1153-Br  
Aug 22/23, 1979  
103aO + GG385  
45 min

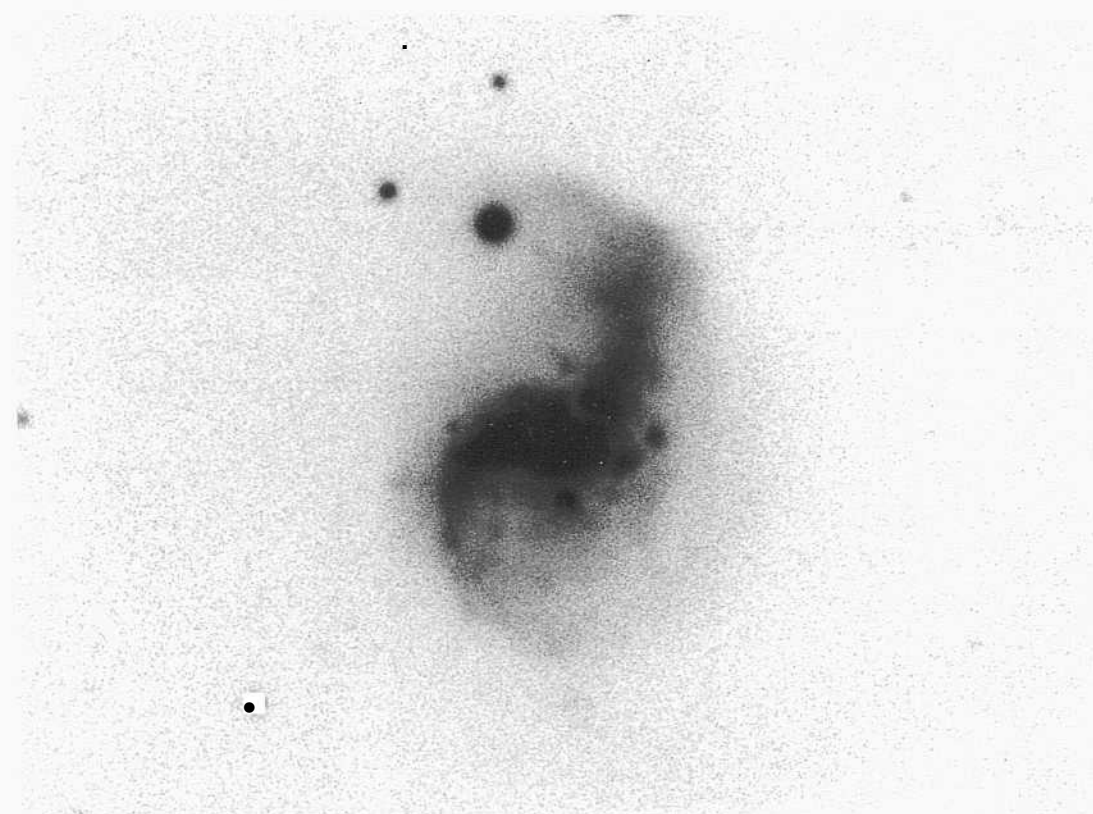
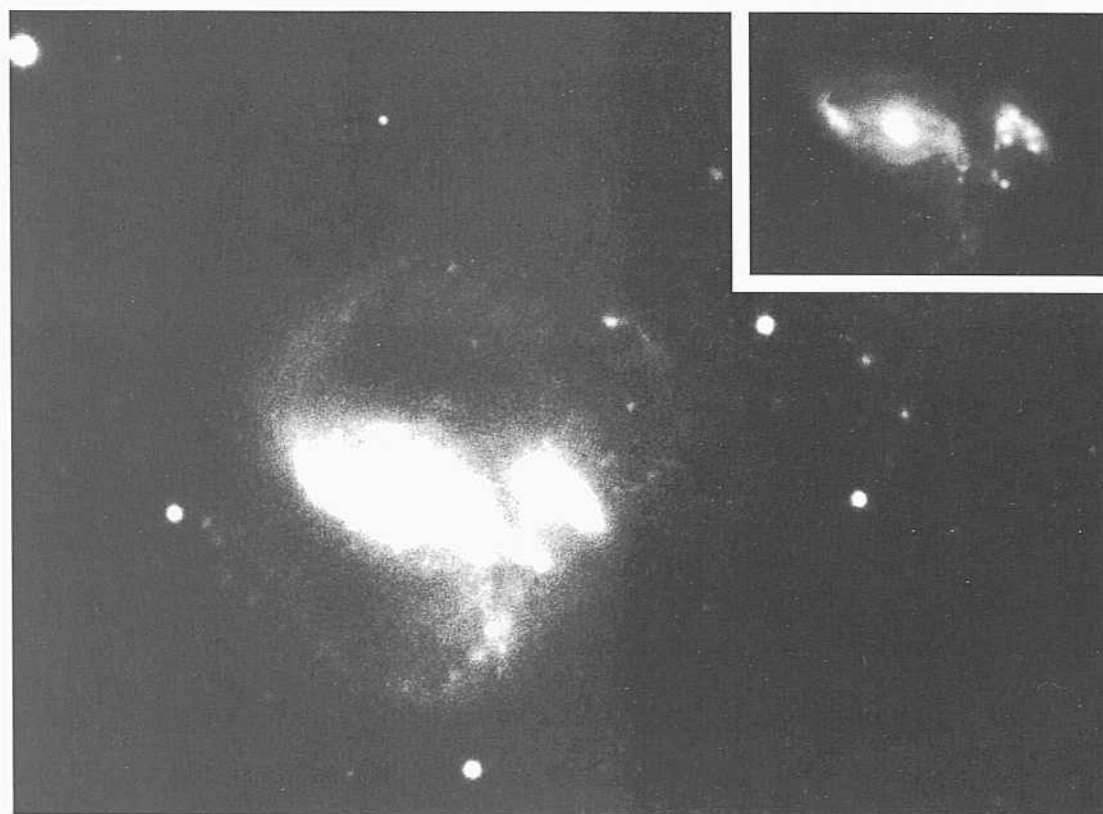
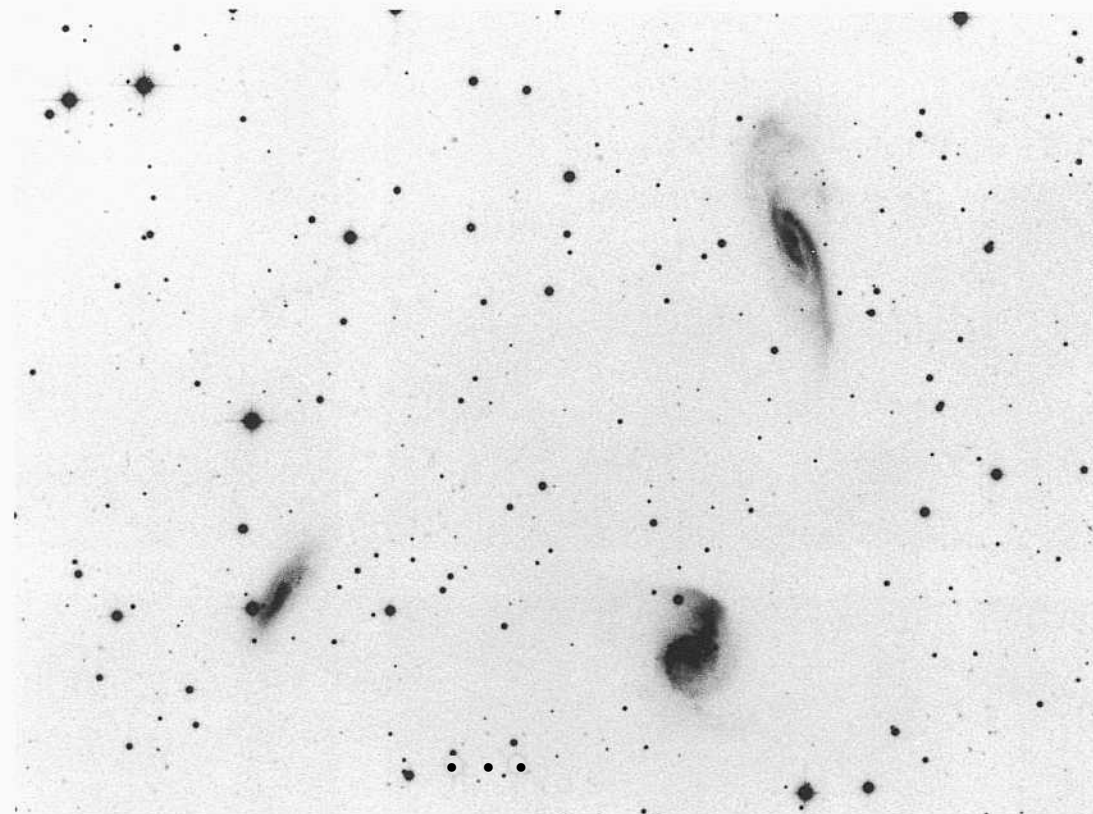
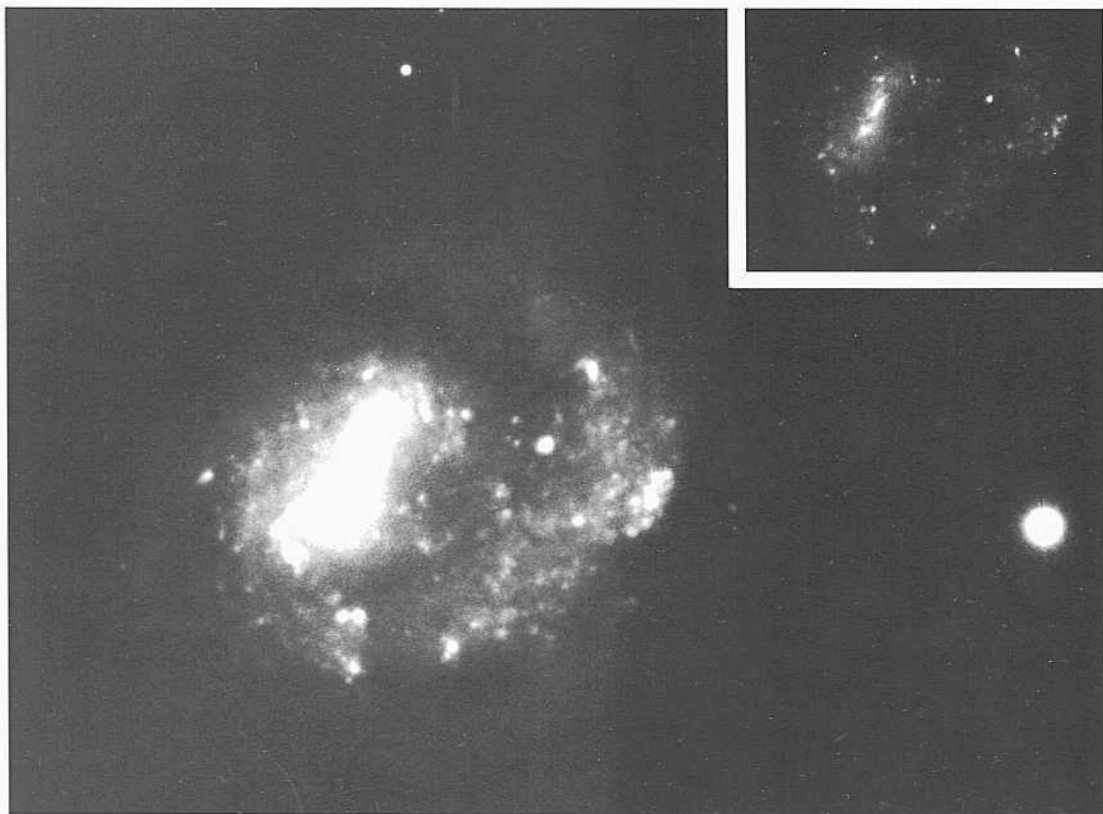
The bar in NGC 5188 is suggested by a straight luminous segment on one side of the image. The form is unusual; NGC 5188 may not, in fact, be a true SB spiral but rather may simply have a semi-chaotic inner spiral morphology where one of its features imitates a bar.

The redshift is  $v_o = 2107 \text{ km s}^{-1}$ .



PANEL  
211

PANEL  
212



**NCC4618 SBbc(rs)II.2 pec M51 Gr**  
**PH-7666-S Karachentsev 349**  
**April 29/30, 1979**  
**103aO**  
**6 min**

NGC 4618 forms a physical pair with NGC 4625 (Sc pec) at a separation of 8.5'. The redshifts are  $u_0(4618) = 563 \text{ km s}^{-1}$  and  $u_0(4625) = 641 \text{ km s}^{-1}$ . At the mean redshift distance of 12 Mpc ( $// = 50$ ) the projected linear separation of the pair is small, at 30 kpc.

Both galaxies show evidence of interaction. Each has an asymmetrical spiral pattern characterized by a single prominent arm, presumably made by the action of tides in the manner calculated by Toomre and Toomre (1972).

Both NGC 4618 and NGC 4625 are well resolved into brightest stars and HII regions. These galaxies are in the nearby complex Ursa Major region, which Tammann (unpublished) has divided into three separate kinematic groups plus the great Ursa Major Cluster at  $\langle v_0 \rangle = 980 \text{ km s}^{-1}$ . The three groups are (1) a very highly resolved nearby group at  $\langle v_0 \rangle = 285 \text{ km s}^{-1}$ , containing NGC 4144, 4214, 4244, 4395, 4449, 4736, and IC 4182 among others, (2) the M51 Group at  $\langle v_0 \rangle = 595 \text{ km s}^{-1}$ , containing NGC 4258, 4490, and 4618, and NGC 4625 here, and (3) a group at  $\langle v_0 \rangle = 750 \text{ km s}^{-1}$ , containing NGC 3675, 4013, 4051, 4085, 4088, 4147, 4242, 4389, and IC 750.

**NGC 5534 SBbc(s)II(tides, merger?)**  
**CD-1330-S/Br**  
**March 13/14, 1980**  
**103aO + GG385**  
**50 min**

NGC 5534 may be a composite image of two galaxies in the process of merger. The main body has a normal SB oval in the central regions. Two small satellite objects exist on one side of the main body from which an apparent tidal plume emerges. The outer thin spiral arms of wide extent may also be a result of a response to tides.

The redshift is  $u_0 = 2483 \text{ km s}^{-1}$ .

**NGC 5915/5916/5916A SBbc(s) pec triplet?**  
**CD-1433-S/Br So pec? panel HI**  
**March 25/26, 1980**  
**103aO + GG385**  
**45 min**

Based on the near equality of their  $r_0$  redshifts,  $2116 \text{ km s}^{-1}$  and  $2165 \text{ km s}^{-1}$ , NGC 5915 and NGC 5916 (panel 81) form an obvious physical pair. The group may be a triplet formed also with NGC 5916A, but the redshift of this galaxy is presently (1990) unknown.

At the mean redshift distance of 43 Mpc ( $// = 50$ ), the projected linear separations of both NGC 5916 and NGC 5916A from NGC 5915 are small at 59 kpc.

The morphologies of both NGC 5915 and NGC 5916 appear disturbed, presumably due to tidal interaction. Note that the form of NGC 5916 (Sa) is similar to that of NGC 3211 (Sa; panel 65) in the Antlia Cluster.

**NGC 5915 SBbc(s) pec**  
**CD-1433-S/Br**  
**March 25/26, 1980**  
**103aO + GG385**  
**4-5 min**

NGC 5915 is outside the classification system. It is called SBbc(s) based on the "arms" that spring from the ends of the central region in the manner of NGC 1300. However, the form may be due to tidal interaction with NGC 5916, shown above.



# The Sc Classification Section

## THE SCI SUBCLASS

**S**c galaxies of luminosity class I are shown on this and the next eight panels. Galaxies with two principal arms of the grand design are on the first three panels; those with multiple arms are on panels 216—221.

NGC4321      Sc(s)I      VCC 596  
 PH-742-S      HA, pp. 28, 31  
 April 8/9, 1954      M100  
 103aE + RG2  
 90 inin

Two of the largest spirals in the Virgo Cluster are shown on this page. As listed in the RC2, the angular sizes of NGC 4321 and NGC 4303 are 6.9' and 6.0', respectively, measured to an isophote of 25 mag arc sec<sup>2</sup>. Photographs of many Virgo Cluster spirals are shown elsewhere (Sandage, Binggeli, and Tammann 1985a), printed to a common angular scale, showing thereby that the two galaxies on this panel are among the largest spirals in the cluster.

The print shown here of NGC 4321 is from a red plate sensitive to Ha radiation. It was from this plate, taken in 1954, that it came to be understood that most of the knots in spiral galaxies which Hubble (1936a) had used with his calibrations of brightest stars are **HII** regions (Humason, Mayall, and Sandage 1956, Appendix C). From this it was evident that Hubble's distance scale must be revised upward by a much larger factor than the correction determined by Baade for M31.

The two principal arms in NGC 4321 begin near the center as dust lanes. A side of one lane attaches smoothly to the beginning of one of the principal luminous arms. The principal dust lane on the other side cuts across the beginning of the first luminous arm at a steep angle.

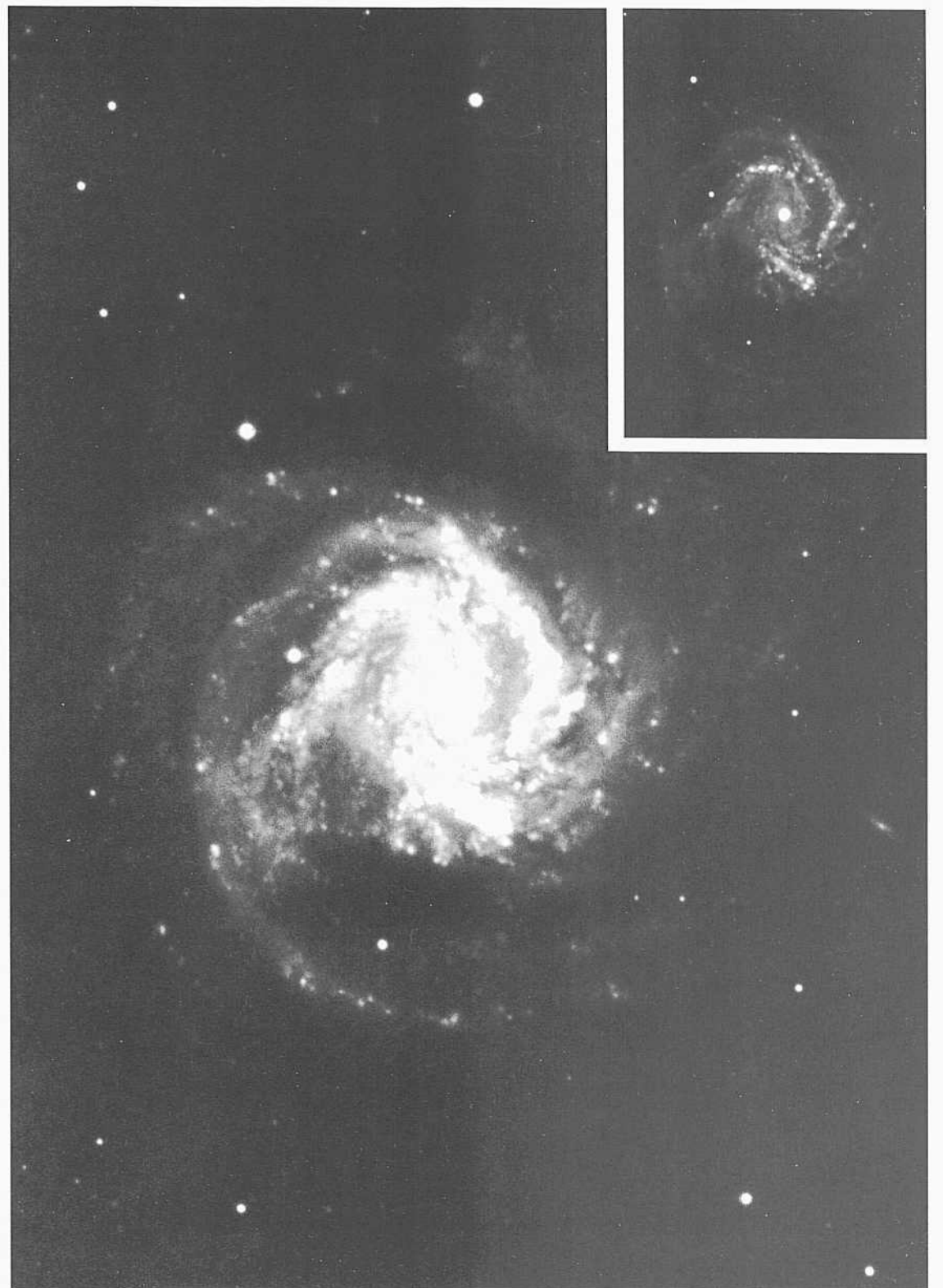
The largest **HII** regions resolve at about the 2" level. Individual brightest stars are difficult to separate from **HII** regions on blue or red plates. On yellow plates, where no **HII**-region emission lines exist, brightest-star candidates may exist, starting at apparent magnitude about  $V = 21.5$ .

NGC 4303      Sc(s)1.2      VCC 508  
 CD-2136-S      HA, p. 29  
 March 22/23, 1982      M61  
 103aO  
 50rain

As with NGC 4321 at the left, NGC 4303 is among the largest-angular-sized spirals in the Virgo Cluster region. Both are considered members of the cluster. Both have redshifts larger than the Virgo Cluster mean of  $\langle v_o \rangle = 976 \text{ km s}^{-1}$  (Sandage and Tammann 1990). The redshift of NGC 4321 is  $v_o = 1464 \text{ km s}^{-1}$ ; that of NGC 4303 is  $v_o = 1404 \text{ km s}^{-1}$ .

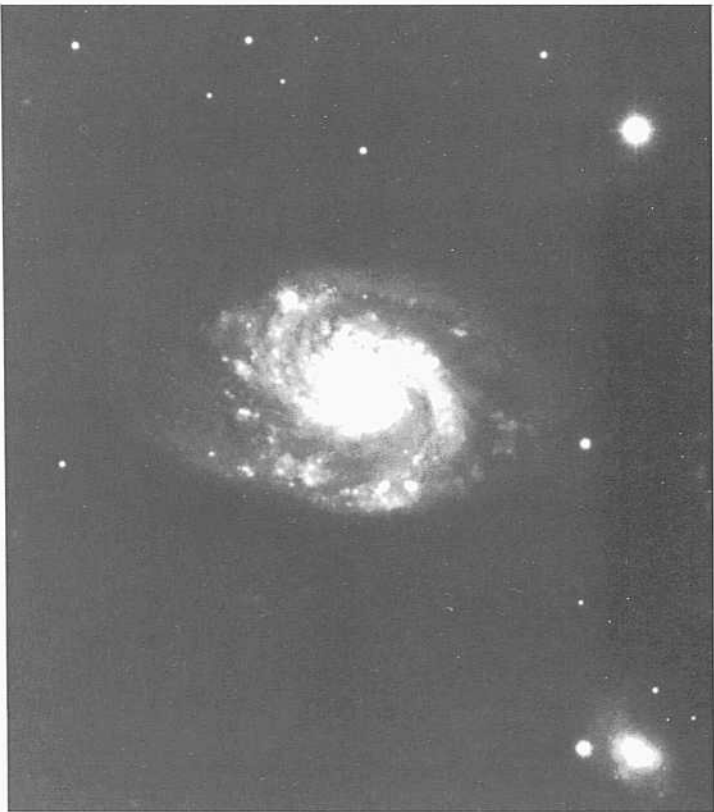
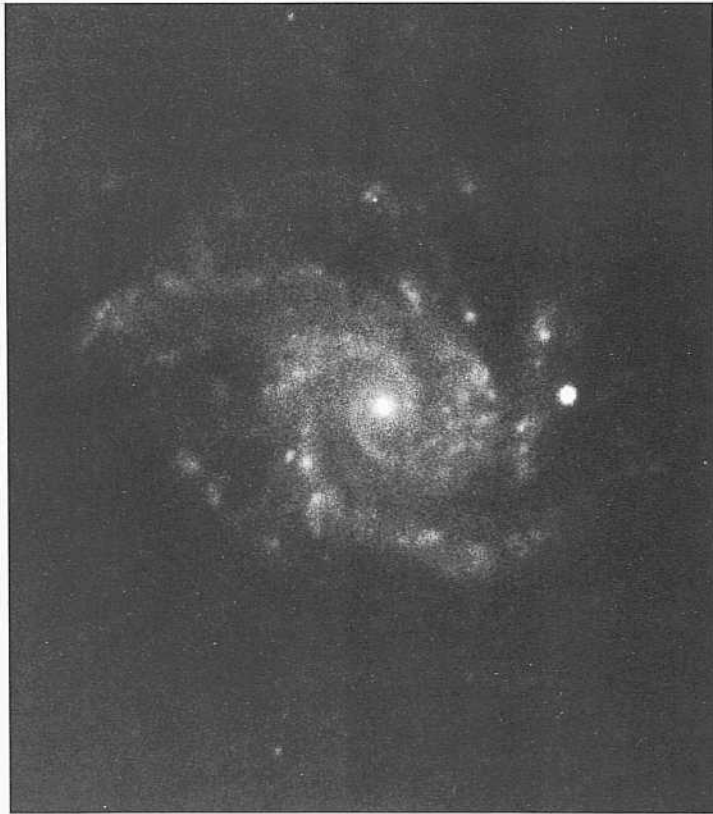
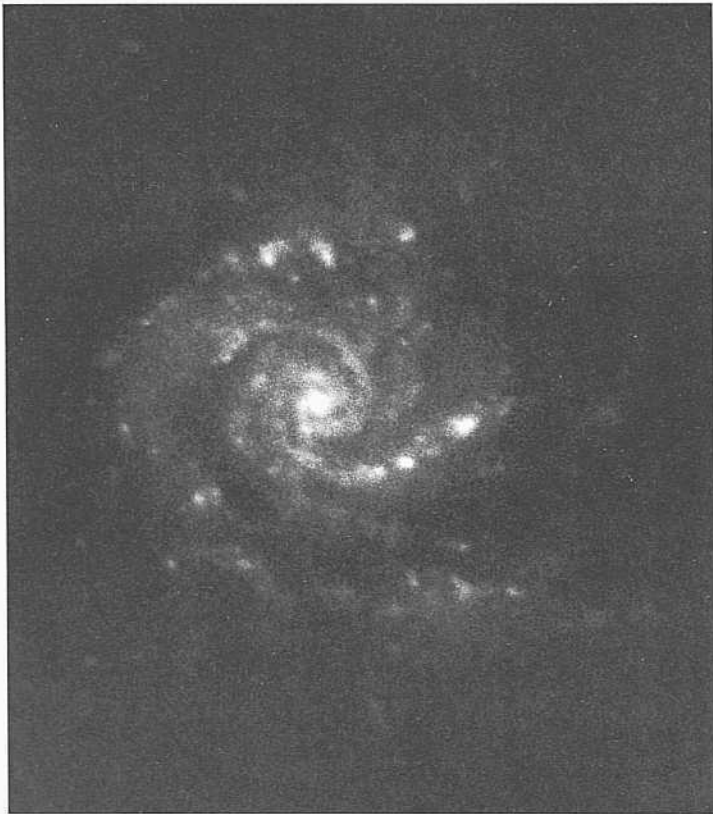
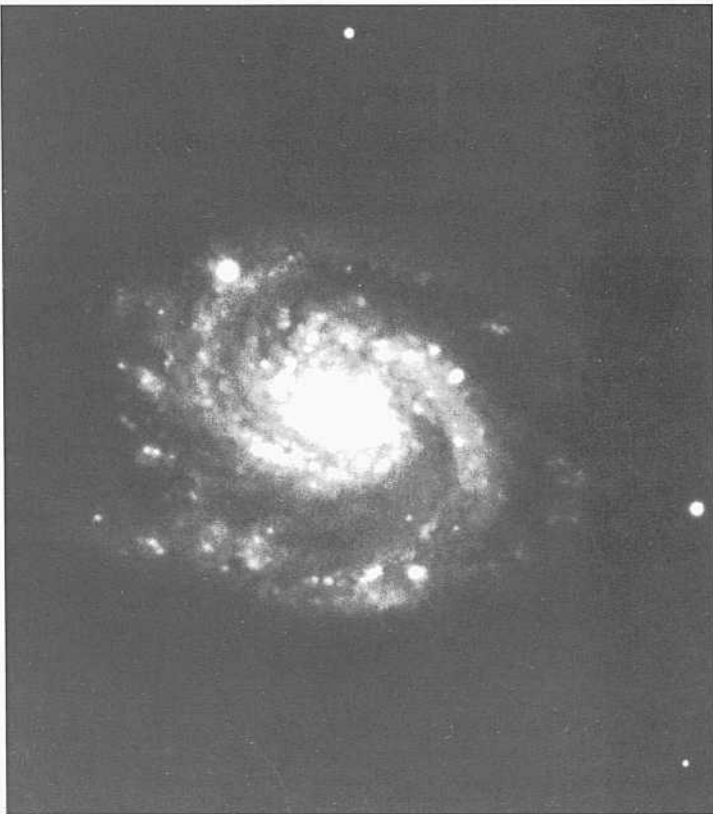
The arm pattern in NGC 4303 begins at the center as two thin dust lanes that wind outward through the inner disk, meeting the two principal luminous arms of the grand design type at the edge of the bright part of the disk. One of the principal arms is bent into two straight sections that meet at a sharp angle.

The arms are filled with **HII** regions that must be identified and eliminated from a candidate list before a survey of the brightest stars can be made.



PANEL  
213

PANEL  
214



Sc Classification Section (continued)

NGC 3893 Sc(s)1.2 Karachentsev 313  
 PH-7636-S Ursa Major Cluster  
 April 28/29, 1979  
 103aO  
 12 min

NGC 3893 and its companion, NGC 3896, are members of the Ursa Major Cluster, whose mean redshift is about  $\langle v_r \rangle = 980 \text{ km s}^{-1}$ . The angular size of the galaxy is large at  $D_{95} = 4.4'$  listed in the RC2. The size is slightly smaller than the largest galaxies in the Virgo Cluster such as NGC 4321 and NGC 4303 on the preceding panel.

The spiral pattern of NGC 3893 is of the grand design type having two principal spiral arms, both of high surface brightness for at least half a turn from their place of origin near the center. The largest of the numerous HII regions in the arms resolve (core + halo) at about the 2" level.

NGC 3893/3896 Sc(s)1.2 Karachentsev 313  
 PH-7636-S BCD Ursa Major Cluster  
 April 28/29, 1979  
 103aO  
 12 min

NGC 3896 (BCD, for blue compact dwarf) is a companion to NGC 3893 at an angular separation of  $3.7'$ . At the mean redshift distance of 19.6 Mpc for the cluster ( $l = 50$ ) the projected linear separation of the pair is small, at 21 kpc.

NGC 5660 Sc(s)1.2 pair?  
 PH-7864-S  
 Sep 5/6, 1980  
 I03aO  
 12 min

NGC 5660 may form a wide pair with NGC 5676 (Sc; panel 245) at a separation of  $30.5'$ . It also has a likely dwarf hIII companion of unknown redshift at the small separation of  $2.6'$ . The redshifts are  $z(5660) = 2433 \text{ km s}^{-1}$  and  $z(5676) = 2239 \text{ km s}^{-1}$ . At the redshift distance of 47 Mpc ( $l = 50$ ) the projected linear separations are 41.7 kpc for NGC 5676 and 3.5 kpc for the hIII companion.

The spiral pattern in NGC 5660 is prototype Sc(s) of the grand design type where the two main arms begin at the center.

NGC 34-64 Se(rs)I/SBc(s)I  
 CD-199-S  
 Feb 8/9, 1978  
 103aO + GG385  
 45 min

NGC 3464 is shown in the Se section here rather than with the SBc galaxies because we decided in preparing the KSA2 that the bar (or central oval) is weak enough to ignore. However, our sober second opinion is that the bar is strong enough, as viewed at this favorable inclination angle, to acknowledge. If the galaxy were viewed from an angle such that the central near-ring, which is almost complete, would appear circular, the bar would be considered to be as weak as those of others classed simply as Sc with arms starting from the edge of the inner disk.

The redshift is  $v_r = 3571 \text{ km s}^{-1}$ .

NGC 2912 Sc(a)1.3  
 PH-771 I-S  
 Feb 11/12, 1980  
 103nO  
 12 min

The spiral arms in this highly symmetric early-luminosity-class prototype Sc(s)I galaxy are well-formed, thin, and of the grand design type. The galaxy is remote by KSA standards. The redshift is  $v_r = 4399 \text{ km s}^{-1}$ .

NGC 2207/IC 2163 Se(s)1.2 pair  
 CD-580-S Sc(s)II-III  
 Oct 8/9, 1971!!  
 I03aO + GG385  
 55 min

The pair is clearly interacting, based both on the morphological distortion of IC 2163 (note the outward sweep on one side of the spiral pattern) and on the near equality of the redshifts. The redshifts derived from the Huchtmeier/Richter Catalog (1989) are  $z(2207) = 2597 \text{ km s}^{-1}$  and  $z(2163) = 2118 \text{ km s}^{-1}$ .

The angular separation of the centers of the pair is  $1.5'$ . At the mean redshift distance of 50 Mpc ( $l = 50$ ), the projected linear separation is small, at 22 kpc. However, it may be that the true separation is larger than this, and that the separation is mostly in the line of sight. The plane of NGC 2207 may be warped, but because the image is nearly face on, the warp, if present, would not be visible.

Note that although IC 2163 shows evidence of tidal distortion, NGC 2207 does not. This point illustrates that interaction cannot be judged by morphological distortion, at least in some cases.

Sc Classification Section (continued)

NGC 958            Sc(s)1.2  
PH-7843-S  
Sep 3/4, 1980  
103aO  
12 min

NGC 958, with redshift  $u_0 = 5738 \text{ km s}^{-1}$  is one of the most distant galaxies in the RSA (see the distribution of redshifts set out in RSA2, Fig. 2, p. 92). There are two major arms of the grand design type. Their beginning near the center is difficult to trace because of the high inclination to the sight line: the (s)-subtype designation is uncertain for that reason.

NGC 2955            Se(s)I            Racine wedge  
PH-8071-S  
Feb 5/6, 1981  
103aO  
12 min

NGC 2955, with  $v_r = 7051 \text{ km s}^{-1}$ , has the second-largest redshift in the RSA: consequently the number of resolution elements in the image is among the smallest in this atlas. (The galaxy with the largest redshift is NGC 7119, Sell, panel 282, with  $v_r = 9825 \text{ km s}^{-1}$ .)

There are two main arms of the grand design type beginning at the center in NGC 2955.

NGC 3478            Sc(s)I  
PII-8074-S  
Feb 5/6, 1981  
103aO  
12 min

The redshift of NGC 3478 is  $v_B = 6730 \text{ km s}^{-1}$ , the sixth-largest in the RSA, giving a distance of 135 Mpc ( $z = 50$ ). Hence the resolution of the image here is poorer than for most galaxies in this atlas.

The unusual feature of NGC 3478 is its six principal arms, each of which is thin and well defined. Each starts from the center and is generally smooth, although a few III1 regions exist in the outer parts of three of the arms.

New 6 = A2120-46    Sc(s)I  
CD-1543-S/Br  
Aug 7/8, 1980  
103aO + GG385  
45 min

The nearly edge on inclination of New 6 makes the classification of a grand design spiral pattern uncertain; what is evident is that the arms are thin, well defined, and well separated.

The redshift of New 6 is  $u_0 = 2600 \text{ km s}^{-1}$ .

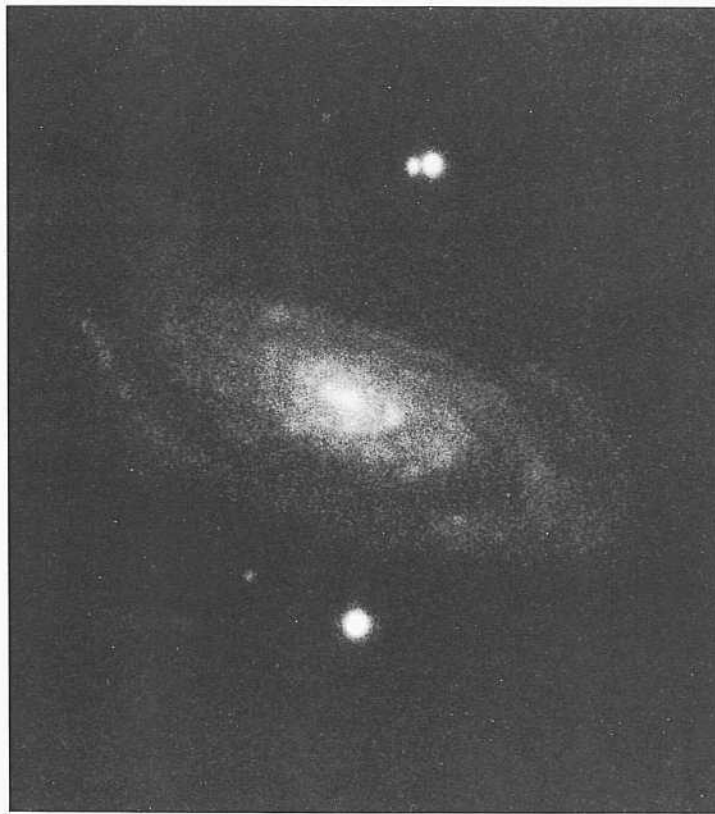
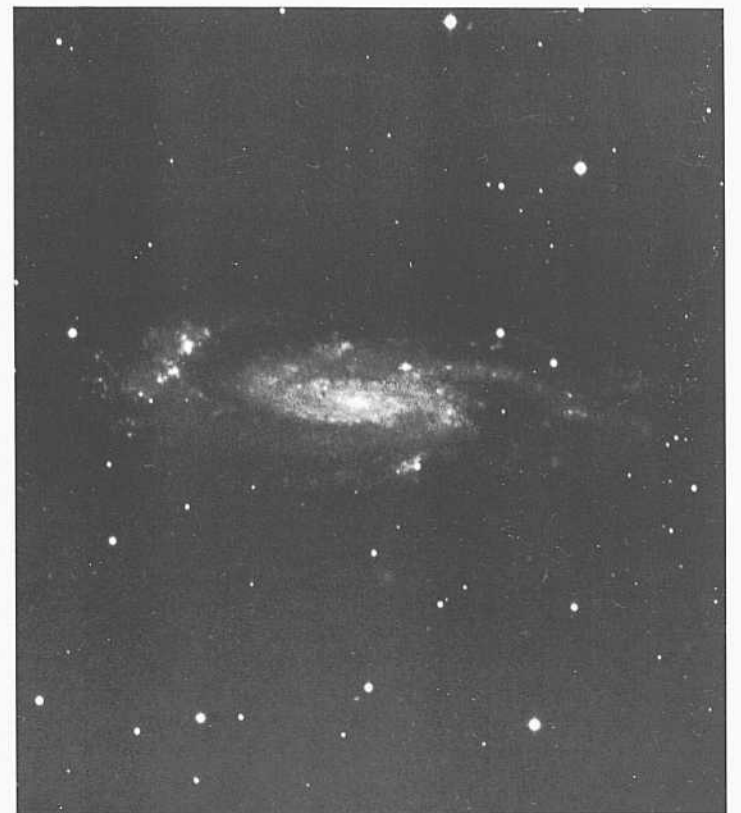
IC 764                Sc(s)1.2  
CD-1706-S  
Jan 5/6, 1981  
103aO + GG385  
45 min

The spiral arms in IC 764 are well defined and begin at the center. A central bulge is absent; the center is defined by a very small nucleus; hence the Sc classification is required.

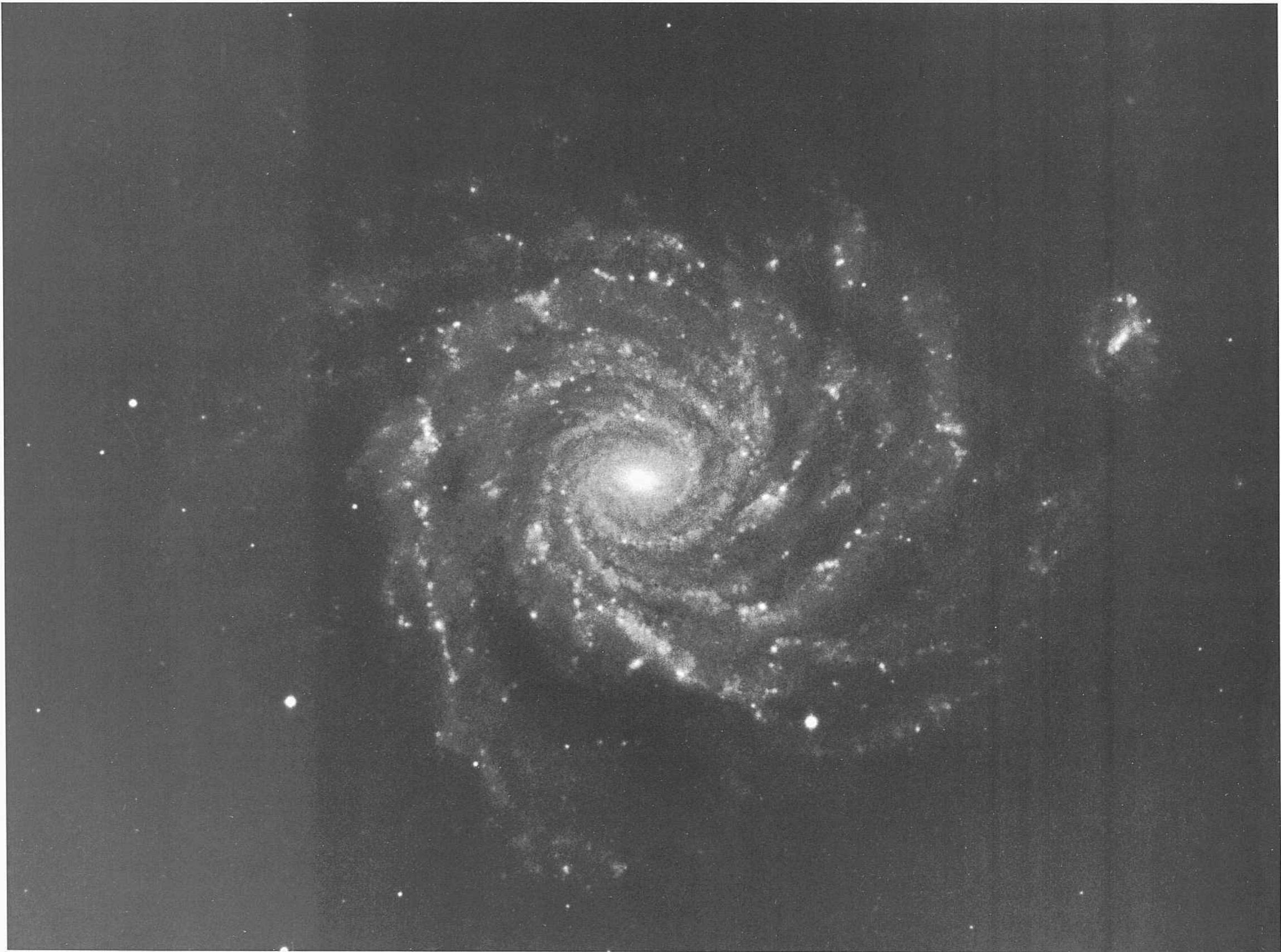
Many HII regions exist in one of the two principal arms. The largest have core + halo diameters of about 3". The redshift of IC 764 is  $v_r = 1851 \text{ km s}^{-1}$ .

NGC 3095            Sc(s)I-II pec            pair  
CD-128-HB  
Jan 5/6, 1978  
103aO + GG385  
80 min

NGC 3095 forms a wide apparent pair with NGC 3100 (SO<sub>1</sub> prolate; not in the RSA) at an angular separation of 10'. The redshift of NGC 3095 is  $v_r = 2564 \text{ km s}^{-1}$ ; the redshift of NGC 3100 is unknown. If the pair is physical rather than optical in the line of sight, the projected linear separation is 149 kpc. If the pair is in fact binary it is important because the large difference in morphological type (Sc vs. SO) would have important implications for the yet-unsolved problem of galaxy formation and subsequent evolution as related to the classification sequence.



PANEL  
216



*Sc Classification Section (continued)*

NGC 1232/1232A      Sc(ra)I      HA, p. 32  
CD-679-Br          SBmIII      panel S13  
Jaii 26/27, 1979  
103nO + GG385  
45 niin

NGC L232 is one of the wonders in the sky. It is the prototype of a highly regular multiple-armed spiral of the earliest luminosity class.

The arms start at the edge of a high-surface-brightness disk. Only two major arms begin at this rim. After about one-quarter revolution, each branches into two fragments which after further unwinding branch again until a highly multiple armed structure spreads over the outer disk.

Each fragment is well separated from the others; the geometrical entropy of the pattern is as low as in any galaxy in the RSA, equal or somewhat lower than in other highly regular Sc galaxies such as NGC 309 (Hubble Atlas, p. 32; panel 22 1 here) and NGC 536 1 (Hubble Atlas, p. 32; panel 2 1 7 here).

The arms are filled with III] regions and candidates for brightest stars. The largest III] regions have core + halo diameters of 3". The redshift is  $v_0 = 1775 \text{ km s}^{-1}$ .

The SBm III companion to the east is separated from NGC 1232 by 4.0'. There is confusion (c. 1992) as to whether this highly resolved galaxy is at the same distance as NGC 1232. The redshift of NGC 1232 A measured by Welch, Chincarini, and Rood (1975) of  $v_0 = 1780 \text{ km s}^{-1}$  was rejected by de Vaucouleurs, de Vaucouleurs, and Nieto (1979) in favor of  $u_0 = 6496 \text{ km s}^{-1}$  measured by them from an I let line. However, a 2.1-cm III redshift of  $v_0 = 1772 \text{ km s}^{-1}$  by Reif, Mebold, Goss, van Woerden, and Siegman (1982) confirmed the early value by Welch *et al.* But an even later 2.1-cm redshift confirms the larger redshift near  $v_0 = 6500 \text{ km s}^{-1}$ .

The resolution of NGC 1232A into star's and III] regions at the same level as in NGC 1232 itself makes no sense in the conventional interpretation of redshifts as a precise distance indicator if the high redshift value is correct. The case remains an important mystery (c. 1992).

At the mean redshift distance of 35 Mpc, the projected linear separation of NGC 1232 A from NGC 1232 is small at 4.1 kpc if they are at the same distance. If not, the mystery remains.



*Sc Classification Section (continued)*

NGC 5364            Sc(r)I            triplet  
PH-193-MH                            HA, p. 32  
May 13/11, 1950  
103aO  
30min

NGC 5364 has one of the most regular spiral patterns of all the RSA galaxies. The arms start tangent to a complete inner ring. The ring is not made by the near overlapping of opposite principal arms, as is the usual case. It is fed by two spiral arcs that start near the center. The description in the Hubble Atlas of the outer arms is still valid and is not repeated here.

NGC 5364, with a redshift  $v_n = 1140 \text{ km s}^{-1}$ , forms a physical triplet with NGC 5360 (BCD: not in the RSA:  $v_o = 1060 \text{ km s}^{-1}$ ) at a separation of 7.7', and with NGC 5363 (SO<sub>3</sub> in the RSA but not shown in this atlas:  $v_o = 1018 \text{ km s}^{-1}$ ) at a separation of 14.4'. At the mean redshift distance of 2.1 Mpc ( $z = 50$ ) the projected linear separations from NGC 5364 are 47 kpc and 88 kpc, respectively. The large morphological difference between NGC 5363 (SO) and NGC 5364 (Sc) is noteworthy.



PANEL  
217

PANEL  
218





*Sc Classification Section (continued)*

NGC 3938      Sc(s)I      Ursa Major Cluster  
PH-4523-S                      panels 220, S5

April 15/16, 1964

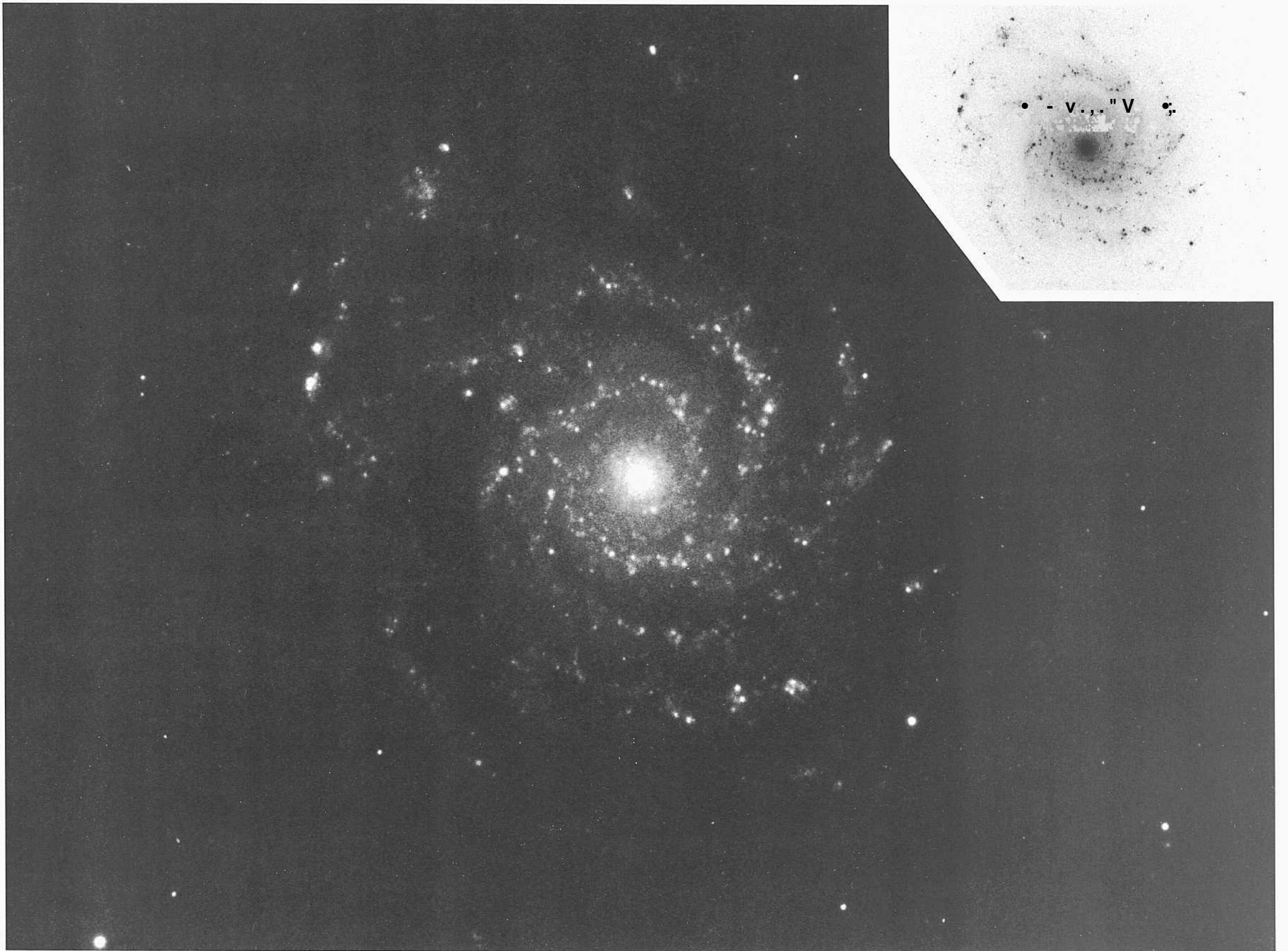
103aE + H $\alpha$  interference

120 min

NGC 3938 is a millipie-armed, early luminosity class Sc(s) galaxy- similar to NGC 1232 and M101 on the preceding panels. The **print** here is from a **Palomar** 200-inch **Hex** interference red plate. The image in the blue **continuum** is **on the** following panel at the upper **left** (panel 220).

The **HII** regions define the arms as beads on a string. As in M51 and M101, the two principal arms begin near the center and unwind for about half a revolution, branching thereafter. Thin dust lanes are present throughout the inner arm region, the inner disk, and the inside of the **principal** luminous arms.

The largest **HII** regions have diameters (core + halo) of about 5". The **redshift** of NGC 3938 is  $v_o = 844 \text{ km s}^{-1}$ .



PANEL  
219

PANEL  
220



Sc Classification Section (continued)

NGC 3938            Sc(s)I            **panels 219, S5**  
 PH-7637-S  
 April 28/29, 1979  
 103aO  
 12 min

The image here is made from a blue plate taken with the Hale 200-inch telescope at Palomar. The resolution into individual brightest stars is not as evident as, and will be more difficult to identify and measure photometrically than, in M101 or NGC 628. Nevertheless, the size of the largest HII regions at 5" shows that the low redshift of  $v_0 = 844 \text{ km s}^{-1}$  correctly indicates that the galaxy is close enough to permit study of the brightest stars at a level more favorable than in the Virgo Cluster ScI spirals, where the HII-region diameters are not larger than about 3".

NGC 628            Sc(s)I            HA, p. 29,31  
 PH-1151-S  
 Oct 24/25, 1955  
 103aO + GG13  
 25 min

The spiral pattern in NGC 628 is the prototype of a highly regular, two-principal-arm, grand design type. The central parts of the two major arms begin at the center as dust lanes. The lanes accompany luminous arms after about a quarter-rotation. The thin dust lanes then are generally on the inside of the luminous ridge-lines of the star-forming arm regions.

The resolution into individual stars begins at the bright apparent magnitude of about  $B = 20$ . This galaxy is one of the prime candidates wherein we must obtain (c. 1990) brightest-star photometry; the background surface brightness of the luminous arms is low compared with the much more difficult cases of M51 (panels 172, 177) and M83 (panels 300, 301), making this galaxy ideal for study.

The largest HII regions in NGC 628 are complex. Several with multiple nuclei have core + halo diameters of 5". The redshift of NGC 628 is  $v_0 = 861 \text{ km s}^{-1}$ . The resolution into stars is easier seen in NGC 628 than in the Virgo Cluster and Ursa Major Cluster spirals, but is more difficult than in M101 and its satellites, consistent with the intermediate value of its redshift.

NGC 3614            Sc(r)I            **pair:<sup>1</sup>**  
**PH-8051-S**                            **Racine wedge**  
 Feb 1/5, 1981  
**103aO**  
 12 min

The spiral pattern in NGC 3614 is that of the multiple-armed type, starting with two main arms that begin from an internal ring and that branch after about three-quarters of a revolution. The arms are thin and can be well traced, requiring the early luminosity classification.

A candidate for a close companion exists at a separation of 2.6'. Its redshift is presently (1990) unknown. If it is similar to the value for NGC 3614 of  $v_0 = 2362 \text{ km s}^{-1}$ , the projected lineal separation of the pair would be small, 36 kpc at the redshift distance of 47 Mpc ( $z = 0.05$ ). The brightnesses of the HII-region knots in the two galaxies are similar enough to argue for equality of distances.

NGC 5161            Sc(s)I  
 CD-1478-S/Br  
 May 11/12, 1980  
 103aO + GG385  
 45 min

Two opaque dust lanes begin at the small nucleus in a prototypical (s) pattern. These lanes change into luminous arms close to the center, whereupon the arms soon branch into a multiple-arm pattern similar to that in M31 (panel 149). Going outwards, the arms cross the major axis five times on one side of the major axis; on the other side four crossings are definite. An arm fragment that would provide the fifth crossing is present, but is of very low surface brightness.

The numerous HII regions in the arms are unresolved. The redshift of NGC 5161 is  $v_0 = 2113 \text{ km s}^{-1}$ .



Many of the galaxies on this panel are more distant than most RSA galaxies. As a consequence, the prints have fewer resolution elements than do most prints on preceding panels. Despite the relative lack of resolution, it is evident that all galaxies here have very regular spiral patterns of small geometrical entropy, requiring the luminosity class I category.

NGC 309            Sc(x)I            HA, p. 32  
 PH-15-MH  
 Nov 15/16, 1949  
 103aO  
 20 min

The internal ring from which the highly branched multiple arms begin in NGC 309 is almost complete. The ring may attach to the ends of a central bar, similar to the pattern in the prototype SBbc(rs)II galaxy NGC 1073 (Hubble Atlas, p. 49; panel 294 here), but any bar that is present in NGC 309 is weak.

Many HII regions are present in the arms, but none are resolved. The distance is large, as is also shown by the high redshift of  $v_o = 5786 \text{ km s}^{-1}$ .

NGC 2776            Sc(rs)I  
 PH-7991-S  
 Feb 2/3, 1981  
 103aO  
 12 niin

The reproduction here is made from a weak 200-inch Palomar plate taken through clouds.

The spiral arms start from the outer edge of a smooth inner disk of moderately high surface brightness [not a luminous inner ring as in most (r) subtypes]. Three, rather than two, arms begin from this edge. None of the HII regions resolve into disks at the 1" level. The redshift of NGC 2776 is  $v_o = 2673 \text{ km s}^{-1}$ .

NGC 2280            Sc(s)1.2  
 CD-664-Br  
 Jan 22/23, 1979  
 103aO + GG385  
 45 min

As in the pattern of NGC 5161 on the preceding panel, the multiple-armed pattern of NGC 2280 can be traced to show five crossings of the major axis on one side and four on the other. Six crossings on either side of the *minor* axis can be counted.

The redshift is  $v_o = 1709 \text{ km s}^{-1}$ .

NGC 2989            Sc(s)I  
 CD-683-Br  
 Jan 26/27, 1979  
 103aO + GG385  
 45 min

The angular diameter of NGC 2989 is small at 1.4": the redshift is  $v_o = 3916 \text{ km s}^{-1}$ . The spiral pattern is regular and of the multiple-armed type, similar to all others on this panel.

NGC 1376            Sc(s)I  
 PH-7919-S  
 Nov 7/8, 1980  
 103aO  
 12 min

The spiral pattern of NGC 1376 is similar to that of NGC 309 at the upper left except that the inner ring is absent; the inner arms begin at the nucleus as in M101 (Hubble Atlas, pp. 27, 31; panel 218 here) rather than in the (r) pattern as in prototype NGC 309.

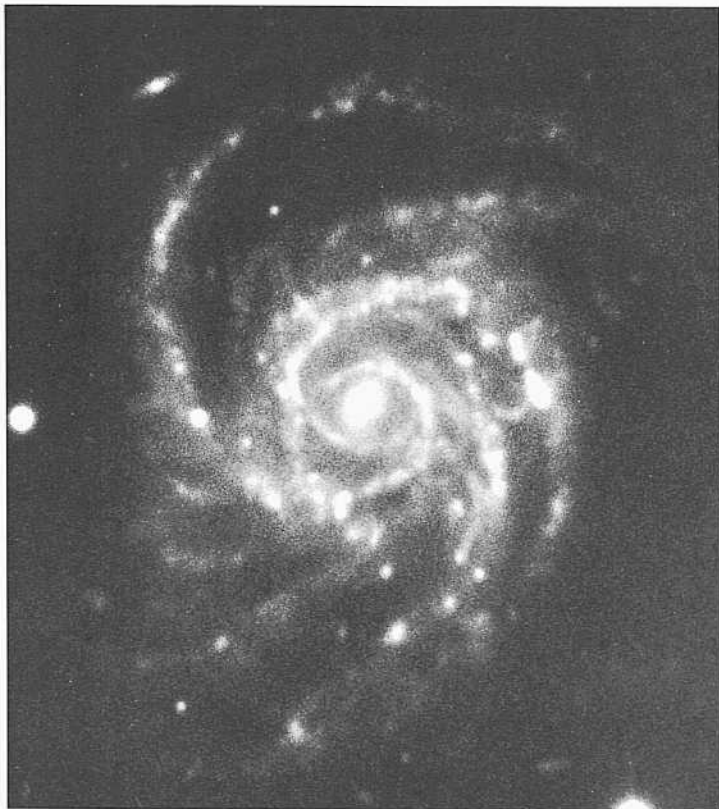
The redshift of NGC 1376 is  $v_o = 4198 \text{ km s}^{-1}$ .

NGC 2998            Sc(rs)I  
 H-2346-H  
 Nov 27/28, 1946  
 103aO  
**30 niiii**

The spiral pattern of NGC 2998 is of the same type as that of the other five galaxies on this panel. Five arm crossings can be counted on each side of the major axis. The arms are thin and very well defined, requiring the early luminosity class.

The reproduction here is made from a plate taken in excellent seeing with the Hooker 100-inch telescope on Mount Wilson.

The redshift of NGC 2998 is large, at  $v_o = 4813 \text{ km s}^{-1}$ .



PANEL  
221



PANEL  
222



*Sc Classification Section (continued)*

NGC2997      Sc(s)1.3      panel S5

CD-710-S

Feb 3/1, 1979

103aO + GG385

15 min

The spiral pattern in NGC 2997 is of the **grand design** type; **two main arms** in the central region branch into **thick fragments covering the outer disk**, filling it much as in NGC 5194 (MS I; Hubble Atlas, pp. 26, 171; plates 172, 177 here), but **less extreme here**.

The inner disk is covered with thin, tightly wound spiral **dust lanes**. The **two most** opaque lanes **begin at the center** [(s) type] silhouetted against the **high-surface-brightness** inner disk. The **two** main luminous arms associated with these dust lanes begin some **distance from the center**, each after about half a turn **outward from** the parent dust lanes. The **arms** become luminous on the outside of the **accompanying** spiral dust pattern.

A group of "hot spots" **exist in the complex center** (Sersic and Pastoriza L965).

Many **till** regions exist in the high-surface-brightness luminous arms. The largest are complexes of several centers.

As in M51, the identification and **photometry** of individual stars will be difficult because of the problem of identification and elimination of the small **III** regions. The **high surface** brightness of the **arms** also will make **photometry** difficult.

The **redshift** is  $v_{\text{sr}} = 199 \text{ km s}^{-1}$ .

## THE SCI-II SUBCLASS

NGC 5247      Sc(s)I-II      panel S5  
CD-908-IIB  
April 29/30, 1979  
103aO + GG385  
45 mill

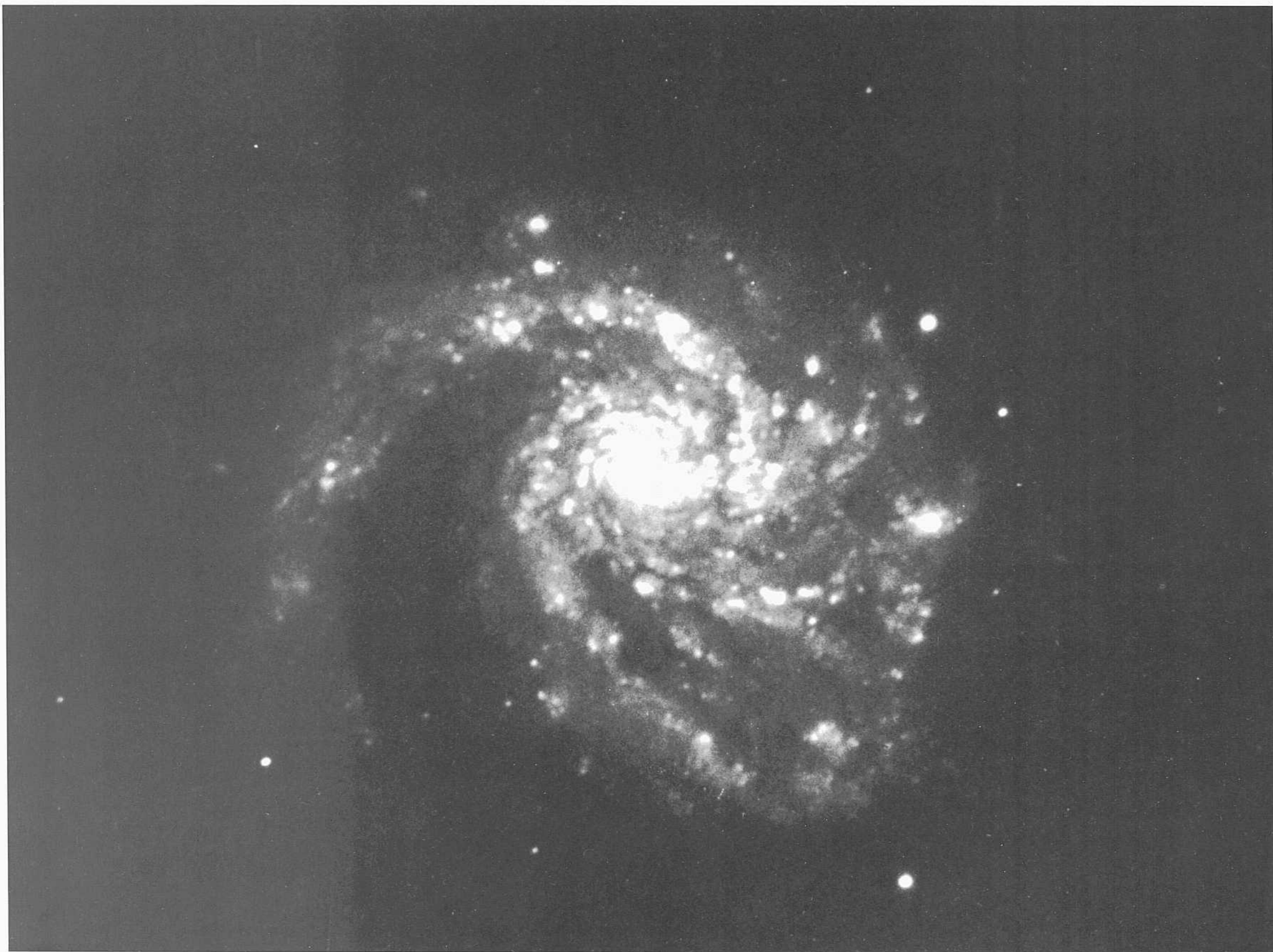
NGC 5247 is a prime example of spiral **structure** of the grand design type. Two very-well-defined principal arms start as narrow luminous spiral lanes at the center and can be traced at **high** surface brightness for slightly more than half a revolution. A set of **fainter-surface-brightness** arms exist **inside** the main **set**. These also begin near the center, but are thicker and less well defined.

The largest **HII-region** complexes in the main arms have core + halo diameters of about 4". No resolution into individual stars is evident brighter than about magnitude  $V = 22$ . The redshift of NGC 5247 is  $v_0 = 1143 \text{ km s}^{-1}$ .



PANEL  
223

PANEL  
224







Sc Classification Section (continued)

NGC 157      Sc(s)II-III      HA, p. 29  
 PH-1054-S  
 Aug 24/25, 1955  
 103aO  
 SO min

Although the spiral pattern in NGC 157 consists of two main grand design arms of high surface brightness beginning near the center, the entire disk is filled with thick arm fragments. The pattern differs from that of NGC 5247 two panels back, where the grand design arms are thin and cover only a small fraction of the disk area.

The main arms in NGC 157 branch such that eventually three crossings of separate arm fragments occur on one side of the major axis, proceeding outward. On the other side, spiral dust fragments cover the disk. The geometrical entropy is high. The luminosity class given in the HSA2 is I-II. It is revised here to II-III because of the disorder in the arms.

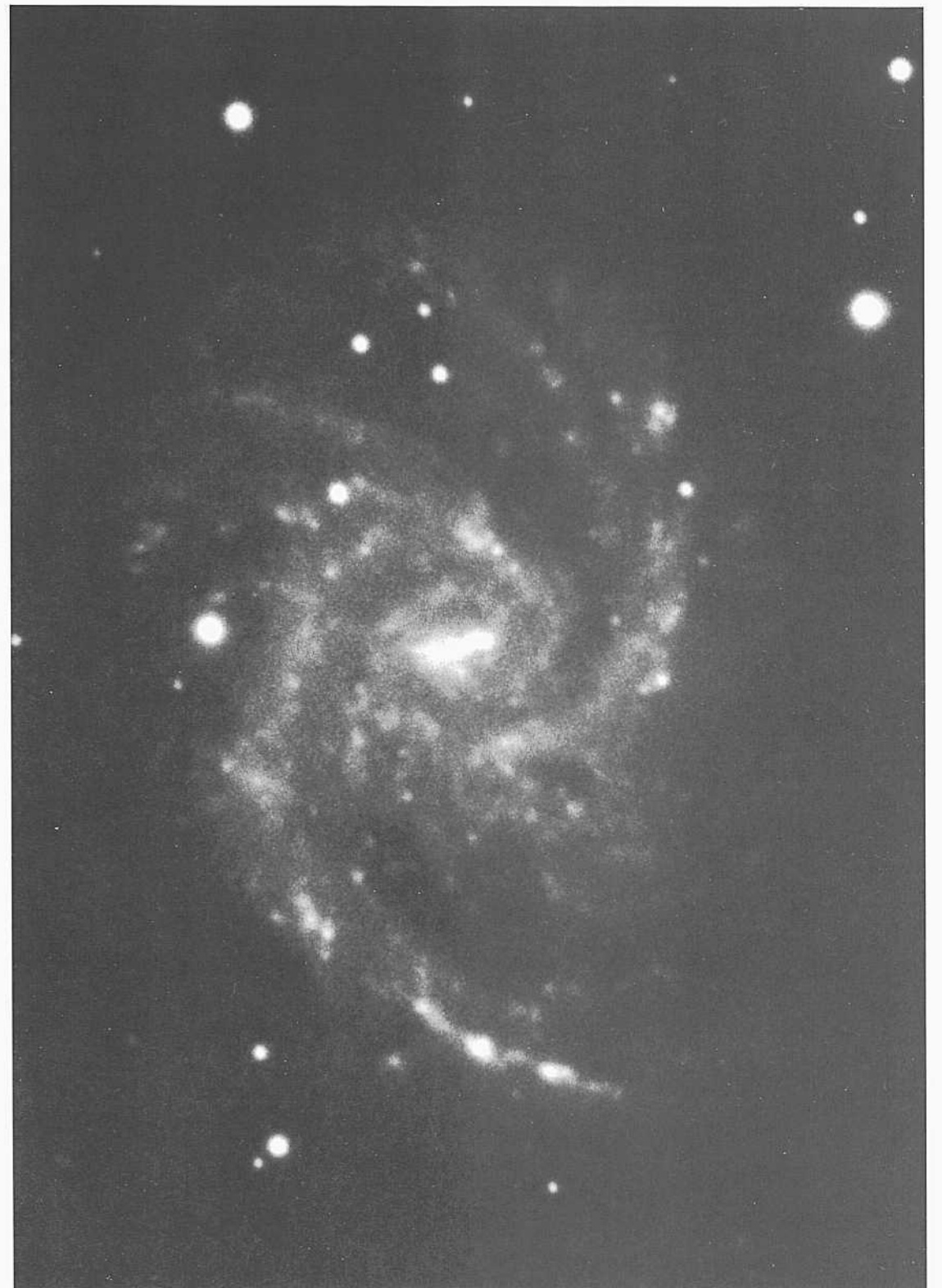
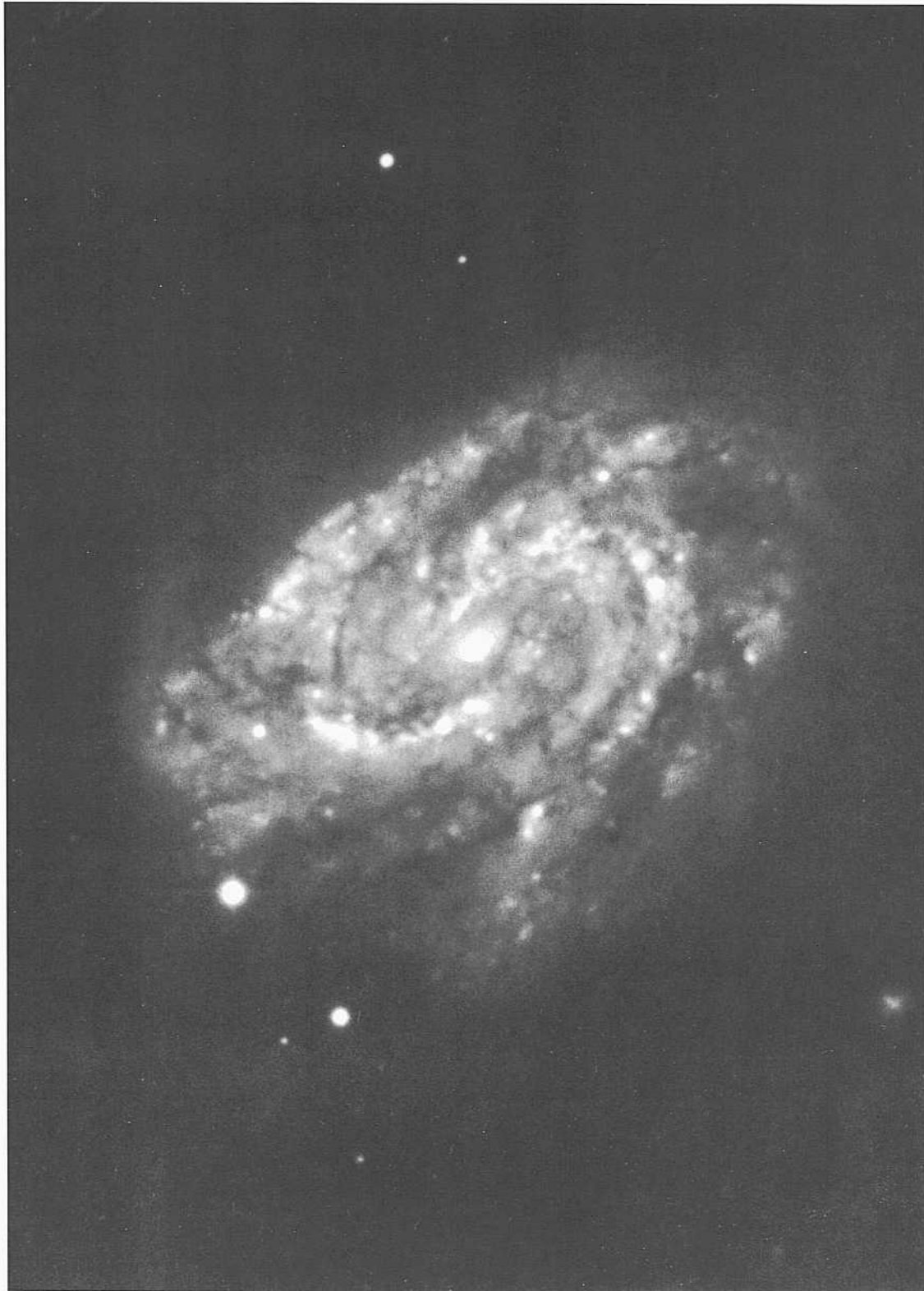
The III regions are unresolved at the 2" level. Brightest stars are not easily resolved on the high-surface-brightness background. The redshift is  $v_r = 1813 \text{ km s}^{-1}$ .

NGC 7125      Sc(rs)I-II/SBc(s)I-H      pair  
 CD-1520-S/Br  
 Aug 5/6, 1980  
 103aO + GG385  
 45 min

NGC 7125 forms a physical pair with NGC 7126 (Sab: panel 1 1 1) at 6.2' separation. The redshifts are  $v_r(7125) = 2910 \text{ km s}^{-1}$  and  $v_r(7126) = 2888 \text{ km s}^{-1}$ . At the mean redshift distance of 5.8 Mpc ( $z = 0.05$ ), the projected linear separation is 105 kpc.

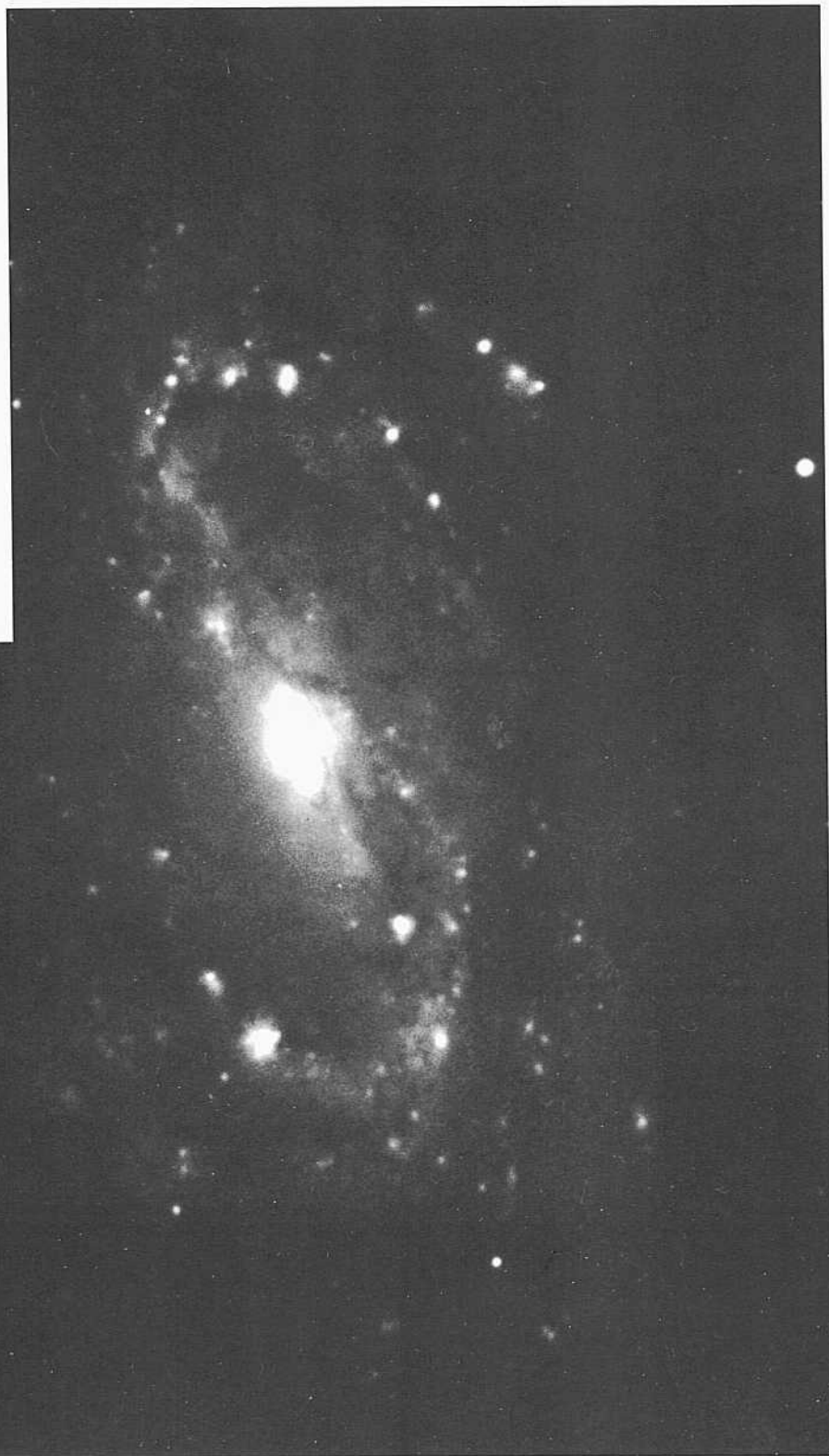
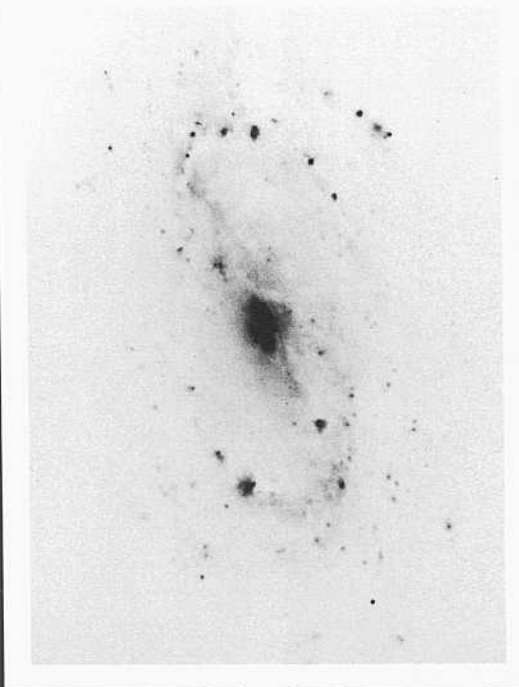
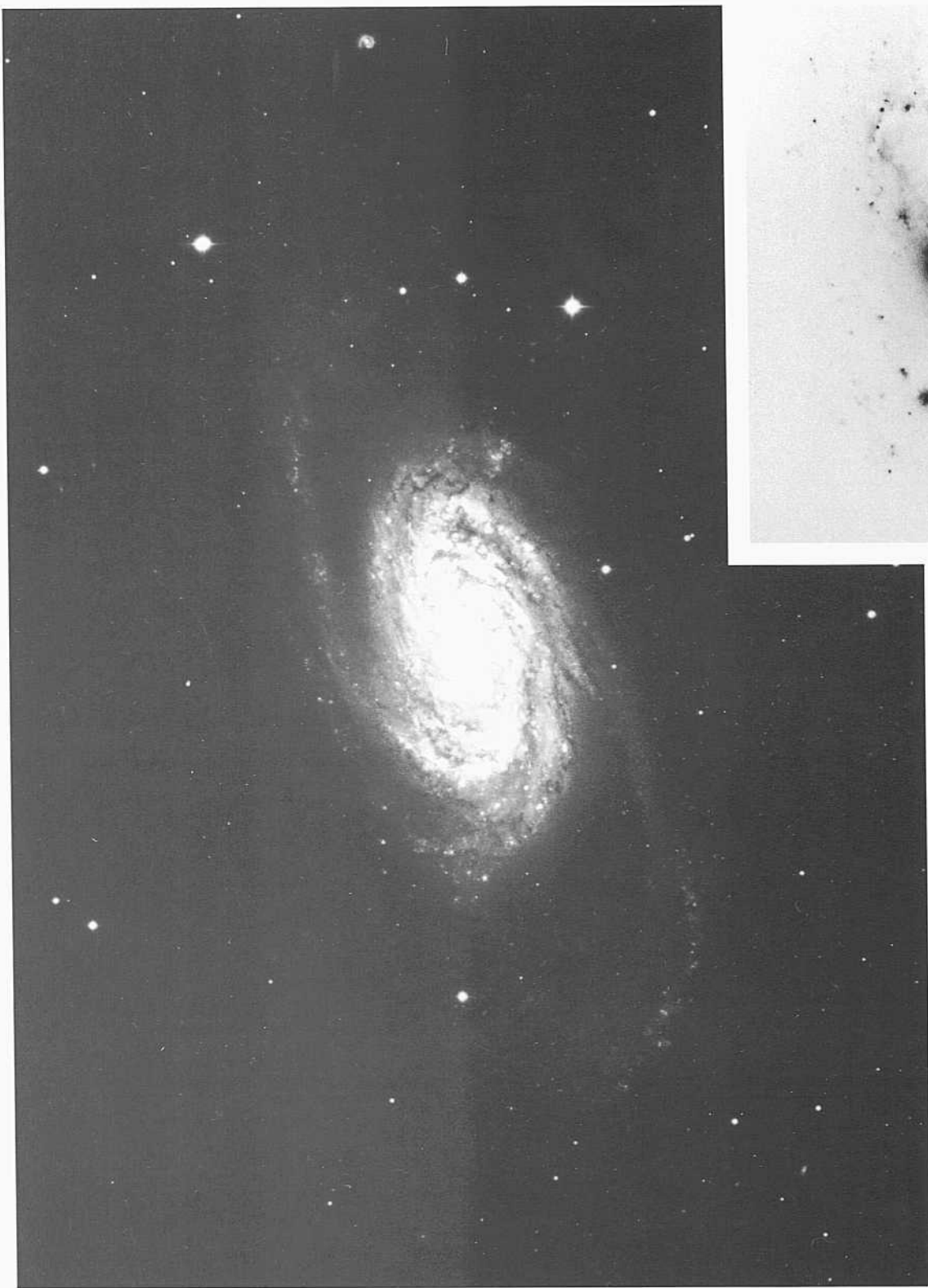
A short bar exists in the central region of NGC 7125 from which the two principal arms begin at each end. The two main arms can be traced for a complete revolution as the principal spiral features, albeit with branching into fragments that generally parallel the main pattern as it unwinds outward.

The III regions are unresolved. No candidates for brightest stars exist to this plate limit.



PANEL  
225

PANEL  
226



NGC 2903      Sc(s)I-II      HA, p. 35  
 PH-71-MH  
 Feb 15/16, 1950  
 103aO  
 30 min

NGC 2903 is nearby, as judged by the degree of resolution **into individual stars beginning** at about  $B = 22$  in the two very-low-surface-brightness outer **spiral** arms. Resolution is not as easy as in M101, but is much easier **than** in any of the Virgo Cluster spirals **such as M100. The redshift of NGC 2903 is  $v_0 = 472 \text{ km s}^{-1}$ .**

The surface brightness of the inner **spiral** pattern is exceptionally high. The arm **pattern** is thick. **In addition to the two main arms, well** seen in the print at the right, the outer arm pattern **is multiple**, filling the disk. On the short exposure on the right, the **central** pattern is a weak **bar** from which one of the **two principal arms** springs. The opposite arm forms part of the slightly curved bar on that side.

The dust lanes throughout the disk are **spiral** fragments. Their opening (pitch) angles near the edges of the bar are very steep (**the** lanes begin almost **perpendicularly** to the bar), flattening to the pitch angles of an ordinary **non-barred** spiral in the outer pattern. These dust lanes undoubtedly trace the flow pattern of the interstellar medium as its **hydrodynamic** response to the gravitational potential of the **rotating** bar, including shocks near the **leading** edges of the bar (e.g., Huntley 1978, 1980, and references therein).

NGC 2903      SC(B)I-II      HA, p. 35  
 PH-3902-S  
 Feb 5/6, 1962  
 L03aE + Ha interference  
 90 min

The weak bar pattern is seen **well** in this Ho. interference filter photograph taken **with the Palomar 200-inch Hale Telescope**. The bar is **not** well defined **but** is definite. U ran **also** lie seen as an intensity enhancement across the disk in the **continuum** photograph on the left.

The dust lanes along the bar on either side, situated as usual on the **leading edges** of the bar **relative to the direction of rotation, are characteristic** of dusty barred spirals. **They are thought to be the result of shocks in the vicinity of the bar caused by the bar's rotation (Prendergast 1962, 1983; Peterson and Huntley 1980; Huntley 1978, 1980).**

The **largest HII-region complexes** seen here have **core + halo diameters** of about 6". The redshift of NGC 2903 is small, at  $v_0 = 472 \text{ km s}^{-1}$ .

Note **the difference in the** enlargement of this image **compared with** that at the left.

The four galaxies on this panel and the six on the next continue the spiral pattern of two principal arms. In the galaxies here, the arms either fragment themselves or are joined near the center by lower-surface-brightness secondary (fossil) arms which, together with the two main arms, cover the disk with a high-surface-brightness spiral pattern. Yet the arms and their fragments are definite, not filamentary as in NGC 2841 (panels 142, S4, S12).

NGC 2441      Sc(r)I-II  
 PH-7551-S  
 Nov 6/7, 1978  
 103aO  
 12 min

At first glance the spiral pattern in NGC 2441 seems similar to that in NGC 309 (panel 221), where an almost-complete internal ring exists from which the spiral arms originate. The impression, however, is deceptive. Very-low-surface-brightness, luminous thin inner arms in NGC 2441 connect with the center, together with two associated dust lanes. After half a revolution the nearly invisible arm on one side increases in surface brightness and, after nearly overlapping a segment of the opposite bright arm, winds outward for another nearly half-revolution. At that point it overlaps with a section of the other arm which, in the meantime, has itself branched at nearly right angles to form part of the apparent inner ring. Hence the pattern is disturbed on one side with overlapping arms, which, however, still are narrow and well defined as fragments.

The redshift is high, at  $v_r = 3815 \text{ km s}^{-1}$ .

NGC 7412      Sc(s)I-II  
 CD-1510-S/Br  
 Aug 4/5, 1980  
 103aO + GG385  
 45 min

The spiral pattern is similar to that of M51 (panels 172, 177). The arms are of the grand design type and are massive in the sense of Reynolds (1927a.ii). The two major arms start at the center, each dominated at the beginning by a thin dust lane which continues outward on the inside of each luminous arm. Secondary, lower-surface-brightness arms exist, one inside of one of the main arms and the other outside of the opposite main arm.

None of the MI! regions are resolved at the 1.5" level. The redshift of NGC 7412 is  $v_r = 1691 \text{ km s}^{-1}$ .

NGC 908      Sc(s)I-II  
 CD-1513-S/Br  
 Aug 4/5, 1980  
 103aO + GG385  
 45 min

As in NGC 7412 below at the left, the arms are massive in the sense of Reynolds (1927a,b). Although the spiral pattern is of the grand design, there are more than two dominant arms. Going outward along the major axis, four crossings of the major axis can be counted on either side.

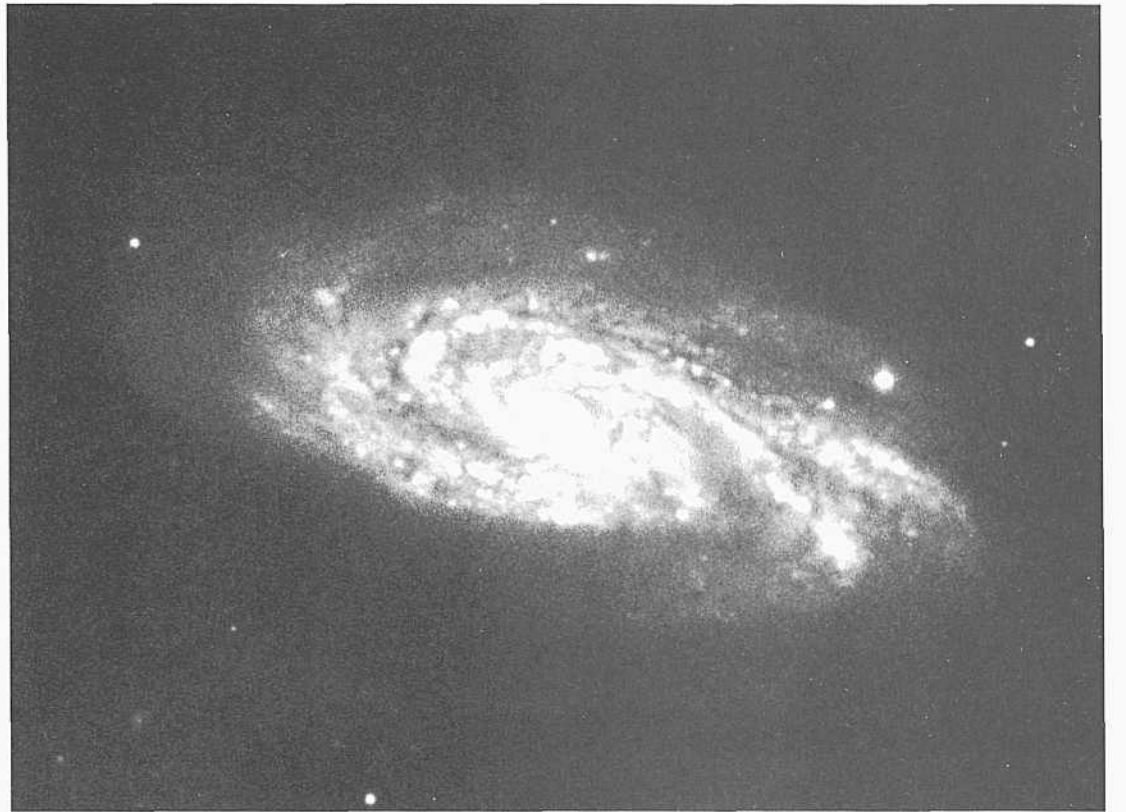
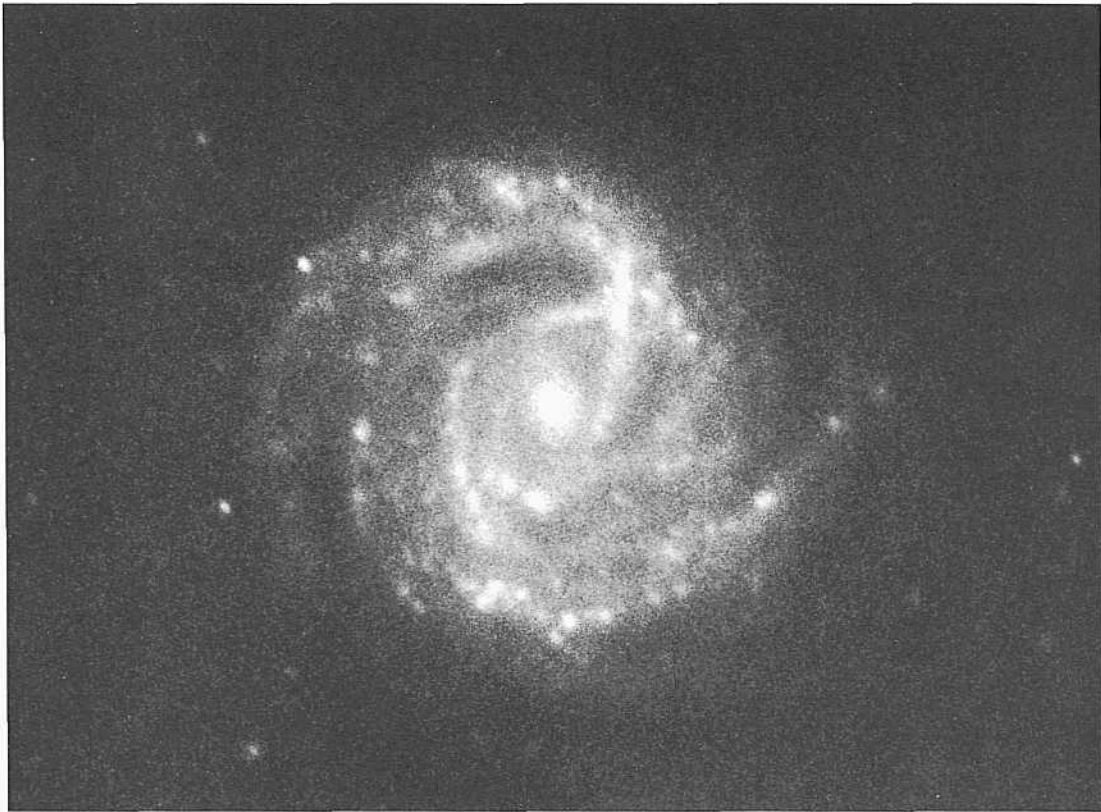
The redshift of NGC 908 is  $v_r = 1563 \text{ km s}^{-1}$ .

NGC 1042      Sc(rs)I-U      pair  
 CD-1579-S/Br  
 Aug 10/11, 1980  
 103aO + GG385  
 45 min

NGC 1042, redshift  $v_r = 1436 \text{ km s}^{-1}$ , forms a probable physical pair with NGC 1035 (Sc; panel 291) whose redshift is  $v_r = 1307 \text{ km s}^{-1}$ . The angular separation of  $22.5'$ , at a mean redshift distance of 27 Mpc ( $H = 50$ ), gives the projected linear separation of 177 kpc.

Two principal arms begin near the center but on the rim of a smooth central disk. The arms branch into fragments, one after a quarter revolution outward, the other after half a revolution.

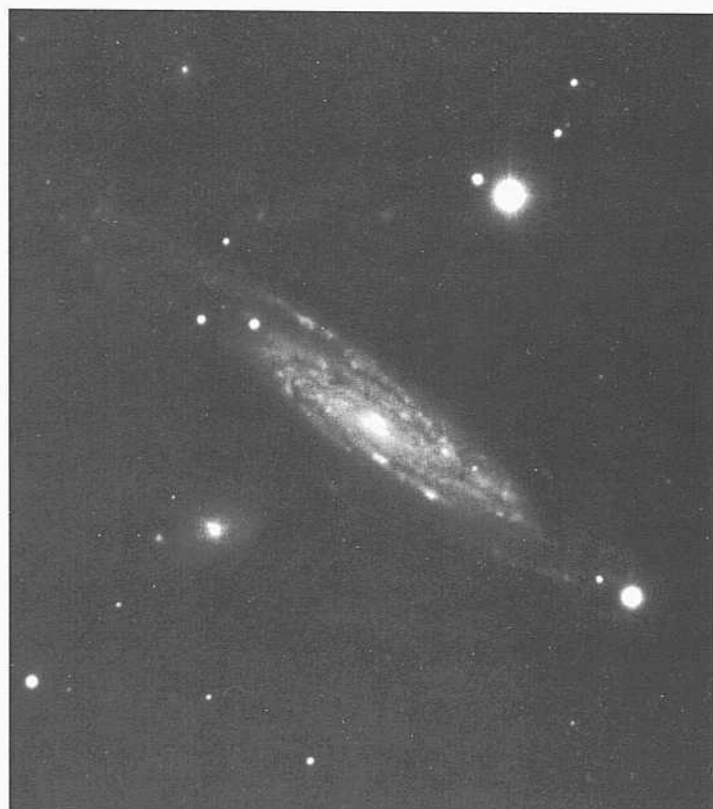
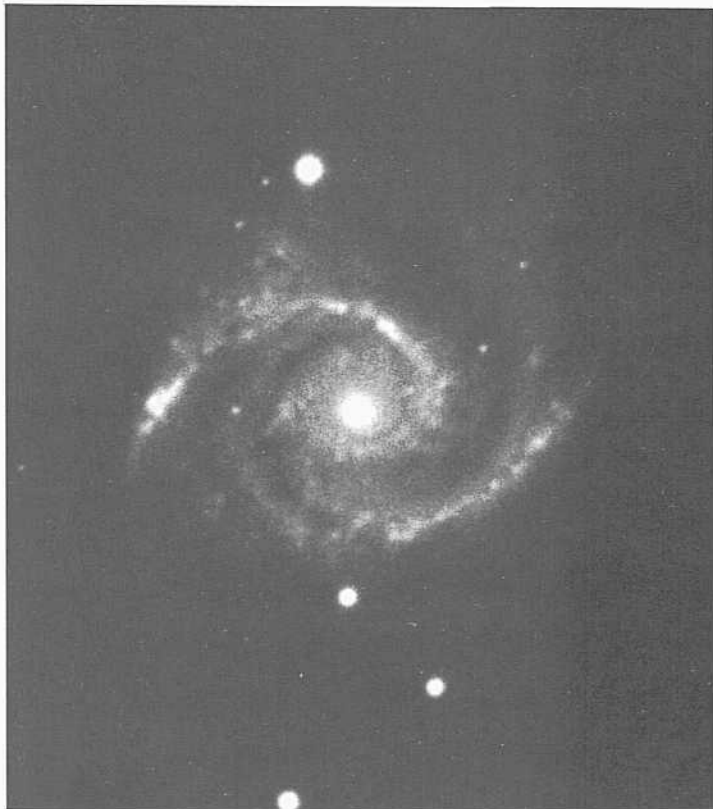
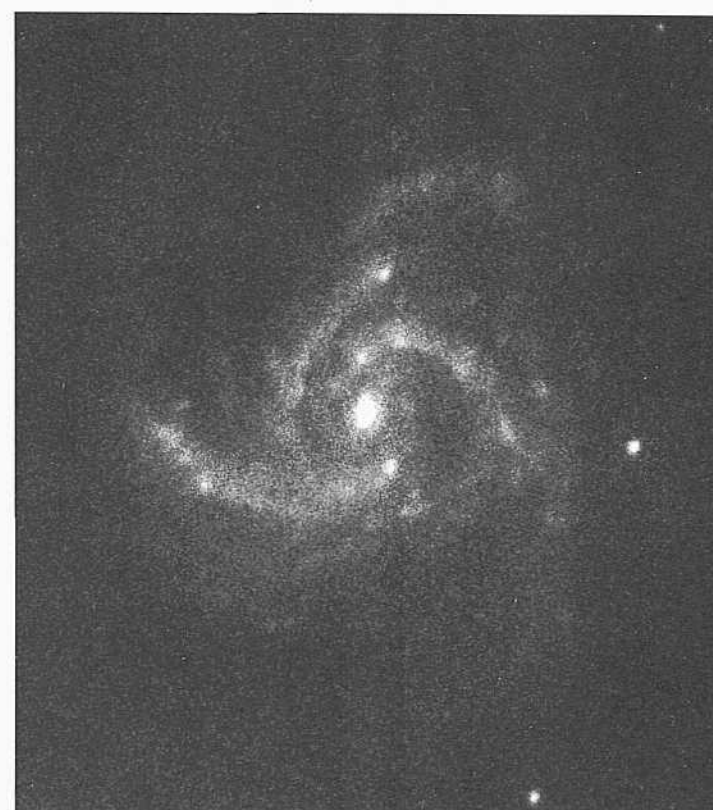
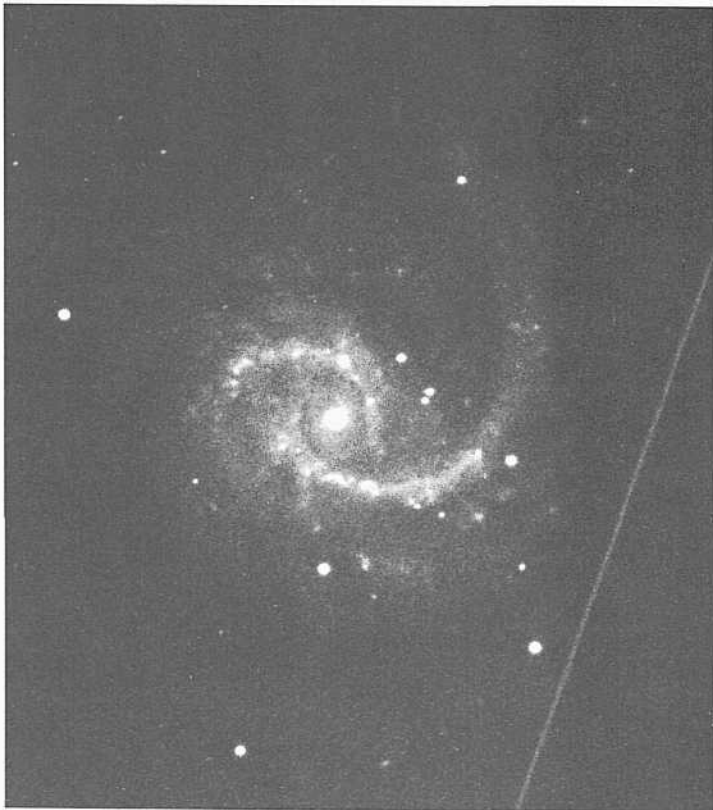
The largest of the **HII-region** complexes is about 1" in diameter (core + halo).



PANEL  
227



PANEL  
228



**T**  
 I. In six galaxies on this panel show spiral patterns of the grand design type, although four have multiple arms rather than simply two principal arms.

IC 2627            Sc(rs)I-II

CD-1666-S

Dec 30/31, 1980

103aO + GG385

45 min

IC 2627 has only two principal arms, which are thin and do not branch into secondary arms of the kind that cover the underlying disk in other galaxies of this type. The disk here is threaded only by the two high-surface-brightness principal arms.

The arms begin near the center, yet on the edge of the small smooth central disk.

The redshift of IC 2627 is  $v_0 = 1804 \text{ km s}^{-1}$ .

NGC 6878            Sc(r)1.3            group?

CD-1107-Br

Aug 18/19, 1979

103aO + GG385

45 min

This exquisite spiral is of small angular diameter,  $D_{95} = 1.6'$ ; its redshift is large, at  $v_0 = 5791 \text{ km s}^{-1}$ . It is in a field of several other galaxies of similar angular diameter, which may form a physical group. NGC 6878A (RSab11) is at a separation of  $10.3'$  toward the north (the declination in the RC2 is incorrect) at a projected linear separation of 347 kpc. An anonymous high-surface-brightness closer candidate companion (unknown redshift) at a separation of  $6.7'$  has a projected linear separation of 226 kpc. Many other galaxies of similar angular size over a wider but still nearby field are seen on the Palomar Schmidt survey prints. However, this field is in the neighborhood of the Telescopium Group, whose mean redshift is  $\langle v_0 \rangle = 2733 \text{ km s}^{-1}$  (Sandage 1975b); NGC 6878 may simply be in the background.

The spiral pattern is prototypical ScI; two principal arms start at the edge of a smooth, central high-surface-brightness inner disk.

NGC 7300            Sc(s)I-II

CD-1573-S/Br

Aug 10/11, 1980

103aO + GG385

45 min

The multiple arms in this highly inclined galaxy are thin and well developed. The nucleus is small, characteristic as a classification criterion for Sc galaxies.

The redshift is  $v_0 = 5021 \text{ km s}^{-1}$ .

NGC 5297            Sc(s)I-II            Racine wedge

PH-8093-S

Karachentsev 394

Feb 6/7, 1981

103aO

12 min

NGC 5297 forms a close physical pair with an anonymous (SO pec) companion at an angular separation of  $88''$ . The redshift from the RSA is  $v_0 = 2654 \text{ km s}^{-1}$ . Karachentsev (1987) lists  $v_0 = 2755 \text{ km s}^{-1}$  for the SO companion. At the redshift distance of 53 Mpc, the projected linear separation of the pair\* is very small at 23 kpc.

The multiple arms in NGC 5297 are thin and well defined but the pattern is mostly hidden by the high inclination.

NGC 7309            Sc(rs)I-II

P11-7688-S

Sep 26/27, 1979

103aO

10 min

The angular size of this remote ( $r_0 = 4082 \text{ km s}^{-1}$ ) exquisite spiral is small at  $\theta_{95} = 2.1'$ . Three principal, high-surface-brightness arms exist: fragments of lower-surface-brightness outer arms are present. The nucleus is small.

NGC 5936            Sc(r)I-II

S-1601-II

April 23/24, 1936

Imp. Eel.

60 min

The reproduction here is from a plate taken in excellent seeing by Hubble with the 60-inch telescope on Mount Wilson. The angular size of the galaxy is small at  $D_{95} = 1.5'$ ; the number of resolution elements in this image is smaller than for most other prints in this atlas. The redshift of NGC 5936 is  $v_0 = 3995 \text{ km s}^{-1}$ .

The arm pattern is peculiar in a similar way to NGC 2441, described on the preceding panel.



**G**alaxies on this and the next five pages, all of early luminosity class **I-II**, have multiple arms rather than two major ones as in the extreme examples of the grand design spiral type. Some of the multiple-armed galaxies still have elements of the grand design, while many are totally of the flocculant type (Elmegreen and Elmegreen 1982, 1987), having arm fragments such as those in NGC 488 (panels 115, 116, S3,S12) and NGC 2841 (panels 142, S4, S12).

NGC 6070      Sc(s)I-II  
 PH-7830-S  
 Sep3/4, 1980  
 103aO  
 12 niin

Five arm crossings on one side of the major axis and seven on the other define the multiplicity of the well-defined arm pattern in NGC 6070. Although the outer pattern is multiple, all arms are branched from two main arms that begin near the small central region.

The redshift of NGC 6070 is  $v_o = 1979$  km  $s^{-1}$ . Two of the largest HII-region complexes may resolve (core + halo) at about 1.5".

NGC 4100      Sc(s)I-II  
 S-1982-H  
 Feb 20/21, 1947  
 103aO  
 60 niin

The reproduction of NGC 4100 here is from a plate taken with the 60-inch telescope on Mount Wilson. The spiral structure near the small nucleus is defined by thin dust lanes. Three major luminous arms can be identified in the outer disk on each side of the major axis.

The redshift of NGC 4100 is  $v_o = 1135$  km  $s^{-1}$ .

NGC 6118      Sc(s)1.3  
 CD-1403-S/Br  
 March 22/23, 1980  
 103aO + GG385  
 10 niin

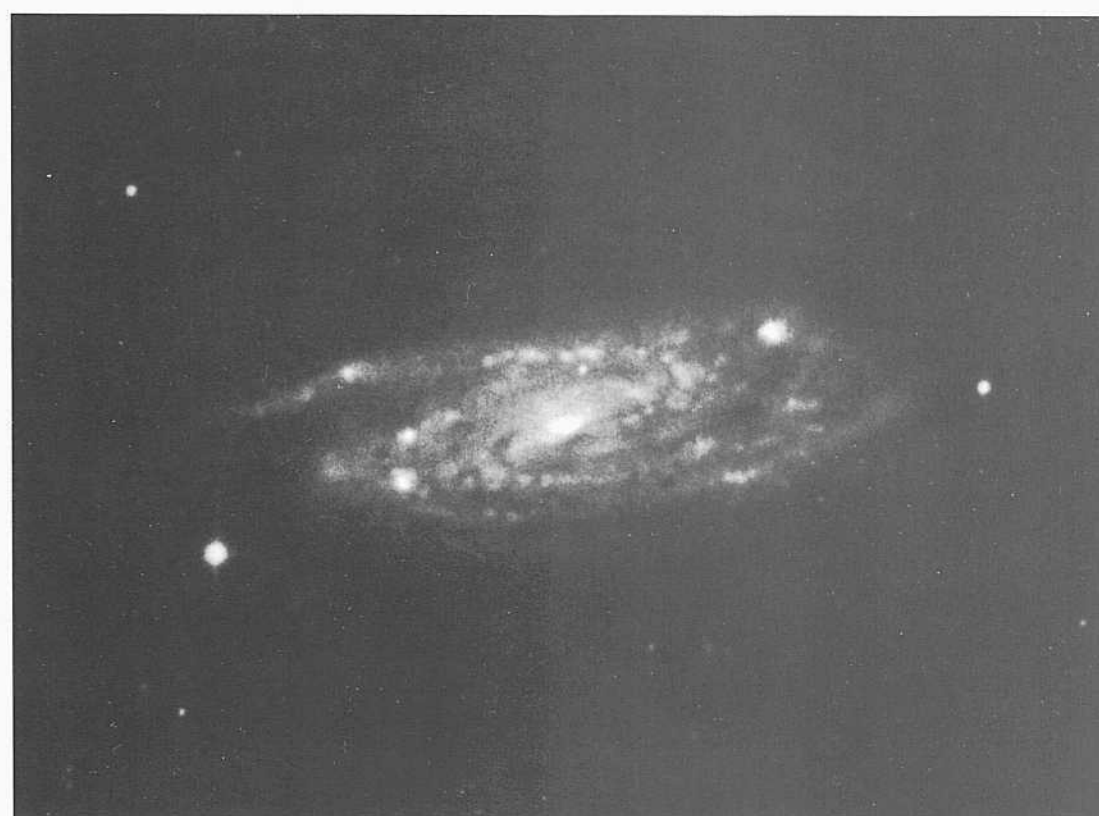
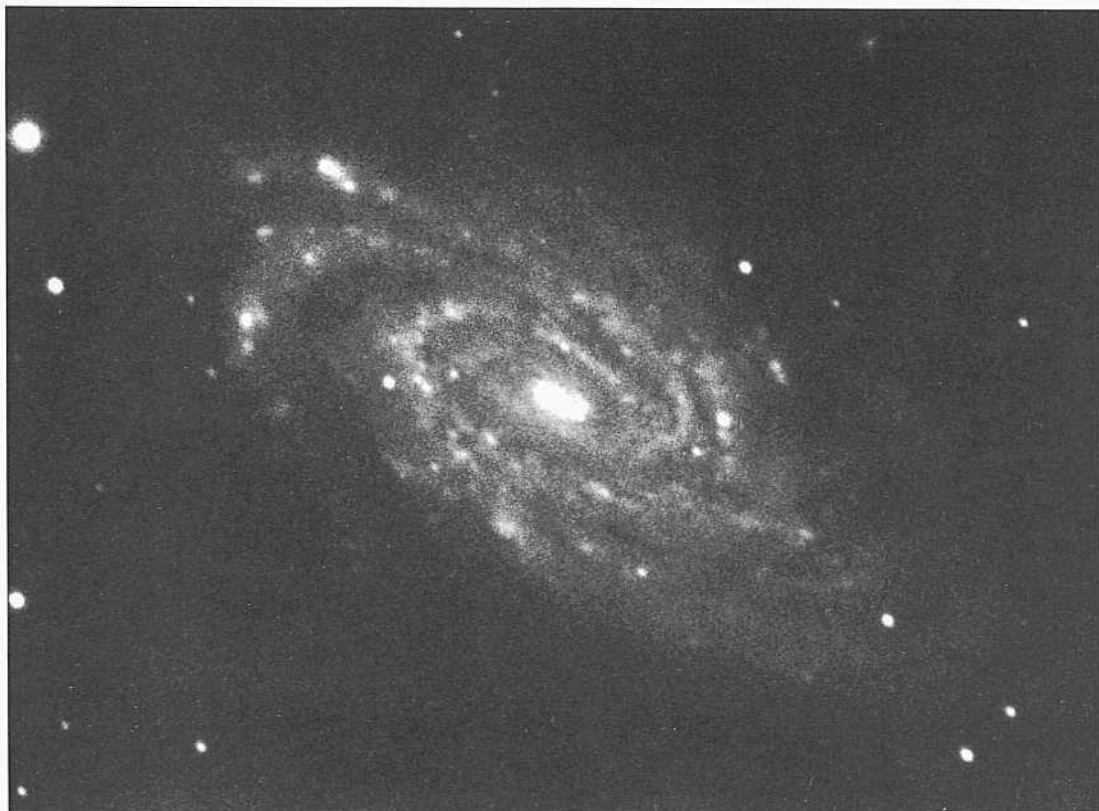
The spiral pattern consists of two principal arms, which begin at the center and branch into fragments which constitute the outer multiple spiral pattern.

The redshift is  $v_o = 1535$  km  $s^{-1}$ .

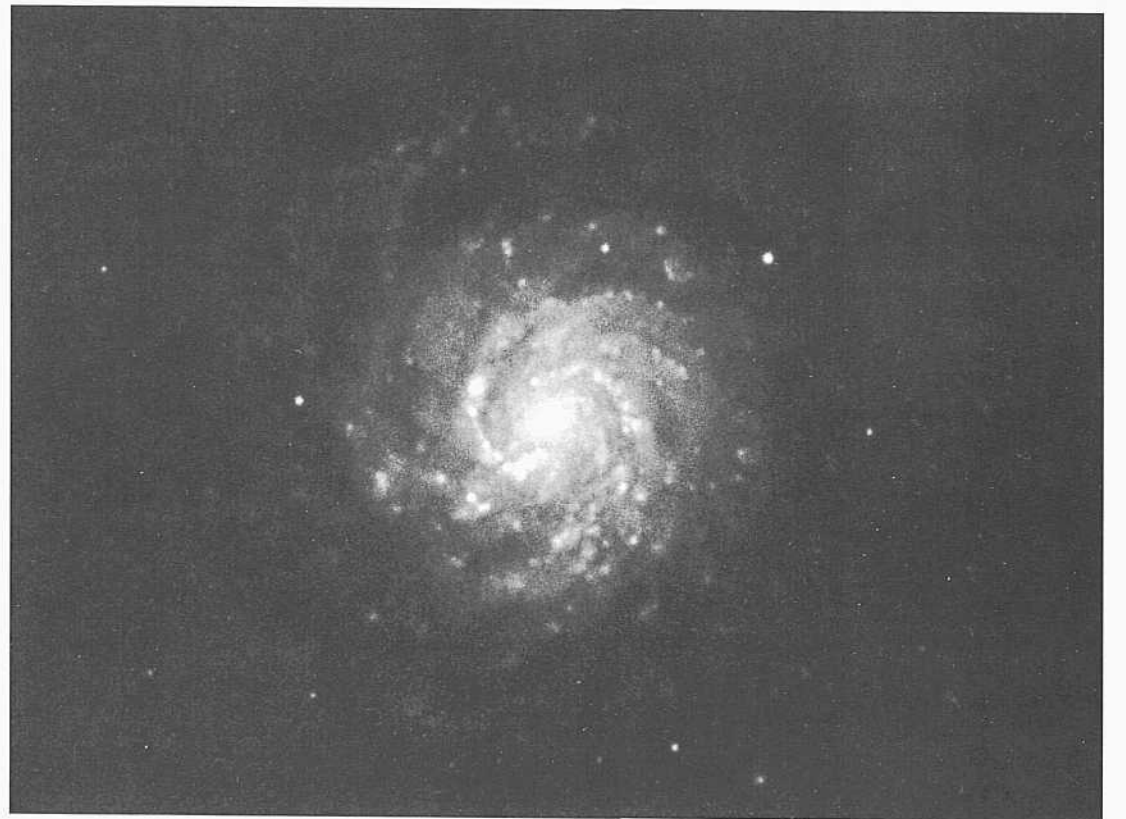
NGC 4602      Sc(r)MI  
 CD-1400-S/Br  
 March 22/23, 1980  
 103aO  
 75 niin

The spiral pattern of multiple outer arms fed by two major arms which start near the center is similar to that of the other three galaxies on this page. The high inclination of NGC 4602 obscures the details of the pattern near the center, but two thin dust lanes emerge from the center in a manner similar to the straight lanes along the bar in SBb and SBbc galaxies, suggesting here a mild bar.

The redshift is  $v_o = 2347$  km  $s^{-1}$ .



PANEL  
230



NGC 4653      Sc(rs)1.3      pair  
 CD-1411-S/Br  
 March 23/24, 1980  
 103aO  
 75 min

NGC 4653, with redshift  $v_r = 2433 \text{ km s}^{-1}$ , forms a close physical pair with NGC 4642 (Sc nearly on edge; not in the RSA), with  $v_0 = 2471 \text{ km s}^{-1}$ . The angular separation of the pair corresponds to a projected linear separation of 140 kpc at the redshift distance of 49 Mpc ( $z = 50$ ).

The outer spiral arms are branches from two main arms that begin on opposite sides of a central disk, similar to the (s)-type arm origins in SBb galaxies such as NGC 1300 (panels 154, S8). However, there is no additional evidence of a bar or of a strong oval central region.

NGC 4136      Sc(r)1-II  
 PH-8029-S  
 Feb 3/1, 1981  
 103aO  
 12 min

The inner spiral pattern begins tangent to an almost-complete inner ring similar to the pattern in NGC 309 (Hubble Atlas, p. 32; panel 221 here) and NCC 5364 (Hubble Atlas, p. 32; panel 217 here).

The outer arms are more massive in the sense of Reynolds (1927a,b) than in NGC 309; hence the slightly later luminosity class is required here.

Brightest stars begin to resolve in the arms at about magnitude  $m_i = 22$ , much more easily than in the Virgo Cluster spirals such as NGC 4321 (M100; Hubble Atlas, pp. 28, 31; panel 213 here), but not as easily as in M101 (Hubble Atlas, pp. 27, 31; panel 218 here) which has nearly the same redshift. The redshift of NGC 4136 is  $v_{rl} = 409 \text{ km s}^{-1}$ ; that of M101 is  $v_0 = 372 \text{ km s}^{-1}$ . However, the absolute magnitudes of these two galaxies differ by 3.2 mag, NCC 4136 being very faint at  $M_g = -18.3$ . Because the absolute  $B$  magnitude of the brightest resolved blue stars is a strong function of the absolute magnitude of the parent galaxy (Sandage and Tammann 1974b; Sandage and Carlson 1988) the difference between NGC 4136 and NGC 4321 in ease of resolution into stars is understood. That the distance determined from redshift is reliable within this range of very small redshift values follows from the low random velocities about a linear redshift-distance relation for the nearby galaxies (Sandage and Tammann 1975a, Sandage 1986a).

The five largest HI regions each resolve at about the 5" level, showing again that the galaxy is nearby.

[C2537      Se(s)1-II  
 CD-1327-S/Br  
 March 13/1 I, 1980  
 I(0)3a(0) + GG385  
 45 min

The two main arms in IC 2537 begin near the center, along with their associated thin dust lanes, branch outward until about fifth arm crossings of the major axis can be counted on each side.

The redshift is  $v_r = 2523 \text{ km s}^{-1}$ .

NGC 2967      Sc-(rs)1-II  
 CD-1358-S/Br  
 March 16/17, 1980  
 I03a0 + GG385  
 45 min

The spiral pattern in NGC 2967 is remarkably similar to the pattern and the character of the arms in M101 (Hubble Atlas, pp. 27, 31; panel 211 here), requiring no further description here.

The redshift of NGC 2967 is  $v_r = 2065 \text{ km s}^{-1}$ .

Sc Classification Section (continued)

NGC 3756      Sc(s)I-II      Racine wedge  
PH-7127-S  
Jan 31/Feb 1, 1976  
103aO + GG13  
30 min

Three arms emerge from the **central** region of NGC 3756. As **the** arms wind outward they fill the area of the disk, being of the massive variety in the sense of Reynolds (1927a,b) lacking a thin, well-defined form.

The **redshift** of NGC 3756 is  $v_o = 1372 \text{ km s}^{-1}$ . The galaxy is in the region of the Ursa Major Cluster but is considered to be a probable background galaxy.

NGC 3198      Sc(s)I-II  
PH-7960-S  
Nov 8/9, 1980  
103aO  
12 min

The arms in NGC 3198 **are** moderately thin and fairly well defined. However, the inclination angle is so high that the pattern, although regular, is not easily traced. If one views the image at an angle and at an **optimum** orientation by tipping and rotating the panel to compress the major axis until it is **equal** to the minor axis, the image presents two principal arms that start at the center [the (s)-type attachment to the center]. Each can be traced for about half a revolution before each branches to form the multiple pattern.

The redshift of NGC 3198 is small, at  $702 \text{ km s}^{-1}$ , but the HII regions remain unresolved at the 2" level.

NGC 3672      Sc(s)I-H      HA, p. 30  
CD-1832-HB  
April 1/2, 1981  
103aO + GG385  
45 min

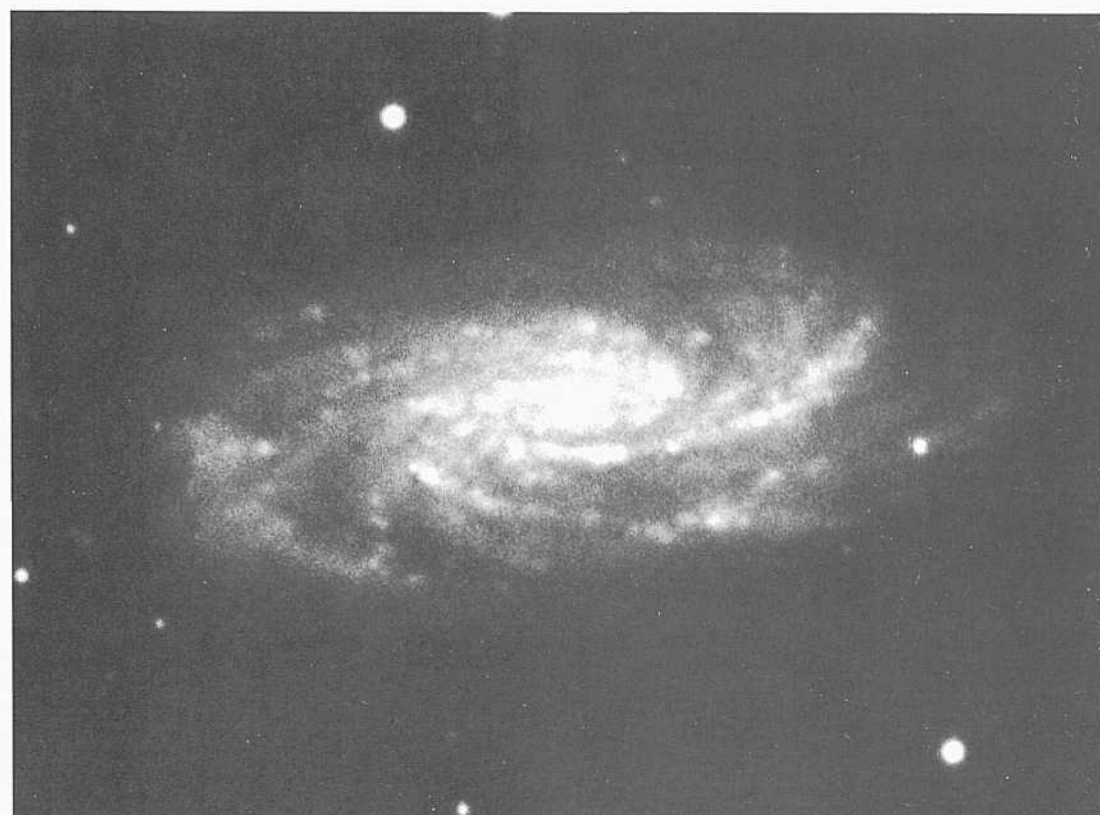
Although the spiral pattern here has multiple arms, it is not filamentary (**flocculent**; Elmegreen and Elmegreen 1982, 1987) but rather is of the grand design: four rather ill-defined arms start near the center and wind outward to cover the disk.

The redshift is  $v_o = 1633 \text{ km s}^{-1}$ .

NGC 1337      Sc(s)I-II  
PH-7699-S  
Sep 26/27, 1979  
103aO  
12 min

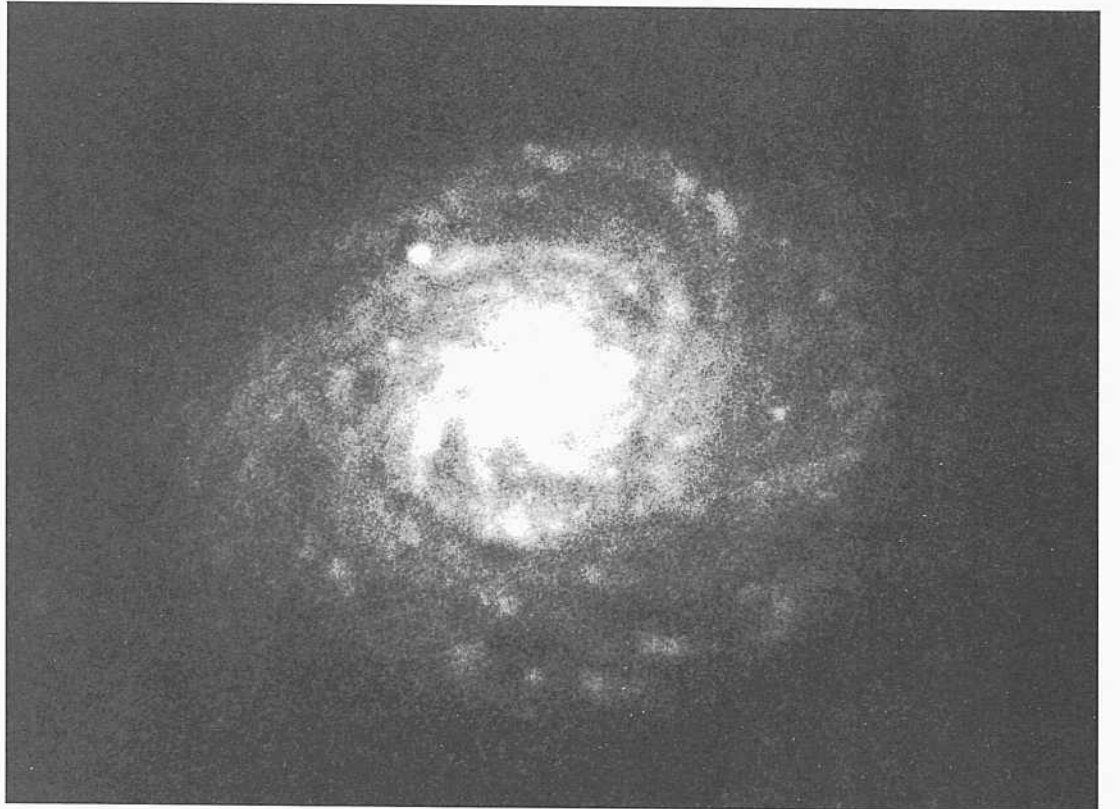
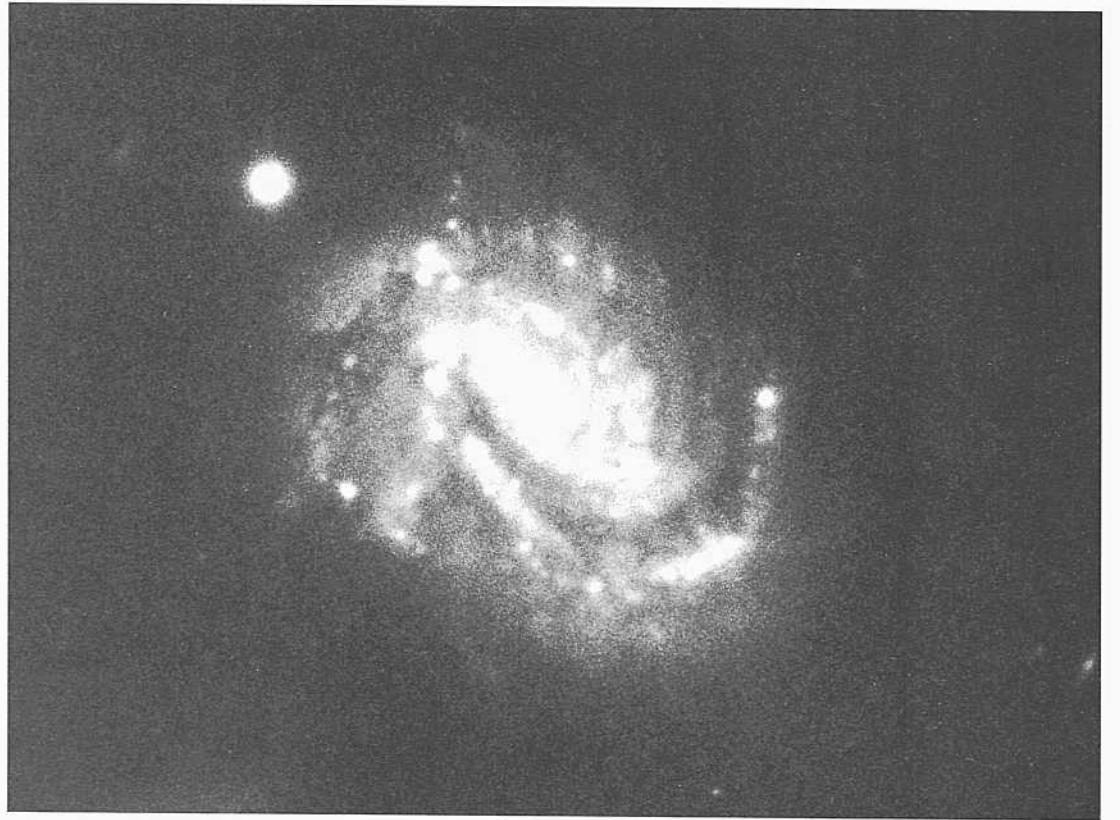
NGC 1337 is seen only about  $10^\circ$  from edge on, making the spiral pattern difficult to trace. It is evident that the nucleus is small (the type, therefore, is Sc). The arm pattern is multiple, similar to the other highly inclined galaxies on this panel.

The redshift is  $v_o = 1270 \text{ km s}^{-1}$ .



PANEL  
231

PANEL  
232



*Sc Classification Section (continued)*

NGC 3294            Sc(s)I.3  
H-2330-H  
Oct31/Nov I, 1946  
I03a0  
30 mill

NGC 3294 and NGC 877 to the right have spiral arms of the grand design type, albeit with a multiple-arm outer pattern. The two galaxies below arc of the flocculent type whose prototypes are NGC 488 and NGC 284 i.

The one highest-surface-brightness arm which starts at the center in an (s)-type configuration can be traced for a full I 1/2 revolutions outward before it fades below detectability on this 100-inch Hooker Telescope plate. The corresponding opposite arm can be traced for a whole revolution, which is unusual.

The redshift of NGC 3294 is  $1566 \text{ km s}^{-1}$ .

NGC 4899            Sc(s)I-II            triplet  
CD-1842-HB  
April 2/3, 1981  
I03a0 + GG385  
75 min

NGC 4899 is the middle galaxy of a wide triplet, with NGC 4891 (SBbc; panel 205) to the north by 30' at a redshift of  $v_0 = 2418 \text{ km s}^{-1}$ , and NGC 4902 (SBb; panel 162) to the south by 34' at a redshift of  $v_0 = 2426 \text{ km s}^{-1}$ . The redshift of NGC 4899 is  $v_0 = 2437 \text{ km s}^{-1}$ . At the mean redshift distance of 48 Mpc, the projected linear separations of NGC 4891 and NGC 4902 from NGC 4899 are 419 kpc and 475 kpc, respectively. The group is of a similar size to the Local Group.

The arms are flocculent. of the NGC 284] type.

NGC 877            Sc(s)I-II            group  
PH-7531-S  
Nov 4/5, 1978  
I03a0 + GG13  
15 mill

NGC 877 is the brightest galaxy in a field of other Dreyer galaxies (NGC 870, 871, 1176, and 877) within I 2' of each other, it seems likely that at least some of these form a physical group. The  $v_0$ , redshifts are similar at  $3830 \text{ km s}^{-1}$  for NGC 871 (low-surface-brightness Sc at 8.1' separation),  $4006 \text{ km s}^{-1}$  for NGC 876 (edge-on S0<sub>3</sub>? at a separation of 2.2'), and  $4010 \text{ km s}^{-1}$  for NGC 877 itself. At the mean redshift distance of 79 Mpc ( $H_0 = 50$ ), the projected linear separations of NGC 871 and NGC 876 from NGC 877 are 193 kpc and 50 kpc, respectively.

The arms in NGC 877 are semi-massive in the sense of Reynolds (1927a,b). The arm pattern is of the grand design, although not prototypical.

NGC 4047            Sc(s)I-II  
PH-7642-S  
April 28/29, 1979  
I03a0  
12 min

The exquisitely fine, multiple-spiral pattern of NGC 4047 is similar to the MAS patterns in NGC 488 and NGC 284 1 but is farther along the classification sequence. A better match, later in the sequence but still earlier than NGC 4047, is with NGC 5055 (She: Hubble Atlas, p. Z5; panels 19 I, S5 here) and NGC 352 1 (She: Hubble Atlas, p. 15; panel 188 here).

The redshift of NGC 4047 is  $v_0 = 3416 \text{ km s}^{-1}$ .



**T**he six galaxies on this panel and the four on the next complete the Sc section of luminosity class I-II. Most are of the grand design type, but many have more than two arm fragments in the outer regions.

NGC 3888      Sc(s)I-II  
 PH-7635-S  
 April 28/29, 1979  
 103aO  
 12 min

The **high-surface-brightness** parts of each of the **two** inner **luminous** arms in NGC 3888 begin a\* dust lanes near the center. They become luminous after about a **quarter** of a **turn** from the center. The arms arc thin and do not branch into as many multiple fragments outward as in the prototype MAS pattern of M1 01. The pattern in NGC 3888 is primarily two-armed throughout.

The redshift is  $v_o = 2454 \text{ km s}^{-1}$ .

NGC 4651      Sc(r)I-II  
 H-2534-H  
 May 4/5, 1948  
 103aO  
 30 min

NGC 4651 is in the Virgo Cluster region, 4° north of NGC 4486, which is near the center of Virgo **subcluster** A. This position is just outside the survey area for the Virgo Cluster Catalog (Binggeli, Sandage, and Tammann 1985), so that NGC 4651 is not listed in the VCC.

Four crossings by the arms of the major axis on both sides can be counted. The arms are thin and well **defined, requiring** the early luminosity classification.

The small redshift of  $v_o = 723 \text{ km s}^{-1}$  **indicates, but does not require,** a small redshift **distance** of 14 Mpc ( $m - M = 30.8$ ) ( $// = 50$ ) because the resolution into stars and **III regions** is similar" to that in Virgo Cluster **spirals** such as NGC 4321. The large velocity dispersion of the Virgo **Cluster** members **accounts** for the small observed redshift of NGC 4651. despite its large indicated **resolution-distance** of  $m - M$  of about 31.8.

NGC 237      Sc(s)I-II  
 PH-7833-S  
 Sep 3/4, 1980  
 103aO  
 12 min

NGC 237 is a two-armed spiral where each arm can be traced for nearly a whole revolution, causing two crossings of the major axis on each side. Faint spiral fragments from mild branching also exist in the outer regions.

The redshift is  $v_o = 4308 \text{ km s}^{-1}$ .

NGC 753      Sc(s)I-II      Racine wedge  
 PH-7850-S  
 Sep 4/5, 1980  
 103aO  
 12 min

The spiral pattern is extremely regular in the inner region of NGC 753 where the two grand design arms of very high surface brightness originate. The regularity of the **pattern** is similar to that of the inner arms of NGC 1566 (She; panels 171, S5), which is one of the most symmetrical galaxies in the RSA.

The arms branch into well-defined fragments at the place where the surface brightness of the principal arms decreases rather abruptly after about three-fourths of a turn.

The redshift of NGC 753 is  $v_o = 5145 \text{ km s}^{-1}$ . The absolute magnitude is bright at  $M_g = -22.7$ , similar to  $M_B = -22.3$  for NGC 1566.

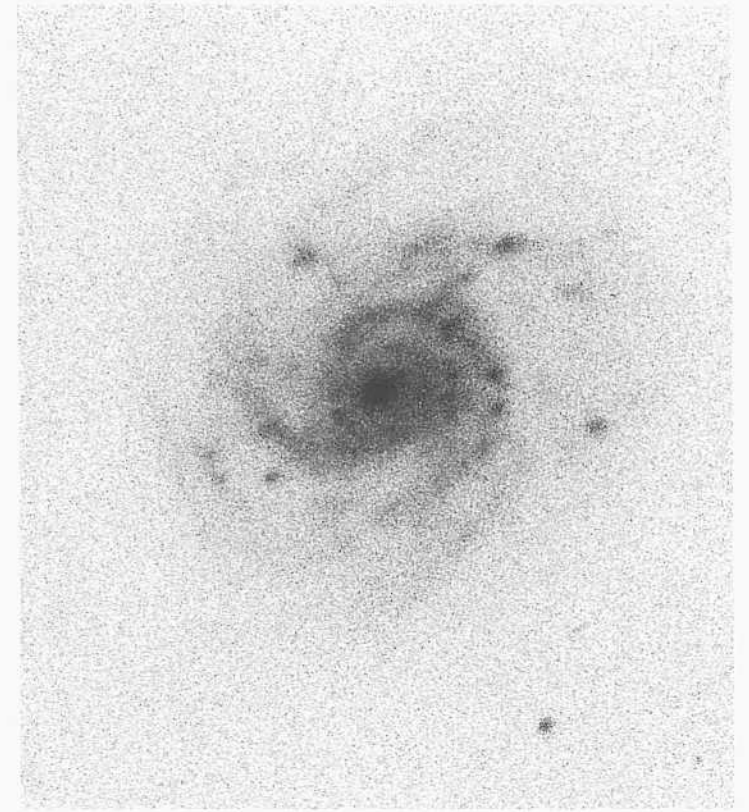
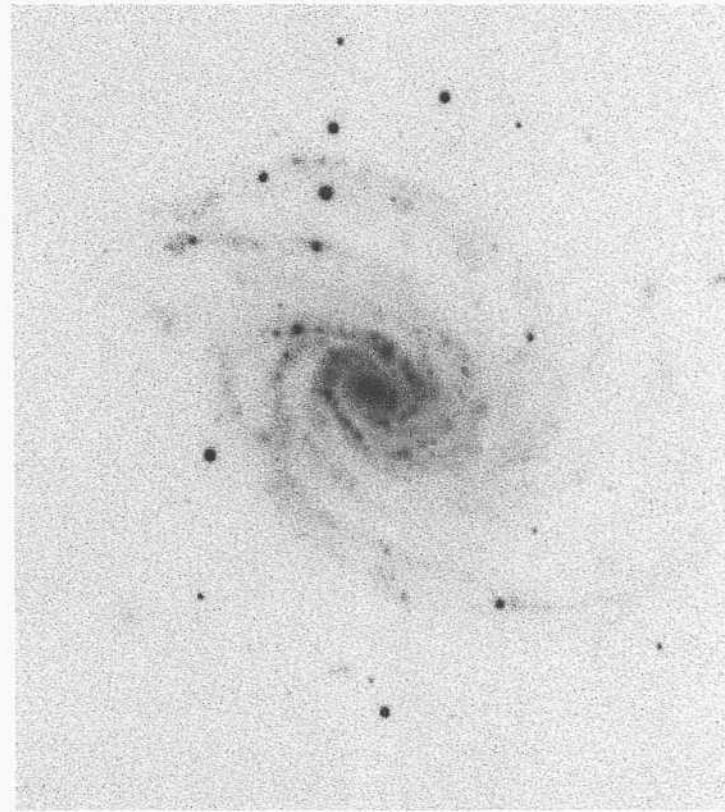
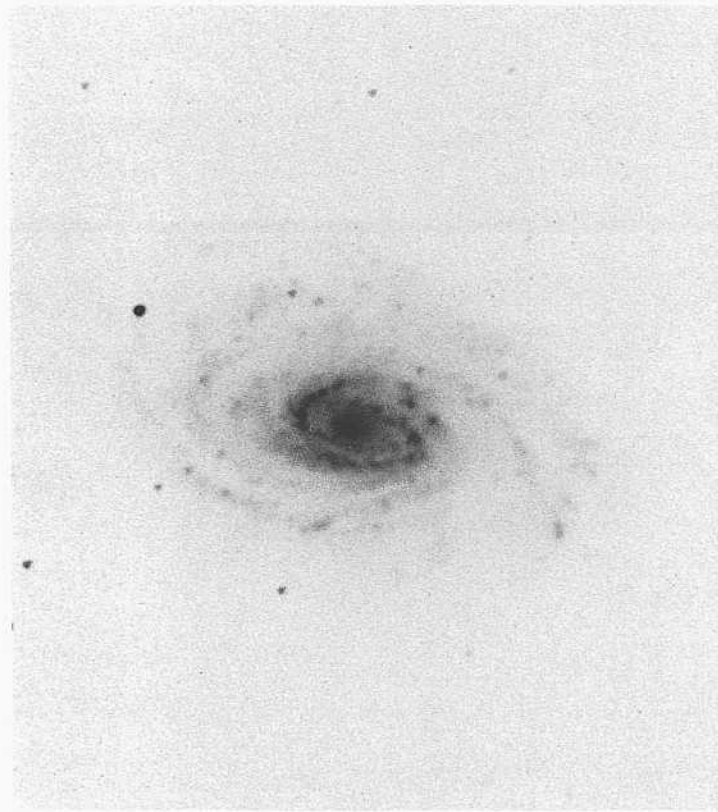
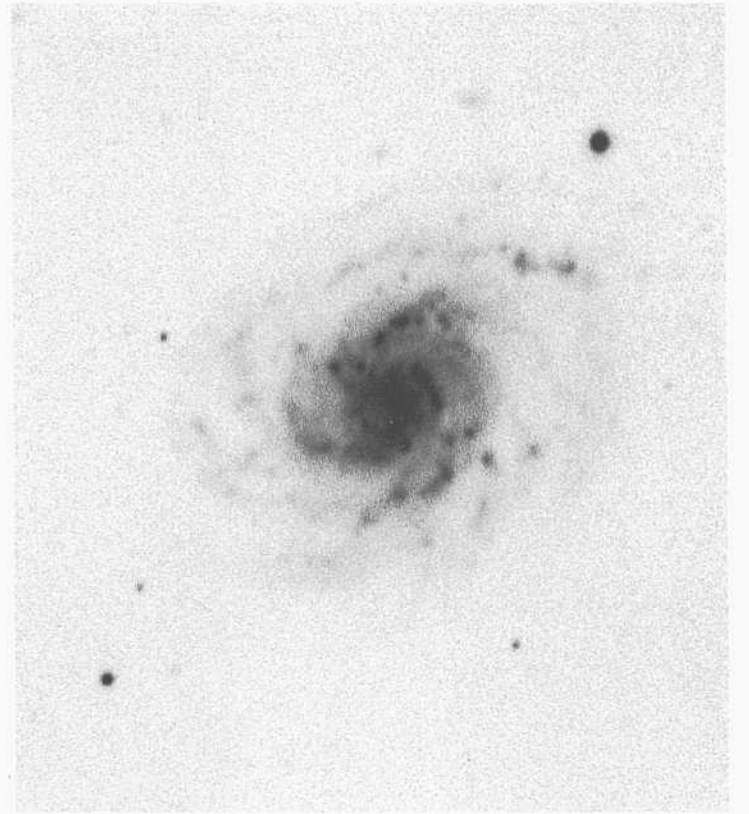
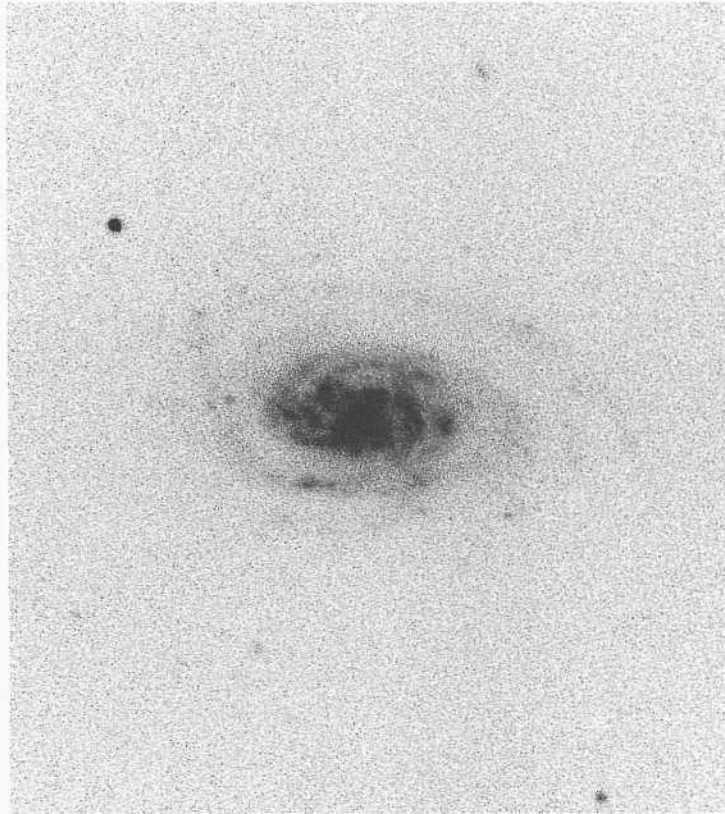
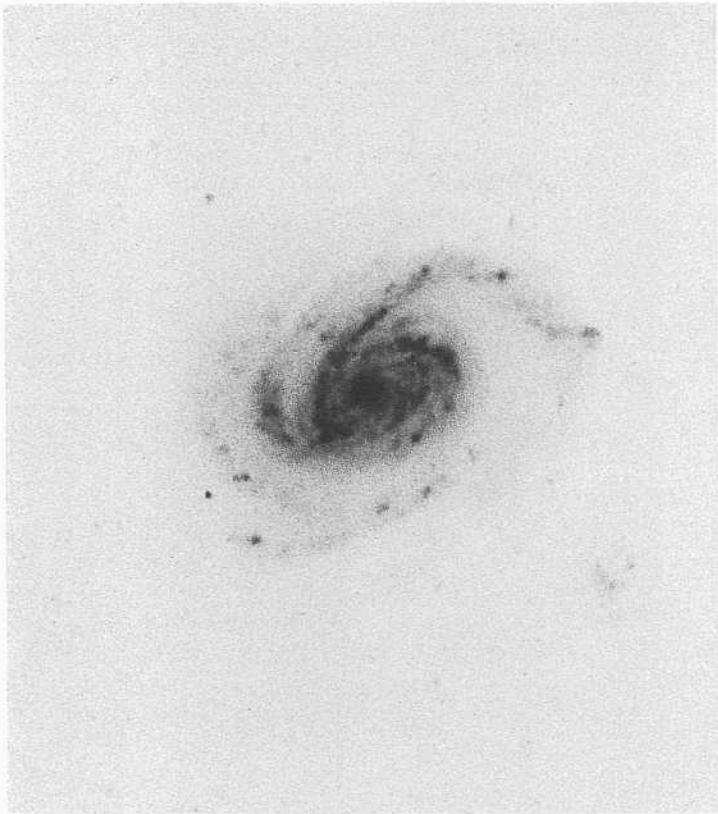
NGC 4152      Sc(r)I.4      VCC 25  
 CD-2137-S  
 March 22/23, 1982  
 103aO  
 50 min

NGC 4152 is listed in the VCC, though no decision is given there on membership. It is located in the extreme northwestern corner of the survey field. The redshift is large, at  $v_o = 2055 \text{ km s}^{-1}$ , but is not higher than the upper **redshift** cutoff of  $v_o = 2700 \text{ km s}^{-1}$  adopted in the VCC for cluster membership (justified by a symmetrical velocity distribution), with the low-velocity cutoff observed to be at  $v_o = -700 \text{ km s}^{-1}$  (Binggeli, Sandage, and Tammann 1985).

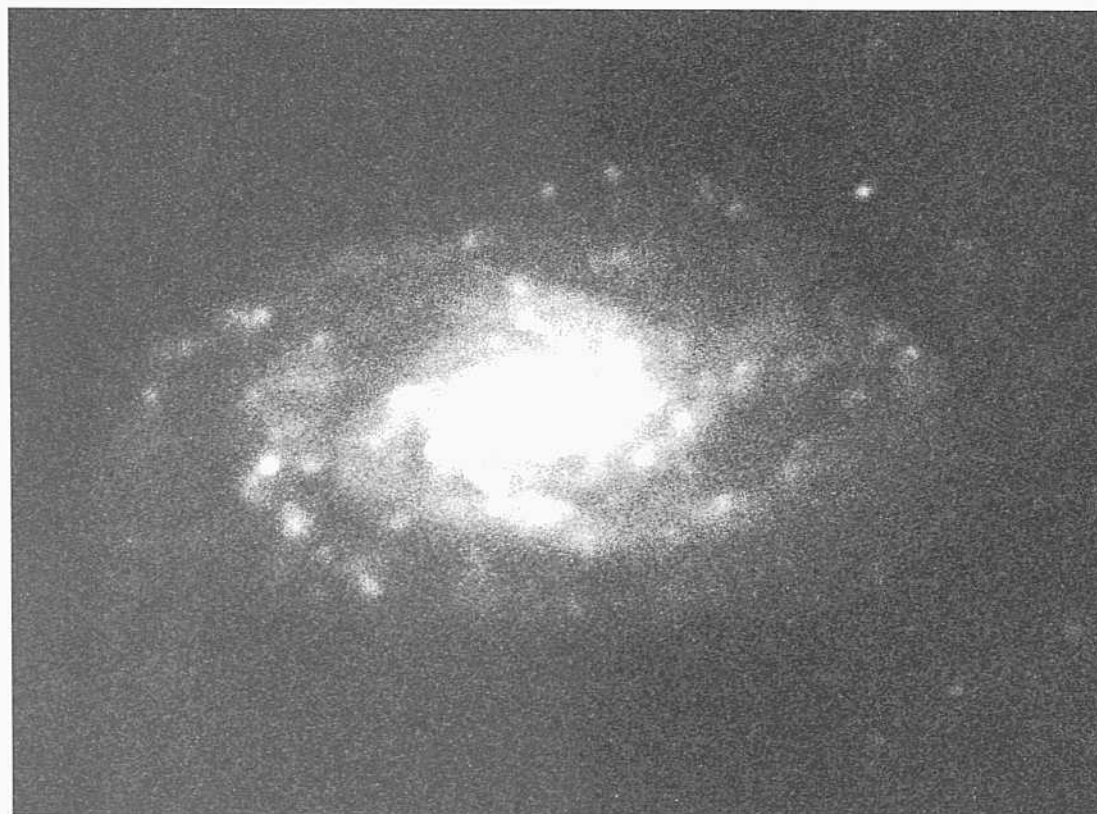
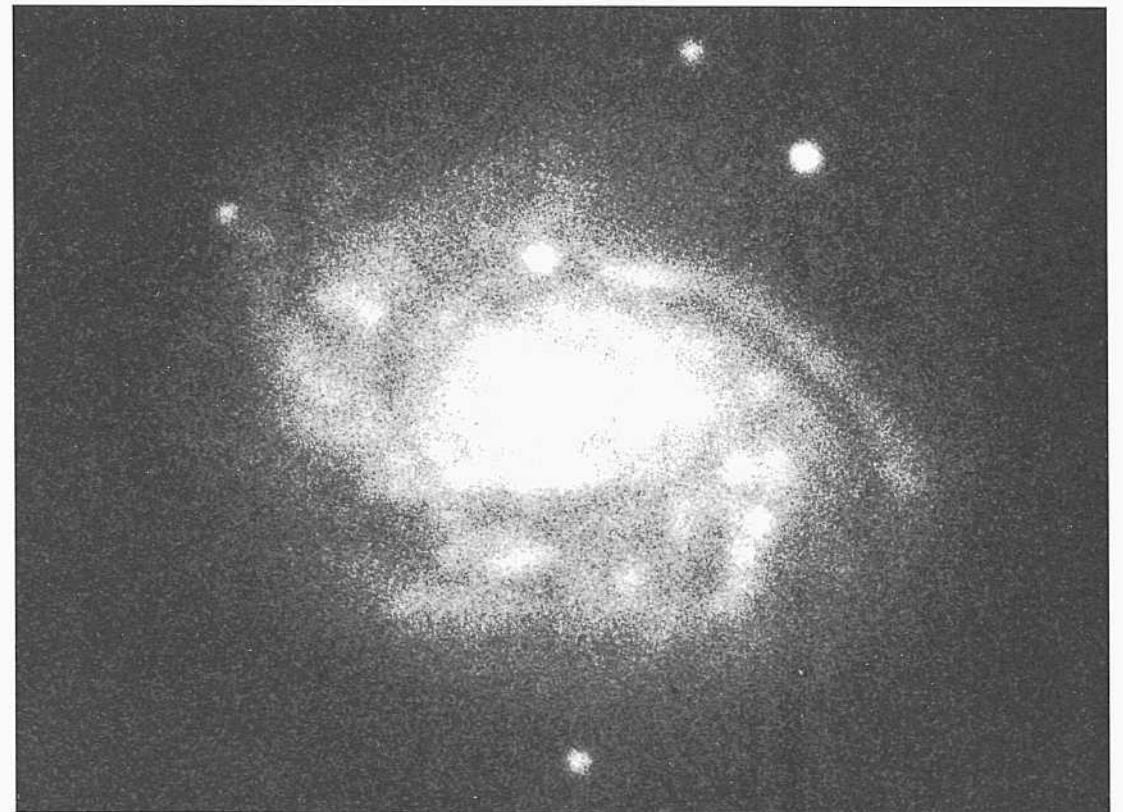
The arms in NGC 4152 start **from** an internal ring similar to the pattern in NGC 309 (Hubble Atlas, p. 32: panel 221 here).

NGC 3512      Sc(rs)I-II      group  
 H-2347-H  
 Nov 27/28, 1946  
 103aO  
 30 min

NGC 3512 is at the center of an apparent group of three **bright** galaxies; the other two are NGC 3504 (Sb/SBb; panel 169) at an **angular** separation of 12',  $v_o = 1480 \text{ km s}^{-1}$ , and NGC 3515 (She, not in the RSA) at an angular separation of 13.7' but whose redshift is presently unknown (e. 1990). The redshift of NGC 3512 is  $v_o = 1340 \text{ km s}^{-1}$ . At the mean redshift distance of 27 Mpc, the **projected** linear **separation** of NGC 3512 and NGC 3504 is 96 kpc.



PANEL  
234



The four galaxies on this panel complete the S<sub>r</sub>I-II luminosity class illustrations.

NGC 4162            Sc(i-)MI  
H-2390-H  
Feb 23/24, 1947  
103aO  
**30 miii**

The spiral pattern in NCC 4 162 is multiple-armed throughout the image. There are not two principal arms from which a multiple pattern develops; rather, the arms begin tangent to an inner disk at many places on the rim.

The redshift is  $v_0 = 2481 \text{ km s}^{-1}$ .

NGC 3370            Sc(s)I-II  
PH-8019-S  
Feb 3/4, 1981  
103aO  
12 min

Four arms (three of which are bright) emerge from the center, forming the multiple-arm pattern on the outside.

NGC 1667            Sc(r)I-II  
**PH-7896-S**  
Nov 6/7, 1980  
**103aO**  
12 min

The three main spiral arms begin tangent to a high-surface-brightness inner ring similar to the pattern in NGC 309 (panel 22 1).

The redshift is  $v_0 = 1562 \text{ km s}^{-1}$ .

NGC 3936            Sc(s)MI  
CD-769-S  
Feb 21/22, 1979  
**103aO + GG385**  
**-15 miii**

NCC 3936 is viewed within  $1^\circ$  of edge on, making assessment of the spiral pattern and the luminosity classification uncertain. The nucleus is small, indicating the Sc (-) class. The arm fragments are narrow and well separated, suggesting the early luminosity class.

The redshift is  $v_{r_0} = 1738 \text{ km s}^{-1}$ .

## THE ScII SUBCLASS

**S** c II galaxies constitute the largest subclass of the Sc section. The RSA galaxies of this type and luminosity class illustrated on the next 24 panels are arranged in two parts. Those where the spiral pattern is predominately of the grand design type, dominated by two principal arms, are set out on the next six panels. Galaxies of the multiple-armed type, some grand design and others of the filamentary (flocculent) type, are on the remaining 18 panels, 241-258.

NGC 4145      Sc(r)II      Ursa Major Cluster

PH-8028-S

Feb 3/4, 1981

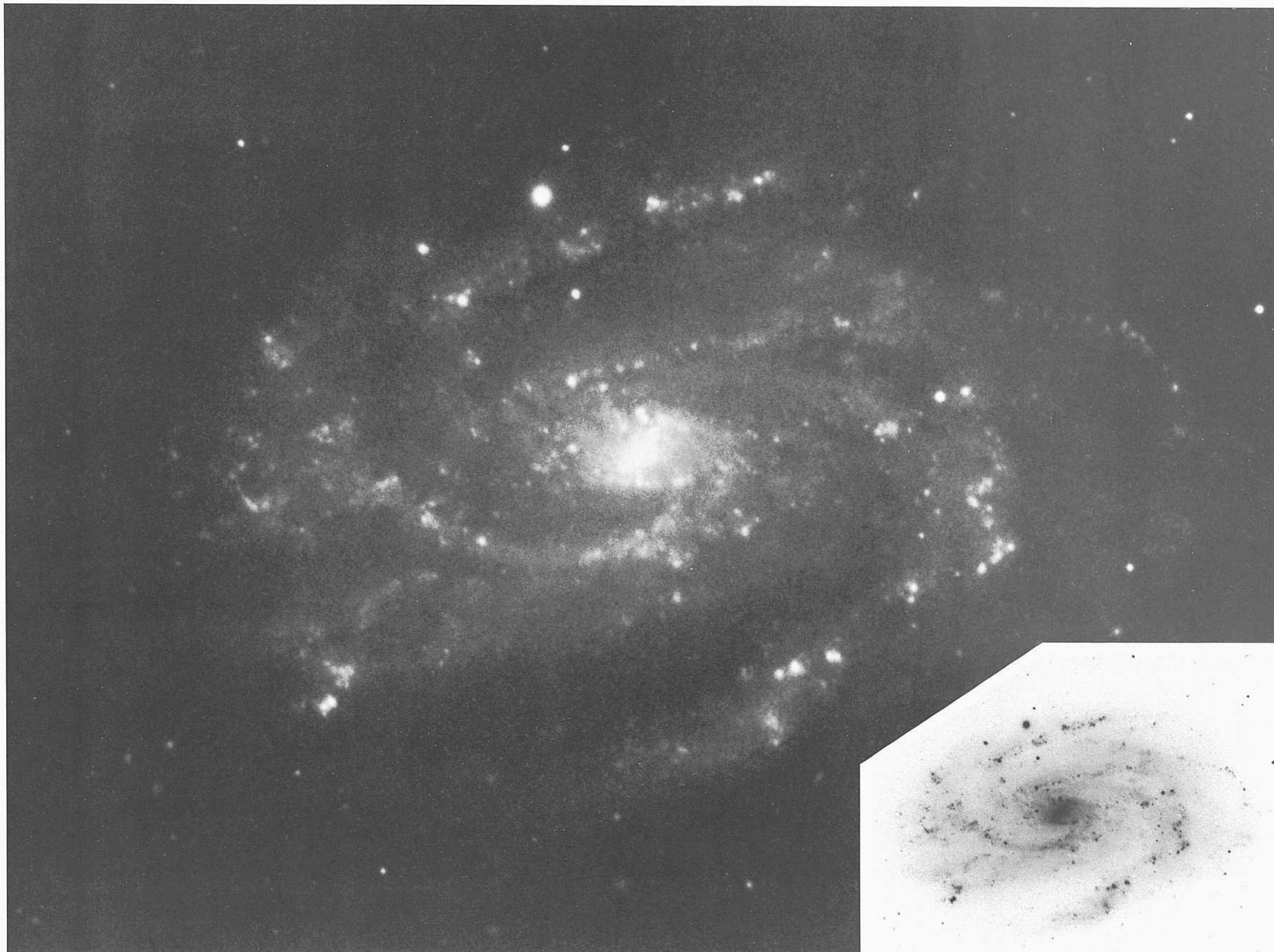
103aO

12 mill

NGC 4145 is a **large-angular-diameter** (O95 = 5.8') spiral. **It is one of the principal** galaxies in the Ursa Major Cluster, which is dominated by spirals. The mean redshift of the cluster is  $\langle z \rangle = 980 \text{ km s}^{-1}$  with a dispersion of about  $100 \text{ km s}^{-1}$ . The redshift of NGC 4145 is  $v_d = 1030 \text{ km s}^{-1}$ .

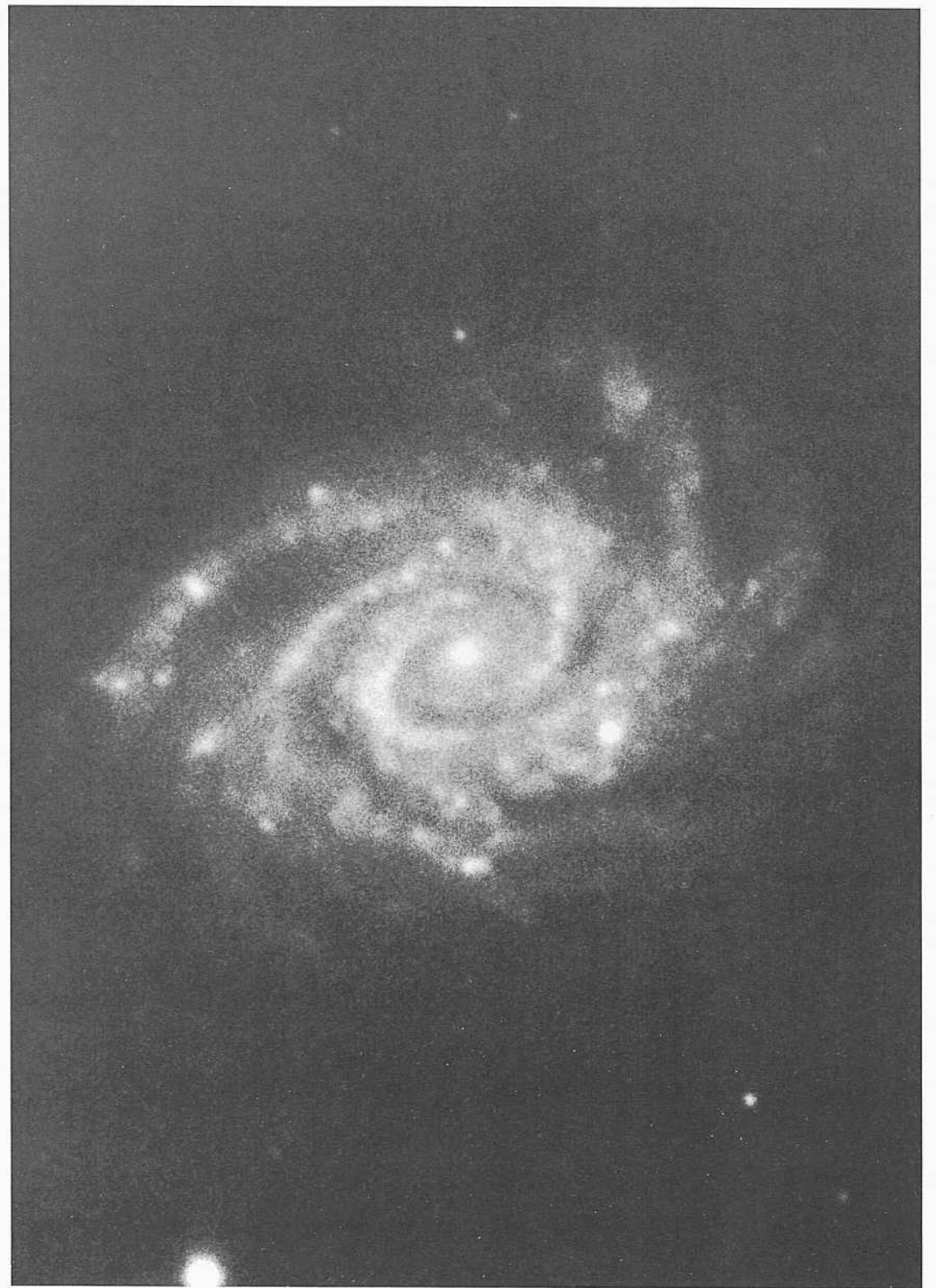
The two principal spiral arms begin on the rim of an inner disk, across which there is a weak bar. Each of **the** arms begins to fragment after about half a revolution, **but** two main fragmented extensions of the original segments can be traced for an additional half rotation.

The arms are well resolved into individual **brightest** stars beginning at about  $B = 22$ . This is somewhat brighter than in the giant **spirals** of the Virgo Cluster, but much fainter than in the galaxies of the M101 Group and the **very nearby** NGC 4395 Group. Many HII regions also exist in the arms, the largest of which resolve at about the 2" level.



PANEL  
235

PANEL  
236



*Sc Classification Section (continued)*

HA 85-1 = A0509-11 Sc(s)II

CD-720-S

Feb 1/2, L979

103aO + GG385

45 niin

The spiral patterns of both galaxies on this page are similar.

The two principal arms in HA 85-1 start near the center at opposite edges of the small central region. Each arm is well defined for more than half a revolution. Major branching occurs in one of the arms beyond that point, giving four arm segments on one side. The branching is less complete on the other side.

The redshift of HA 85-1 is  $v_0 = 2063 \text{ km s}^{-1}$ . The evident HII regions are bright but are unresolved at the 1" level. Individual brightest stars are not identifiable because of their faintness at this distance.

NGC3052 Sc(r)II

CD-8U-S

Feb 26/27, 1979

103aO + GG385

45 mill

The arm pattern of NGC 3052 has very high surface brightness over almost all the image.

Each of the two principal arms near the center are highly symmetrical for the first quarter-turn. One of the inner principal arms branches into two major arms, which retain their thinness and good definition for another half revolution. The opposite arm only widens without becoming double. As a consequence, the outer spiral pattern has three major arms.

The redshift is  $v_0 = 3364 \text{ km s}^{-1}$ . No stars or HII regions are individually resolved.



Sc Classification Section (continued)

NGC 3181      Sc(r)II.2      panel S5  
PH-7993-S  
Feb 2/3, 1981  
103aO  
12 min

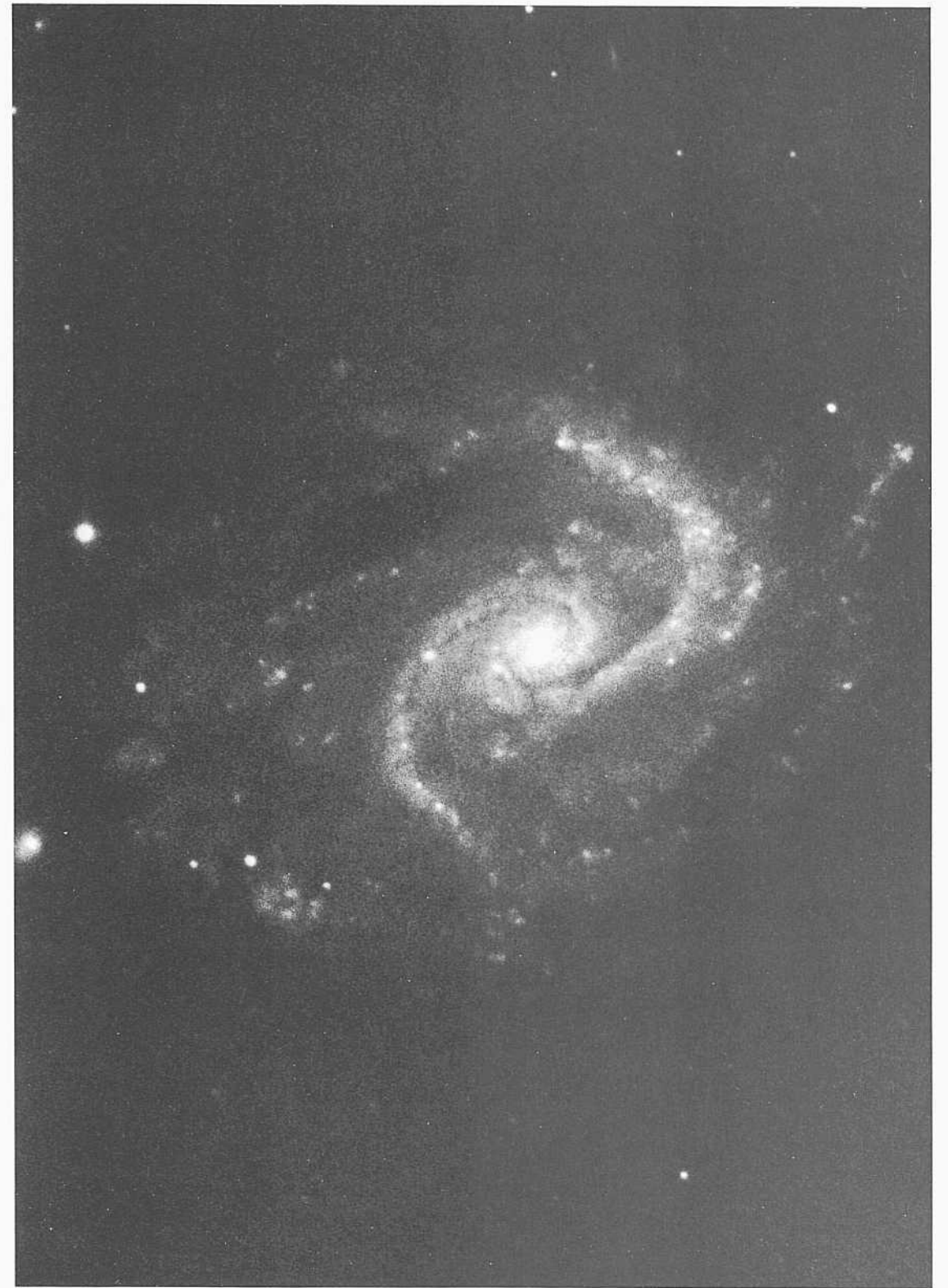
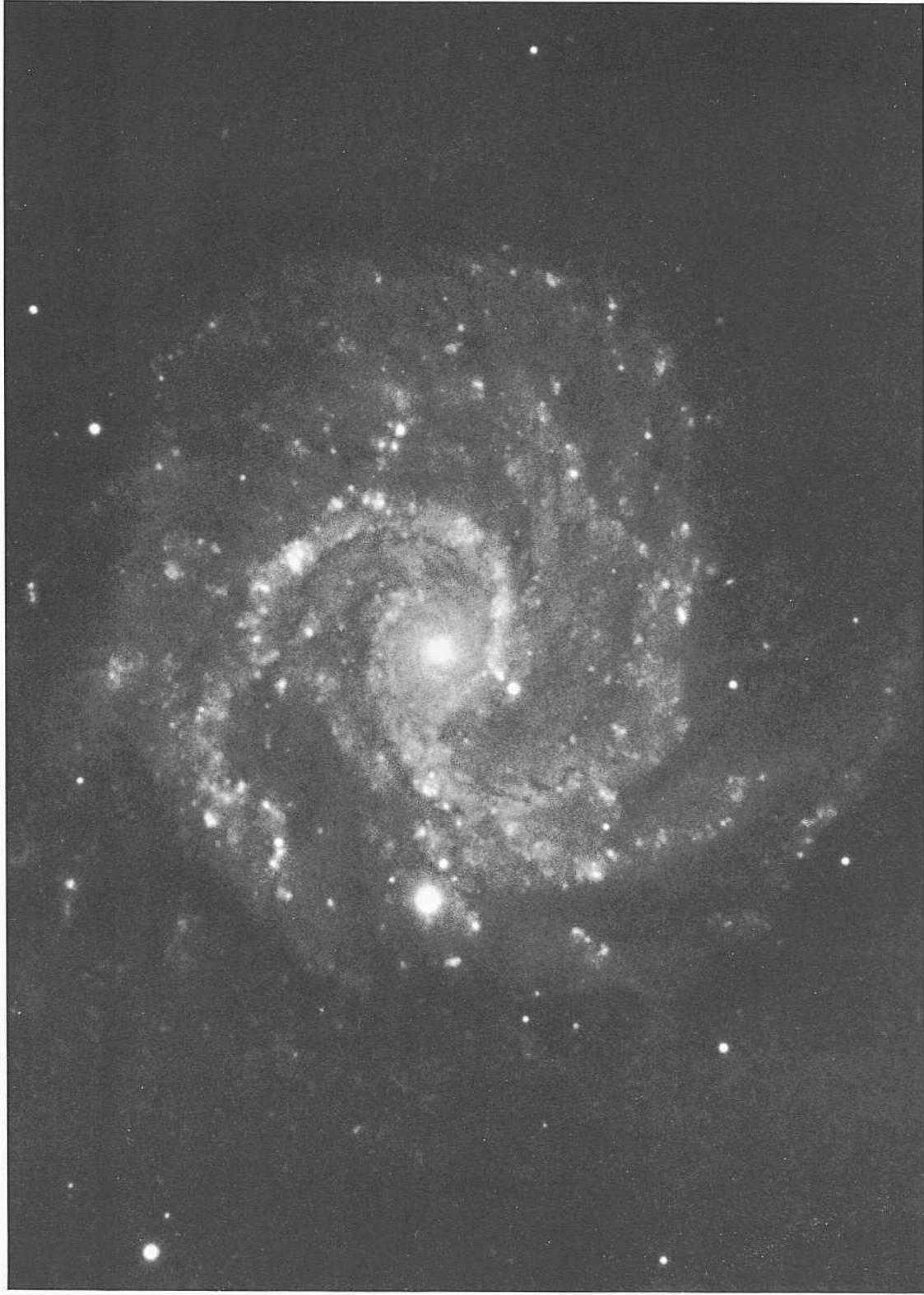
NGC 3184 is **near** enough that individual stars **begin to** resolve **out of** the **background** of the arms **at** about  $B = 22$ , but **the** separation of **the** stars from **the** many **III** regions will **require** the standard identification procedures comparing **Met** and yellow images. The redshift of NGC 3184 is  $v_o = 60.7 \text{ km s}^{-1}$ .

The arms begin tangent to the rim of a small, smooth inner disk, within which two faint spiral dust lanes start at **the** center and connect with the beginnings of the two main luminous arms. The luminous arms branch into several thick **fragments** that spread to cover much of the area of the outer disk. Dust lanes exist throughout the pattern.

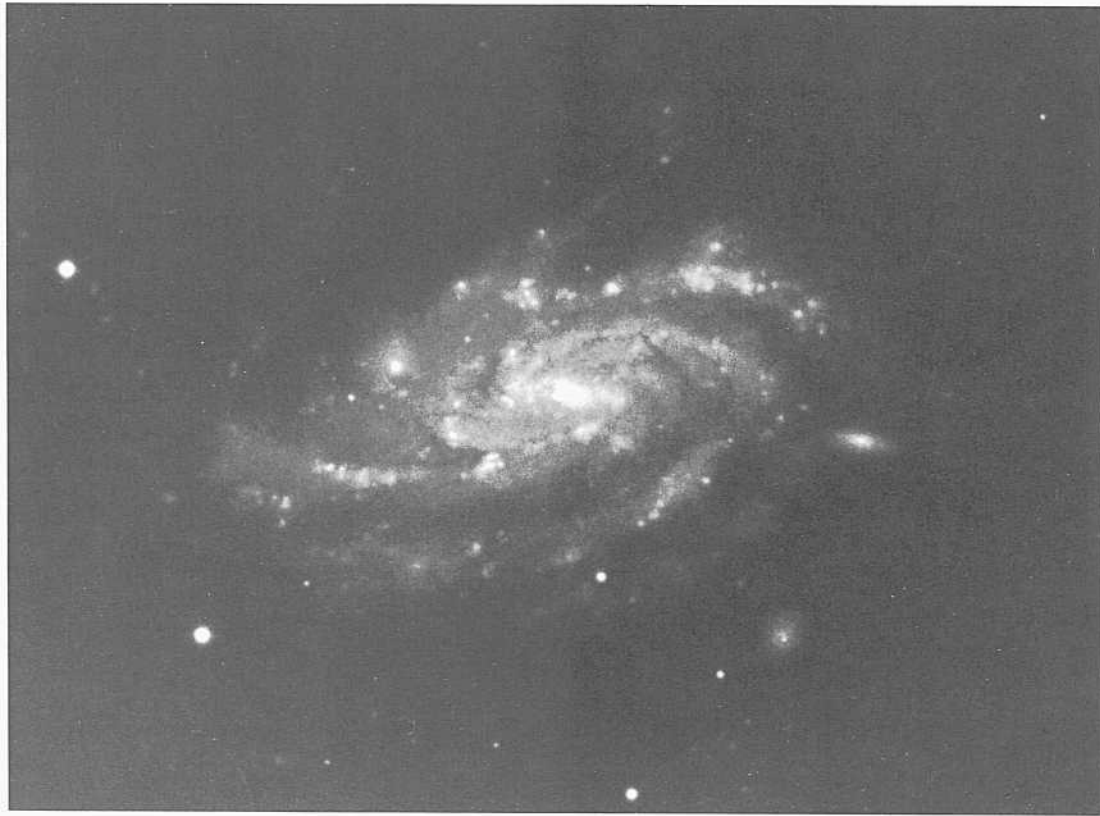
NGC 895      Sc(s)II  
CD-1589-S/Br  
Aug 11/12, 1980  
103aO + GG385  
45 min

The two principal arms can be traced into the center. Well-defined (opaque) dust lanes exist inside these high-surface-brightness dominant arms throughout the region where their surface brightness remains high. **Low-surface-brightness** spiral arm fragments exist over the outer area of the disk on the outside of the principal arms.

The redshift is  $v_n = 2383 \text{ km s}^{-1}$ .



PANEL  
238



The separate arms in each of the galaxies on this panel are easy to trace. Their geometrical entropies are low; hence the moderately early luminosity classes near II for each is required.

NGC 578                      Sc(s)H  
 CD-1523-S/Br  
 Aug 5/6, 1980  
 103uO + GG385  
 45 min

Like NGC 3052 two panels back, NGC 578 is a three-armed spiral. The third arm is not well defined near the center. It becomes prominent, having the highest density of III regions of the three arms, only in its outside segment.

The two largest HII regions are complex, probably composed of overlapping separate centers. They appear to resolve (core + halo) at about 1.5". The redshift of NGC 578 is  $v_r = 1675 \text{ km s}^{-1}$ .

NGC 7418                      Sc(rs)1.8                      Gins Gr?  
 CD-1161-Br  
 Aug 22/23, 1979  
 103aO + GG385  
 45 min

NGC 7418 may be a member of the loose Grus Group, of wide extent and mixed morphology (de Vaucouleurs 1956a; Shobbrook 1966; Sandage 1975b, 1978). The mean  $v_0$  redshift of the group is about  $1580 \text{ km s}^{-1}$ . The redshift of NGC 7418 is  $v_0 = 1451 \text{ km s}^{-1}$ .

Four principal arms exist, yet the galaxy is of the grand design type.

IC L954                      Sc(s)II.2  
 CD-672-Br  
 Jail 24/25, 1979  
 103aO + GG385  
 45 min

The arms in IC 1954 are massive in the sense of Reynolds (1927a.b). As in NGC 578 to the left and NGC 3052 on panel 236, there are three principal arms, two of which start together on one side of the center; the other starts on the opposite side and remains single for the two-thirds of a revolution that can be traced. Opaque dust lanes exist on the inside of each of the three major arms.

The redshift of IC 1954 is  $v_r = 905 \text{ km s}^{-1}$ .

NGC 1084                      Sc(s)II.2                      HA, p. 29  
 PH-7915-S  
 Nov 7/8, 1980  
 103aO  
 2 min

The surface brightness of the arm pattern in NGC 1084 is exceptionally high. The well-exposed image here was obtained in only a two-minute exposure with the Palomar 200-inch Hale Telescope; it is nearly overexposed even so.

The arms are massive in the sense of Reynolds (1927a.b). There are three arms, as in IC 1954 and NGC 578 on this panel and NGC 3052 on panel 23d. The best-developed of the arms is on one side alone. The other two arms on the opposite side in the outer region start as two thin, luminous threads that themselves begin on opposite sides of the center but overlap after unwinding by half a turn, after which the spiral pattern on that side is confused.

The redshift of NGC 1084 is  $v_r = 1471 \text{ km s}^{-1}$ .

**T**  
 The four galaxies on this panel all have spiral patterns of the grand design rather than filamentary (floccular) type, examples of which follow on panels 241-258.

NGC 5861      Sc(s)II  
 CD-1381-S/Br  
 March 20/21, 1980  
 103aO + GG385  
 55 min

The spiral pattern in the inner part of NGC 5861 is one of the most regular in the sky.

One of the two main arms can be traced from its beginning at the center for nearly 11/2 revolutions without branching. The other can be traced for one revolution, at which point it breaks into an outer fragment and a moderately chaotic pattern begins. If this outer pattern were absent, the luminosity class would be I rather than II.

The redshift is  $v_0 = 1725 \text{ km s}^{-1}$ .

NGC 6946      Sc(s)II  
 PH-3832-S  
 Aug 6/7, 1961  
 103aE + RG2  
 120 min

NGC 6946 is among the closest galaxies to the Local Group as judged by the large angular extent ( $D_{95} = 18'$ ), the moderately easy resolution into brightest stars beginning at about  $B = 21$ , and the large angular size of the several largest HII regions at a core + halo diameter of 10". The resolution into stars is not as easy as in M101, whose distance modulus is 29.3, or in members of the NGC 4395/NGC 4214 Group at  $m - M$  of about 28.5, but the Galactic latitude of NGC 6946 is low at  $b = 12^\circ$ , opening the possibility of appreciable Galactic absorption.

Note that the plate used here is red sensitive, favoring the detection of HII regions rather than individual brightest blue stars.

The redshift of NGC 6946 is low at  $u_0 = 336 \text{ km s}^{-1}$ .

NGC 5899      Sc(s)II  
 PH-7648-S  
 April 28/29, 1979  
 103aO  
 12 min

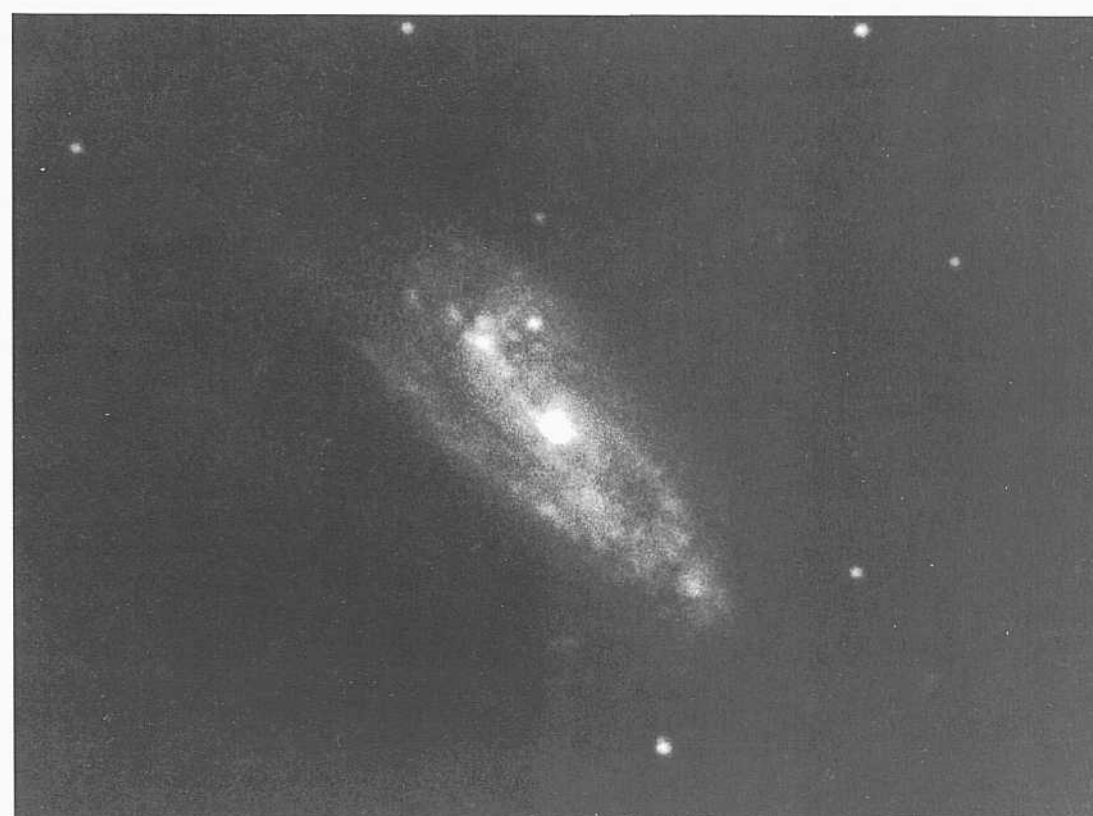
The pattern defined by the two principal arms of this grand design spiral is highly regular. The arms are of high surface brightness, they are thin, and they can each be traced for three-quarters of a turn without branching. Beyond that point, one of the arms branches in a way similar to the pattern in NGC 5861 at the left.

The redshift of NGC 5899 is  $v_n = 2657 \text{ km s}^{-1}$ .

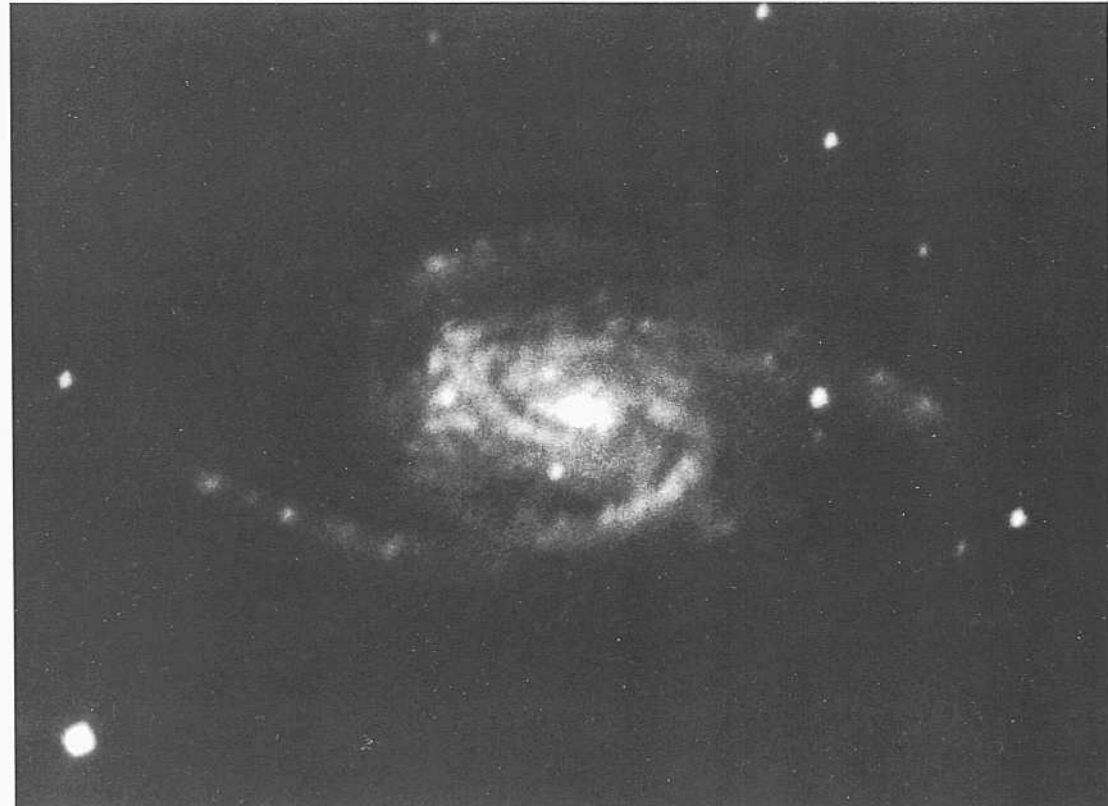
NGC 5756      Sc(s)II      panel 257  
 CD-1471-S/Br  
 May 10/11, 1980  
 103aO + GG385  
 45 min

This galaxy, shown also in a deeper print on panel 257, has a very faint set of regular, smooth outer arms which resemble the outer pattern in the Sa galaxy NGC 1350 (panels 71, 88, S3). These outer arms of exceedingly low surface brightness are extensions of the two principal (s)-type inner arms shown in the low-contrast print here.

The redshift of NGC 5756 is  $v_0 = 2025 \text{ km s}^{-1}$ .



PANEL  
240



The four galaxies on this panel finish the Sill section of galaxies where the spiral pattern is formed by two principal arms.

NGC 2964      Sc(s)II.2      pair?  
 PH-7603-S      panel 251  
 April 3/4, 1979  
 H1aJ + GG385  
 30 min

NGC 2964 may form a physical pair with NGC 2968 (Amorphous or  $S0_{\text{a}}$  pec; panels 49, 337), at an angular separation of 6.2'. The redshifts are  $u_0(2964) = 1292 \text{ km s}^{-1}$  and  $u_0(2968) = 1576 \text{ km s}^{-1}$ . If they are associated at a mean redshift distance of 29 Mpc ( $z = 50$ ), the projected linear separation of the pair is small at 52 kpc, which is the distance of the Large Magellanic Cloud from the Sun.

The arms in NGC 2964 are massive in the sense of Reynolds (1927a,b). The pattern is principally that of two arms, although a third, ill-defined broad arm pattern exists on one side. Opaque dust lanes exist on the insides of the two best-defined luminous arms.

NGC 406      Se(s)II.8  
 CD-2015-Bedke/Gregory  
 Oct 25/26, 1981  
 103aO + GG385  
 4-5 min

The spiral pattern in NGC 406 is not well defined. Although the luminosity class assigned in the RSA2 is II, the diffuseness of the pattern suggests the later luminosity class of II.8 given here.

The redshift is  $v_0 = 1326 \text{ km s}^{-1}$ .

NGC 4712      Sc(s)II  
 H-2286-H  
 May 30/31, 1946  
 103aO  
 40 min

Although NGC 4712 is in the same field as NGC 4725 (Sb/SHII; panel I 68), with an angular separation of 12', the pair is an optical superposition and not a physical association. The redshifts are  $u_0(4712) = 4332 \text{ km s}^{-1}$  and  $r_{\text{c}}(\text{IT25}) = 1167 \text{ km s}^{-1}$ .

The print here is made from a 100-inch plate taken with the Mount Wilson Hooker reflector before the mirror had regained thermal equilibrium from an earlier thermal shock due to rapid temperature change. On such occasions the plate glass mirror is warped and the star images are distorted.

NGC 6181      Se(s)II      HA, p. 29  
 H-1851-II  
 Aug 3/4, 1937  
 Imp. Eel.  
 60 min

The spiral pattern of NGC 6181 is dominated by two principal arms having moderate geometrical entropy. The redshift is  $v_0 = 2438 \text{ km s}^{-1}$ .



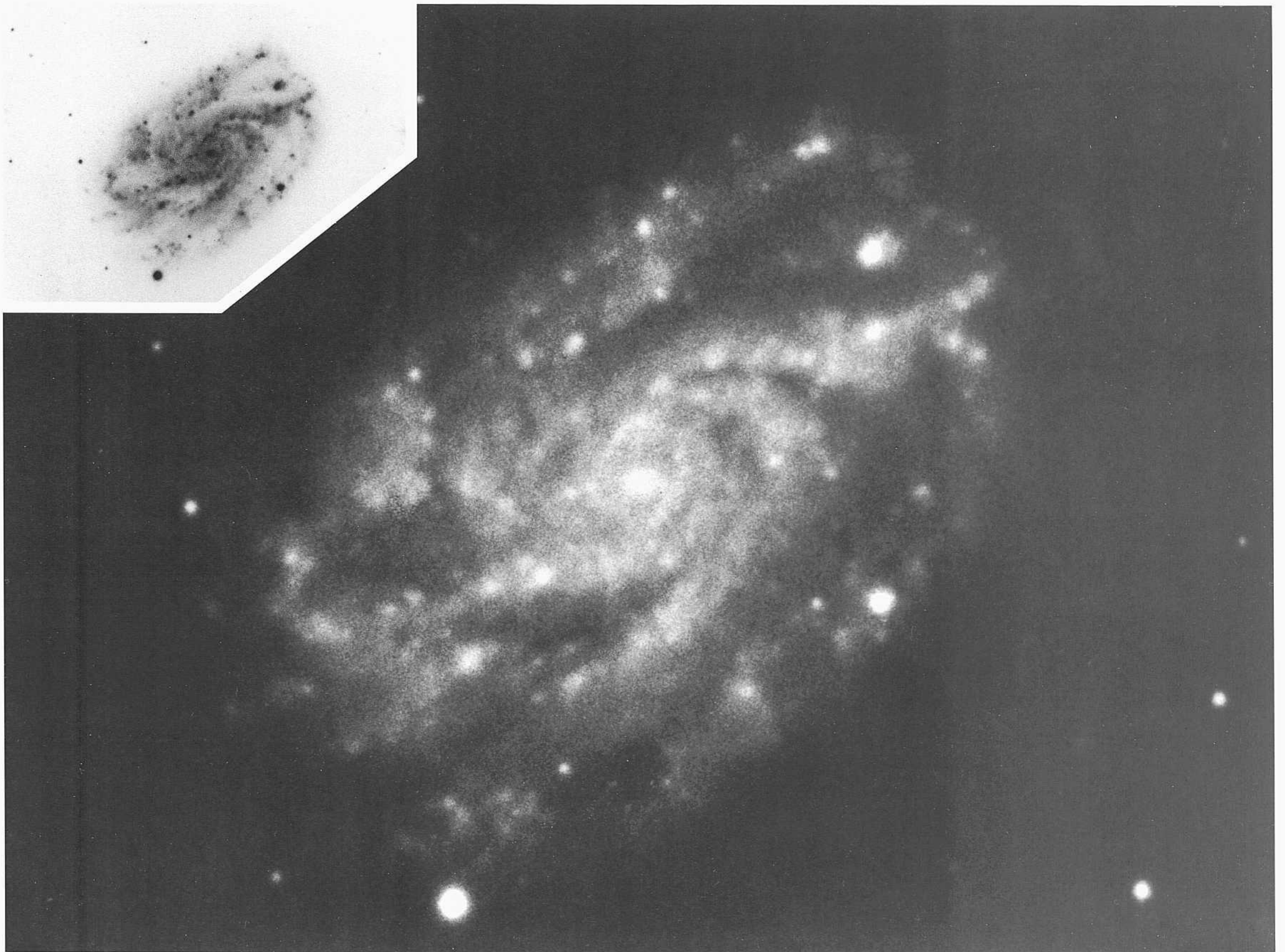
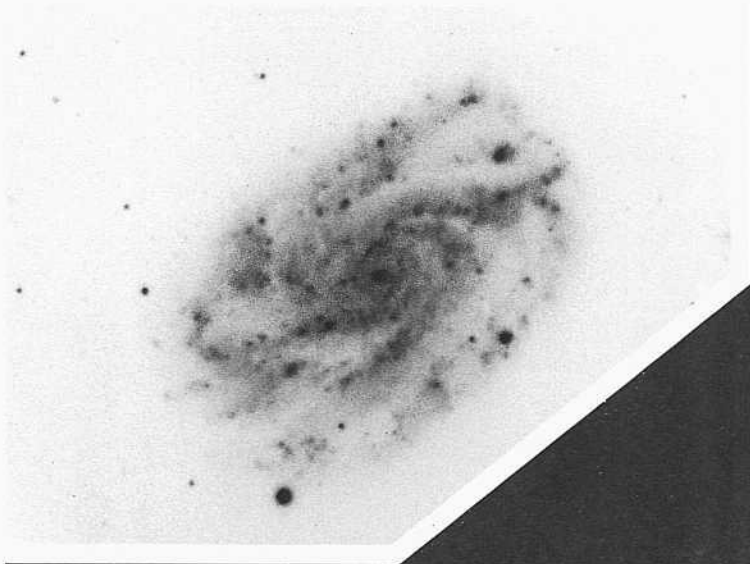
This page begins the section of the Sell galaxies having a primarily multiple-armed pattern. Some have arms of the grand design type; others have a flocculent design of the NGC 2841 (panels 142, S4, S12) type. Galaxies with multiple arms that are thin are on panels 241-247. Galaxies with thicker arms are on panels 248—253.

NGC 7689          Sc(sr)II  
CD-503-S  
Scp 27/28, 1978  
103aO + GG385  
45 mill

Each of the many arms in NGC 7689 begins tangent to a thin luminous inner ring close to the nucleus. The three arms on one side begin near one another on the ring, within about  $15^\circ$  in their position angles. The three arms wind outward and remain moderately well defined over half the outer disk, although one arm abruptly changes direction by about  $120^\circ$  and continues unwrapping. The arm pattern on the other side is more chaotic, becoming more difficult to trace. This may be an aspect effect where the far side is less visible than the near because of silhouetting effects against the background disk.

The arms are massive, covering an appreciable fraction of the disk area.

The redshift is  $v_o = 1681 \text{ km s}^{-1}$ .



PANEL  
241

PANEL  
242



*Sc Classification Section (continued)*

NGC 3423      SC(B)IL2

**CD-1684-S**

**Jan 2/3, 1981**

**103aO + GG385**

15 mill

**The multiple-armed Bpiral pattern in IN(8)!**  
3423 is similar to that in NGC 5457 (M101;  
Hubble Alias, pp. 27, 31; panel 218 here).  
There are no grand design major arms; rather at  
least six arms can be identified starting at the  
center, existing over all position angles around  
the image.

**Brightest individual stars may be beginning  
to resolve at about  $B = 2.1$ . Until they are confused  
on this blue plate with the numerous IIII regions.  
The largest of these regions have core + halo  
diameters of about 2".**

The redshift of NGC 3423 is  $v_r = 845$  km

$s^{-1}$ .

*Sc Classification Section (continued)*

NGC 2763      Sc(s)II

CD-789-S

Feb 23/24, 1979

103aO + GG385

15 min

The two galaxies on this panel have spiral patterns highly similar to that of M10] (ScI; panel 2 18).

Two principal arms in NGC 2763 start near the center. After unwinding for about half a revolution, each arm branches into several segments, which themselves branch again until the outer region is filled with spiral fragments, most of which are of moderately high surface brightness. Many HII regions exist throughout the multiple arms, but individuals must be identified by the usual methods before the brightest stars can be isolated.

The redshift of NGC 2763 is  $v_r = 1\,658$  km

$s^{-1}$ .

NGC 5085      Sc(r)II

CD-1849-HB

April 3/4, 1981

103aO + GG385

45 min

Two principal well-defined arms of low surface brightness begin near the center, tangent to the edge of a small central bulge. Prominent, regular dust lanes exist inside each of the two main arms over about half a revolution from their beginnings.

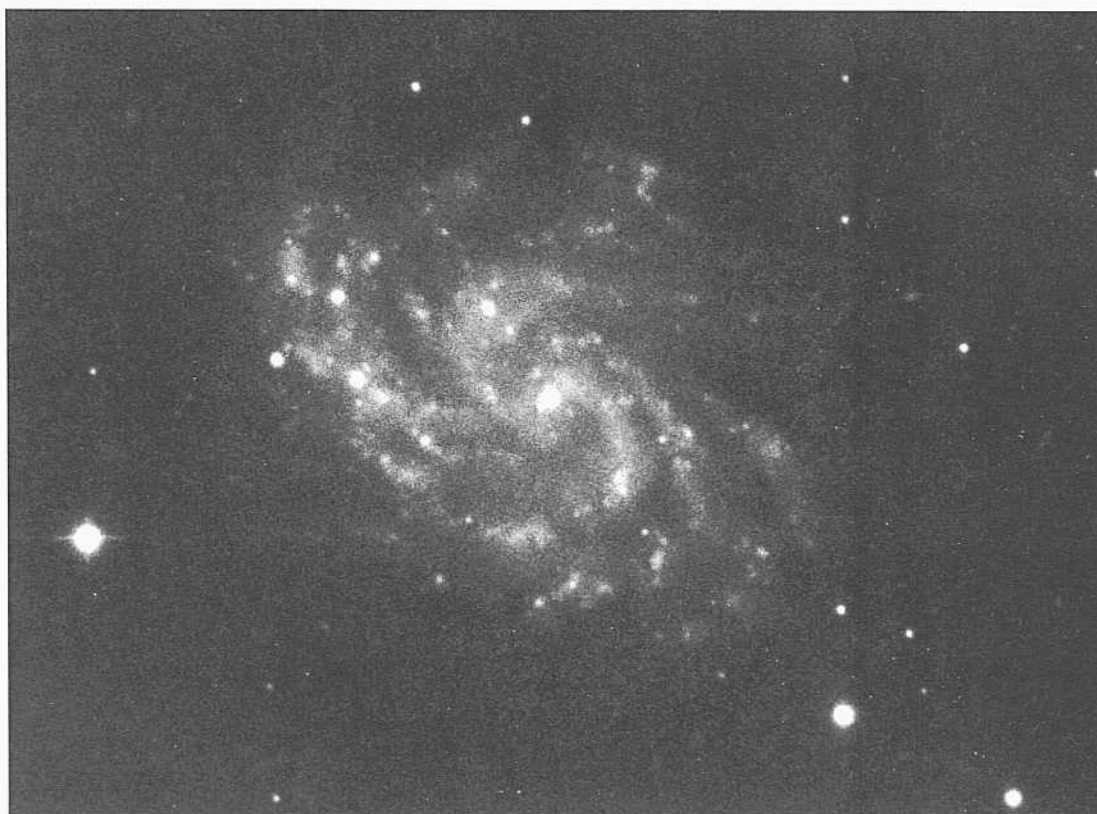
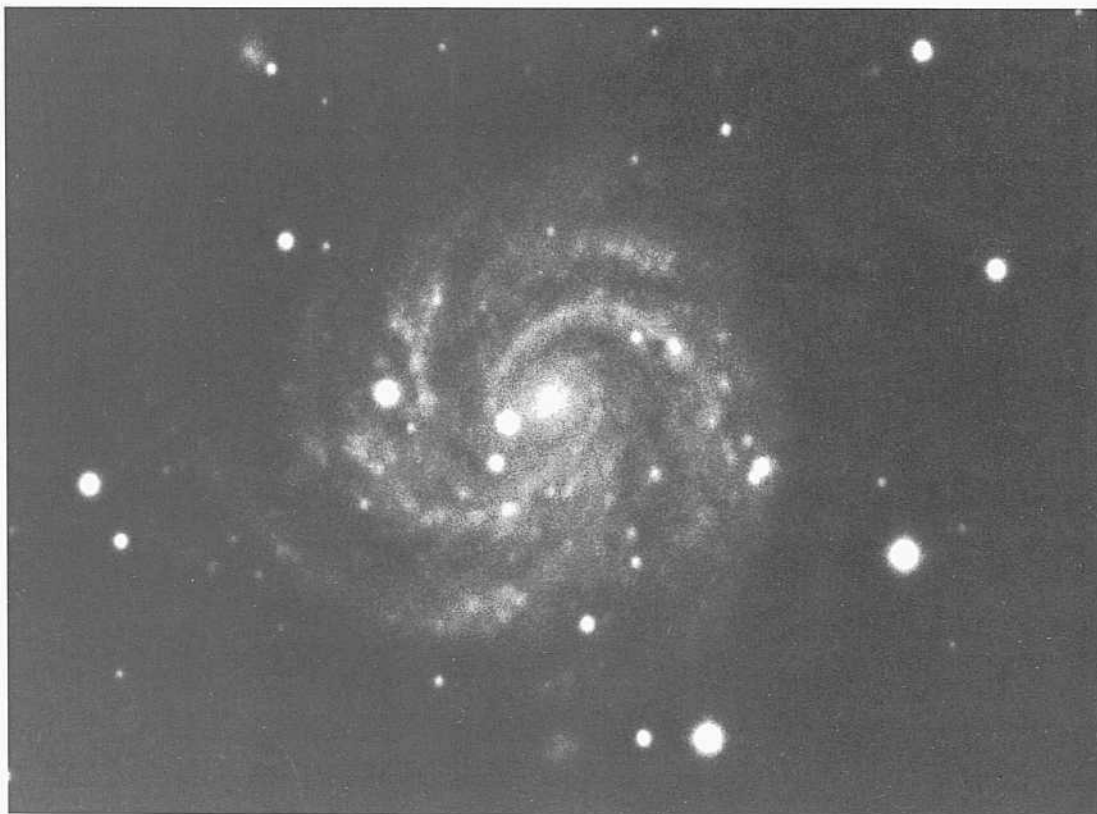
The outer disk is filled with spiral fragments, which originate not as branches of the two main arms but rather as dust lanes covering the disk, as in the NGC 2841 flocculent pattern. These lanes in the outer disk either turn luminous in short segments or are defined by a pattern of HII regions. The pattern is not chaotic, but, aside from the inner parts of the two principal grand design arms, the outer spiral fragments are difficult to trace.

The redshift is  $v_r = 1\,720$  km  $s^{-1}$ .



PANEL  
243

PANEL  
244



The galaxies on this and the following panel continue the pattern of spiral arms that are thin and multiple.

NGC 5494      Sc(s)II  
 CD-1549-S/Br  
 Aug 8/9, 1980  
 103aO + GG385  
 45 min

Two principal arms begin in NGC 5494 near the center on the rim of a small, relatively high surface brightness, smooth disk. They branch almost immediately into secondary arms, which remain of moderately high surface brightness.

The redshift is  $v_0 = 2461 \text{ km s}^{-1}$ . The numerous HII regions are not resolved at the 1" level.

NGC 2848      Sc(s)II      triplet  
 CD-799-S  
 Feb 24/25, 1979  
 103aO + GG385  
 45 min

NGC 2848 forms an apparent triplet with NGC 2851 (S0<sub>3</sub> or very early Sa, not in the RSA) at an angular separation of 5.1', and with an ImlV dwarf irregular at 3.6' from NGC 2848.

The brightest of the HH-region-candidate knots in NGC 2848 and in the ImlV candidate companion are about the same brightness. The same is true of candidates for the brightest individual stars in each galaxy, strengthening the case for a common distance; the redshifts of NGC 2851 and the ImlV dwarf are not yet known (c. 1990). If the triplet is at a common distance of 3.6 Mpc, based on  $v_0 = 1795 \text{ km s}^{-1}$  of NGC 2848, the projected linear separations of the companions from NGC 2848 would be small, at 5.3 kpc and 3.8 kpc.

The two principal well-defined arms in NGC 2848 begin at the center [(s)-type pattern] and branch to form most of the multiple arms over the face of the disk.

NGC 5584      SC(B)L8  
 CD-1836-HB  
 April 1/2, 1981  
 103aO + GG385  
 45 min

Tin' spiral pattern is highly regular although of the multiple-armed type. Some of the arms can be traced for more than half a revolution as individual fragments. Three arms can be said to begin near the center. The two principal ones emerge from the center in an (s)-type connection; the third begins near the center and can be traced for half a revolution outward. Other fragments branch from these main arms farther out in the disk.

The redshift is  $v_0 = 1518 \text{ km s}^{-1}$ .

NGC 4189      SBc(sr)II      VCC 89  
 CD-2118-S  
 March 20/21, 1982  
 103aO  
 50 min

NGC 4189, listed in the Virgo Cluster Catalog, is located 4.2° west of subcluster A associated with NGC 4486 (M87). The morphological type listed in the VCC is SBc(sr)IL2. The evidence for the bar is well seen in the reproduction here. (The galaxy was placed in the Sc section here during an early formatting of the present atlas, based on the RSA classifications. That formatting became fixed early, preventing moving the illustration into the more appropriate SBc section.)

Three principal arms begin near the ends of the bar. Two start at the ends of the short bar in the manner of arms in NGC 1300 (panels L54, S8). The third begins close to but slightly beyond one of the ends of the bar. Branching of all the segments fills the disk with the multiple-arm spiral pattern.



Sc Classification Section (continued)

NGC 5676 Sc(s)II

S-1999-H  
April 12/13, 1948  
103aO  
30 min

The print here of NGC 5676 is from a plate taken with the Mount Wilson 60-inch telescope. The galaxy is unreachable with the Mount Wilson 100-inch because of the high declination.

The spiral pattern is not symmetric on opposite sides of the major axis; the faint and chaotic outer spiral pattern on one side extends over the outer disk to twice the distance from the center, as do the well-defined inner arms on the opposite side, where there are no corresponding outer arms. This pattern is rare but not unknown. NGC 5678 (ScII-III; panel 278) shows the same asymmetry.

The inner arms are thin and well defined. They start from the center in the (s)-subtype configuration.

The redshift of NGC 5676 is  $v_r = 2239 \text{ km s}^{-1}$ .

NGC 3810 Sc(s)II HA, p. 30

H-15-S  
Jan 5/6, 1951  
103aO  
20 min

The spiral pattern of IVGC 3810 resembles that of NGC 1068 (Sb; panel 138). The central disk is filled with very-high-surface-brightness, tightly wound spiral fragments. Lower-surface-brightness arms with more-open pitch angles exist outside the break in the surface-brightness distribution over the inner half of the image.

The largest HII regions may just resolve at the 1" level. Candidates for **individual** brightest stars exist, but they must be verified by standard techniques that separate the stars from HII regions.

The redshift is  $v_r = 860 \text{ km s}^{-1}$ .

NGC 991 Sc(rs)H

PH-7844-S  
Sep 3/4, 1980  
103aO  
12 min

The extremely low surface brightness arms begin at the rim of a central smooth disk that may be an oval; if so, an alternate classification would be SBc.

An unresolved nucleus exists at the center of the oval. The central pattern closely resembles dE,N nucleated dwarf elliptical galaxies (Sandage and Binggeli, 1984, give an atlas of dE,N Virgo Cluster galaxies). Such bright, unresolved nuclei embedded in a smooth disk are characteristic of this type.

The redshift is  $v_r = 1607 \text{ km s}^{-1}$ .

NGC 5468 Sc(s)1.8

CD-1856-HB  
April 4/5, 1981  
103aO + GG385  
45 min

Two thin principal arms can be followed from the center outward, one for half a revolution and the other for a quarter revolution, before they branch into several thin fragments winding through the outer disk. The resulting arm pattern is open. Although the arms are multiple, they remain thin and do not cover a large area of the outer disk because they are so thin.

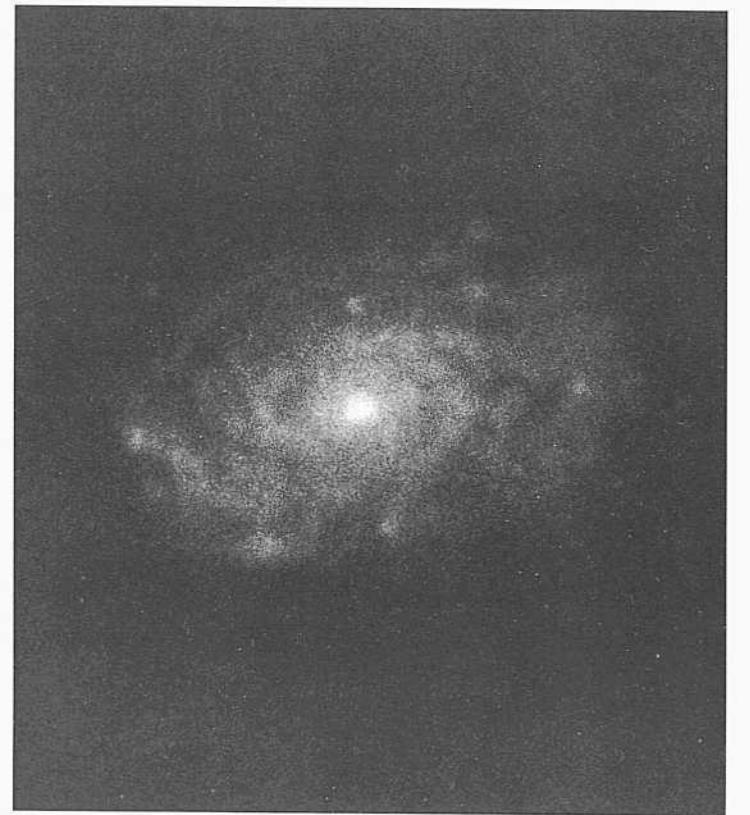
Three high-surface-brightness HII regions and a number of fainter HII regions exist in the arms but are unresolved at the 1" level. The redshift of NGC 5468 is  $v_r = 2696 \text{ km s}^{-1}$ .



PANEL  
245



PANEL  
246



**G**alaxies on this panel continue the illustration of well-organized spiral structure where the arms are moderately thin and the pattern is multiple rather than dominated by two arms of the grand design type.

F-703 = A1511-15      Sc(s)II.2      pair?  
 CD-1420-S/Br  
 March 24/25, 1980  
 103aO  
 75 min

F-703 forms a possible wide physical pair with NGC 5878 (Sb; panel 128) at an angular separation of  $1.2^\circ$ . The redshifts are  $z_o(703) = 2128 \text{ km s}^{-1}$  and  $z_o(5878) = 1974 \text{ km s}^{-1}$ . If the two galaxies are at the same redshift distance of 41 Mpc, the projected linear separation would be 860 kpc (which is the separation of our Galaxy from M31 in the Local Group).

NGC 5605      Sc(rs)II  
 CD-1580-S/Br  
 Aug 11/12, 1980  
 103aO + GG385  
 45 min

Three arms begin near the center of NGC 5605, tangent to the rim of a small, high-surface-brightness, smooth inner disk. These arms branch to form the arm fragments that cover the outer disk.

The redshift is  $v_r = 3196 \text{ km s}^{-1}$ .

NGC 6643      Sc(s)II      HA, p. 35  
 PII-60-H      panel 247  
 April 27/28, 1949  
 103aO  
 40 min

The surface brightness of the inner part of the multiple-arm pattern in NGC 6643 is high. Many bright IIII regions largely define these inner arms. The arm fragments, together with their associated fragmented dust lanes, cover the disk.

A print from a yellow Palomar plate is on the next panel.

The redshift is  $v_r = 1743 \text{ km s}^{-1}$ .

IC 4721      Sc(s)II      pair-  
 CD-1480-S/Br  
 May 11/12, 1980  
 103aO + GG385  
 27 min

IC 4721 forms a physical pair with IC 4720 (Sc) at an angular separation of  $8.5'$ . The redshifts are  $z_o(4720) = 2104 \text{ km s}^{-1}$  and  $z_o(4721) = 2405 \text{ km s}^{-1}$ . At the mean redshift distance of 45 Mpc the projected linear separation of the pair is 111 kpc. An E0 galaxy of unknown redshift exists at the small angular separation of  $2.2'$  from IC 4721. It can be seen on the print here. If it is associated with the pair, its projected linear separation from IC 4721 is small, at 29 kpc.

NGC 2715      Hc(s)II  
 PH-7709-S  
 Fell 1 1/12, 1979  
 103aO  
 12 min

The arm pattern in NGC 2715 is multiple in the sense of NGC 2811 and NGC 488. It is not formed by two principal inner arms that start at the center and then fragment into an outer multiple pattern. Rather, the MAS pattern in NGC 2715 is present from the beginning of the spiral pattern at the center.

The redshift of NGC 2715 is  $z_r = 1540 \text{ km s}^{-1}$ .

NGC 4237      Sc(r)II.2      VCC 226  
 H-1970-H      HA, p. 20  
 April 21/22, 1938  
 E40  
 60 min

The spiral pattern of NGC 4237 is similar to that of NGC 2715, above. The reproduction in the Hubble Atlas was made from the same Mount Wilson 100-inch plate shown here.

The redshift of NGC 4237 is  $v_o = 814 \text{ km s}^{-1}$ . The galaxy is in the region surveyed for the Virgo Cluster Catalog. It is located  $4.5^\circ$  northwest of NGC 4186, associated with Virgo subcluster A.

Sc Classification Section (continued)

NGC 6643      Sc(s)H      HA, p. 35  
PH-5372-S      panel 246  
Sep 11/12, 1969  
103aD + GG11  
40 min

The image here of NGC 6643 is from a 200-inch Palomar 103aD yellow plate rather than from the blue Palomar plate used for the image on the preceding panel.

The description of the spiral pattern is given there for this galaxy. The image on this panel shows a high-surface-brightness continuum disk upon which young spiral arms are superposed. The continuum yellow light shown in this print is from the old stellar component rather than from the young stellar content detected in either blue light or in Ha light, on red-sensitive plates.

NGC 4504      Sc(s)II      pair  
CD-1859-HB  
April 6/7, 1981  
103aO  
75 min

NGC 4504 forms an apparent physical pair with NGC 4487 (Sc; panel 250) at an angular separation of 3.5'. The redshifts of the pair are  $u_o(4487) = 831 \text{ km s}^{-1}$  and  $u_o(4504) = 794 \text{ km s}^{-1}$ . At the mean redshift distance of 1.6 Mpc, the projected linear separation is 165 kpc. The resolution into HII regions and brightest stars is about the same for both galaxies. The largest several HII regions in each galaxy resolve into disks (core + halo) at about the 3" level.

Another nearby spiral exists (UGCA 282; SBbl) at an angular separation from NGC 4487 of 25' at redshift  $v_o = 5460 \text{ km s}^{-1}$ . It is clearly in the background for reasons other than the large redshift difference: its resolution into HII regions is nil, contrary to the case of NGC 4487 and NGC 4504.

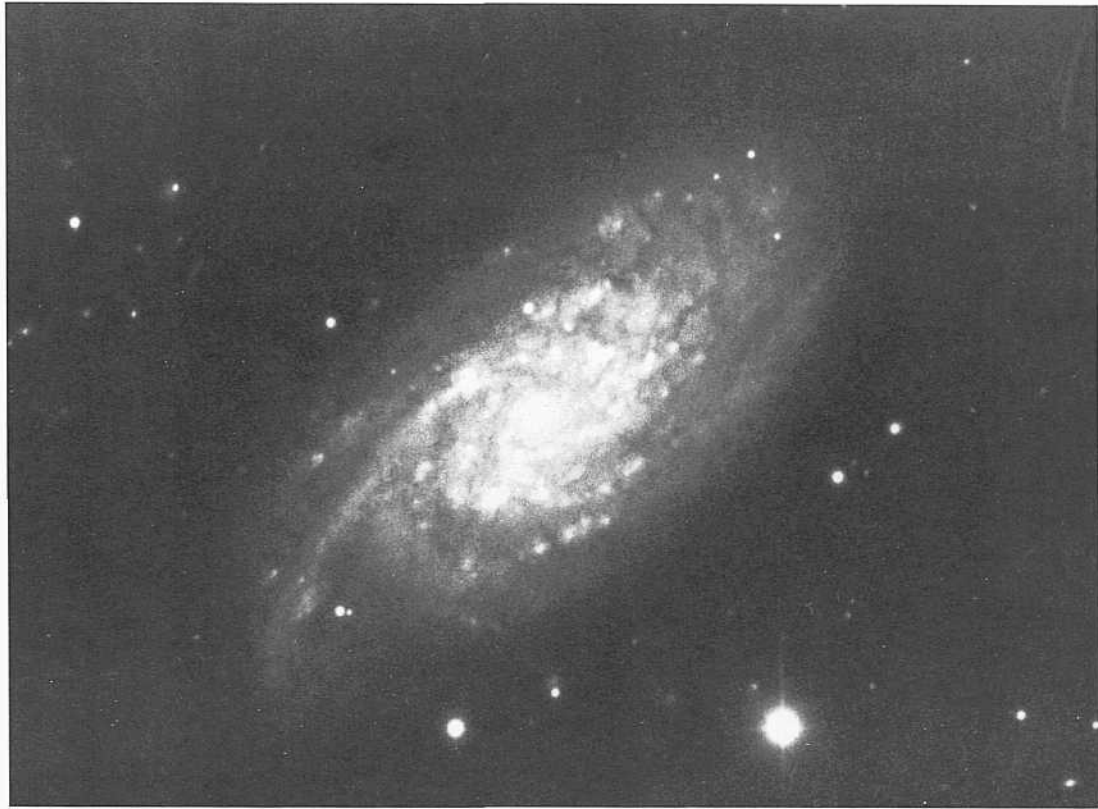
NGC 4559      Sc(s)II  
PH-8003-S  
Feb 2/3, 1981  
103aO  
12 min

NGC 4559 is nearby, judged by the ease of resolution of the HII regions at about the 3" level and the existence of what appear to be individual stars starting at about  $B = 22$  mag. The blue image is given in the upper print here. The Ha interference filter image is below.

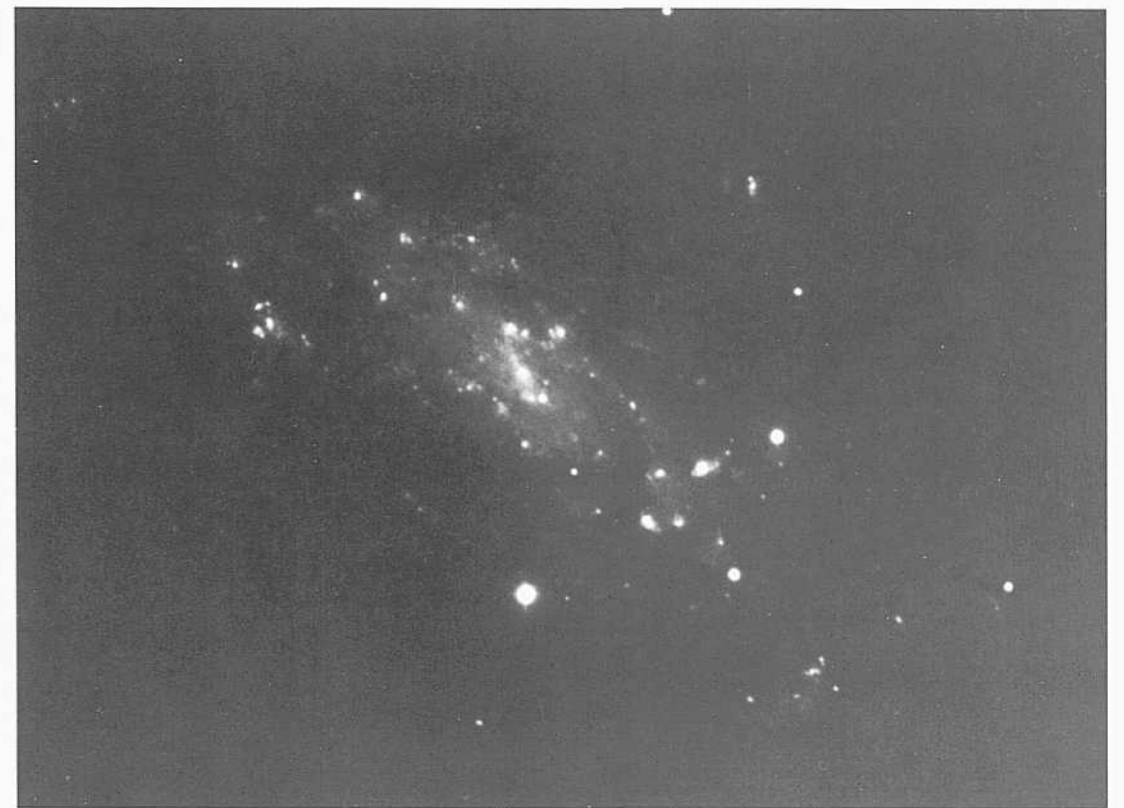
The redshift is  $v_o = 771 \text{ km s}^{-1}$ .

NGC 4559      Sc(s)II  
PH-4516-S  
April 14/15, 1964  
Ha interference filter  
120 min

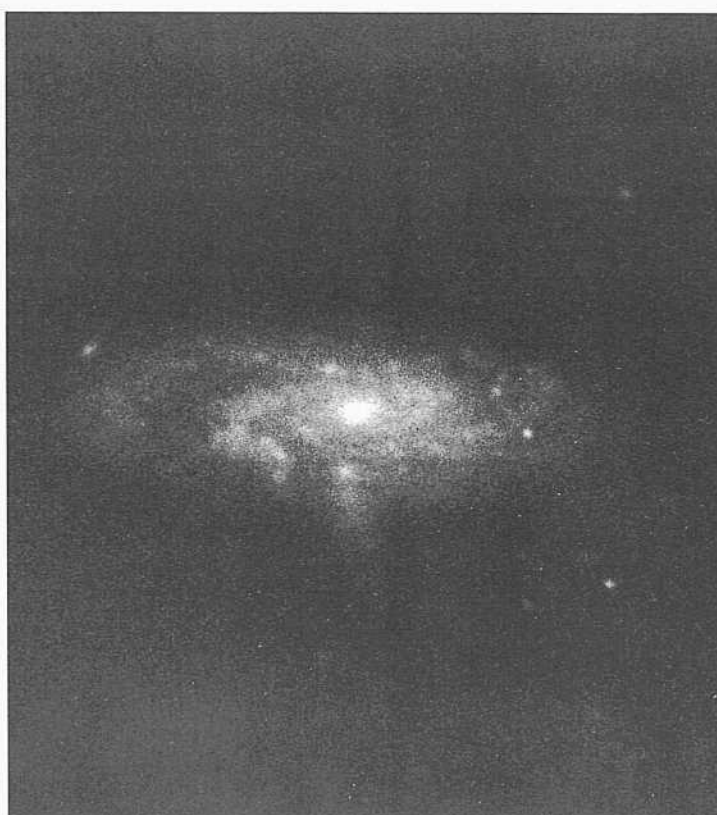
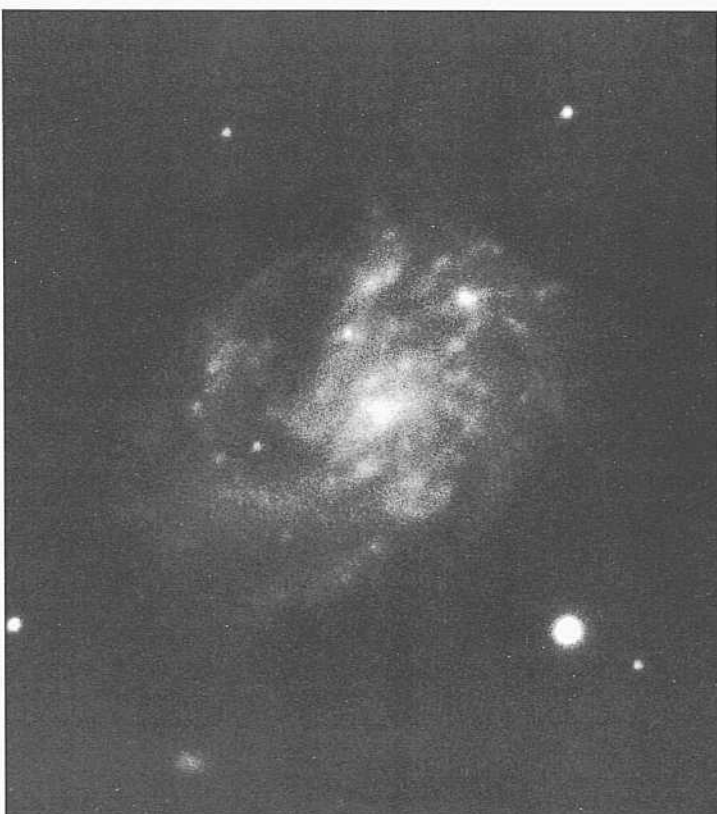
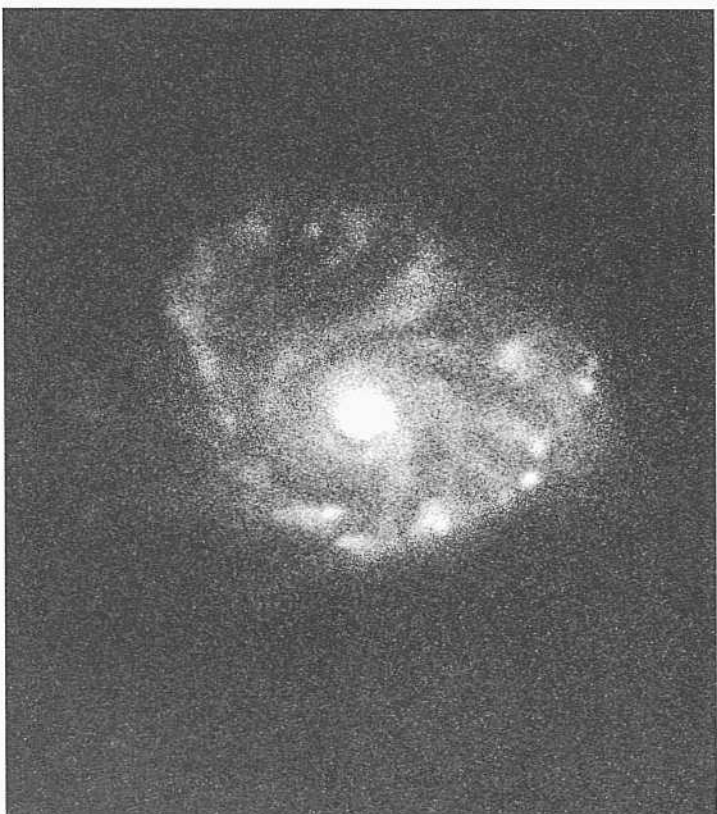
The largest of the individual HII regions in NGC 4559 resolve at about the 3" level. The arms are not as well defined as in the continuum blue image in the print above.



PANEL  
247



PANEL  
248



The six galaxies on this panel continue the Sell morphology among galaxies whose spiral arms are thin and easily traced as individual fragments  $l > 11$  which are multiple and cover much of the underlying disk.

NGC 514            Sc(s)II            Racine wedge  
PH-7698-S  
Sep 26/27, 1979  
103aO  
12 min

The multiple pattern in NGC 514 begins at the small nuclear region, starting as dust lanes closer to the center than where the luminous segments start, after which the dust lanes are generally on the insides of the best-defined arm fragments.

The bright stars show secondary images made by the Racine wedge.

The redshift is  $v_o = 2675 \text{ km s}^{-1}$ .

NGC 5112            Sc(rs)II            Racine wedge  
PH-8063-S  
Feb 4/5, 1981  
103aO  
12 min

An apparent short bar exists at the center of NGC 5112. The bar is strong enough for the type to be SBc in the RC2, based on a Mount Wilson 60-inch plate.

Four arms begin in the vicinity of the ends of the bar. They remain thin but branch into several segments over the outer disk.

The redshift is  $v_o = 998 \text{ km s}^{-1}$ .

NGC 95            Sc(s)1.8            Racine wedge  
PH-7694-S  
Sep 26/27, 1979  
103aO  
12 min

Five arm segments begin at the center and end abruptly at a bright edge, which at lower resolution would appear to be a luminous outer rim.

The redshift is large for RSA galaxies, at  $v_o = 5104$ . Because NGC 95 has an apparent magnitude that is bright enough to be in the RSA, the absolute magnitude of NGC 95 is among the brightest in that catalog, at  $M_B = -22.2$ .

There are evident HII regions, especially along the outer edge of the spiral pattern. These are unresolved at the great distance of the galaxy.

NGC 3041            Sc(s)II            Racine wedge  
PH-7962-S  
Nov 8/9, 1980  
103aO  
12 min

Two faint stubs of luminous spiral arcs begin at the center but fade into the inner disk after a quarter revolution. The larger fragments of arms composing the outer spiral pattern begin farther from the center and have no clear connection with the two inner spiral stubs.

The bright stars show the secondary images made by the Racine wedge, separated from the primary by 18" with an intensity that is 5 mag fainter.

The redshift is  $v_o = 1296 \text{ km s}^{-1}$ .

NGC 3629            Se(s)II.2            Racine wedge  
**PH-8053-S**  
Feb 4/5, 1981  
**103aO**  
12 min

The spiral pattern of NGC 3629 is of the MAS type, similar to that of NGC 2 HI 1 and NGC 488 where many arms on the outside extend 1" the center.

The bright stars show the secondary images made by the Racine wedge, separated by 18" from the primary and fainter by 5 mag.

The redshift of NGC 3629 is  $v_o = 1451 \text{ km s}^{-1}$ .

NGC 5362            Sc(s)II            Racine wedge  
PH-8098-S  
Feb 6/7, 1981  
103aO  
12 min

Although the viewing angle for NGC 5362 is high, it appears that four main arms exist in a grand design pattern starting from the center in an (s)-type central connection.

The most unusual feature is the spike of luminosity on one side of the image, beginning at an unresolved knot on the minor axis. From the direct image alone one cannot locate it in three dimensions: it is not evident if it is in the plane or is above the nucleus in the halo.

Such features are rare elsewhere but not unknown. Evidence exists for a fountain into tin; halo in NGC 1808 (Shi-pec; panel 193). Evidence both from direct imaging and spectroscopy exists for matter being ejected from the plane in NGC 3034 (MK2: panels 333, 334).

The redshift of NGC 5362 is  $u_o = 2321 \text{ km s}^{-1}$ .



Sc Classification Section (continued)

NGC 5967      Sc(rs)II.2      pair  
 CD-923-HB  
 May 3/4, 1979  
 103aO + GG385  
 45 min

NGC 5967 forms a physical pair with NGC 5967A at an angular separation of  $8.3'$ . The  $v_o$  redshifts are  $2657 \text{ km s}^{-1}$  and  $2714 \text{ km s}^{-1}$ , respectively. At the mean redshift distance of 54 Mpc ( $// = 50$ ) the projected linear separation is 130 kpc.

The inclination of NGC 5967 to the sight line is sufficiently high that the central region appears to be oval. However, the major axis of the central image has the same position angle as that of the outer spiral arms. By viewing the image obliquely by holding this page at an angle and rotating for the proper position angle of the major axis, a decision can be made that the morphological type is Sc rather than SBc.

NGC 1292      Sc(s)II  
 CD-577-S  
 Oct 8/9, 1978  
 103aO + GG385  
 40 min

Four arm crossings of the major axis occur on one side of the image of this MAS-type spiral; three crossings occur on the other side. The arms and their associated spiral dust lanes in the inter-arm regions cover much of the area of the disk.

The redshift is  $v_o = 1390 \text{ km s}^{-1}$ .

NGC 7059      Sc(r)II  
 CD-508-S/Br  
 Sep 28/29, 1978  
 103aO + GG385  
 4-5 min

The spiral pattern is not regular in NGC 7059. The arm pattern is difficult to trace both in the center and on the outside. Two thin segments of separate arms cross on one side of the major axis; they either have very different pitch angles or one is out of the main plane. As with other galaxies on this panel, the disk is covered with star-forming regions. The numerous HII regions are unresolved.

The redshift is  $v_o = 1660 \text{ km s}^{-1}$ .

NGC 3021      Sc(s)II      Racine wedge  
 PH-7932-S  
 Nov 7/8, 1980  
 103aO  
 7 min

The set of (s)-type multiple arms is of high surface brightness. Note the secondary images of the bright stars made by the Racine wedge.

The redshift is  $v_o = 1520 \text{ km s}^{-1}$ .

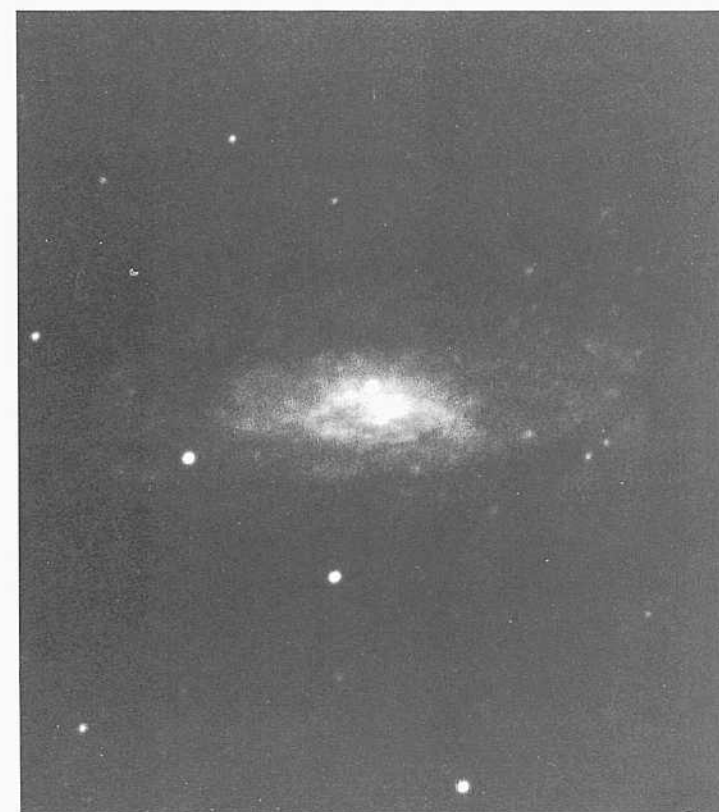
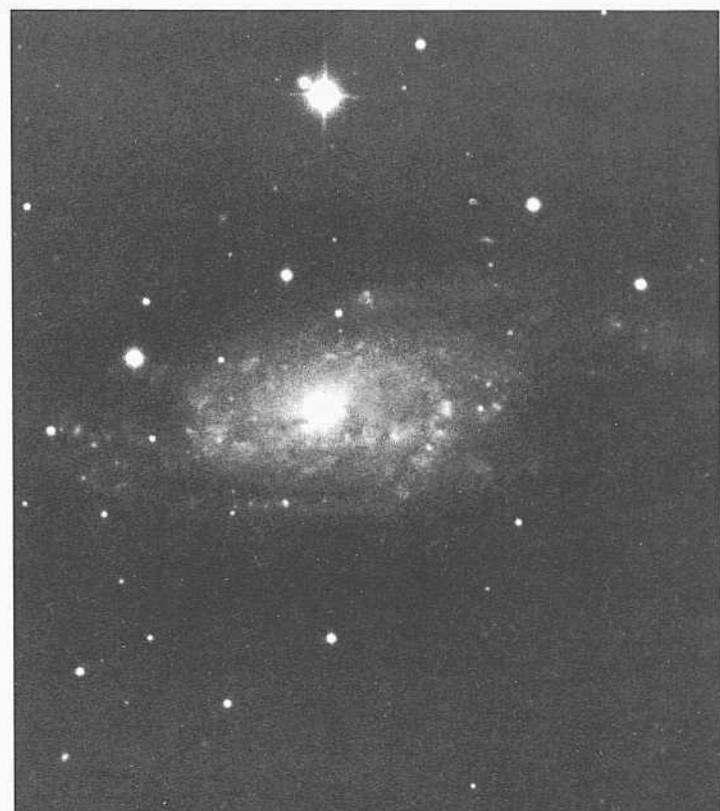
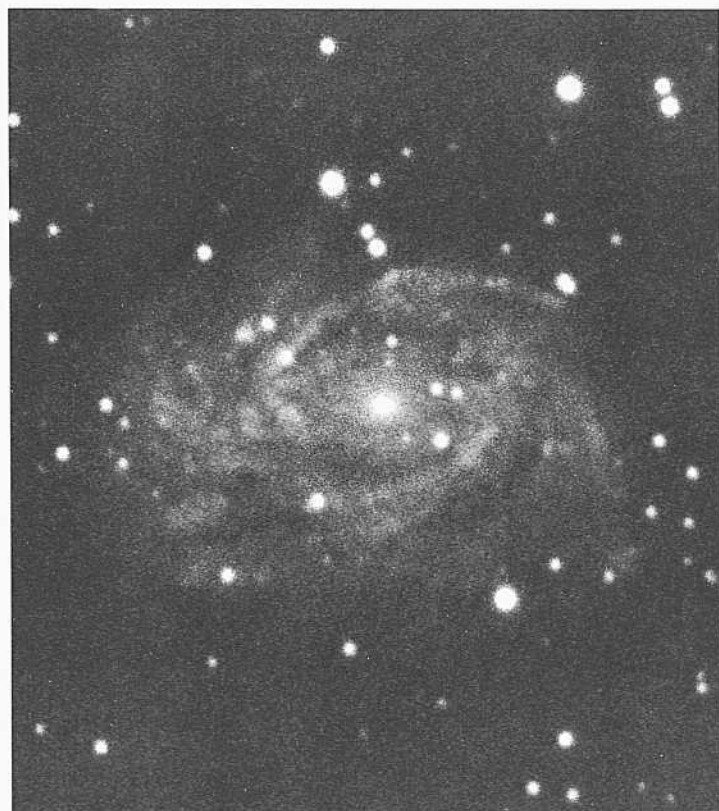
NGC 6574      Sc(s)II  
 H-1403-H  
 July 31/Aug 1, 1932  
 Imp. Eel.  
 60 min

Three principal arms exist in this more-or-less grand design spiral. Two of the principal arms are themselves double. Counting these as separate arms yields four arm crossings of the major axis on one side.

The redshift is  $v_o = 2415 \text{ km s}^{-1}$ .

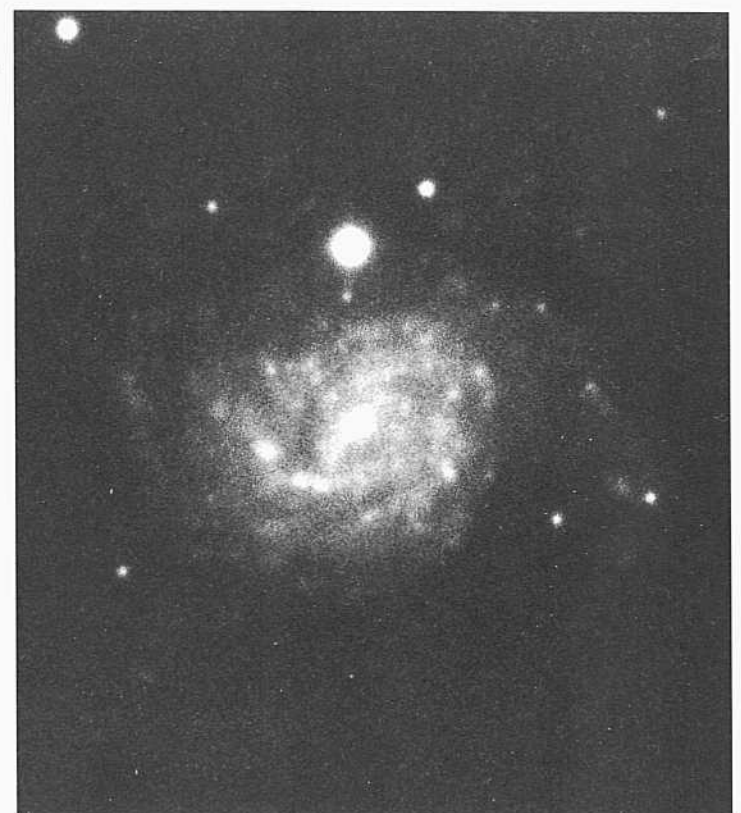
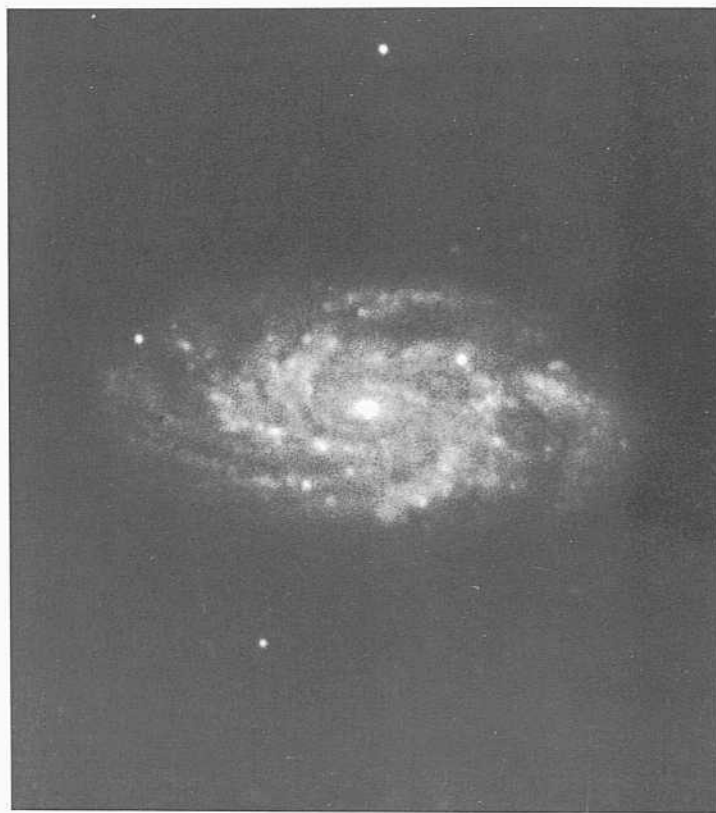
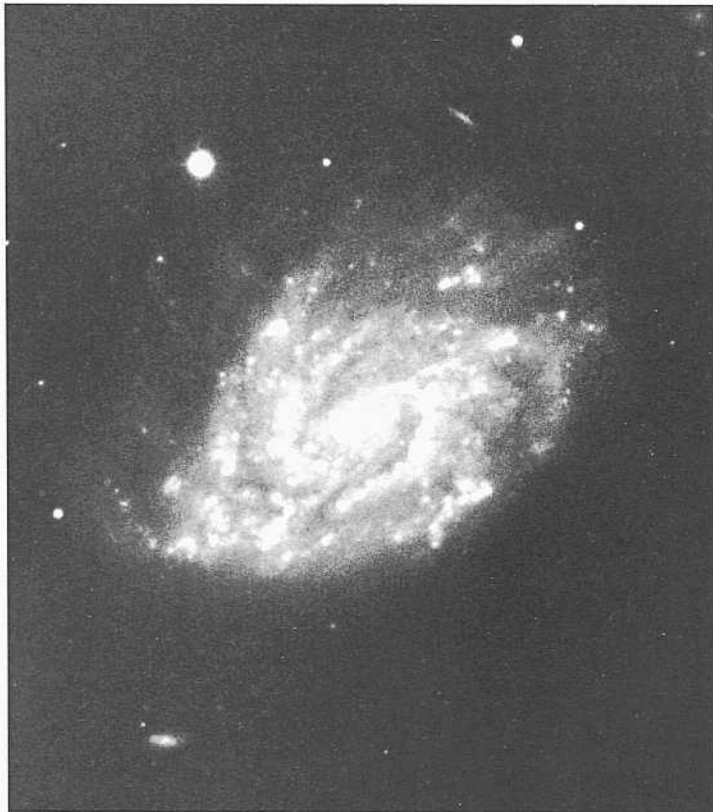
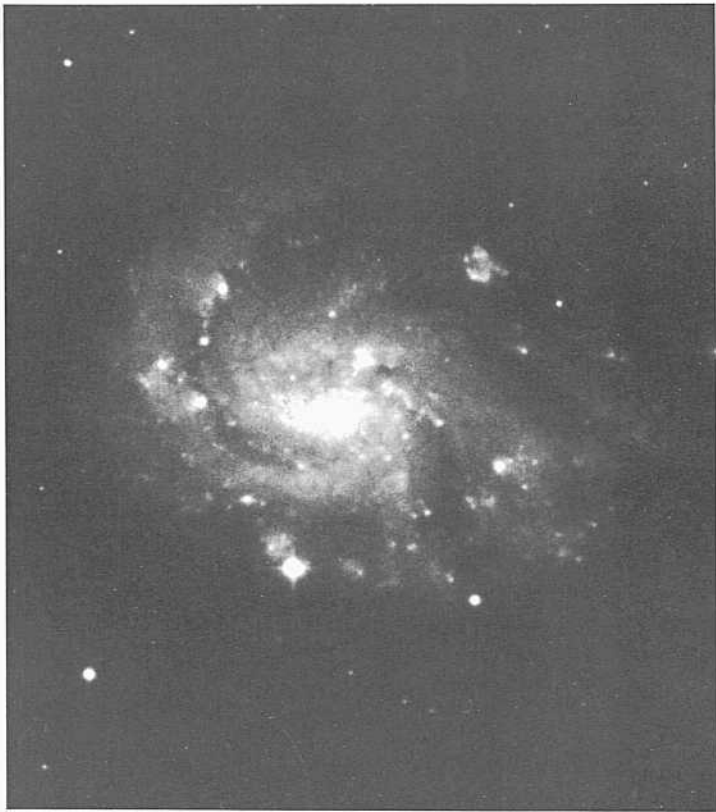
NGC 4951      Sc(s)II      pair:  
 CD-2189-S  
 March 29/30, 1982  
 103aO + GG385  
 45 min

NGC 4951, with  $v_o = 993 \text{ km s}^{-1}$ , may form a physical pair with NGC 4941 (Sab; panel 117), whose redshift is  $v_o = 878 \text{ km s}^{-1}$ . The angular separation of the pair is  $60'$ . At a redshift distance of 19 Mpc the projected linear separation is 332 kpc, or about one-third the diameter of the Local Group.



PANEL  
249

PANEL  
250



**G**alaxies on this and the next three panels are of morphological class Scl and often have the MAS arm pattern. Most have massive arms in the sense of Reynolds (1927a,b); such arms cover much of the disk.

NGC 4487      Sc(s)II.2      pair  
 CD-1859-HB  
 April 6/7, 1981  
 103aO  
 75 min

NGC 4487 forms an **apparent** physical pair with NGC 4504 (Sc; panel 247). The redshift of NGC 4487 is  $v_o = 831 \text{ km s}^{-1}$ ; that of NGC 4504 is  $v_o = 794 \text{ km s}^{-1}$ . The latter has an **angular** separation of  $35'$  from NGC 4487. At the mean redshift **distance** of 16 Mpc the projected linear separation is 165 kpc.

Two principal arms of the grand design type exist in NGC 4487. Dust lanes accompany these arms on the inside of the arm segments. One of the **principal** arms is less well defined than the other; it branches into several, perhaps four, broad segments which cover one side of the disk.

The largest of the many HII-region candidates resolve into disks (core + halo) at the  $3''$  level.

NGC 2742      Sc(rs)II      Racine wedge  
 PH-7710-S  
 Feb 11/12, 1980  
 103aO  
 12 min

The **spiral** pattern in NGC 2742 is beautifully regular. It is multi-armed: five crossings of the major axis can be traced on one side and three or four on the other (depending on whether one counts satellite arm fragments as separate arms).

The original **plate** was taken with a Racine wedge which makes secondary images of the bright stars.

The redshift is  $v_o = 1422 \text{ km s}^{-1}$ .

NGC 1255      Sc(s)H  
 CD-2000-Bedke/Gregory  
 Oct 22/23, 1981  
 103aO + GG385  
 45 min

The arm pattern in NGC 1255 is massive in the sense of Reynolds (1927a,b), covering the disk. Four arm crossings of the major axis can be counted on each side of the image.

The largest of the several HII-region candidates **probably** resolve into disks (core + halo) at about the  $1.5''$  level.

The redshift is  $v_o = 1656 \text{ km s}^{-1}$ .

NGC 450      Sc(s)II.3      Racine wedge  
 PH-7835-S  
 Sep 3/4, 1980  
 103aO  
 12 min

The surface brightness of the multiple-arm pattern in NGC 450 is low. The **brightest** of the many HII-region candidates in the arms may be **complex**. The largest two regions appear to resolve (core + halo) at about the  $2''$  level. The redshift of NGC 450 is  $1911 \text{ km s}^{-1}$ .

Note the small Sc galaxy nestled in the outer arm pattern of NGC 450. There is no evidence for a strong gradient of absorption across the disk of this galaxy. The point is important because the small galaxy is evidently in the background; yet dust absorption, as would be caused by the disk of NGC 450 if it were **optically thick**, is **not** evident. This is taken as evidence **that** the disks of at least some Sc galaxies are optically **thin** at blue (optical) wavelengths, **contrary to** some current (c. 1990) views.

NGC 2090      Sc(s)II      panel 257  
 CD-663-Br  
 Jan 22/23, 1979  
 103aO + GG385  
 45 min

The distance to NGC 2090 is evidently **smaller than the distance to the Virgo Cluster** (adopted here to be  $m - M = 31.7$ ) because the **outer-arms are well resolved into individual brightest-star candidates and IIII regions**. The largest of the IIII regions are resolved into disks (core + halo) at the  $4''$  level.

Although the **resolution into individual brightest stars** is better than in Virgo Cluster spirals, the galaxy is **not** as easily resolved as M101, whose distance modulus, determined from Cepheids, is  $m - M = 29.3$ . An estimate of the distance modulus of NGC 2090 at about  $m - M = 31$  comes from the ease of **resolution into stars**. The redshift is  $v_o = 755 \text{ km s}^{-1}$ .

The arm pattern in NGC 2090 is **multiple**. The inner region of the disk is **covered with** spiral arms that have very high surface brightness. The outer-arm pattern is composed of **arm fragments of low surface brightness**; the resolution into stars and IIII regions is easiest here.

NGC 5768      Sc(s)II  
 CD-1844-HB  
 April 2/3, 1981  
 103aO + GG385  
 45 min

The small **angular size of NGC 5768** ( $D_{25} = 2'$ ) and the **faint apparent magnitude of  $S_f = 12.9$** , combined with the fairly small redshift of  $v_o = 1960 \text{ km s}^{-1}$  gives the faint absolute magnitude  $M_{H\beta} = -20.4$ .

The HII regions and individual brightest stars are unresolved.

The spiral arms in the six galaxies on this panel are massive in the sense of Reynolds (1927a,b). The arm pattern in each is regular enough for assignment of luminosity class II.

NGC 7448      Sc(r)II.2  
 PH-7689-S  
 Sep 26/27, 1979  
 103aO  
 12 min

As in NGC 2090 on the preceding panel, the spiral pattern in NGC 7448 is composed of two regions of quite different surface brightness. The inner region of the disk has tightly wound, **high-surface-brightness** spiral fragments. Individual arms are **not** easily identified. The surface brightness decreases abruptly at the edge of this inner zone. Outer individual arm fragments and a general inter-arm spiral pattern in weak dust lanes can be traced over the outer disk.

A cluster of unresolved **III** regions exist in one of the most conspicuous of the outer arms.

The redshift is  $u_0 = 2485 \text{ km s}^{-1}$ .

NGC 3055      Sc(s)II  
 CD-1698-S  
 Jan 4/5, 1981  
 103aO + GG385  
 45 min

NGC 3055 has weak features of a barred spiral. Two high-surface-brightness inner arms start from the ends of the bar and, by branching, give rise to the luminous, massive arm fragments that cover the outer disk.

The redshift is  $v_0 = 1747 \text{ km s}^{-1}$ .

NGC 3089      Sc(s)II  
 CD-1315-S/Br  
 March 12/13, 1980  
 103aO + GG385  
 45 min

The two principal arms of this (s)-type spiral begin as low-surface-brightness features with associated dust lanes near the center. These features, moderately ill-defined, connect with the **very-high-surface-brightness**, massive, well-defined principal outer luminous arms at a distance of about half a disk length from the center.

A third, lower-surface-brightness arm begins also at the place that one of the two principal **high-surface-brightness** arms starts. The pitch angle of this third arm is different from the others.

The redshift is  $v_0 = 2375 \text{ km s}^{-1}$ .

NGC 2964      Sc(s)II.2      Karachentsev 210  
 PH-7603-S      panel 240  
 April 3/4, 1979  
 IIIaJ + GG385  
 30 min

NGC 2964 forms a close physical pair with NGC 2968 (S0<sub>8</sub> or Amorphous; panels 49, 337) at a separation of 5.8'. The redshifts are  $u_0(2964) = 1292 \text{ km s}^{-1}$  and  $f_0(2968) = 1576 \text{ km s}^{-1}$ . At the mean redshift distance of 2.9 Mpc ( $H = 50$ ) the projected linear **separation** is small, at 49 kpc.

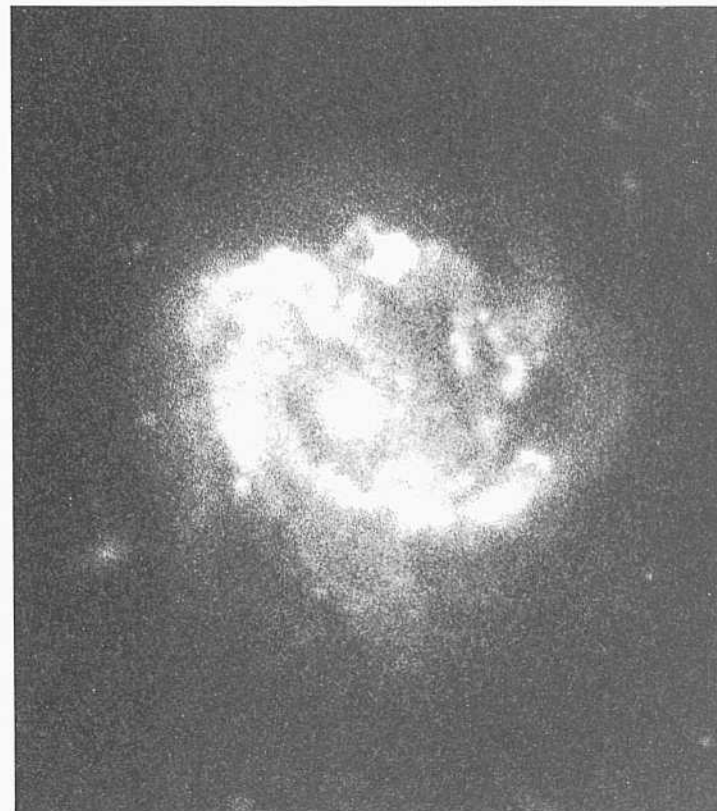
NGC 245      Sc(s)II pec  
 PH-7834-S  
 Sep 3/4, 1980  
 103aO  
 12 min

There are three main arm connections with the center in NGC 245, but, as in NGC 3089 to the left, the surface brightness of these connections is low. The central structures become the bright principal arms at about a third of a disk radius from the center. Four main bright arms are evident near the outside of the pattern.

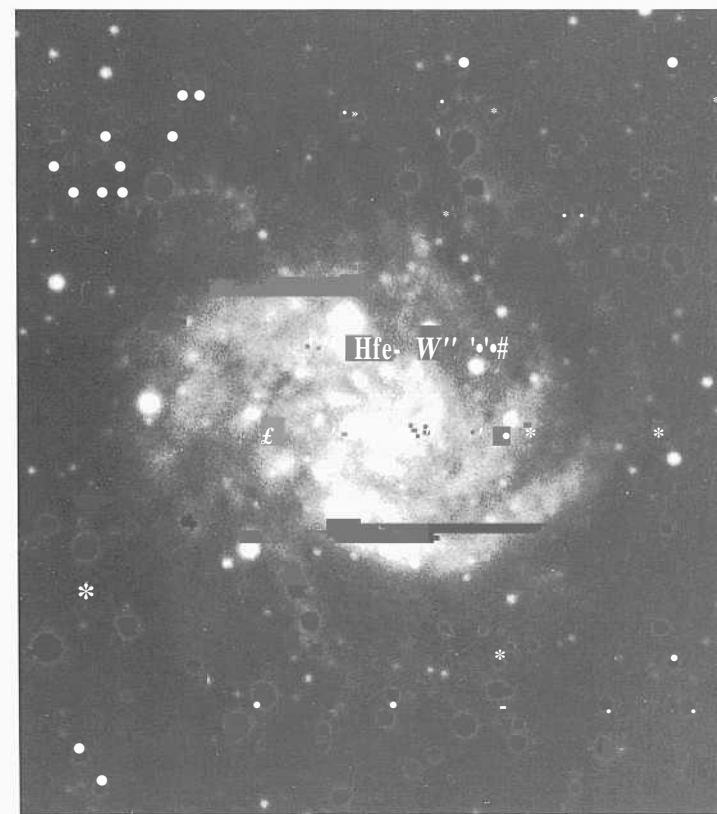
The redshift is  $v_0 = 4275 \text{ km s}^{-1}$ .

NGC 6215      Sc(s)II      pair  
 CD-1582-S/Br  
 Aug 11/12, 1980  
 103aO + GG385  
 45 min

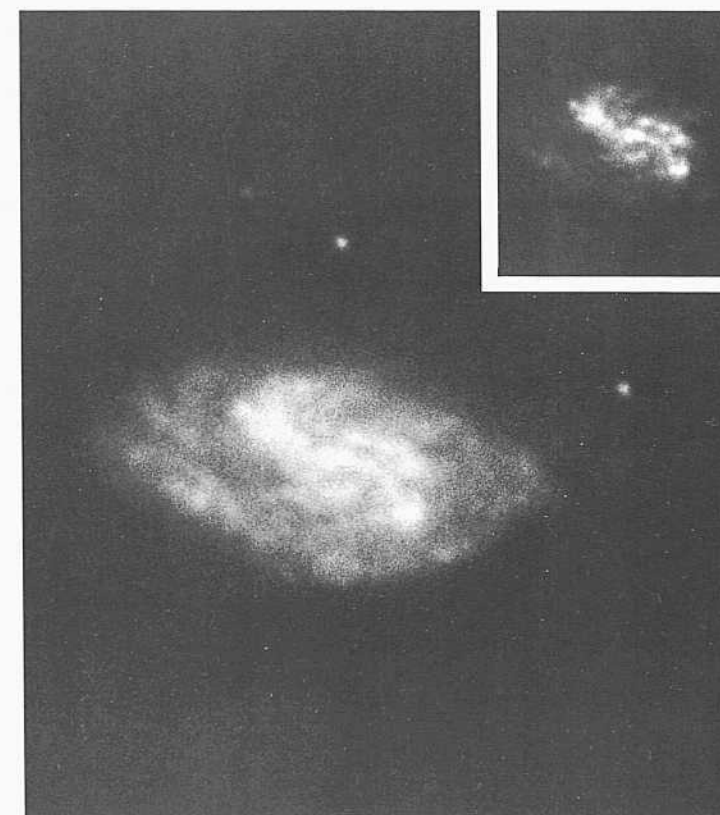
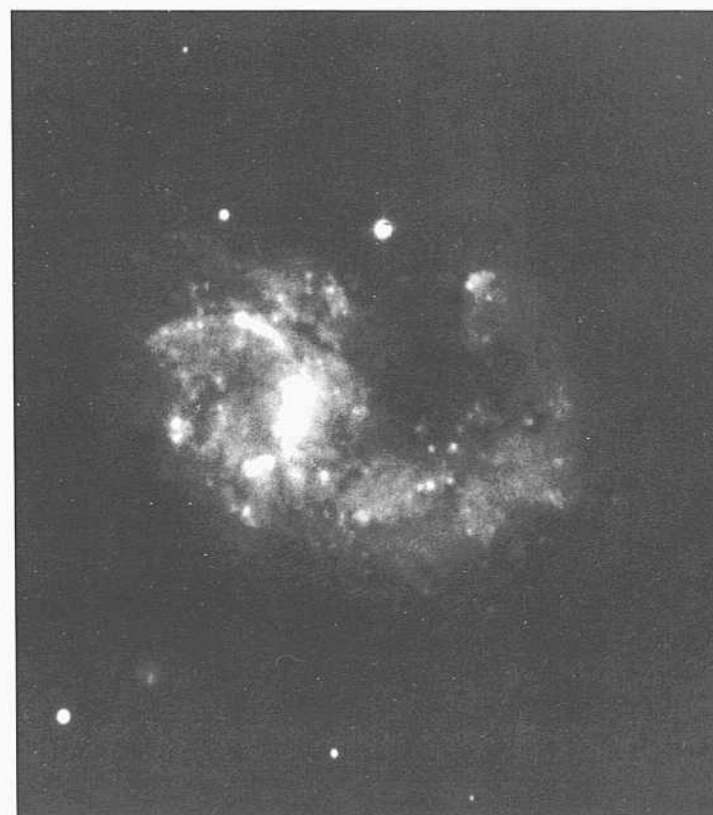
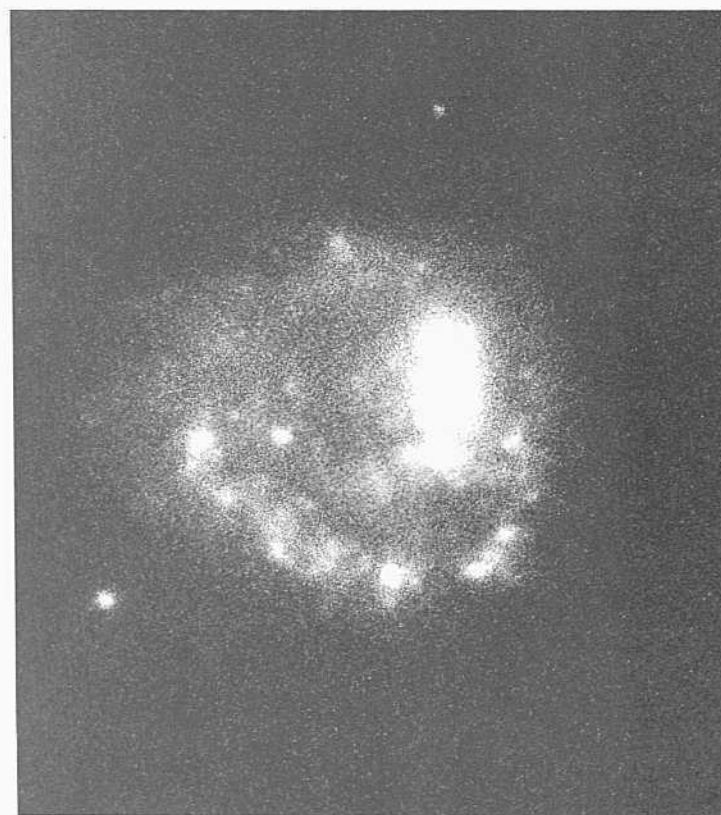
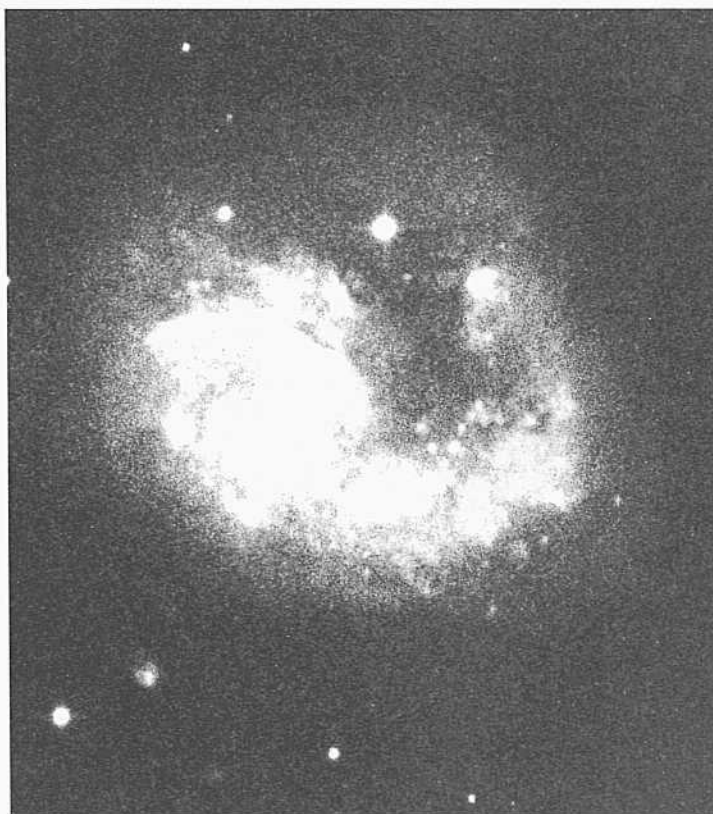
NGC 6215 forms a physical pair with NGC 6221 (Sbc; panel 189) at an angular separation of 18.3'. The redshifts are  $u_0(6215) = 1355 \text{ km s}^{-1}$  and  $u_0(6221) = 1270 \text{ km s}^{-1}$ . At the mean redshift distance of 2.6 Mpc ( $H = 50$ ), the projected linear separation of the **pair** is 140 kpc. There are several candidate low-surface-brightness **companion dwarfs** in the field.



PANEL  
251



PANEL  
252



**T**  
 The five galaxies on this panel continue the examples of spiral patterns that cover the disk because of their massive nature in the sense of Reynolds (1927a,b).

NGC 337      Sc(s)II.2 pec      merger?  
 PH-7672-S  
 Sep 25/26, 1979  
 103aO  
 12 min

The arms in NGC 337 cannot be well traced from the nucleus. Perhaps part of the central pattern is a bar, from whose opposite ends originate two of the arm fragments, but the pattern is not regular. The association of the other segments with any overall spiral pattern as a whole is even less obvious.

The irregular morphology of the arm segments may be clue to a close encounter; this might be established if the small structure with a central knot (a nucleus?) and associated bar with its associated stubby (s)-type arms can be identified as a companion. But it is not certain that this galaxy is in fact a companion, or even if so, if it is ready to merge.

The comment in the RC1 on the morphology of NGC 337 that NGC 337 "resembles NGC 1313" may be appropriate; NGC 1313 (SBIII-IV; panel 309) has been suggested to be in a close encounter.

NGC 2793      SclI pec  
 PH-7931-S  
 Nov 7/8, 1980  
 103aO  
 12 min

The unusual morphology of NGC 2793 is similar to NGC 337 above and NGC 4027 to the right. The partial-ring morphology is also similar to the ring galaxies attributed by Theys and Spiegel (1976, 1977) and Lynds and Toomre (1976) as due to plunging encounters, as discussed on earlier pages of this atlas. A small, undisturbed galaxy exists at the close separation of 90", but its redshift is unknown and it may be in the background. If so, the unusual morphology of NGC 2793 would be endemic to the system, not due to an encounter.

NGC 4027      Sc(s)II.2      group  
 CD-1679-S  
 Jail 1/2, 1981  
 103aO  
 60 min

NGC 4027 is in an apparent small group of galaxies contained within a 2°-diameter circle, all having similar redshifts within  $10 \text{ km s}^{-1}$  of the mean redshift.  $\langle v_r \rangle = 1382 \text{ km s}^{-1}$ , of the five brightest group members. These five brightest members, all in the RSA, are NGC 4024 (SO; panel 31), NGC 4027 here (Sc), NGC 4033 (SOj; panel 35), and the famous interacting pair NGC 4038/4039 (Sc/Sc tides; panel 280). If the angular radius of the group is  $1^\circ$ , its linear radius is 480 kpc, based on a mean redshift distance of 28 Mpc. Therefore the group is a field example of the Local Group. It contains late-type spirals, early-type galaxies, and Magellanic Cloud-type Im galaxies. Two of these are close to NGC 4027, here. A well-resolved ImIII exists at an angular separation (south) of 4.0' (projected linear separation of only 33 kpc); a BCD exists at an angular separation (northwest) of 16.4' (projected linear separation of 133 kpc).

Although NGC 4027, shown here and below, has a peculiar morphology because of the nonsymmetry due to its one bright, massive arm, there is no evidence of an encounter or a merger; there is no perturbing galaxy nearby.

It must be considered a coincidence that NGC 4038/4039, the galaxies that provide the most direct evidence anywhere in the sky of a close encounter, are in this group and are separated from NGC 4027 by only 41'. The projected linear separation of the NGC 4038/4039 pair from NGC 4027 is 334 kpc.

NGC 4027      Sc(s)II.2      group  
 CD-1679-S  
 Jim 1/2, 1981  
 103aO  
 60 min

The resolution of NGC 4027 into IIII-region candidates and perhaps a few brightest stars is visible in this short-exposure print from the same original plate used for the heavy print above.

NGC 3985      Sc(s)II pec      Racine wedge  
 PH-8055-S      Ursa Major Cluster  
 Feb 4/5, 1983  
 103aO  
 12 min

Its position and redshift,  $v_0 = 1004 \text{ km s}^{-1}$ , suggest that NGC 3985 is a member of the Ursa Major Cluster.

In a way similar to NGC 4427 shown at the left, the spiral structure in NGC 3985 is unusual because of its one-armed pattern.

NGC 2990      Sc(s)II.2  
 CD-1692-S  
 Jan 3/4, 1981  
 103aO + GG385  
 45 min

NGC 2990 insert  
 CD-1691-S  
 Jim 3/4, 1981  
 103aO + GG385  
 7 min

The inner spiral pattern in NGC 2990 has an unusually high surface brightness, as seen in the insert. The arms are massive, covering much of the area of the disk.

The redshift is  $v_0 = 3006 \text{ km s}^{-1}$ .



The six galaxies on this panel complete the illustration of Sell objects having massive arms in the sense of Reynolds (1927a,b). Most are of the two-armed variety with the arms beginning at the center [the (s) subtype].

IC 4444            Sc(s)II pec  
 CD-1875-HB  
 April 10/11, 1981  
 103aO + GG385  
 45 min

The surface brightness of the central region and the two inner spiral fragments beginning therein is very high. The arm pattern is not symmetrical, yet the spiral feature of the three (perhaps four) arm segments is definite.

The redshift is  $u_0 = 1760 \text{ km s}^{-1}$ . Only a very few (if any) HH-region candidates have been identified.

NGC 5595            Sc(s)II            pair  
 CD-1569-S/Br  
 Aug 10/11, 1980  
 103aO + GG385  
 45 min

NGC 5595 forms a close physical pair with NGC 5597 (SBe: panels 298, S10) at an angular separation of  $4.0'$ . The redshifts are  $i_0(5595) = 2501 \text{ km s}^{-1}$  and  $i_0(5597) = 2444 \text{ km s}^{-1}$ . At the mean redshift distance of 59 Mpc, the projected linear separation of the pair is small, at 58 kpc.

The surface brightness of the arms in NGC 5595 is unusually high.

NGC 3389            Sc(s)II.2            Leo Gr #28  
 PH-270-S  
 Dec 10/11, 1952  
 103aD + GG11  
 25 min

NGC 3389 is listed as a member of the Leo Group in the catalog of Ferguson and Sandage (1990), where the morphological type is given as Scd(s)II.

NGC 3389 is in a triplet of the brightest Leo Group galaxies, which form the center of the aggregate. The other two galaxies are NGC 3379 (E0; panel 1) at a separation of  $9.8'$ , and NGC 3384 (SBO j; panels 54, S7) at a separation of  $6.4'$ . The mean redshift of the group listed in the Leo Cluster Catalog is  $\langle v_0 \rangle = 909 \text{ km s}^{-1}$ . At a redshift distance of 18 Mpc, the projected linear separations of NGC 3379 and NGC 3384 from NGC 3389 are small, at 51 kpc and 34 kpc, respectively. The redshift of NGC 3389 itself is  $v_0 = 1277 \text{ km s}^{-1}$ .

NGC 6970            Sc(s)II  
 CD-1532-S/Br  
 Aug 6/7, 1980  
 103aO + GG385  
 15 min

NGC 6970 insert  
 CD-1110-Br  
 Aug 19/20, 1979  
 103aO + GG385  
 15 min

The angular size of this remote galaxy is small, at  $35''$ . The redshift is  $v_0 = 5207 \text{ km s}^{-1}$ .

The two major spiral arms have very high surface brightness. The arm pattern is of the grand design, the arms being of the massive type.

IC 2056            Sc(s)II  
 CD-135-S  
 Jan 31/Feb 1, 1978  
 103aO + GG385  
 60 min

IC 2056 insert  
 CD-172-S  
 Feb 6/7, 1978  
 098-04 + GG385  
 10 min

The inner disk of IC 2056, filled with spiral segments, has a very high surface brightness and surrounds a nearly pointlike nucleus. The spiral arms are tightly wound.

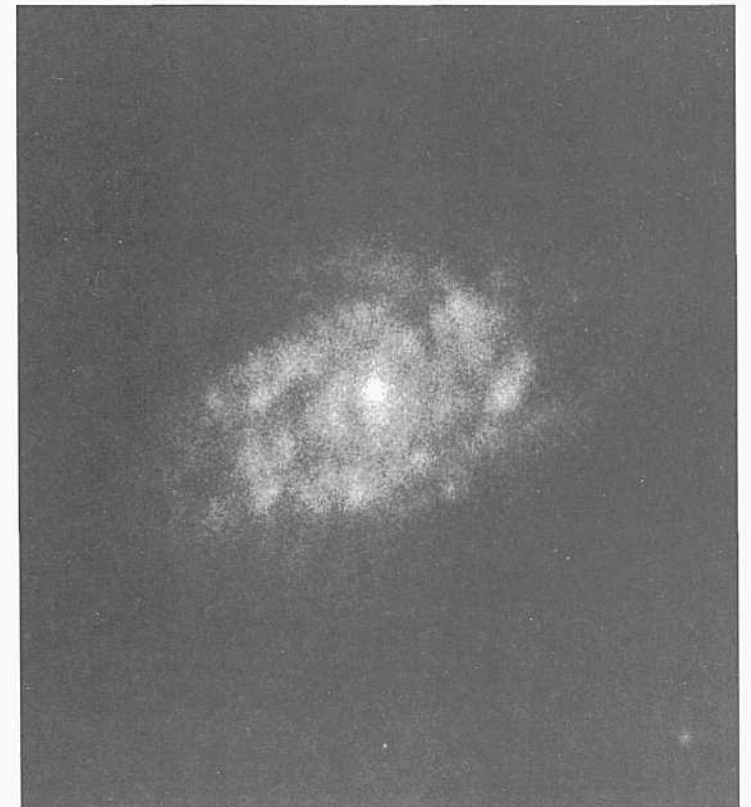
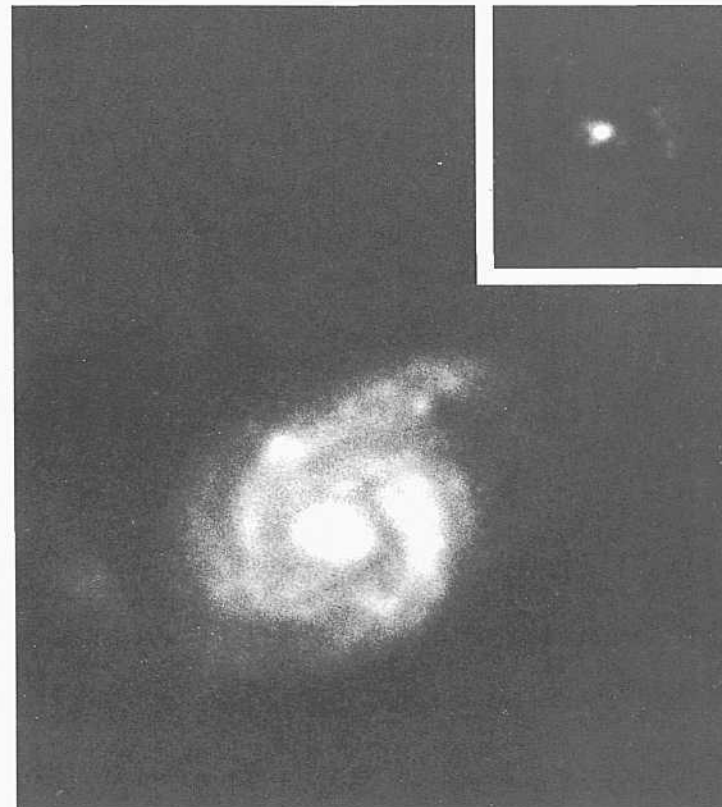
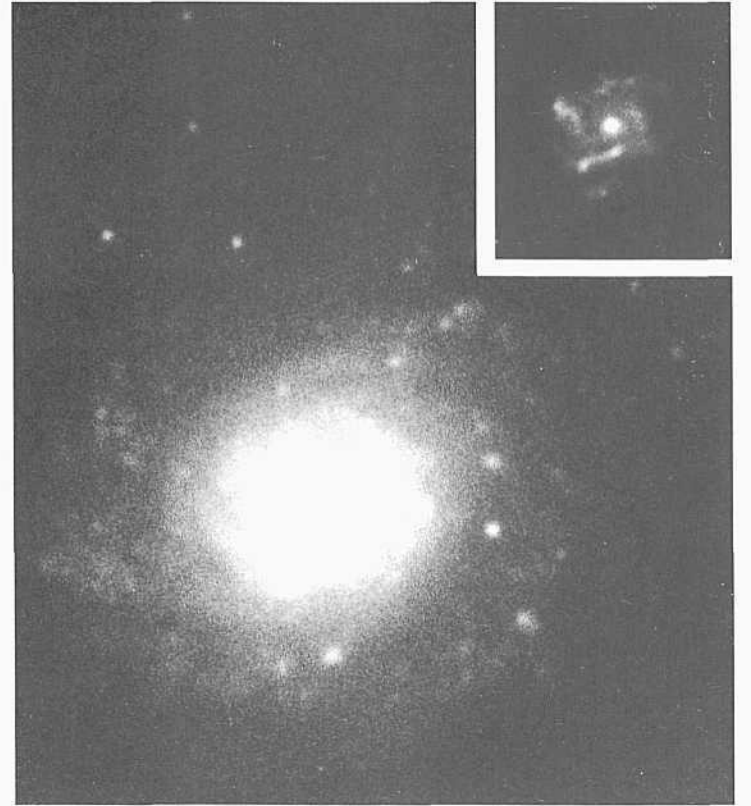
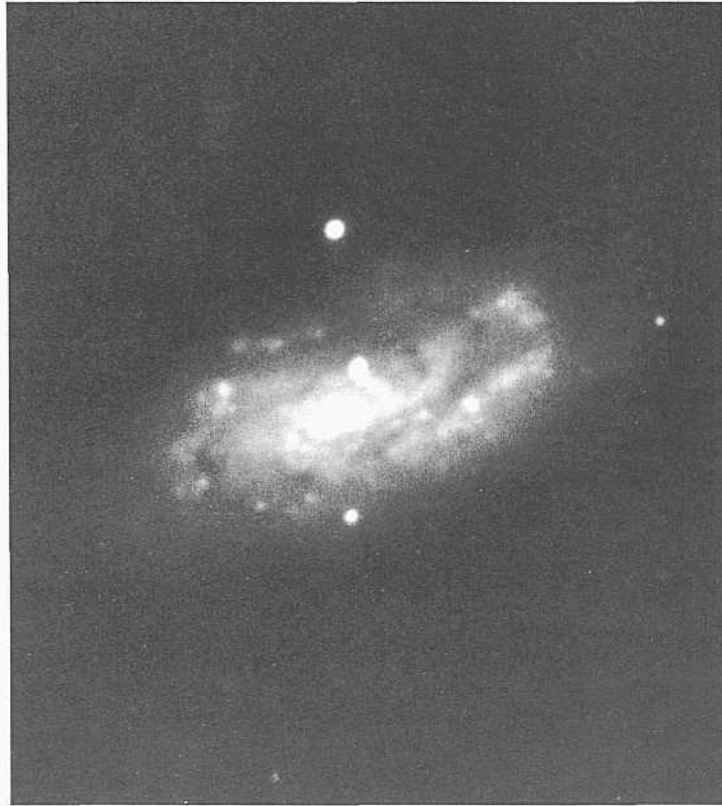
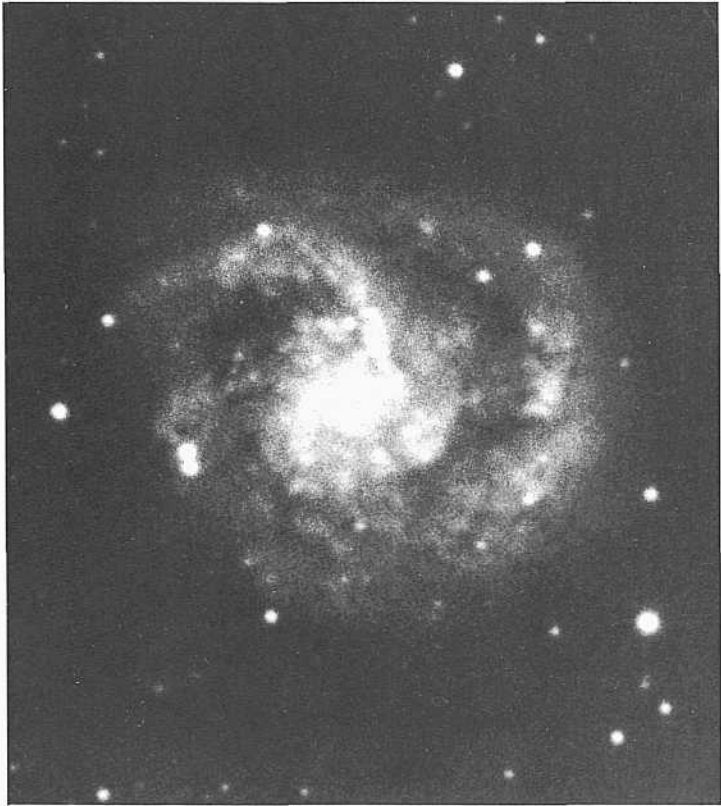
Lower-surface-brightness segments of a spiral pattern exist in the outer disk, shown in the heavy main print. Many knots in these outer arms are candidates for Mil regions. The redshift of IC 2056 is  $v_0 = 934 \text{ km s}^{-1}$ .

The high-surface-brightness inner arms and the small, intense nucleus are well seen in the insert print made from a red-sensitive plate and a wide-bandwidth filter.

NGC 5633            Sc(s)II  
 PH-7862-S  
 Sep 5/6, 1980  
 103aO  
 2 min

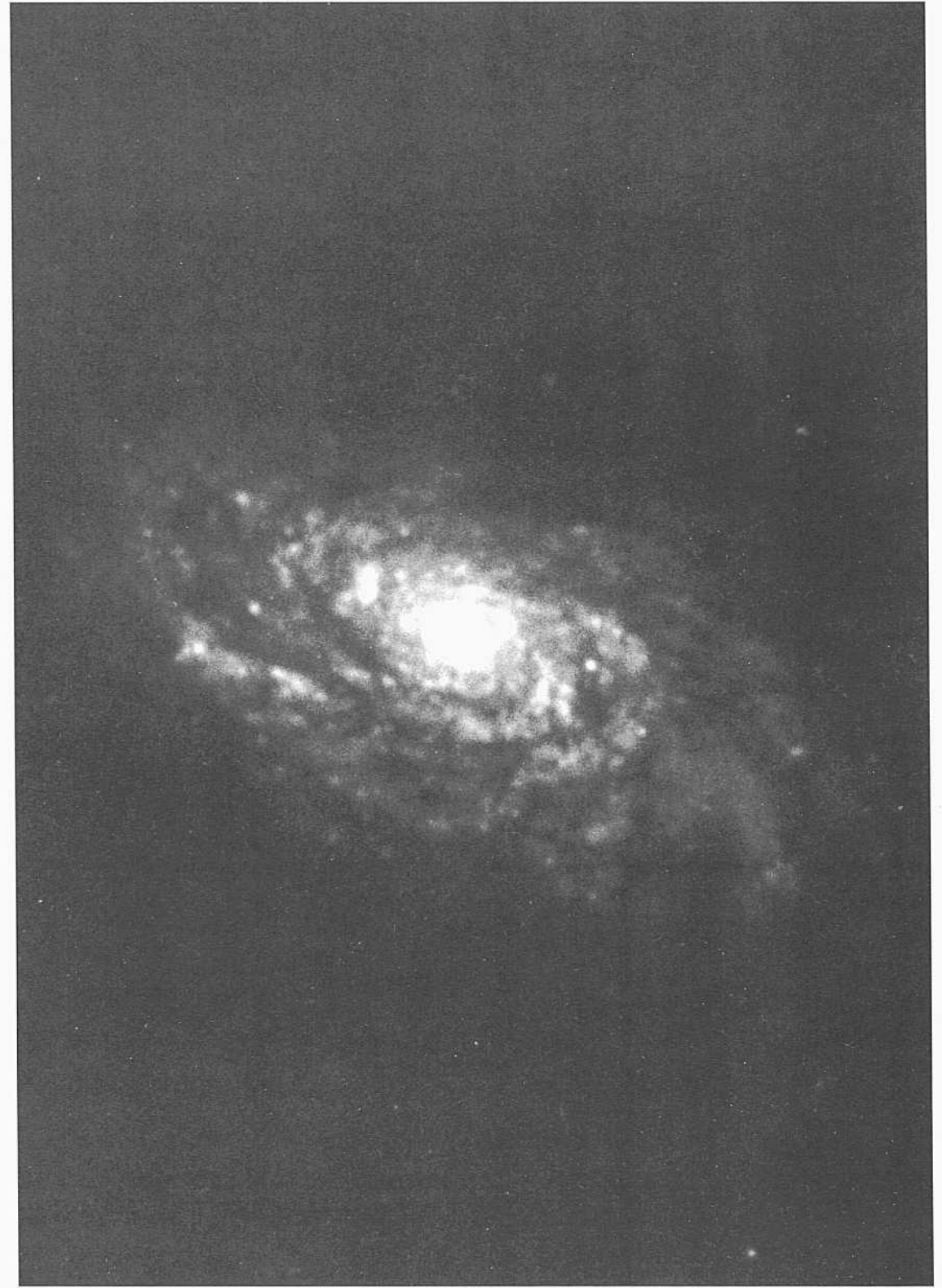
Two sets of arms exist in NGC 5633. The inner set, of extremely high surface brightness, is shown in the print here, made from a very-short-exposure Palomar plate. The outer set of much-fainter-surface-brightness arms is not seen here.

The redshift is  $v_0 = 2437 \text{ km s}^{-1}$ .



PANEL  
253

PANEL  
254



**G**alaxies on this and the next panel are grouped together as Sell galaxies with multiple-arm morphologies similar to the arm patterns of NGC 488 (Sa); panels L15, S3, SI 2) and NGC 2841 (Sb; panels 142, S4, SI 2).

NGC 1437      Sc(s)II      FCC 290  
 CD-192-S  
 FeI>8/9, 1978  
 103aO + GG385  
**45 mill**

NGC 1437 is listed as a member in the Fornax Cluster Catalog (Ferguson 1989). It is located about  $1^\circ$  southeast of the center (nominally at the position of NGC 1399). Its redshift is  $v_0 = 1067 \text{ km s}^{-1}$ . The adopted mean redshift of the Fornax Cluster is  $\langle v_0 \rangle = 1366 \text{ km s}^{-1}$  (Ferguson and Sandage 1990).

The Fornax Cluster is 0.2 mag more distant than the Virgo Cluster (Ferguson and Sandage 1988, Sandage and Tammann 1990) and therefore has a distance modulus near  $m - M = 32$ . Resolution of NGC 1437 into individual stars occurs about half a magnitude above the plate limit of this image ( $B = 2.3$ ) made with the Las Campanas du Pont 100-inch reflector; therefore the absolute magnitude of these brightest stars is about  $MB = -9.5$ . The several IUI-region candidates are unresolved at the 1" level.

NGC 441-1      Sc(sr)H.2  
 [-1-2384-11  
 Feb 21/22, 19-17  
 IIaO  
**10 iiiiin**

The multiple-armed spiral structure is well developed in NGC 4414. Dust accompanies the luminous arm fragments and is well silhouetted against the near side of the underlying disk. The IIII regions are unresolved, as are the brightest stars on this plate taken with the Mount Wilson 100-inch Hooker reflector. The redshift of NGC 4414 is  $v_B = 702 \text{ km s}^{-1}$ .

Sc Classification Section (continued)

NGC 1792            Sc(s)II  
 CD-129-HB  
 Jaii 6/7, 1978  
 103aO + GG385  
 60 niin

The surface brightness of the spiral fragments covering the disk is exceptionally high. The arms are massive in the sense of Reynolds (1927a,b), and the spiral pattern is multiple, as in NGC 488, but NGC 1792 here is of later morphology; the arms are not thin or as easily traced as they are in NGC 488.

The redshift is  $v_o = 1055 \text{ km s}^{-1}$ .

NGC 1792            Sc(s)II  
 CD-1347-S/Br  
 March 15/16, 1980  
 103aO + GG385  
 7 niin

This print from the short-exposure plate shows the high-surface-brightness ridge positions of multiple arms. HII-region candidates are numerous along the ridge lines. Note the small nucleus.

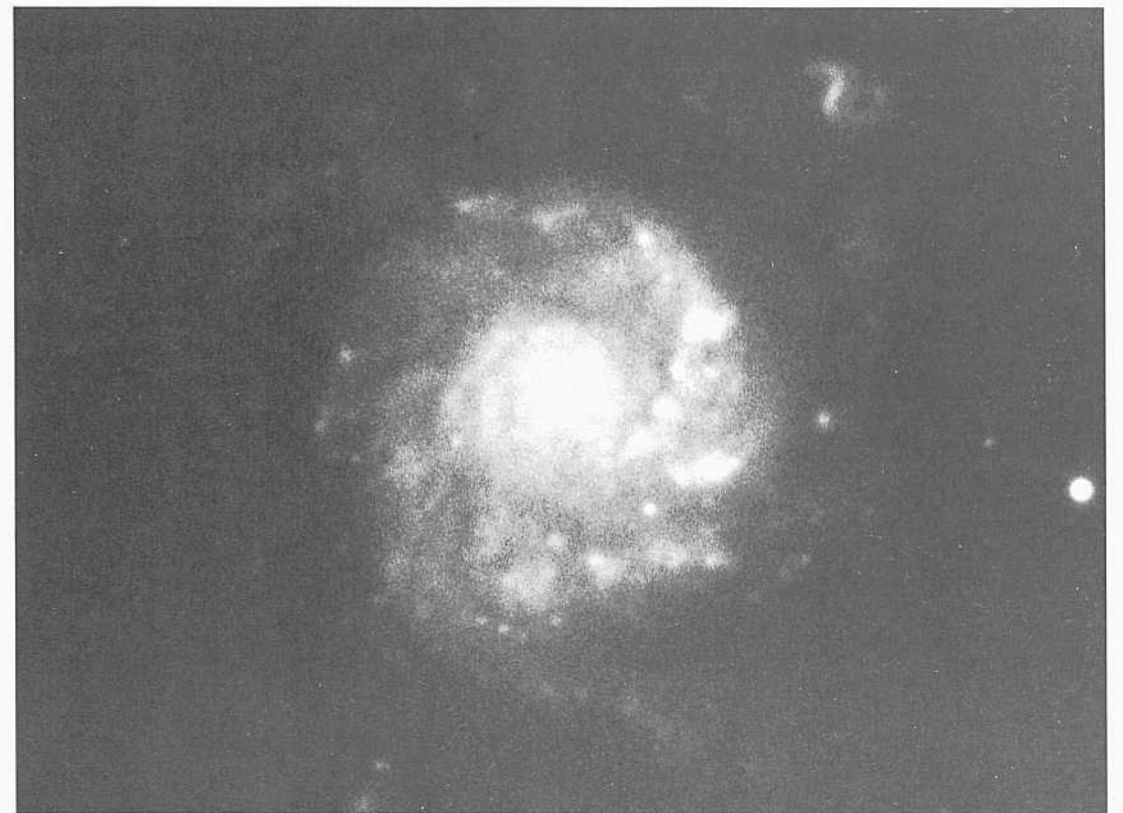
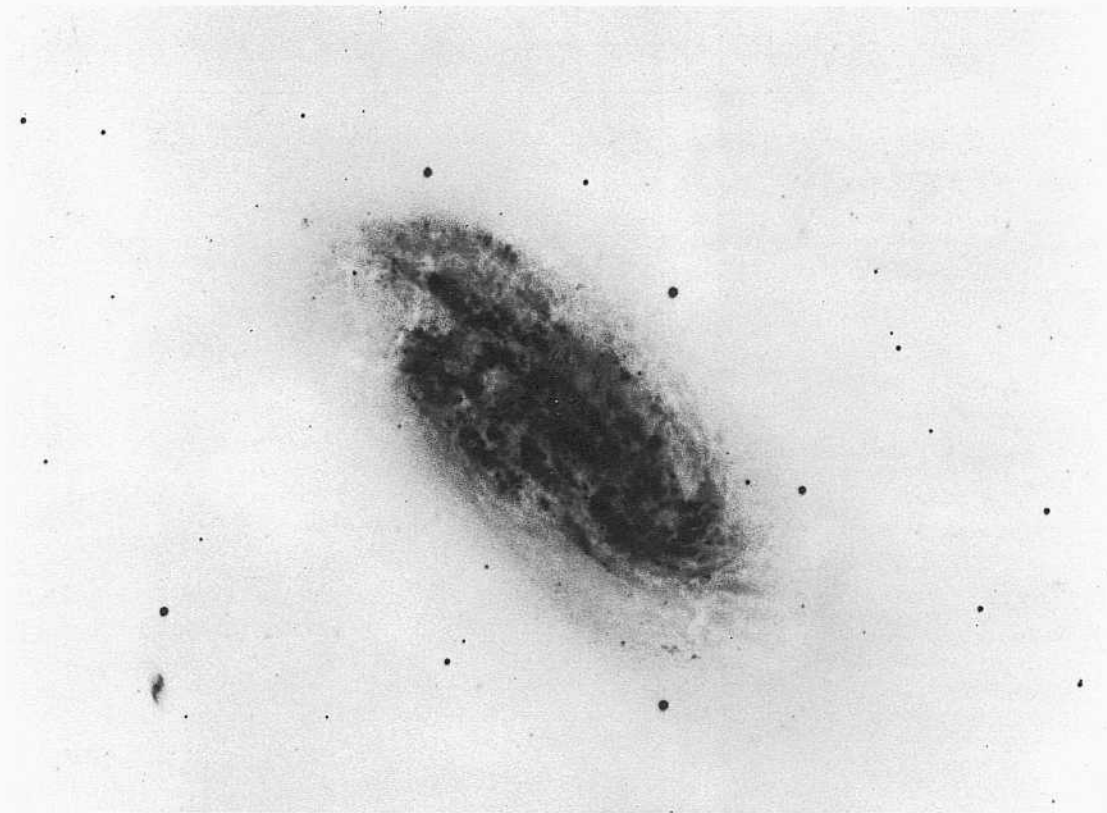
NGC 1309            Sc(s)II            Racine wedge  
 PH-7918-S  
 Nov 7/8, 1980  
 103aO  
 12 niin

The spiral arms are regular and are very tightly wound. The inner-arm pattern is of high surface brightness. One of the principal arms is brighter than the other. Both begin at the edge of the inner disk, which itself is filled with luminous arm segments that begin at the center.

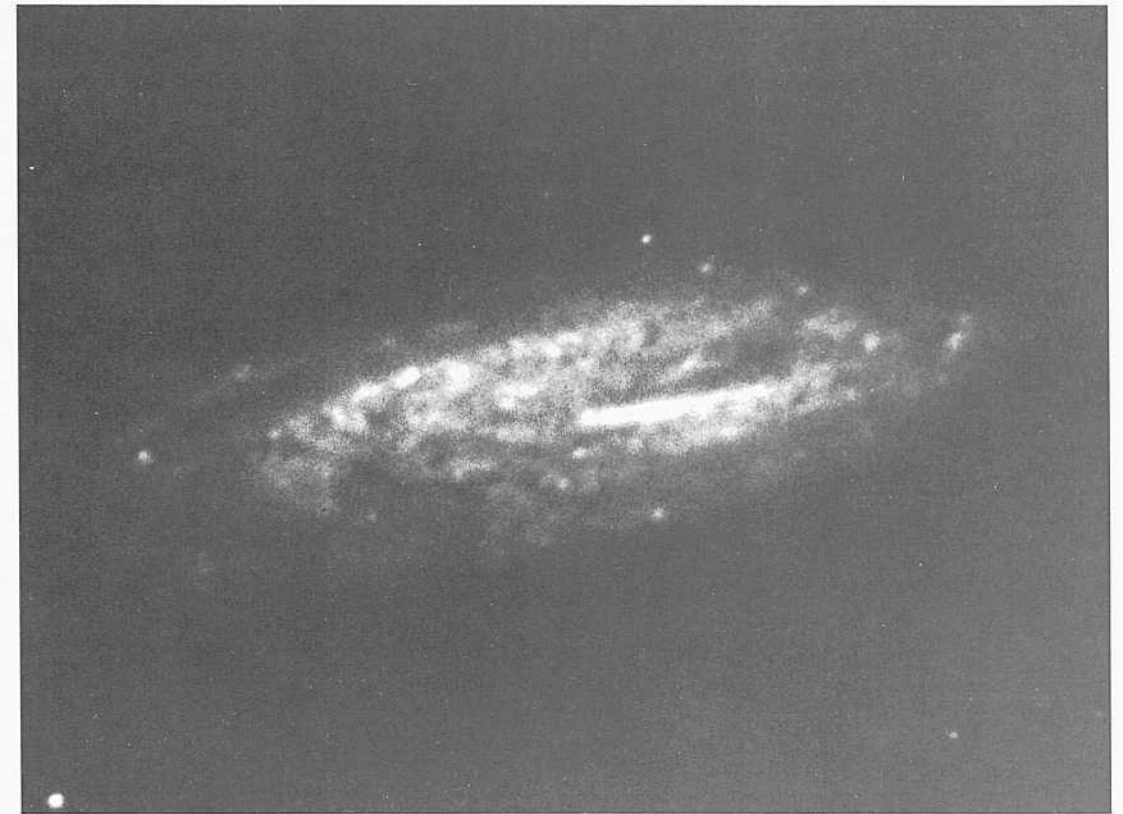
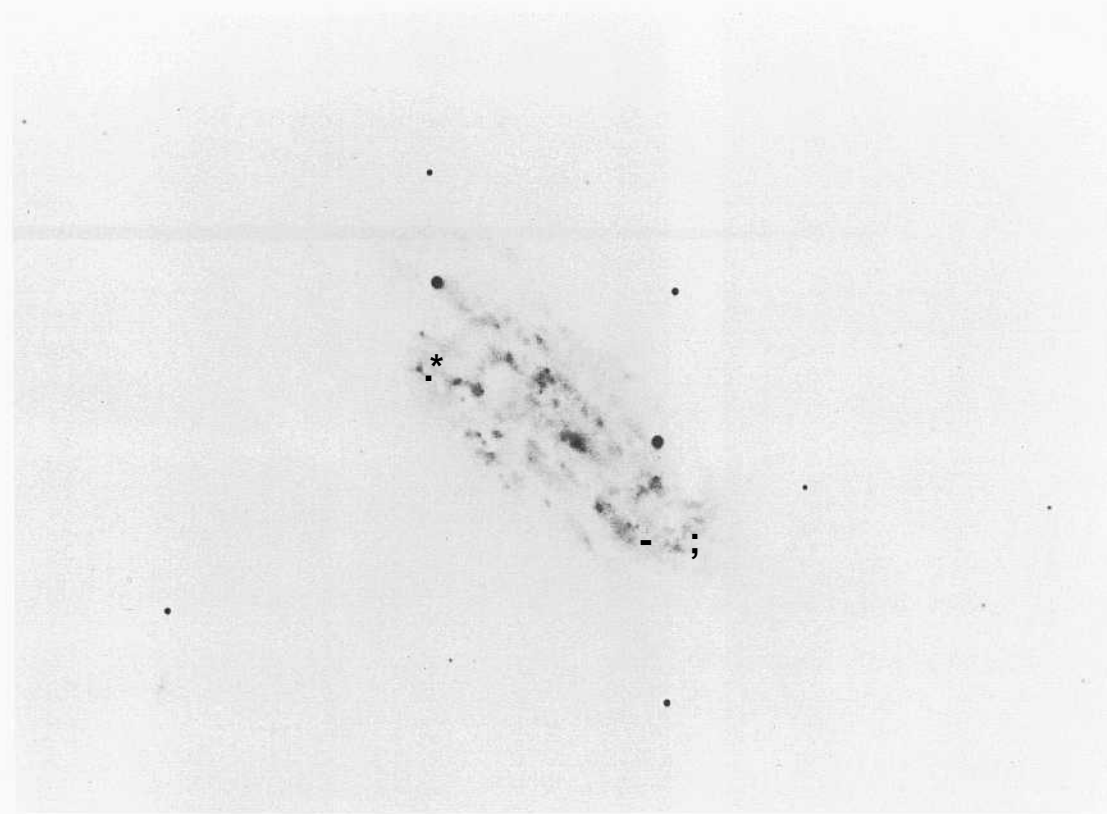
HII-region candidates exist. A few candidates for individual brightest stars also exist in the low-surface-brightness parts of the outer arm system, but identification as stars must yet be done by the standard methods that separate stars and HII regions. The redshift is  $v_o = 2143 \text{ km s}^{-1}$ . At the redshift distance of  $m - M = 33.2$  a star of absolute magnitude  $M_g = -10$  has a blue magnitude of  $B = 23.2$ , which is fainter than the candidate stars; the starlike candidates are therefore interesting, as they may be HII regions.

NGC 754-1            Sc(s)II            Karachentsev 578  
 H-945-Dunear                            panel 282  
 Sep 2/3, 1945  
 103aO  
 60 niin

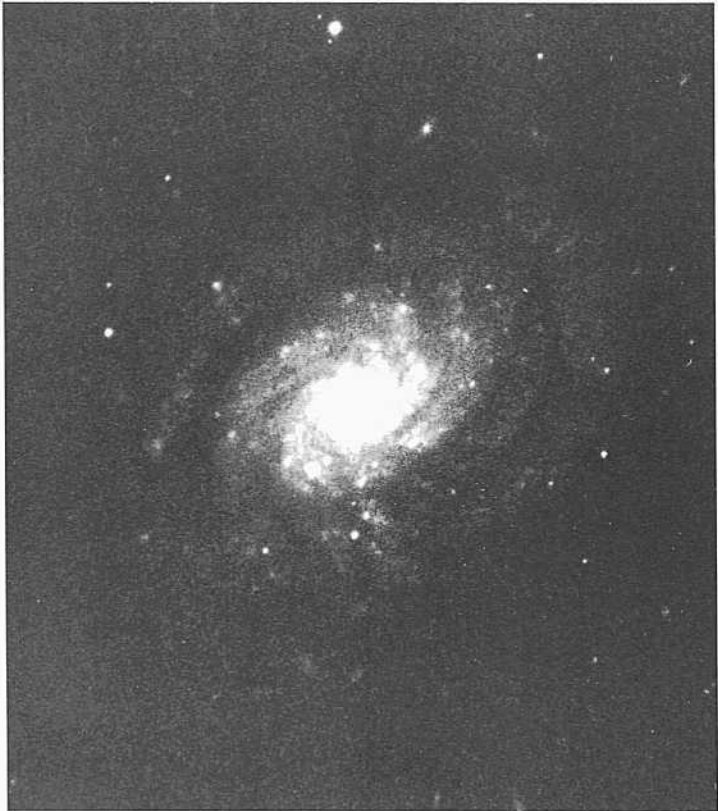
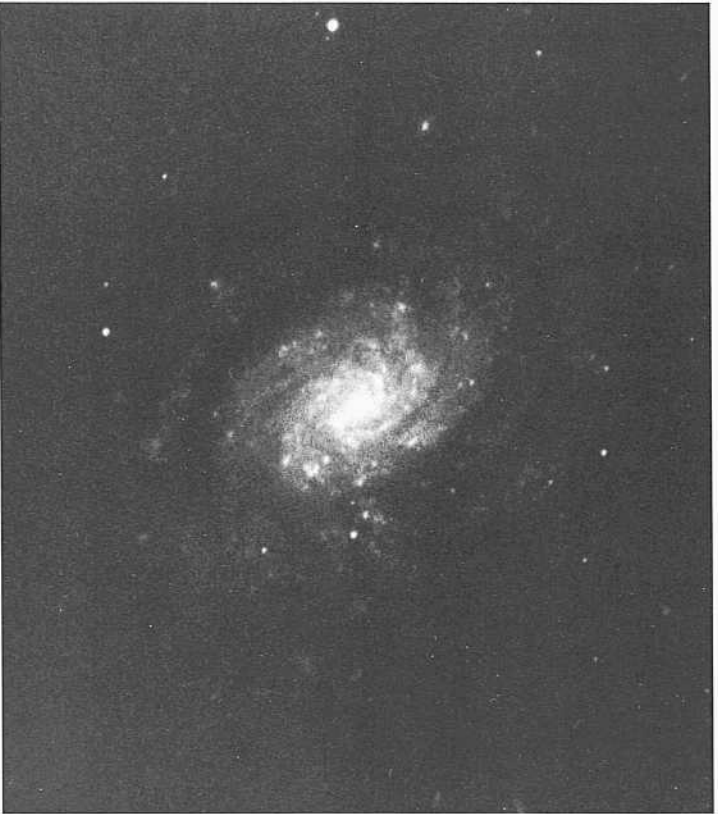
NGC 7541 forms a physical pair with NGC 7537 [Sc(s)] at an angular separation of  $2.7'$ . Karachentsev (1987) gives redshifts of  $v_o(7537) = 2834 \text{ km s}^{-1}$  and  $v_o(7541) = 2793 \text{ km s}^{-1}$ . At the mean redshift distance of  $5.6 \text{ Mpc}$  the projected linear separation is small, at  $44 \text{ kpc}$ . There is no evidence for morphological distortion in either galaxy, despite this apparent closeness.



PANEL  
255



PANEL  
256



*Sc Classification Section (continued)*

**NGC3684**                      **Sc(s)II**                      group  
CD-1811-**IIK**  
April 2/3, 1981  
103a0  
7 $\frac{1}{2}$  mill

NGC 3684 is **IIK**- center  $\langle r \rangle$  ; small group of seven confirmed members (based on similarity of redshifts). The number of candidate group members is  $\approx 15$ . Many of the fainter candidates are dwarf **Sm** and **Im** morphological types.

The confirmed group members listed in *Ilie RSA* are NGC 3681 (**SBb**; panel L64;  $v_o = 1135$  km s $^{-1}$ ), NGC 3686 (**SBbc**; panel 20\*);  $v_o \approx 1034$  km s $^{-1}$ ), and NGC 3693 (**Scd**; panel 317;  $v_o = 947$  km s $^{-1}$ ). Other members have 21-cm redshifts are listed in Hoffman *et al.* (1987). The mean redshift of the seven confirmed group members is  $\langle v_o \rangle = 1021$  km s $^{-1}$ .

The group is more compact than the Local Group. The members are within  $1^\circ$  of each other, a linear diameter of 35.6 kpc (about one-third the size of the Local Group).

The three images of NGC 3684 on the opposite page have been made from a single original *du Pont* 100-inch plate taken at Las Campanas hut printed to different densities to show the inside spiral pattern [(s) type] and the very-low-surface brightness outer-arm structure, which has at times been called a fossil-arm pattern.



The four galaxies on this panel continue the pattern of two sets of arms seen on the preceding panel. An inner set has very high surface brightness; an outer set of very faint outer arms exhibits the form of what is often called a fossil-arm pattern, common in many galaxies. Earlier-type galaxies having this pattern include NGC 1068 (Sb; panel 138) and NGC 3981 (Sbc; panel 178).

NGC 4793      Sc(s)H.2      HA, p. 35  
**H-2273-H**  
 May 5/6, 1946  
 103aO  
 40 niin

A possible dwarf companion (type Sm?) to NGC 4793 exists at an angular separation of  $1.3'$ . The redshift of NGC 4793 is  $v_o = 2460 \text{ km s}^{-1}$ . If the satellite is a companion, the projected linear separation from NGC 4793 is small at 1.9 kpc, based on a redshift distance of 49 Mpc ( $H = 50$ ). One of the outer low-surface-brightness fossil arms appears to connect with the satellite.

NGC 3403      Sc(s)II      Racine wedge  
 PH-8015-S  
 Feb 3/4, 1981  
 103aO  
 12 niin

There is an abrupt change of surface brightness between the inner and outer sets of multiple arms in NGC 3403.

The redshift is  $v_o = 1422 \text{ km s}^{-1}$ .

NGC 5756      Sc(s)II      panel 239  
 CD-1471-S/Br  
 May 10/11, 1980  
 103aO + GG385  
 45 iiiin

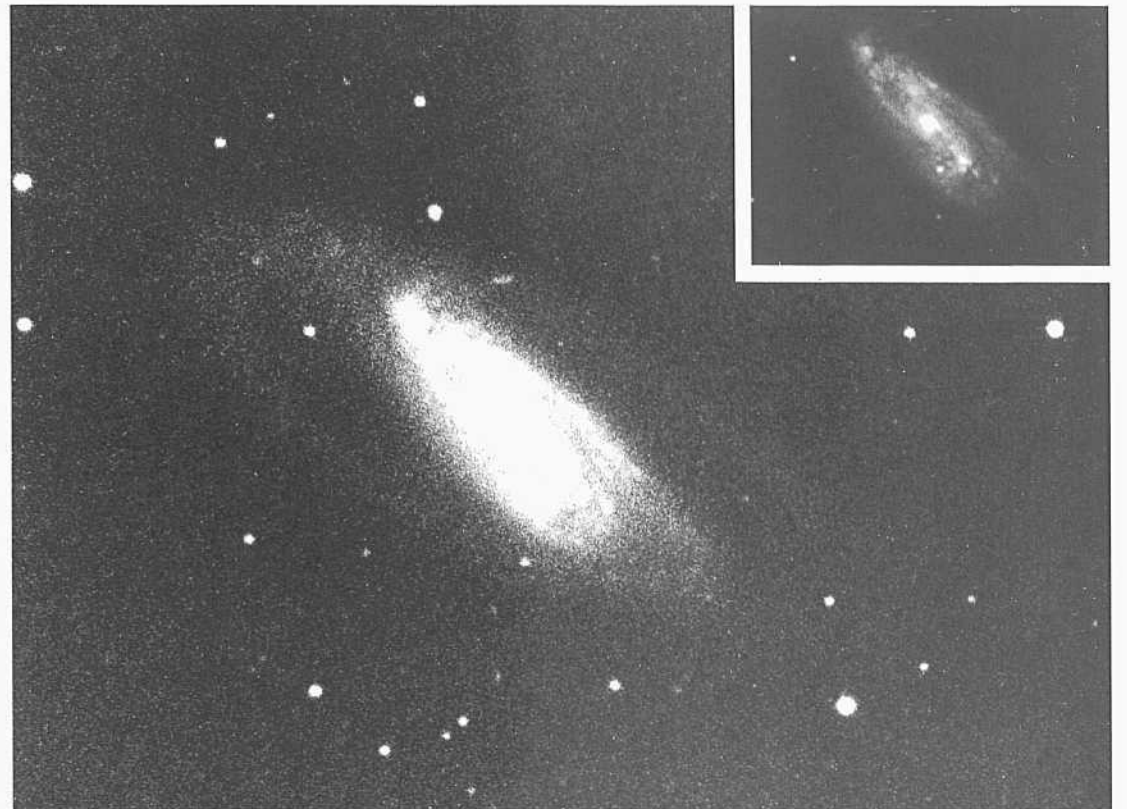
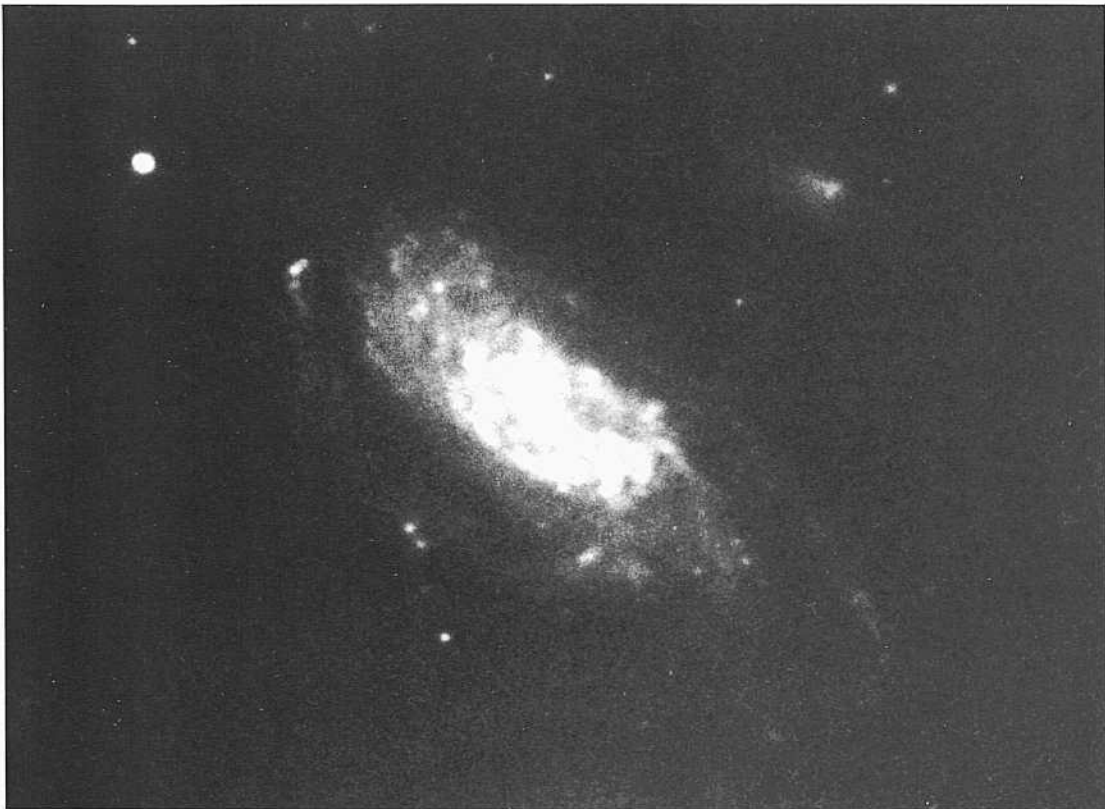
The very-faint-surface-brightness outer arms in NGC 5756 are smooth, showing no evidence of recent star formation. The two main high-surface-brightness inner arms start at the small nucleus in a prototype (s) pattern.

The redshift is  $v_o = 2025 \text{ km s}^{-1}$ .

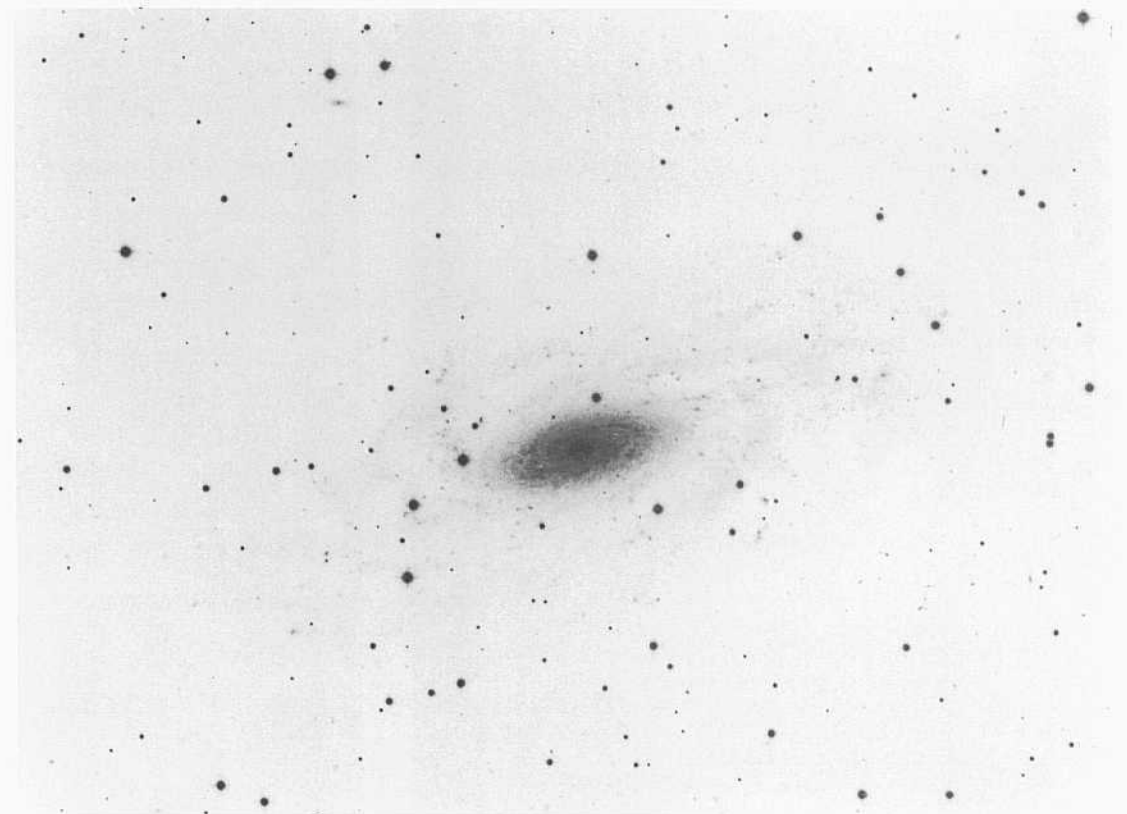
NGC 2090      Sc(s)II      panel 250  
**CD-663-Br**  
**Jan 22/23, 1979**  
**103aO + GG385**  
 45 niin

NGC 2090 is repeated here from panel 250 to illustrate and compare the pattern of high-surface-brightness inner arms and low-surface-brightness outer arms with the similar pattern shown by other galaxies on this page. The pattern is similar to that in such prototype cases as NGC 1068 (Sb; panel 138) and NGC 3981 (Sbc; panel 178).

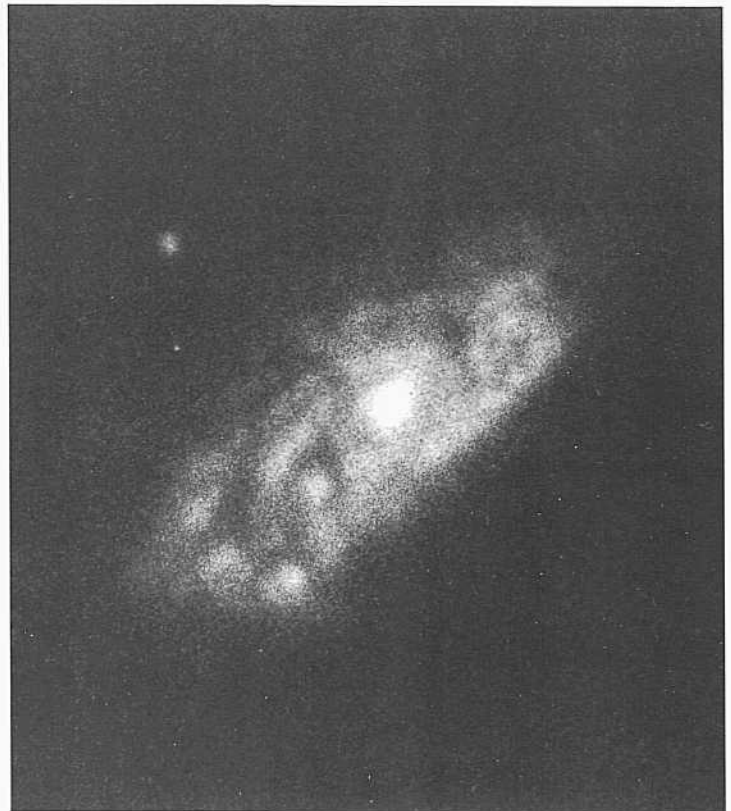
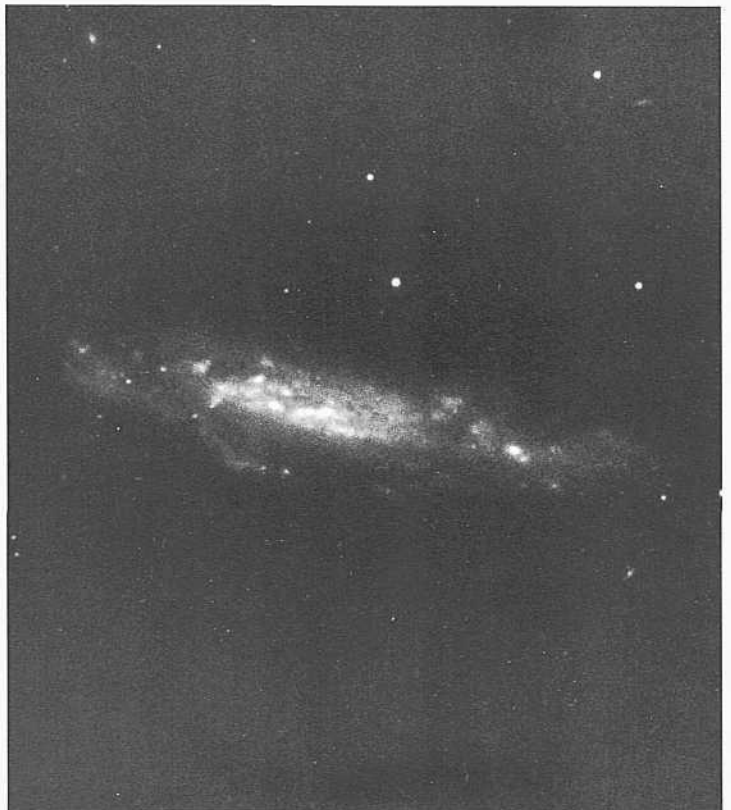
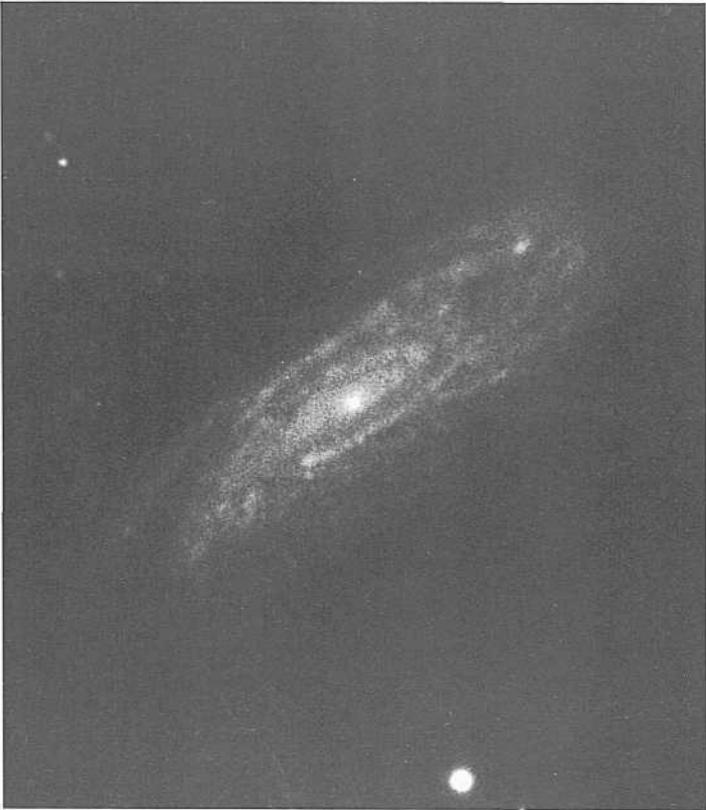
The redshift is  $u_o = 755 \text{ km s}^{-1}$ .



PANEL  
257



PAXEL  
258



The six galaxies on this panel complete the Sell morphological bin of RSA galaxies whose arm pattern is generally filamentary, often similar to the pattern in NGC 488 but later in the classification sequence. All six galaxies here are highly inclined to the line of sight, showing well the absence of a central bulge and the presence of only a small nucleus.

NGC 3549            Sc(rs)II  
 PH-8073-S  
 Feb 5/6, 1981  
 103aO  
 12 niin

The multiple arms in NGC 3549 are thin, regular, and multiple. The redshift is  $v_0 = 2921 \text{ km s}^{-1}$ .

NGC 3437            Sc(s)II            Racine wedge  
 PH-8021-S  
 Feb 3/4, 1981  
 103aD  
 2 ruin

The image of NGC 3437 here is from a yellow plate (no filter) with a very short exposure, designed to see the semi-chaotic spiral pattern over the high-surface-brightness inner disk. The redshift of NGC 3437 is  $v_0 = 1201 \text{ km s}^{-1}$ .

NGC 3956            Sc(s)II            group  
 CD-1672-S  
 Dec 31/Jan 1, 1980/1981  
 103aO  
 60 niin

NGC 3956 is in a rich field that includes the RSA galaxies NGC 3957 (S0<sub>3</sub>; panel 44), at a separation from NGC 3956 of 59.2' with a redshift of  $v_0 = 1583 \text{ km s}^{-1}$ , and NGC 3981 (Sbc; panel 178), at a separation of 50.0' with a redshift of  $v_0 = 1554 \text{ km s}^{-1}$ . The redshift of NGC 3956 itself is  $v_0 = 1394 \text{ km s}^{-1}$ . If the three galaxies are physically related with mean redshift of  $\langle v_0 \rangle = 1510 \text{ km s}^{-1}$  at a redshift distance of 30 Mpc ( $r = 50$ ), the projected linear separations from NGC 3956 are 516 kpc and 436 kpc from NGC 3957 and NGC 3981, respectively. These dimensions are similar to the size of the Local Group.

The field around and between these three bright galaxies contains many (IE, Im, and Sm dwarf galaxy candidate members of the group.

IC 5039            Sc(s)II            pair  
 CD-1529-S/Br  
 Aug 6/7, 1980  
 103aO + GG385  
 45 niin

IC 5039 forms a physical pair with IC 5041 [SBbc(s)II; not in the RSA] at a separation of 9.8'. The redshifts are  $v_0(5039) = 2723 \text{ km s}^{-1}$  and  $v_0(5041) = 2739 \text{ km s}^{-1}$ . At the redshift distance of 55 Mpc ( $r = 50$ ), the projected linear separation is 157 kpc.

NGC 3003            S-(s)H  
 PH-7958-S  
 Nov 8/9, 1980  
 103aO  
 12 mill

NGC 3003 is seen nearly on edge, making its spiral pattern difficult to trace. The absence of a halo and (the smallness of the central nucleus is evident.

The redshift of is  $v_0 = 1161 \text{ km s}^{-1}$ .

NGC 6808            Sc(s)II  
 CD-480-S  
 Sep 23/24, 1978  
 103aO + GG385  
 60 mill

Three principal arms can be traced in NGC 6808, two on one side and one on the other. The arms are intermediate in width between narrow and massive in the sense of Reynolds (1927a,b).

The redshift is  $v_0 = 3281 \text{ km s}^{-1}$ .

## THE SCII-III SUBCLASS

**G**alaxies on the next 16 panels are of the late-luminosity classes II-III and III. Many are nearby and are highly resolved into individual stars and HII regions, making them especially useful for calibration of the extragalactic distance scale. Many of the disks are of low surface brightness; hence photometry of the resolved stars will be relatively straightforward.

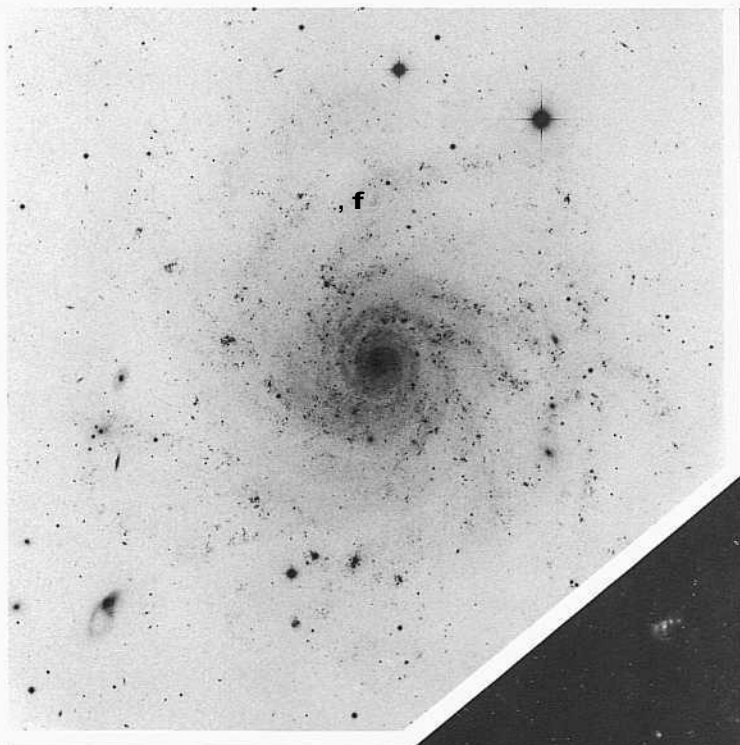
**IC 5332**            **Sc(s)H-III**            **pair**  
**CD-539-S**  
**Oct 1/2, 1978**  
**103aO + GG385**  
**45 niin**

IC 5332 forms a wide pair with NGC 7713 (Sc; panel 267) at a separation of  $1.9^\circ$  and at redshifts of  $713 \text{ km s}^{-1}$  and  $684 \text{ km s}^{-1}$ . At a mean redshift distance of 14 Mpc ( $H = 50$ ), the projected linear separation of the pair is 464 kpc, similar to the distances within the Local Group.

IC 5332 resolves easily into individual stars starting at about  $B = 19$ . The surface brightness of the disk is low, making IC 5332 a prime candidate for detailed photometric study.

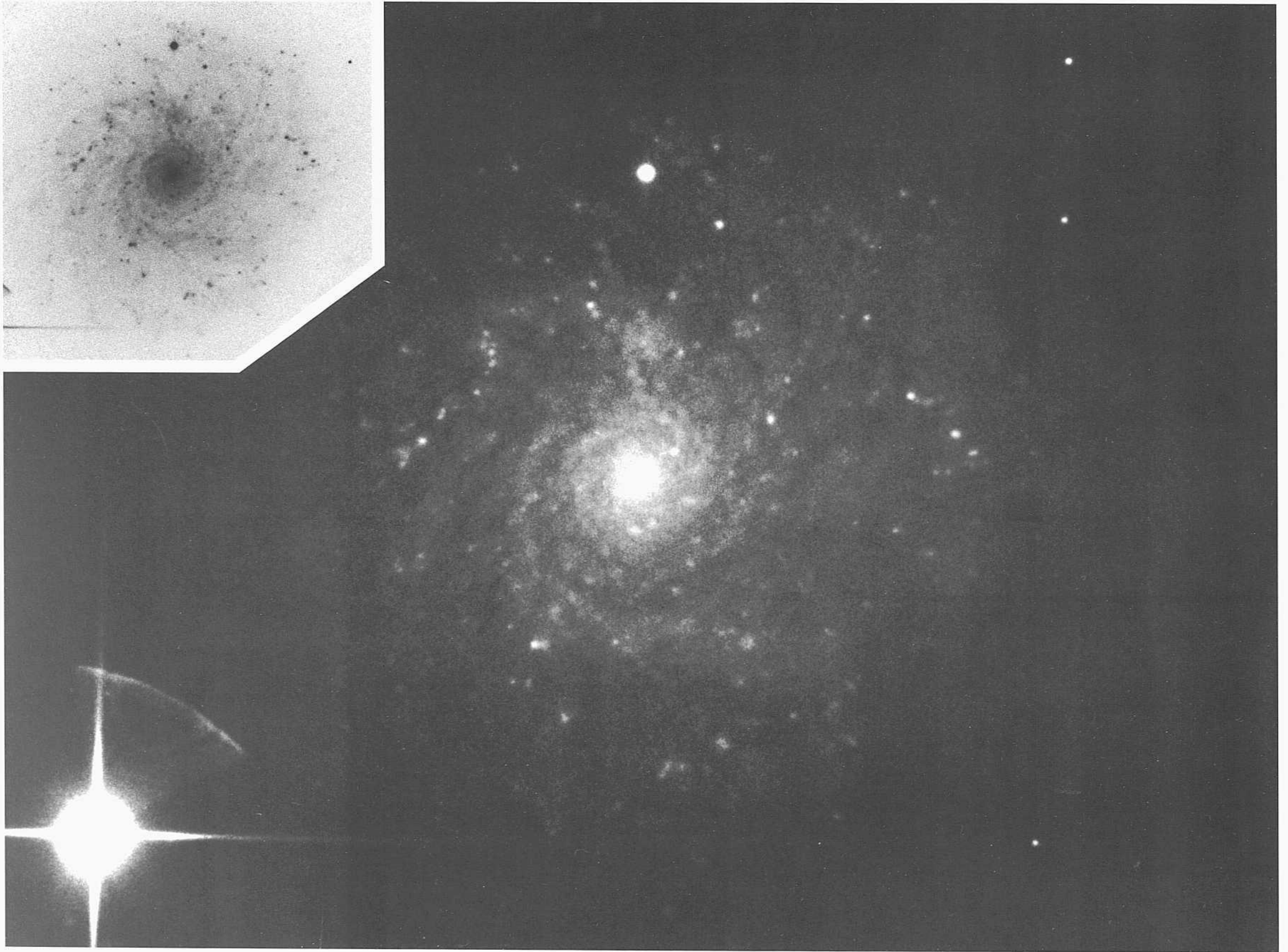
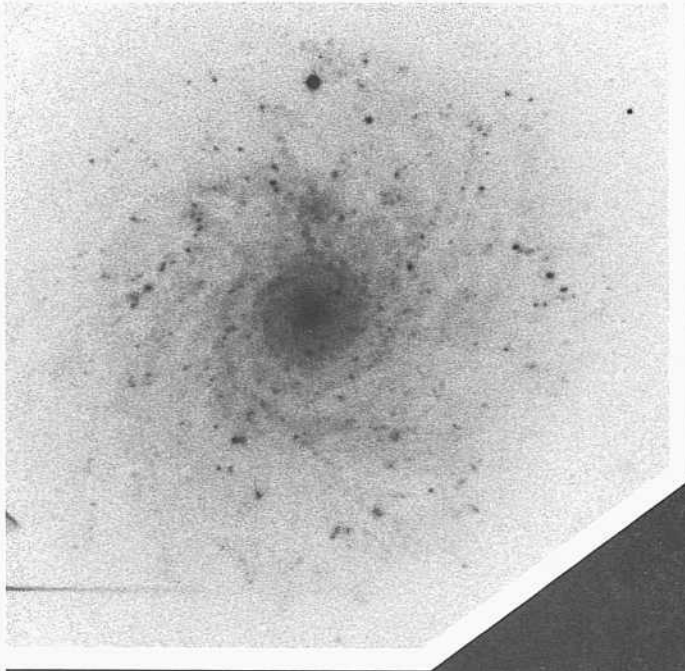
The largest **HII** region in a faint outer arm has a disk diameter (core + halo) of  $6''$ . If it conforms to the linear halo diameter of 500 pc from the calibration of first-ranked **HII** regions in **ScII-III** galaxies (Sandage and Tammann 1974a), the **inferred** HH-region-based distance is 1.7 Mpc, similar to the adopted redshift distance given above. A similar distance is obtained from the ratio of the halo diameter  $6''$  here to that of NGC 604 (the first-ranked HII region in M33, with a halo diameter of  $100''$ ).

Because of the very low disk **surface** brightness and the easy resolution into individual stars, a detailed study of the stellar content would be of great importance.



PANEL  
259

PANEL  
260



*Sc Classification Section (continued)*

NGC4571      SC(B)II-IU      VCC 1696  
CD-756-S

**Feb4/5, 1979**

**103aO + Wr2c**

**50 inin**

NCC 4571 is an Sc galaxy in the Virgo Cluster whose potential for significant resolution into individual stars and IIII regions from  $\text{tin}^*$  ground is good, owing to the low surface brightness of the disk and the openness of  $\text{tin}^*$  spiral arms.

The arm pattern resembles M101 but is of lower surface brightness. It is similar to but later than that in the prototype multiple-armed spiral NGC 488 (Sab; panels L15, 116, S3, S12).

NGC 4571 is in the northeastern part of the Virgo Cluster region, about  $2.5^\circ$  from the core of Virgo subcluster A associated with [NGC 4486]. Its redshift is  $v_0 = 342 \text{ km s}^{-1}$ , which differs from the cluster mean of  $\langle v_0 \rangle = 976 \text{ km s}^{-1}$ , presumably because of the large internal velocity dispersion of the Cluster and/or the streaming motions of the system of Virgo spirals relative to the Virgo core ellipticals. Spirals may be falling into the older cluster core, composed of ellipticals and dE dwarfs.



*Sc Classification Section (continued)*

NGC 300            Sc(s)II.8     South Polar Gr  
CD-2044-Bedke/Gregory            panel S6  
Nov2/3, 1981  
103aO  
**90rain**

NGC 300 is a member of the South Polar Group (de Vaucouleurs 1959a), which also contains the well-resolved galaxies NGC 55, NGC 147, NGC 253, and NGC 7793. The distance modulus of NGC 300 is small, at  $m - M = 26.5$  ( $D = 2.9$  Mpc), determined from **Cepheids** (Graham 1984). Because the distance is so small, resolution into individual brightest stars in many well-defined associations is exceptionally easy, **beginning** at about  $B = 18$  (estimated).

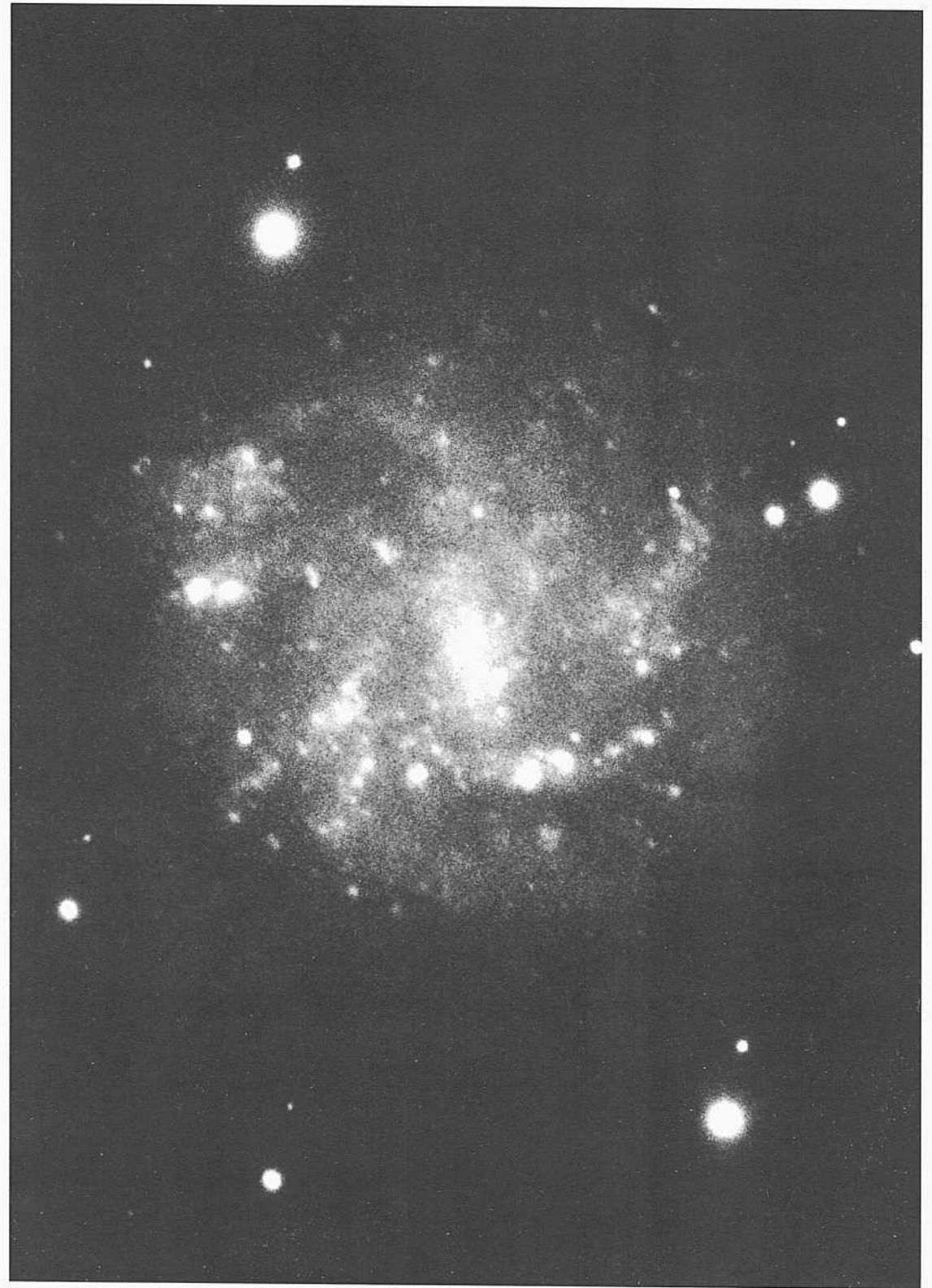
The brightest stars are contained in the associations. \et. only slightly fainter stars that are also young are spread throughout the inter-arm region.

The spiral-arm pattern is massive in the sense of Reynolds (1927a,b). At least two major arms exist on each side of the minor axis. Three arm crossings of the major axis can be traced on each side of the image.



PANEL  
261

PANEL  
262





Sc Classification Section (continued)

NGC 3780      Sc(r)II.3  
PH-7634-S  
April 28/29, 1979  
103aO  
12 niin

The spiral pattern in NGC 3780 is similar to the multiple arms in the prototype multiple-armed galaxy M101 (Sc; Hubble Atlas, pp. 27, 37; panel 218 here). Both galaxies are later versions of the multiple-armed pattern of NGC 488 (Sab; panels 115, 116, S3, S12).

The arms in NGC 3780 are thin but highly branched. Most can be traced as individual fragments for only about a half-rotation.

The many individual HII regions are unresolved at the 1" level. The redshift of NGC 3780 is  $v_o = 2481 \text{ km s}^{-1}$ .

NGC 2276      Sc(r)II-III      Karachentsev 127  
S-1879-H  
Dec 4/5, 1939  
103aO  
60 min

NGC 2276 forms a pair with NGC 2300 (E3; panel 6). The redshifts measured by Karachentsev are  $u_o(2276) = 2598 \text{ km s}^{-1}$  and  $i_o(2300) = 2332 \text{ km s}^{-1}$ . The separation of 6.3' corresponds to a projected linear separation of 90 kpc at the mean redshift distance of 49 Mpc.

The difference in morphological type of the pair is particularly to be noted (Sc and E3) if the two galaxies form a bound system. Other listed nearby Dreyer galaxies are IC 455 (SO) and IC 469. Many fainter early-type galaxies and several candidates for dwarf dE galaxies also exist in the field.

The image here of this field near the celestial pole is from a plate taken with the Mount Wilson 60-inch telescope. For comparison, an image from a plate taken with the Palomar 200-inch Hale reflector is shown at the right.

NGC 1659      Sc(s)II-III  
H-44-S  
Feb 8/9, 1951  
103aO  
25min

The multiple spiral arms form an asymmetrical pattern over the outer disk. The asymmetry is similar to that in NGC 2276, below, but unlike in that galaxy there is no evidence in NGC 1659 for a close (tidal) encounter. NGC 1659 appears to be isolated.

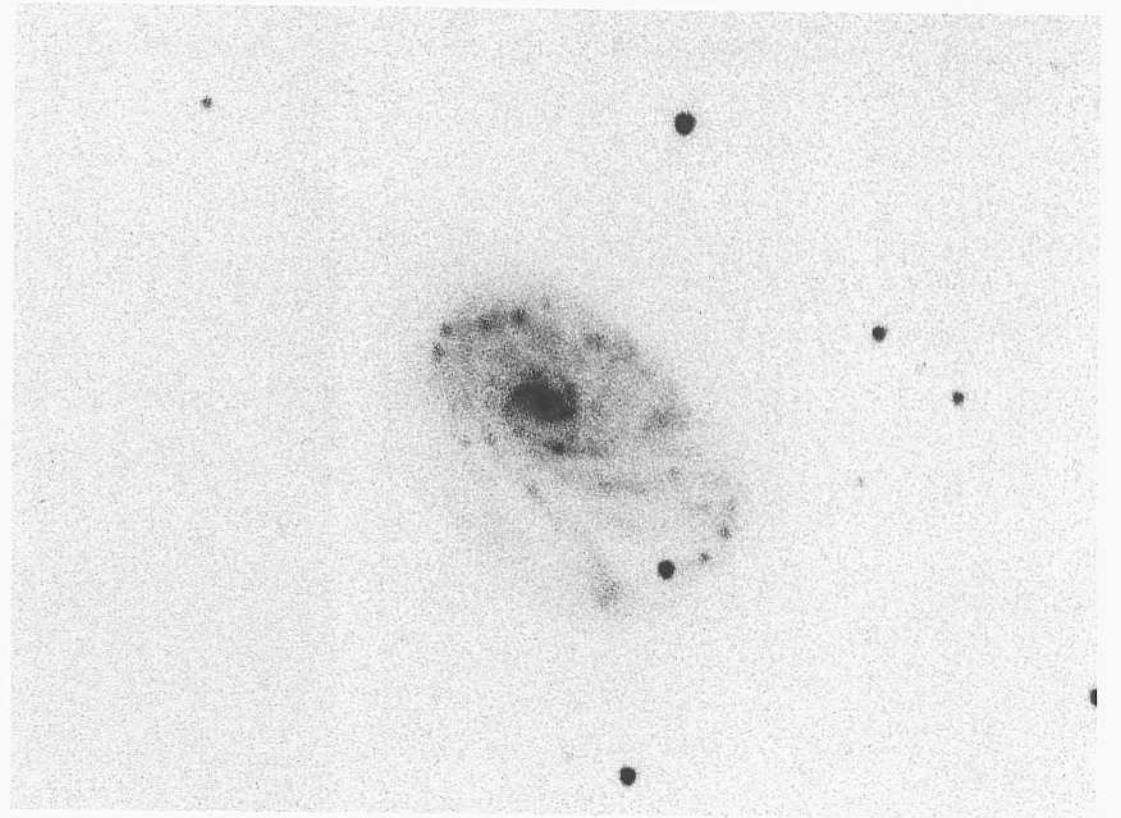
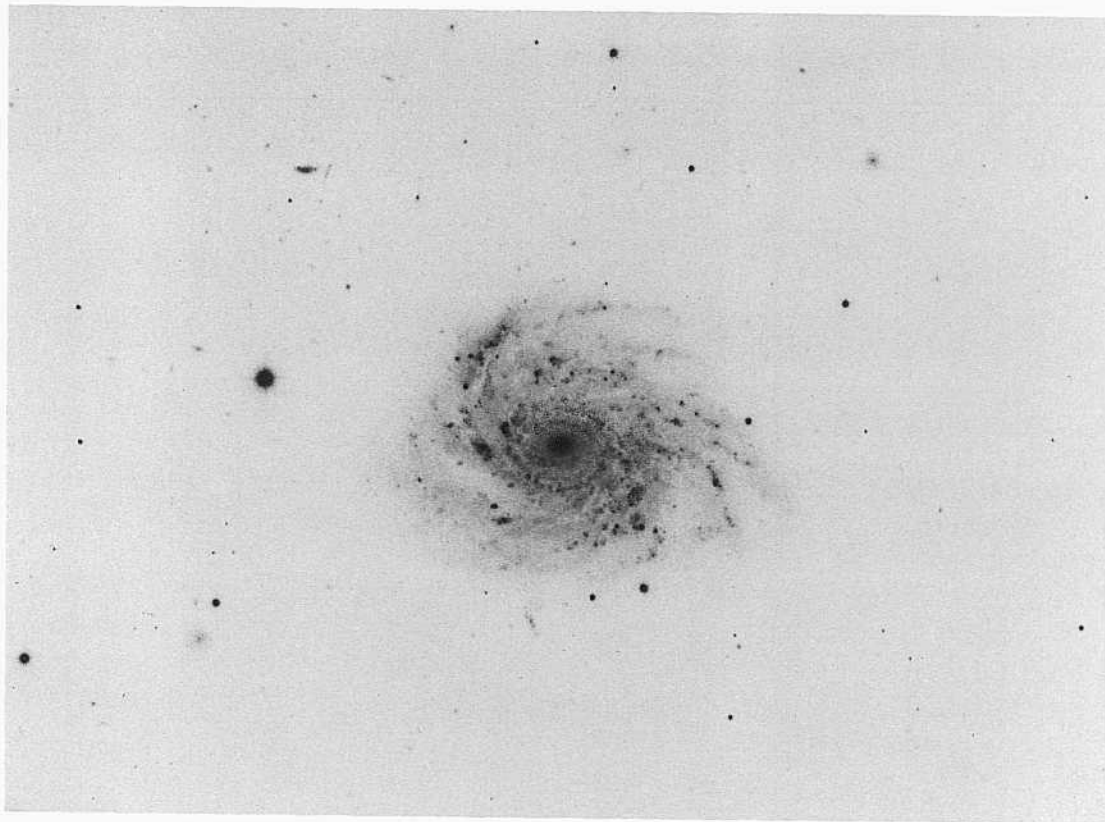
The multiple-arm pattern, which is asymmetric in the region where the arms end abruptly at an outer edge, is nearly identical with that of NGC 95 (Sc; panel 248). The pattern is also similar to that in NGC 5605 (Sc; panel 246).

The redshift of NGC 1659 is  $v_o = 4522 \text{ km s}^{-1}$ .

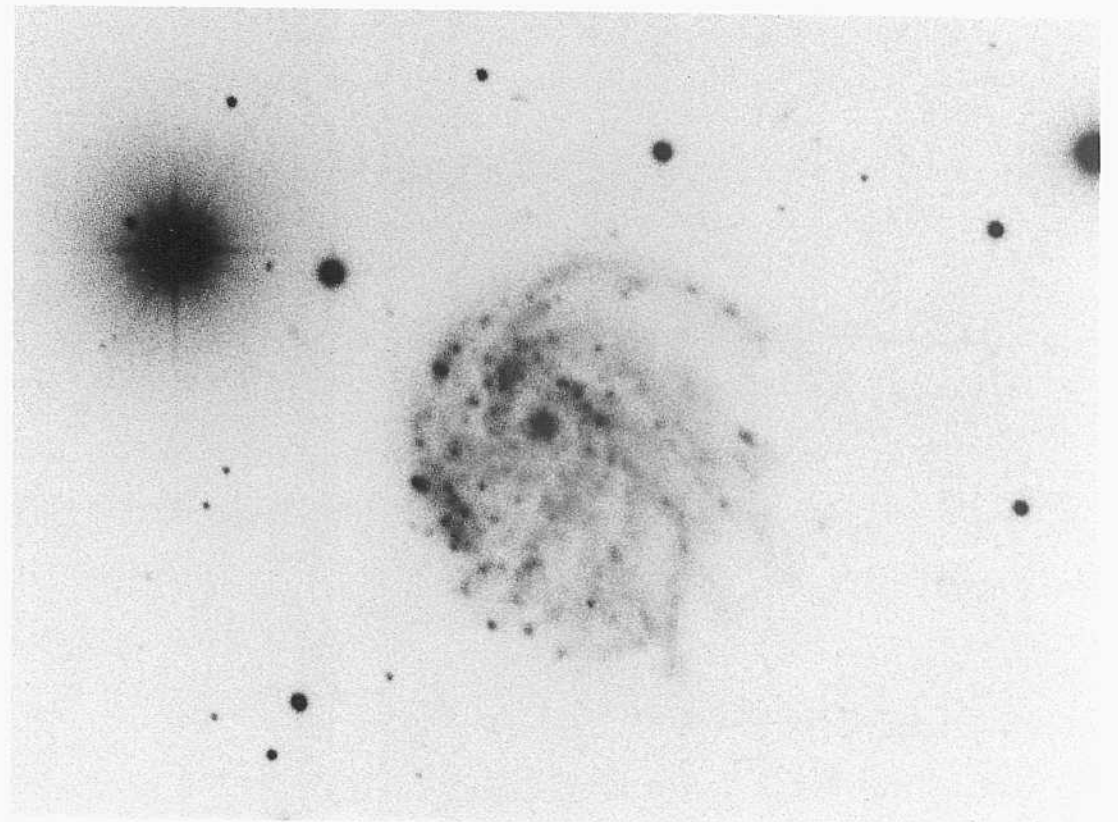
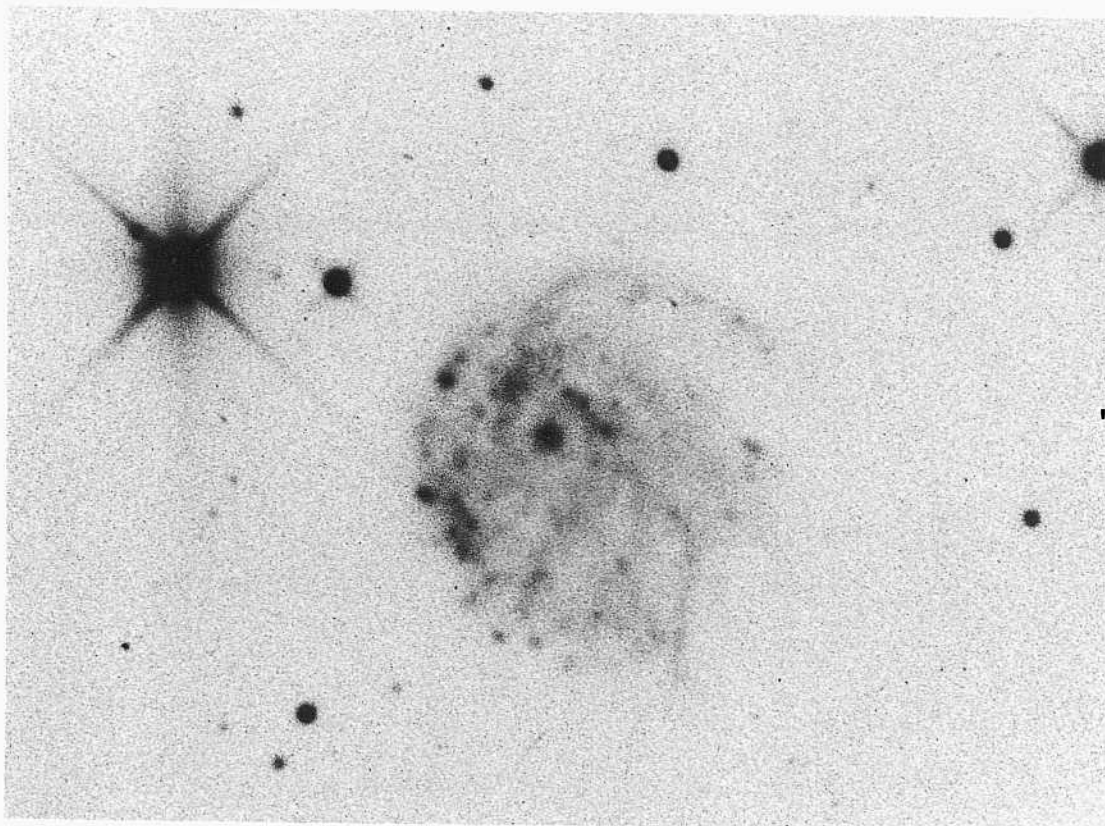
NGC 2276      Sc(r)II-III      Karachentsev 127  
PH-7566-S  
Nov 7/8, 1978  
103aO  
12 min

Compare the image of NGC 2276 taken with the Palomar Hale 200-inch telescope in the print here with that taken with the Mount Wilson 60-inch reflector in the print to the left.

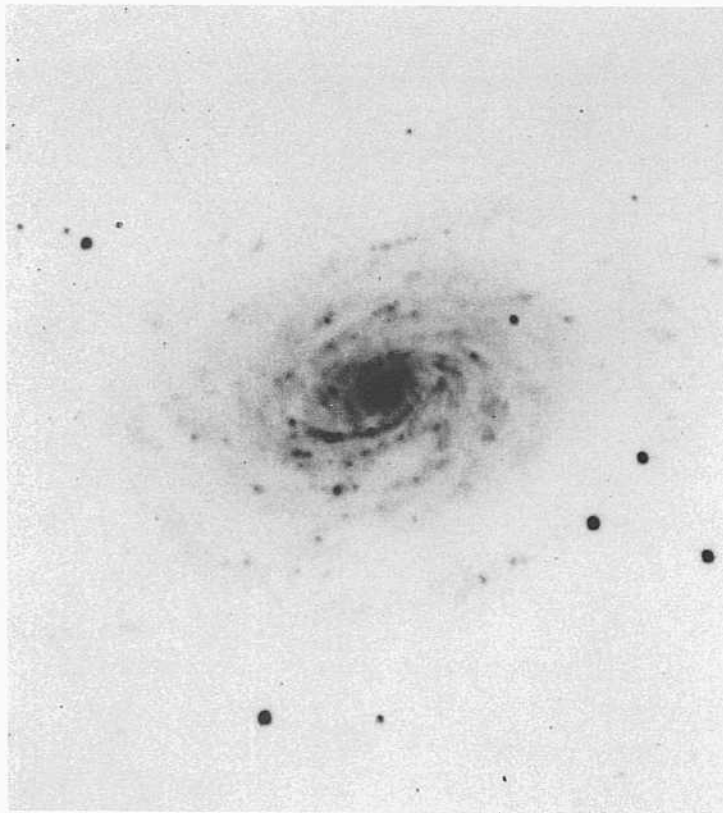
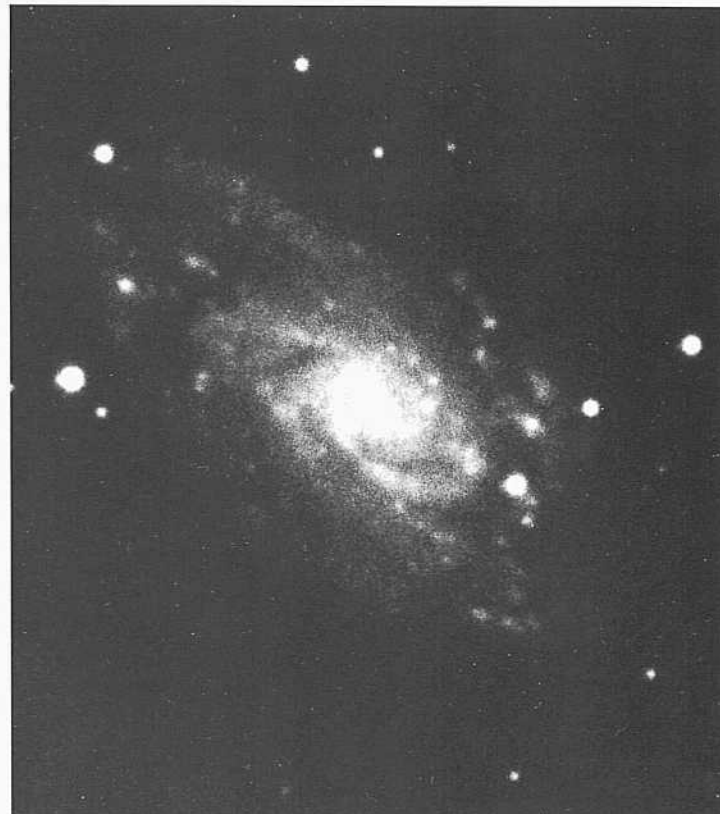
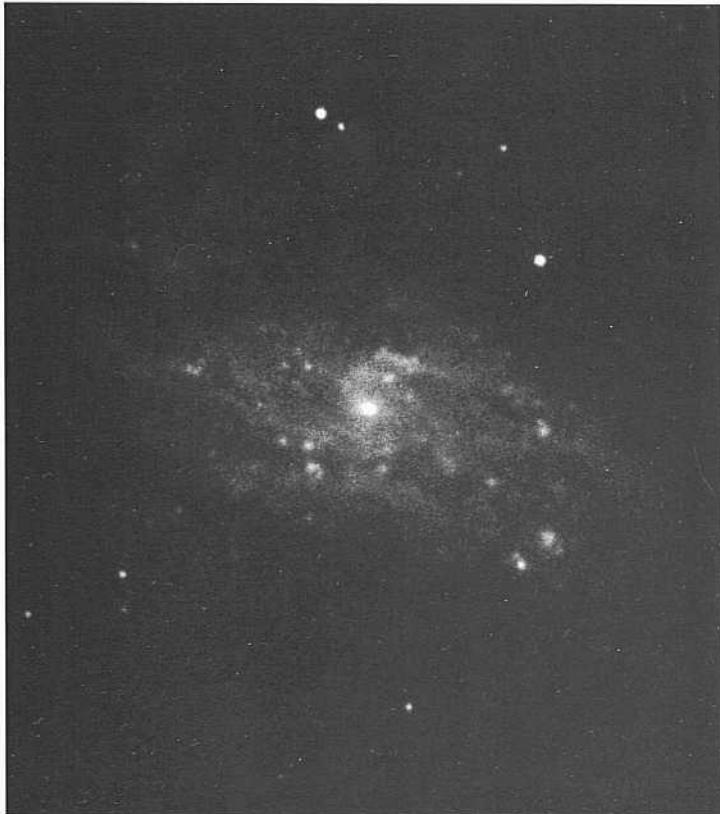
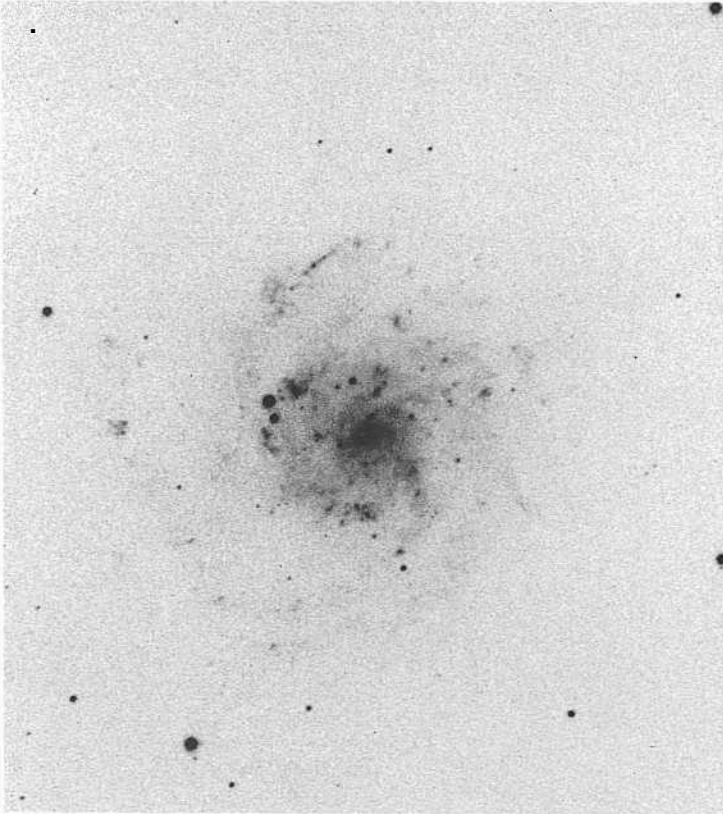
The spiral pattern is unusual, perhaps because of a tidal encounter with the probable companion NGC 2300 (E3; panel 6), whose projected linear separation is small at 90 kpc.



PANEL  
263



PANEL  
264



## T

lie six galaxies on this panel continue the late-luminosity class, Sc morphological type, where the arm pattern is multiple and where the arm fragments are thin. The arm pattern in each galaxy has similarities to the spiral pattern in M10 1 (Sc; panel 2 18) and the geometrical entropy is higher (more chaotic) here; hence the later-luminosity class is required.

NGC 5668      Sc(s)II-III      panel 268  
 CD-2114-S  
 March 19/20, 1982  
 103aO + GG385  
 35 min

The brightest HII region in NGC 5668 is double, apparently resolving at about the 2" level. The numerous other HII regions are unresolved at 1". The redshift of NGC 5668 is  $v_0 = 1491 \text{ km s}^{-1}$ .

NGC 5962      Sc(rs)II.3      HA, p. 30  
 II-2295-H  
 July 2/3, 1946  
 ItaO  
 30 min

The HII-region candidates are unresolved at the 1" level. The redshift of NGC 5962 is  $v_0 = 1972 \text{ km s}^{-1}$ .

New 4 = A 1252+00      S(s)II-III  
 CD-2167-S  
 March 27/28, 1982  
 103aO + GG385  
 45 min

The largest of the several HII regions appears to be a composite of several separate but overlapping regions, presenting a disk of about 2" diameter. The other regions are unresolved. The redshift of New 4 is  $v_0 = 1160 \text{ km s}^{-1}$ .

NGC 2541      Sc(s)III      group  
 PH-93-MH  
 March 16/17, 1950  
 103aO  
 10 min

NGC 2541 is highly resolved into individual HII regions. The largest three of the more than 50 such regions identifiable on this short-exposure Palomar 200-inch plate have resolved disks at the 3"-diameter level.

NGC 2541 is near the middle of a loose group of at least four highly resolved late-type galaxies, all in the HSA, already mentioned in the description of NGC 2500 (Sc; panel 262). The mean redshift of the group is  $\langle v_0 \rangle = 595 \text{ km s}^{-1}$ . The individual redshifts are  $v_0(2500) = 615 \text{ km s}^{-1}$ ,  $v_0(2537) = 513 \text{ km s}^{-1}$ ,  $v_0(2541) = 646 \text{ km s}^{-1}$ , and  $v_0(2552) = 607 \text{ km s}^{-1}$ . The angular separations and corresponding projected lineal separations from NGC 2541, based on a mean redshift distance of 11.9 Mpc ( $\theta = 50$ ), are  $2.6^\circ$  and therefore 540 kpc for NGC 2500,  $3.1^\circ$  and 644 kpc for NGC 2537, and  $1.2^\circ$  and 219 kpc for NGC 2552. These projected linear separations are similar to distances within the Local Group.

Note the similarity of the HII-region brightness distribution and the spiral pattern in all members of the group, seen on panels 262, 275, and 322 in addition to the panel here.

NGC 6106      Sc(rs)II.3  
**CD-910-HB**  
 April 29/30, 1979  
 103aO + GG385  
 40 min

The redshift of NGC 6106 is  $v_0 = 1459 \text{ km s}^{-1}$ . The HII regions are unresolved at the 1" level.

NGC 7456      Sc(s)II-III  
 CD-549-S  
 Oct 2/3, 1978  
 103aO + GG385  
 15 min

The surface brightness of the disk is low. There is no central bulge: as in all Sc galaxies on this and previous pages, the nucleus is either small or often unresolved at the 1-2" level, as here. The redshift of this galaxy is  $v_0 = 1199 \text{ km s}^{-1}$ .



The six galaxies on this panel complete the late-luminosity class (II-III/III) of the Sc classification section for galaxies with thin arms. The ScII-III and ScIII galaxies with intermediate or massive arms follow on panels 266-272.

NGC 4062      Sc(s)II-III      HA, p. 20  
H-2246-H  
March 7/8, 1946  
103aO  
60 min

The multiple-armed structure of the NGC 488 type begins at the small nucleus of NGC 4062 and, together with associated spiral dust lanes, spreads throughout the moderately low surface brightness disk. A few HH-region candidates exist, which, despite the low redshift of  $v_0 = 745 \text{ km s}^{-1}$ , are unresolved at the I" level.

The plate used for the image here was taken with the Mount Wilson 100-inch Hooker reflector.

NGC 3949      Sc(s)III  
S-476-H  
June 16/17, 1925  
E40  
40 min

NGC 3949 is in the highly complex Ursa Major region, within which at least four separate kinematic groups can be identified. The lowest-redshift group contains the highly resolved late-type spirals NGC 4144, 4214, 4244, 4449, 4736, and IC 4182. The mean redshift of this group is  $\langle v_0 \rangle = 285 \text{ km s}^{-1}$ . The second kinematic group at  $\langle v_0 \rangle = 595 \text{ km s}^{-1}$  is associated with M51, and contains also NGC 4258, 4490, 4616, and others. A group with  $\langle v_0 \rangle$  near  $750 \text{ km s}^{-1}$  contains NGC 3675, 3769, 3782, IC 750, NGC 4051, 4242, and NGC 3949 shown here. The fourth group is the great Ursa Major Cluster, with  $\langle v_0 \rangle$  about  $980 \text{ km s}^{-1}$ .

The image here of NGC 3949 is from a Mount Wilson 60-inch plate. The surface brightness of the disk is high. Useful resolution into stars from the ground seems unlikely.

The redshift is  $u_0 = 857 \text{ km s}^{-1}$ .

NGC 6015      Sc(s)II-III  
PH-5543-S  
June 6/7, 1970  
103aO + GG385  
20 min

The multiple-arm pattern of NGC 6015 starts at the center in a prototype (s)-type configuration. There is no evidence of a central bulge. The nucleus is small, characteristic of the Sc morphology. The redshift of NGC 6015 is  $v_0 = 1018 \text{ km s}^{-1}$ .

NGC 4428      Sc(s)II.3  
H-2263-S  
May 4/5, 1946  
103aO  
40 min

NGC 4428 forms a physical pair with NGC 4433 (See; panel 194) at an angular separation of  $7.2'$  and  $v_0$  redshifts of  $2828 \text{ km s}^{-1}$  and  $2771 \text{ km s}^{-1}$ , respectively, giving a mean redshift distance of 56 Mpc. The projected linear separation is 117 kpc.

The print here is from a Mount Wilson 100-inch plate. The print of NGC 4433 on panel 194 is from a Palomar 200-inch plate. Note the similar morphology of the two galaxies of this pair\*.

NGC 4595      Sc(s)II-III      VCC 1811  
H-1729-H  
Dec 25/26, 1935  
Imp. Eel.  
60 min

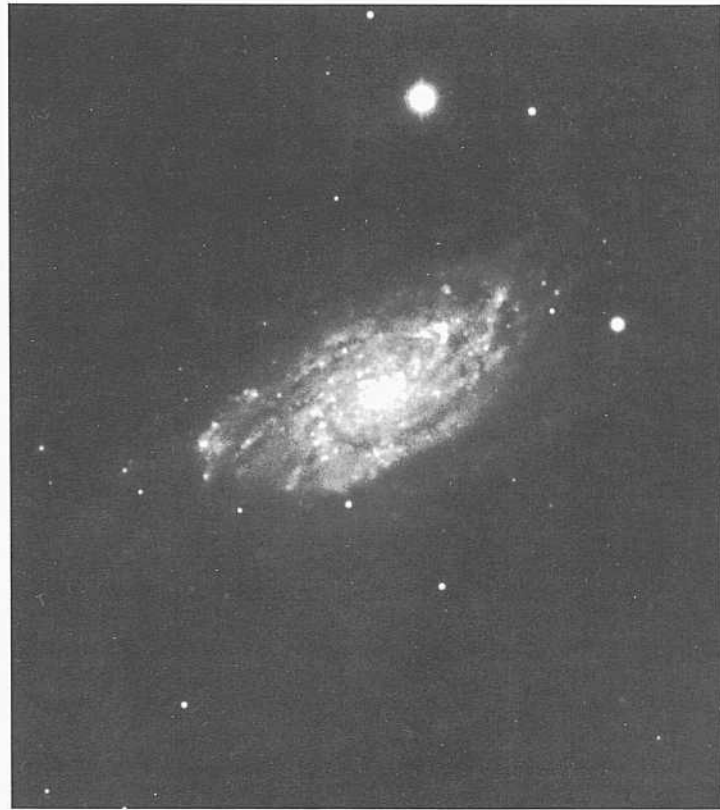
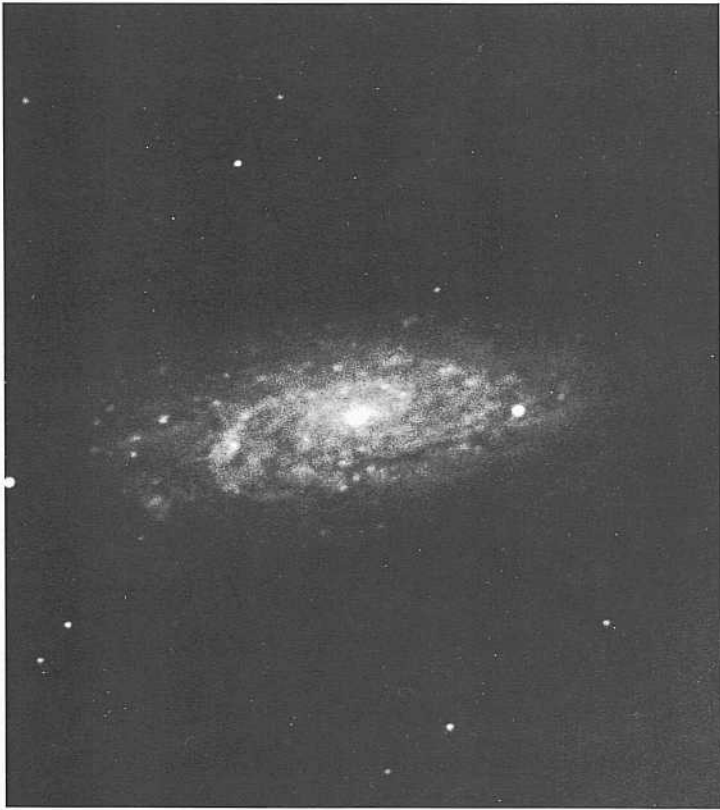
NGC 4595 is a small galaxy located  $3.7^\circ$  northeast of NGC 4486, which is the brightest galaxy associated with the Virgo subcluster A. A comparison of the angular size of NGC 4595 with other Virgo Cluster galaxies is made in the atlas of such galaxies printed to a common scale (Sandage, Binggeli, and Tammann 1985a).

The redshift of NGC 4595 is  $v_B = 559 \text{ km s}^{-1}$ .

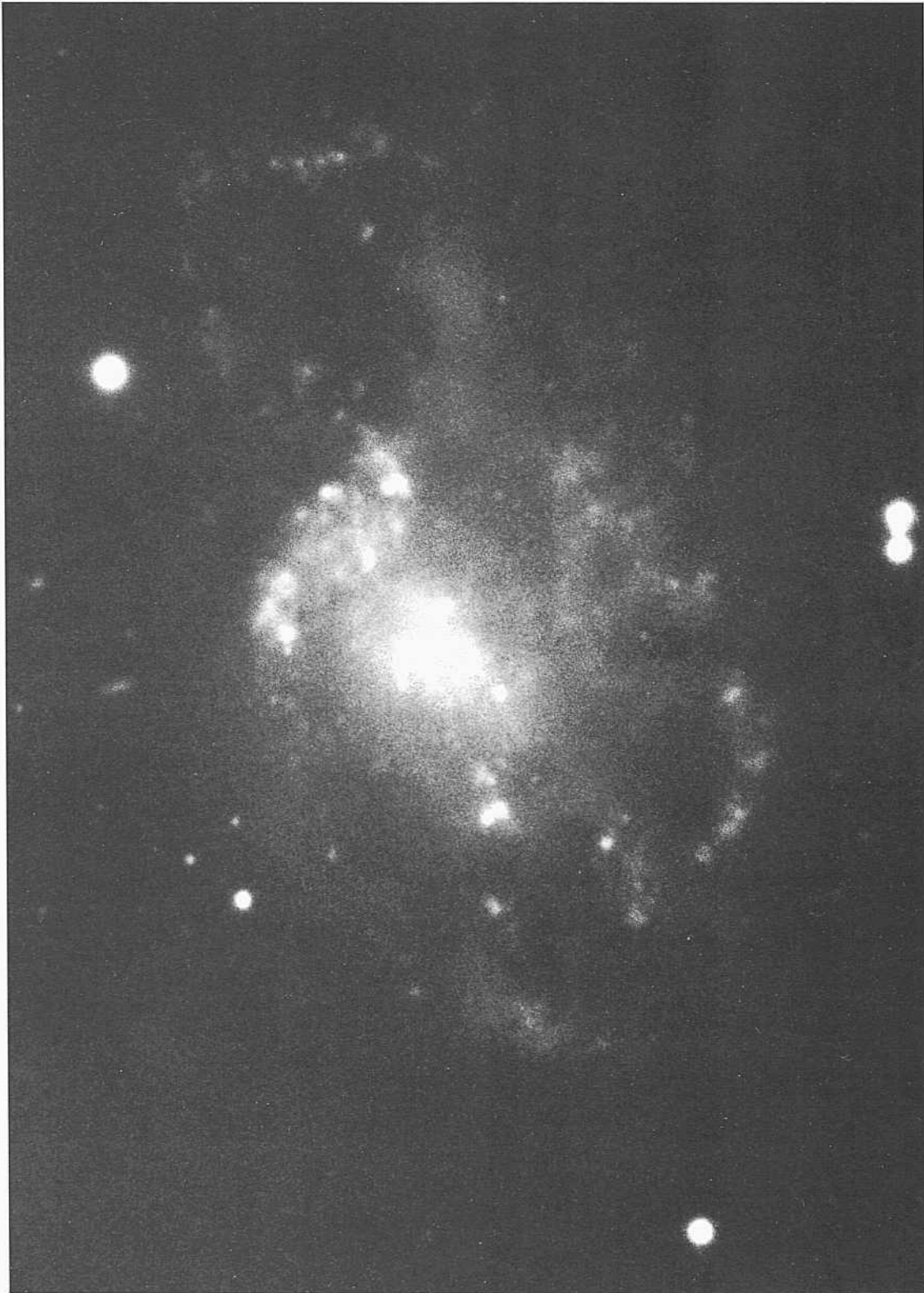
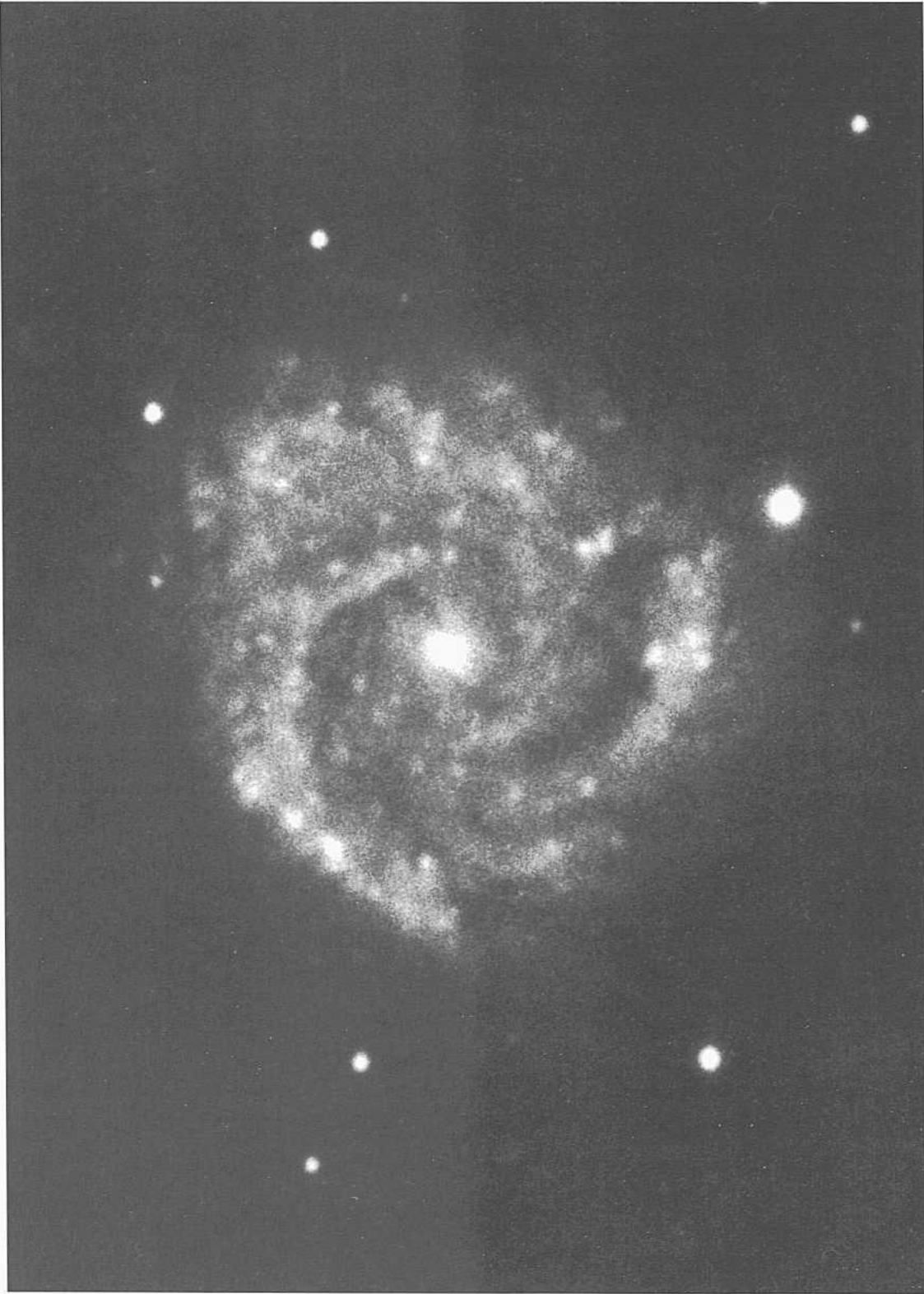
NGC 5645      Sc(s)II-III  
CD-1868-HB  
April 9/10, 1981  
103aO  
75 min

The spiral pattern in NGC 5645 is less regular than in other galaxies of luminosity class II-III on this panel. The pattern has a similar geometrical entropy to that in NGC 428 (ScIII) on the next panel, and hence the luminosity classification might have been placed at III. Note, however, that the arms are still moderately thin in contrast to the massive arms in, say, NGC 2427 (Sc; panel 269).

The redshift of NGC 5645 is  $v_0 = 1375 \text{ km s}^{-1}$ .



PANEL  
266



The spiral arms of the 12 galaxies on this and the next two panels are intermediate in thickness between the thin arms shown on the preceding seven panels of .Sell-III types, and the massive arms in the sense of Reynolds (1927a,b) in galaxies on panels 2 69-2 72.

NGC 7137      Sc(rs)II.8  
 PH-5-S  
 Sep 24/25, 1951  
 103aO  
 30min

For its relatively small redshift,  $v_0 = 1951$  km  $s^{-1}$ , the angular diameter to the edge of the spiral pattern in NGC 7137 is very small, at  $D = 0.9'$ . At a redshift distance of 39 Mpc ( $H = 50$ ), this corresponds to a linear diameter of only 10 kpc. Despite the small size (and the consequent relatively faint absolute magnitude,  $(V_B = -20.4)$ , the arm pattern is well formed and indeed almost exquisite.

The disk is filled with arms which on one side break into six separate fragments; in contrast there is but one major arm on the opposite side.

NGC 428      Sc(s)III  
 PH-7562-S  
 Nov 7/8, 1978  
 103aO  
 12min

The semi-chaotic pattern seen here is similar to that in NGC 5645 on the preceding panel. The surface brightness of the inner disk is high. Many Mil regions exist in the bright part of one of the major arms on one side of the image. Useful resolution into individual stars from the ground seems difficult.

The redshift of NGC 428 is  $v_0 = 1311$  km  $s^{-1}$ .

Sc Classification Section (continued)

NGC 3320      Sc(s)II-III      Racine wedge  
PH-7713-S  
Feb 11/12, 1979  
103aO  
12 min

The **arm pattern is multiple**, beginning at the center in a characteristic (s) mode. The disk is covered **with arm** fragments. **The few individual** HH-region candidates are unresolved at the 1" level. The redshift of NGC 3320 is  $v_o = 2380 \text{ km s}^{-1}$ .

The original plate was made with a Racine wedge, making **multiple** images of the bright stars whose secondary component is 5 mag fainter than the primary.

NGC 7713      Sc(s)II-HI      pair  
CD-1522-S/Br  
Aug 5/6, 1980  
103aO + GG385  
45 min

NGC 7713 forms a wide pair with IC 5332 (Sc; panel 259) at an angular separation of  $1.9^\circ$ . The redshifts are  $u_o(5332) = 713 \text{ km s}^{-1}$  and  $u_o(7713) = 684 \text{ km s}^{-1}$ . At the mean redshift distance of 14 Mpc ( $\mu = 50$ ) the projected linear separation is 464 kpc.

The resolution of NGC 7713 into individual stars and HII regions is more difficult than in IC 5332 for two reasons: (1) the background surface brightness of the NGC 7713 disk is higher than that in IC 5332, and (2) the problem is made worse by the high inclination of NGC 7713 to the line of sight.

The largest of the several HH-region candidates resolve into disks at about the 2" level.

NGC 701      Sc(s)II-III  
CD-1558-S/Br  
April 8/9, 1980  
103aO + GG385  
45 min

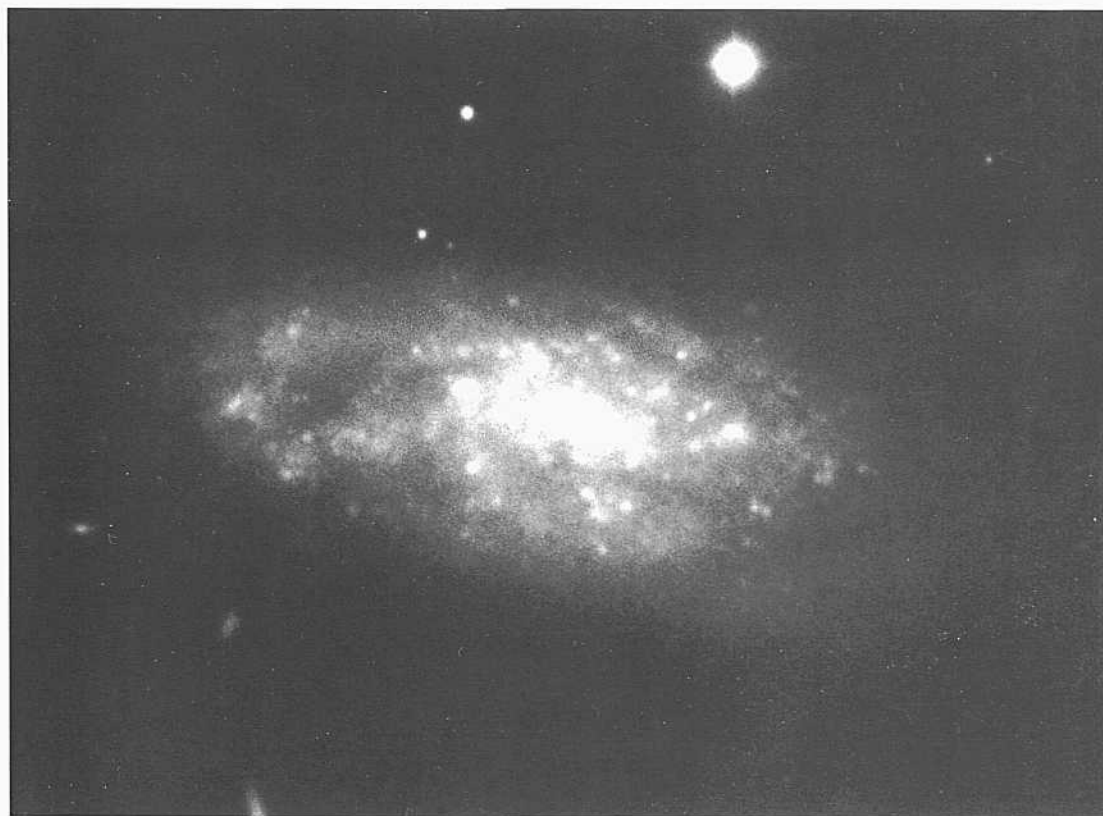
The multiple-armed pattern in NGC 701 is similar to the **spiral** morphology of the arms in NGC 7713, at the lower left.

The **HII** regions are unresolved. The redshift of NGC 701 is  $v_o = 1923 \text{ km s}^{-1}$ .

IC 3253      Sc(s)II-III  
CD-207-S  
Feb 9/10, 1978  
103aO + GG385  
45 min

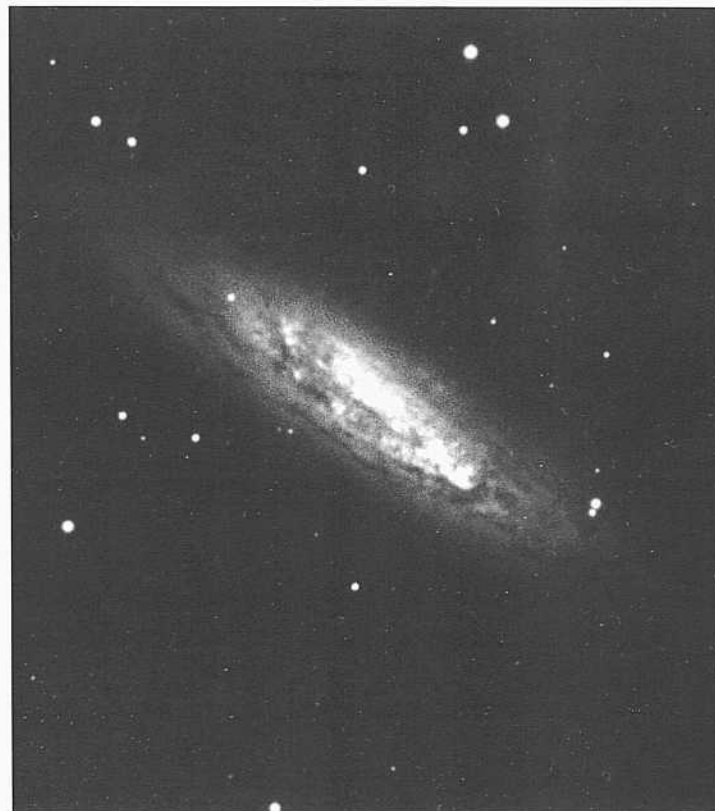
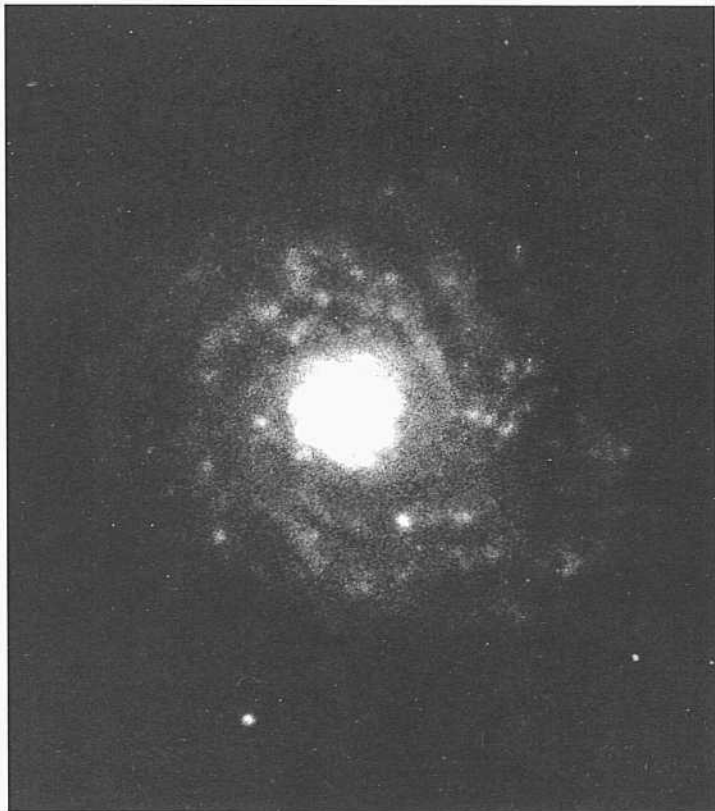
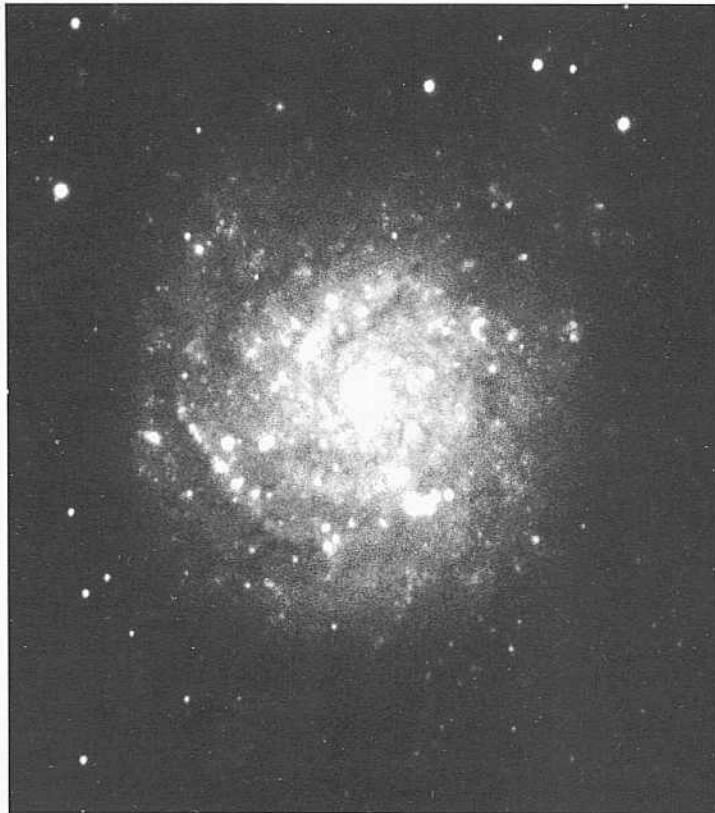
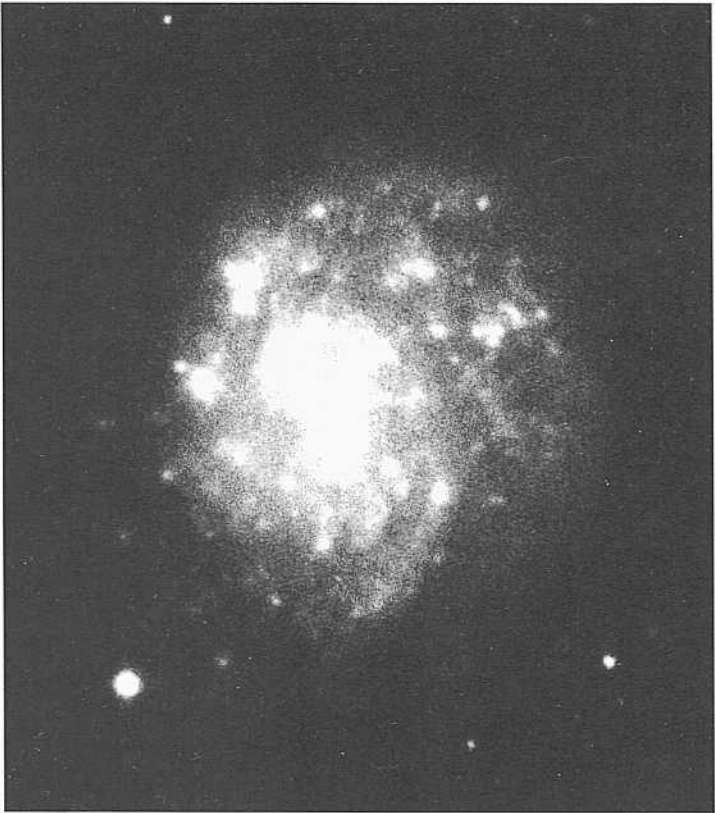
IC 3253 has the standard morphology of a multiple-armed **spiral** pattern in a highly inclined galaxy of late-luminosity class, of the M101 type. The disk surface brightness is high; the arms fill the disk.

The **HII** regions will not usefully resolve from the ground. The redshift is  $v_o = 2582 \text{ km s}^{-1}$ .



PANEL  
267

PANEL  
268





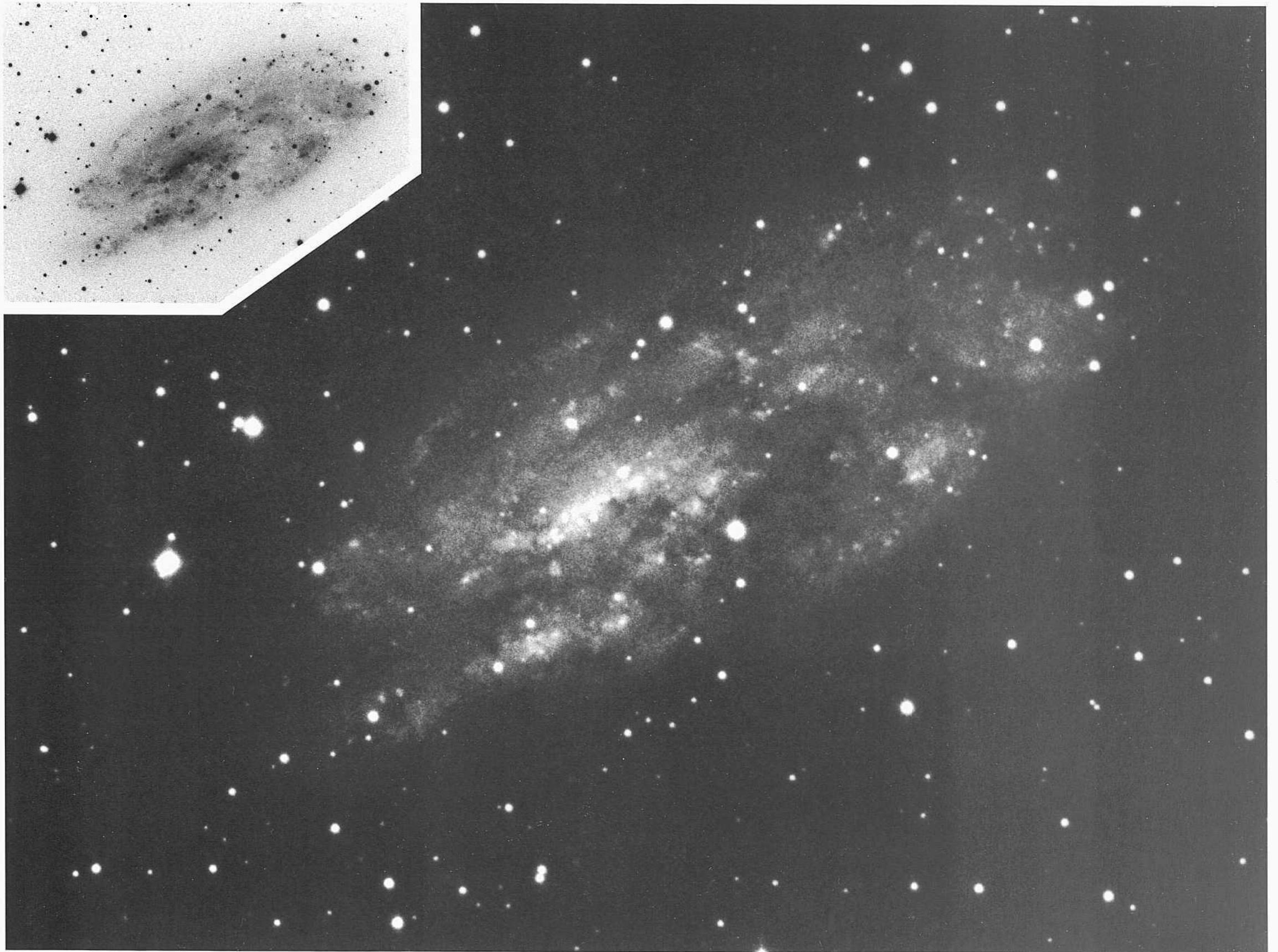
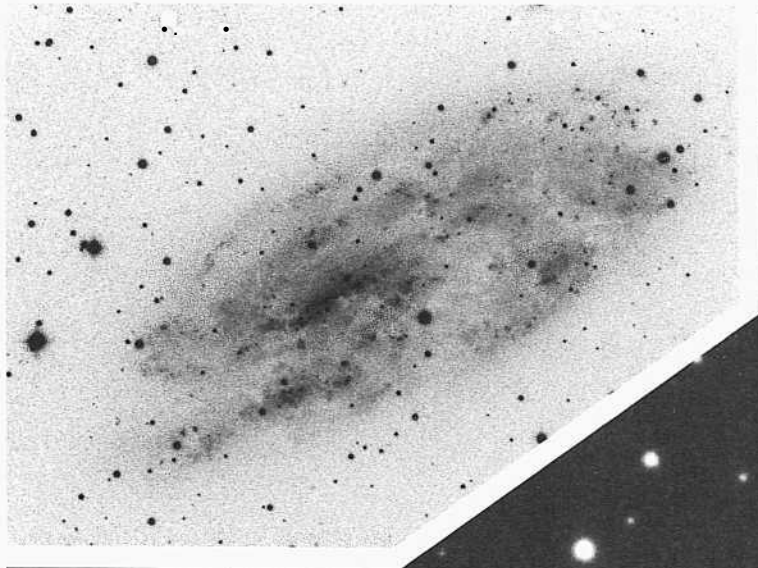


**M**ost of the galaxies on this and the next three panels have massive arms in the sense of Reynolds (1927a,b). Such arms cover the disk and provide a high-surface-brightness background against which it is difficult to identify individually resolved stars.

**NGC 2427      Sc(s)H-III**  
**CD-798-S**  
**Feb 24/25, 1979**  
**103aO + GG385**  
**45 min**

NGC 2427 is a very late Sc; it is near the StI edge of the Sc morphological box in the classification progression. There is no central bulge or identifiable nucleus. **Individual** stars may begin to resolve at about  $B = 22$ . The redshift is  $v_o = 707 \text{ km s}^{-1}$ .

The mixed classification SAB(s)dm, between ordinary and barred spiral, given in the RC2, emphasizes the bar characteristics but assigns a later galaxy type (Sdm) than we have done here.



PANEL  
270



*Sc Classification Section (continued)*

NGC 5530      Sc(s)II.8  
CD-1412-S/Br  
March 23/24, 1980  
103aO + GG385  
4.5 min

The disk of NGC 5530 is filled with fragments of thick arms and their associated dust lanes. The arm pattern is multiple. There is only a small central nuclear region. Most of the pattern is dominated by the arms.

Resolution into individual stars and III regions does not occur on the available plate material. The redshift is  $v_r = 943 \text{ km s}^{-1}$ .

NGC 2082      Se(s)II-III  
CD-167I-S  
Dec. **31/Jan 1, 1980/1981**  
**103aO + GG385**  
4.10 min

NGC 2082 is in a rich field of LMC disk stars. It is located about  $5^\circ$  north of the bar of the LMC, close to Shapley's Constellation II of the LMC.

No resolution into stars or III regions occurs. The redshift is  $v_r = 1038 \text{ km s}^{-1}$ .

The six galaxies on this panel and the two on the next complete the section showing late-luminosity-class Sc galaxies with massive arms.

NGC 4088 Sc(s)II-III/SBc Ursa Major Cluster  
**S-1971-H** HA, p. 30  
 Feb 19/20, 1947  
 103aO  
 15 niin

NGC 4088 forms a pair with NGC 4085 (Sc; panel 291) at a separation of  $11''$ . The redshifts are  $v_r(4088) = 820 \text{ km s}^{-1}$  and  $v_r(4085) = 823 \text{ km s}^{-1}$ . Both are considered to be members of the Ursa Major Cluster, whose mean redshift is  $\langle v_r \rangle = 980 \text{ km s}^{-1}$ . At a redshift distance of 20 Mpc ( $H = 50$ ), the projected linear separation of the pair is 64 kpc.

NGC 2701 Sc(s)II-IH  
 PH-7552-S  
 Nov 6/7, 1978  
 103aO  
 12 min

One of the two major arms of NGC 2701, which begin near the center with the (s) arm configuration, is considerably brighter than the other. In addition, the arm pattern is asymmetric about the small bright nucleus. There is no evidence of a close encounter or a merger (no close companion is seen). The asymmetry of the pattern appears to be natural, endemic to the galaxy.

The redshift is  $v_r = 2421 \text{ km s}^{-1}$ .

IC5179 Sc(s)II-III  
 CD-1563-S/Br  
 Aug 9/10, 1980  
 103aO + GG385  
 45 niin

The nucleus of IC 5179 is unresolved (it is starlike, seen in the insert) at the  $1''$  level. The redshift is  $v_r = 3453 \text{ km s}^{-1}$ .

NGC 1359 Sc(s)H-III  
 CD-2008-Bedke/Gregory  
 Oct 23/24, 1981  
 103aO + GG385  
 45 min

NGC 1359 is close to but just outside the catalog boundaries of the NGC 1400 Group (Ferguson and Sandage 1990) whose mean redshift is  $\langle v_r \rangle = 1581 \text{ km s}^{-1}$ . The redshift of NGC 1359 itself is  $v_r = 1972 \text{ km s}^{-1}$ .

Active star formation is occurring throughout the arms, evidenced by the many bright HII regions in the central bar and especially in the one well-developed major arm.

A bright asteroid trail is evident in the reproduction.

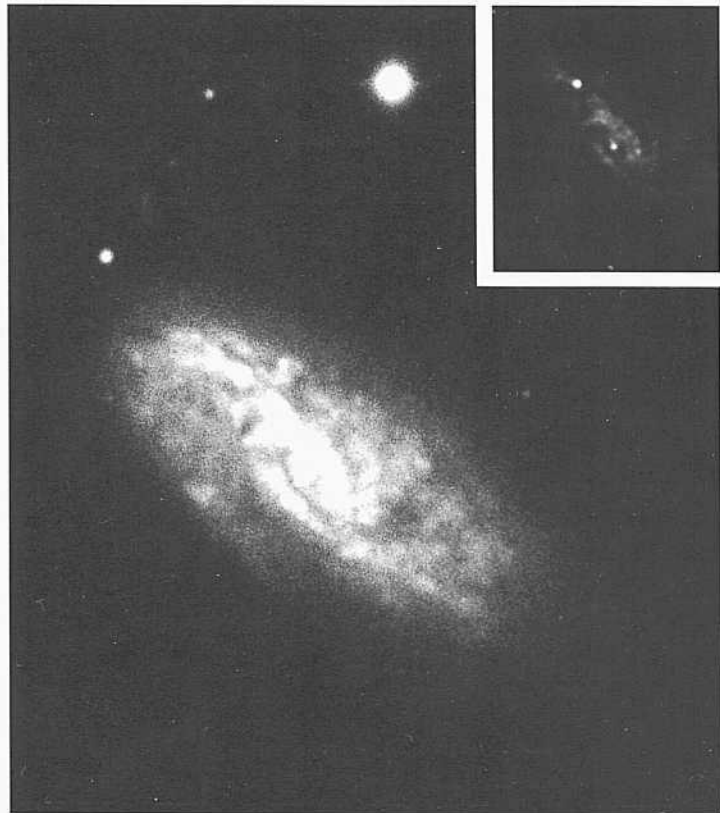
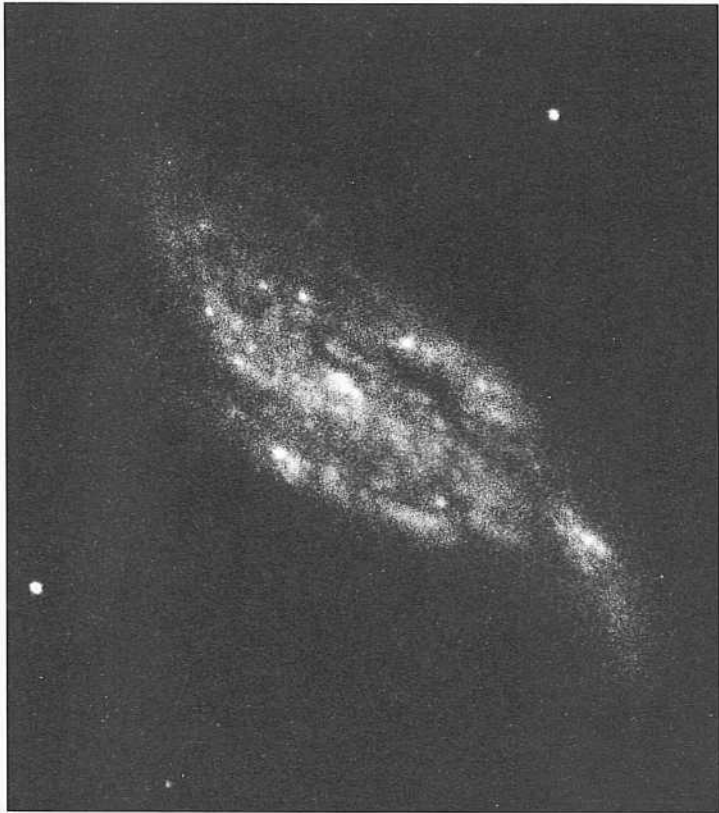
HA 72 = A1357 Sc(s)II-IH  
 CD-1538-S/Br  
 Aug 7/8, 1980  
 103aO + GG385  
 45 niin

Galactic foreground stars in this low-latitude field ( $b = 16^\circ$ ) contaminate the face of the galaxy, complicating the identification of the stellar and the HII components of HA 72. Nevertheless, the existence of HH-region candidates is evident in each of the two principal arms.

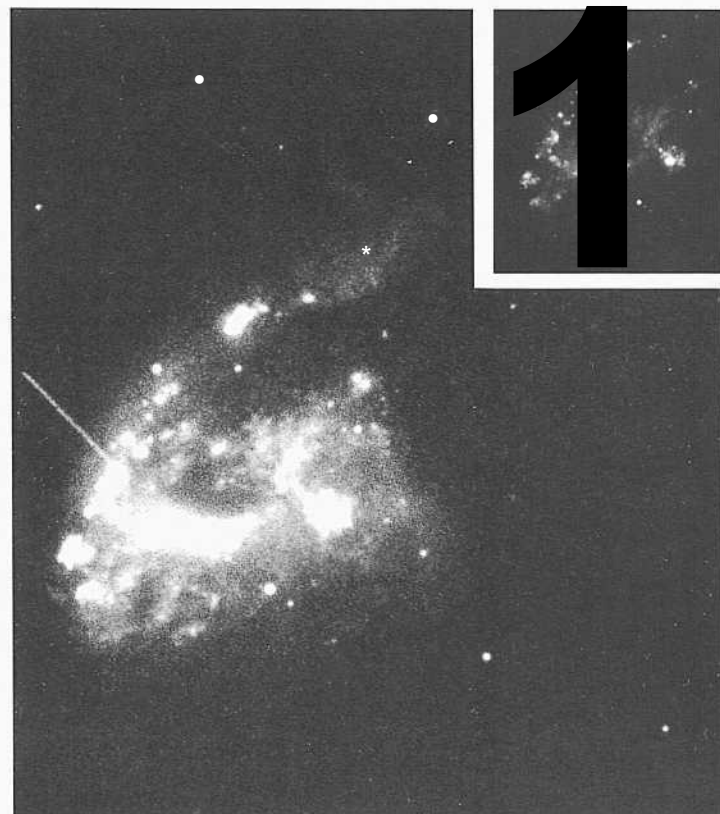
The redshift of HA 72 is  $v_r = 1192 \text{ km s}^{-1}$ .

NGC 7218 Sc(s)II.8  
 CD-1509-S/Br  
 Aug 4/5, 1980  
 103aO + GG385  
 45 niin

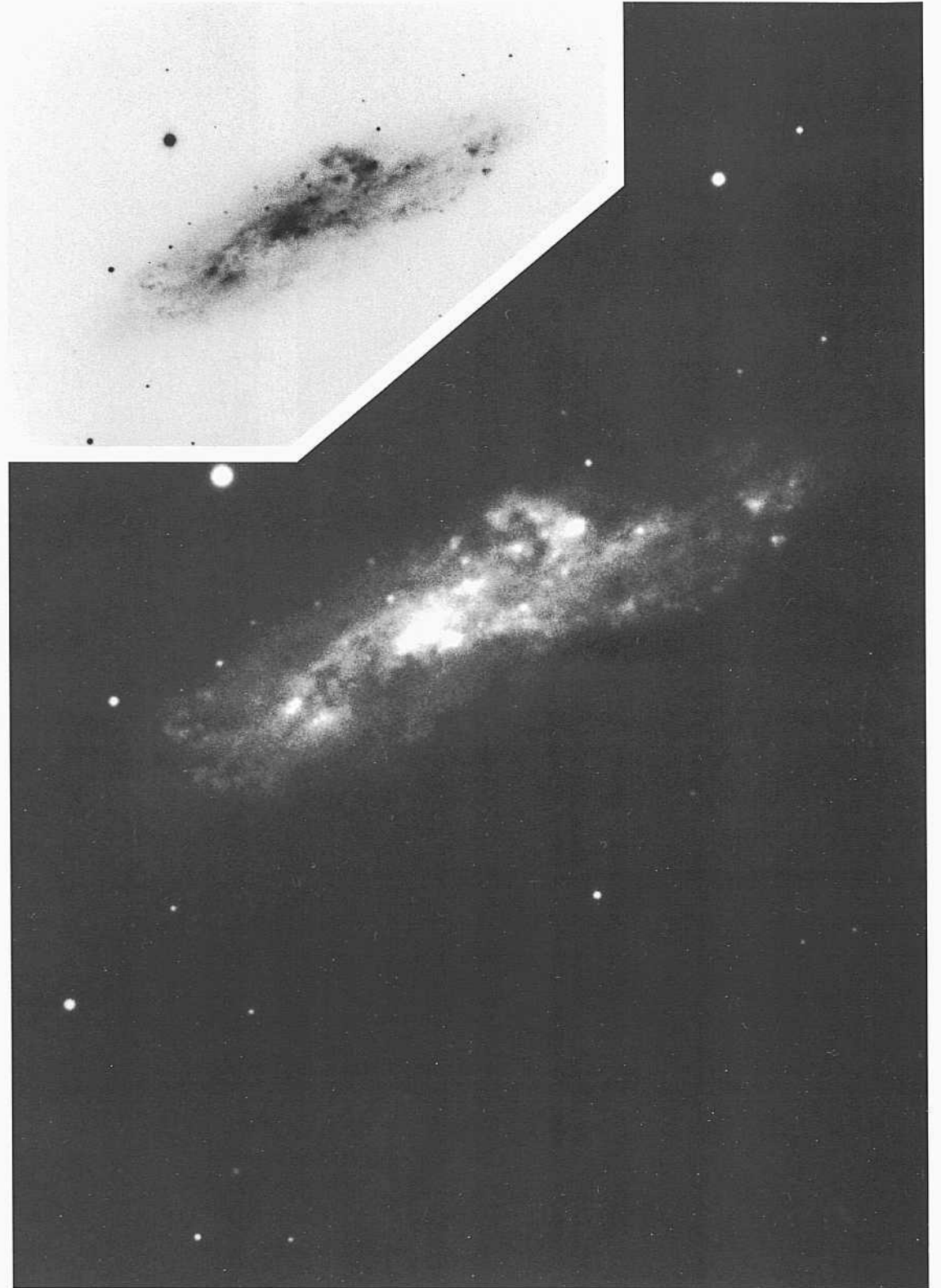
The surface brightness of the arms of NGC 7218 is very high. No useful resolution into HII regions is evident on the available plate material. The redshift of NGC 7218 is  $v_r = 1781 \text{ km s}^{-1}$ .



PANEL  
271



PANEL  
272



THE Sell I SUBCLASS

NGC 1518      ScIII  
CD-2009-Bedke/Gregory  
Oct 23/24, 1981  
103aO + GG385  
45 min

NGC 1518 is nearly on edge, making it impossible to trace the spiral pattern or accurately to classify the galaxy. There is no central bulge; hence the late-type classification is required. There is possibly a bar and an arm structure, as in NGC 1300 (but later), where the arms spring from the ends of the bar.

The arms contain many HII-region candidates and possibly individual resolved stars. The redshift is  $v_r = 914 \text{ km s}^{-1}$ .

IC 2995      S<(s)III  
CD-218-S  
Feb 11/12, 1978  
103aO + GG385  
40 min

The pattern of IC 2995 is similar to that of NGC 1518 at the left. The largest of the many III regions resolve at about 2". No resolution into individual stars is seen on the available plate material. The redshift is  $v_r = 1566 \text{ km s}^{-1}$ .



Galaxies of luminosity classes III and III-IV are shown on this and the next two panels. A spiral pattern is still evident and traceable, but the regularity of the arms is generally poor. Although the chaos in the pattern is great (large geometrical entropy), the surface brightness of most of the 18 galaxies on these

three panels is very high; yet the absolute magnitudes of many of these galaxies are faint. Evidently, surface brightness is not an indicator of absolute luminosity in the ScIII galaxies as defined here. The opposite is true, however, for Sd, Sm, and Im types in the later sections of the classification.

NGC 3511      Sc(s)II.8      pair  
CD-722-S      HA, p. 35  
Feb 1/2, 1979  
103aO + GG385  
4-5 min

NGC 3511 forms a close pair with NGC 3513 (SBc; panel 299) with a separation of 10.5'. The redshifts are  $P_o(3511) = 951 \text{ km s}^{-1}$  and  $r_o(3513) = 845 \text{ km s}^{-1}$ . At the mean redshift distance of 1.8 Mpc ( $H = 50$ ), the projected linear separation is small, at 5.5 kpc.

The surface brightness of the spiral pattern overlaying the entire disk is very high, as shown in the print at the upper left. A lighter print from the same plate is shown at the lower left.

The arms are massive in the sense of Reynolds (1927a,b). The pattern is similar to that in NGC 2427 (Sc; panel 269) and NGC 4088 (Sc; panel 271) although slightly less regular.

NGC 3511      Sc(s)II.8      HA, p. 35  
CD-722-S  
Feb 1/2, 1979  
103aO + GG385  
4-5 min

The image here is made from the same plate used for the print above, but printed more thinly to show the spiral pattern and the associated heavy dust lanes that are predominantly on the insides of the heavy luminous arms.

NGC 3621      Sc(s)II.8  
CD-811-S  
Feb 25/26, 1979  
103aO + GG385  
4-5 min

NGC 3621 is highly resolved into individual brightest stars, beginning at about  $B = 20$  in some of the outer associations. The HII regions are not numerous but are present, the largest of which have halo diameters of about 4". The galaxy is similar in its spiral pattern to NGC 2403 in the print below. It also resolves into brightest stars in the same way but at a level about 1.5 mag fainter. This more-difficult resolution is consistent with the larger redshift of  $u_o(3621) = 435 \text{ km s}^{-1}$  compared with  $i_o(2403) = 299 \text{ km s}^{-1}$ .

NGC 2403      Sc(s)IH      HA, p. 36  
PH-344-B  
Nov 6/7, 1950  
103aO  
30 min

The stellar content of NGC 2403, including its brightest stars, the HII regions, the bright irregular blue variables, and the Cepheids require a distance modulus of  $m - M = 27.6$  (Tammann and Sandage 1968). This value was confirmed in a modern study by Freedman and Madore (1988).

The brightest blue stars begin to resolve at  $B = 18$ ; the brightest red supergiants begin at  $V = 19.5$  (Sandage 1984b). NGC 2403 was the first galaxy beyond the Local Group in which Cepheid variables were found. It was the first step in taking the distance scale outward into the true expansion field. The large difference in the distance modulus obtained from Cepheids of  $m - M = 27.6$ , compared with Hubble and Humason's (1931) value of  $m - M = 24.0$ , was a major correction that eventually led to a stretching of Hubble's original scale at large distances by a factor of slightly more than ten, giving the global value of the Hubble constant as near  $H = 50 \text{ km s}^{-1} \text{ Mpc}^{-1}$ .

NGC 4781      Sc(s)IH  
CD-1848-HB  
April 3/4, 1981  
103aO + GG385  
75 min

NGC 4781 ( $u_o = 689 \text{ km s}^{-1}$ ) is in a complex field where, within a radius of about  $1^\circ$ , are NGC 4742 (E4; panel 10;  $v_o = 1114 \text{ km s}^{-1}$ ), NGC 4760 (SO; panel 30;  $u_o = 4451 \text{ km s}^{-1}$ ), and NGC 4790 (Scd; panel 315;  $v_o = 1154 \text{ km s}^{-1}$ ). NGC 4742 and NGC 4790 may be kinematically related to NGC 4781, although a spread in redshift larger than  $400 \text{ km s}^{-1}$  is relatively rare. (See the later comment on resolution of the stellar content in the description of NGC 4790 on panel 315, in the Scd section.)

Also in the field are a number of partially resolved late-type dwarf galaxies (Sm and Im types) which may be related to NGC 4781.

The surface brightness of the thick spiral fragments that cover the disk is high. HII regions exist, and a few brightest stars may begin to resolve out of the background at about  $B = 2.15$ .

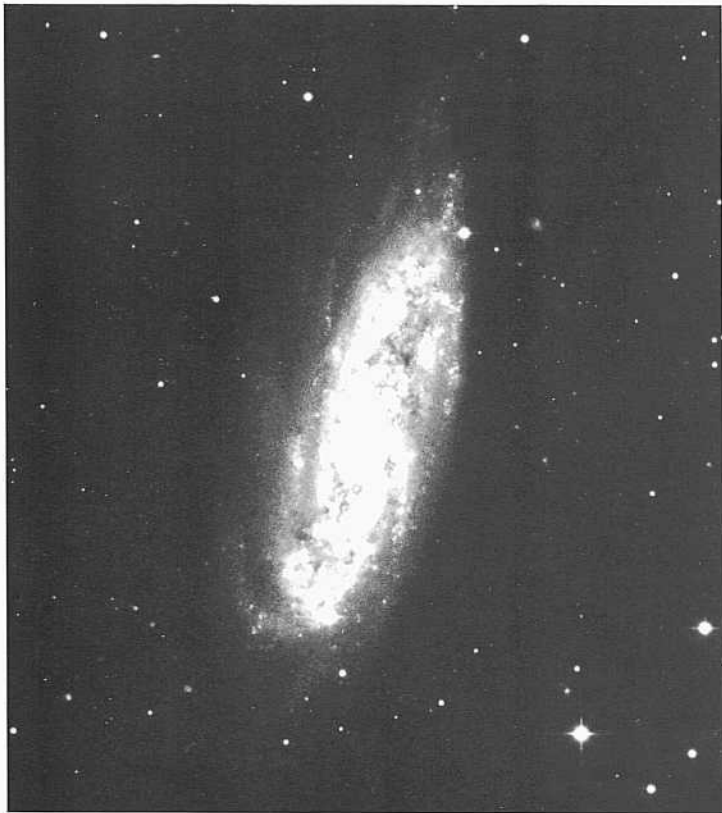
NGC 1546      Sc(s)III  
CD-219-S  
Feb 12/13, 1978  
103aD + GG495  
4-5 min

NGC 1546 insert      Sc(s)III  
CD-1675-S  
Jan 1/2, 1981  
103aO + GG385  
10 min

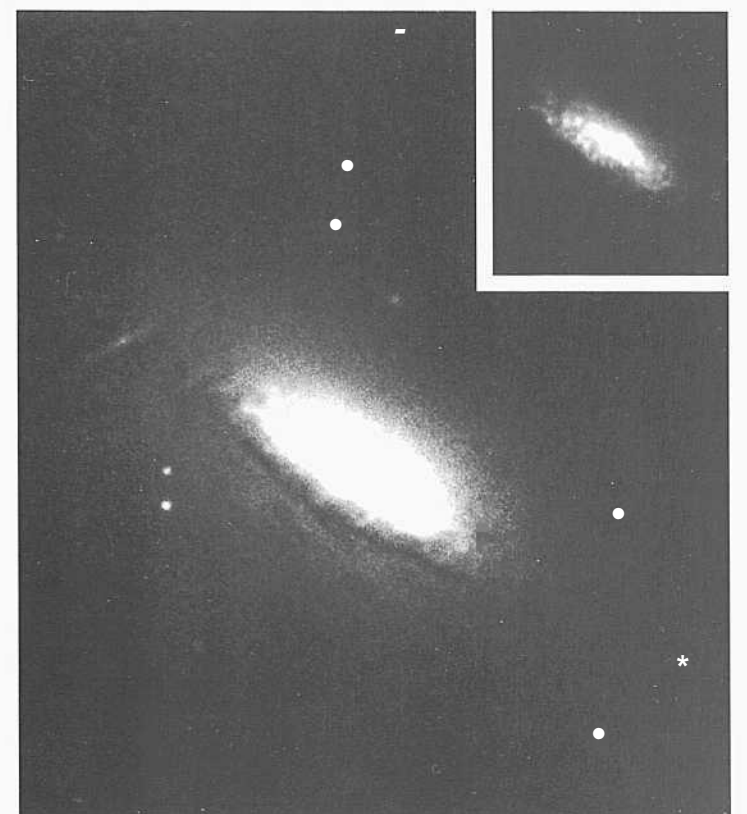
NGC 1546 has a very-high-surface-brightness arm pattern, seen almost edge on. The surface brightness is so high that on low-resolution photographs the image would appear to be an SO galaxy having no structure. In both the RC1 and RC2 the classification is listed as SO?, based on a 30-inch Stromlo reflector plate. But the pattern is that of a nearly edge on Sc spiral with multiple arms, similar to the morphology of NGC 3511 and NGC 4781 on this page.

The redshift of NGC 1546 is  $v_o = 1007 \text{ km s}^{-1}$ .

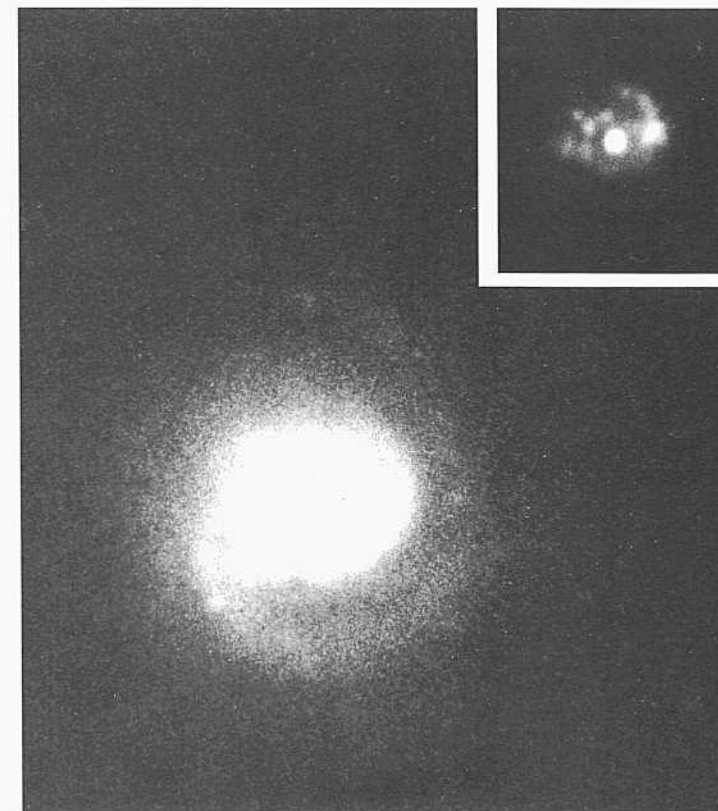
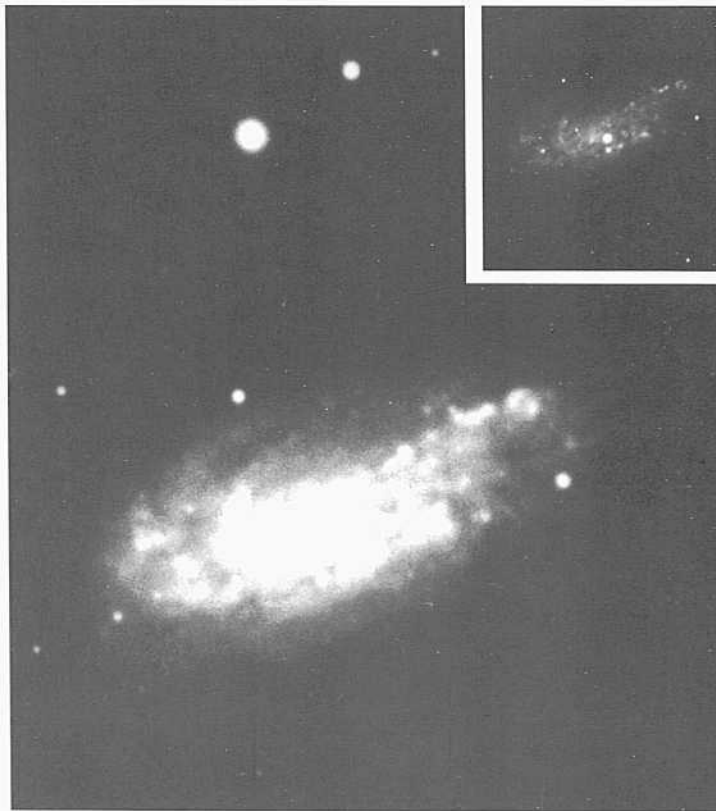
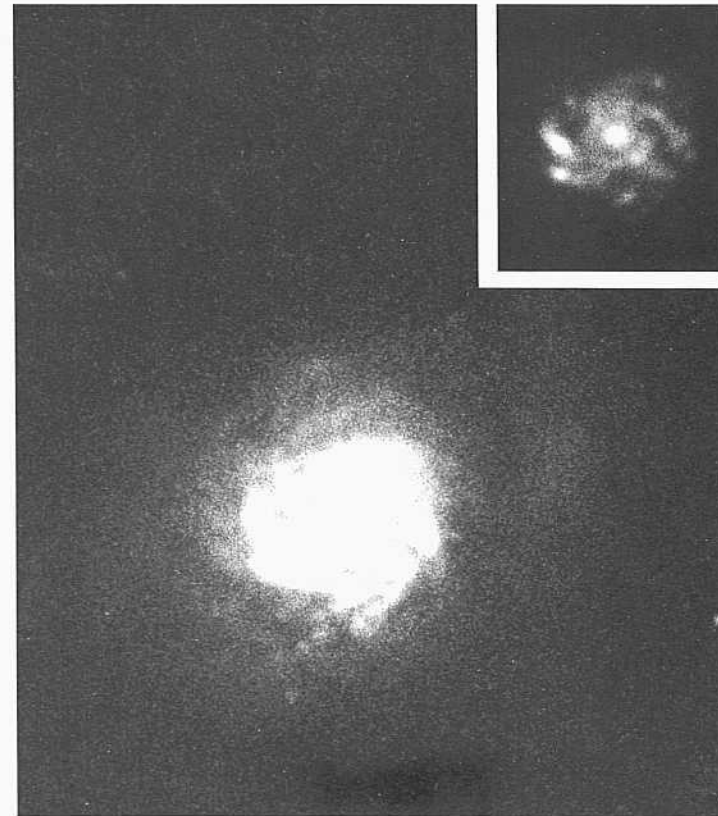
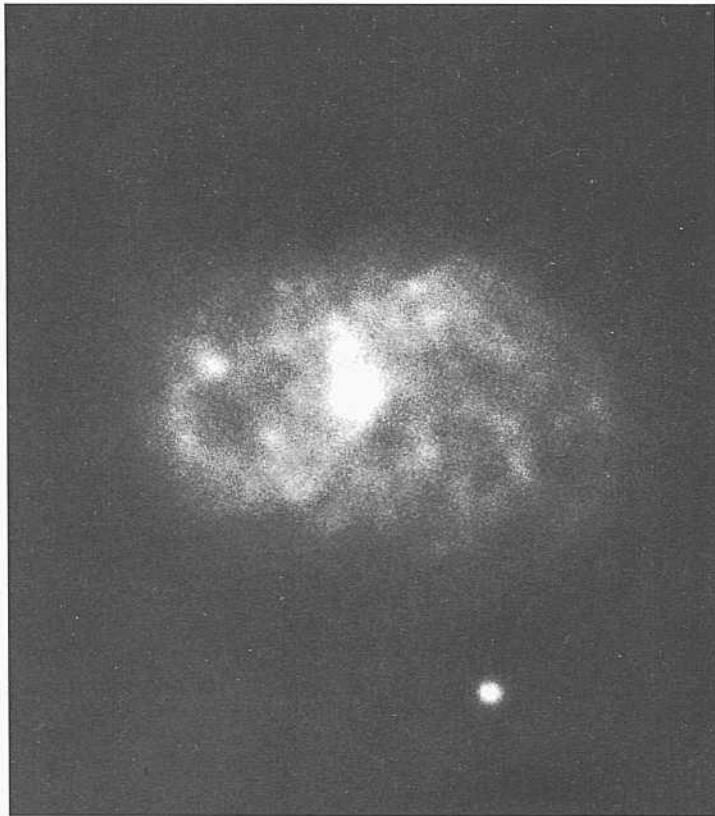
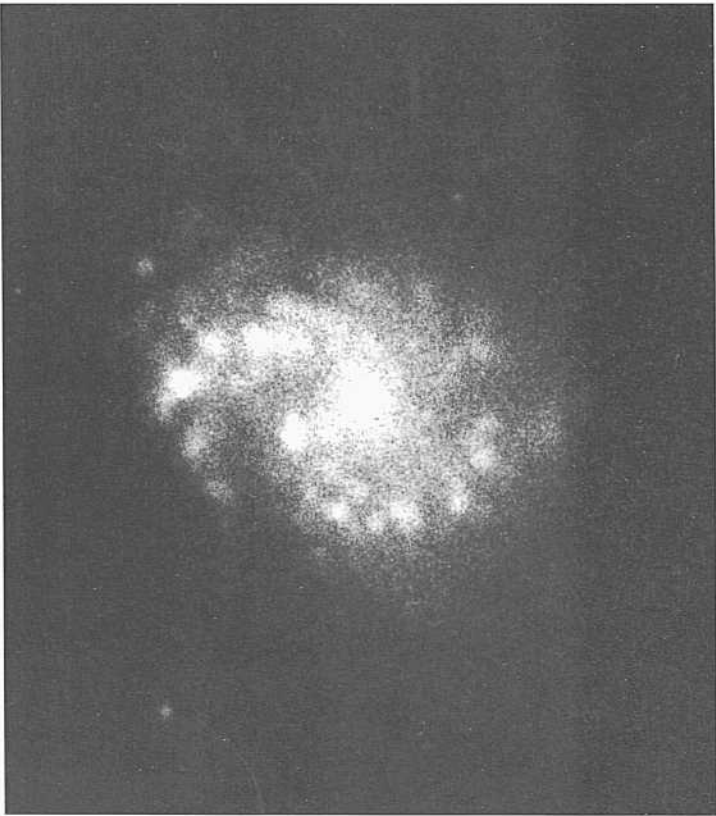
The image in the insert frame is made from a different Las Campanas plate than was used for the heavier main print. The thick-armed, multiple-spiral-arm pattern that begins at the center is hinted at in this print.



PANEL  
273



PANEL  
274



The six galaxies on this panel continue the pattern of high-surface-brightness arm fragments, often massive, that cover the disk in a way similar to the galaxies illustrated on the preceding panel.

NGC 4928      Sc(s)III.3  
H-2387-H  
Feb 21/22, 1947  
103aO  
30 iniii

NGC 4928 is a two-armed spiral where the arms are massive. Many HH-region candidates exist in the arms. The surface brightness of the luminous parts of the arms between the III regions is high; evidently the current rate of star formation is robust.

The redshift is  $v_o = 1434 \text{ km s}^{-1}$ .

NGC 6207      Sc(s)III  
PH-775-S  
Aug 24/25, 1954  
103aO + GG385  
30 min

NGC 6207 insert  
PH-7683-S  
Sep 26/27, 1979  
103aO  
8 min

NGC 6207 is similar to NGC 2403 (Sc; panel 273) in the character of the spiral arms and the high surface brightness over the inner disk. The redshift of NGC 6207 is  $v_o = 984 \text{ km s}^{-1}$ .

The insert print of NGC 6207 is made from a different original plate of shorter exposure than the one used for the heavy main print.

NGC 5480      Sc(s)IH      Racine wedge  
PH-7740-S                      Karachentsev 416  
June 11/12, 1980  
103aO  
12 min

NGC 5480 forms a close pair with NGC 5481 (EO/SO; not in the RSA) at a separation of 3.1'. The pair is number 416 in the catalog of close pairs by Karachentsev. He gives the redshifts of  $u_o(5480) = 2023 \text{ km s}^{-1}$  and  $u_o(5481) = 2143 \text{ km s}^{-1}$ . At the mean redshift distance of 42 Mpc ( $H = 50$ ), the projected linear separation of the pair at 38 kpc is small.

The pair is especially important because of the vast difference in the morphological types (E/SO vs. ScIII); yet they are obviously associated kinematically.

The arm pattern of NGC 5480 is multiple. Five arm fragments can be identified, four on one side and one on the other, all originating near the center.

NGC 4420      Sc(s)III      VCC 957  
CD-2174-S  
March 28/29, 1982  
103aO  
50 min

NGC 4420 is at the southern edge of the Virgo Cluster survey area used in the Virgo Cluster Catalog (Binggeli, Sandage, and Tammann 1985), but it may not be a member of the cluster.

The galaxy is illustrated in the atlas of Virgo Cluster candidates where the photographs are enlarged to the same angular scale (Sandage, Binggeli, and Tammann, 1985a; panel 10 there).

The surface brightness over the disk is high. The angular diameter is small. No useful resolution into individual stars is evident on the available plate material.

The redshift is  $v_o = 1515 \text{ km s}^{-1}$ .

NGC 5653      Sc(s)III pec  
H-2258-H  
May 3/4, 1946  
I03aO  
40 mill

NGC 5653 insert  
H-2302-H  
July 3/4, 1946  
103aO  
10 min

The surface brightness of the multiple-arm pattern over the inner disk of NGC 5653 is exceedingly high. Most of the detail of these arms is burned out in the main print. The five arm fragments, resembling a pinwheel, are seen in the insert. Very faint, smooth outer arms are visible in the overprinted main image here.

The redshift is  $v_o = 3587 \text{ km s}^{-1}$ .

The insert print showing the main multiple spiral arms of NGC 5653 has been made from a different original plate than the one used for the main print. Both plates were taken with the Mount Wilson 100-inch Hooker reflector.

NGC 3732      Sc(r) pec  
CD-1376-S/Br  
March 20/21, 1980  
103aO + GG385  
20 min

NGC 3732 insert  
CD-1377-S/Br  
March 20/21, 1980  
103aO + GG385  
10 min

The inner spiral pattern is tightly wound about a small nucleus seen only in the insert. A set of faint, smooth outer (fossil?) arms, brighter on one side than the other, is seen in the main print. No useful resolution into stars or III regions is evident on the available plate material. The spectrum is rich in emission lines (Sandage 1978), evidence of the high rate of star formation suggested by the high surface brightness of the arms.

The angular diameter of NGC 3732 of 30" is remarkably small for the small redshift of  $v_o = 1493 \text{ km s}^{-1}$ .

The insert print has been made from an original Las Campanas plate other than the one used for the main print.

**A** galaxies on this page are of the lowest luminosity classes of the Sc galaxies in the RSA. This panel completes the formal Sc illustrations. Special attributes of the Sc class follow, on panels 276-293.

NGC 3445      Sc(s)III      triplet  
PH-8048-S  
Feb 4/3, 1981  
103aO  
12 min

NGC 3445 forms a triplet with NGC 3440 (possible Sbc merger in progress; not in the RSA) at a separation of 9.9', and NGC 3458 (SBO, panel 54) at a separation of 14.0'. The redshifts are  $L_o(3440) = 2021 \text{ km s}^{-1}$ ,  $u_o(3445) = 2083 \text{ km s}^{-1}$ , and  $f_o(3458) = 1899 \text{ km s}^{-1}$ . At the mean redshift distance of 40 Mpc ( $H = 50$ ) the projected linear separations of NGC 3440 and NGC 3458 from NGC 3445 are 115 kpc and 163 kpc, respectively.

The importance of the triplet is that the morphological types for two of the companions are so very different (Sc and SBO). The case is similar to that of NGC 5480/5481 on the preceding panel.

The face of NGC 3445 is covered with a thick spiral pattern within which numerous HII-region candidates exist. At the end of the single principal arm is a shred that may be a separate galaxy (or was at one time). The angular separation of the shred from the center of NGC 3445 is 1.2', which is a projected linear separation of only 14 kpc. This close pair is number 256 in Karachentsev's catalog of pairs. He lists the redshifts of  $i'_o(3445) = 2058 \text{ km s}^{-1}$  and  $v_o = 2004 \text{ km s}^{-1}$  for the shred which he classifies as type Sm.

NGC 2537      ScIII pec  
H-2254-H  
May 3/4, 1946  
103aO  
40 miii

The strange morphology of NGC 2537 may be due to an encounter in progress. Both galaxies are visible, one near the center of the arch; the other is the arch itself.

Both segments are filled with bright HII regions, the largest having a halo diameter of about 8" though it may be a complex of several overlapping separate regions. The redshift is small at  $v_o = 513 \text{ km s}^{-1}$ , consistent with the good resolution into disks of the **largest** HII regions.

NGC 4625      Sc(s)H-III pec      Karachentsev 349  
PH-7666-S  
April 29/30, 1979  
103aO  
6 min

NGC 4625 is not in the RSA but is a companion to NGC 4618 (SBbc; panel 212), which is in that catalog. The pair have closely the same redshifts, at  $u_o(4618) = 563 \text{ km s}^{-1}$  and  $u_o(4625) = 640 \text{ km s}^{-1}$ . The angular separation of 8.5' at a redshift distance of 12 Mpc ( $H = 50$ ) gives the small projected linear separation of 30 kpc. The pair<sup>1</sup> is number 349 in Karachentsev's catalog of close pairs.

The morphology of both NGC 4618 (panel 212) and NGC 4625, here, is peculiar. Both galaxies have a single dominant arm, as if pulled out by a tidal encounter. The resolution into stars and HII regions is at the same level in both galaxies. The high degree of resolution is consistent with the low mean redshift of  $\langle v_o \rangle = 602 \text{ km s}^{-1}$  for the pair.

NGC 4630      Sc(s)III      VCC 1923  
CD-2166-S  
March 27/28, 1982  
103aO  
50 min

NGC 4630 is in the extreme southeastern corner of the survey area of the Virgo Cluster Catalog (Binggeli, Sandage, and Tammann 1985). No decision was made in that catalog as to cluster membership.

HII-region candidates are evidently present. The redshift of NGC 4630 is  $v_{\lambda} = 533 \text{ km s}^{-1}$ .

NGC 4540      Sc(s)HI-IV      VCC 1588  
CD-2130-S  
March 21/22, 1982  
103aO  
50 min

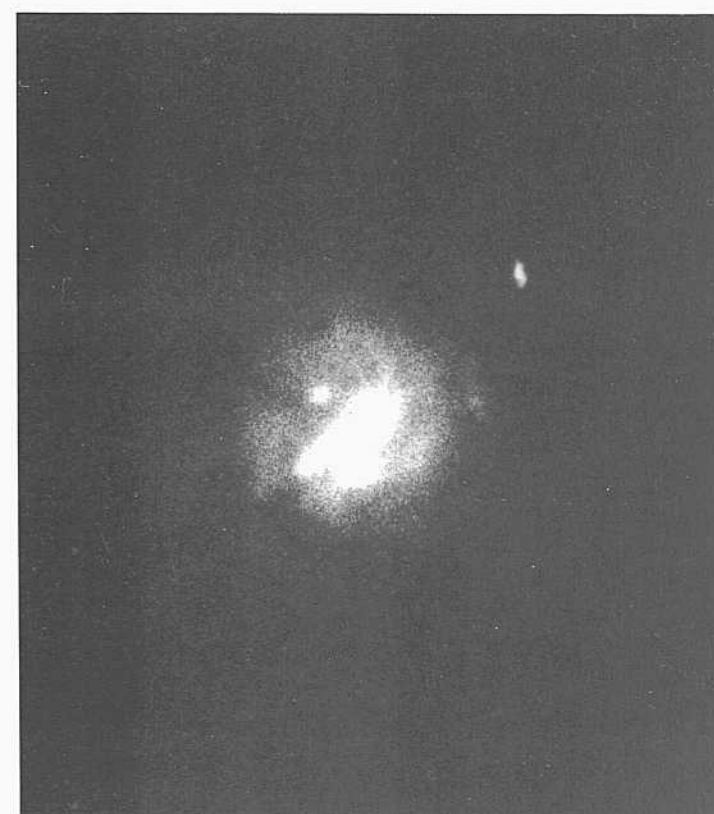
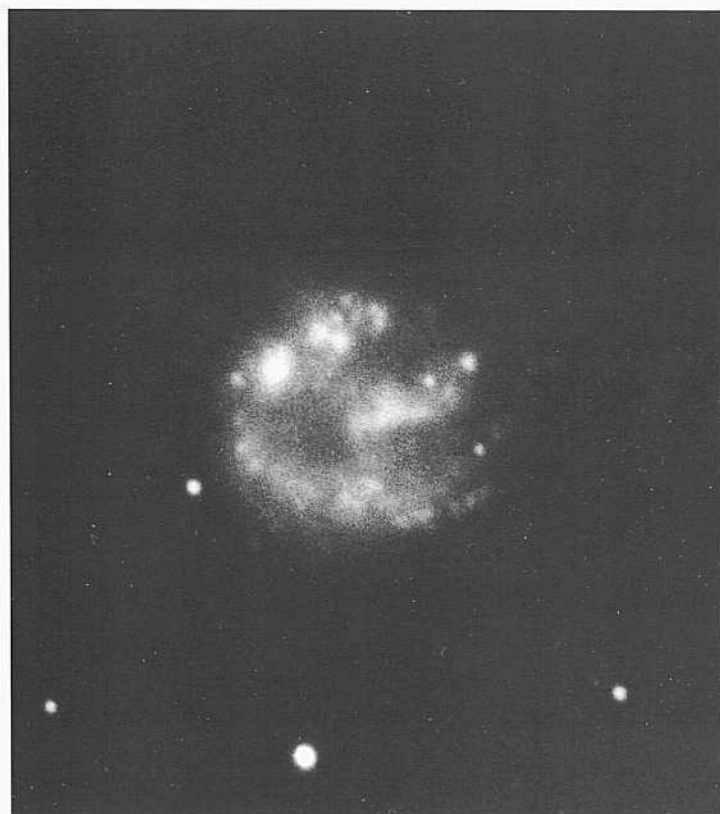
NGC 4540 is about 3.5° northeast of the center of Virgo subcluster A associated with NGC 4486. It is listed as a cluster member in the Virgo Cluster Catalog (Binggeli, Sandage, and Tammann 1985).

NGC 4369      Sc(s)III-IV  
H-2508-H  
March 5/6, 1948  
103aO  
30 min

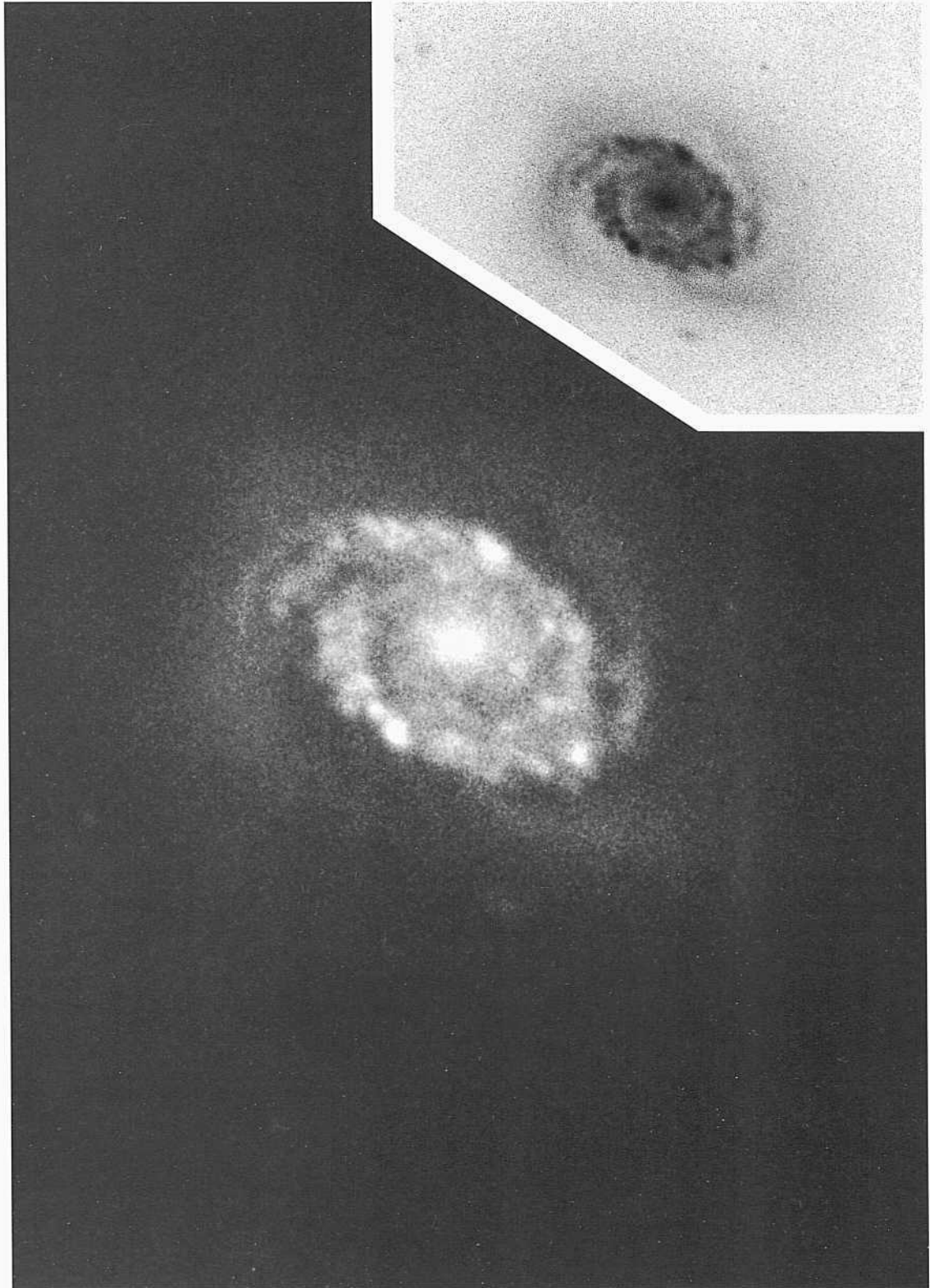
The spiral pattern in NGC 4369 is not well traced in the high-surface-brightness central region of this small, almost irregular spiral. The redshift of NGC 4369 is  $v_{\lambda} = 1069 \text{ km s}^{-1}$ .




PANEL  
275



PANEL  
276



 The two galaxies on this panel are peculiar enough to be outside the classification system. They are placed in the Se section here because of the late stellar content and small nuclear region of both.

NGC 3187            Sc/SBc            quartet  
PH-149-MH  
April 12/13, 1950  
103aO  
30 niin

NGC 3187 (not in the RSA) is a member of the famous quartet whose other members are NGC 3185 (SBa; panel 99;  $v_o = 1151 \text{ km s}^{-1}$ ), NGC 3190 (Sa; panel 76;  $v_o = 1384 \text{ km s}^{-1}$ ), and NGC 3193 (E2; panel 5;  $v_o = 1307 \text{ km s}^{-1}$ ).

NGC 3187 is highly distorted, having two long plumes which are drawn out from the lenticular central region. The closest member of the quartet to NGC 3187 is NGC 3190, which is also distorted, having a tilted fundamental plane in its outer regions. The circumstantial evidence suggests that a close encounter occurred involving NGC 3187 and NGC 3190; the present angular separation of the two is  $4.8'$ . At the mean redshift distance of 27 Mpc ( $H = 50$ ) corresponding to  $\langle u_o \rangle = 1336 \text{ km s}^{-1}$ , the projected linear separation of the pair is small at 38 kpc.

HII-region candidates exist both in the central bar and in each plume. They are unresolved at the  $1''$  level.

NGC 4580            Sc(s)/Sa            HA, p. 21  
CD-2187-S            VCC 1730  
March 29/30, 1982            panel 86  
103aO  
50 niin

NGC 4580 has also been described and illustrated in the Sa section on panel 86. The smooth outer arms are similar to non-star-producing arms in the early section of the Sa types. The small nucleus, the lack of a central bulge, and the obvious HII regions in the inner ring, which is nearly complete, have the character of the content of Sc galaxies.

NGC 4580 is one of the few galaxies in the RSA having these mixed characteristics. The unusual classification assigned here is to identify the combination.



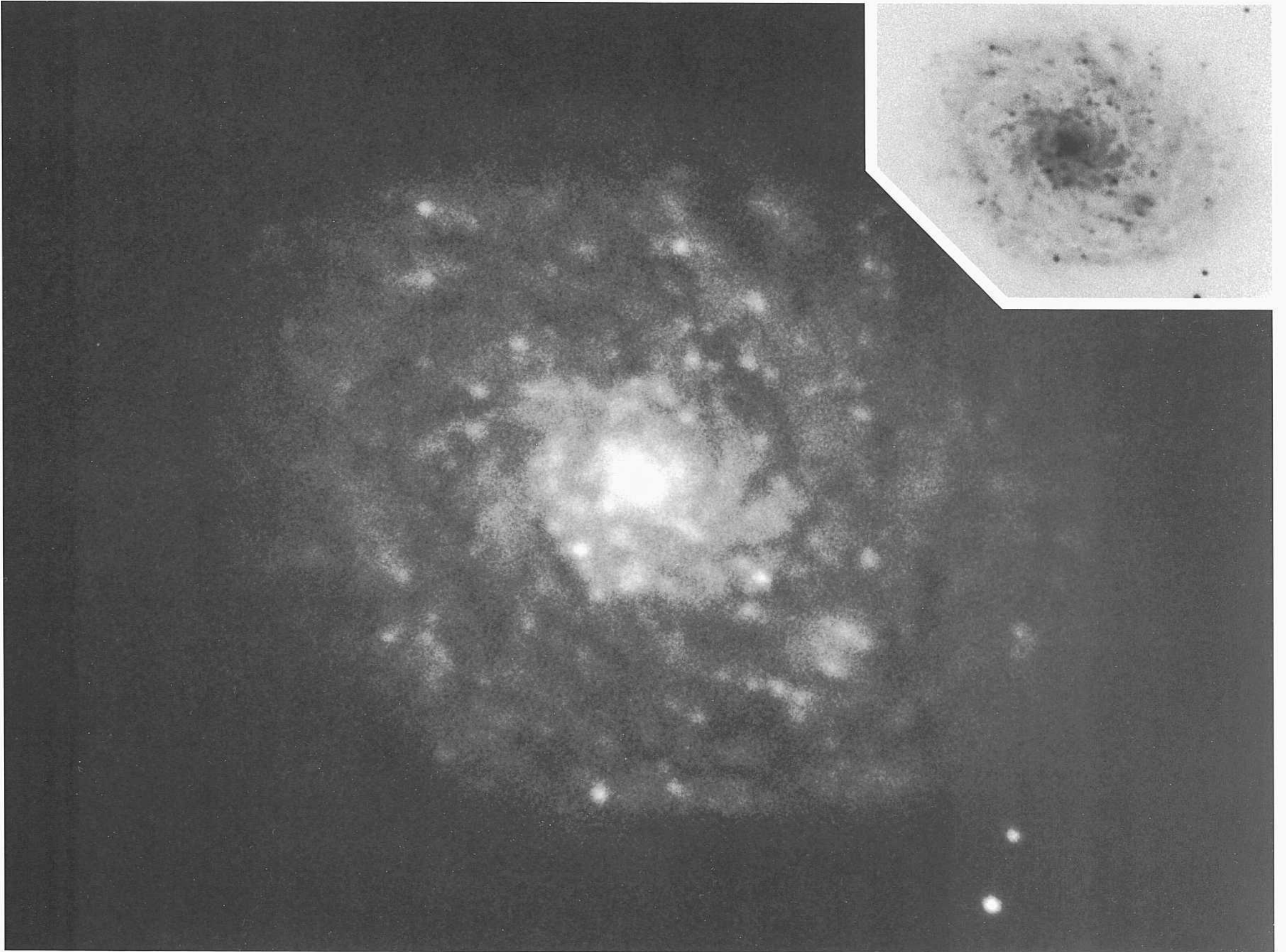
**T**he nine galaxies on the next three panels have Sc multiple-arm spiral patterns that are similar to but later in stellar content than that of NGC 488 (Sab; panels 115, 116, S3, S12), the prototype example of the form. The galaxies are arranged on these panels to show the development of the form along the classification sequence. A similar summary of the development of the NGC 488 type along the sequence is shown in the Summary, panels S12 and S13, but with less morphological resolution than is given in the next three panels.

NGC 4689-S      Sc(s)IL3      VCC 2058  
CD-2138-S  
March 22/23, 1982  
103aO  
50 miii

NGC 4689 is in the extreme northeastern corner of the survey area for the Virgo Cluster Catalog (**Binggeli**, Santiago, and Tammann 1985). It is listed as a cluster member, at redshift  $z = 0.034$ . It is listed as a cluster member, at redshift  $v_0 = 1508 \text{ km s}^{-1}$ . A **photograph** printed to a common angular scale with other members is given in the photographic atlas of the Virgo Cluster (Sandage, Binggeli, and Tammann 1985a, panel 6) showing that NGC 4689 is among the **largest** of the Sell-luminosity-class galaxies in the cluster.

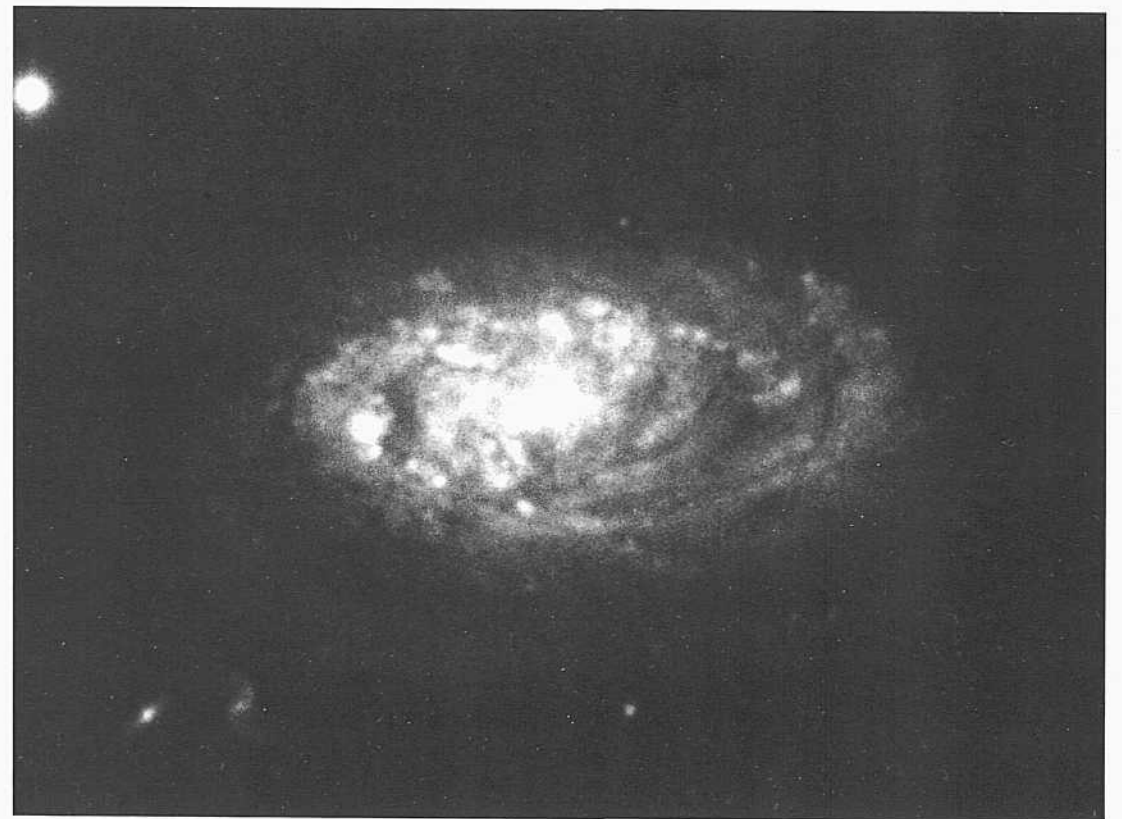
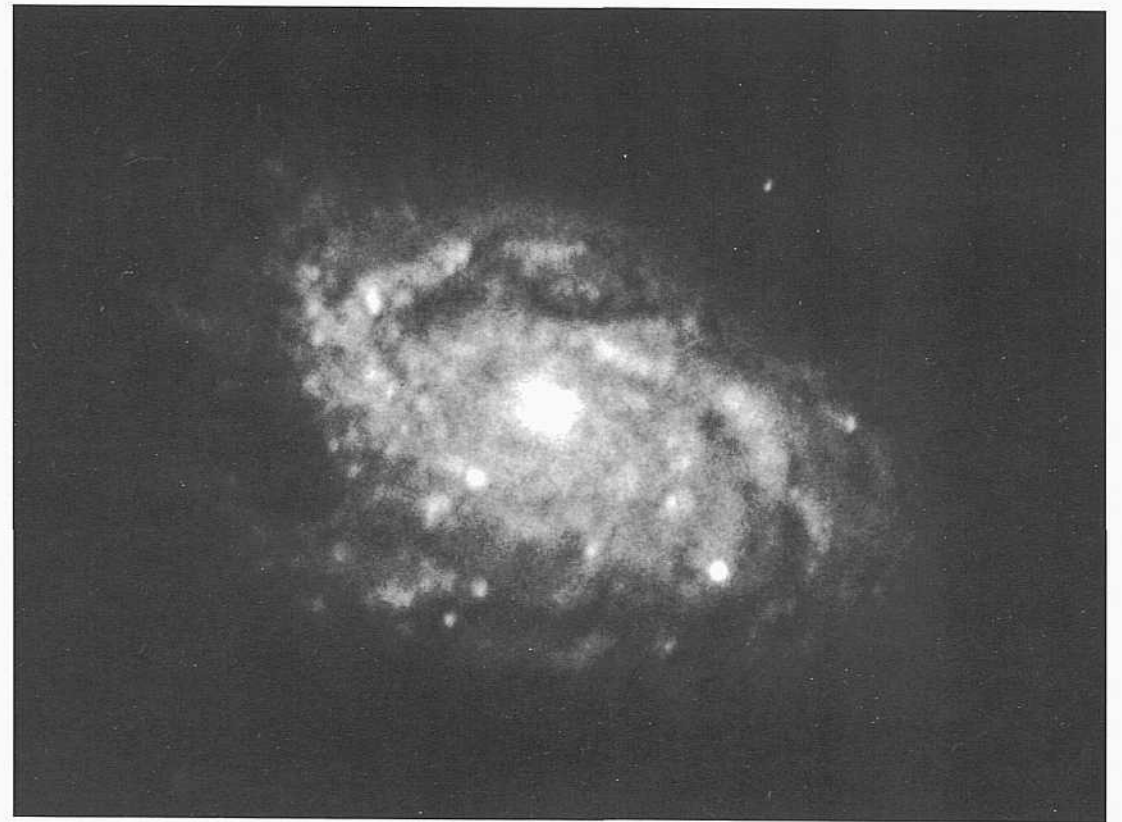
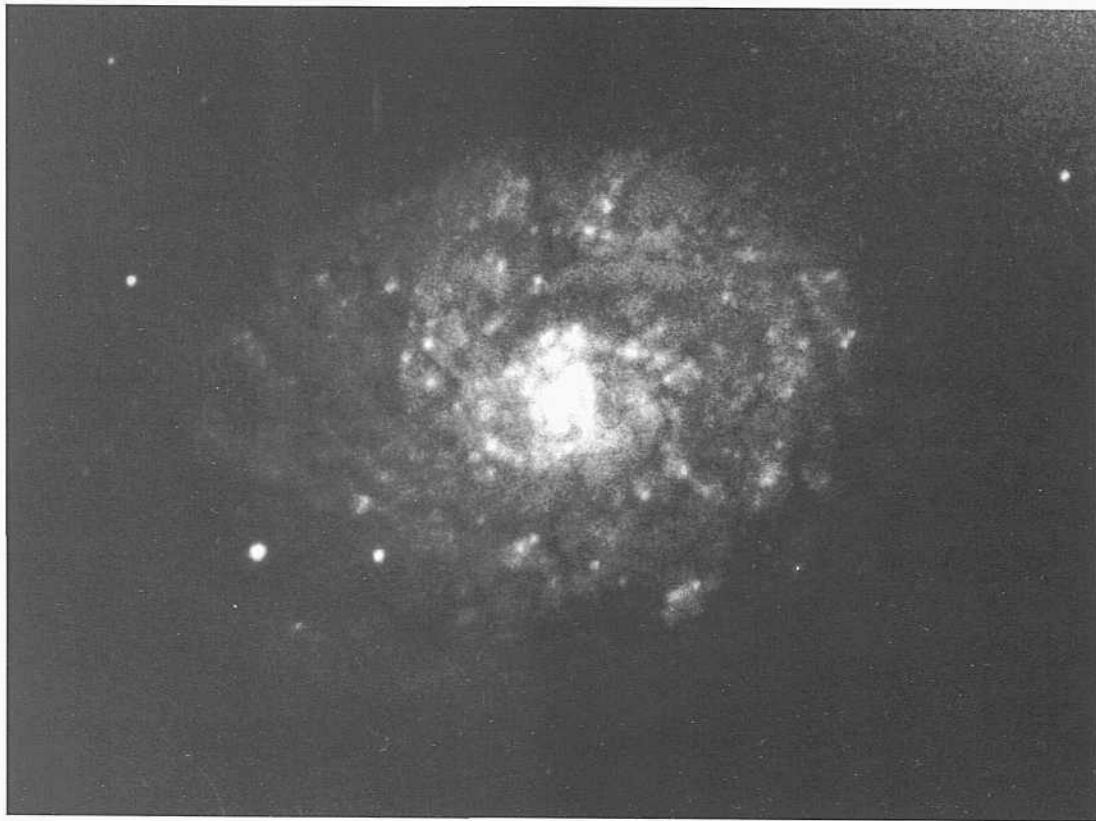
The HH-region candidates in many of the arm fragments are unresolved at the 1.5" level on the available plate material.

Upon inspecting this image on this plate, one viewer commented, "When man creates a sharper telescope, God will create a fuzzier object."



PANEL  
277

PANEL  
278



*Sc Classification Section (continued)*

NGC 4647      Sc(rs)III      pair  
 CD-802-S      VCC 1972  
 Feb 24/25, 1979      panels 51, S14  
 103aO + Wr2c  
 45 min

NGC 4647 with  $v_0 = 1331 \text{ km s}^{-1}$  forms a close (physical?) pair with NGC 4649 (M60; SO;; panel 51;  $v_0 = 1142 \text{ km s}^{-1}$ ). The pair is shown in panel 10 of the Virgo Cluster photographic atlas of spirals (Sandage, Binggeli, and Tammann 1985a). The angular separation of the pair is 2.8', which corresponds to a small projected linear separation of 18 kpc at a distance of 21.8 Mpc if the galaxies are physically associated.

Numerous EQI-region candidates exist in some of the arm fragments. The largest resolve into disks at about the 1.5" level.

NGC 7314      Sc(s)HI      HA, p. 30  
 CD-1574-S/Br  
 Aug 10/11, 1980  
 103aO + GG385  
 45 min

The small nucleus, the absence of a central bulge, and the evident presence of HII regions in some of the multiple arm fragments are the classification characteristics of the Sc morphology.

The redshift is  $v_R = 1491 \text{ km s}^{-1}$ .

NGC 4212      S<(s)II-III      VCC 157  
 CD-793-S  
 Feb 23/24, 1979  
 103aO + Wr2c  
 55 min

NGC 4212 is located in the northwestern corner of the Virgo Cluster survey area, about 4° from the center of Virgo subcluster A associated with NGC 4486. It is listed as a member in the Virgo Cluster Catalog and is illustrated in a common scale with other cluster members in the Virgo Cluster atlas of spirals (Sandage, Binggeli, and Tammann 1985a, panel 1).

NGC 5678      Sc(s)II-III  
 PH-7647-S  
 April 28/29, 1979  
 103aO  
 12 min

The numerous Mil regions in the multiple arms are unresolved at the 1" level. Hic redshift of NGC 5678 is  $v_0 = 2446 \text{ km s}^{-1}$ .

*Sc Classification Section (continued)*

NGC 5949                      Sc

**PH-58-H**

**April 27/28, 1949**

103aO

**30 min**

The arm pattern in NGC 5949, composed as in NGC 488 of **multiple** fragments hut later in the classification sequence, begins at a poinllikc nucleus. There is no **centra]** bulge or evidence of a halo.

The **redshift** is small,  $v_p = 624 \text{ km s}^{-1}$ , yet the few HII-region candidates are unresolved. And there is no sign of resolution into individual stars, as would be expected at such a small redshift by comparison with galaxies of similar redshift such as NGC 5194 (M5 1; panels 172, 177) at  $v_n = 541 \text{ km s}^{-1}$ .

NGC 4298                      Sc(s)III                      VCC 483

CD-1399-S/Br    pair

**March 22/23, 1980**    panel 289

103aO

75 niin

NGC 4298 forms an apparent pair with NGC 4302 (**Sc** on edge; panel 289) at a separation of 2.4'. The redshifts listed in the RSA are identical at  $v_o = 1004 \text{ km s}^{-1}$ . However, as the pair is in the Virgo Cluster, the similarity of redshifts does not assure a dynamical relation because of the large virial velocities of parts of the cluster complex. If the pair is at the same distance of 21.9 Mpc ( $m - M = 31.7$ ), their **projected** linear separation is small at 1.5 kpc.

As in NGC 5949 above, and NGC 7314 on the preceding panel, the nucleus of NGC 4298 is pointlike. There is no central bulge or evidence of a halo.

NGC 2397                      **Sc(s)IH**

**CD-159-S**

**Feb 4/5, 1978**

**103aO** + GG385

**45 min**

The spiral pattern in NGC 2397 is similar to that in NGC 5949 and NGC 4298, also on this panel.

The redshift of NGC 2397 is  $v_o = 1044 \text{ km s}^{-1}$ .

Several candidates for Im dwarf companions exist within  $0.5^\circ$  of NGC 2397.

**NGC 1087                      Sc(s)III.3                      HA, p. 35**

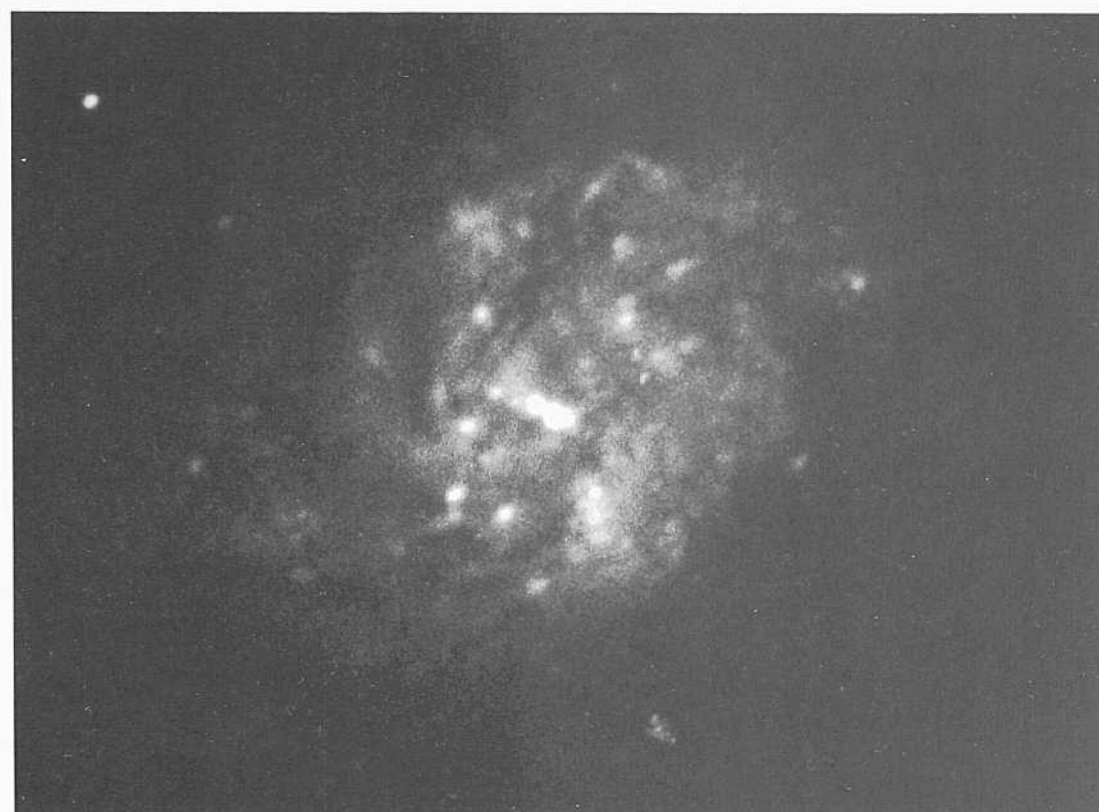
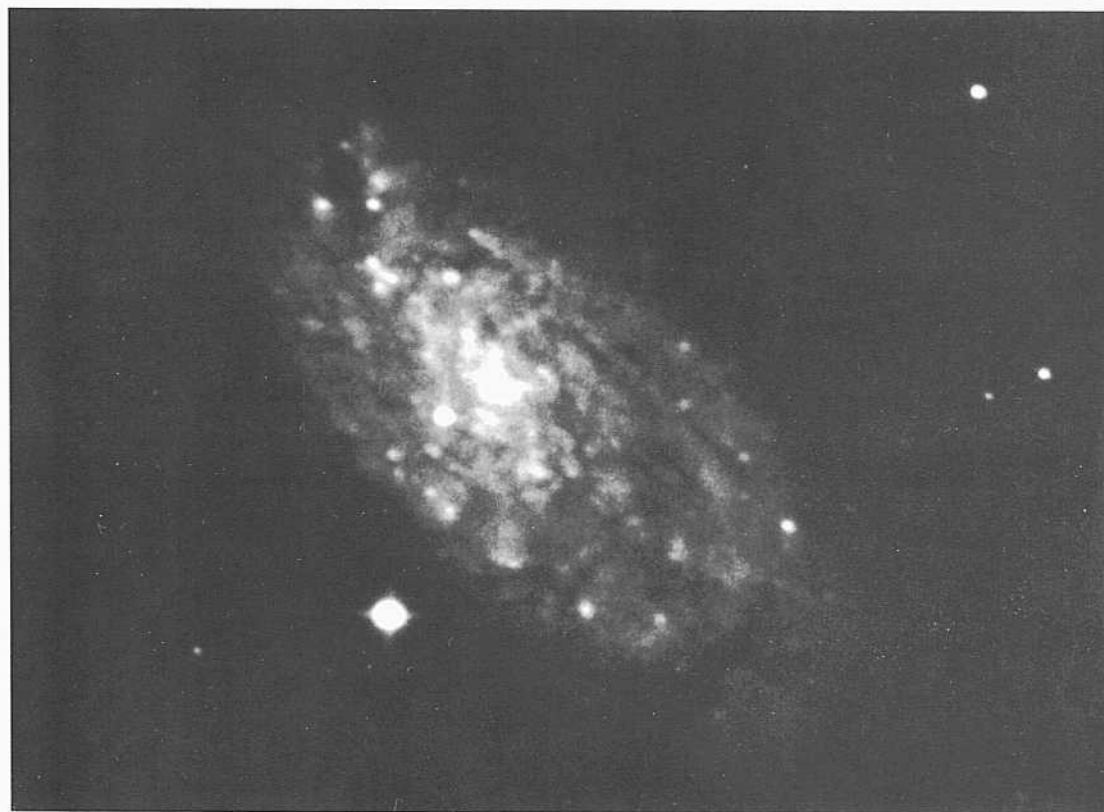
**H-2337-H**

**Nov 27/28, 1946**

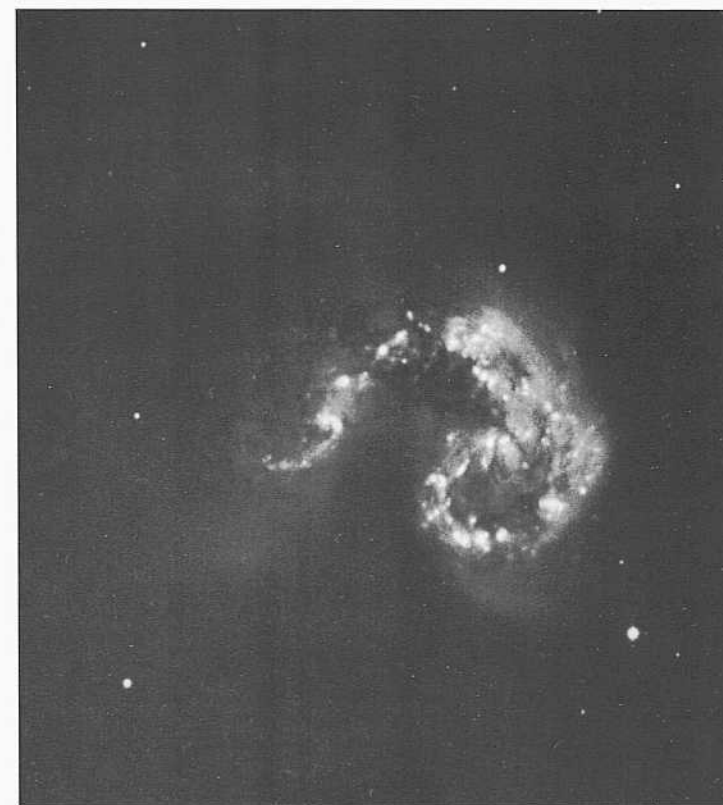
103aO

**10 min**

HII-region candidates exist within the disordered spiral pattern of the multiple-armed type. The redshift of NGC 1087 is  $v_n = 162.8 \text{ km s}^{-1}$ .



PANEL  
280



The next five panels show Sc galaxies that are in pairs and in some cases in close encounters. The illustrations here for Sc types are similar to the illustrations of such pairs and/or encounters in earlier sections describing galaxies of type K (panels 21-23), SO (panels 51, 52), Sa (panels 81-86), SBa (panel 105), SB (panel 153), Sbc (panel 198), and SBbc (panel 212).

NGC 1038/1039 Sc(tides) group  
 CD-1679-S Sc(tides)  
 Jan 1/2, 1981  
 103aO  
 60 min

This well-known interacting pair with its tidal plumes was simulated in the famous N-body calculation by Toomre and Toomre (1972). They gave the first convincing proof that such morphological features as tails are due in tidal interactions in a close encounter.

This interacting pair is in a loose group of five other RSA galaxies and several fainter non-Dreyer galaxies that may be kinematically associated. The five bright group members with their redshifts and separations from NGC 4038/4039 are NGC 3957 (SO; panel 44:  $v_o = 1583 \text{ km a}^{-1}$ ; separation  $2.1^\circ$ ), NGC 3981 [Sbc-II (tides?); panel 178;  $v_o = 1554 \text{ km s}^{-1}$ ; separation  $1.7^\circ$ ], NGC 4024 (SO; panel 31;  $v_o = 1444 \text{ km s}^{-1}$ ; separation  $58'$ ), NGC 4027 (Scl.2; panel 252;  $v_o = 1419 \text{ km s}^{-1}$ ; separation  $41'$ ), and NGC 4033 (SO; panel 35;  $v_o = 1273 \text{ km s}^{-1}$ ; separation  $65'$ ). The redshift of NGC 4038 is  $v_o = 1391 \text{ km a}^{-1}$ .

The mean redshift of the six galaxies is  $\langle v_o \rangle = 1444 \text{ km s}^{-1}$ . At the redshift distance of 29 Mpc ( $\mu = 50$ ) a separation of  $1^\circ$  corresponds to a projected linear separation of 506 kpc. Hence all projected distances of the five listed galaxies from NGC 4038/4039 are less than about 1 Mpc. The group is similar in size to the Local Group and may be a good model.

The three prints on the facing page have all been made from the same original photograph taken at Las Campanas with the 100-inch reflector. Robust recent star formation is evident in the central regions of the apparently merging configuration.



*Sc Classification Section (continued)*

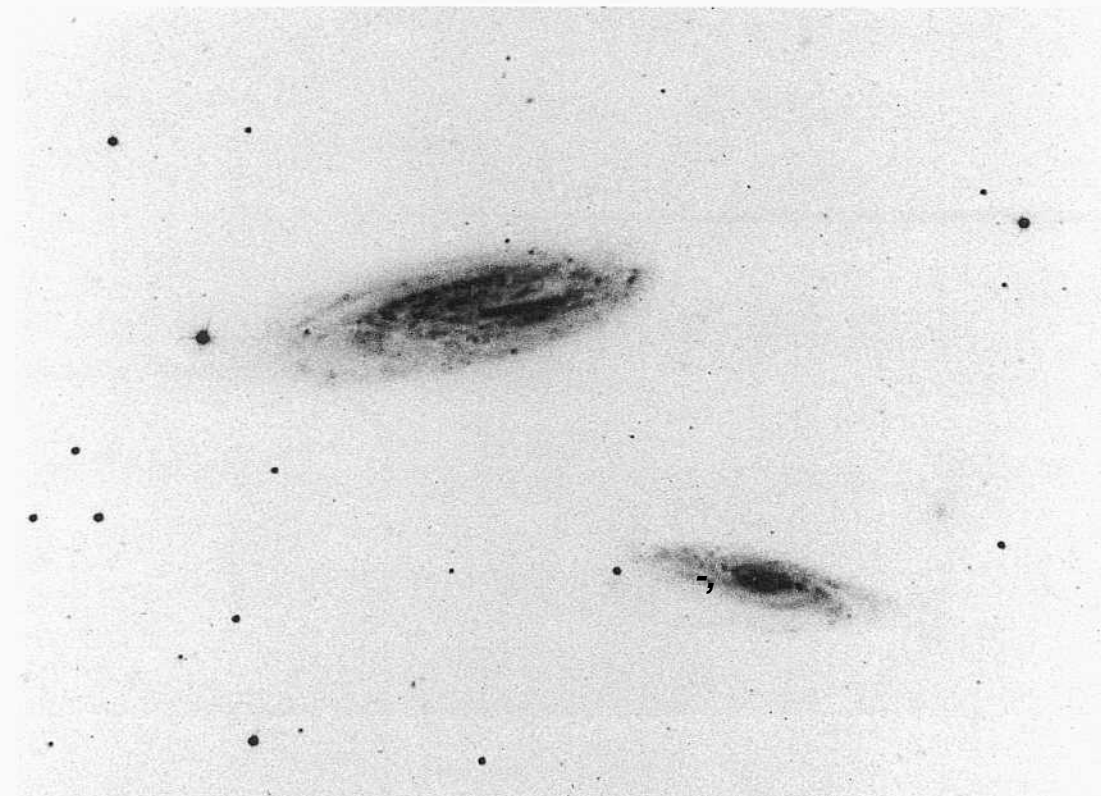
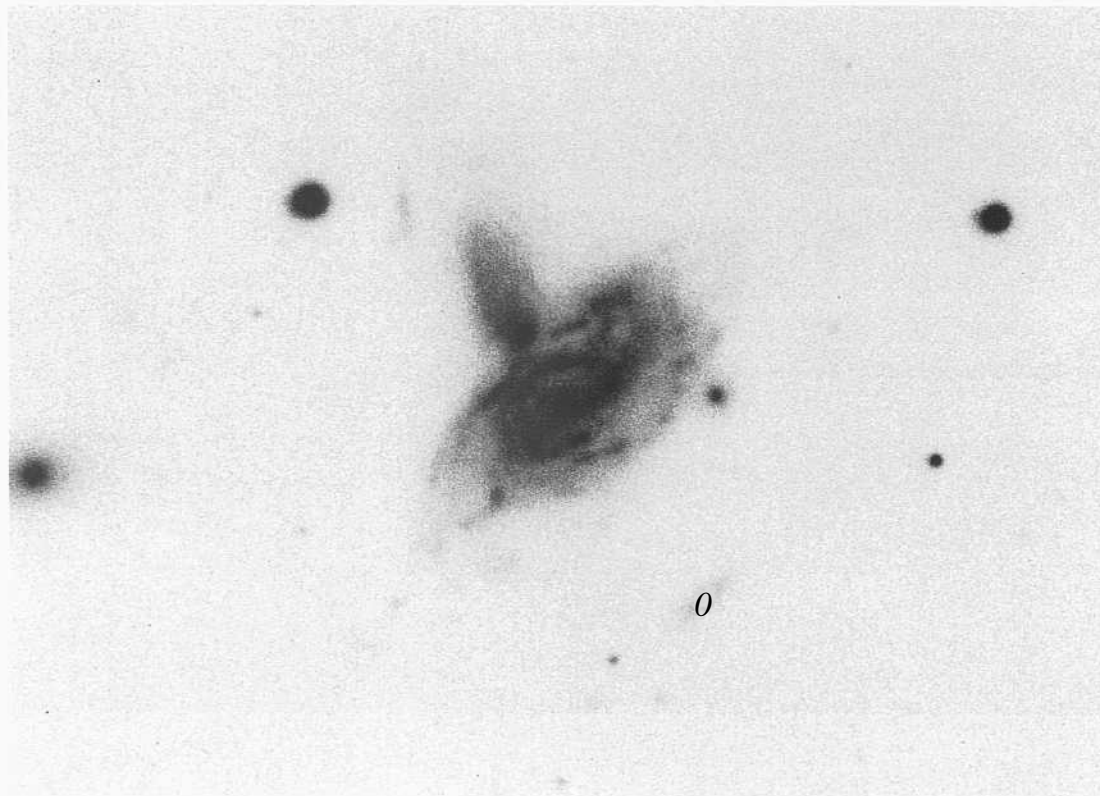
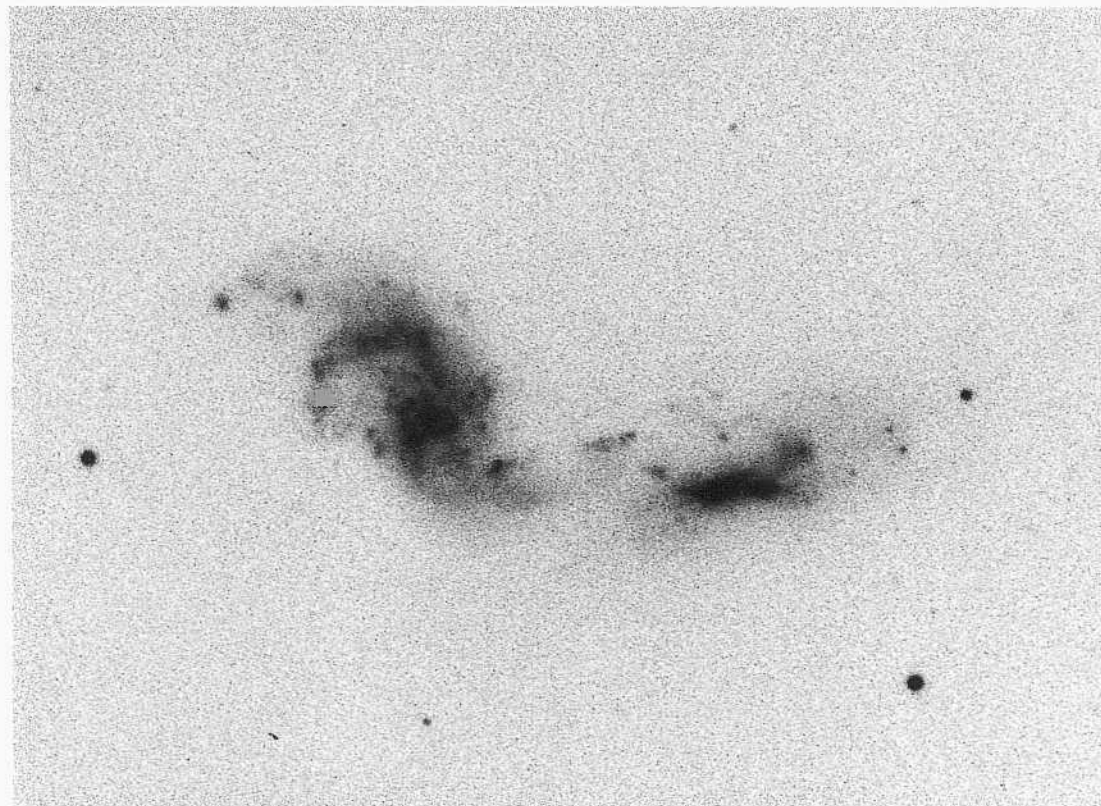
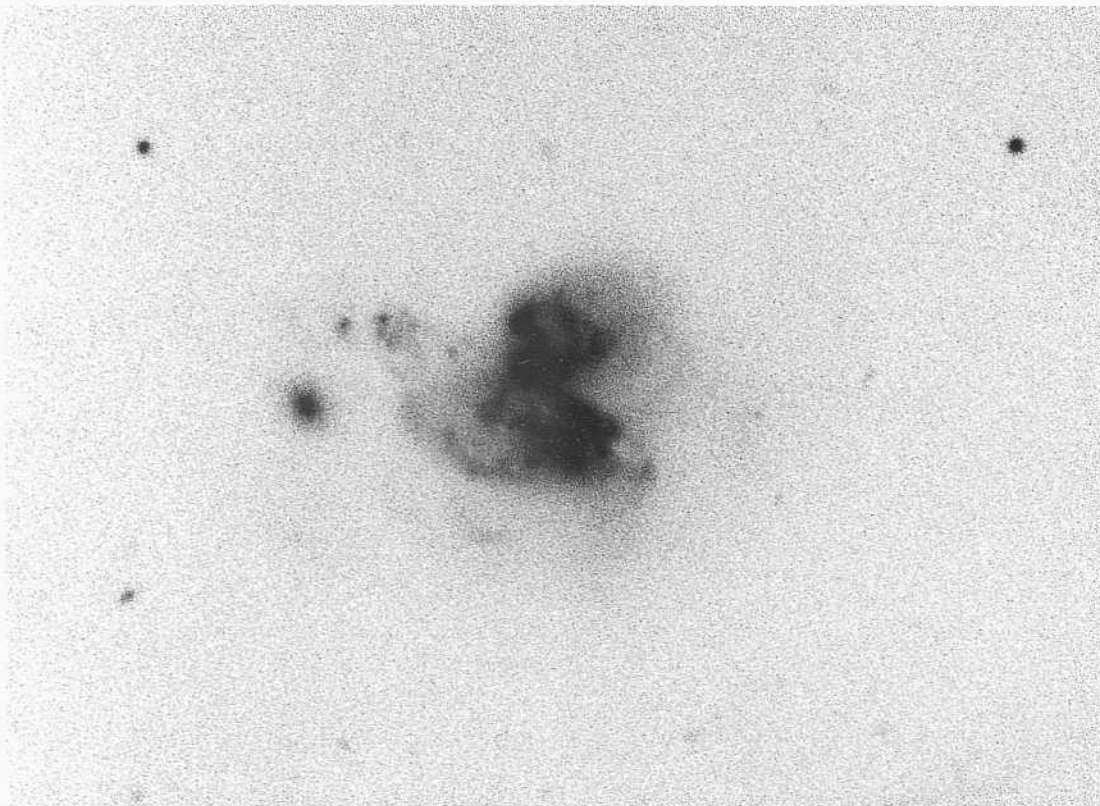
NGC 4567/4568 Sc(s)II-III VCC 1673  
CD-733-S Sc(s)H-III VCC 1676  
Feb 2/3, 1979 W 219  
103aO + Wr2c Karachentsev 347  
45 mill

The redshifts of the components of this pair are  $u_o(4567) = 2136 \text{ km s}^{-1}$  and  $v_o(4568) = 2199 \text{ km s}^{-1}$ . The separation of centers is  $1.3'$ . If the pair is in the Virgo Cluster at a distance of 21.9 Mpc, the projected linear separation is small at 8 kpc.

A most interesting aspect of the combined morphology is the lack of evidence for tidal distortion in either member of the pair. Each galaxy has the morphology of a normal Sc galaxy of intermediate luminosity class. Each has a small nucleus and well-developed multiple spiral arm fragments of the NGC 488 type. Either the separation is large in the line of sight or the orbital circumstances of the encounter are unfavorable for tidal plumes (orbital angular momentum could be opposite to the direction of the individual spin angular momenta).



PANEL  
282



Sc Classification Section (continued)

NGC 3690 Sc(tides) Karaehcilsev 288  
 PII-8058-S  
 Feb4/5, 1981  
 103aO  
 12min

A close encounter is clearly in progress in this close pair whose separation of centers is 26". Karachentsev lists the individual  $v_0$  redshifts as 3156 km s<sup>-1</sup> and 3196 km s<sup>-1</sup>. At the redshift distance of 64 Mpc ( $H = 50$ ) the projected linear separation is 8 kpc. A possible third E companion exists at a separation of 66", but it may be in the background.

The morphology of each companion is highly disturbed. Faint outer plumes are associated with each galaxy.

NGC 7119 Sc(s)II pair?  
 CD-1121-Br  
 Aug 20/21, 1979  
 103aO + GG385  
 4.5 min

NGC 7119 and its possible companion, with a separation of only 2.1", may be a chance superposition in the line of sight. Other galaxies of the same small angular diameter as the companion exist in the surrounding field as if there is a background group.

There is no distortion of the morphology of either member of the pair, again suggesting a chance alignment.

The redshift listed in the RSA2,  $v_0 = 9825$  km s<sup>-1</sup>, is suspect because of its very high value for RSA galaxies. It is based on a single measurement quoted in a private communication. The kinematics of the system are clearly of interest. There is, of course, the possibility that the high redshift applies to the small companion and that the redshift of NGC 7119 itself is unknown (e. 1990).

NGC 3395/3396 Sc(s)II-III Karachentsev 219  
 PH-7995-S Sc(tid.-s)  
 Feb2/3, 1981  
 103aO  
 12min

Clearly a close encounter is in progress. The redshifts listed in the HSA2 are  $u_0(3395) = 1599$  km s<sup>-1</sup> and  $u_0(3396) = 1619$  km s<sup>-1</sup>. The angular separation of 68" corresponds to a projected linear separation of 10 kpc at the redshift distance of 32 Mpc ( $H = 50$ ).

The pair is apparently connected by a faint (tidal?) plume. The fainter of the pair appears to be partially disrupted. Robust star formation may be occurring in the center of the fainter member.

NGC 7541/7537 Sc(s)II Karachentsev 578  
 H-915-Dimcan Sc(s) panel 255  
 Sep 2/3, 1945  
 103aO  
 60 mill

NGC 7541, shown on panel 255, is the brighter member of a physical pair with NGC 7537. The redshifts listed by Karachentsev are  $u_0(7537) = 2834$  km s<sup>-1</sup> and  $u_0(7541) = 2793$  km s<sup>-1</sup>. The angular separation of 2.7' corresponds to a projected linear separation of 44 kpc at the redshift distance of 56 Mpc ( $H = 50$ ). The spiral pattern of neither member of the pair shows evidence of an encounter.

Two Im candidates for dwarf companions to the pair exist within 11' of NGC 7541. They have HII-region candidates at the same brightness as the HII knots in the two main Sc galaxies and are therefore very likely at the same distance. Three candidates for dK dwarf companions also exist in the immediate field.

*Sc Classification Section (continued)*

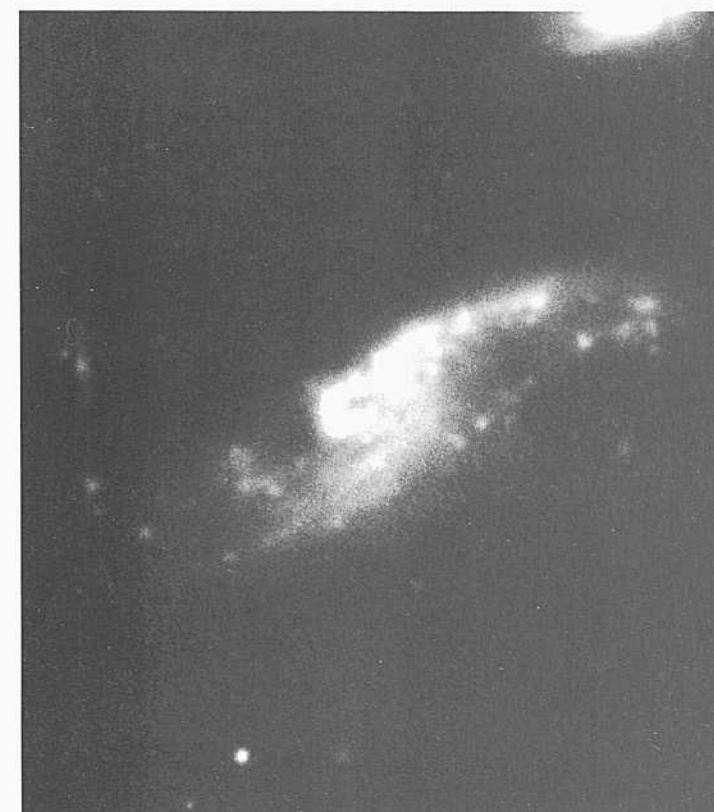
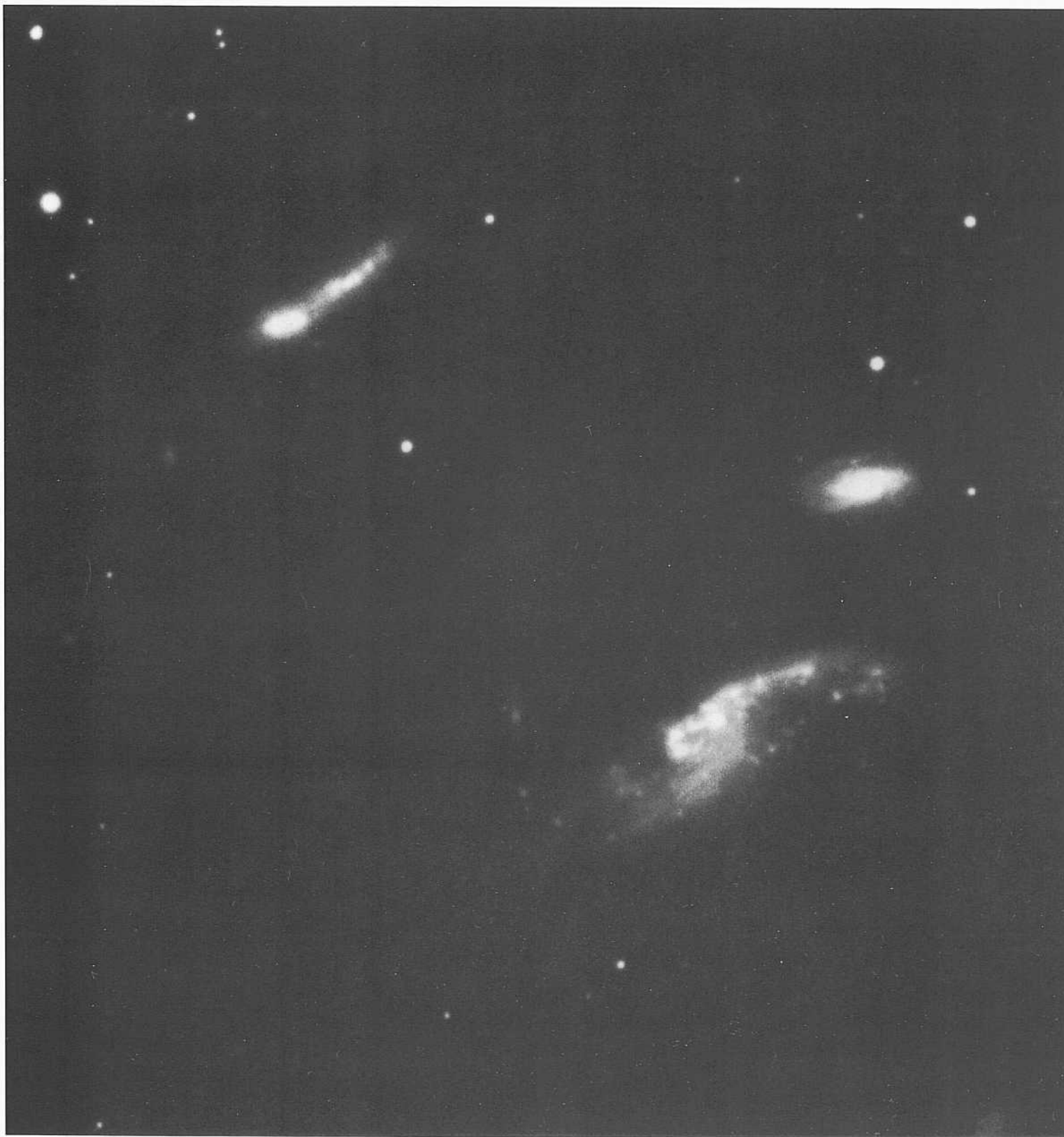
NGC 3995/3991/3994      Karachentsev 311  
PH-8054-S      Sc(tides)      Racine wedge  
Feb 4/5, 1981      Pec(tides)      Arp 313  
103aO      Sbc or Sc  
12 inin

NGC 3995 is the brightest galaxy of a multiple interacting group whose next-brightest members are NGC 3994 (She: it is the closest galaxy to NGC 3995) and NGC 3991. The morphology of NGC 3991 is dominated by a thin tidal plume in which very bright HH-region candidates are present. Karachentsev lists redshifts of  $r_{c}(3394) = 3086 \text{ km s}^{-1}$  and  $u_{c}(3395) = 3232 \text{ km s}^{-1}$ . The redshift listed for NGC 3991 by Palumbo *et al.* (1983) is  $3256 \text{ km s}^{-1}$ . From these three redshift values, the mean redshift distance of the group is 64 Mpc ( $H = 50$ ).

The angular separations of NGC 3994 and NGC 3991 from NGC 3995 are 1.9' and 3.7', respectively. The corresponding projected linear separations are 35 kpc and 68 kpc.

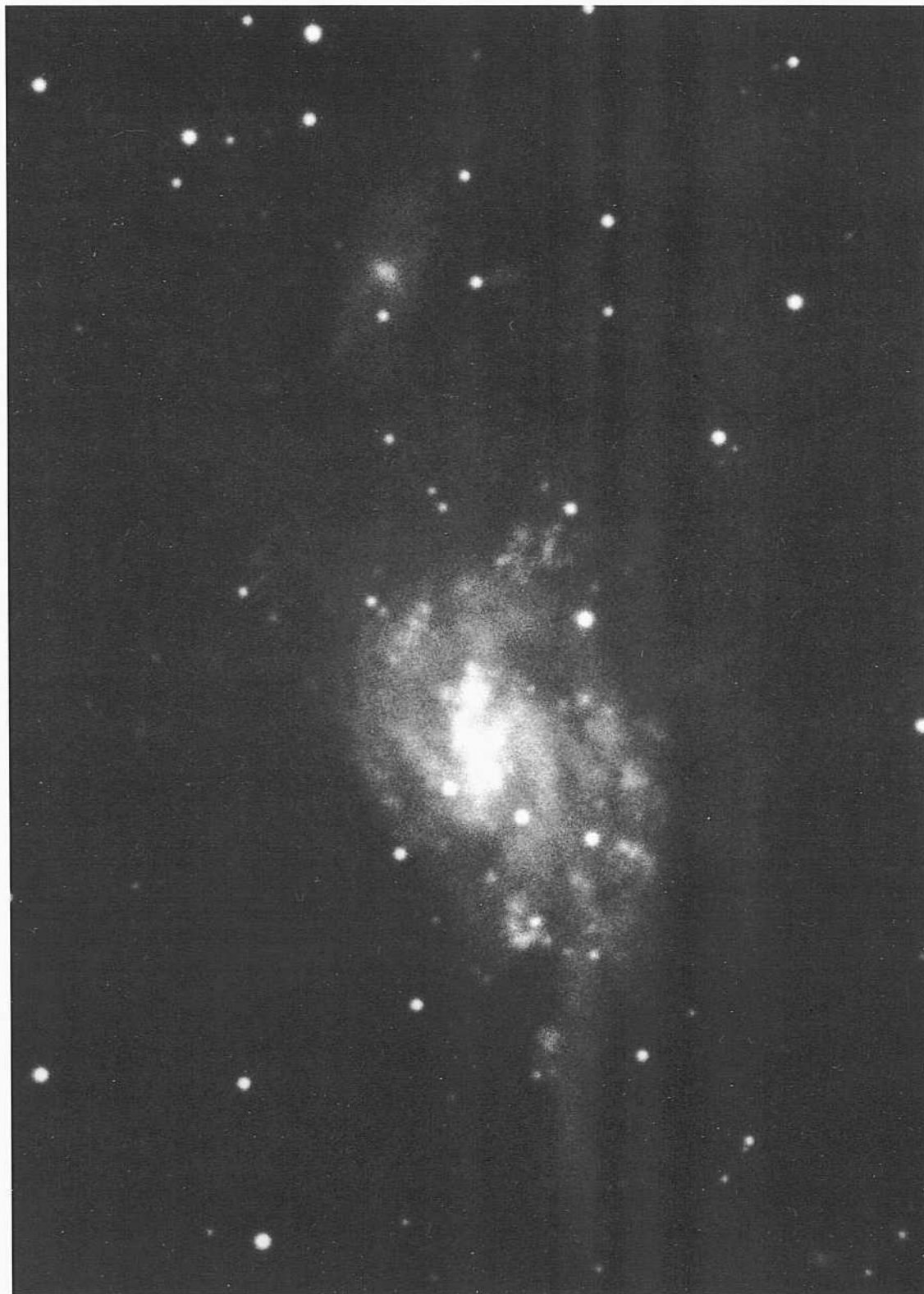
The morphology of NGC 3994 (the fainter of the close pair) is normal for a late-type Sbc or Sc. There is no evidence of tidal distortion despite its apparent closeness to NGC 3995. However, tidal disruption is clearly evident in NGC 3991, the more distant in projection of the triplet.

The two main prints of NGC 3995 (the brightest galaxy of the group) also show evidence of morphological distortion. It would seem that the interaction has been between NGC 3995 and NGC 3991, not involving NGC 3994.



PANEL  
283

PANEL  
284



*Sc Classification Section (continued)*

IC 1837/1839      S<(s)II-III  
CD-537-S          **Sab(a)1.2**  
Oc11/2, 1978  
103aO + GG385  
45 mill

The pair has an angular separation of 3.4'. Only IC 4837 (the late-type Sc) is in the Shapley-Ames, although IC 3839 (the more regular Sab) is nearly as bright. No redshift is known for IC 4839 (e. 1990). The redshift for IC 4837 is  $v_D = 2575 \text{ km s}^{-1}$ , as listed in the RSA2. [If IC 4839 is at the same redshift distance of 52 Mpc, the projected linear separation of the pair is 55 kpc.

The spiral morphology of IC 4837 (shown alone at the right) is too normal to provide evidence of tidal interaction. The extension of the outer arm on one side of the pattern, although asymmetric, is not unusual even in isolated galaxies.



**G**alaxies on this and the next six panels are Sc types that are either highly inclined or are nearly edge on. They are grouped together at the end of the Sc section to illustrate the smallness of the nuclear region, the absence of a central bulge, and the absence of an appreciable luminous halo. These characteristics separate the Sc class from the Sb types. The three criteria are best seen in galaxies that are nearly edge on.

NGC 247      Sc(s)III-IV      South Polar Gr  
 CD-512-S  
 Sep 28/29, 1978  
 103aO + GG385  
 45 min

NGC 247 is a highly resolved nearby galaxy in the South Polar Group (de Vaucouleurs 1959a). Among members of the group are NGC 55, NGC 247, NGC 253, NGC 300, and NGC 7793. all in the RSA and all shown in this atlas.

The stellar content of NGC 247 is easily resolved into individual stars, star clusters, associations, and a few small HII regions. The resolution begins at about  $B = 17$  for the blue supergiants. The distance modulus must be nearly the same as that of NGC 300 (panels 261, S6) at  $m - M = 26.5$  from Cepheids (Graham 1984). Hence the brightest blue supergiants have absolute magnitudes of about  $M_g = -9.5$ , consistent with the calibration given elsewhere (Sandage and Carlson 1988). The redshift is small at  $v_0 = 227 \text{ km s}^{-1}$ , consistent with the small distance modulus.

The type is very late Sc. Note the small nucleus and the absence of a central bulge.

NGC 4945      Sc  
 CD-144-S  
 Feb 1/2, 1978  
 103aO + GG385  
 30 min

NGC 4945 is seen nearly edge on, hiding the spiral **pattern**. The heavy dust on the near side, silhouetted against the background disk, obscures whatever nucleus may be present, but it is certain that there is no central bulge and that the nuclear region is small.

No useful resolution into individual stars is achieved on the available plate material. Although individual stars can be identified in parts of the arms, peeking out of the dust, they are much fainter than in NGC 247, which has nearly the same redshift. Contamination by Galactic stars is also a problem at the low galactic latitude  $\text{offc} = 13^\circ$ .

The redshift of NGC 4945 is small,  $v_0 = 275 \text{ km s}^{-1}$ . Closeness is also indicated by the large angular size ( $D_{95} = 2.0'$ ), consistent with the small redshift. Although the distance is evidently small, the high inclination and the dust obscuration prevent NGC 4945 from being useful for the calibration of distance indicators normally used for measurements of extragalactic distances.



PANEL  
285

PANEL  
286



*Sc Classification Section (continued)*

NGC 253                      Sc(a)                      South Polar Gr  
CD-2036-Bedke/Gregory                      HA, p. 34  
Oct31/Nov 1, 1981  
098-04  
90min

NGC 253 is a member of the South Polar Group. Its redshift is small at  $v_D = 293 \text{ km a}^{-1}$ . The estimate of the distance modulus in the RSA2 is  $m - M = 27.5$ . As suggested there, the group may extend in distance from the nearest members such as NGC 55, NGC 247, and NGC 300 at about  $m - M = 26.6$ , to more-distant members such as [NGC, 253 here, and then to NGC 7793 (Sd; panels 321, S6), which may be a magnitude more distant.

Resolution into individual stars is more difficult than in NGC 247 on the preceding panel, but is not as difficult as in NGC 4945, also on that panel. The brightest stars are in associations; they resolve beginning at about  $H = 11!$ . But the dust obscuration is very heavy. Limiting their use in NGC 253 for calibration purposes in measurements of the extragalactic distance scale. Yet star clusters, associations, and HII regions are clearly evident in the regions which have a small optical depth in the dust.

The nucleus is small. There is no central bulge. The type is prototypical Sc(s), but there is much more dust than in NGC 247 and NGC 55 (Se; panel 318).

**T**

The four galaxies on this panel are similar to NGC 253 but are at much greater distances, masking the details of the dust lanes. This apparent lack of dust gives a false security that obscuration and dust-dimming of the stellar content are unproblematic in photometry of individual stars and HII regions. Because of this, caution is in order using stars in these galaxies for addressing the problem of the distance scale.

**NGC 3877**      **Sc(s)II**    **Ursa Major Cluster**  
**PH-8081-S**  
**Feb 5/6, 1981**  
**103aO**  
**12 min**

A few HII-region candidates are present in some of the arm fragments of NGC 3877. The spiral pattern is multiple armed. There is a small nucleus and no central bulge. The redshift of NGC 3877 is  $v_o = 939 \text{ km s}^{-1}$ . It is considered to be a member of the Ursa Major Cluster.

**NGC 3495**      **Sc(s)II-III**      **panel SI 1**  
**CD-1840-HB**  
**April 2/3, 1981**  
**103aO + GG385**  
**45 min**

The morphology of NGC 3495 is almost identical to that of NGC 3877, above. The redshift is  $v_o = 970 \text{ km s}^{-1}$ .

**NGC 4096**      **Sc(s)II**      **M51 Gr?**  
**S-1979-H**  
**Feb 20/21, 1947**  
**103aO**  
**30 min**

Thin, multiple spiral arms are well defined, but the high inclination of NGC 4096 makes luminosity classification uncertain. Because of the rather-well-defined nature of the arms, the luminosity class has been reassigned here relative to the **II-III** class listed in the RSA2.

The redshift of NGC 4096 is  $v_o = 616 \text{ km s}^{-1}$ . The galaxy is tentatively assigned to the M51 Group, which also contains NGC 4258 ( $v_o = 520 \text{ km s}^{-1}$ ), NGC 4460 ( $v_o = 605 \text{ km s}^{-1}$ ), NGC 4490 ( $v_o = 601 \text{ km s}^{-1}$ ), NGC 4618 ( $v_o = 563 \text{ km s}^{-1}$ ), and M51 ( $v_o = 552 \text{ km s}^{-1}$ ). Whether these galaxies actually form a physical group, as suggested by the similarity of their small redshifts, is uncertain. The maximum separation of  $16^\circ$  on the sky of the suggested members corresponds to a projected linear diameter of the group of 3.4 Mpc at the mean redshift distance of 12 Mpc. If M51 is excluded from consideration of membership, the linear diameter of the remaining group is smaller, at 2.2 Mpc.

The original plate from which this print was made was taken with the 60-inch reflector at Mount Wilson.

**NGC 1448**      **Sc(s)II**  
**CD-1590-S/Br**  
**Aug 11/12, 1980**  
**103aO + GG385**  
**45 min**

HII-region candidates exist in the arms of NGC 1448. On this plate, taken with the Las Campanas 100-inch telescope in excellent seeing, the brightest stars seem almost ready to resolve individually.

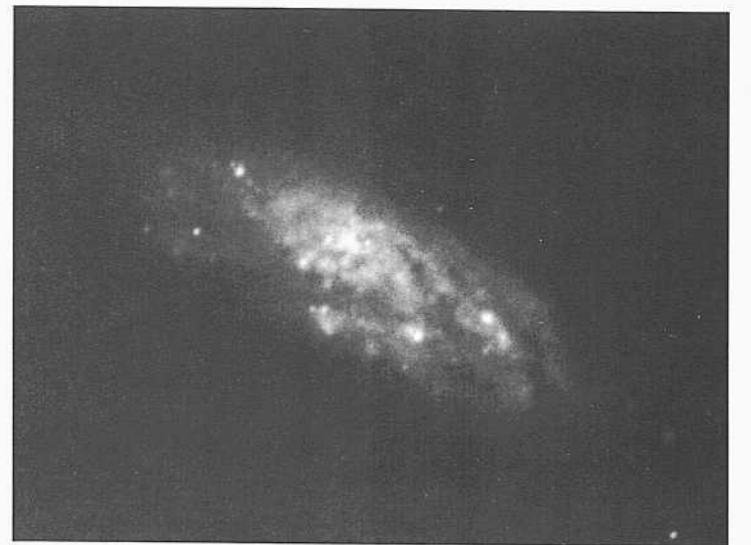
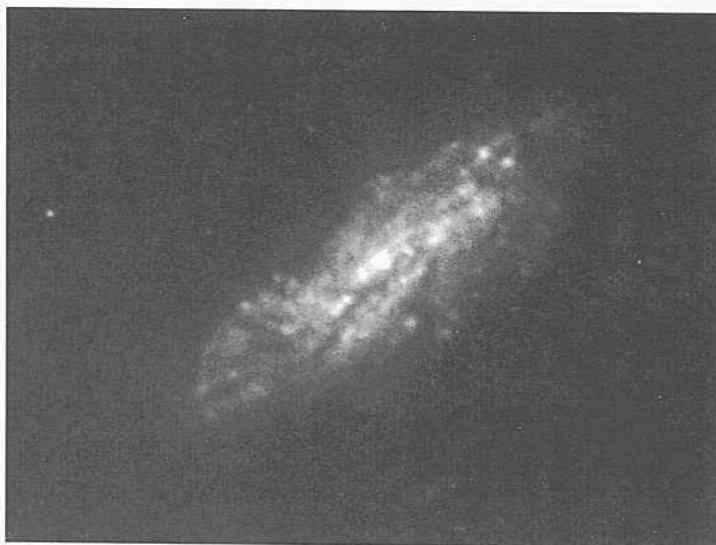
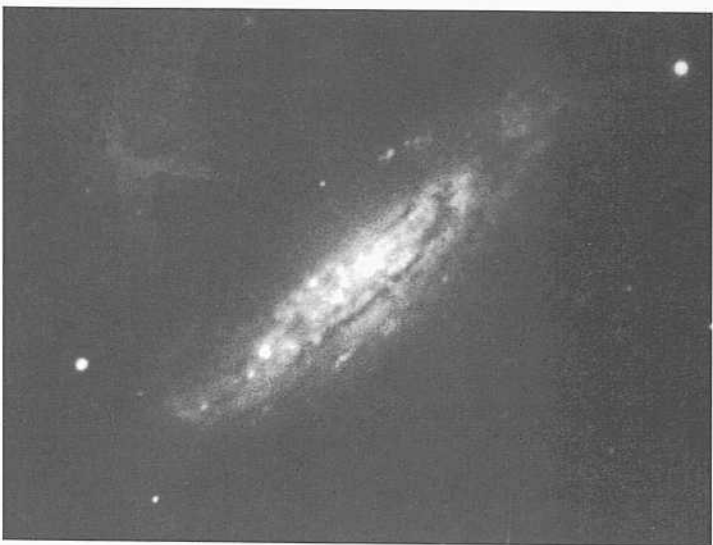
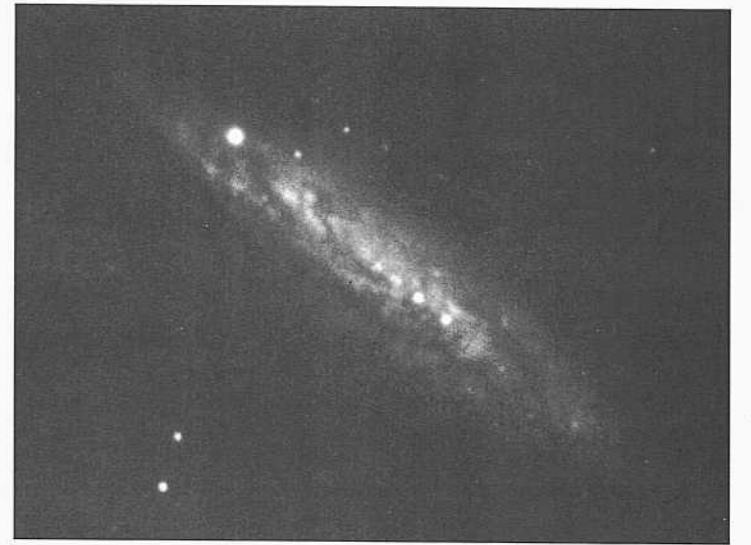
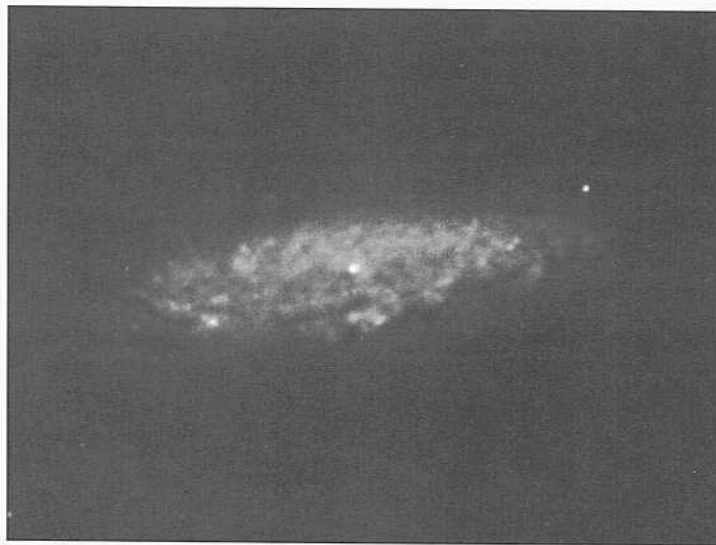
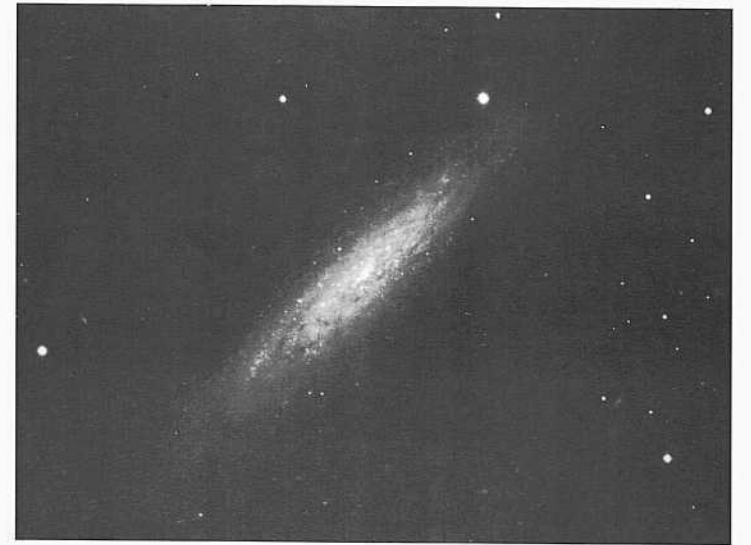
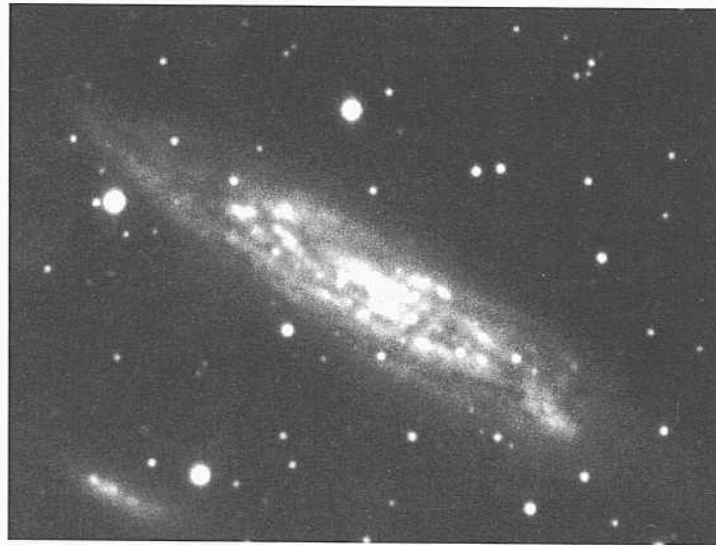
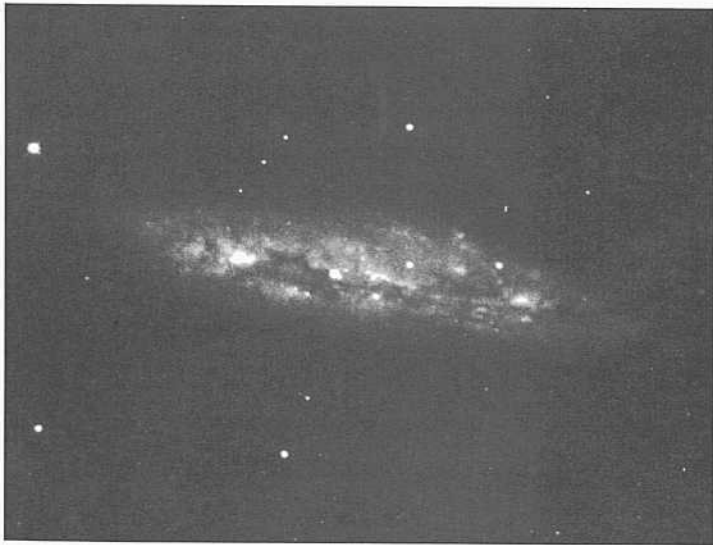
The redshift is  $v_o = 1038 \text{ km s}^{-1}$ .



PANEL  
287



PANEL  
288



The nine galaxies on this panel have similar morphologies. They have multiple-arm spiral patterns of the NGC 488-NGC 2841 type but are later in the sequence; they generally have small, pointlike nuclei or none at all; they have no central bulge or evidence of a luminous halo. These attributes are characteristic of late Sc galaxies.

NGC 3556 Sc(s)III HA, p. 35  
S-1742-H  
Dec 6/7, 1937  
Imp. Eel.  
60 min

The original Mount Wilson 60-inch plate used for NGC 3556 here is the same used in the Hubble Atlas. The description there suggests the morphological similarity of NGC 3556 and NGC 253.

Several HII-region candidates exist in parts of the arms not obscured by the dust lanes on the near side. The largest of these regions may begin to resolve at about the 2" level. The redshift of NGC 3556 is  $v_o = 790 \text{ km s}^{-1}$ .

NGC 7361 Sc(s)II-III  
CD-1545-S/Br  
Aug 7/8, 1980  
103aO + GG385  
45 min

The largest of the several HII regions may just begin to resolve at the 1" level. The redshift of NGC 7361 is  $v_o = 1276 \text{ km s}^{-1}$ .

NGC 2748 Sc(s)II  
PH-7930-S  
Nov 7/8, 1980  
103aO  
12 min

The morphology of NGC 7361 is similar to that of NGC 253. The HII regions are unresolved at 1". The redshift is  $v_o = 1634 \text{ km s}^{-1}$ .

NGC 4835 Sc(s)H pair  
CD-2148-S  
March 23/24, 1982  
103aO + GG385  
45 min

NGC 4835 forms an apparent pair with a dwarf shred (Im or BCD; classified as dIBm in the RC1) as a possible companion visible on this print near the lower-left border, at 1.6' separation. The resolution into knots (presumed HII regions) in the companion and in NGC 4835 itself is the same, suggesting a common distance.

The redshift of NGC 4835 is  $v_o = 1973 \text{ km s}^{-1}$ . At the redshift distance of 39 Mpc ( $H = 50$ ) the projected linear separation of the pair is small, at 18 kpc.

NGC 6503 Sc(s)II.8 Racine wedge  
PH-7687-S  
Sep 26/27, 1979  
103aO  
5 min

The spiral pattern in NGC 6503 is similar to the multiple-armed structure of NGC 488, but is much later, and the arms are not as well defined.

The well-determined redshift of NGC 6503 is small, at  $v_o = 303 \text{ km s}^{-1}$ . Individual stars and HII regions resolve out of the high-surface-brightness background on a red-sensitive plate taken with the Palomar 200-inch telescope, but the resolution in the blue on the print here is not nearly as prominent. Incipient resolution into stars occurs in one of the outer arms that is not silhouetted against the high-surface-brightness disk, but the exposure on the original plate used here is short, made to see the central regions rather than the individual stars that begin to resolve out at about  $\theta = 20$ .

NGC 4808 Sc(s)III  
H-2265-H  
May 4/5, 1946  
103aO  
40 min

The original plate used for the print here was taken with the Mount Wilson 100-inch Hooker reflector.

The surface brightness of the multiple-arm pattern that covers the disk is high. The nucleus is either small and faint or is nonexistent. The redshift of NGC 4808 is  $630 \text{ km s}^{-1}$ .

NGC 24 Sc(s)II-III  
CD-530-S  
Sep 30/Oct 1, 1978  
103aO + GG385  
45 min

The outer regions of NGC 24 that arc silhouetted against the highly inclined bright disk are highly resolved into individual stars beginning at about  $B = 21$ .

The redshift of NGC 24 is  $v_o = 621 \text{ km s}^{-1}$ .

NGC 5690 Sc(s)H:  
CD-1850-HB  
April 3/4, 1981  
103aO + GG385  
45 min

The redshift of NGC 5690 is  $v_o = 1653 \text{ km s}^{-1}$ .

NGC 4632 Sc(s)II.3 triplet  
CD-1411-S/Br  
March 23/24, 1980  
103aO  
75 min

NGC 4632 forms an apparent triplet with NGC 4666 (Six; panel 194;  $v_o = 1474 \text{ km s}^{-1}$ ) and NGC 4668 (SBc; panel 313;  $v_o = 1531 \text{ km s}^{-1}$ ). The redshift of NGC 4632 is  $v_o = 1557 \text{ km s}^{-1}$ . The angular separation of NGC 4666 from NGC 4632 is 45.9'. At the mean redshift distance of 30 Mpc ( $H = 50$ ) for the triplet, the projected linear separation of NGC 4666 from NGC 4632 is 400 kpc, similar to distances within the Local Group.



**M**ost of the galaxies on this and the next two panels are more nearly on edge than those on preceding panels of the ScII-III section. The thinness of the disk and the absence of a strong central bulge are the classification criteria.

NGC 5907      So(on edge)      panel SI 1  
PH-186-MH  
May 10/11, 1950  
103aO  
40 iiiin

NGC 5907 shows the absence of the central bulge particularly well because of its high inclination.

The redshift is  $v_o = 779 \text{ km s}^{-1}$ .

NGC 4302/4298      Sc(on edge)      VCC 497  
CD-1399-S/Br      Sc(s)III      VCC 483  
March 22/23, 1980      panel 279  
103aO      Karachentsev 332  
75 niin

NGC 4302 and NGC 4298 in the Virgo Cluster may form a physical pair. Their redshifts are identical at  $v_o = 1004 \text{ km s}^{-1}$ , as listed in the RSA2. The angular separation of 2.4' corresponds to a projected linear separation of only 1.5 kpc at the distance of 21.9 Mpc. There is no evidence for tidal distortion in either NGC 4298 or NGC 4302. Note that the thin disk seen edge on in NGC 4302 is not warped; yet NGC 4298, in projection, is nearly in the pole of NGC 4302.

The lack of morphological distortion in either galaxy suggests that the true separation is considerably larger than the projected separation. Similarity of redshift in the Virgo Cluster does not necessarily mean a common distance because of the large (virial) spread in the velocities of cluster members.

NGC 5775      Sc(on edge)      Karachentsev 440  
CD-1884-HB  
April 11/12, 1981  
103aO + GG385  
45 niin

NGC 5775 forms a physical pair with NGC 5774 [SBc(s)II] at a separation of 4.2'. The redshifts are similar at  $u_o(5774) = 1488 \text{ km s}^{-1}$  and  $y_o(5775) = 1687 \text{ km s}^{-1}$ , as listed by Karachentsev. At the mean redshift distance of 31 Mpc ( $H = 50$ ) the projected linear separation of the pair is small at 38 kpc.

No morphological distortion is evident in either galaxy. In particular, the thin disk in NGC 5775, seen nearly edge on, is not warped.

NGC 5301      Sc(s)      Racine wedge  
PH-7719-S  
Feb 11/12, 1979  
103aO  
12 niin

The original plate used for the print here was taken with a Racine wedge, giving secondary images that are 5.0 mag fainter than the primary and separated from the primary image by 18".

NGC 5301 is nearly on edge, showing the thinness of the disk.

The redshift is  $v_o = 1709 \text{ km s}^{-1}$ .

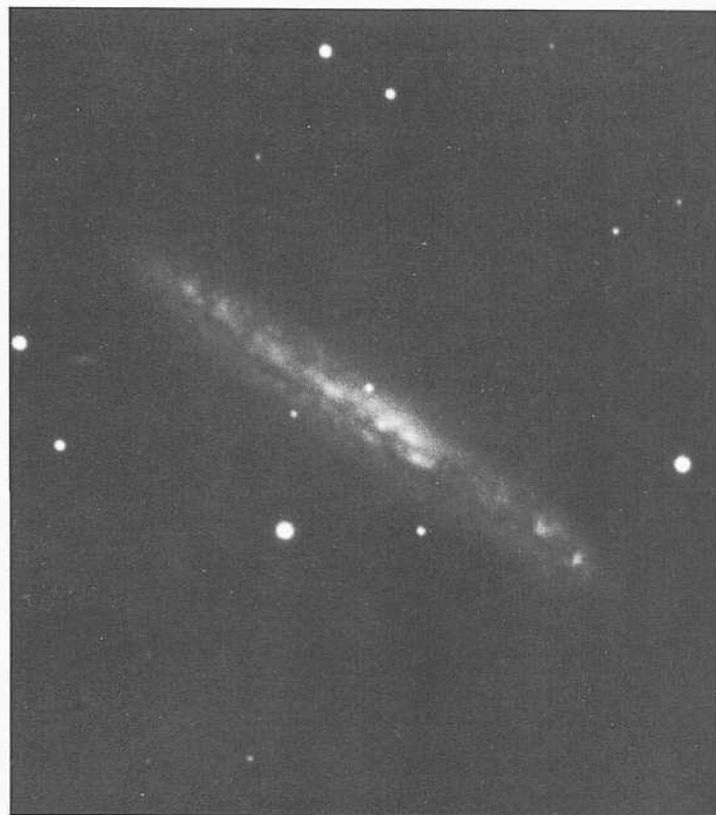
NGC 5496      Sc(s)II  
CD-1591-S/Br  
Aug 12/13, 1980  
103aO + GG385  
45 niin

NGC 5496, seen nearly on edge, may have a small luminous bar near the center, seen well in the print here.

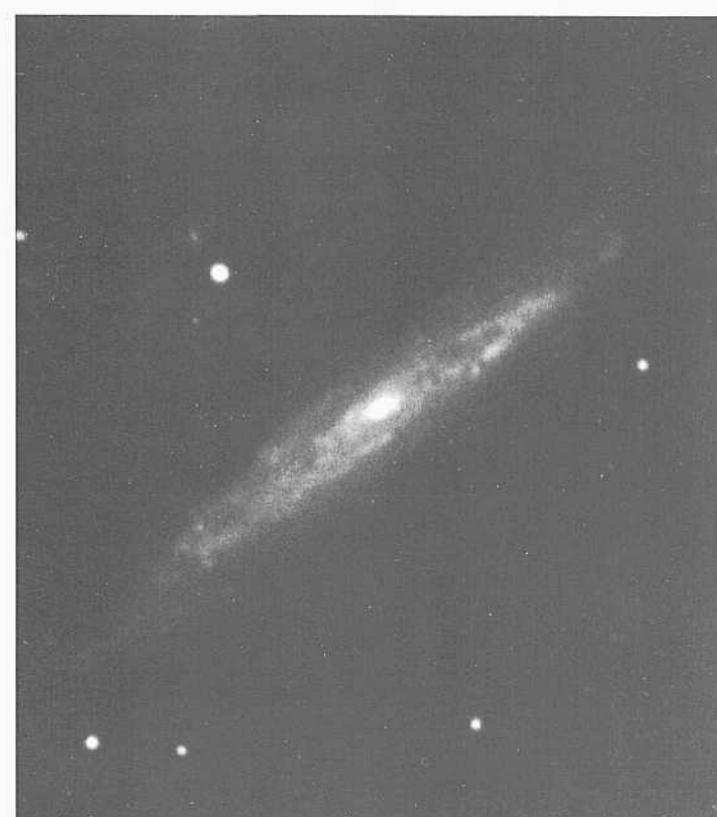
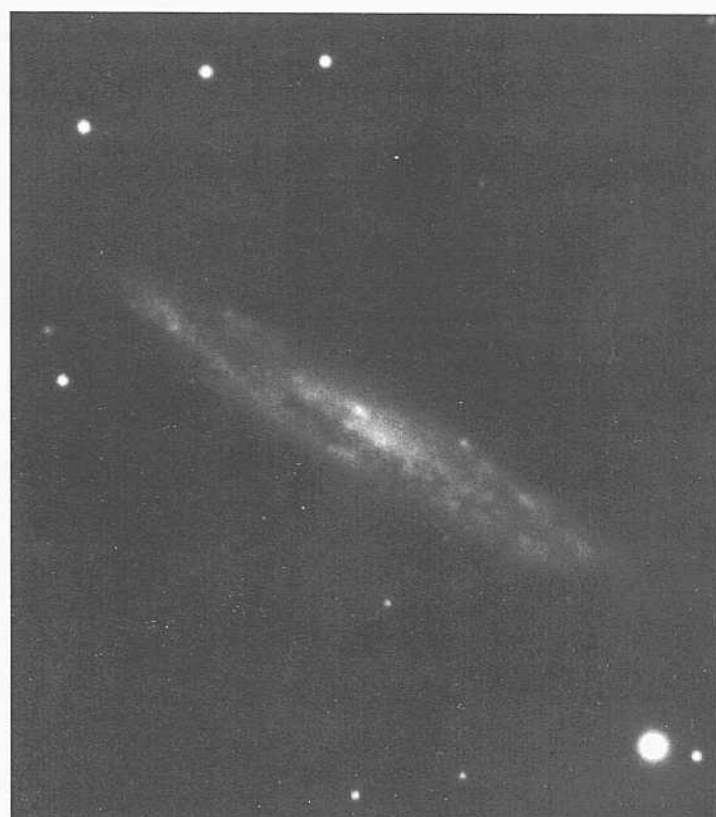
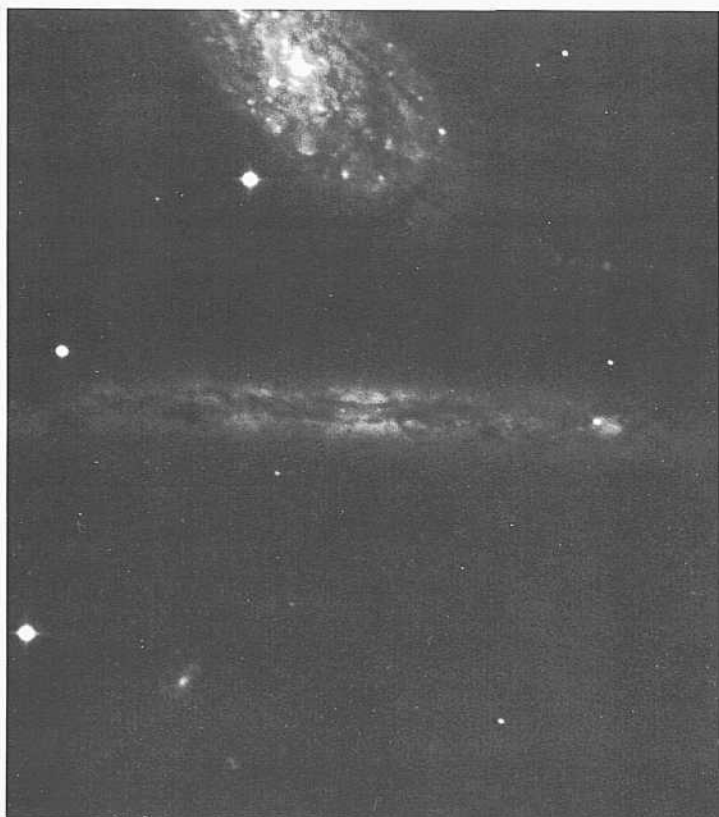
The redshift is  $v_o = 1398 \text{ km s}^{-1}$ .

NGC 3735      Sc(s)I      Racine wedge  
PH-8110-S  
Feb 7/8, 1981  
103aO  
12 mm

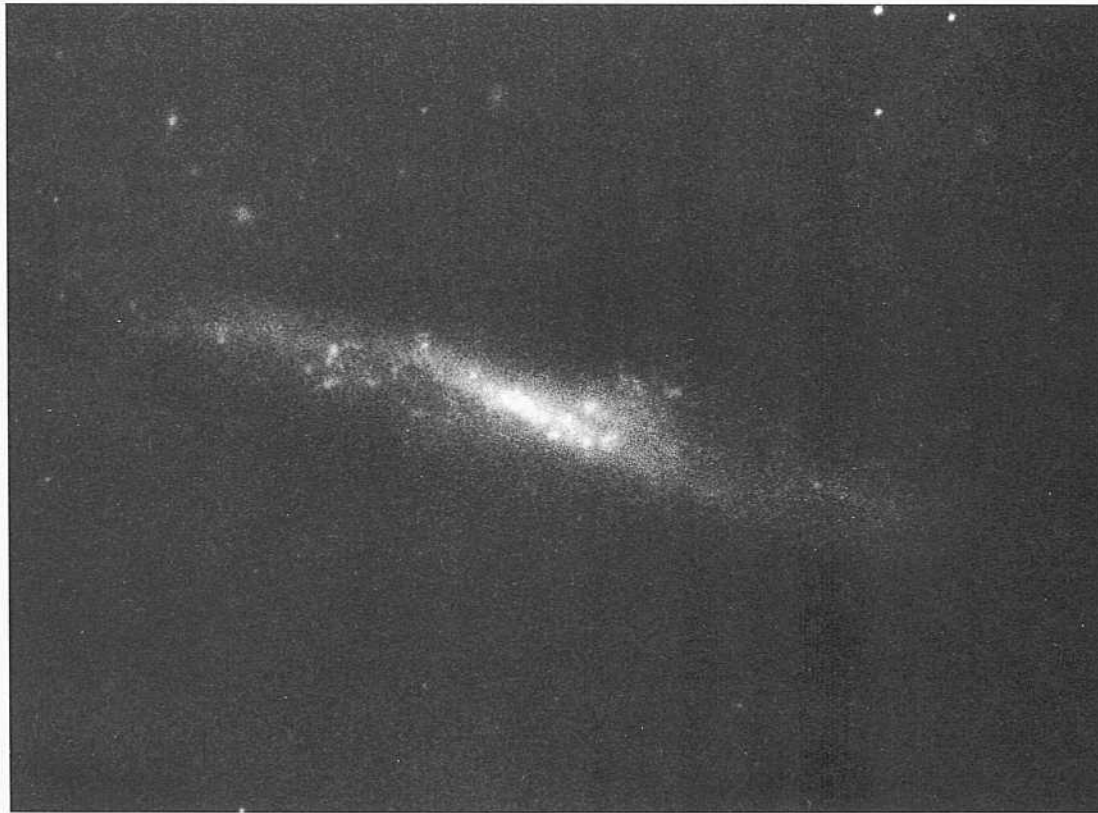
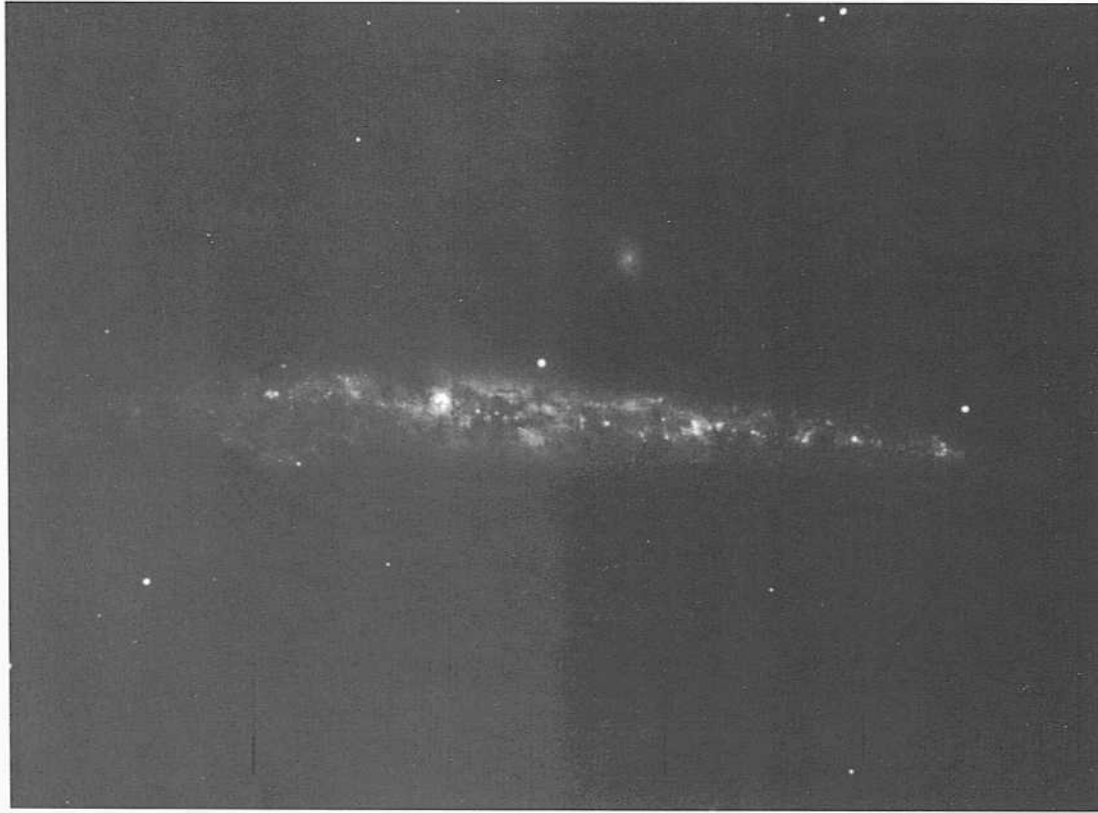
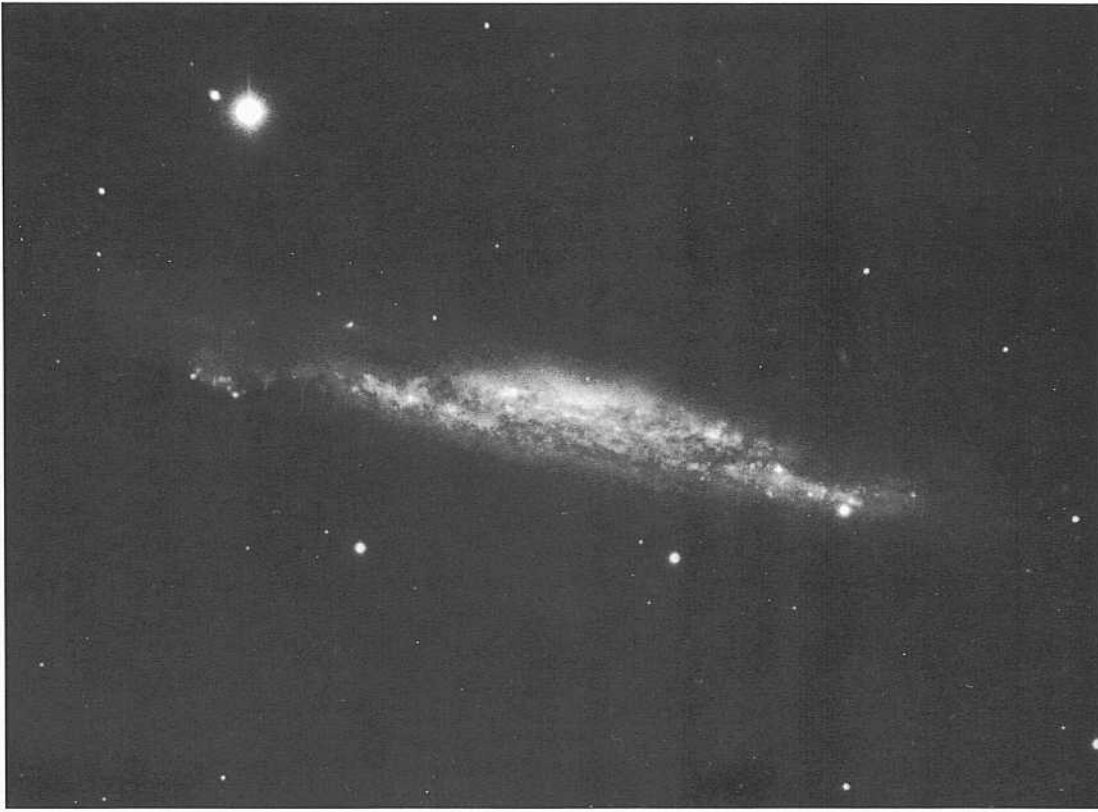
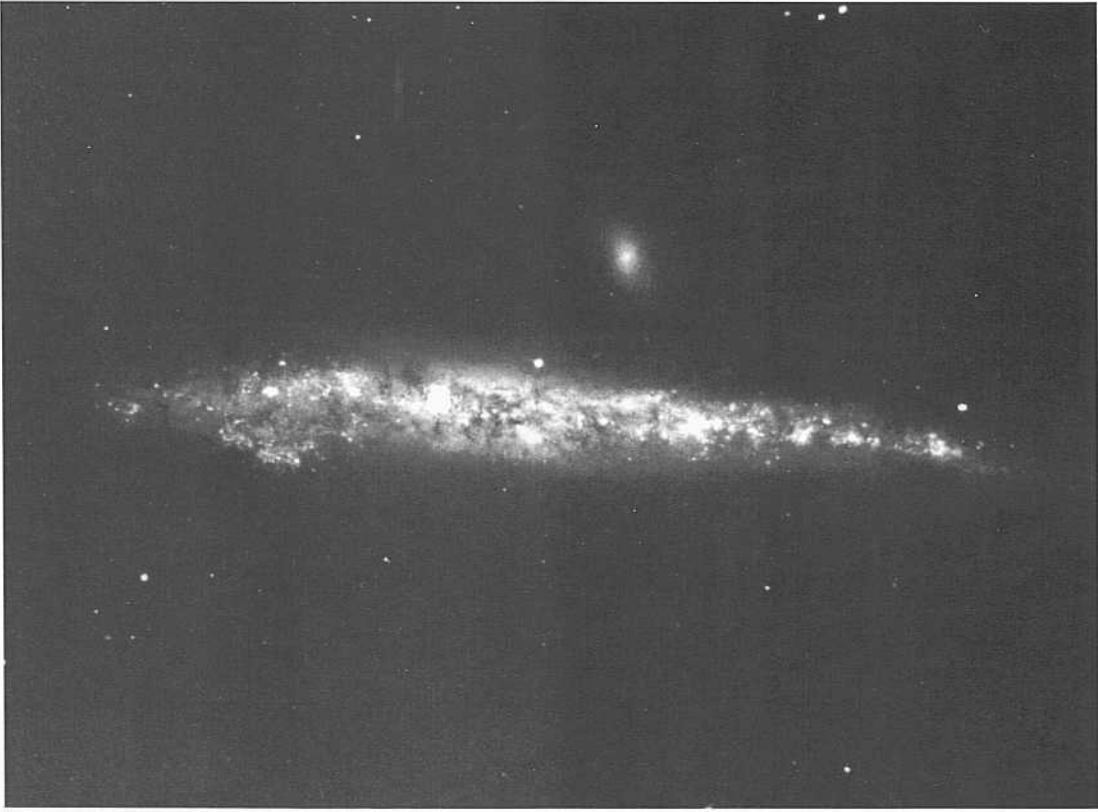
NGC 3735, seen nearly on edge, has a redshift of  $v_o = 2838 \text{ km s}^{-1}$ .



PANEL  
289



PANEL  
290



NGC 4631/4627 Sc(on edge) pair  
 H-2161-II dE5,N HA, p. 25  
 Jaii 29/30, 1941  
 CrHiSpSp  
 120 min

NGC 4631 forms a close pair with the dwarf elliptical NGC 4627 (dE,N) at a separation of 2.7', and a wide pair with NGC 4656 (Im; panels 32.7, S6) with a separation of 31'. These galaxies are in the nearby group called the CnV II Cloud (de Vaucouleurs 1975; Sandage and Tammann 1975a), which has  $\langle v_o \rangle$  of about 750 km s<sup>-1</sup>.

A study of the 21-cm HI content of the wide NGC 4631/4656 pair (Weliachew, Sancisi, and Guélin 1978) gave evidence that a tidal encounter had occurred or is now occurring (Combes 1978) between this apparent pair. At an assumed redshift distance of 12 Mpc ( $H = 50$ ) the projected linear separation of NGC 4631 from NGC 4656 is 108 kpc. If a smaller distance of 5 Mpc is used, based on the stellar content (Sandage and Tammann 1974d), the projected linear separation is 44 kpc. At this distance, the projected linear separation of the much closer NGC 4631/4627 pair is only 4 kpc.

NGC 4631 is highly resolved into bright stars starting at about  $B = 1.9$ . However, because the galaxy is viewed nearly edge on, the dust obscuration is high and variable, making photometric studies of the stellar content difficult and the results uncertain.

NGC 4631/4627 Sc(on edge) pair  
 H-3634-S cE5,N HA, p. 25  
 Feb 18/19, 1963  
 103aO + GG13  
 25 min

The dwarf companion NGC 4627 has a nucleus and is surrounded by a swarm of about ten images brighter than  $B = 22$ . These may be globular clusters similar to the case in NGC 205 (panel 25), the companion to M31. Also like NGC 205, NGC 4627 has tidal tails pointing toward and away from its larger companion. This is clear evidence of a close encounter, pointed out and shown well in the deep photograph in the *Atlas of Peculiar Galaxies* (Arp 1966). A similar case is the pair NGC 1531/1532 (panels 197, 337).

NGC 4627 has nearly the same redshift as NGC 4631. Ulrich, quoted by Weliachew *et al.* (1978), has measured  $v_o(4631) = 647$  km s<sup>-1</sup>. Chinearini and Rood (1971) quote  $v_o(4627) = 727$  km s<sup>-1</sup>. Combes (1978), who has calculated encounter parameters for the three-galaxy interaction, suggests that NGC 4627 was once a recent star-producing Im dwarf whose HI was swept out, leaving a nucleated dwarf E galaxy from the encounter.

NGC 3079 Se(s)II-III triplet?  
 PH-7933-S Racine wedge  
 Nov 7/«, 1980  
 103aO  
 12 min

NGC 3079 (iNCC 3079)( $\langle v_o \rangle = 1225$  km a<sup>-1</sup>) forms a pair with NGC 3073 (SO pec!;  $v_o = 1271$  km s<sup>-1</sup>; not in the USA), at a separation of 10.1'. A third anonymous galaxy (Im or lid) of unknown  $v_o$  exists in the field, separated by 6.6' from NGC 3079. From its stellar content, this candidate companion appears to be at the same distance as NGC 3079.

At the mean redshift distance of 25 Mpc ( $H = 50$ ) the projected linear separations of the two supposed companions from NGC 3079 are small, at 73 kpc and 48 kpc, respectively.

The plane of NGC 3079 is warped in the outer regions. Furthermore, the morphology of the two companions is abnormal, suggesting an earlier encounter.

A few individual stars (or more probably III regions) resolve out of the background light in the outer regions of the image starting at about  $B = 21$ .

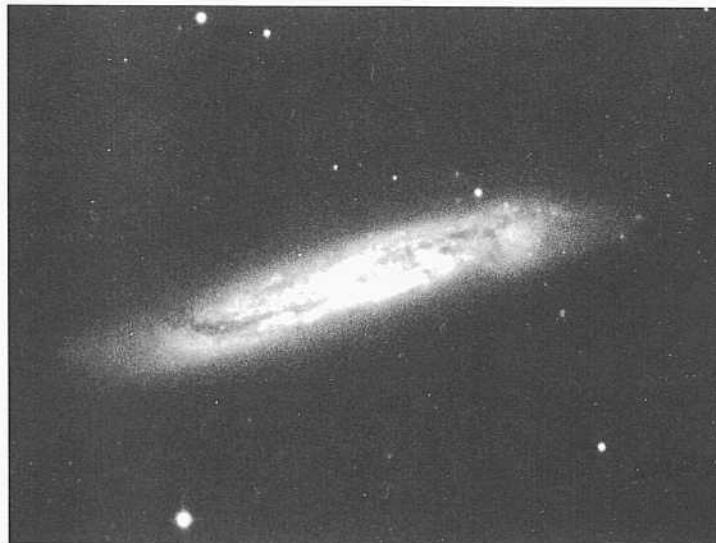
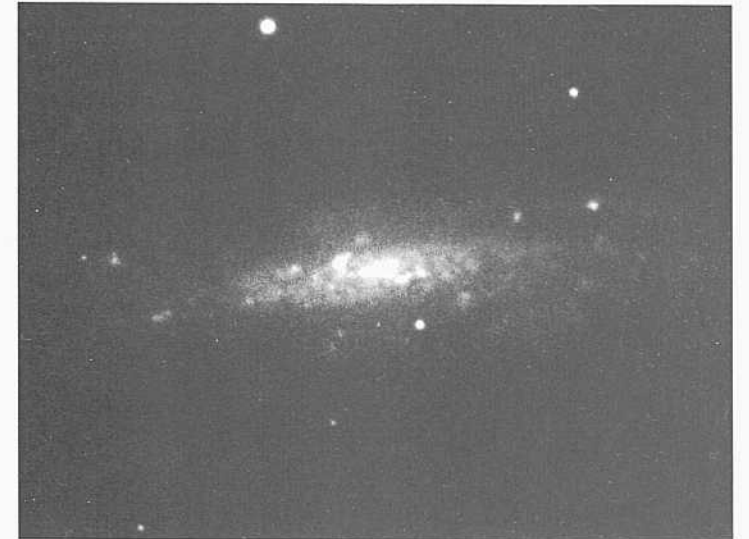
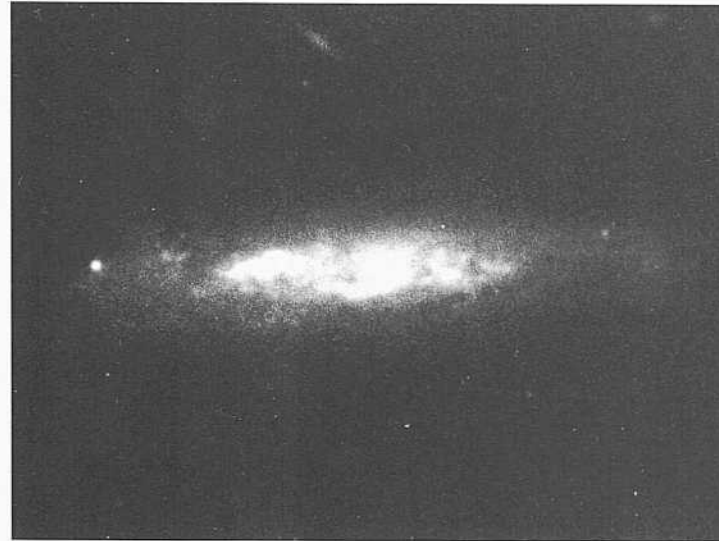
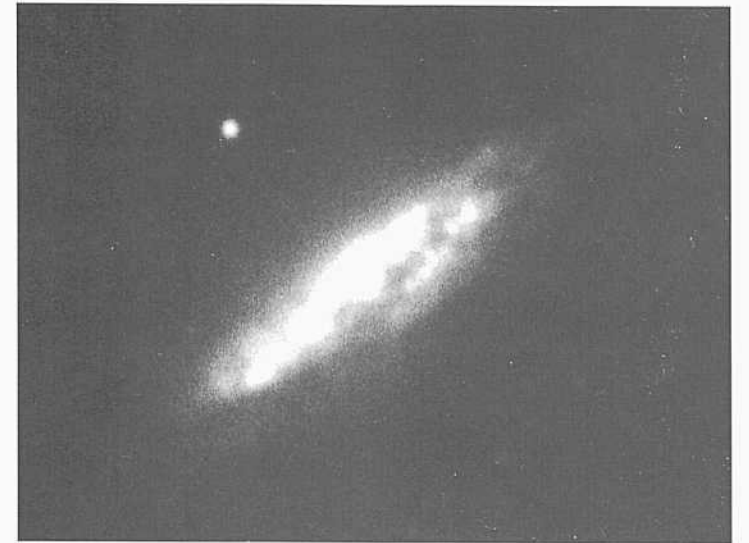
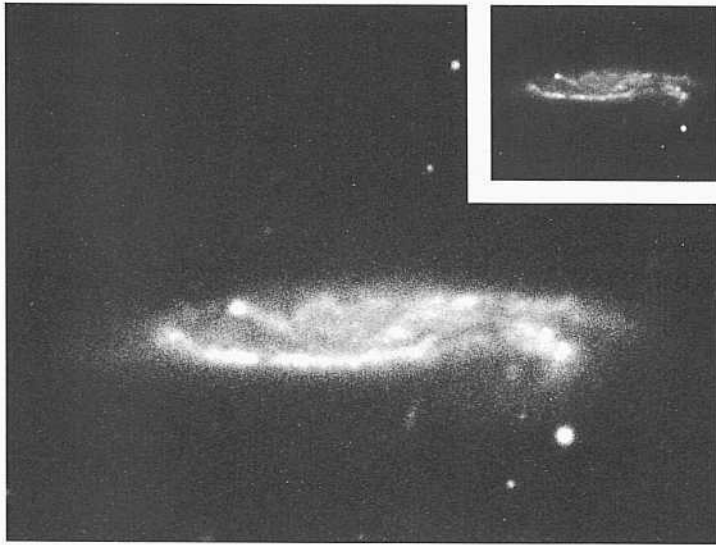
A Racine wedge has produced secondary images to the bright stars 5 magnitudes fainter than the primary at 1.8" separation.

NGC 3510 Sc(warped plain-)  
 PH-8079-S  
 Feb 5/6, 1981  
 103aO  
 12 min

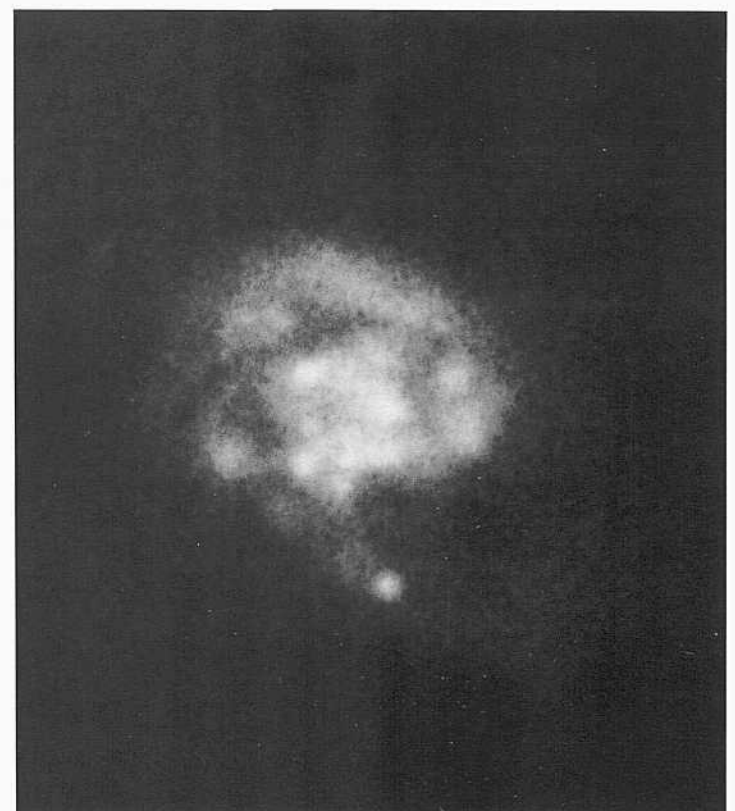
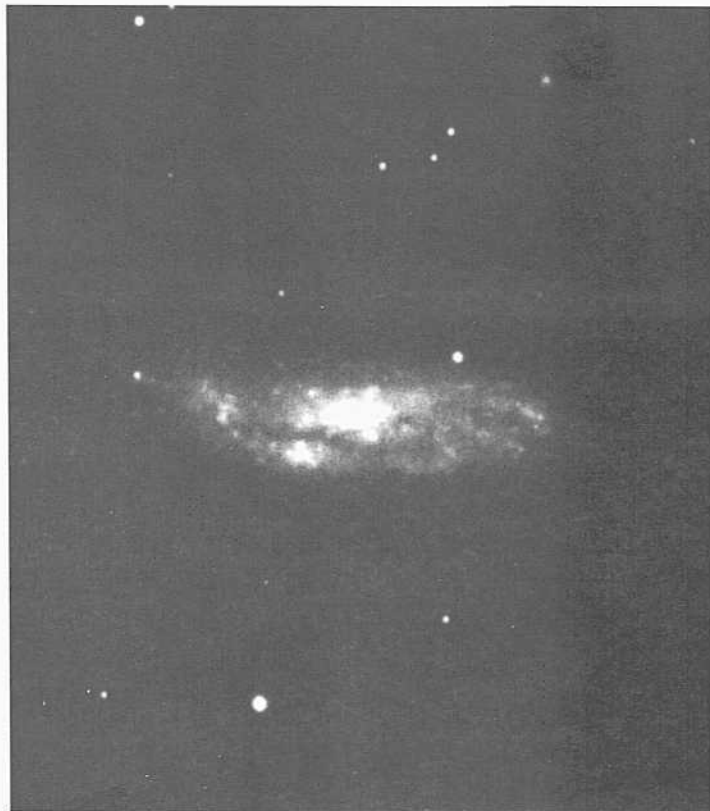
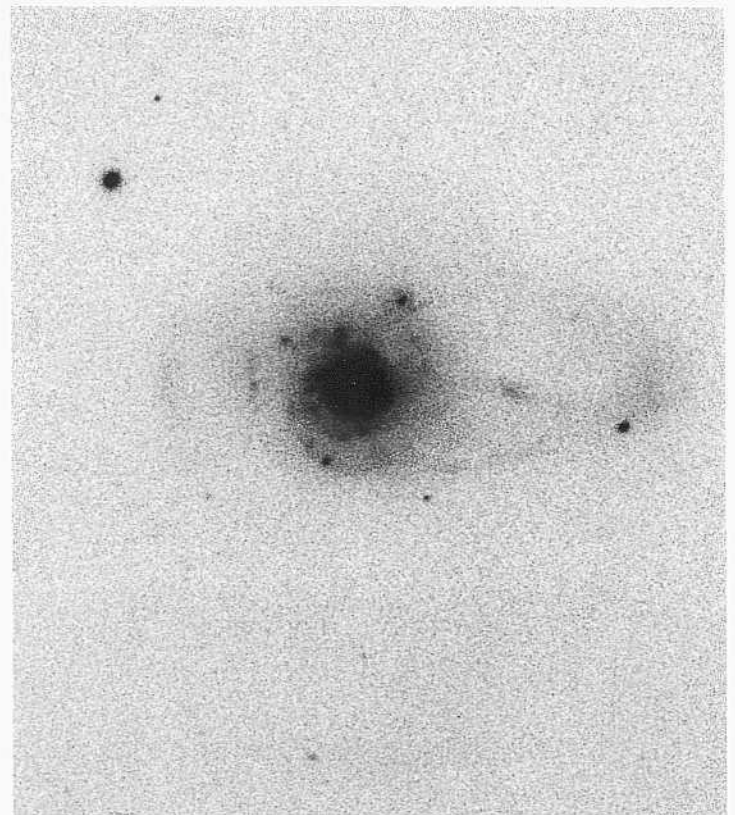
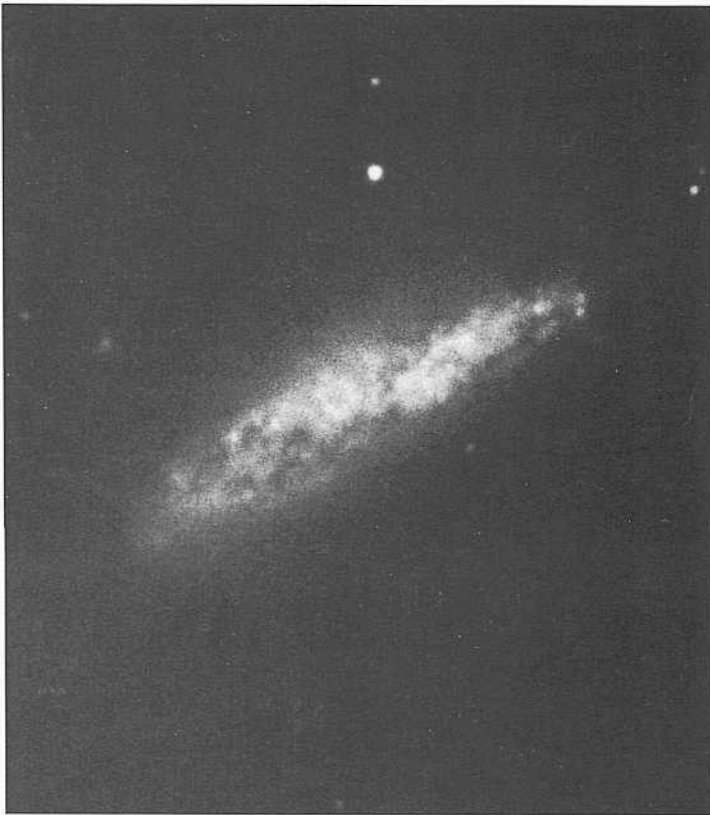
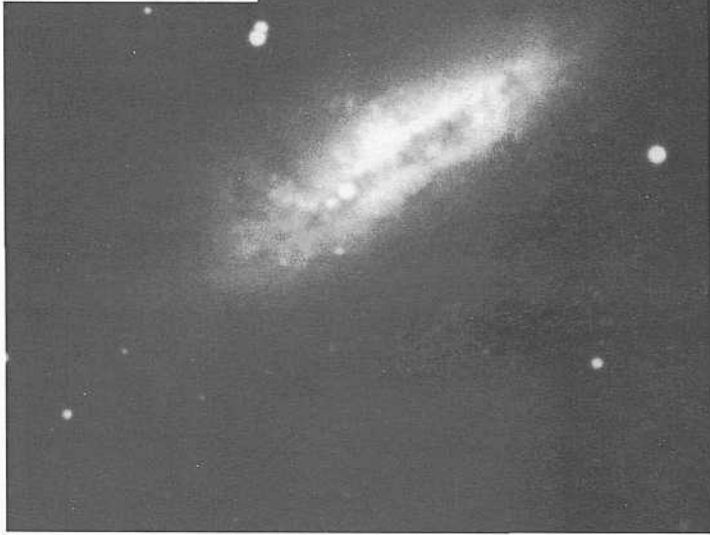
The outer regions of NGC 3510 show a warped plane. There are no nearby companions upon which to blame the warping.

Many individual knots, supposed unresolved III regions, exist in the inner (bar-like) central part of the image. Individual slurs begin to resolve at about  $B = 22$ . The redshift of NGC 3510 is  $\langle v_o \rangle = 660$  km s<sup>-1</sup>.





PANEL  
292



**T**he Se section is concluded on this panel with four nearly edge on galaxies, continuing the illustrations begun on panel 285. The section is concluded with final galaxies that have peculiar morphologies, combining features of Sa and Sc systems.

NGC 1511 Sc pec or Amorphous? triplet?  
 CD-759-S  
 Feb 20/21, 1979  
 103aO + GG385  
 45 niin

NGC 1511 insert  
 CD-1744-S  
 Jaii 12/13, 1981  
 103aO + GG385  
 7 mill

NGC 1511 is an apparent triplet with NGC 1511A (Amorphous or BCD; not in the RSA) at a separation of 11.1' and NGC 1511B (Sd or Sm on edge; also not in the RSA) at a separation of 7.6'. The known redshifts are  $v_o(1511) = 1142 \text{ km s}^{-1}$  and  $v_o(1511B) = 1101 \text{ km s}^{-1}$ . At the redshift distance of 22 Mpc ( $H = 50$ ) the projected linear separations from NGC 1511 are 71 kpc and 49 kpc.

The complex line of presumed HI! regions at the edge of the thick opaque dust lane is well seen in the short-exposure insert print.

NGC 5088 Se(s)II  
 CD-1874-HB  
 April 10/11, 1981  
 103aO  
 75 niin

NGC 5088 is in the neighborhood of the NGC 5077 group (mean redshift of about  $v_o = 2500 \text{ km s}^{-1}$ ; Humason, Mayall, and Sandage 1956), but is in the foreground with a redshift of  $v_o = 1230 \text{ km s}^{-1}$ . HII-region candidates are abundant but are probably unresolved at the 1.5" level.

NGC 4605 Se(s)III  
 S-1921-H  
 April 3/4, 1946  
 103aO  
 55 niin

The sense of the spiral pattern can be determined from the lower-surface-brightness side of the image where the multiple-arm pattern can be seen opening up.

The redshift is  $v_o = 273 \text{ km s}^{-1}$ .

NGC 3067 Sc(dust)  
 PH-7992-S  
 Feb 2/3, 1981  
 103aO  
 12 niin

The classification of NGC 3067 is difficult because of the dust and the inclination. Star formation is obviously occurring. Several HII-region candidates are visible.

The redshift is  $v_o = 1429 \text{ km s}^{-1}$ .

NGC 7679 Sc(s)/Sa(lides?) pair  
 PII-7816-S panel 86  
 Sep2/3, 1980  
 103aO  
 12 mill

NGC 7679, also illustrated in the Sa section (panel 86), forms a physical pair with NGC 7682 (SBa) at a separation of 1.5'. The redshifts are  $v_o(7679) = 5397 \text{ km s}^{-1}$  and  $v_o(7682) = 5333 \text{ km s}^{-1}$ . At the mean redshift distance of 107 Mpc ( $H = 50$ ) the projected linear separation is 139 kpc.

The smooth outer arm that is pulled out on one side of NGC 7679 may be due to a tidal encounter with NGC 7682. However, the morphology of NGC 4682 is undistorted.

NGC 5665 Sa/Sc panel 86  
 CD-1868-HB  
 April 9/10, 1981  
 103aO  
 75 min

NGC 5665 is also illustrated in the Sa section (panel 86).

The smooth outer arms are devoid of star-forming regions but the inner parts of the image are filled with HII-region candidates. There is no nucleus or central bulge. There is a thin, single-inner-arm pattern that can be traced for 1/2 revolutions.



## The SBc Classification Section

The division between the SBbc and SBc morphological boxes is arbitrary and therefore subjective, defined by the examples themselves. There is considerable width to the SBc section from early, near the SBbc section, to late, merging into the SBcd section.

The characteristics of SBc galaxies are (1) a high degree of resolution of the bar and of the spiral arms into knots (HH-region candidates) and associations, (2) smallness or absence

of a high-surface-brightness inner disk associated with the central regions, and (3) openness of the spiral arms.

The 76 SBc galaxies on the next 21 panels are generally arranged in order of luminosity class, from the most-regular arm patterns of the class I galaxies to patterns with the most chaos (high geometrical entropy) of class III near the end of the section at panel 313.

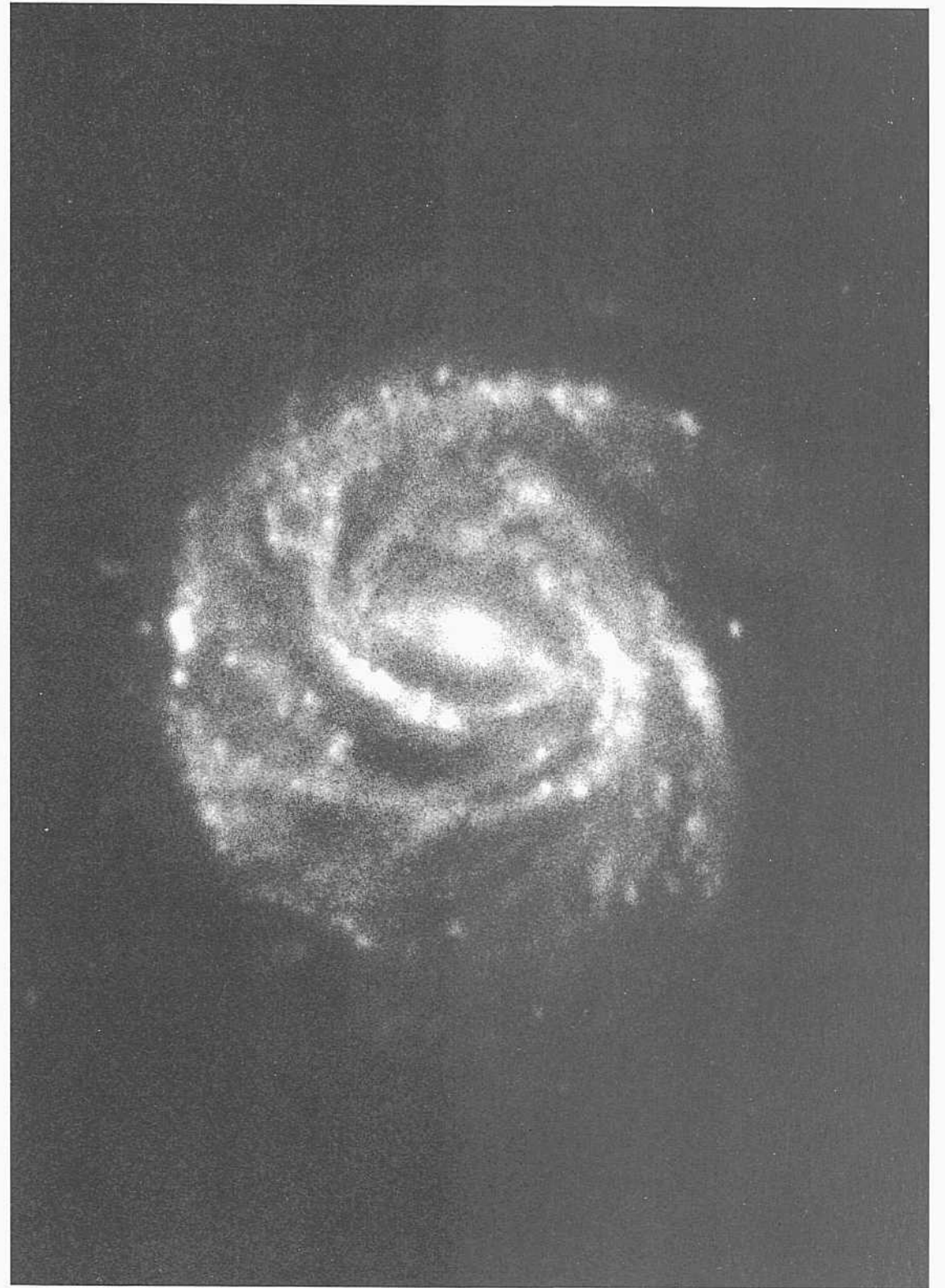
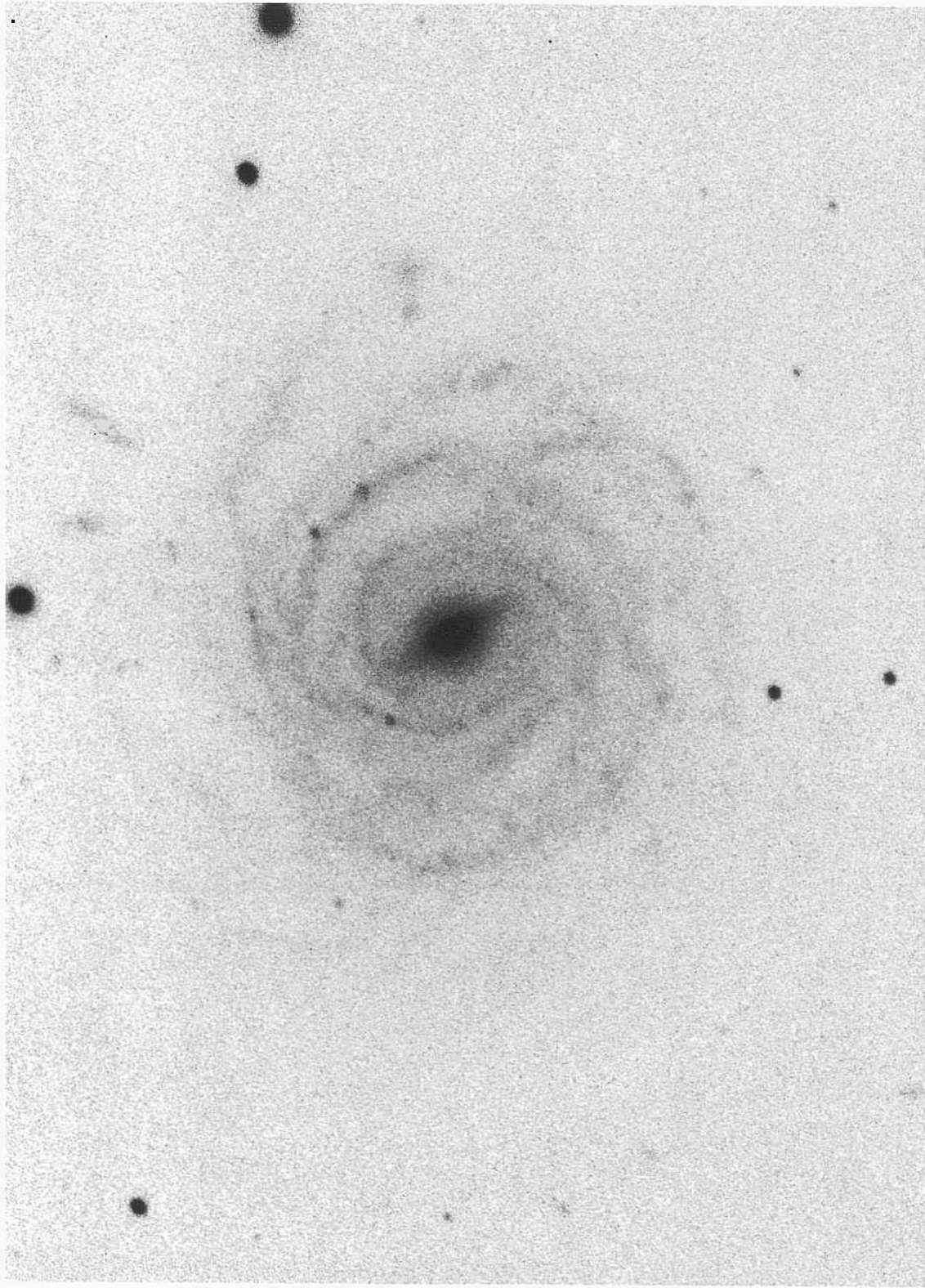
**NGC521**            **SBc(rs)I**            **group**  
**PH-7547-S**  
**Nov 6/7, 1978**  
103aO  
**12 min**

NGC 521 is the earliest of the SBc galaxies in this atlas, close to the edge of the SBbc morphological section. It may form a physical pair with NGC 533 (E3; panel 8) at a separation of 14.5'. The redshifts are  $u_o(521) = 5223 \text{ km s}^{-1}$  and  $r_o(533) = 5664 \text{ km s}^{-1}$ . At a mean redshift distance of 109 Mpc ( $H = 50$ ) the projected linear separation is 460 kpc if the association is real. NGC 533 is the brightest member of a rich group of fainter E and SO galaxies within a radius of about 20'.

NGC 3367            SBc(s)II.2            HA, p. 49  
CD-1731-S  
Jan 10/11, 1981  
103aO  
75 min

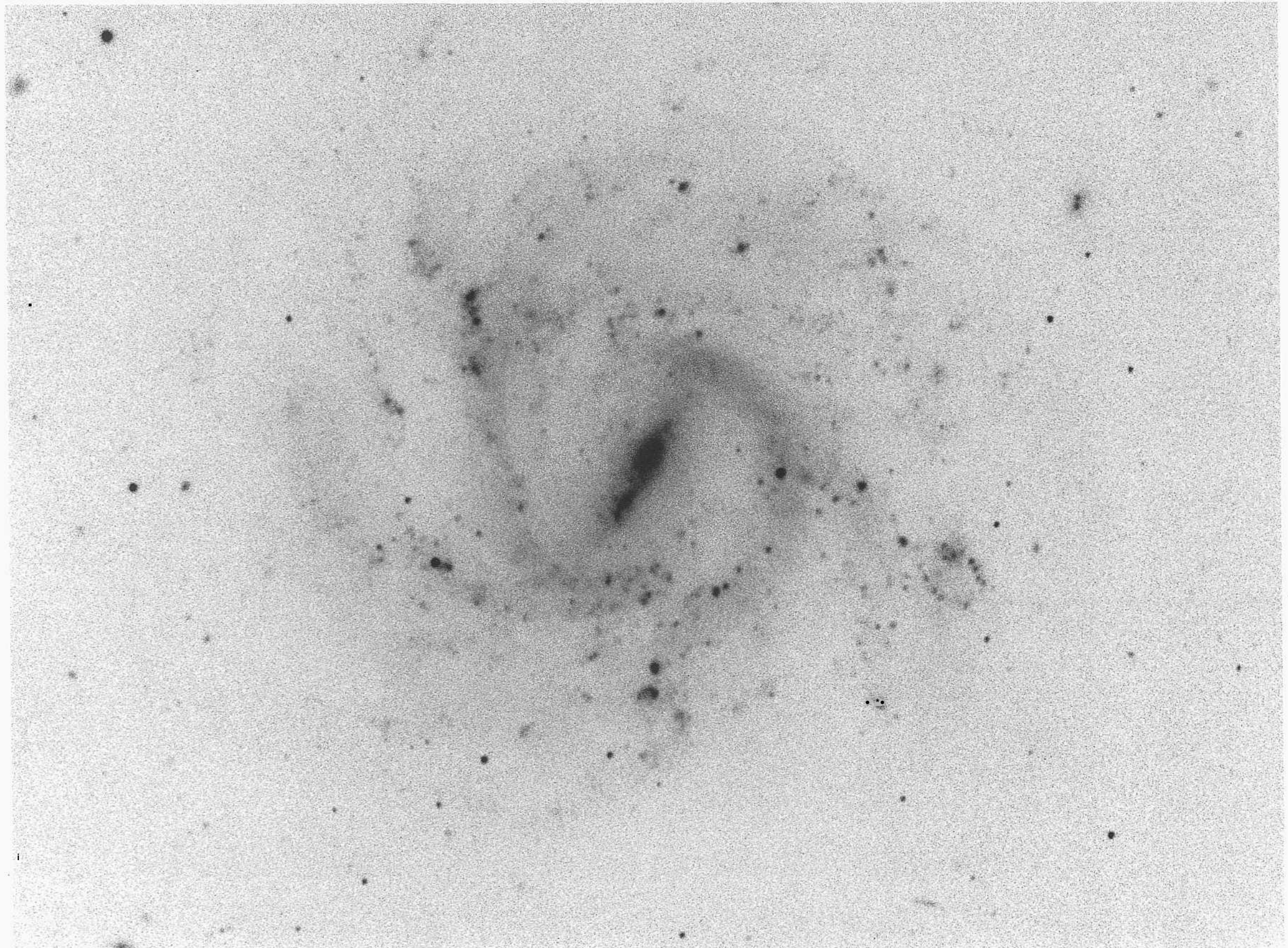
NGC 3367 is in the field of the Leo Group (Ferguson and Sandage 1990) but is judged to be in the background based on its high redshift of  $v_o = 2906 \text{ km s}^{-1}$ . The mean redshift of the Leo Group proper is  $\langle v_o \rangle = 909 \text{ km s}^{-1}$ .

Many bright HII regions are strung along the inner parts of the two major arms that begin at the ends of the bar in the (s) configuration whose prototype is NGC 1300 (SBb; panels 154, S8). The two major arms fragment after about half a revolution, creating the multiple-arm pattern in the outer regions.



PANEL  
293

PANEL  
294





T

The four galaxies on this panel have similar morphology. In each, the arm pattern begins near the ends of the bar, thereafter fragmenting into the multiple-arm pattern in the outer regions.

NGC 7424 Sc(rs)II.3/SBc(s)II.3 panel S9  
 CD-1511-S/Br  
 Aug 4/5, 1980  
 103aO + GG385  
 10 min

NGC 7424 is of very large angular diameter ( $D_{95} = 7.6'$ ) and clearly is nearby, judging from the high degree of resolution of the arms into spiral regions and individual stars. The largest of the many HII-region candidates have angular diameters (halo) of about  $2''$ . The individual stars that can be guessed not to be HII regions start to resolve at about  $B = 2.2$ . The stars and the HII regions have yet (1991) to be identified by standard means.

The redshift is  $v_r = 92.5 \text{ km s}^{-1}$ .

NGC 3359 SBc(s)L8 pec HA, p. 49  
 PH-1144-S  
 Oct 23/24, 1955  
 103aO + WG2  
 25 min

HII-region candidates and perhaps brightest stars are present in the well-developed but late-type bar in NGC 3359. The thin, multiple arms are full of HII-region candidates, only two of which resolve into disks at the  $1.5''$  level. Individual stars have not yet been distinguished from the HII regions by standard methods.

The redshift is  $v_r = 1138 \text{ km s}^{-1}$ .

NGC 1179 SBc(r)II.2  
 CD-1653-S  
 Dec 29/30, 1980  
 103aO + GG385  
 45 min

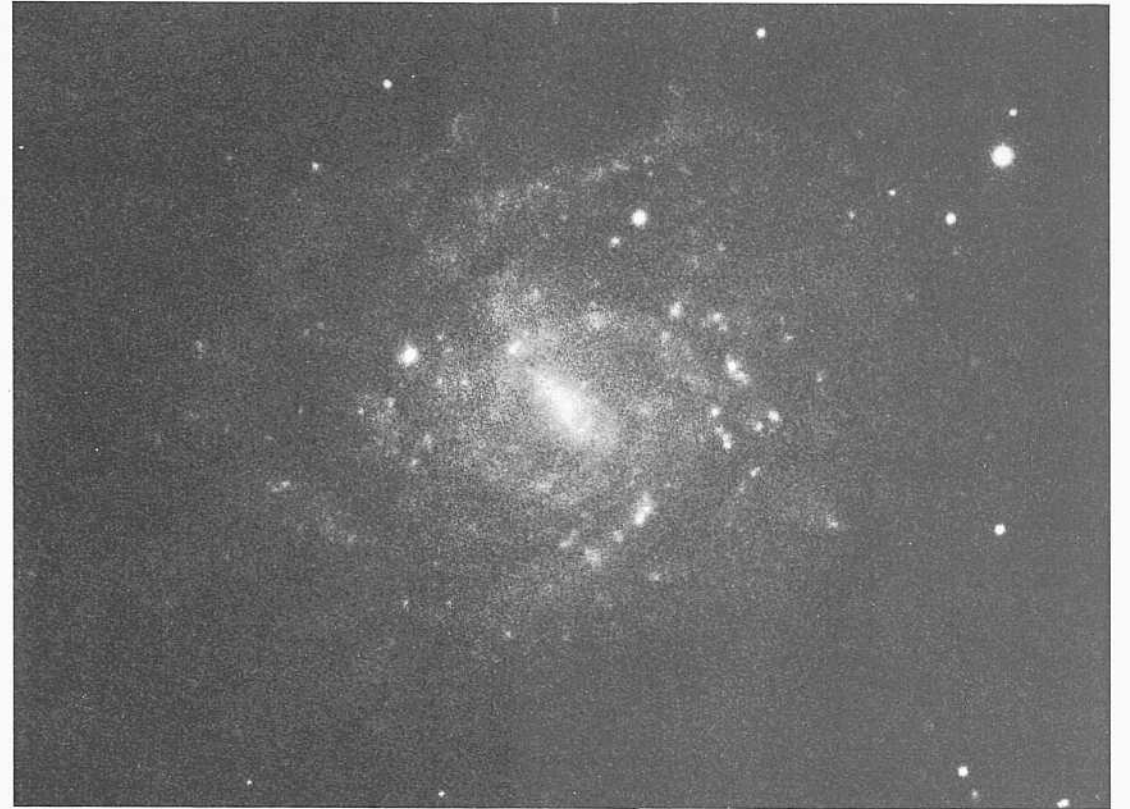
HII-region candidates exist in the central bar as well as in all the arm fragments of NGC 1179. Three particularly bright bill-region candidates are very compact and do not resolve at the  $1.5''$  level. No individual stars resolve to the plate limit.  $B = 2.3$ .

The redshift is  $v_r = 1776 \text{ km s}^{-1}$ .

New 1 = A 0102-06 SBc(s)II.2 Racine wedge  
 PH-7673-S  
 Sep 25/26, 1979  
 103aO  
 10 min

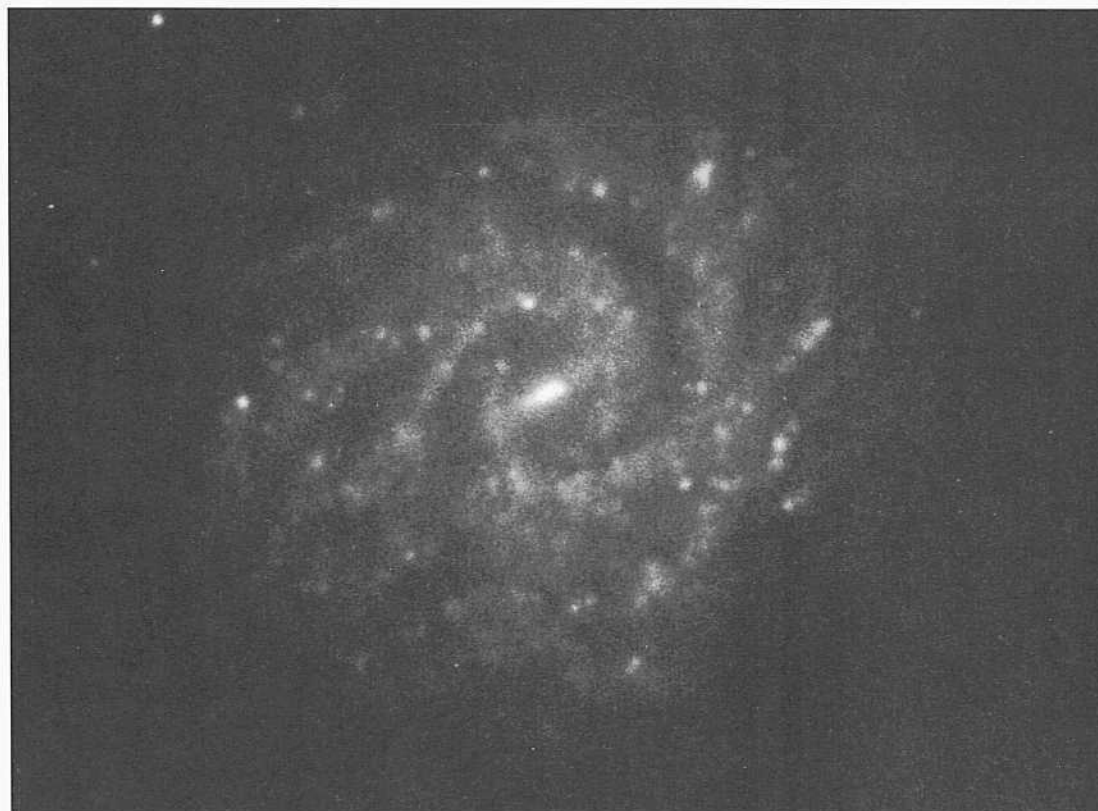
The image here is from an underexposed original plate which, nevertheless, shows a number of HII regions in the weak central bar and in the several multiple arms.

A low-surface-brightness shred (Im on edge) exists at a separation of  $4.1'$ . Its HII-region candidates are of comparable brightness to those in the main galaxy. The redshift of New 1 is  $v_r = 1116 \text{ km s}^{-1}$ . At the redshift distance of 22 Mpc ( $// = 50$ ) the projected linear separation of the shred from New 1 is small at 2.6 kpc.



PANEL  
295

PANEL  
296



*SBC Classification Section (continued)*

NGC 2835      SBC(rs)I.2      pair  
 CD-767-S  
 Feb 21/22, 1979  
 103aO + GG385  
 45 inin

NGC 2835 at a redshift of  $v_o = 624 \text{ km a}^{-1}$  may form a wide physical pair with the S0i(4) galaxy NGC 2784, which has a similar redshift of  $v_o = 451 \text{ km s}^{-1}$ . The separation of the galaxies is  $2.2^\circ$ , giving a projected linear separation of 422 kpc at a mean redshift distance of 10.8 Mpc (similar to separations within the Local Group).

The arms of NGC 2835 are filled with III1-region candidates and stellar associations. The several largest of the HII-region complexes resolve into halo diameters of  $5''$ . Individual stars begin to resolve at about  $B - 21$ .

The Galactic latitude is low at  $b = 18.5^\circ$ , suggesting that some Galactic obscuration may be present over the field.

NGC 2835      SBC(rs)I.2      pair  
 CD-767-S  
 Feb 21/22, 1979  
 103aO + GG385  
 45 inin

This light print from the same original plate used above shows the high incidence of III1 regions in the high-surface-brightness inner arms as well as in the bar.

NGC 33-16      SBC(rs)II.2  
**H-14-S**  
 Jan 5/6, 1951  
 103aO  
 20 min

The two principal arms begin as a partial ring upon which the bar terminates. On one side of the bar the ring-segment begins about  $30^\circ$  downstream (relative to the direction of rotation determined from the sense of the spiral arms) from the inner end of the bar; on the other end of the bar the ring begins  $90^\circ$  downstream. Upon winding outward for less than half a revolution, each arm fragments into the multiple-arm pattern that covers the outer disk.

The redshift is  $v_o = 1138 \text{ km a}^{-1}$ . The III1 regions are unresolved. Individual stars are undoubtedly present beginning at about  $B = 22$ , but a proper separation from the HII-region candidates has not been done (c. 1991).

NGC 1090      SBC(s)I.8      Racine wedge  
 PH-7916-S  
 Nov 7/8, 1980  
 103aO  
 12 inin

The bar in NGC 1090 is weak and subtle. However, two thin, straight dust lanes exist starting from the center: one dust lane crosses in front of the nucleus and the other behind, as in the classical dust pattern in SBb galaxies such as a prototype example NGC 5383 (SBb; panel 168). The presence of these dust lanes, thought to be shock patterns in the gas resulting from highly non-circular motions in the neighborhood of a bar, accounts for the SBC classification.

The two principal inner arms begin at the ends of the bar in the (s) configuration of the NGC 1300 type. A few HII-region candidates exist. The redshift is  $v_o = 2835 \text{ km s}^{-1}$ .



*Sbc Classification Section (continued)*

NGC 4535      **Sbc(s)I.3**      VCC 1555  
CD-801-S  
Feb 24/25, 1979  
103aO +**Wr2c**  
**45** niin

NGC 4535 is one of the largest spirals considered to be a member of the Virgo Cluster. It is shown with other cluster members, enlarged to a common scale, in the Virgo Cluster atlas (Santiago, Bingeli, and Tamiliann 1985a), where it is evident that this galaxy is among the seven largest galaxies associated with the cluster.

HII regions are prevalent in the thin, well-formed, regular arms, the largest of which begin to resolve at about 1".

The nucleus is bright and is star like (unresolved at 0.1"), similar to Seyfert (AGN) nuclei.

Two thin dust lanes winding outward from the central regions are evident. They are curved rather than straight, as in the prototype Sb galaxy NGC 1300, but the pattern as a shock in the central oval potential seems clear.

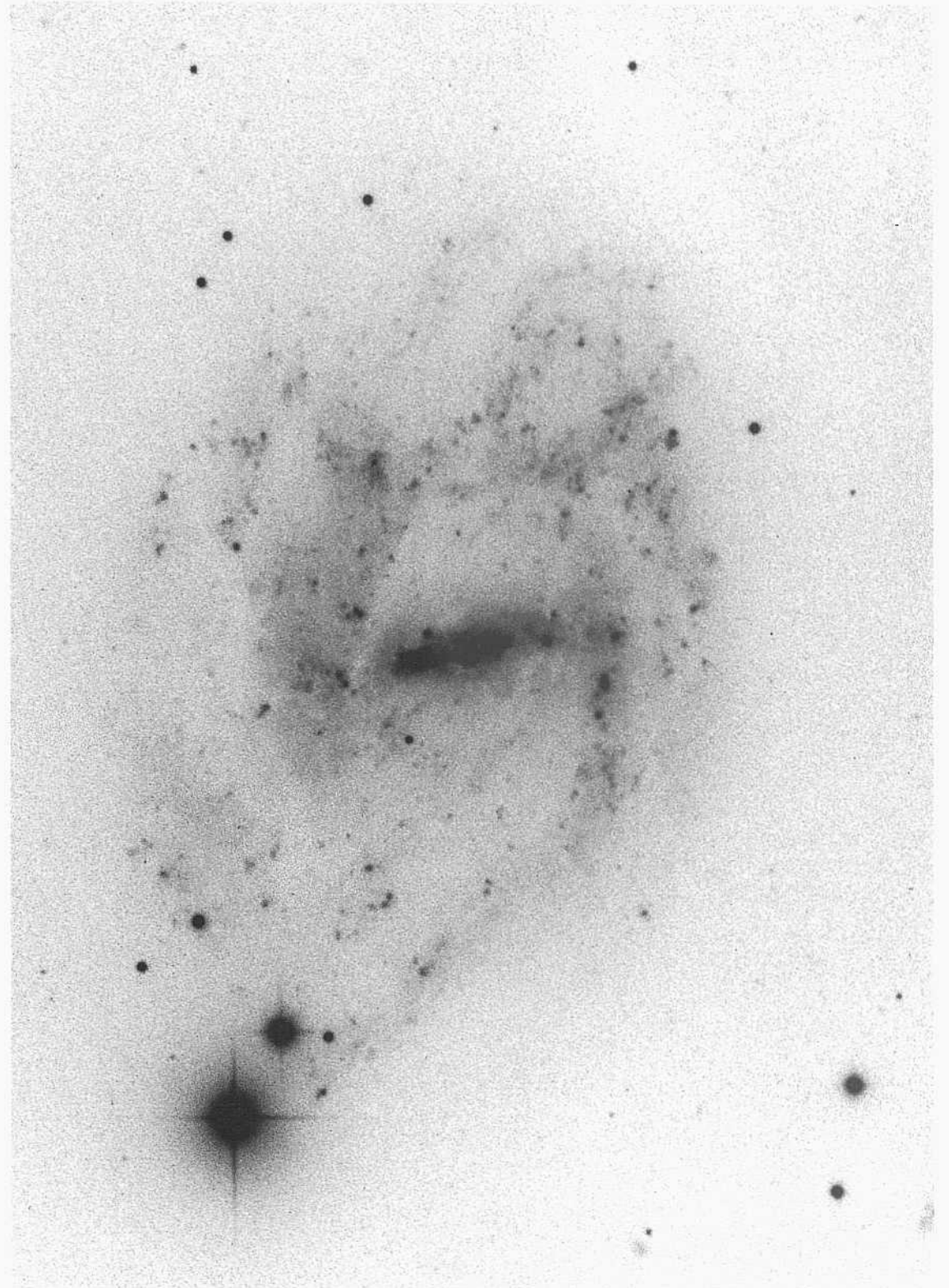
**NGC 7741**      **Sbc(s)H.2**      **HA, p. 49**  
**PH-66-H**      panel S10  
Oct 13/14, 1950  
**103aO**  
30 min

Star formation is occurring throughout the well-formed bar in NGC 7741. It is also occurring everywhere in the arms, which are massive in the sense of Reynolds (1927a,b), in contrast to the thin arms in NGC 4535 shown at the left.

Individual stars are easily resolved and are **identified** as stars by comparing red plates (sensitive to the HII-region Ha emission) and yellow plates (insensitive to emission lines but sensitive to the stellar continuum light). The brightest stars begin to resolve at about  $B = 2.15$ .

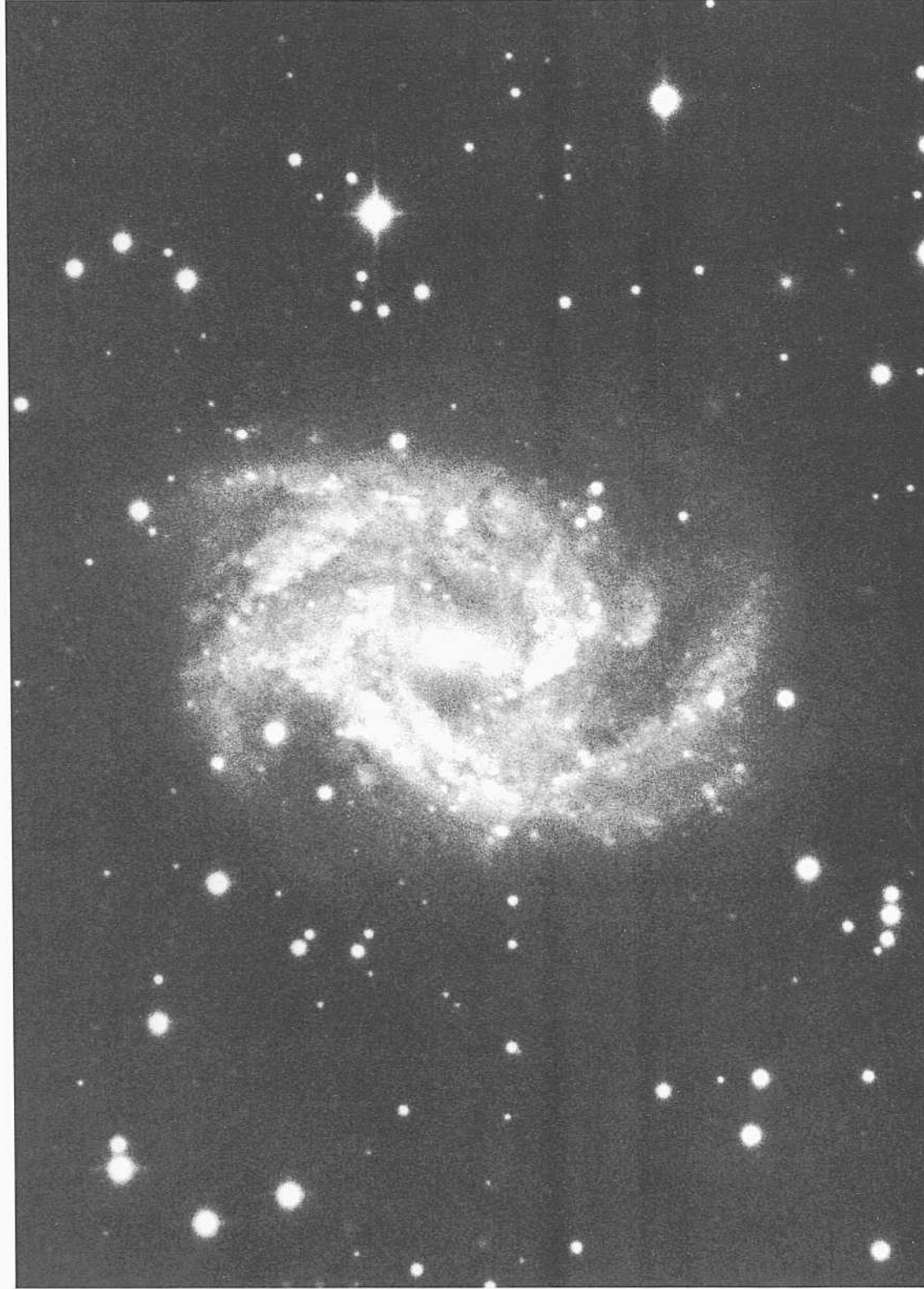
The largest **HII** complex is a superposition of two regions. It has a (halo) major axis diameter of about 3".

The redshift is  $v_{\text{r}} = 1030 \text{ km s}^{-1}$ .



PANEL  
297

PANEL  
298



*SBC Classification Section (continued)*

NGC 5597            SBC(s)II            pair  
 CD-1569-S/Br                            panel S10  
 Aug 10/11, 1980  
 103aO + GG385  
 45 niin

NGC 5597 forms a close physical pair with NGC 5595 (Sc; panel 253) at a separation of 4.0'. The redshifts are  $v_0(5595) = 2501 \text{ km s}^{-1}$  and  $w_0(5597) = 2444 \text{ km s}^{-1}$ . At the mean redshift distance of 49 Mpc ( $z = 0.015$ ) the projected linear separation is small at 58 kpc.

The largest of the several HII regions in NGC 5597 appears to be complex; its halo diameter is about 1.5". Star formation is occurring throughout the arms and in the central bar.

NGC 2525            SBC(s)II            HA, p. 49  
 CD-779-S                            panel S 10  
 Feb 22/23, 1979  
 103aO + GG385  
 45 niin

The two principal arms in NGC 2525 are classic prototypical (s) type in the sense of NGC 1300 but are much later in the classification sequence. The arms are massive in the sense of Reynolds (1927a.li)-

The surface brightness of the arms is very high, making study of the evidently numerous HII regions difficult. The HII regions are unresolved at 1". Individual stars are undoubtedly observed starting at about  $B = 22$ . The redshift of NGC 2525 is  $v_0 = 1395 \text{ km s}^{-1}$ .

The nucleus is starlike at 0.7" resolution.

*SBC Classification Section (continued)*

NGC 1559      **SBC(s)II.2**      **pair?**  
**CD-1676-S**  
**Jan 1/2, 1981**  
**103aO + GG385**  
**7 min**

NGC 1559 is in the complex Dorado region. It is located about 6° south of the center of the dense Dorado Group (de Vaucouleurs 1975, No. G16) and has about the same redshift. Ferguson and Sandage (1990) list  $\langle v_o \rangle = 1056 \text{ km s}^{-1}$  as the mean redshift of the Group. The redshift of NGC 1559 is  $v_o = 1093 \text{ km s}^{-1}$ .

NGC 1559 may form a wide physical pair with IC 2056 (Sc; panel 253) at a separation of 2.6°. The redshift of IC 2056 is  $u_o = 934 \text{ km s}^{-1}$ . At the mean redshift distance of 20 Mpc ( $H = 50$ ) the projected linear separation is 909 kpc, somewhat larger than the distance from our Galaxy to M31 in the Local Group.

HII regions exist throughout the spiral pattern in NGC 1559. The largest are complex, with halo diameters of about 6". Individual stars appear to resolve out of the background at about  $B = 22$ .

NGC 5669      **SBC(s)II**      **companion**  
**CD-2113-S**  
**March 19/20, 1982**  
**103aO + GG385**  
**35 min**

Current star formation is occurring in the bar: HII-region candidates exist there. The brightest HII-region candidate in the arms is compact, bright, and unresolved at the 1.5" level.

The redshift is  $v_u = 1304 \text{ km s}^{-1}$ . A dwarf (BCD?) candidate companion exists at a separation of 6.2' which, at the redshift distance of 26 Mpc ( $H = 50$ ), corresponds with a projected linear separation of 47 kpc.

NGC 3513      **SBC(s)II.2**      **pair**  
**CD-722-S**  
**Feb 1/2, 1979**  
**103aO + GG385**  
**45 min**

NGC 3513 has a similar morphology to NGC 1559 at the upper left.

The galaxy forms a close physical pair with NGC 3511 (Sc; panel 273) at a separation of 10.5'. The redshifts are  $u_o(3511) = 951 \text{ km s}^{-1}$  and  $u_o(3513) = 845 \text{ km s}^{-1}$ . At the mean redshift distance of 18 Mpc ( $H = 50$ ) the projected linear separation is small, at 55 kpc.

The brightest part of the stellar content in NGC 3513 resolves well. The brightest stars individually begin to resolve at about  $B = 21.5$ . The largest of the numerous HII regions resolve into disks at the 2" level.

NGC 1688      **SBC(s)II**  
**CD-1683-S**  
**Jan 2/3, 1980**  
**103aO + GG385**  
**43 min**

As with NGC 1559 at the left, NGC 1688 is in the complex Dorado region and is listed as an extended member of the Dorado Group by Sandage (1975a). The mean redshift of the central part of this group is given by Ferguson and Sandage (1990) as  $\langle v_o \rangle = 1056 \text{ km s}^{-1}$ . The redshift of NGC 1688 is  $v_o = 1040 \text{ km s}^{-1}$ .

The galaxy is listed by Maia, da Costa, and Latham (1989) as a member of their group number 7 in the Dorado region.

HII-region candidates exist in the central bar. The largest of the several HII regions in the arms are unresolved at the 1.5" level. Individual stars have not begun to resolve to the limit of the available plate material at about  $B = 23$ .

NGC 268      **SBC(s)I-H**  
**CD-1557-S/Br**  
**Aug 8/9, 1980**  
**103aO + GG385**  
**45 min**

The thinness, order, and regularity of the arms in this distant galaxy require the early luminosity classification. The nucleus is bright and starlike at the 1" level, as in AGNV.

The redshift is  $v_o = 5659 \text{ km s}^{-1}$ .

NGC 2339      **SBC(s)II**  
**CD-688-Br**  
**Jan 27/28, 1979**  
**103aO + GG385**  
**45 min**

The bar is very weak in NGC 2339, and there is no evidence for recent star formation in it. Few HII regions exist in the multiple-arm pattern. An alternate, better classification might be SBbcII.2, as in the RSA2.

The redshift of NGC 2339 is  $v_o = 2229 \text{ km s}^{-1}$ .

IC 2522      **Sc/SBC(s)I-II**      **pair**  
**CD-198-S**  
**Feb 8/9, 1978**  
**103aO + GG385**  
**40 min**

IC 2522 forms a close apparent physical pair with IC 2523 (ScII-III; not in the RSA) at a separation of 4.4'. A redshift is not available for IC 2523, but the brightness of the HII-region candidates is similar in both galaxies, suggesting equal distances.

The redshift of IC 2522 is  $u_o = 2701 \text{ km s}^{-1}$ . At a redshift distance of 54 Mpc ( $H = 50$ ), the projected linear separation is small at 69 kpc.

IC 1933      **SBC(s)II-III**  
**CD-200-S**  
**Feb 9/10, 1978**  
**103aO + GG385**  
**45 min**

The largest HII regions in IC 1933 are complex with a combined (overlapping) diameter of about 3". Star formation is occurring in the bar as well as robustly in the arms.

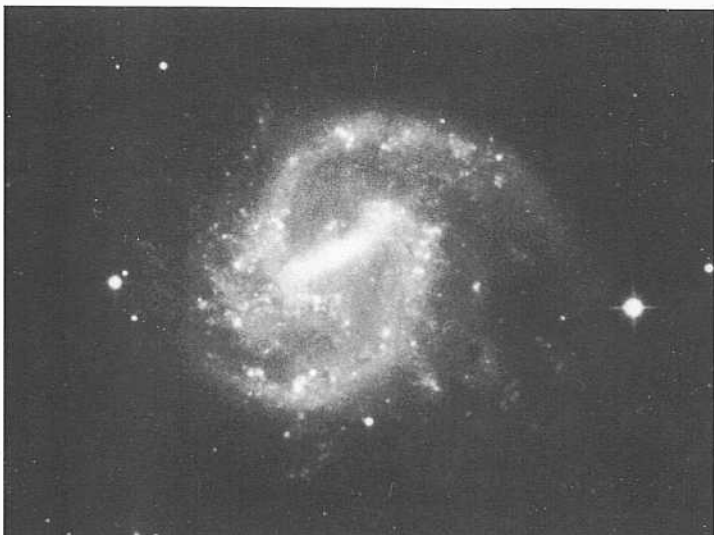
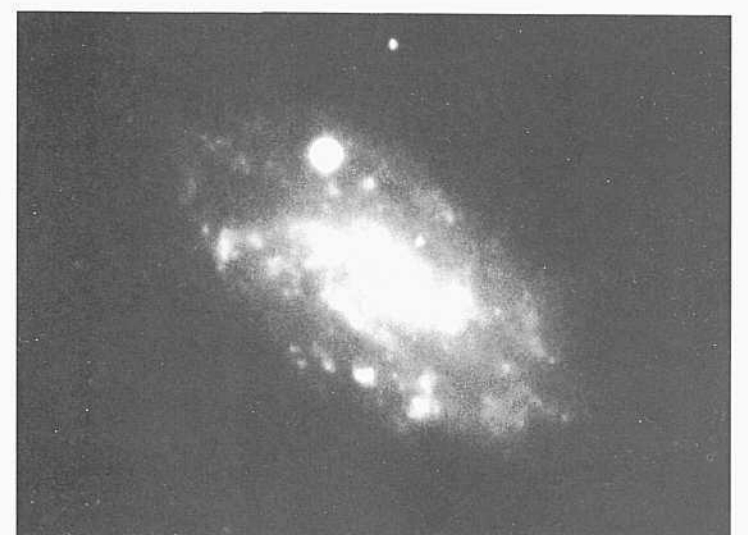
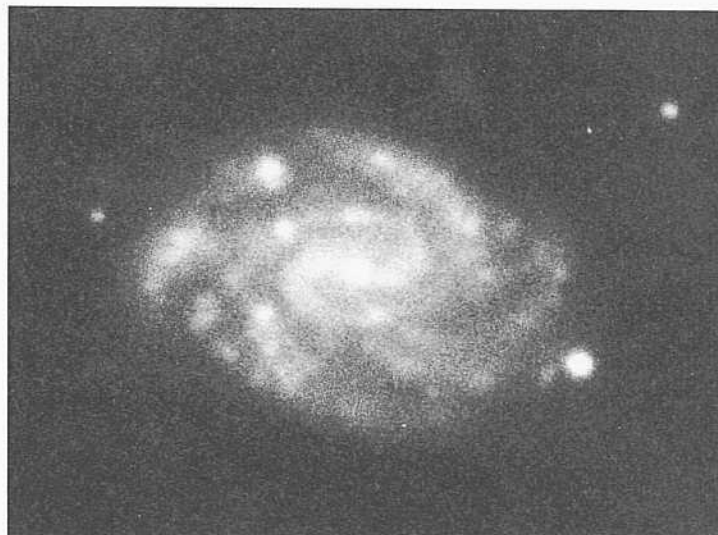
The redshift of IC 1933 is  $v_o = 914 \text{ km s}^{-1}$ .

NGC 3287      **SBC(s)II-III**  
**PH-8018-S**  
**Feb 3/4, 1981**  
**103aO**  
**12 min**

The redshift is  $v_o = 1219 \text{ km s}^{-1}$ .



PANEL  
299



PANEL  
300



*SBC Classification Section (continued)*

NGC 5236	SBC(s)II	Cen A Gr
CD-1320-S/Hr		HA, p. 28
March 12/13, 1980		M83
103aO + GG385		panel 301
45 miii		

NGC 5236 is the brightest spiral in tin-nearby group whose brightest member is NGC 5 128 (Cen A; SO + S pec; panels 45, 46). The mean redshift of the group is about  $\langle v_r \rangle = 2 \text{ HO km s}^{-1}$ . Because the group is so nearby, most members are highly resolved and are important for the calibration of the extragalactic distance scale.

The surface brightness of NGC 5236 is exceedingly high in the arms, which are massive in the sense of Reynolds (1927a,b) and therefore cover most of the disk.

The dust lanes are intricate and, in general, are closely associated with the luminous arms on the insides of these arms, as usual.

The range of the surface-brightness scale is so large that two levels of the image from the original negative are illustrated. The heavy image is on this panel; a lighter print showing the dust lanes and the central regions is on the following panel.

Far-outlying associations exist beyond the borders of this print. They are similar to the associations in M31 Field TV of Baade and Swope (1963), which is 96' from the center of M31. It is in these outlying fields, where the surface brightness of the background disk of M83 is low and the dust is negligible, that searches for Cepheids will be made. Several such remote associations exist; the farthest, easily visible on the Las Campanas 100-inch plates, is at a radial distance of 11' from the center, off the borders of this print. At the estimated distance of 6 Mpc for M83 this angular distance corresponds to a linear distance from the center of 20 kpc. The distance of Field IV from the center of M31 is similar, at 24 kpc.



*SBC Classification Section (continued)*

NGC 5236	SBC(s)H	Cen A Gr
CD-1320-S/Br		HA, p. 28
March 12/13, 1980		M83
103aO + GG385		panel 300

45 mill

This light **print** of M83 shows the intricate dust lanes and the central oval luminosity **distribution requiring** the barred classification. Consistent **with** this classification are the two major **thin** dust lanes in the central oval. The dust lane pattern, the signature of a bar potential, is due to the response of the interstellar gas to that potential, resulting in two hydrodynamic shock fronts that appear as straight dust lanes. The **pattern** has been discussed in many of the previous descriptions of prototypical SBb galaxies such as NGC 1300 (panels 154, S8).

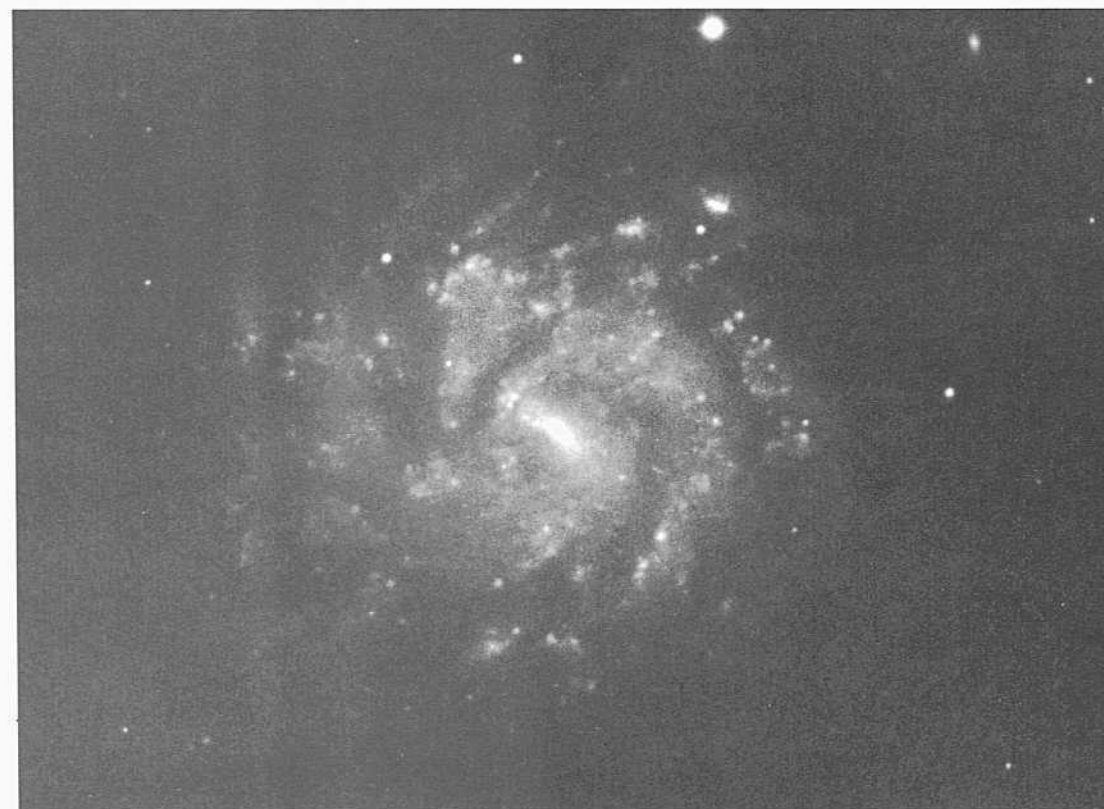
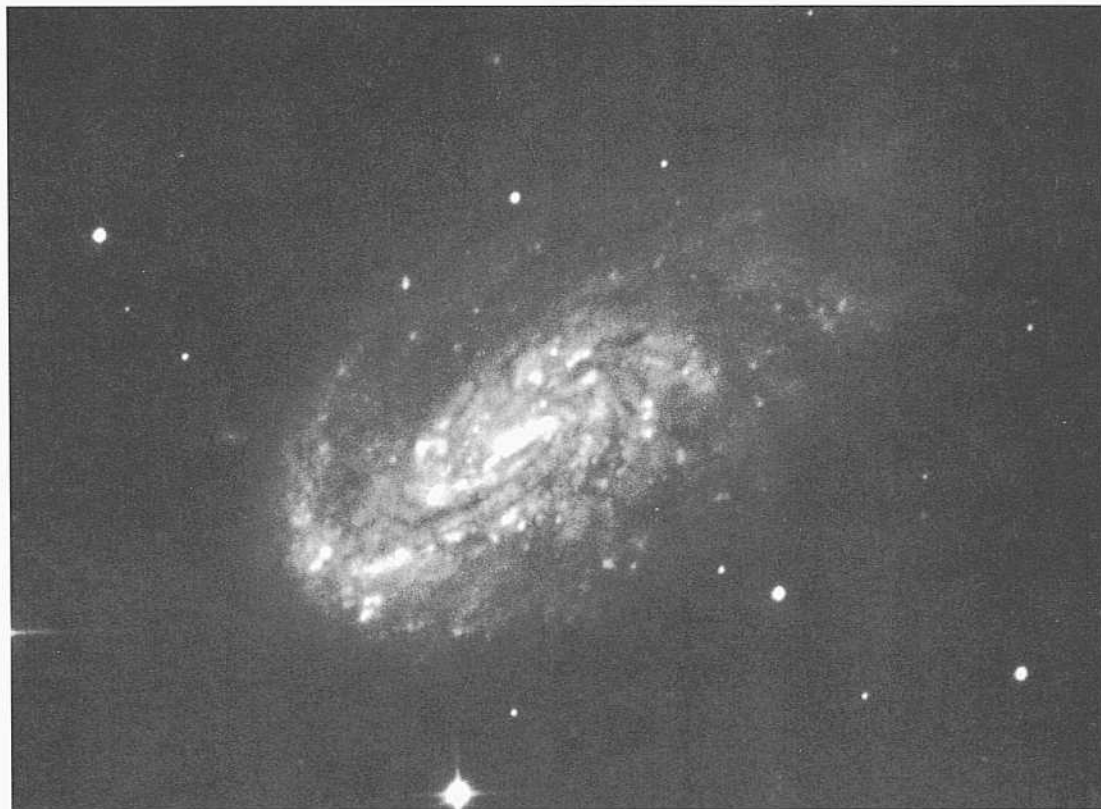
One of the central dust lanes cuts across the front of the nuclear region; the other appears to duck behind. The pattern is identical to that in the prototypical SBb galaxy NGC 5383 (panel 168).

The brightest individual stars are easily resolved throughout the image of **M83**. However, their photometry in the high-surface-brightness central regions is difficult to interpret because of the evident high internal absorption throughout the inner disk and arms. We estimate that the brightest stars begin to resolve at about  $B = 17$ .



PANEL  
301

PANEL  
302



*SBc Classification Section (continued)*

NGC 5334 SBc(rs)II  
 CD-1514-S/Br  
 Aug 5/6, 1980  
 103aO + GG385  
 45 min

NGC 5334 may be IC 4338 listed in Dreyer's Second Index Catalog, although the RA positions differ by 1.5 seconds of time.

The surface brightness of NGC 5334 is exceptionally low, enhanced in this print by contrast control in the darkroom in progressing from the original negative to the final image.

There are a few IHI-region candidates in the bar and in the arms, but none are resolved at the 1.5" level. The redshift of NGC 5334 is  $v_o = 1237 \text{ km s}^{-1}$ .

NGC 685 SBc(rs)II  
 CD-2016-Bedke/Gregory  
 Oct 25/26, 1981  
 103aO + GG385  
 45 min

Many individual knots are present in the bar and in the massive arms of NGC 685. These are likely to be HII regions and brightest resolved stars, but the distinctions have not yet been made (1991) by standard techniques. The resolution is sufficiently promising and the surface brightness is low enough in the arms to make NGC 685 a prime galaxy for more-detailed study of its stellar content.

The largest HII regions probably begin to resolve into disks at about the 1" level. The redshift of NGC 685 is  $v_o = 1306 \text{ km s}^{-1}$ .

NGC4654 SBc(rs)II-IH VCC 19JS7  
 CD-2176-S  
 March 28/29, 1982  
 103nO  
 50 min

NGC 4654 is among the 15 largest spirals considered to be members of the Virgo Cluster. Its isophotal diameter is large at  $l \rightarrow r = 4.7'$ . A comparison of its angular size with other large spirals in the cluster can be seen in the atlas of Virgo Cluster spirals (Sandage, Binggeli, and Tammaun 1985a, panel 6).

As with the other large spirals in this cluster, NGC 4654 is in the outskirts of the cluster, away from either subcluster A or B (compare Binggeli, Tammann, and Sandage 1987). It is located  $3.3^\circ$  east (and slightly north) of NGC 4486, which is associated with Virgo subcluster A.

Mil regions are present in the bar. The nucleus is brilliant and starlike at the 1" level. The brightest HII regions in the arms are abundant and have a heterochromatic blue magnitude of about  $B = 20$ . The galaxy is a good candidate for resolution into individual stars using a high-resolution telescope.

The redshift is  $v_o = 926 \text{ km s}^{-1}$  but, being in the Virgo Cluster, this is as much a virial velocity as a distance indicator.

NGC 5885 SBc(s)II  
 CD-1392-S/Br  
 March 21/22, 1980  
 103aO + GG385  
 45 min

NGC 5885 is a beautifully symmetric barred spiral, similar to but not quite as regular as its Sc counterpart NGC 1232 (Sc; panels 2.16, S1.3), or more closely similar to NGC 3184 (Sc; panels 23.7, S5) or IC 5332 (Sc; panel 2.59).

The bar is short. The two principal inner arms spring from the ends of the bar, as in NGC 1300 (SBb; panels 15.4, S8). They then branch into the thick multiple-armed structure in the outer regions.

Many Mil regions exist, defining the centers of the luminous arms. The regions are unresolved at the 0.7" level. The redshift of NGC 5885 is  $v_o = 1879 \text{ km s}^{-1}$ .

*SBC Classification Section (continued)*

NGC 3319      SBC(s)II.4  
 PH-7126-S  
 Jan 31/Feb 1, 1976  
 103aO + GG385  
 35 niin

NGC 3319 is a **highly** resolved, nearby galaxy, in which **robust star formation is occurring** in the **high-surface-brightness**, lumpy bar. The two spiral arms spring from the ends of the **bar** in the (s) configuration of the NGC 1300 (SBb; panels **154, S8**) type. The arms are moderately **chaotic**; hence the late luminosity class is shown.

Individual **brightest** stars are clearly resolved in the arms, starting at about  $B = 19$ , but more-precise data **require** photometry and the separation of stars from the several **bright HII-region** candidates using standard methods.

The largest of the **HII** regions **probably** resolve into disks at the 2" level. The **redshift** of NGC 3319 is  $v_r = 776 \text{ km s}^{-1}$ .

NGC 7496      SBC(s)II.8      MCL Gr #40  
 CD-1163-Br      panel S10  
 Aug 22/23, 1979  
 103aO + GG385  
 45 niin

NGC 7496 is in a complex region of galaxies whose redshifts are about  $u_0 = 1400 \text{ km s}^{-1}$ . The **region** has been mapped in redshift space by Maia, da Costa, and Latham (1989). They assign NGC 7496 to a group of more than 30 galaxies **for** which they have redshifts within projected linear distances of less than 2 Mpc. Among the RSA galaxies assigned to the group are IC 5325 (Se; panel 268), NGC 7462 (SBc; panel 311), NGC 7496 (here), NGC 7531 (She; panel 175), NGC 7552 (SBb; panel 156), NGC 7582 (SBab; panel 122), NGC 7590 (Sc), and NGC 7599 (Sell). The mean redshift assigned to the group by Maia, da Costa, and Latham is  $\langle v_r \rangle = 1390 \text{ km s}^{-1}$ .

**HII regions** are abundant in one of the arms near one end of the bar of NGC 7496. This is the region where the maximum shock **pressure** occurs, often seen in the hydrodynamic simulations (compare **Prendergast** 1962, 1983; Huntley, Sanders, and Roberts 1978; Huntley 1978, 1980).

A few **individual brightest** stars are probably identifiable, starting at about  $B = 20$ . The redshift of NGC 7496 is  $v_r = 1444 \text{ km s}^{-1}$ .

IC 5273      SBC(s)II-III      Grus Gr  
 CD-1546-S/Br  
 Aug 7/8, 1980  
 103aO + GG385  
 45 niin

IC 5273 has high-surface-brightness, **tightly** wound massive arms that cover most of the disk. It has been assigned to the loose, widely separated Grus Group (Sandage 1975b) whose mean redshift is listed as  $\langle v_r \rangle = 1581 \text{ km s}^{-1}$ . The redshift of IC 5273 is  $v_r = 1296 \text{ km s}^{-1}$ .

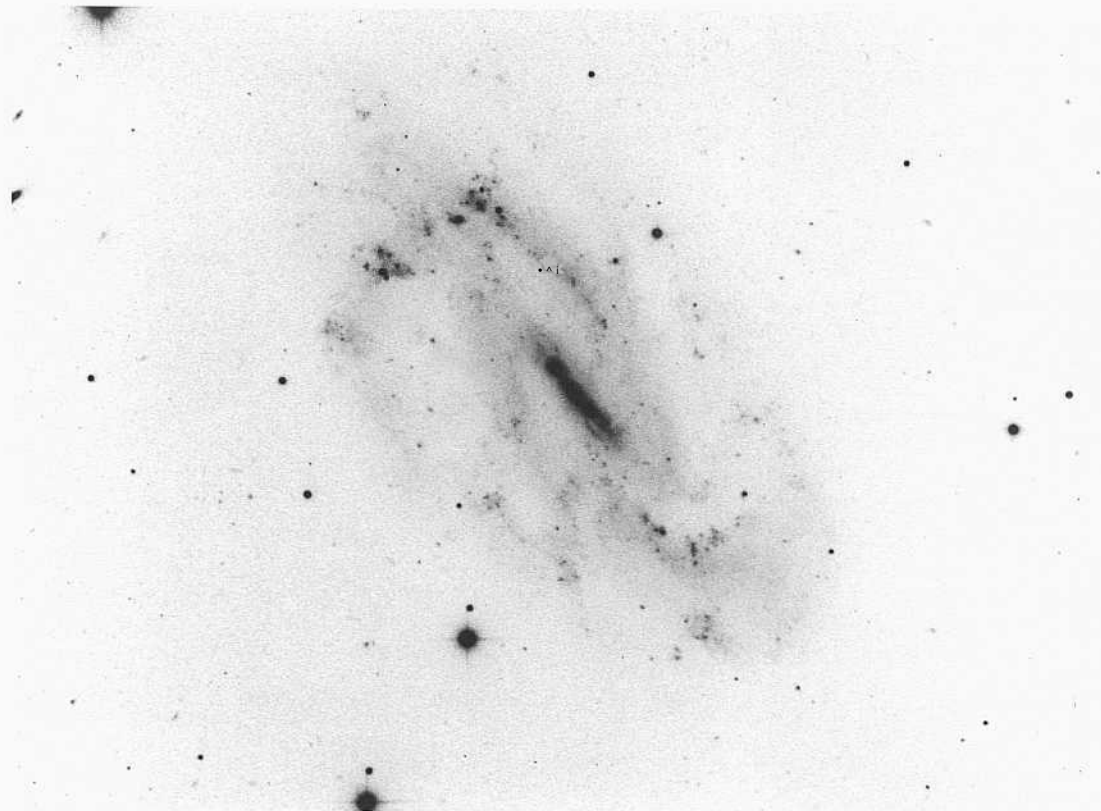
Several of the brightest **HII** regions are complex and resolve at about the 2" level.

NGC 925      SBC(s)II-III      HA, p. 37  
 PH-71-S  
 Dec 26/27, 1951  
 103aO + WG2  
 15 niin

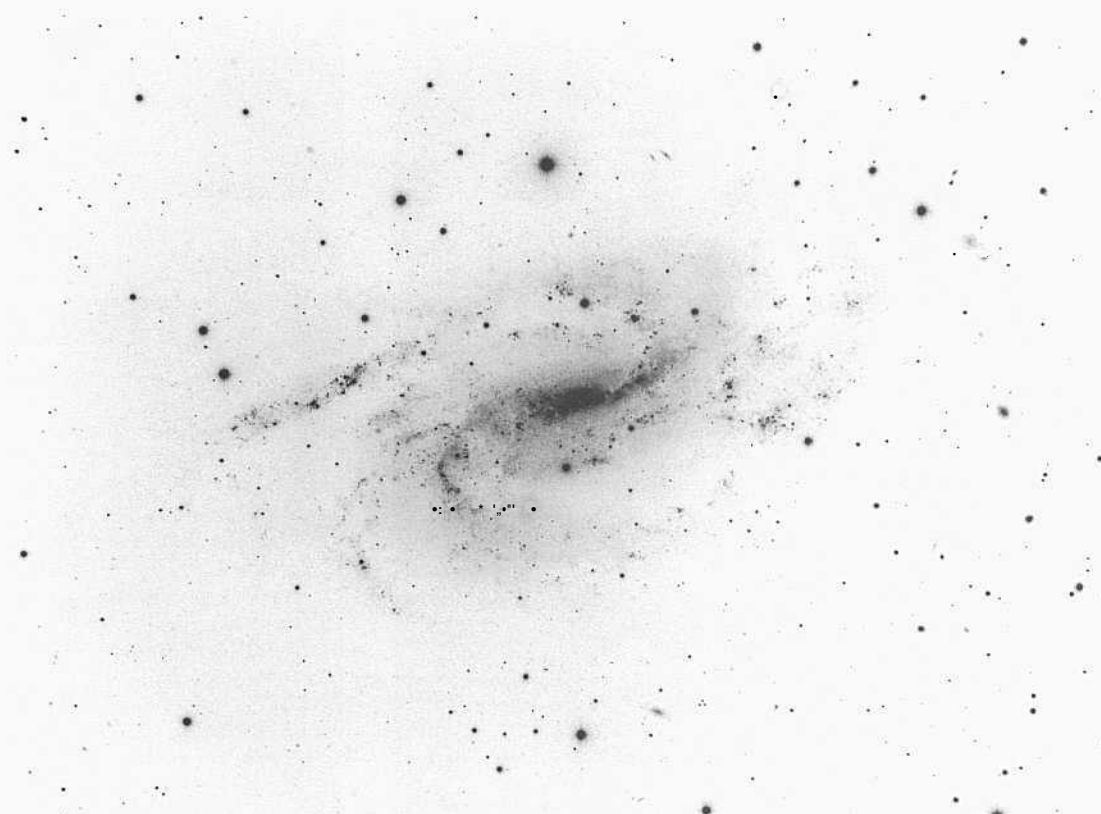
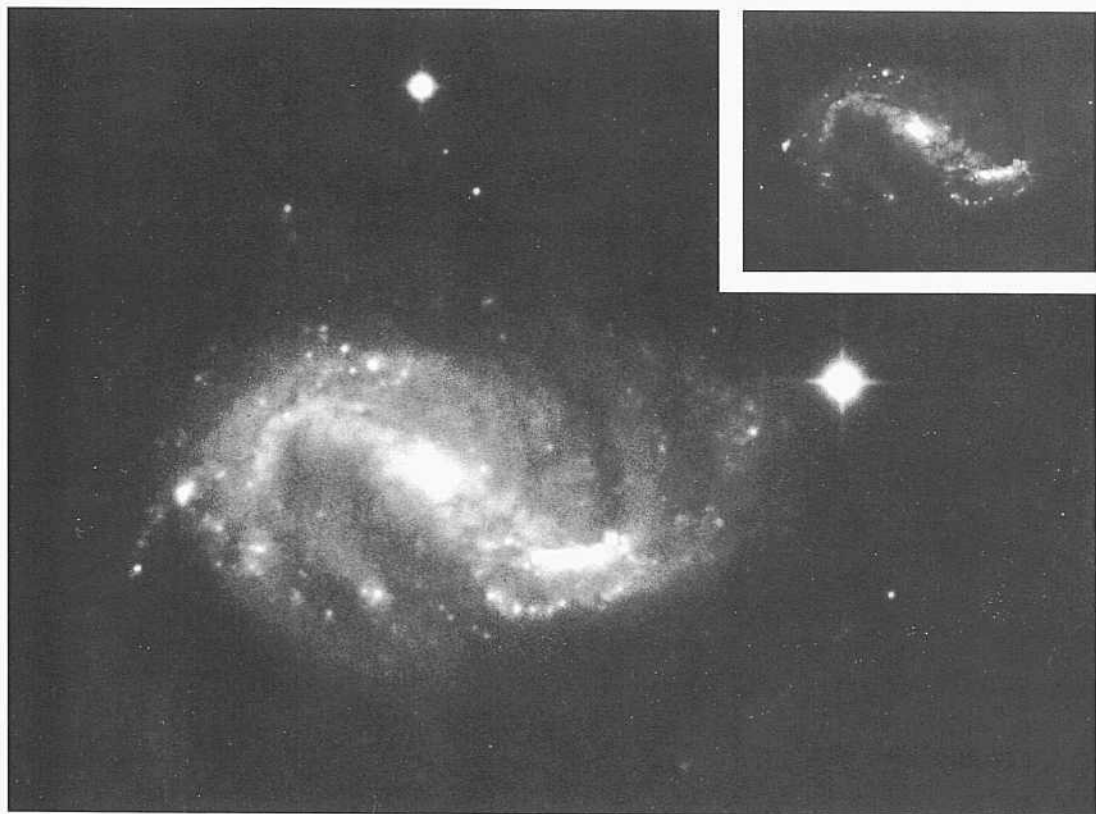
NGC 925 is one of the gems in the sky. It is highly resolved into individual stars starting at about  $B = 20$ . Numerous HII-region complexes exist, the largest of which have angular diameters of about 5".

Stellar associations can be identified in the arms. The bar is full of **HII** regions and resolved stars. NGC 925 is one of the premier galaxies **not** far beyond the Local Group where studies of the stellar content will be important for the distance-scale problem. Cepheids should be easy to detect if the **photometry** can be pushed to  $B = 26$ .

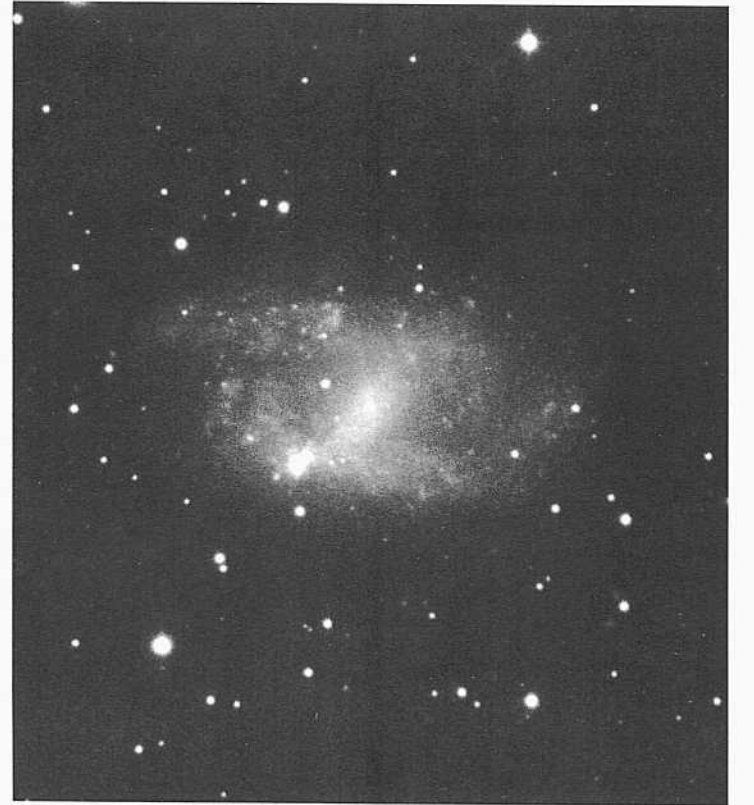
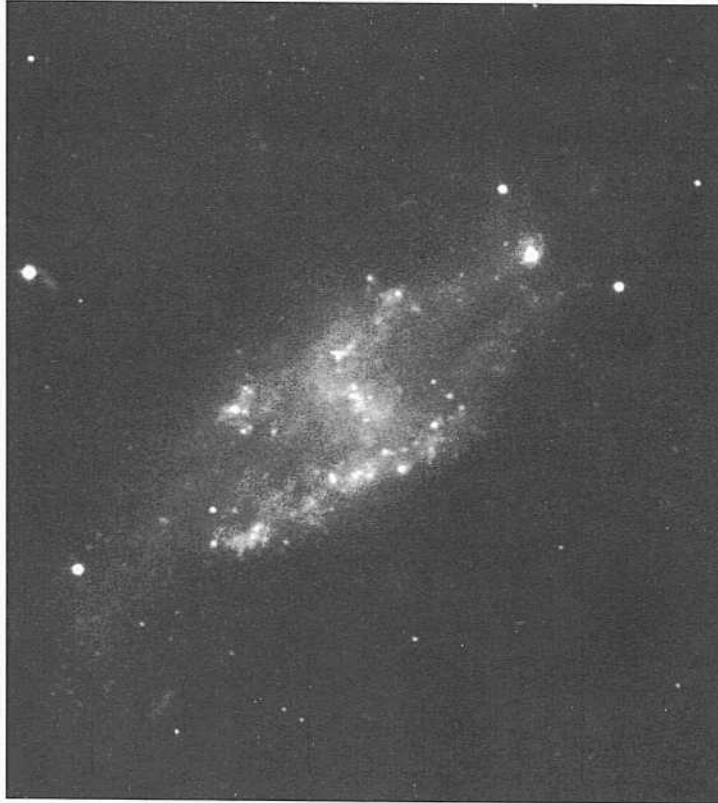
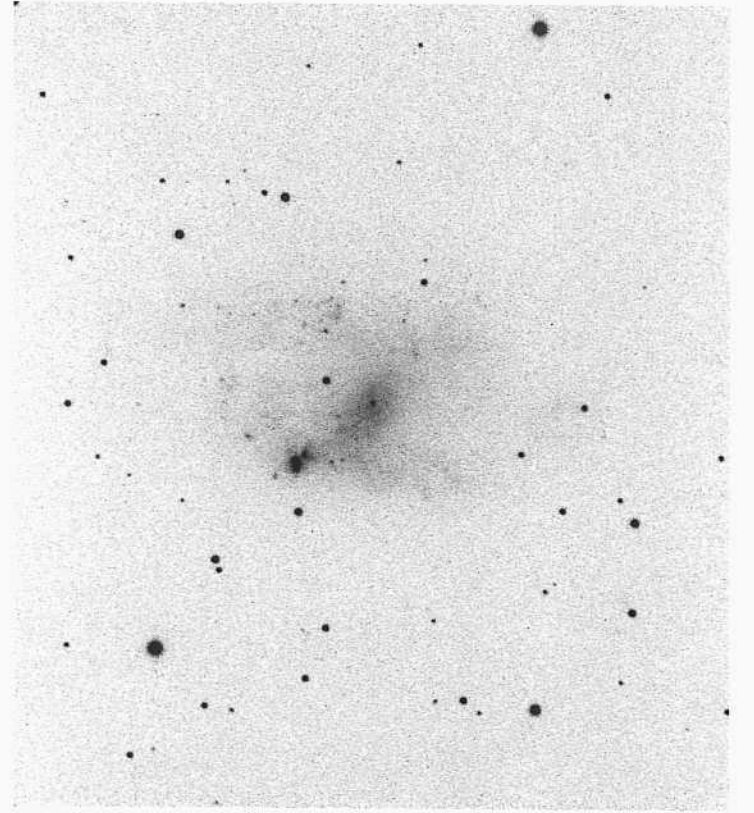
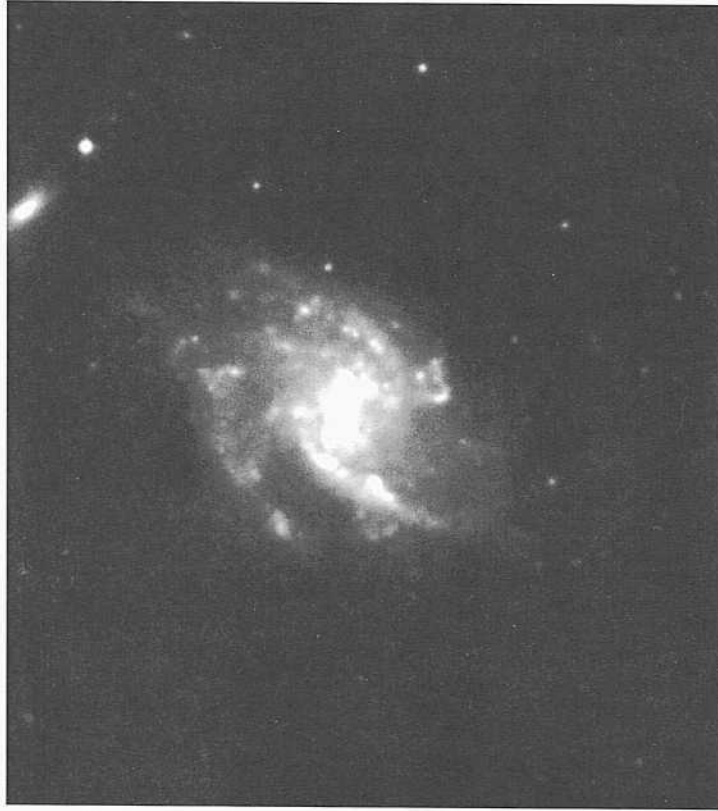
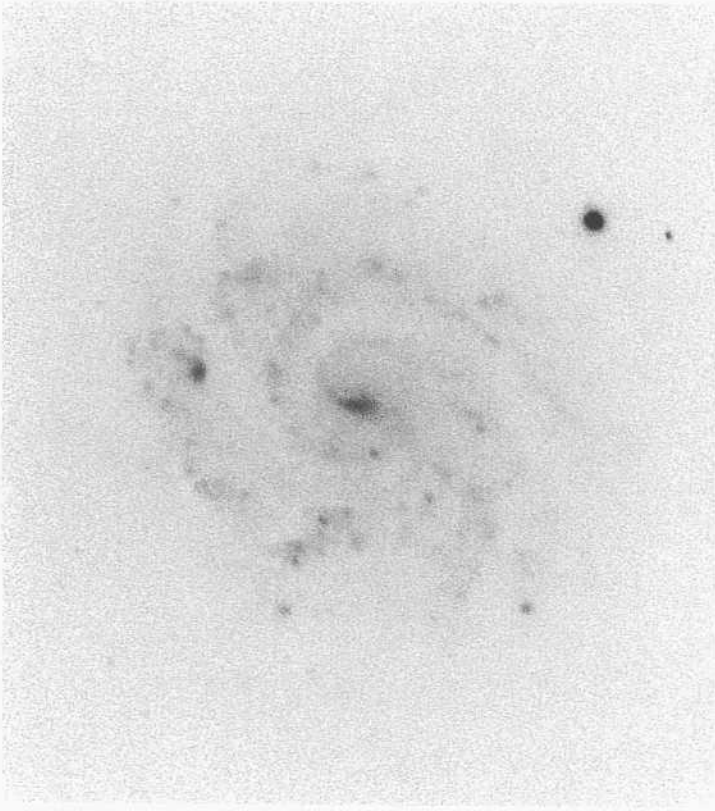
The redshift of NGC 925 is  $v_r = 792 \text{ km s}^{-1}$ .



PANEL  
303



PANEL  
304



NGC 6412 SBc(s)/Sc(s)I-II  
PH-7685-S  
Sep 26/27, 1979  
103aO  
10 min

The arms of the **multiple-spiral** pattern in NGC 6412 are thin and regular, similar to the pattern in NGC 1232 (Se; panels 216, S13); hence the early luminosity class is **required**. The surface brightness of the arm pattern is low.

The bar is short. The two principal arms near the center spring from the ends of the bar in the (s) pattern.

The largest of the several **HII** regions has a halo diameter of about 3". The redshift of NGC 6412 is  $v_r = 1568 \text{ km s}^{-1}$ .

NGC 1341 SBc(s)H-III FCC 62  
CD-1667-S  
Dec 31/Jan 1, 1981  
103aO  
75 min

NGC 1341 is listed as a member of the Fornax Cluster in the Fornax Cluster Catalog (Ferguson 1989). It is located  $2.7^\circ$  (which is 3.8 cluster core radii) southwest of NGC 1399, which is the cluster center. The redshift at  $v_o = 1793 \text{ km s}^{-1}$  is high compared with the adopted mean velocity of  $\langle v_o \rangle = 1366 \text{ km s}^{-1}$  (Ferguson and Sandage 1990).

NGC 4519 SBc(rs)H.2 VCC 1508  
CD-801-S  
Feb 24/25, 1979  
103aO + Wr2c  
45 min

NGC 4519 is near NGC 4472, which is the central galaxy of **subcluster B** of the Virgo Cluster (Binggeli, Tammann, and Sandage 1987). It is **illustrated** in [the Atlas of Virgo Cluster Spiral Galaxies (Sandage, Binggeli, and Tammann 1985a), where it can be **compared** with other cluster members because all images are enlarged to a common scale.

The spiral pattern is similar to that in NGC 4597, below, and NGC 5398, shown in **the two** prints at the right. A central bar exists from which the arms spring, **but** the arms exist on both sides of the ends of the bar. It is the same pattern of a broken (incomplete) ring seen in earlier barred SBa and SBb(rs) types, **but** the **stellar** content is much later in NGC 4519 here and in the two remaining galaxies on this page.

Many **HII** regions exist in the bar and in the arms of NGC 4519. The largest of these resolve at about the 2" level. The redshift is  $v_o = 1094 \text{ km s}^{-1}$ , close to the adopted mean redshift of the Virgo Cluster,  $\langle v_o \rangle = 976 \text{ km s}^{-1}$  (Sandage and Tammann 1990).

NGC 4597 SBc(r)III:  
CD-1400-S/Br  
March 22/23, 1980  
103aO  
75 min

NGC 4597 is in the complex region once called the southern extension of the Virgo Cluster but now called the ridge-line region of the Local Supercluster, south of subcluster B of the Virgo Cluster.

The brightest parts of the stellar content of NGC 4597 are highly resolved into many **HII** regions and perhaps even brightest stars. The largest HII region, similar to NGC 604 in M33, has a core diameter of 5" and a halo diameter of 11". The redshift is  $v_o = 851 \text{ km s}^{-1}$ .

Because the disk surface brightness is low, NGC 4597 is a prime candidate for a major effort to study its bright stellar content for calibration purposes.

NGC 5398 SBc(s)II-III  
CD-1364-S/Br  
March 16/17, 1980  
103aO + GG385  
50 min

NGC 5398 has a **spiral-arm morphology** that is **remarkably** similar to that of NGC 4519\* at tin- left and NGC 4597. below in **the middle column**.


The heavy print here shows tin<sup>1</sup> resolution into stars and **III** regions in the thick massive arms, which, **nevertheless** have a low surface brightness. The **resolution** into stars begins at about  $\{ = 2.1$ .

The largest of the many III regions is complex, with a halo **diameter** of about 6". Measurement of the short-exposure plate used for the print below shows each of the components to have diameters of about 2". The redshift of NGC 5398 is  $v_r = 984 \text{ km s}^{-1}$ .

NGC 5398 SBc(s)II-III  
CD-1365-S/Br  
March 16/17, 1980  
103aO + GG385  
10 min

The bar is oval-like and is of low surface brightness. The nucleus is unresolved at the 0.7" level. It and the oval (which is the bar) **resemble** the dE,N dwarf elliptical morphology. The form would be classified as dE,N if the spiral arms were absent.




 The two galaxies on this panel are the Sbc prototype examples of the multiple-arm pattern seen in the Sc counterparts NGC 1232 (Scl; panels 216, S13) and M101 (Sd; panel 218).

NGC 5643      Sbc(s)II-III  
 CD-1342-S/Br  
 March 14/15, 1980  
 103aO + GG385  
 40 niin

Although NGC 5643 is in low Galactic latitude ( $b = 1.5^\circ$ ) with attendant high foreground contamination, it is nevertheless clear that robust current star formation is occurring in the nearly **circular** arms; very many **MII**-region candidates exist. **Individual** stars also begin to resolve at about  $B = 22$ .

The central region is oval **rather** than bar-like. The straight, thin dust lane on one side of **the** center, characteristic of barred spirals, is evidence for strong **noncircular** motions in the neighborhood of the central oval potential; the lane is the response of the gas to hydrodynamic shocks due to these noncircular motions.

The faintness of a corresponding straight lane on the opposite side of the center may be an aspect effect; these lanes may not lie entirely in the plane of the disk, evidenced also by **their** crossing over and under the nuclear region, as is clear in NGC 5383 (SBb; Hubble Atlas, p. 46; panel 168 here).

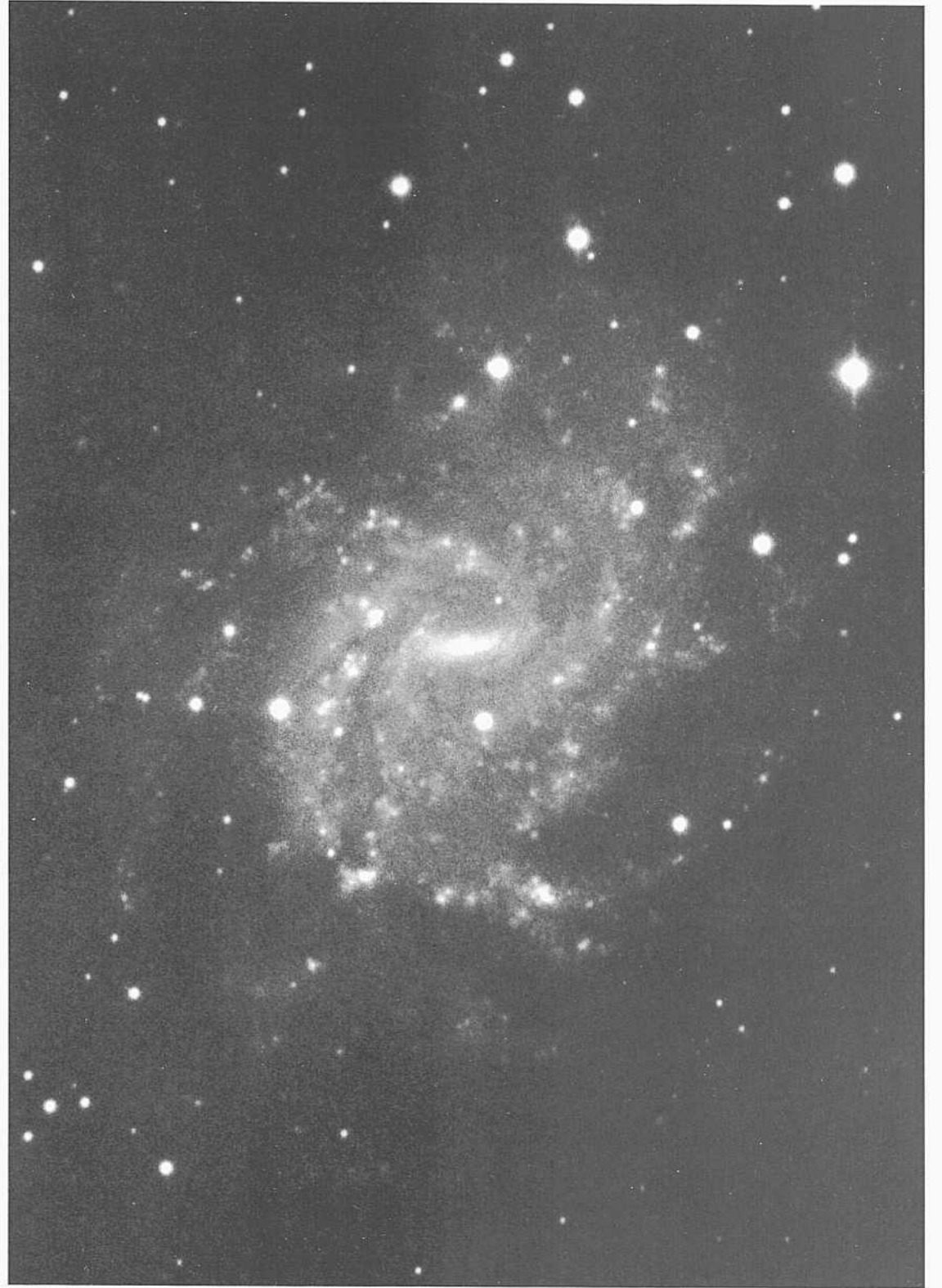
The redshift of NGC 5643 is  $v_r = 947 \text{ km s}^{-1}$ .

NGC 5556      Sbc(sr)II-III      companions  
 CD-1353-S/Br  
 March 15/16, 1980  
 103aO + GG385  
 45 iiiin

The bar in NGC 5556 is short but real. Current star formation is occurring in it. The two main inner arms spring from the ends of the bar and thereafter fragment almost immediately into the multiple-arm pattern of moderate geometrical entropy in the outer regions.

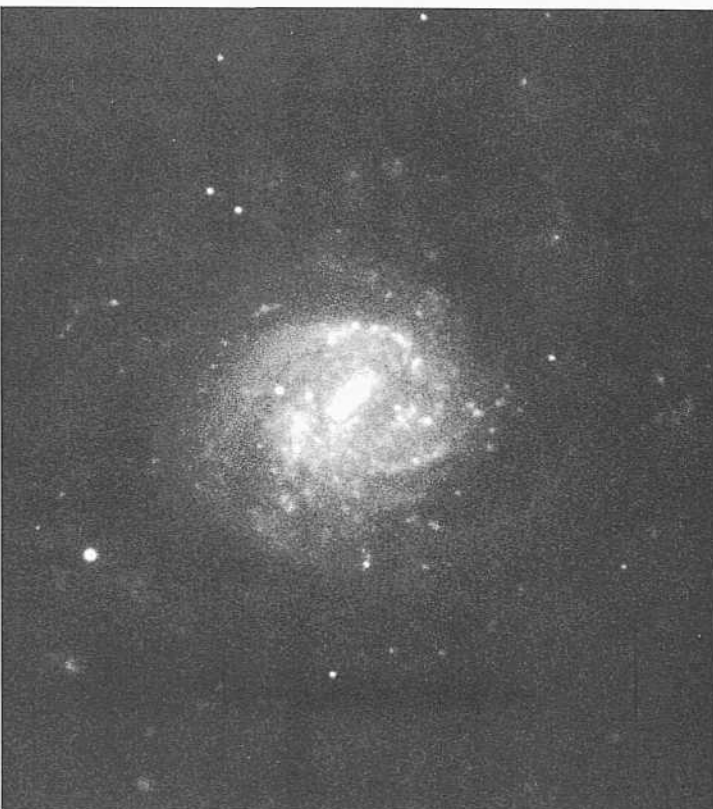
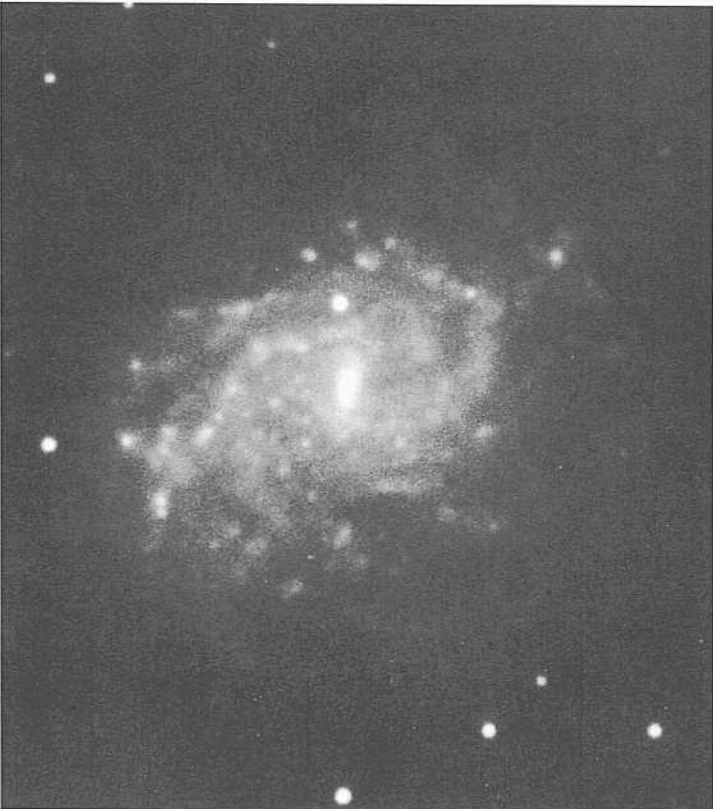
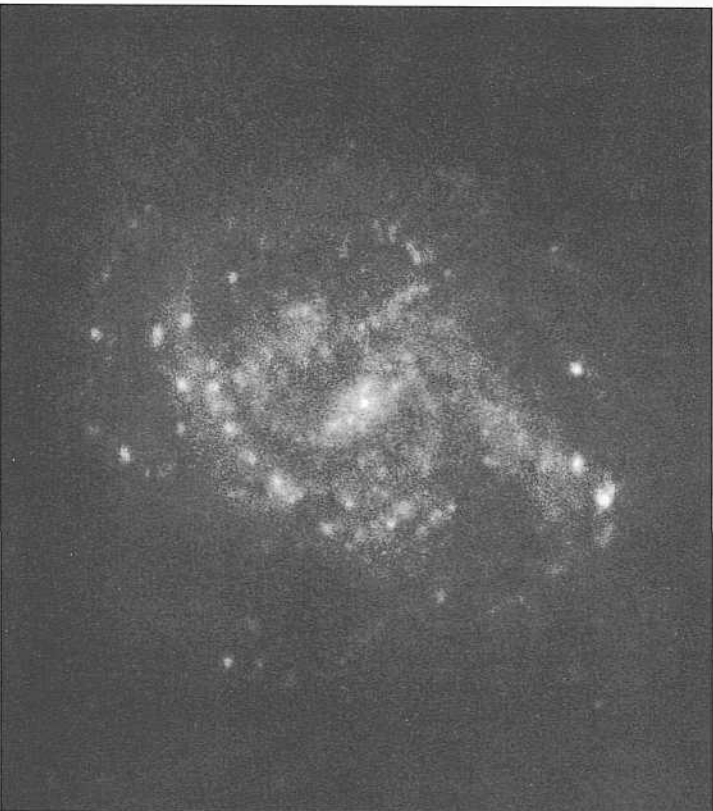
Very many **III** regions exist in the spiral pattern, **the** largest of which begin to resolve at about the 1" level. Individual brightest stars are evident in the image beginning at about  $B = 22$ . The redshift of NGC 5556 is  $v_r = 1163 \text{ km s}^{-1}$ .

A likely **companion** (Anonymous; SniII), with similar resolution of its stellar content, exists at a separation of  $9.4'$ . The projected linear separation is 64 kpc at a redshift distance of 23 Mpc ( $// = 50$ ). Several additional dwarf candidate companions exist in the immediate field. The galaxy and its companions are prime objects to study at higher resolution and brightness levels for the calibration of the extragalactic distance scale.



PANEL  
305

PANEL  
306



**M**any of the galaxies on this panel are highly resolved into individual stars, and are therefore useful for calibration studies of the extragalactic distance scale.

NGC 1637 SBc(s)II.3 HA, p. 30  
 PH-68-MH  
 Feb 15/16, 1950  
 103aO  
 30 niin

The central region of NGC 1637 has no bar but has an oval luminosity distribution. One nearly straight dust lane exists on one side of the center, characteristic of barred spirals.

Individual brightest stars clearly begin to resolve at  $B$  brighter than 22 mag, but the confusion with very many HII-region candidates must be solved before precise data can be interpreted.

The largest HII regions resolve into disks at about the 1.5" level. The redshift of NGC 1637 is  $v_o = 715 \text{ km s}^{-1}$ .

NGC 5068 SBc(s)II-III  
 CD-1855-HB  
 April 4/5, 1981  
 103aO  
 75 niin

The angular size of NGC 5068 is large at  $\theta_{25} = 6.9'$ . It is highly resolved into HII-region candidates and individual brightest stars that could be as bright as  $B = 18.5$  but which must be individually separated from the HII-region candidates before the data can be interpreted.

Star formation is occurring in the bar. Many classical OB associations can be identified in the arms. The largest HII region resolves at a diameter (halo) of about 4". The redshift of NGC 5068 is  $v_o = 443 \text{ km s}^{-1}$ .

IC 749 SBc(rs)II-III Karachenteev 313  
 PH-7641-S  
 April 28/29, 1979  
 103aO  
 12 min

IC 749 forms a close physical pair with IC 750 (Sb?; panel 195) at a separation of 3.3'. The respective  $v_o$  redshifts are  $u_o(749) = 827 \text{ km s}^{-1}$  and  $u_o(750) = 742 \text{ km s}^{-1}$ . The pair may be part of the extended  $\langle v_o \rangle = 750 \text{ km s}^{-1}$  group in the Ursa Major region that also contains NGC 3675 (Sb; panels 139, S4, S13, S14), NGC 3769 (SBc; panel 311), NGC 3782 (SBcd; panel 328), NGC 3949 (Sc; panel 265), NGC 4051 (Sbc; panel 180), NGC 4242 (SBd; panel 322), and others listed in Group 10 by de Vaucouleurs (1975) and called the CVn II Cloud there.

At an adopted redshift distance of 16 Mpc ( $H = 50$ ), the projected linear separation of IC 749 and IC 750 is small at 15 kpc. There is little or no evidence for tidal interaction between the pair; the true linear separation must be considerably larger than this minimum projected distance.

Many HII-region candidates exist in the well-formed arms of IC 749. Resolution into individual stars is also present, starting probably near  $B = 22$ .

NGC 7070 SBc(s)H pair  
 CD-1155-Br  
 April 22/23, 1979  
 103aO + GG385  
 45 niin

NGC 7070 forms an apparent pair with NGC 7072 (Sell, high surface brightness) at a separation of 4.5'. The redshift of NGC 7070 is  $v_o = 2365 \text{ km s}^{-1}$ . The redshift of NGC 7072 is unknown (c. 1990), but the resolution of its stellar content is similar to that in NGC 7070, suggesting a common distance. At a redshift distance of 47 Mpc ( $H = 50$ ) the projected linear separation would be 62 kpc.

The arms of NGC 7070 are thin and regular. The luminosity class of II, assigned here, differs from the II-II class listed in the RSA.

NGC 4116 SB«(i)II-III pair  
 CD-1847-HB  
 April 3/1, 1981  
 103aO  
 75 mill

NGC II I 6 forms a physical pair with NGC 4123 (Sm.c; panels 201, Hii) at a separation of 14'. The respective redshifts are  $u_o(1116) = 1140 \text{ km s}^{-1}$  and  $u_o(4123) = 1157 \text{ km s}^{-1}$ . At a redshift distance of 23 Mpc ( $H = 50$ ) the projected linear separation of the pair is 94 kpc.

Many HII-region candidates exist in the bar and in the arm pattern. The nucleus in the center of the bar is starlike; it is unresolved at the 0.7" level.

NGC 255 SBc(rs)II-III  
 PH-7836-S  
 Sep 3/4, 1980  
 103aO  
 12 niin

The many HII-region candidates in NGC 255 are unresolved at the 1" level. Individual brightest stars may begin to resolve at about  $B = 22.5$ . The redshift is  $v_o = 1726 \text{ km s}^{-1}$ .

*Sbc Classification Section (continued)*

NGC 672      SBe(s)III      Racine wedge  
PH-7697-S      Karachentsev 40  
Sep 26/27, 1979  
103aO + GG385  
12 min

NGC 672 forms a close pair with IC 1727, shown at the right, at a separation of 8.3'. The respective redshifts are  $u_o(672) = 647 \text{ km s}^{-1}$  and  $v_o(1727) = 576 \text{ km s}^{-1}$ . At the mean redshift distance of 12 Mpc ( $z = 50$ ) the projected linear separation is small at 29 kpc.

The resolution into individual stars in the arms of NGC 672 is easy. The brightest begin to resolve near  $B = 22$ . The bar also contains bright stars and several HII-region candidates.

There are only a few HII regions in the arms and none resolve into disks at the 1.5" level.

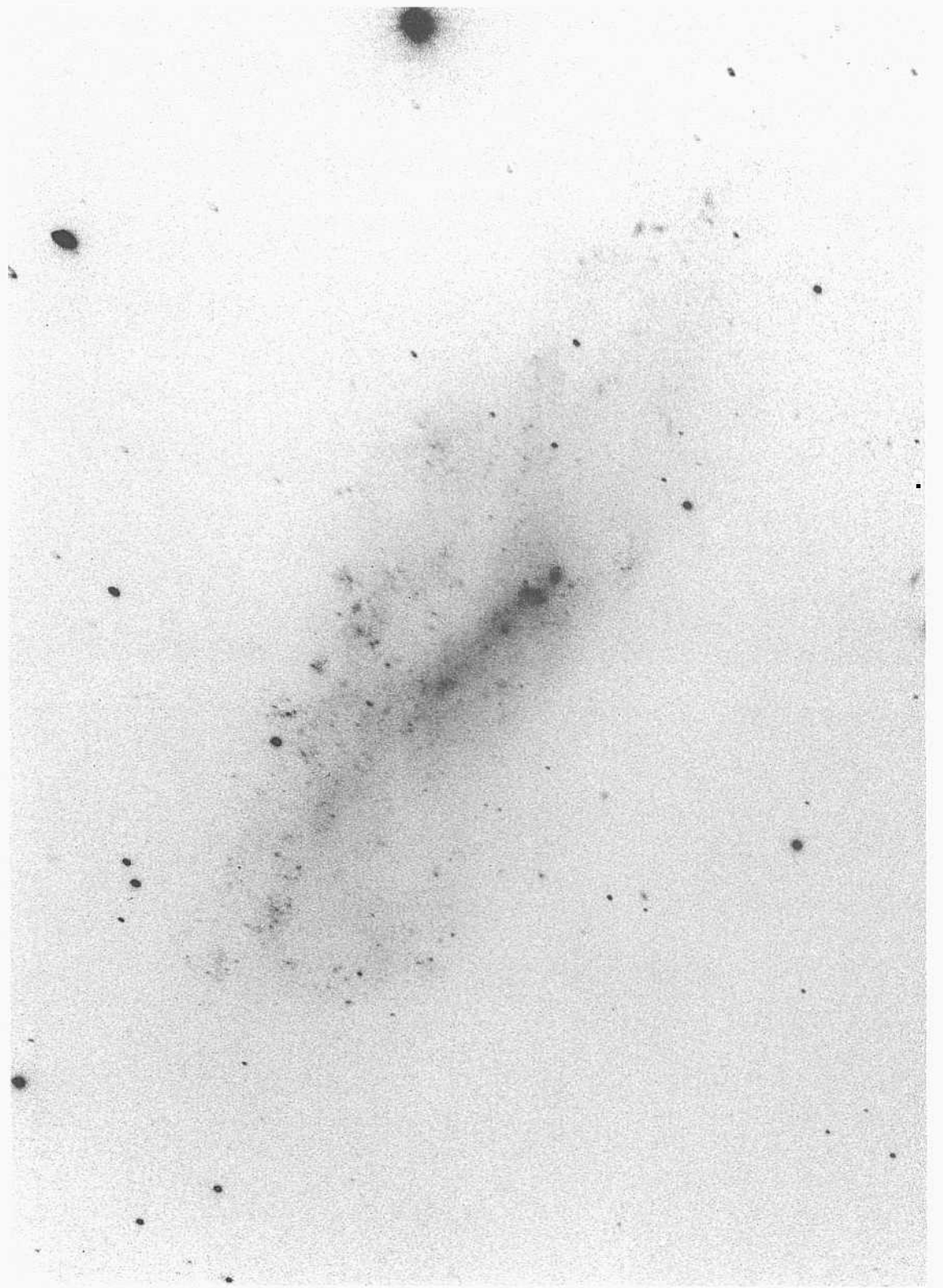
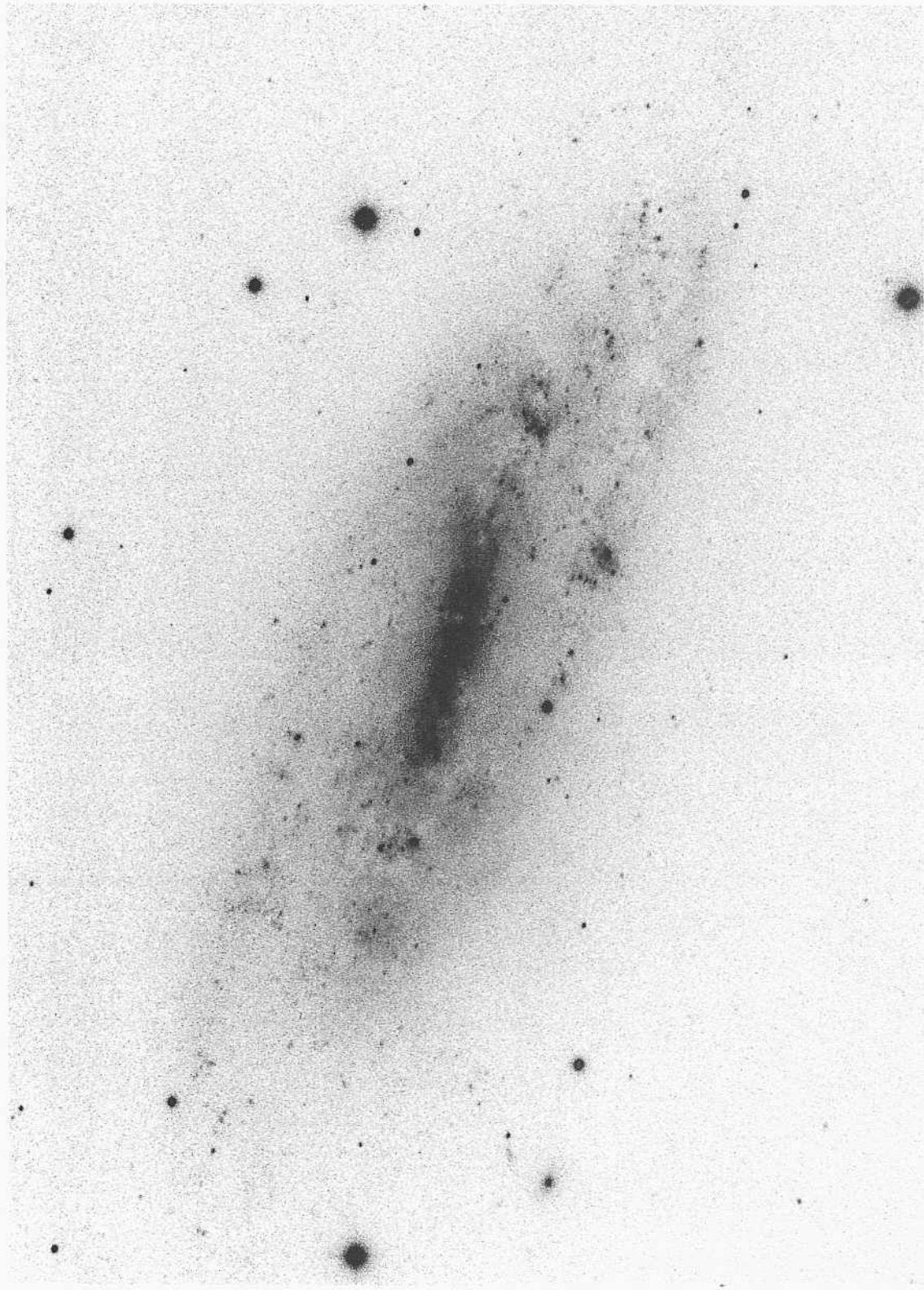
Note that the bright stars in this reproduction have Racine wedge secondary images that are 5 mag fainter and L8" removed from their primaries.

IC 1727      SBed(s)III      Racine wedge  
PH-7697-S      Karachentsev 40  
Sep 26/27, 1979  
103aO + GG385  
12 min

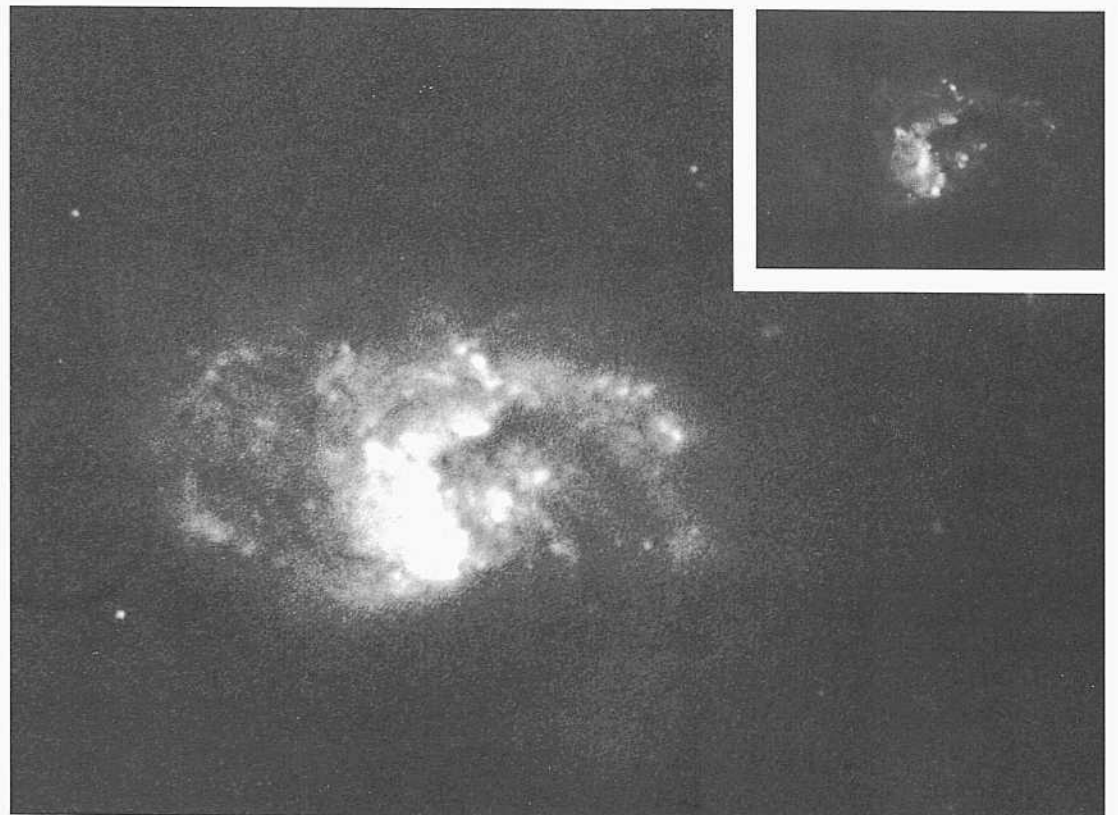
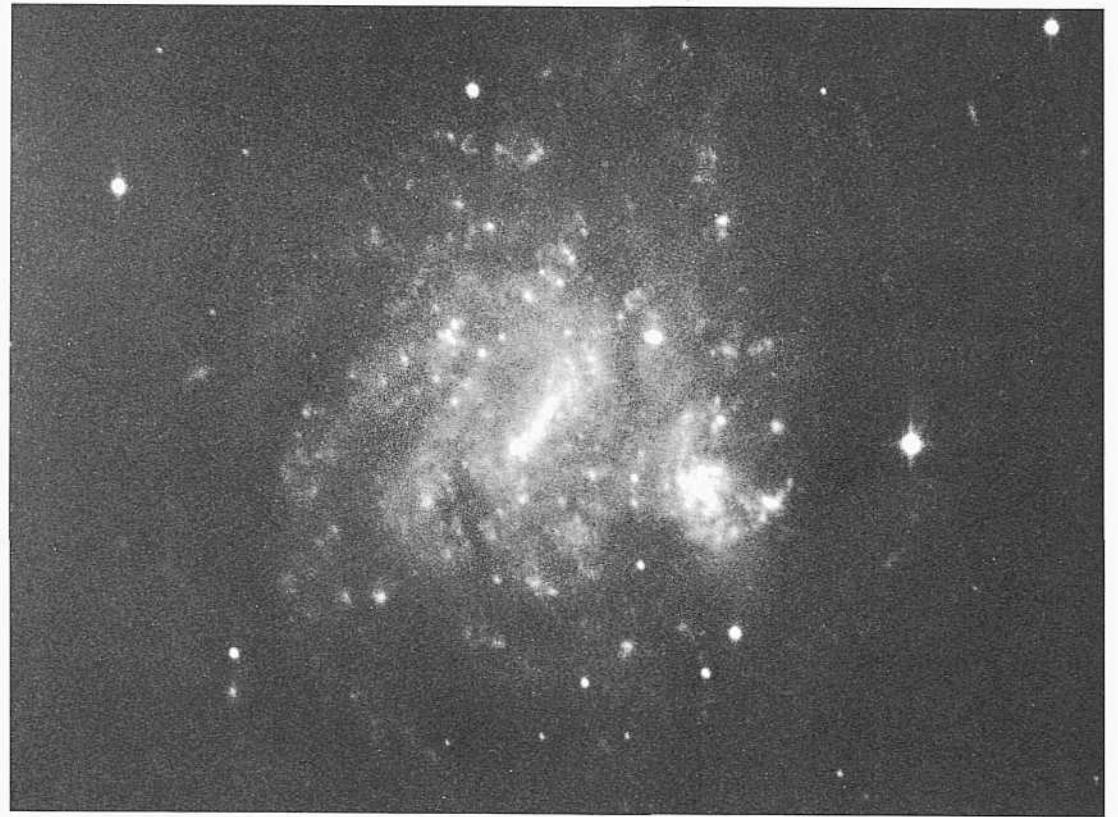
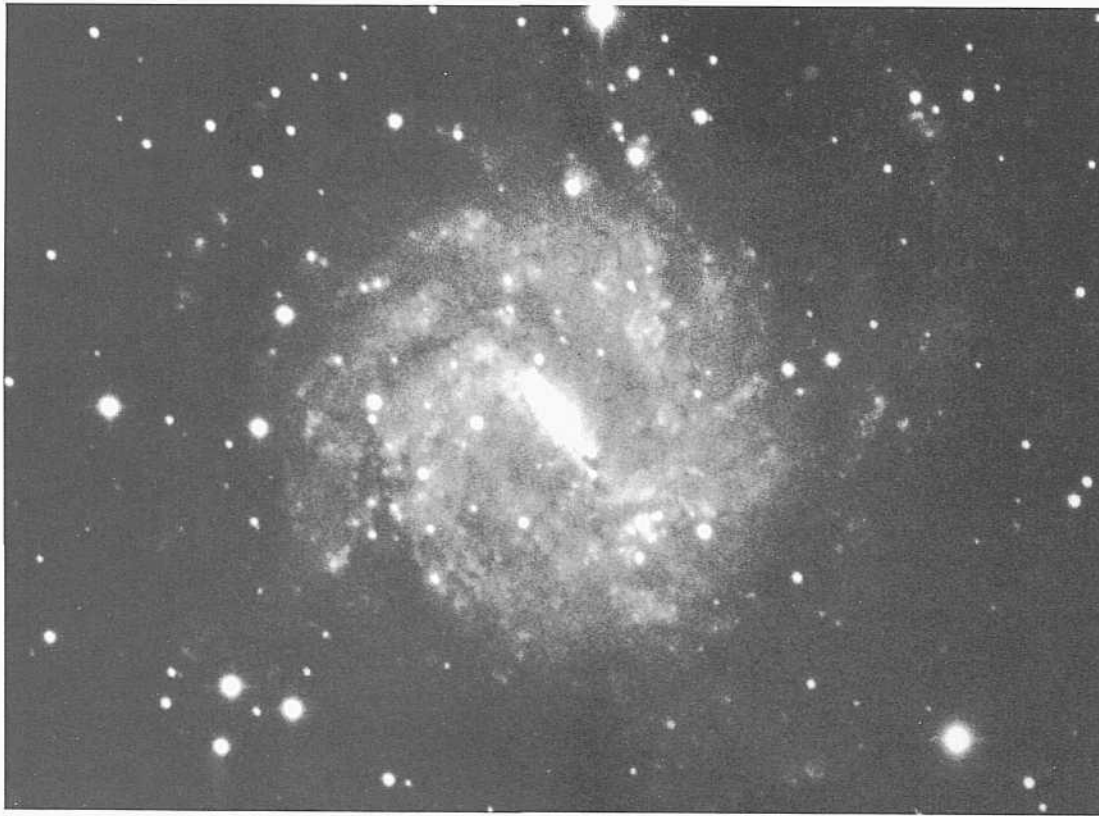
The resolution into individual brightest stars occurs at the same level, about  $B = 22$ , in IC 1727 as in its companion NGC 672, shown at the left. The surface brightness of the arms and of the underlying disk is low in both IC 1727 and NGC 672, making this nearby pair ideal for future studies of the brightest resolved stars, including Cepheids, useful for calibrations of the extragalactic distance scale.

The print of IC 1727 here is made from the same Palomar 200-inch plate used for NGC 672 at the left. IC 1727 is near the edge of the plate whose coma-free field is smaller than the area covered by IC 1727. The images on one side of the print show coma at this break point in the field.

The original plate was taken with a Racine wedge, which produced secondary images to the bright, stars.



PANEL  
308



*Sbc Classification Section (continued)*

NGC 3059      SBc(s)III      panel S9  
 CD-742-S  
 Feb 3/4, 1979  
 103aO + Wr2c  
 45 min

The spiral arms in NGC 3059 are massive in the sense of Reynolds (1927a,b); they cover most of the disk and are of moderate surface brightness. The Galactic latitude of NGC 3059 is low ( $b = -15^\circ$ ), explaining the high density of foreground contaminating stars.

The redshift is  $v_o = 991 \text{ km s}^{-1}$ .

NGC 1493      SBc(rs)III  
 CD-201-S  
 Feb 9/10, 1978  
 103aO + GG385  
 45 min

Mi-region candidates exist throughout the bar and the multiple-arm spiral pattern. The largest of the MI candidates resolves at about the 1.5" level. Individual brightest stars are probably present starting at about  $B = 21.5$ . The redshift of NGC 1493 is  $v_o = 910 \text{ km s}^{-1}$ .

A probable companion (Anonymous: ImlV) exists at a separation of 9.6'. The companion has two HII-region candidates, both of which have disks whose angular diameters are about 2". At the redshift distance of 1.8 Mpc ( $H = 50$ ) for NGC 1493 the projected linear separation of the pair would be 50 kpc.

NGC 4496A/149615      SBcIII-IV      VCC 1375  
 CD-2201-S      VCC 1376  
 March 31/April 1, 1982      Karachentsev 343  
 103aO  
 50min

The image of NGC 4496A overlaps that of NGC 4496B: the centers have an angular separation of 0.9'. The redshifts listed by Karachentsev,  $u_o(4496A) = 1131 \text{ km s}^{-1}$  and  $u_o(4496B) = 4509 \text{ km s}^{-1}$ , would put the companion far in the background. This is curious because the brightnesses of the numerous HII-region candidates in both galaxies seem closely the same, suggesting that the two galaxies are at nearly the same distance. Additional data are needed, but an apparent confirmation of the large redshift of NGC 4496B is given by the 21-cm redshift listed in the VCC of  $u_{mn} = 1548 \text{ km s}^{-1}$  (or  $v_o = 4391 \text{ km s}^{-1}$ ) attributed to unpublished observations by Hoffman, Helou, and Salpeter (1984, private communication). This may be the same measurement published by Hoffman *et al.* (1989), where  $v_{sim} = 4546 \text{ km s}^{-1}$  is listed for NGC 4496B.

Both NGC 4496A and 4496B are listed in the VCC as non-members of the Virgo Cluster.

NGC 1385      SBc(s)III  
 CD-1741-S  
 Jan 12/13, 1981  
 103aO + GG385  
 30min

Vigorous star formation is occurring throughout NGC 1385, as judged by the many bright HII regions in the bar and in the arms. The detected candidates for brightest individual stars in the outer regions do not resolve brighter than  $B = 22$ .

The redshift is  $v_o = 1968 \text{ km s}^{-1}$ .



*Sbc Classification Section (continued)*

NGC 1313      SBc(s)III-IV  
CD-564-S  
Oct4/5, 1978  
103aD + Wr12  
60 min

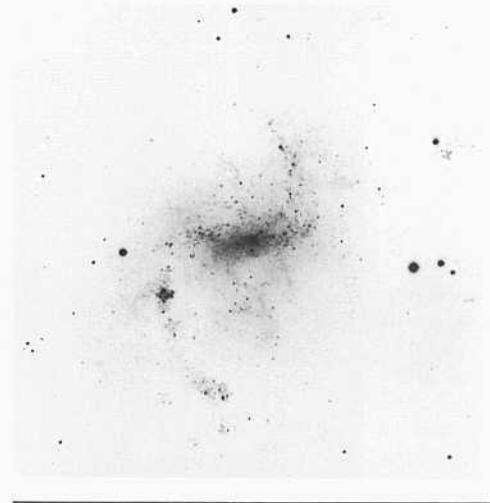
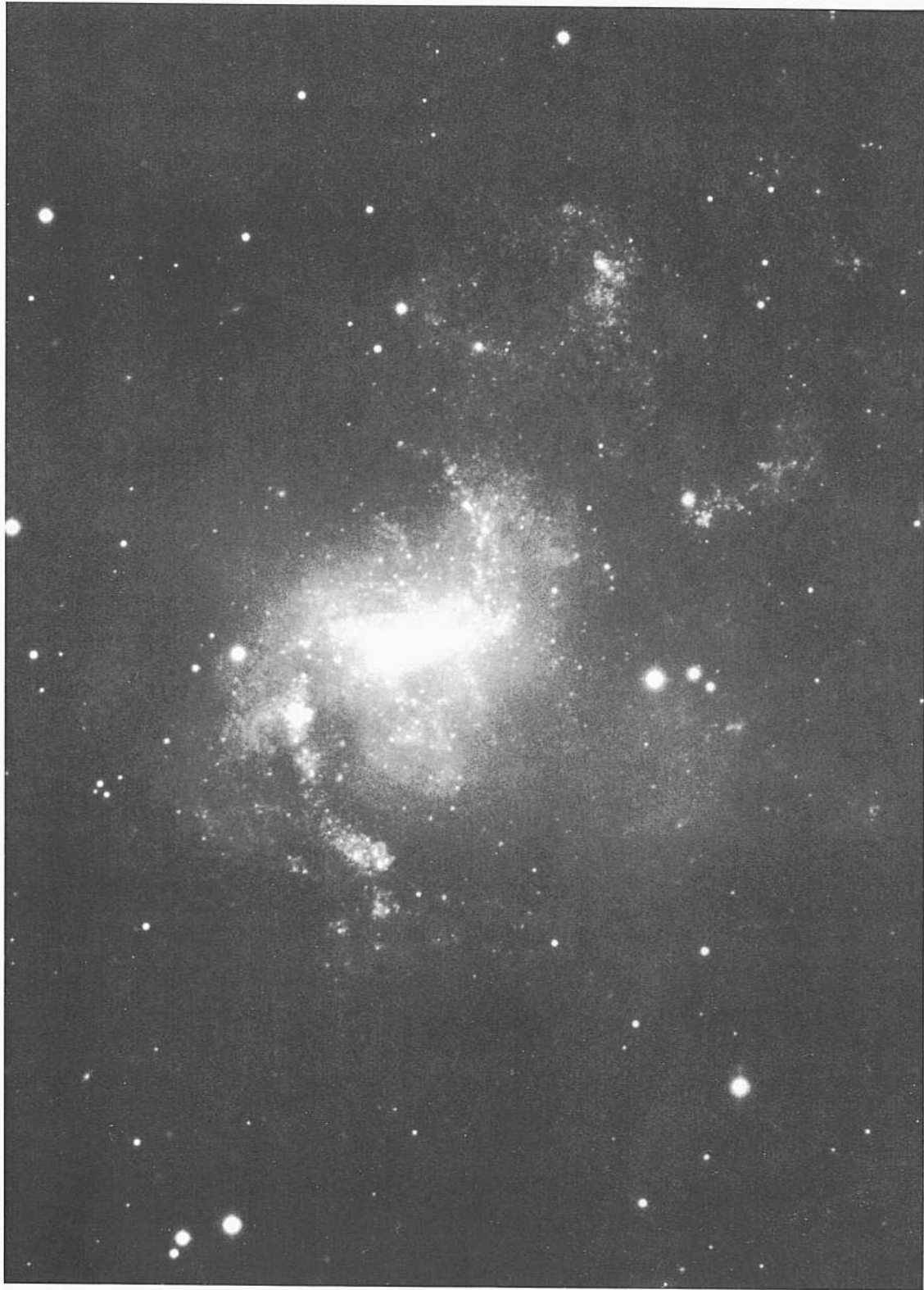
The resolution into individual stars in NGC 1313 is exquisite. Brightest stars begin to resolve at about  $B = 17$ , similar to the level in members of the South Polar Group such as NGC 55, NGC 247, and NGC 300 for which distance moduli of about  $m - M = 26.5$  have been **adopted**.

The brightest stars occur in the bar and in a compact association in one of the two stubby inner arms that start from the ends of the bar. These arms, and **the** resolution of stars in the bar, are seen best in the shallow print on the **right**. Both **prints** here have been made from the same original plate taken in the V photometric passband.

The chaotic nature of the outer regions of NGC 1313 is seen in the heavy print on the left. A semicircular arc near the upper border of the print, similar to Constellation III in the LMC, contains a bright association and provides good resolution into stars. Similar resolution into fainter stars continues to the plate limit over the entire face of the galaxy.

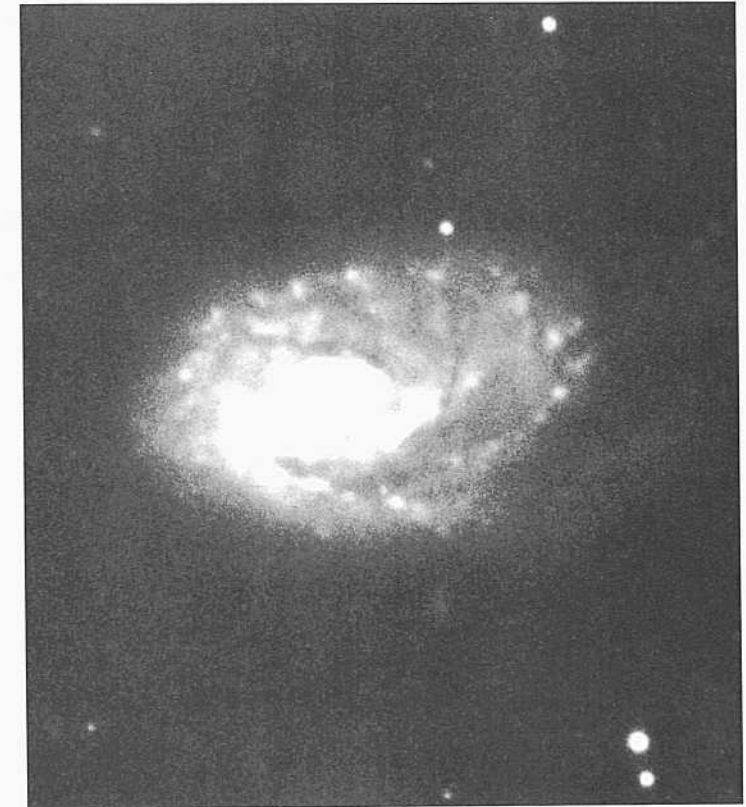
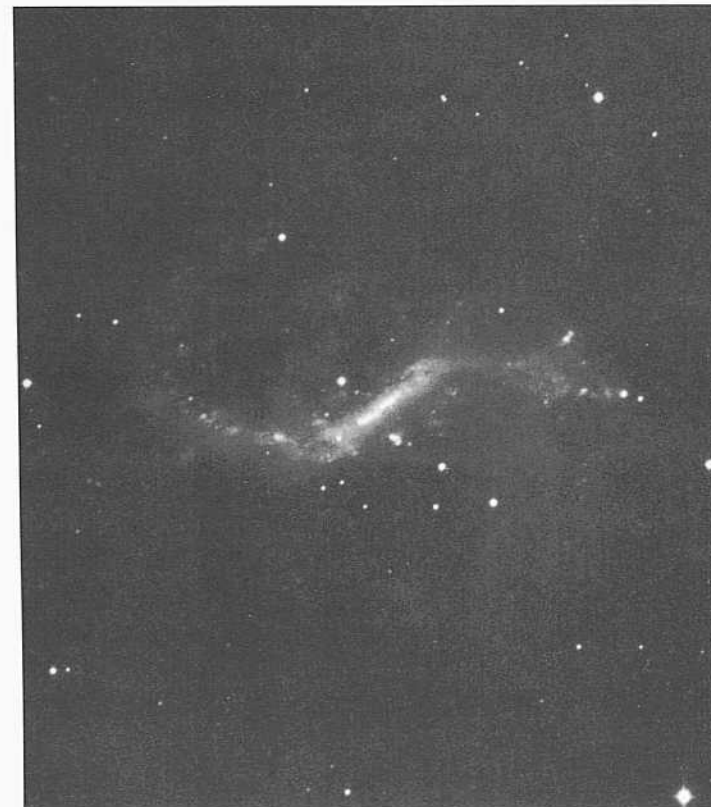
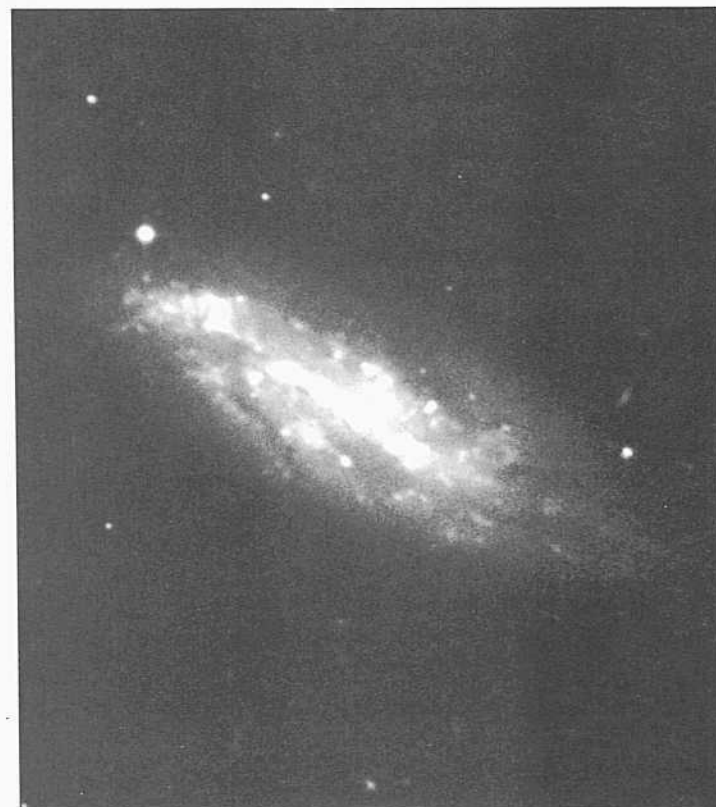
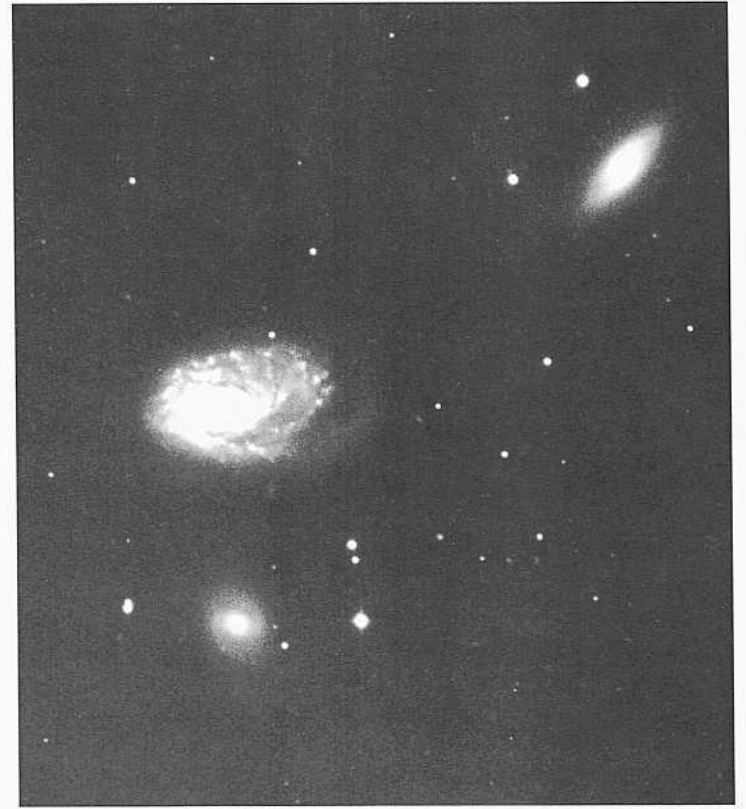
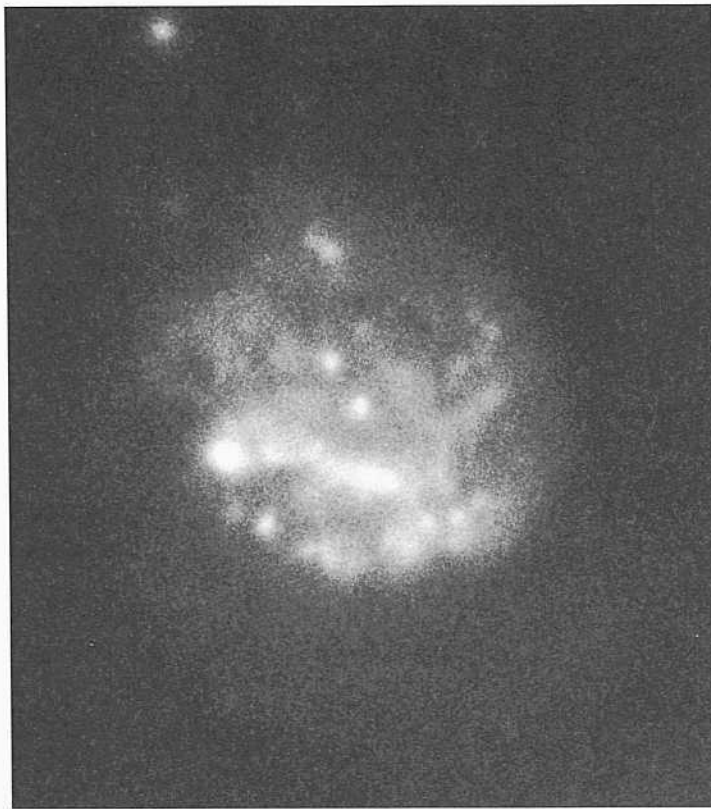
The small redshift  $\langle v_r \rangle = 261 \text{ km s}^{-1}$  is consistent with the small distance inferred from the magnitude of  $B = 17$  for the brightest resolved stars.

Note that the prints here have been made from a yellow-sensitive emulsion rather than blue. This tends to suppress the contrast between the young blue individual stars and the underlying older disk.



PANEL  
309

PANEL  
310



NGC 6239 SBcIII pec  
PH-59-H  
April 27/28, 1949  
103aO  
30 niin

The original plate from which this image was made was one of the earliest taken with the 200-inch Palomar reflector, before the prime-focus Ross corrector was installed. There is, therefore, appreciable coma extending to the center of the field because the  $f$ /ratio of the primary mirror is so small. However, the angular size of NGC 6239 is small enough ( $D_{25} = 2.7'$ ) to avoid much image degradation near the center, where the HII-region candidates exist.

Current star formation is occurring in the bar but little exists in the faint arms. None of the HII-region candidates resolve at the 1" level. The redshift of NGC 6239 is  $v_o = 1110 \text{ km s}^{-1}$ .

NGC 4294 SBc(s)IMII VCC 465  
CD-1318-S/Br pair  
March 12/13, 1980  
103aO  
75 inin

NGC 4294 in the Virgo Cluster forms a close (probable) physical pair with NGC 4299 (Sd; panel 328) at a separation of 5.6'. Both are in the Virgo Cluster and are located about a third of the distance between Virgo subclusters A and B.

Closeness of angular separation in the cluster region is not usually good evidence of physical association. However, the circumstance here is unusual because the redshifts of both galaxies are so nearly the same and each is far from the cluster mean redshift, showing the same (nearly 30) large virial velocity deviation from the mean. This is so improbable as to suggest that the galaxies are, in fact, a binary pair.

The redshifts are  $u_o(4294) = 227 \text{ km s}^{-1}$  and  $u_o(4299) = 107 \text{ km s}^{-1}$ . At the cluster distance of 21.9 Mpc, the projected linear separation of the pair is small at 36 kpc.

HII-region candidates exist both in the bar and in the arms of NGC 4294. However, none resolve into disks, nor is there evidence of resolution into brightest stars in the arms. This lack of resolution is consistent with membership in the Virgo Cluster, which lies at a much greater distance than that indicated by the small redshifts of the two galaxies. This is direct evidence for the large virial velocity dispersion in the Virgo Cluster because, from the stellar content, there is no question that the two galaxies are cluster members.

The pair is shown in the Virgo Cluster Atlas of Spirals (Sandage, Binggeli, and Tammann 1985a, panel 15), enlarged to a common scale for other Virgo galaxies.

NGC 4234 SBcIII.4 VCC 221  
CD-2157-S  
March 26/27, 1982  
103aO  
50 niin

NGC 4234 is in the Virgo Cluster Catalog but is listed there as a non-member. It is located in the southwestern corner of the survey area; it may be a member of the background W Cloud (Binggeli, Tammann, and Sandage 1987). Its redshift is  $v_n = 1981 \text{ km s}^{-1}$ .

NGC 4731 SBc(s)IH(lides?) triplet?  
CD-2188-S  
March 29/30, 1982  
103aO  
4-6 niin

NGC 4731 forms a wide pair with NGC 4697 (E6; panels 13, 19) at a separation of 36'. It also forms a closer pair with an anonymous BCD galaxy at 10.4' that resolves into HII regions at the same brightness as in NGC 4731. The redshifts are  $u_o(4697) = 1033 \text{ km s}^{-1}$  and  $u_o(4731) = 1303 \text{ km s}^{-1}$ . If the galaxies are at a common redshift distance of 23 Mpc ( $H = 50$ ), their projected linear separation is 241 kpc.

The redshift of the closer BCD companion is not known (c. 1990) but there is little doubt that the pair forms a physical association. Their projected linear separation is small at 70 kpc. Many other dwarf E and Im candidate companions exist in the field of NGC 4697 and NGC 4731.

Star formation is occurring in the bar of NGC 4731, judging by the HII-region candidates there. The arm pattern is that of tidal plumes, perhaps due to a close encounter with the BCD companion, which also has a near (so-called) starburst morphology.

NGC 4273 SBc(s)II VCC 382  
CD-1339-S/Br  
March 14/15, 1980  
103aO  
75 min

NGC 4273 is in a busy region in the southwestern corner of the Virgo Cluster Catalog area. It and its companions are probably in the W cloud in the background (Binggeli, Sandage, and Tammann 1985; Binggeli, Tammann, and Sandage 1987). The bright companion galaxies in the wide-angle view in the upper-right photograph are NGC 4277 (SBa; VCC 386;  $v_o = 2345 \text{ km s}^{-1}$ ) and NGC 4268 [S0<sub>2</sub>(6); VCC 371;  $v_n = 2164 \text{ km s}^{-1}$ ]. The redshift of NGC 4273 is  $v_o = 2232 \text{ km s}^{-1}$ . The dwarf elliptical galaxy VCC 390 (dE3) is also present in the field shown here.

NGC 4273 SBc(s)H VCC 382  
CD-1339-S/Br  
March 14/15, 1980  
103aO  
75 min

The spiral arms of NGC 4273 terminate at a sharp outer boundary whose elliptical outline is not centered on the galaxy's center. The pattern of a sharp outer termination is moderately common, shared for example by NGC 95 (panel 248), NGC 491 (panel 211), NGC 1637 (panel 306), NGC 2701 (panel 271), and NGC 4647 (panels 51, 278, 314), among others.

The asymmetry in the arm brightness between the two sides of the major axis is not the normal pattern. Nevertheless there are numerous examples in this atlas. These include IC 1953 (panel 208), NGC 5065 (panel 246), NGC 95 (panel 248), NGC 1569 (panel 263), NCC 2276 (panel 263), NGC 2701 (panel 271), NGC 4781 (panel 273), NGC 4298 (panel 279), NGC 4096 (panel 287), NGC 3367 (panel 293), NGC 1637 (panel 306), the prototypes of NGC 5676 (panel 245) and NGC 5678 (panel 278), NGC 1536 (panel 313), perhaps NGC 922 (panel 313), and NGC 5474 (panel 315).

The six galaxies on this panel have moderate-to-high inclination. All feature a central bar, although the bar is less definite in the last three galaxies than in the first three.

NGC 7640      SBc(s)II:      HA, p. 49  
 PH-115-H  
 Sep 24/25, 1951  
 103aO  
 30 min

NGC 7640 is very highly resolved into individual stars and a few large HII-region complexes. From the degree of resolution into stars, the distance modulus must be smaller than  $m - M = 3.1$  but larger than  $m - M = 30$ . The brightest stars begin to resolve at about  $B = 21.5$ . Star formation is occurring in the central region as well as in the two major arms.

The redshift is  $v_0 = 669 \text{ km s}^{-1}$ .

NGC 4178      SBc(s)II      VCC 66  
 CD-2100-S  
 March 18/19, 1982  
 103aO + GG385  
 75 min

NGC 4178 is listed as a cluster member in the Virgo Cluster Catalog (Binggeli, Sandage, and Tammann 1985). It is illustrated on a common scale with other cluster members in the Atlas of Virgo Cluster Spirals (Sandage, Binggeli, and Tammann 1985a, panel 6). The angular diameter is large at  $D_{2.5} = 5.0'$ . The redshift of NGC 4178 is  $v_0 = 224 \text{ km s}^{-1}$ , illustrating the large virial velocity variation among the Virgo Cluster members. From the characteristics of the HII regions and the lack of individual resolved stars brighter than  $B = 23$ , there is no question that the galaxy is much more distant than its small redshift would indicate.

The bar consists of HII regions in a thin straight pattern. Two large HII-region complexes exist in one of the arms. Halo diameters of these compound associations are about  $5''$ .

NGC 1249      SBc(s)II  
 CD-704-S  
 Jan 30/31, 1979  
 103aO + GG385  
 45 min

The halo diameters of the largest of the HII-region complexes in NGC 1249 are about  $3''$ . Resolution into individual stars is difficult but may begin at about  $B = 22.5$ . The redshift of NGC 1249 is  $v_0 = 887 \text{ km s}^{-1}$ .

NGC 3769      SBc(s)II      Karachentsev 294  
 PH-7633-S  
 April 28/29, 1979  
 103aO  
 12 min

NGC 3769 forms a close pair with a companion (NGC 3769 A; Sin; not in the RSA) which is evidently at the same distance judging by its similar resolution into stars and HII regions. The separation of the pair is  $1.2'$ . The individual  $v_0$  redshifts listed by Karachentsev are  $791 \text{ km s}^{-1}$  for NGC 3769 and  $845 \text{ km s}^{-1}$  for its companion. At the mean redshift distance of  $16 \text{ Mpc}$  ( $H = 50$ ) the projected linear separation is very small at  $6 \text{ kpc}$ . It can be guessed from the distorted morphology that a close encounter is, in fact, in progress.

NGC 7462      SBc(s)  
 CD-1535-S/Br  
 Aug 6/7, 1980  
 103aO + GG385  
 45 min

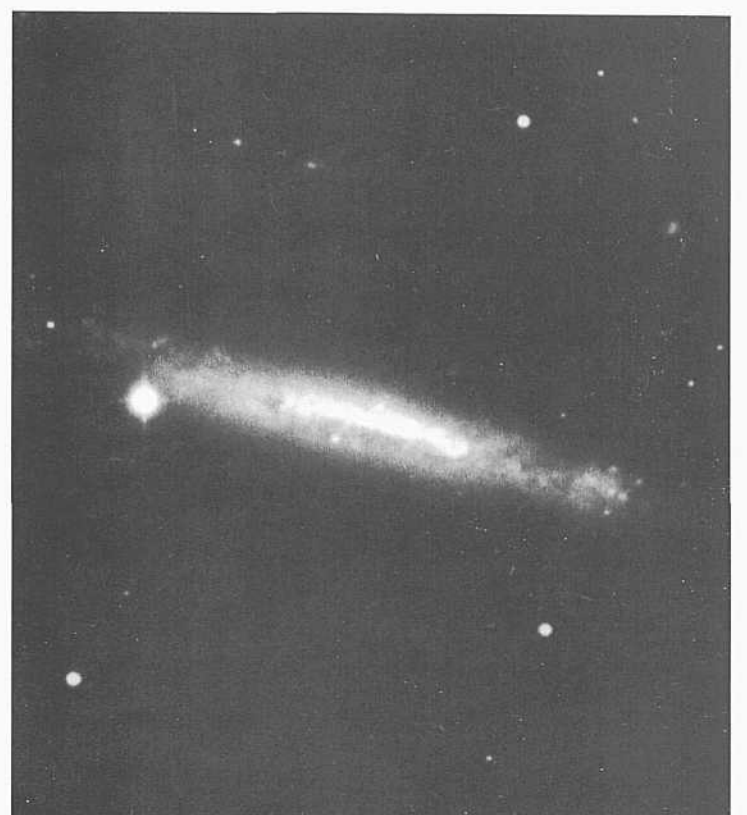
NGC 7462 is nearly on edge. The brightness distribution at the center suggests the presence of a bar, but this is uncertain. HII regions exist, most easily seen on one side of the image in the outer region of lower projected surface brightness.

The redshift is  $v_0 = 1022 \text{ km s}^{-1}$ .

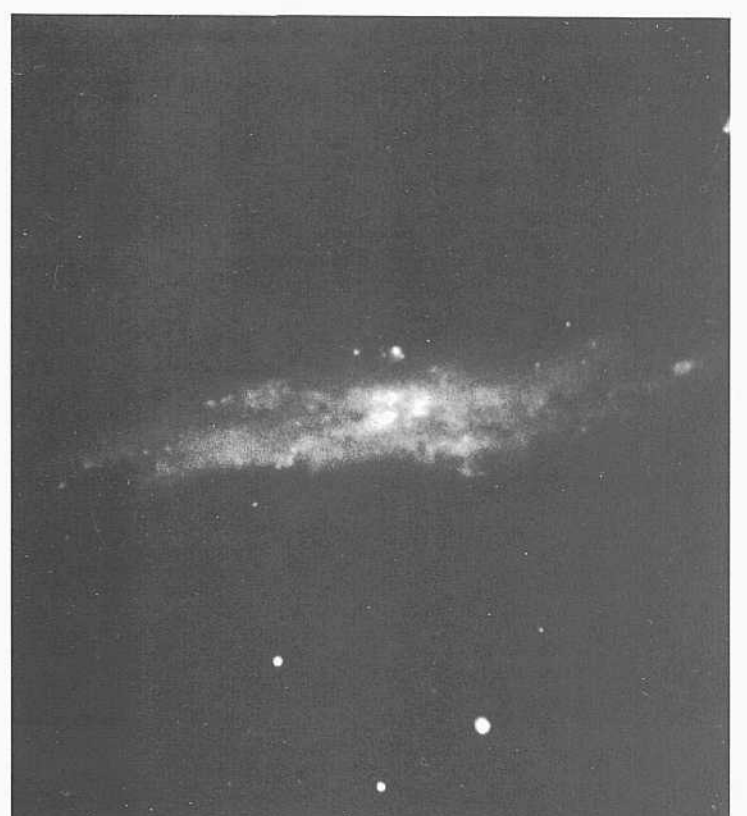
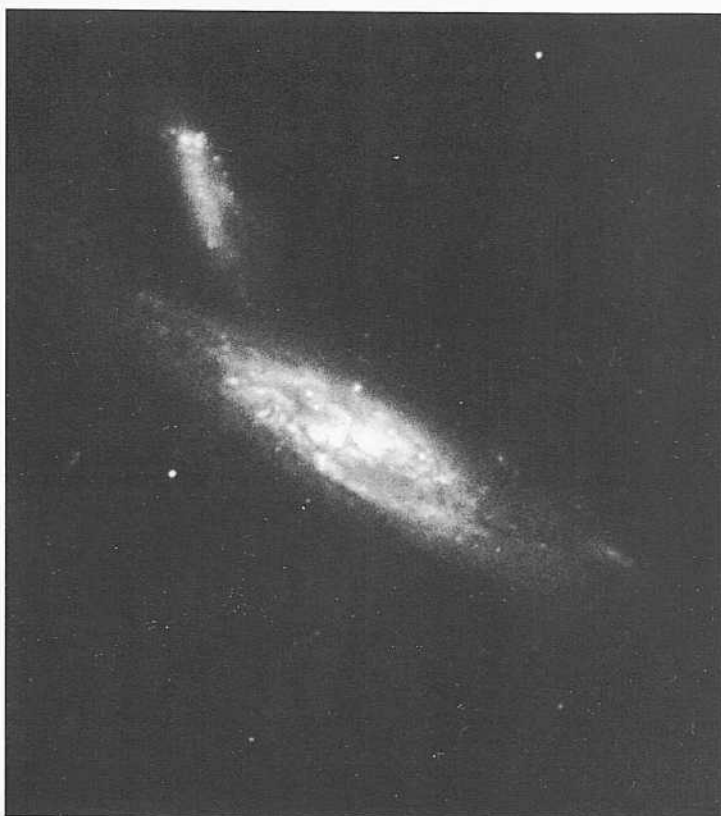
NGC 7307      SBc(s)II  
 CD-1125-Br  
 Aug 20/21, 1979  
 103aO + GG385  
 45 min

Incipient resolution into stars and HII regions exists across the high-surface-brightness face of NGC 7307, but the nearly edge-on inclination to the line of sight makes this information only qualitative.

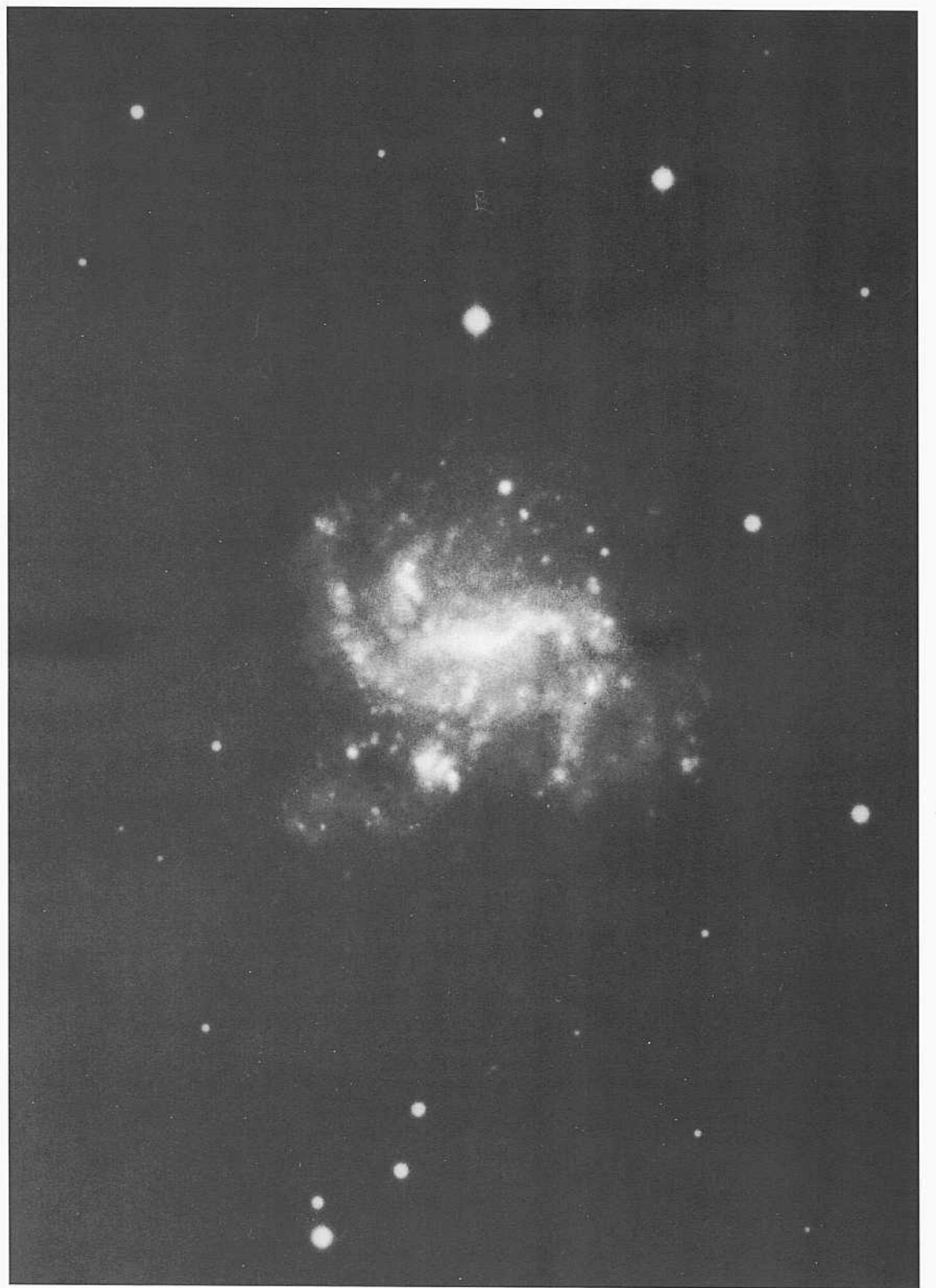
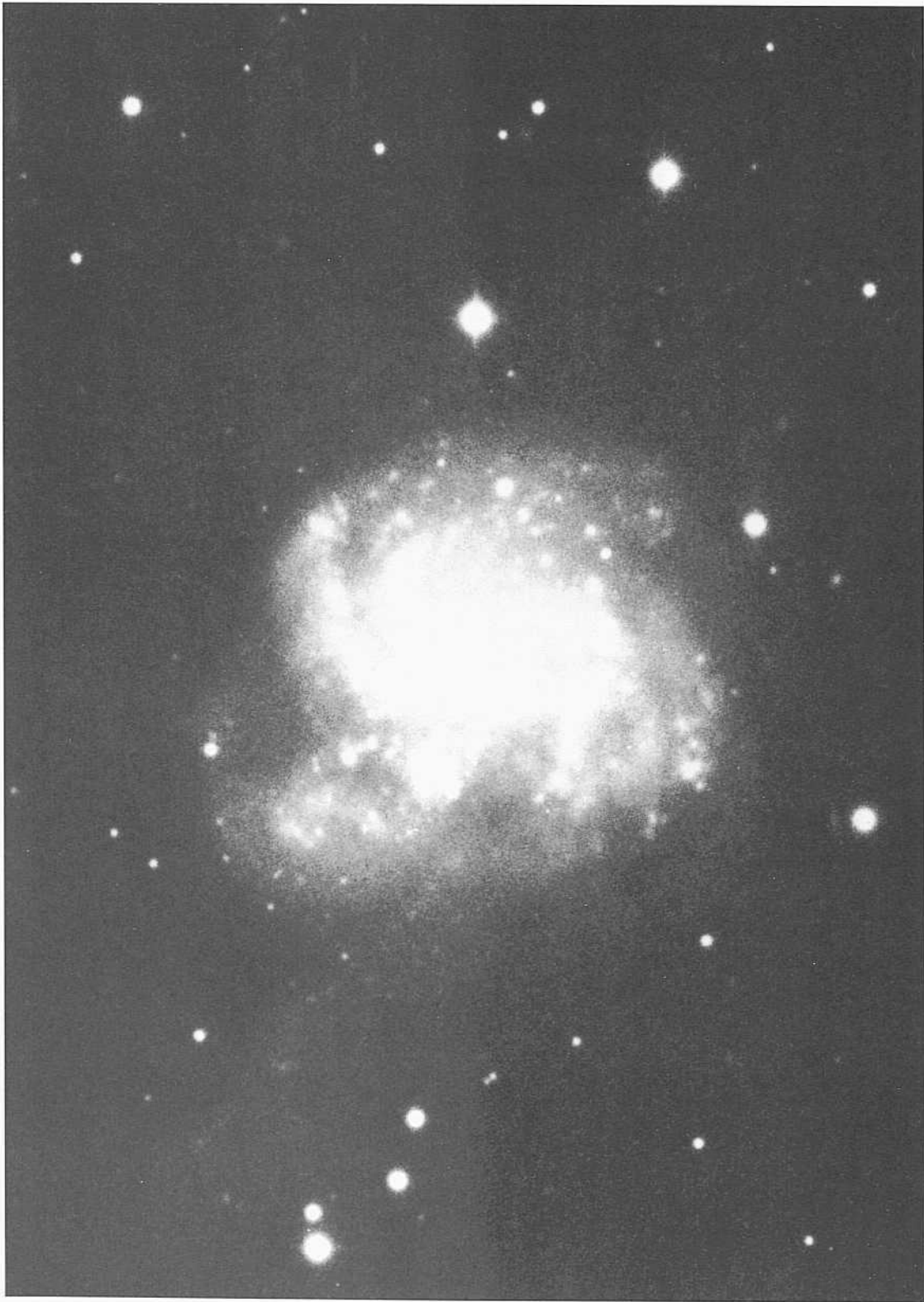
The redshift is  $v_0 = 1865 \text{ km s}^{-1}$ .



PANEL  
311



PANEL  
312



*Sbc Classification Section (continued)*

NGC2139          SBc(s)H.3  
CD-766-S  
Feb 21/22, 1979  
103aO + GG385

15 iiiii

NGC 2139 is in clear evidence of a merger in progress. The small satellite on one side of the larger galaxy near its minor axis is seen best in this light print on the right. The nuclear region of this smaller galaxy is intact, and it has many HII [region] candidates along with evidence of robust star formation. However its outer regions appear to be tidally disrupted.

The main galaxy is also generally intact, having a strong, chaotic bar and massive spiral arms in which robust star formation is occurring. However, there is a low-surface-brightness straight (tidal?) plume extending about one galaxy diameter beyond the main body of the large galaxy, starting near the apparent point of overlap of the two respective central regions.

The stellar content is about equally well resolved in both galaxies.

The redshift, presumably of the central region of the larger galaxy, is  $v_o = 1688 \text{ km s}^{-1}$ .



The nine galaxies on this panel complete the SBc section of the classification. Most are moderately inclined to the sight line and/or are peculiar in some moderate fashion.

NGC 1796 SBc(s)III  
CD-221-S  
Feb 12/13, 1978  
103aO + GG385  
45 min

The disk of NGC 1796 is covered with star-producing regions, causing the high surface brightness over the entire image. A central bar is present; HII-region candidates exist in it as well as in the tightly wrapped arms.

The redshift is  $v_n = 771 \text{ km s}^{-1}$ .

NGC 4668 SBc(s)III pair  
CD-1411-S/Br  
March 23/24, 1980  
103aO  
75 min

NGC 4668 forms a close pair with NGC 4666 (Sbc:  $v_0 = 1474 \text{ km s}^{-1}$ ; panel 194) at a separation of  $7.8''$ ; it also has a wider association with NGC 4632 (Sc:  $v_0 = 1557 \text{ km s}^{-1}$ ; panel 288) at a separation of  $52''$ . The redshift of NGC 4668 is  $v_0 = 1530 \text{ km s}^{-1}$ . At the mean redshift distance of 30 Mpc ( $z = 50$ ) the projected linear separations of NGC 4666 and NGC 4632 from NGC 4668 are 68 kpc and 454 kpc, respectively.

Many HII regions exist over the face of NGC 4668, which is small and chaotic but has a high-surface-brightness disk. The resolution into HII regions is at the same level as in the close companion NGC 4666 and in NGC 4632. There is little question that all three galaxies are at the same distance.

NGC 3912 SB late pec  
PH-7607-S  
April 3/4, 1979  
IIIaJ + GG385  
30 min

The bar and parts of one of the arms of NGC 3912 are filled with HII regions. The redshift is  $v_0 = 1733 \text{ km s}^{-1}$ .

NGC 1536 SBc(s) pec  
C D-2040-Bedke/Gregory  
Nov 1/2, 1981  
103aO + GG385  
45 min

The bar and the region of each arm just beyond the ends of the bar contain many HII-region candidates. The disk is covered with very broad, massive, ill-defined arms nearly devoid of HII regions. The arms are not symmetrical about the bar; one side sweeps out more widely than the other, but there is no evidence for tidal interaction by a companion. NGC 1536 is isolated; its redshift is  $v_0 = 1168 \text{ km s}^{-1}$ .

NGC 5074 SBc(s)II  
PH-8092-S  
Feb 6/7, 1981  
103aO  
12 min

NGC 5074 has a small angular diameter ( $D_{95} = 1.0''$ ) and moderately high surface brightness in its inner region. This region contains a bar and two bright arms that start from the ends of the bar. One arm remains bright for about one-quarter revolution; the other remains bright only for a short stub of a beginning. A fainter, low-surface-brightness outer arm surrounds the inner region.

The redshift of NGC 5074 is  $v_0 = 5675 \text{ km s}^{-1}$ ; the absolute magnitude is bright, at  $M_B = -21.3$ .

NGC 4064 SBc(s):  
H-2213-H  
May 17/18, 1942  
103aO  
60 min

NGC 4064 is difficult to classify because it is seen nearly edge on, but the existence of a bar is certain. HII regions define the bar in the same way as in NGC 1536 at the top of this column, in NGC 4731 (panel 310), and especially in NGC 4178 (panel 311).

Dust patches exist on either side of the major axis. The galaxy may resemble NGC 4389, at the upper right, if it were viewed from an angle about  $10^\circ$  less nearly edge on.

The redshift of NGC 4064 is  $v_0 = 937 \text{ km s}^{-1}$ .

NGC 4389 SBc(s)III pec  
PH-8059-S  
Feb 4/5, 1981  
103aO  
12 min

NGC 4389 has a bright bar filled with discrete HII regions. Its spiral pattern is difficult to trace because of the large inclination angle. Its morphology may be similar to that of NGC 4178 (panel 311), NGC 3059 (panels 308, S9), NGC 4116 (panel 306), NGC 3319 (panel 303), and NGC 4654 (panel 302), all of which are shown in this SBc section and all of which have less-steep inclination angles.

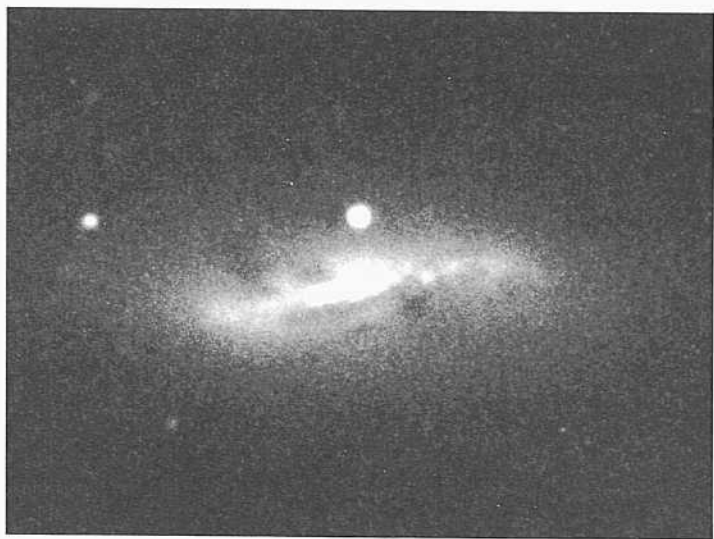
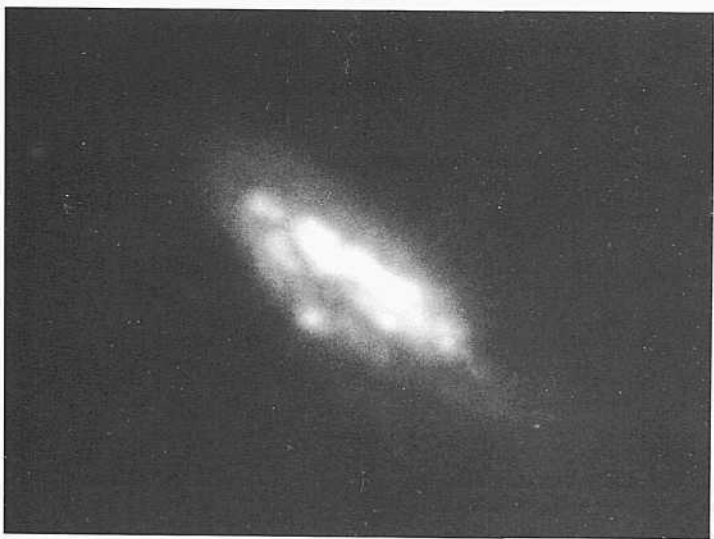
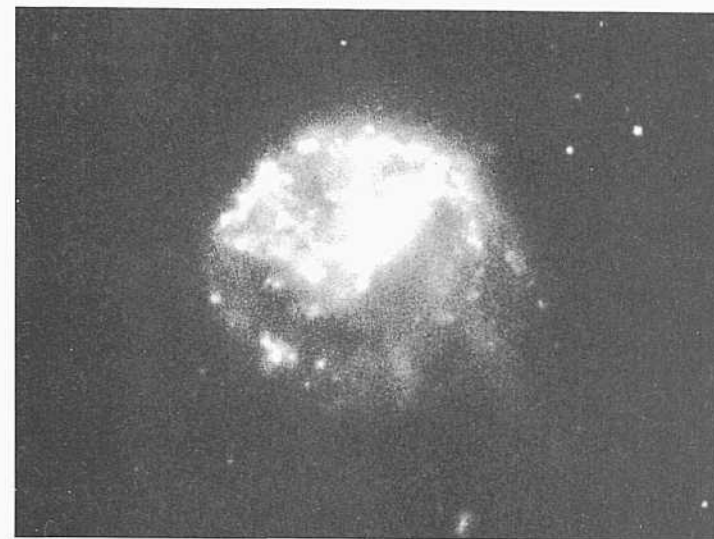
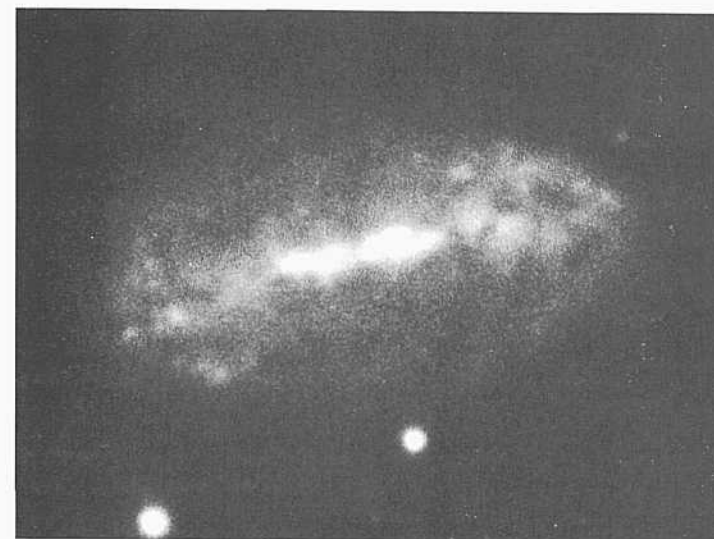
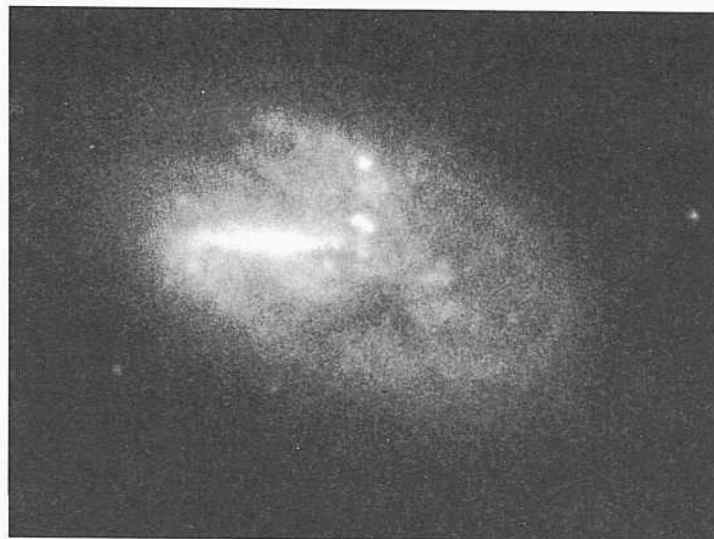
The redshift of NGC 4389 is  $v_n = 767 \text{ km s}^{-1}$ .

NGC 922 SBc(s) pec  
CD-1600-S/Br  
Aug 12/13, 1980  
103aO + GG385  
45 min

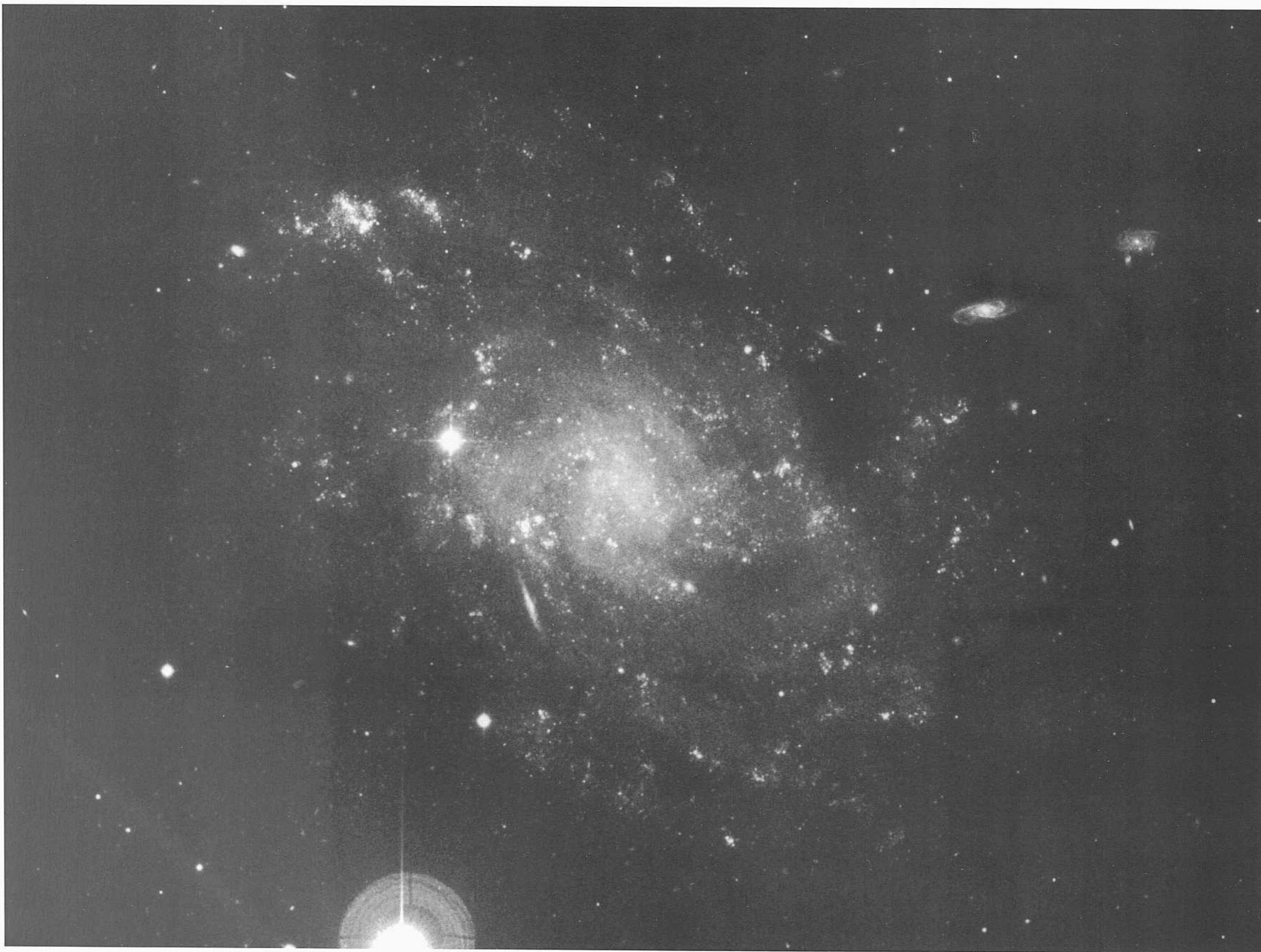
The morphology of NGC 922 is so peculiar as to be outside the classification system. It would be called a sport by nineteenth-century animal breeders. The reason for its inclusion in this section is because it appears to have a central bar from which spiral fragments are attached, primarily on one side. These fragments spiral outward at very large pitch angles, abruptly stopping at an edge. HII regions exist throughout this half of the image. The other half is devoid of high-surface-brightness features, although smooth, low-luminosity plumes exist there.

Two prints of NGC 922 are shown here. In the heavy print above, the smooth, low-surface-brightness features are easily seen. The light print below, made from the same original plate, shows well the HII-region candidates in the bar and in the high-surface-brightness parts of the image.

NGC 922 has no evident companion at the same distance that can be blamed for the peculiar morphology from a supposed close encounter. The redshift of NGC 922 is  $v_0 = 3061 \text{ km s}^{-1}$ . The absolute magnitude of the galaxy is bright at  $M_B = -21.7$ .



PANEL  
314





Scd Classification Section (continued)

NCC 1494            Scd(s)II  
 CD-711-S  
 Jan 31/Feb 1, 1979  
 103aO + GG385  
 4-5 niin

The surface brightness of the disk and arms in NGC 1494 is higher than in NGC 45 shown on the preceding panel. The redshift is larger, at  $v_o = 95.7 \text{ km s}^{-1}$ , consistent with the lack of resolution into individual stars at a level brighter than about  $V = 22$ . Brightest stars begin to resolve at about this level, but confusion with the numerous III regions that, are both brighter and fainter than this level is serious; the two types of objects must be discriminated from one another by standard methods before their photometry can be interpreted.

No nucleus or central bulge is seen on the available plate material. The arms are moderately well formed and are easily traced; hence the relatively high luminosity classification is required.

NGC 5474            Scd(s)IV pec            M101 Gr  
 PH-82-B  
 June 9/10, 1950  
 103aO  
 30 min

NGC 5474 is one of the five late-type dwarf companions to M101. The others are NGC 5204 (SdIV; panel 324), NGC 5477 (not in the RSA; panel 326 here), NGC 5585 (SdIV; panel 323), and Ho IV (not in the RSA or this atlas), all shown together for comparison, as enlarged nearly to a common scale (Sandage and Tammann 1974c, Fig. 1).

NGC 5474 is well resolved into individual stars beginning at  $V = 20.5$ . This is about 2 mag fainter than in M101, which is at the same distance. This magnitude difference for the brightest stars illustrates the dependence of  $M$  (brightest star) on the absolute luminosity of the parent galaxy.

Many Mil regions exist across the disk. The largest several are complex and have total (halo) diameters of about  $10''$ .

The asymmetrical pattern of the multiple-armed system may be due to tidal interaction with M101, at an angular separation of  $44'$ . At the distance of 7.2 Mpc ( $m - M = 29.3$ ) the projected linear separation is small at 92 kpc.

NGC 4790            Scd(s)II            group  
 CD-1848-HB  
 April 3/4, 1981  
 103aO  
 75 niin

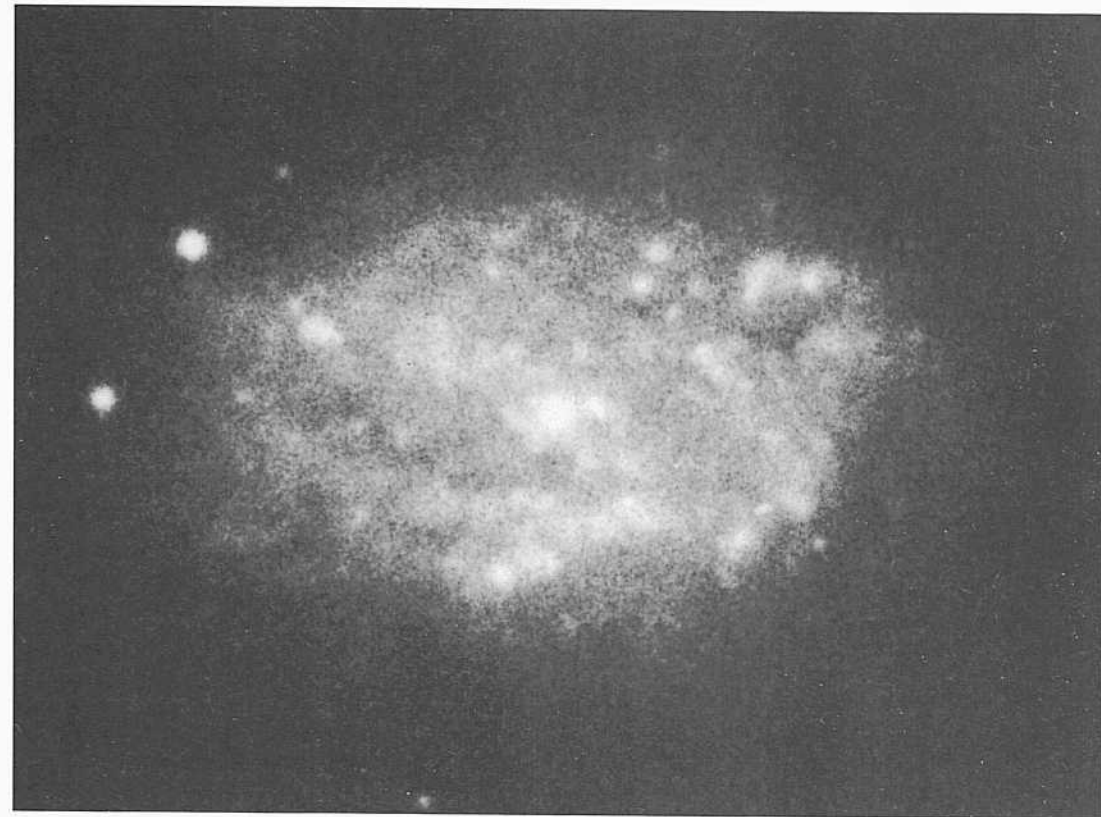
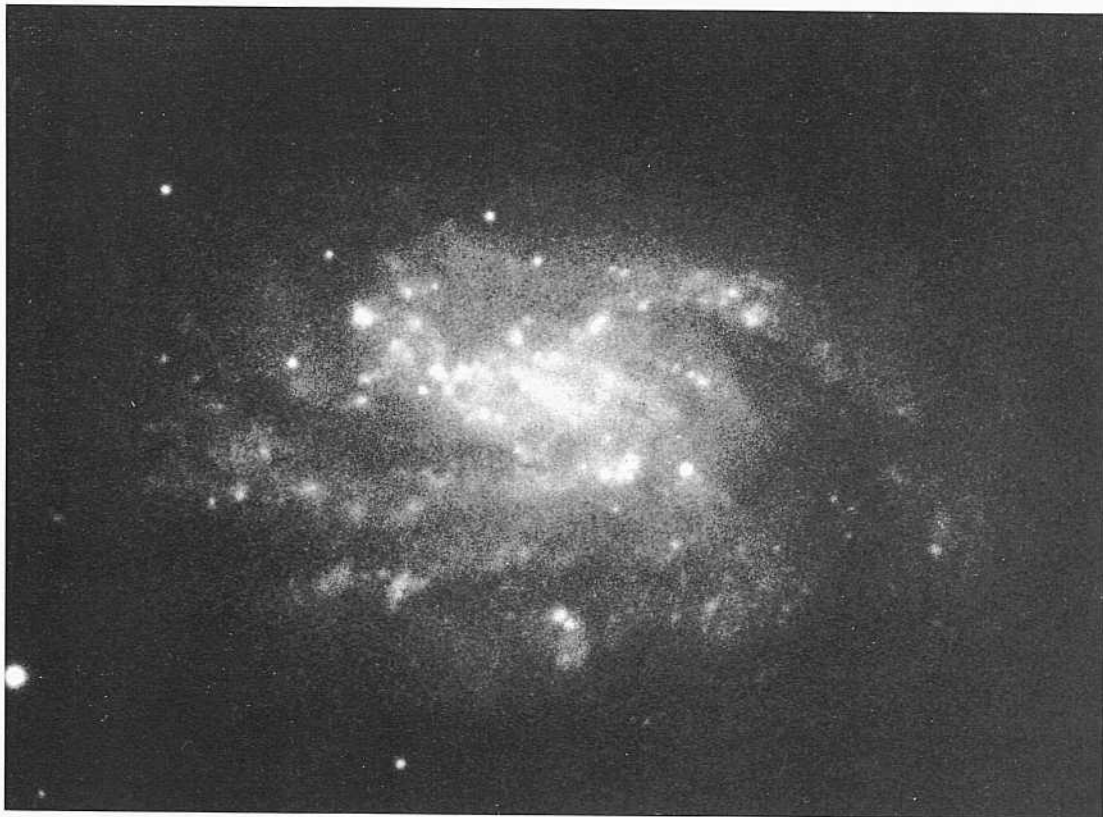
NGC 4790, with  $v_o = 115.4 \text{ km s}^{-1}$ , is in a complex field that also contains NGC 4742 (E4; panel 10;  $v_o = 111.4 \text{ km s}^{-1}$ ) at a separation of  $47'$ , NGC 4781 (Sc; panel 273;  $u_o = 68.9 \text{ km s}^{-1}$ ) at a separation of  $18'$ , and NGC 4760 (SO or cD; panel 30;  $v_o = 44.51 \text{ km s}^{-1}$ ), which obviously is in the background. Although the redshift difference between NGC 4790 and NGC 4781 is large at  $46.5 \text{ km s}^{-1}$ , suggesting different distances, the stellar contents of each resolve into individual stars at about the same level beginning near  $V = 21.5$ ; further, the III regions in each are of about the same brightness, and the largest Mil regions in each resolve at about  $3''$  diameter. In addition, there is a dwarf SmIII-IV galaxy between NGC 4790 and NGC 4781, separated from NGC 4790 by only  $13.3'$ . It has HII regions at the same brightness level as the other two galaxies of the pair.

If NGC 4742 (E4), NGC 4781 (Sc), NGC 4790 (Scd), and the SmIII-IV dwarf arc in a group at a mean redshift of  $\langle v_o \rangle = 98.6 \text{ km s}^{-1}$ , giving a redshift distance of 20 Mpc ( $H = 50$ ), the respective projection linear separations from NGC 4790 are 273 kpc for NGC 4742, 105 kpc for NGC 4781, and 77 kpc for the SmIII-IV dwarf, all smaller by a factor of four than the diameter of the Local Group.

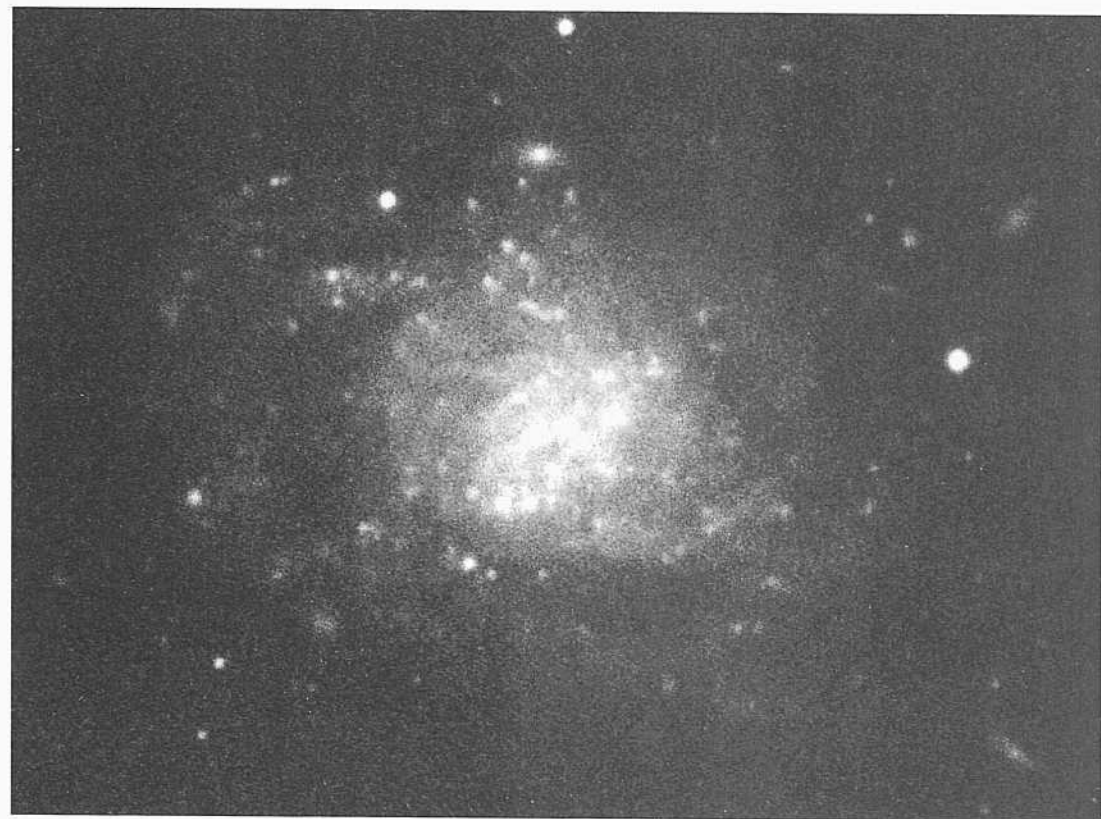
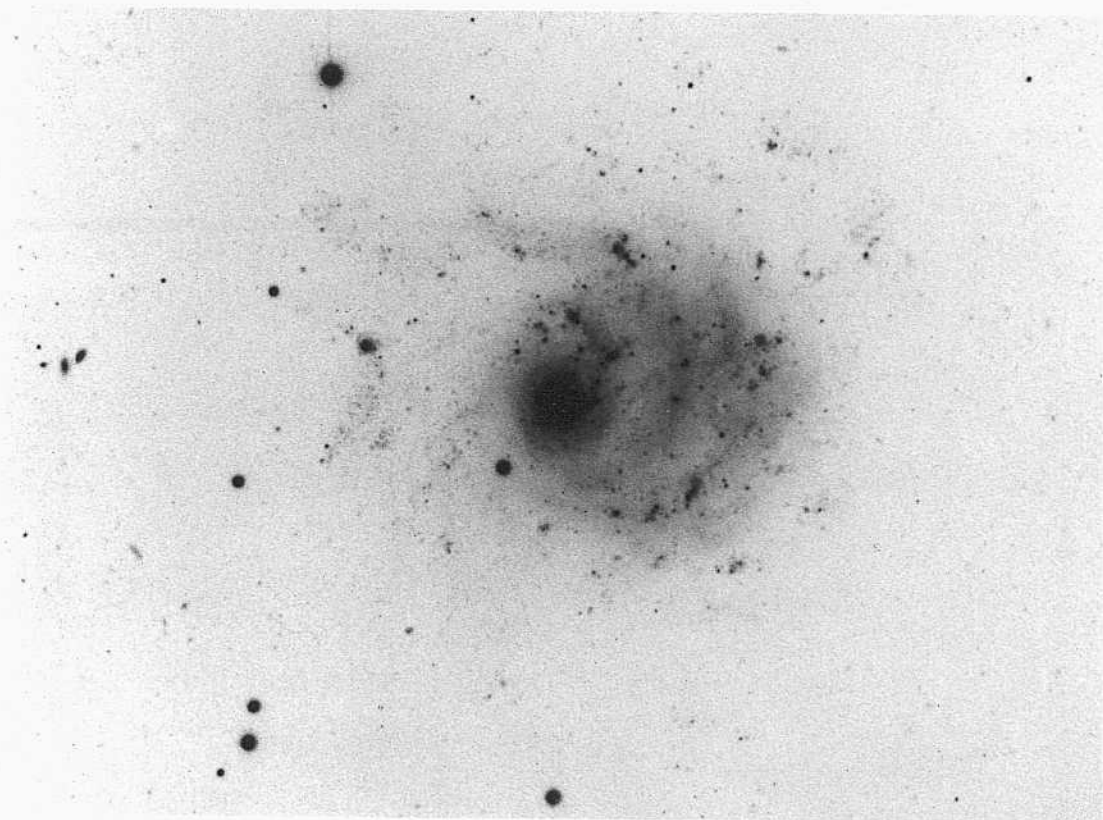
NGC 941            ScdHI            group  
 CD-494-S  
 Sep 26/27, 1978  
 103aO + GG385  
 45 niin

NGC 941 is in an apparent group with NGC 936 (SB0<sub>2/3</sub>/SBa; panels 90, 106, S9) at a separation of  $12.6'$ , and with an anonymous SBcd at a separation of  $12.3'$  whose stellar content resolves at the same level as in NGC 941, and as a wide pair with NGC 955 (Sb; panel 150) at a separation of  $3.1'$ . The redshifts are  $U_o(936) = 151.2 \text{ km s}^{-1}$ ,  $\langle v_o \rangle(941) = 171.7 \text{ km s}^{-1}$ , and  $u_o(955) = 164.1 \text{ km s}^{-1}$ . At the mean redshift distance of 32 Mpc ( $H = 50$ ), the respective projected linear separations from NGC 941 are 117 kpc for NGC 936, 288 kpc for NGC 955, and 114 kpc for the anonymous SBcd companion. These separations are all smaller than the radius of the Local Group.

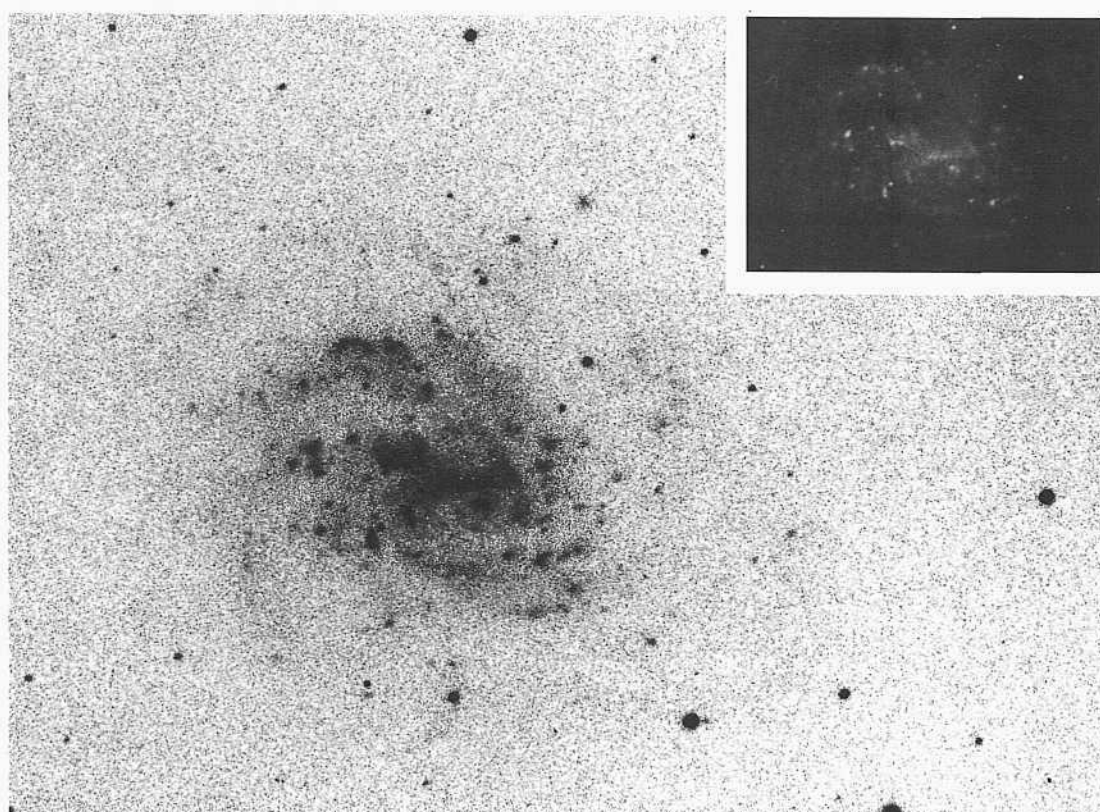
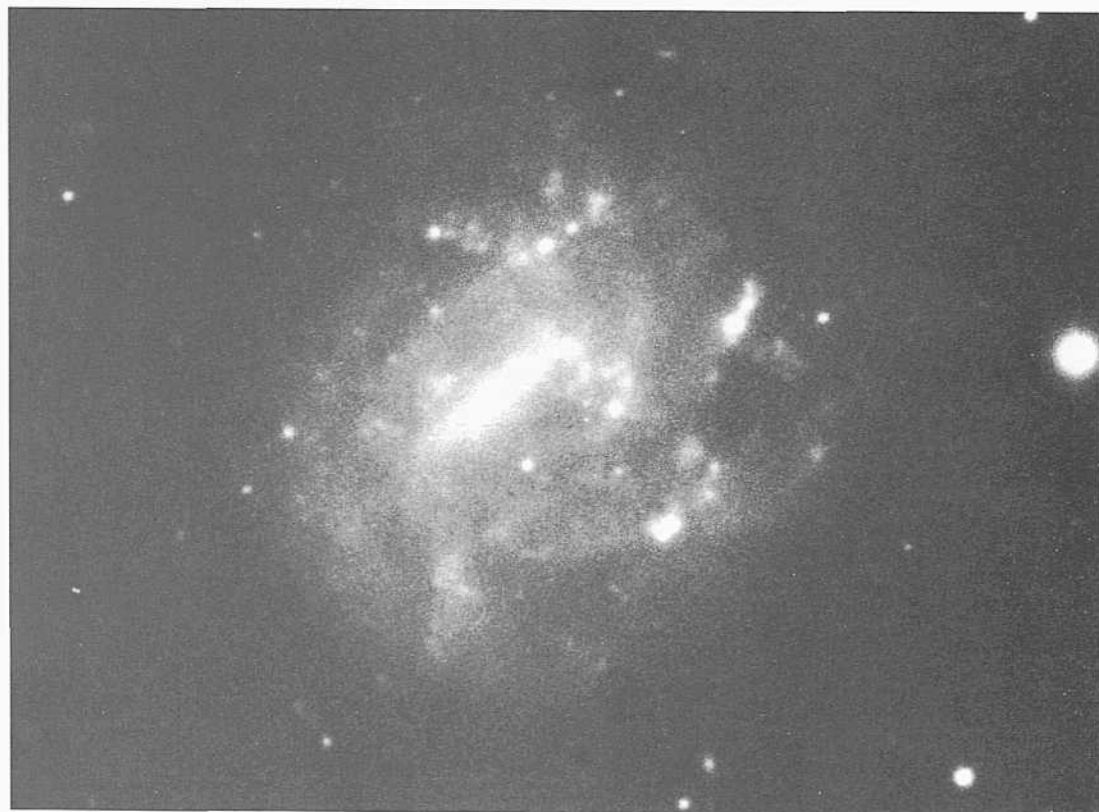
Individual stars may begin to resolve in both NGC 941 and the SBcd companion at about  $V = 22$ ; discrimination and individual identification of the stars and the numerous Mil regions will be necessary by the standard methods.



PANEL  
315



PANEL  
316



*Scd Classification Section (continued)*

IC5201 SBcd(s)II panel S10  
 CD-1533-S/Br  
 Aug 6/7, 1980  
 103aO + GG385  
 45 min

The multiple thin arms are clearly resolved into individual stars beginning at about  $B = 21.5$ , and the arms are also filled with a multitude of Mil regions, the largest of which have diameters of about 5". The redshift from Huchtmeier and Richter (1989) is  $v_0 = 875 \text{ km s}^{-1}$ .

NGC 7107 SBe(s)/SBmIH-IV  
 CD-529-S  
 Sep30/Oct 1, 1978  
 103aO + GG385  
 45 min

There is clear evidence of a bar containing HII-region candidates, indicating recent star formation. The spiral structure is not well defined, resembling more the pattern in the LMC than in a regular spiral; hence the mixed classification is required.

The redshift is  $v_h = 2446 \text{ km s}^{-1}$ .

NGC 1744 SBcd(s)II-III  
 CD-1334-S/Br  
 March 14/15, L980  
 103nO + GG385  
 60 min

Brightest stars begin to resolve in abundance in NGC 1744 about 1 mag above the plate limit, which is near  $H = 23$ . The very brightest star may have  $i_i = 20.5$ , but the numerous III regions must be separated from the stellar candidates before the brightest-star data are secure. Star-formation and III regions exist over the central oval and inner disk.

The redshift is  $v_{ii} = 639 \text{ km s}^{-1}$ . The resolution into stars is not as pronounced as in NGC 45 (two panels back), which has a smaller redshift by a factor of 1.2. If the redshift-distance relation were noiseless, the magnitude difference between the brightest stars in NGC 1744 and NGC 45 would be 0.4 mag. However, the observed difference in the resolution level of the brightest stars is about 1 mag, suggesting noise in the velocity field of about  $\pm 100 \text{ km s}^{-1}$ . Such a random velocity about the Hubble flow is, of course, small. This method has important promise and can be used out to distances of about three-fourths the distance to the Virgo Cluster.

New 3 = A 1246-09 SBcd(s)II.2  
 CD-1883-HB  
 April 11/12, 1981  
 103aO  
 60 min

The surface brightness of New 3 is very low, which is the reason it was not included in the NCC listing. A small bar exists from whose ends the multiple-arm pattern begins.

Many III regions cover the face of the disk. A few exist in the bar.

The redshift of New 3 is  $v_{ii} = 1105 \text{ km s}^{-1}$ .



*Scd Classification Section (continued)*

NGC 4485/4490 S(tidal) Karachentsev 341  
 H-1458-B ScdIII pec  
 May 24/25, 1944  
 103aO  
 75 niin

Both components of this obviously interacting pair show massive, robust star formation over each of their faces. Individual stars begin to resolve at about  $V = 18$  in each galaxy, but the surface brightness is so high over most of their disks as to make the photometry of individual stars difficult. Also there is much dust over the face of NGC 4490, the brighter of the pair.

The redshifts listed in the RSA2 are  $z_o(4485) = 817 \text{ km s}^{-1}$  and  $z_o(4490) = 601 \text{ km s}^{-1}$ . The plate used for the heavy exposure at the top left was taken by Baade with the Mount Wilson 100-inch Hooker reflector.

NGC 4485/4490 S(tidal) Karachentsev 341  
 S-657-B ScdIII pec  
 March 3/April 1, 1938  
 E40  
 60 min

The light print of the NGC 4485/4490 pair at the bottom left was made from an original plate taken by Baade with the Mount Wilson 60-inch reflector.

The morphologies of the galaxies are abnormal, presumably due to the close encounter.

NGC 3691 Scd(s)HI  
 CD-2135-S  
 March 22/23, 1982  
 103aO + GG385  
 45 niin

NGC 3691 is small ( $D_{25} = 1.3'$ ) and is not well resolved into stars or HII-region candidates. Its surface brightness is low.

Deeming that a weak spiral pattern is traceable, we have classified the galaxy as an Scd, but an InIII classification would also be possible.

The redshift is  $v_o = 947 \text{ km s}^{-1}$ .

NGC 3274 ScdIII  
 PH-7934-S  
 Nov 7/8, 1980  
 103aO  
 12 min

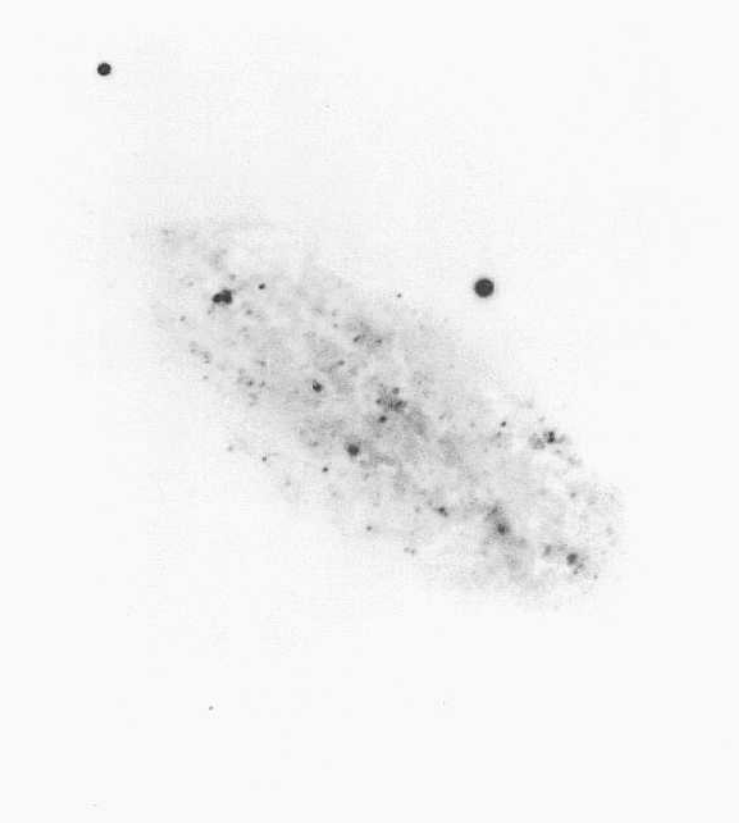
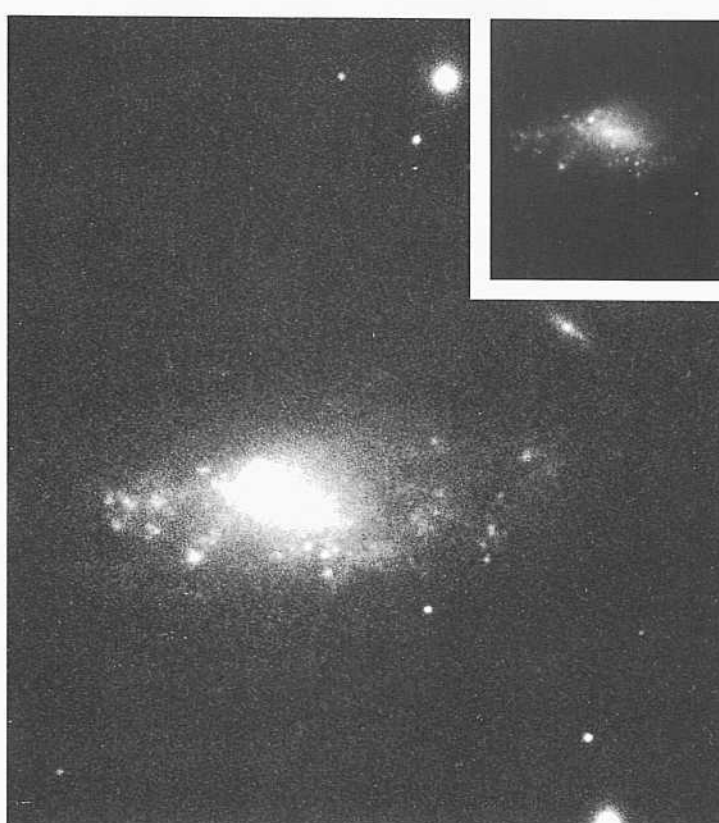
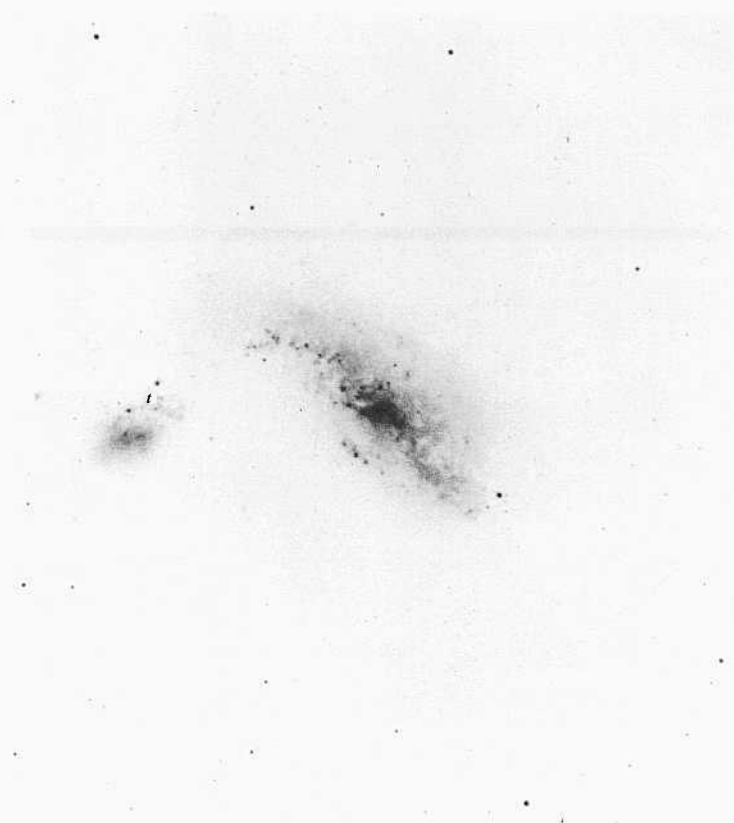
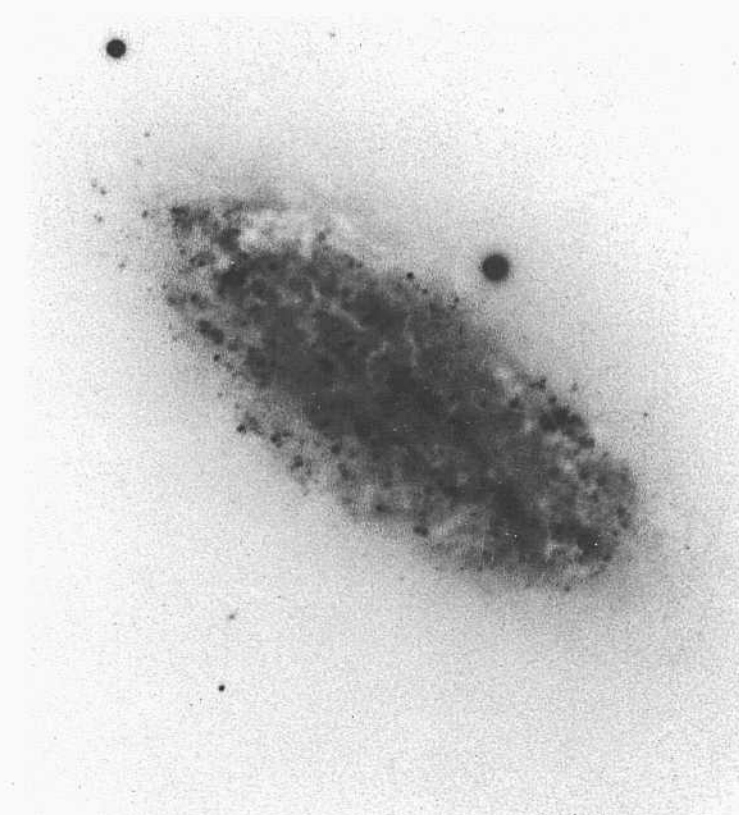
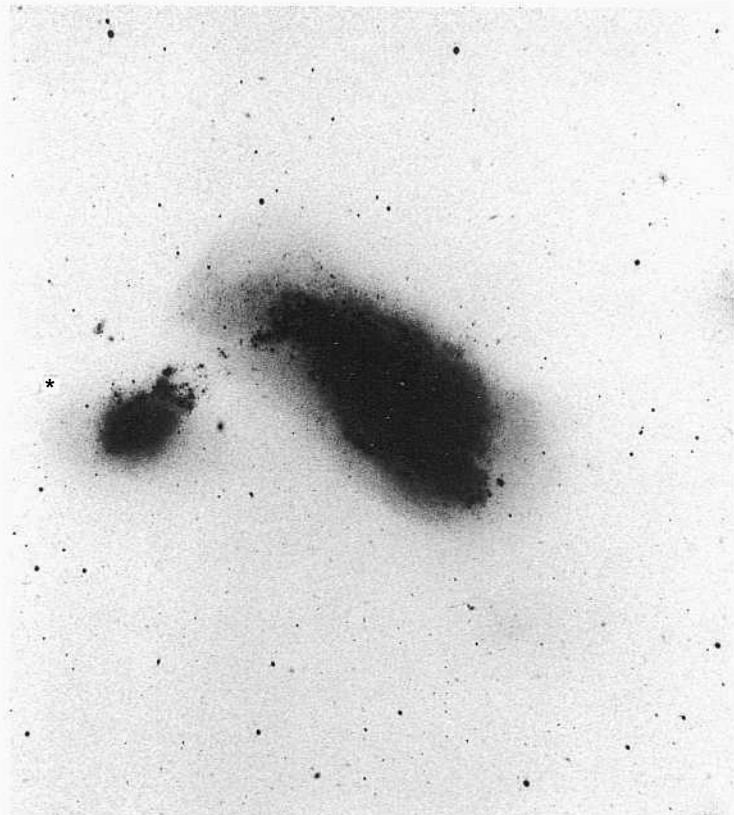
NGC 3274 is resolved into individual stars beginning at about  $B = 19$ . However, discrimination of the stars from the HII-region candidates is necessary before secure photometry of the stars can be done.

The redshift is  $v_o = 486 \text{ km s}^{-1}$ .

NGC 2976 SdHI-IV M81 Gr  
 PH-470-S  
 March 17/18, 1953  
 103aO + GG385  
 10 min

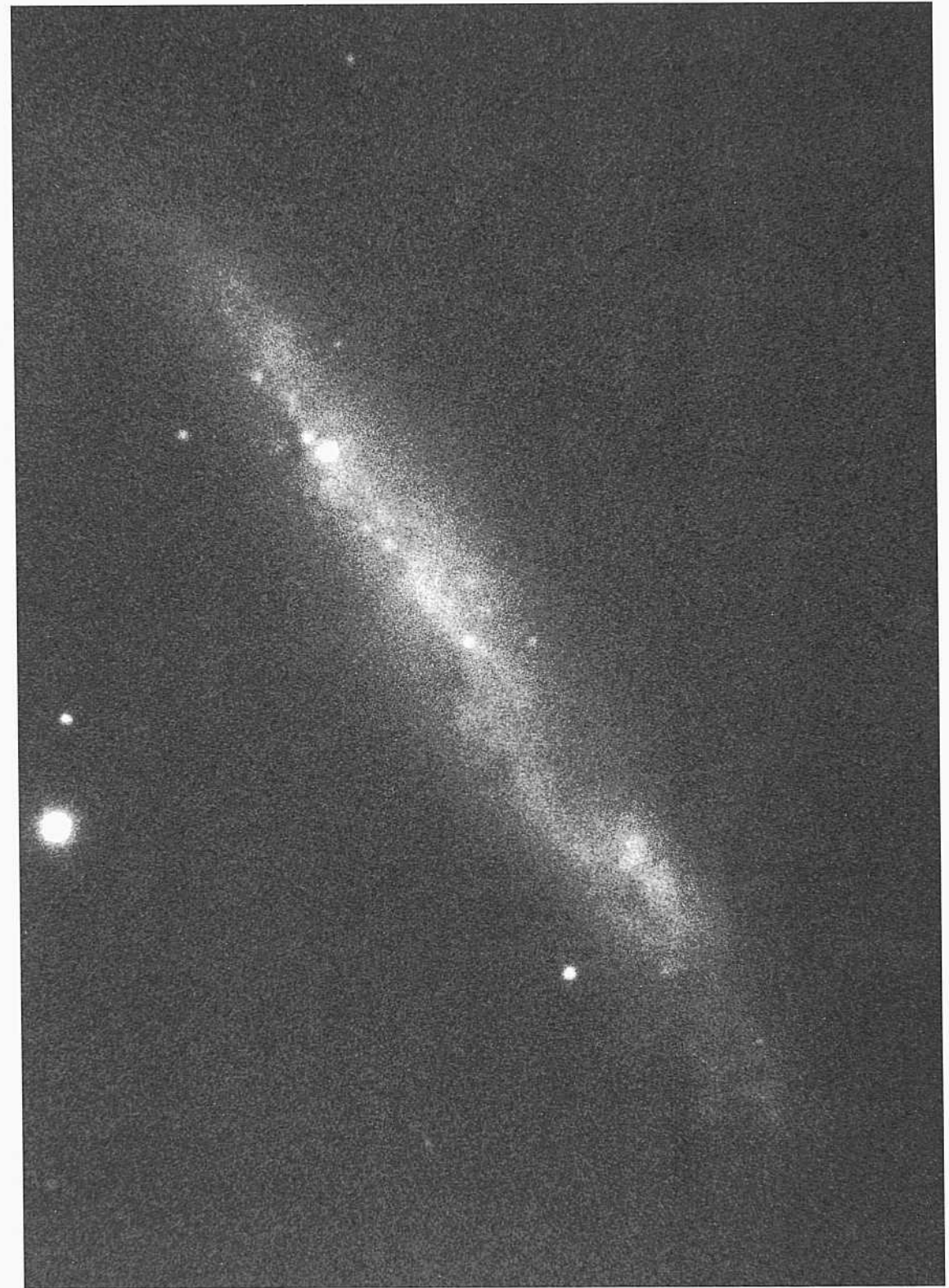
NGC 2976, long considered a member of the M81/NGC 2403 Group (Holmberg 1950), has a large angular diameter ( $D_{95} = 4.9'$ ) and a small redshift,  $v_o = 168 \text{ km s}^{-1}$ , consistent with membership in the Group, whose mean redshift is  $\langle z_o \rangle = 240 \text{ km s}^{-1}$ , as listed in the RSA2.

Both prints on the facing panel have been made from the same short-exposure blue plate taken at Palomar with the 200-inch reflector. The surface brightness is high, making photometry of the individual stars difficult, although they begin to resolve as individuals at about  $B = 18.5$ . A spiral pattern is difficult to trace but it does exist; hence the Sd classification is required.



PANEL  
317

PANEL  
318



The 14 galaxies on this and the next two panels are nearly edge on. All are classified as Sc, Sbc, or Sd, based on the absence of evidence for a nucleus and central bulge and, for the Sbc and Sd types, by the lack of a discernible spiral pattern, often indicated in earlier on-edge Sc types by the particular luminosity distribution at the ends of the disk.

NGC 55                      Sc                      South Polar Gr  
 CD-556-S  
 Oct 4/5, 1978  
 103aO + GG385  
 45 min

NGC 55 is very highly resolved into individual stars, about equally well as other galaxies of the South Polar Group such as NGC 247 and NGC 300. The resolution is also similar to that in the nearby galaxy NGC 3109, where Cepheid variables give a modulus of  $m - M = 26.4$  (Sandage and Carlson 1988). This is nearly the same value measured by Graham (1984) for NGC 300, also using Cepheids.

The brightest stars in NGC 55 begin to resolve at about  $B = 17.5$ . The redshift is  $v_o = 115 \text{ km s}^{-1}$ . Evidently, NGC 55 is just beyond the Local Group and has the small cosmological expansion redshift characteristic of galaxies with distance moduli near  $m - M = 26$  (Sandage 1986a).

NGC 1507                      Sd(on edge)  
**PH-7845-S**  
**Sep 3/4, 1980**  
**103aO**  
 12 min

NGC 1507 is seen on edge and, therefore, is of uncertain morphological type. The Sd classification is made because of the absence of both a nucleus and a central bulge, and because of the lack of the characteristic hooks at the ends of the edge-on image; such hooks are often seen in edge-on Sc galaxies that have strong spiral patterns.

The redshift is  $v_o = 898 \text{ km s}^{-1}$ . A few HII-region candidates are present.

Scd Classification Sectioji (continued)

NGC 4144      ScdIII      CVn II Gr  
PH-7147-S      Raciii wedge  
Feb 1/2, 1976  
103aO + GG13  
30 niin

NGC 4144 is very nearby, judged by the easy resolution into individual stars beginning at about  $B = 20$ . The galaxy is in the complex Ursa Major region wherein at least three separate Kroups can be identified. The mean redshift is about  $\langle v_o \rangle = 285 \text{ km s}^{-1}$  for the CVn I Group, as named by de Vaucouleurs (1975), where he lists five members. The group is called 134 by Kraan-Korteweg and Tammann (1979), where they list 21 members, including NGC 4144.

The second group in the Ursa Major region, called the CVn II Cloud by de Vaucouleurs (1975), has  $\langle v_o \rangle$  of about  $750 \text{ km s}^{-1}$ . It contains such galaxies as NGC 3675 (Sb; panels 139, S4, SI 3, SI 4) and NGC 4051 (She; panel 180) as listed by de Vaucouleurs (1975). It also contains others such as NGC 4242 (SBd; panel 322), IC 749/750 (SBc; Sb?; panels 195, 306), NGC 3782 (SBcd; panel 328), and NGC 3949 (Sc; panel 265). The third aggregate in the region is the loose Ursa Major Cluster, with  $\langle v_o \rangle$  of about  $980 \text{ km s}^{-1}$ .

The redshift of NGC 4144 is small at  $316 \text{ km s}^{-1}$ . The galaxy is clearly in the nearby B4 (or CVn I) Group.

The spiral pattern can be discerned by the characteristic hooks that bend in opposite directions at the ends of the nearly edge on image.

Note that the plate was taken with a Racine wedge; the bright stars have secondary images 5 mag fainter at 1.8" separation.

NGC 2188      ScdIII  
CD-141-S  
Feb 1/2, 1978  
103aO + GG385  
50 niin

Individual stars are beginning to resolve at about  $B = 21$  in this nearly edge on galaxy, but the high-surface-brightness of the image will make photometry difficult.

The redshift is  $v_o = 555 \text{ km s}^{-1}$ .

NGC 4592      ScdIII  
H-2271-H  
May 5/6, 1946  
103aO  
40 niin

NGC 4592 resolves easily into fill-region candidates and brightest stars that begin to appear individually at about  $B = 20$ . This is brighter by about 2 mag than the resolution level of the spirals associated with the Virgo Cluster (NGC 4321, NGC 4535, NGC 4303, NGC 4254, etc.). The mean redshift of the Virgo Cluster of  $\langle v_o \rangle = 976 \text{ km s}^{-1}$  is similar to the redshift of  $v_o = 903 \text{ km s}^{-1}$  of NGC 4592 here, yet the level of resolution of the stellar content is different, suggesting velocity perturbations in the expansion field in the direction of NGC 4592.

The region is complex (NGC 4592 is in the southern extension of the Virgo Cluster), and the redshifts there are not good distance indicators. From the resolution level in NGC 4592 one surmises that the distance modulus to this galaxy is about  $m - M = 30$  on the scale of  $m - M = 31.7$  adopted for the Virgo Cluster.

NGC 4244      ScdIII      CVn I Gr  
PH-124-MH      HA, p. 25  
March 20/21, 1950  
103aO  
30 min

NGC 4244 is a member of the very nearby CVn I Group (de Vaucouleurs 1975), which is the B4 Group of Kraan-Korteweg and Tammann (1979) in the Ursa Major complex. The redshift of NGC 4244 is  $v_o = 249 \text{ km s}^{-1}$ .

The galaxy is highly resolved into individual stars beginning at about  $B = 18$ . However, study of its stellar content will be difficult because the galaxy is almost exactly edge on.

NGC 4244      ScdIII      CVn I Gr  
H-2507-H      HA, p. 25  
March 5/6, 1948  
103aO  
30 min

The image of NGC 4244 in the light print at the bottom of the column was made from a different original plate than was used for the heavy print above it.

The dust lane nearly bisects the very thin plane, showing that the galaxy is closely edge on. There is neither a central bulge nor a luminous halo. HII regions are present, the largest of which resolve at the 5" level.

The angular diameter of the NGC 4244 disk is large, at  $D_{25} = 1.6'$ .

NGC 3044      Scd(on edge)  
CD-1460-S/Br  
May 10/11, 1980  
103aO + GG385  
4.5 niin

NGC 3044 is nearly edge on. It has neither a central bulge nor luminous halo. A few individual knots are either HII regions or individual brightest stars. The magnitude of the brightest of these is about  $B = 21.5$ . The largest HII region resolves into a disk at about the 2" level.

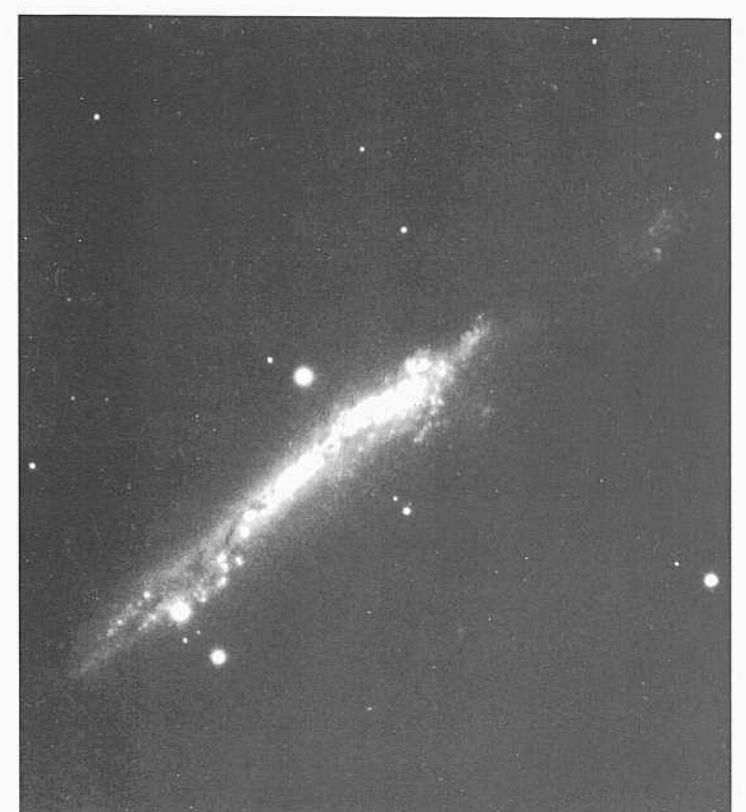
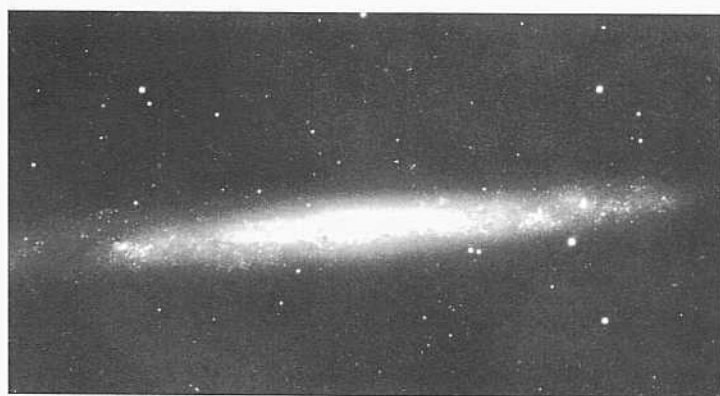
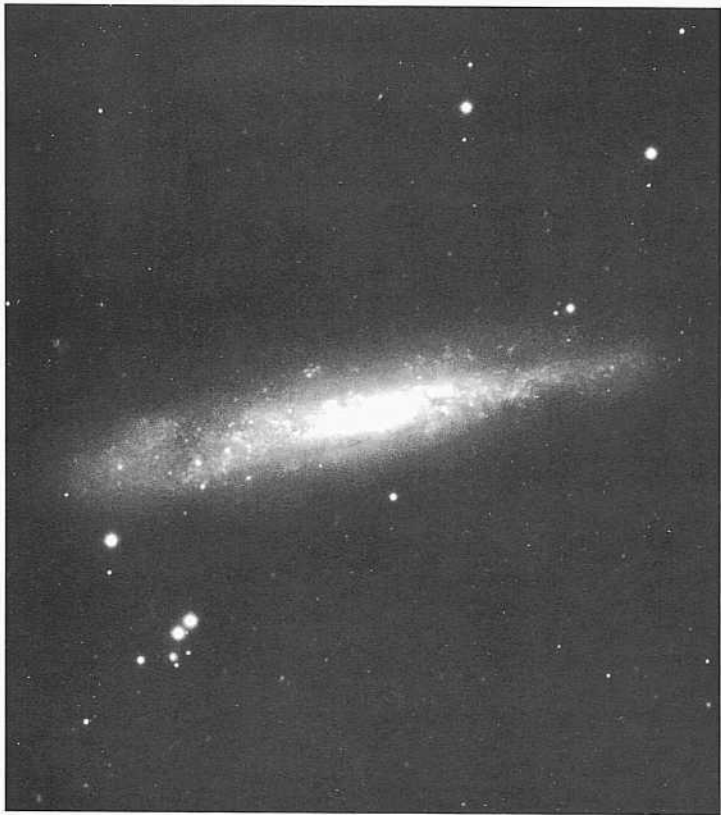
The redshift is  $v_o = 1206 \text{ km s}^{-1}$ .

NGC 3432      Scd(on edge)      NGC 3368 Gr  
PH-8077-S      Racine wedge  
Feb 5/6, 1981      panel 320  
103aO  
5 niin

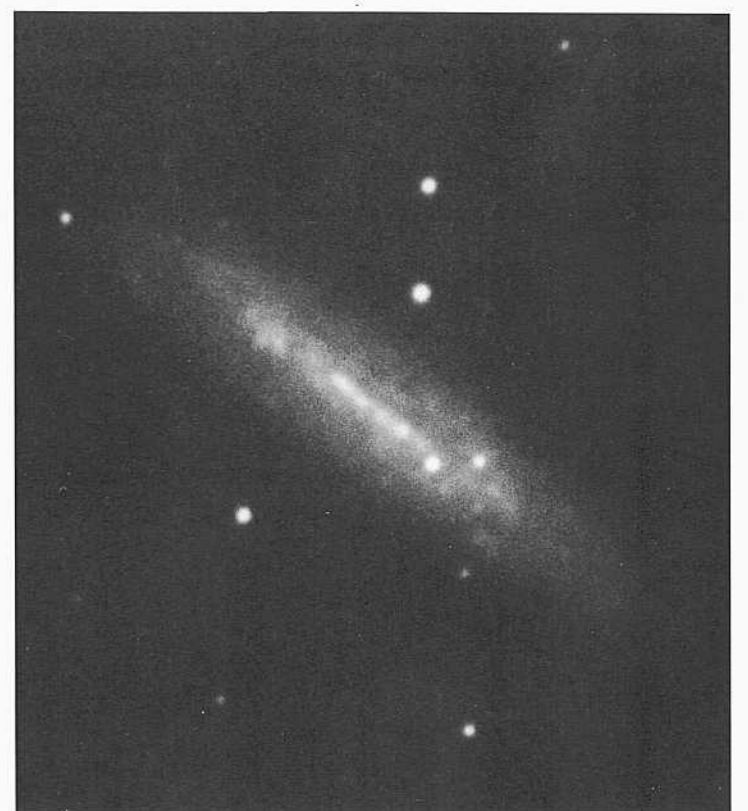
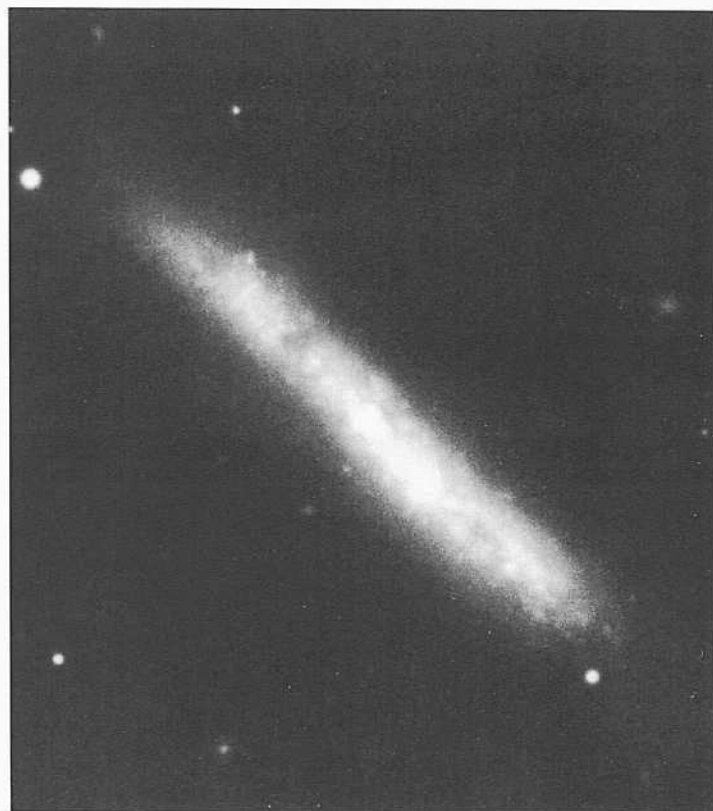
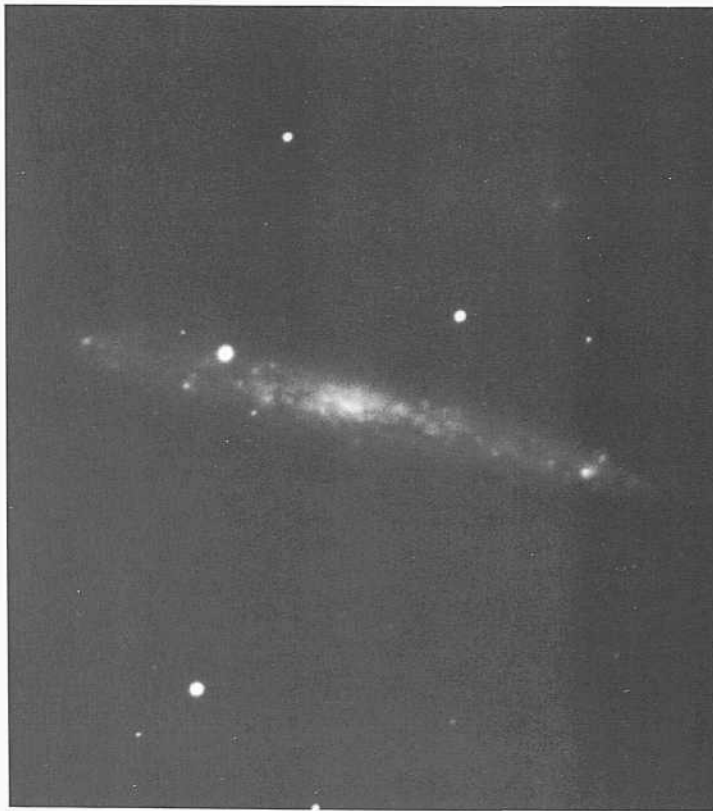
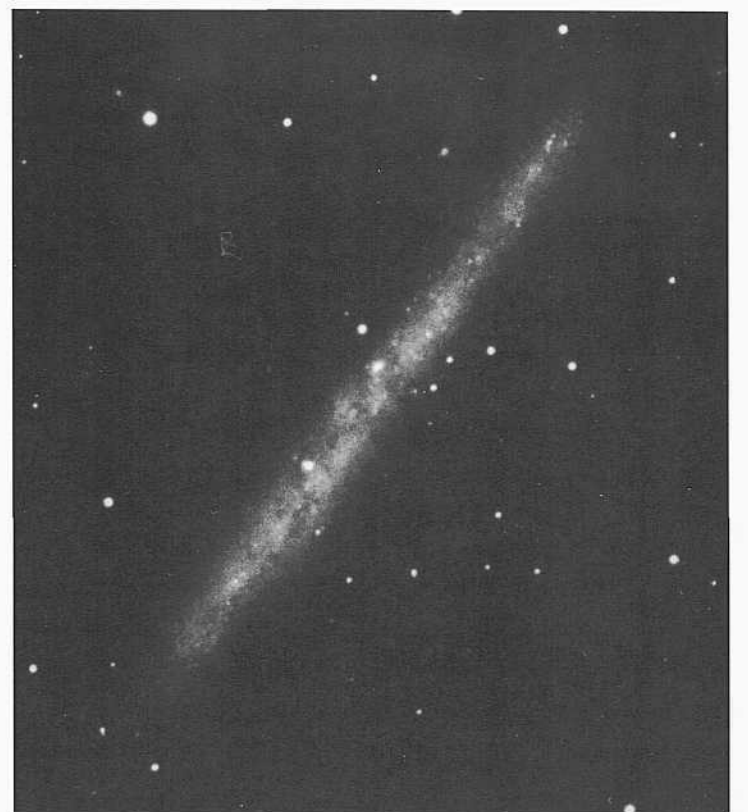
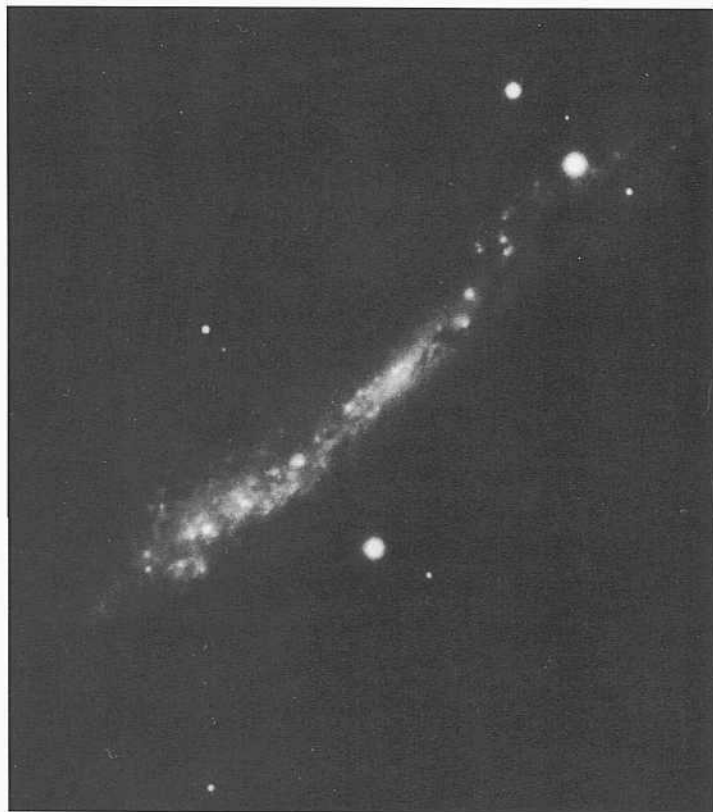
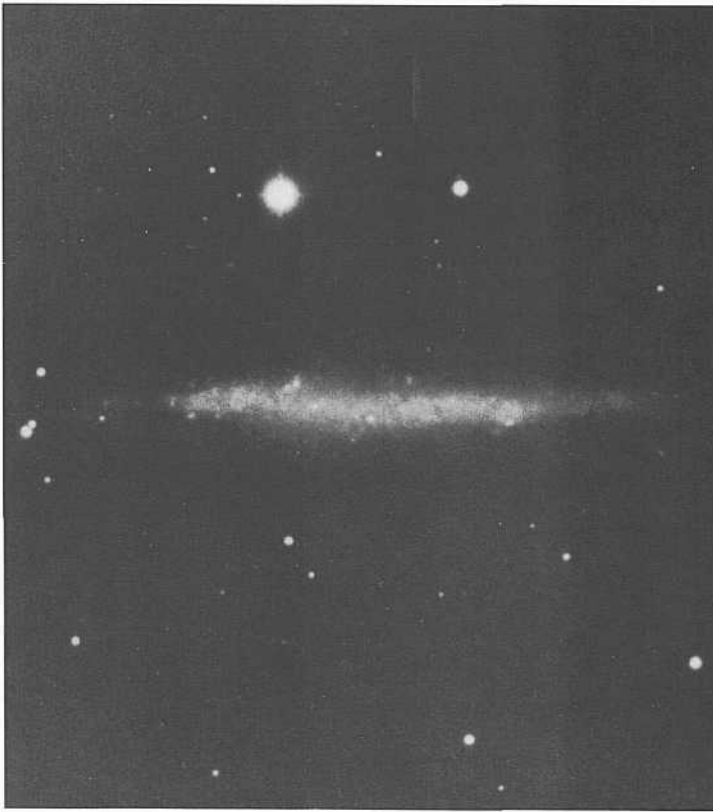
Robust star formation is occurring in the high-surface-brightness disk of NGC 3432. High-surface-brightness HII knots dominate the image. Individual stars probably begin to resolve at about  $B = 21$ .

A large, very-low-surface-brightness dwarf with an unresolved nucleus exists at a separation of  $3.1'$ . It resembles the huge dE.N type in the Virgo Cluster, illustrated elsewhere (Sandage and Binggeli 1984) and listed in the VCC, Table XIV.

NGC 3432 is listed by de Vaucouleurs (1975) as a member of the NGC 3368 Group, whose mean redshift is about  $\langle v_o \rangle = 750 \text{ km s}^{-1}$ . The redshift of NGC 3432 itself is  $v_o = 607 \text{ km s}^{-1}$ . At a redshift distance of 15 Mpc, the projected linear separation of the companion from NGC 3432 is small at 14 kpc.



PANEL  
320



T
 The six galaxies on this panel complete the illustrations of edge-on late-type Sd, Sd, and Sm galaxies in the RSA.

NGC 7064      Scd(on edge)  
 CD-509-S  
 Sep 28/29, 1978  
 103aO + GG385  
 45 min

HII-region candidates begin to appear across the image of NGC 7064 at about  $B = 19.5$ . Individual stars are definitely present at  $B = 21$ , but still-brighter stars are undoubtedly confused with HII regions and must be separately identified before conclusions as to the upper stellar luminosity are secure.

The redshift is  $v_0 = 722 \text{ km s}^{-1}$ .

NGC 4183      Scd(on edge)      Ursa Major Cluster  
 PH-8088-S                              Racine wedge  
 Feb 6/7, 1981  
 103aO  
 4 min

The brightest individual HII-region candidates in NGC 4183 begin to appear at about  $B = 20$ . The two largest probably resolve at about the 1.5" level. Individual stars at least as bright as  $B = 22$  begin to resolve.

The redshift is  $v_0 = 968 \text{ km s}^{-1}$ .

NGC 3432      Scd(on edge)      NGC 3368 Gr  
 PH-8077-S                              Racine wedge  
 Feb 5/6, 1981                              panel 319  
 103aO  
 5 min

The image of NGC 3432 is repeated here from the previous panel, taken from the same original plate.

The redshift is  $v_0 = 707 \text{ km s}^{-1}$ .

NGC 4700      Se or Sin                      panel 291  
 CD-1444-S/Br  
 May 6/7, 1980  
 103aO + GG385  
 45 min

The surface brightness of NGC 4700 is so high as to mask most of the resolution into numerous HII regions seen on the original plate. The galaxy is also illustrated in the Sc section on panel 291.

The redshift is  $v_0 = 1193 \text{ km s}^{-1}$ .

IC5052              Sd(on edge)  
 CD-489-S  
 Sep 26/27, 1978  
 103a(> + GG385  
 45 min

The small redshift  $v_0 = 140 \text{ km s}^{-1}$  listed in the RSA is evidently incorrect because one of the redshifts used in calculating that mean is grossly wrong. An accurate observed 21-cm redshift of  $v_{sun} = 595 \text{ km s}^{-1}$  listed by Huchtmeier and Richter (1989) leads to  $v_0 = 428 \text{ km s}^{-1}$ . This larger redshift is consistent with the level of resolution into stars and HII regions, while the smaller velocity is not.

The largest of the several HII regions resolve at the 2" level. The brightest stars begin to resolve at about  $B = 21$ .

NGC 5984              SBcdIII              Racine wedge  
 PH-7487-S  
 May 11/12, 1978  
 103aO + GG13  
 20 min

The linear pattern of HII-region candidates in the center of the image is the characteristic that suggests the barred morphological classification.

The redshift is  $v_0 = 1122 \text{ km s}^{-1}$ .



## The Sd and SBd Classification Sections

### C

**vXalaxies** of types Sd and SBd at the very late end of the spiral sequence, together with galaxies that are late-type dwarfs of types Sm and Im are shown on the next 12 panels. A spiral pattern can still be traced in the Sd and SBd types, but it is more disorganized than in the earlier morphological boxes of the sequence. A spiral pattern is even less obvious in the Sm types, whose prototype is the Large Magellanic Cloud. All traces of a spiral pattern have disappeared in the Im dwarf class.

NGC 7793      Sd(s)IV      South Polar Gr  
CD-510-S                              panel S6  
Sep 28/29, 1978  
103aO + GG385  
45 nlin

NGC 7793 is highly resolved into individual stars beginning at about  $B = 18$ . A spiral pattern can be discerned, but it is more disorganized than in M33 or NGC 300, which are earlier examples of the same type of massive-armed spiral features.

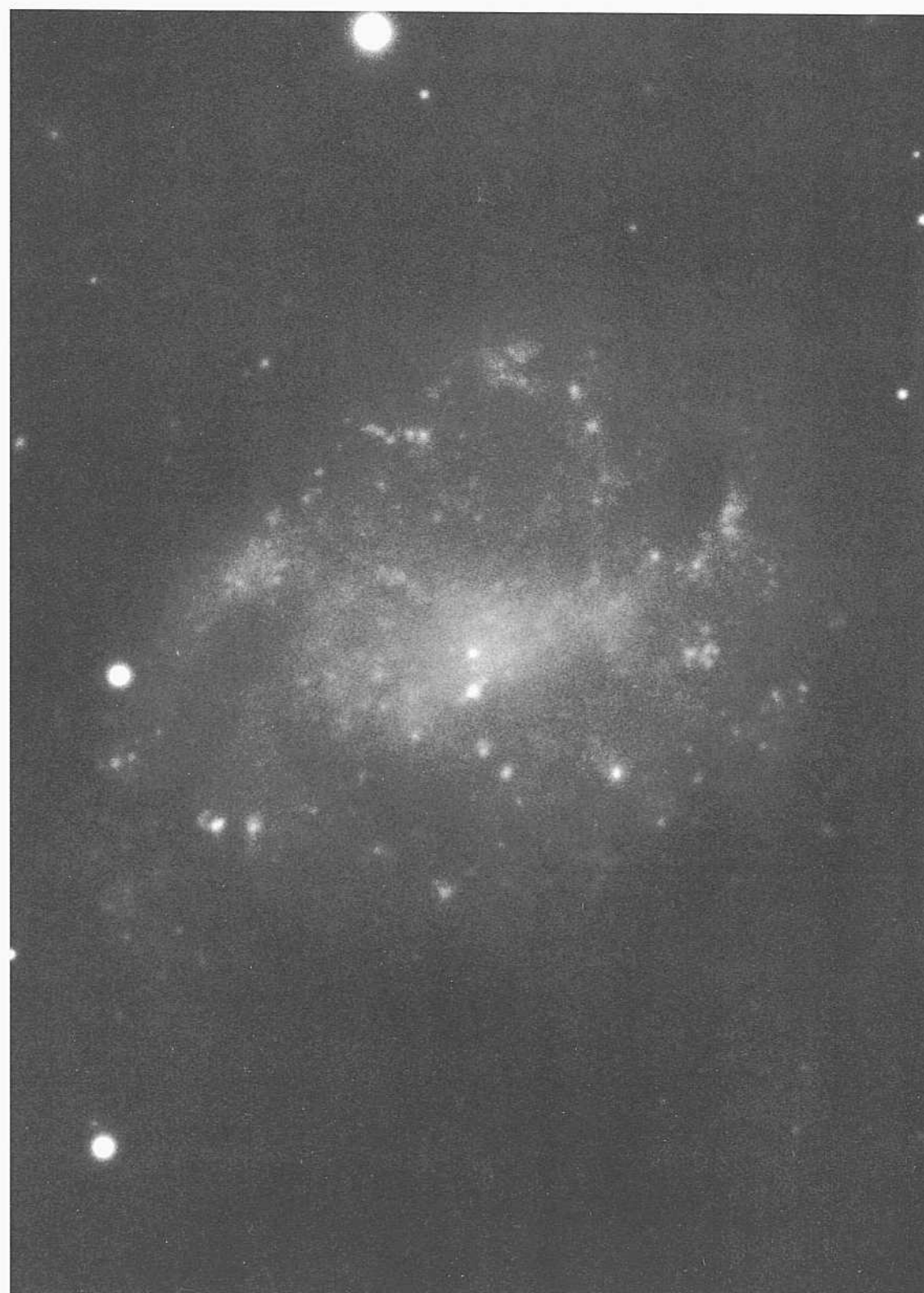
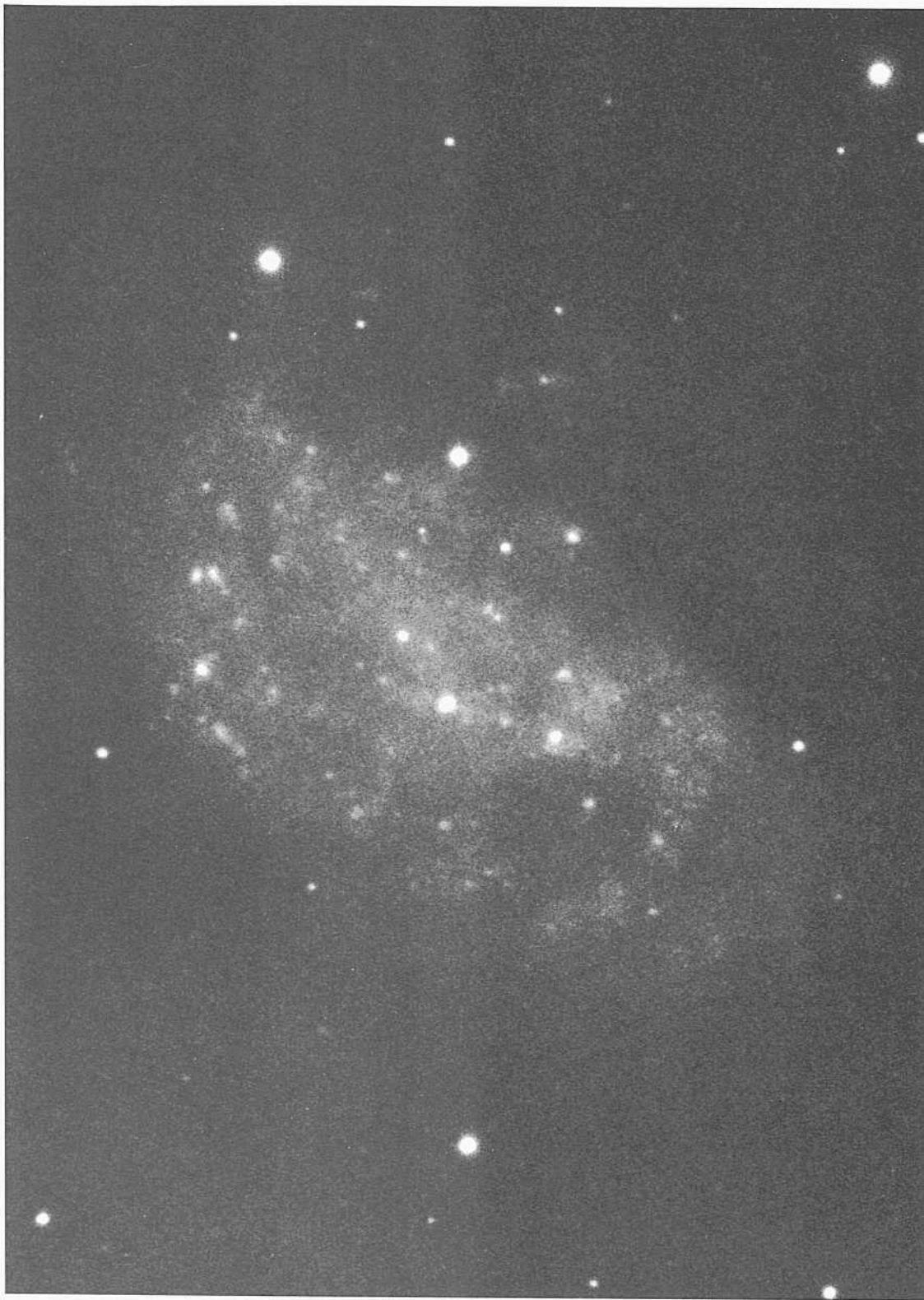
Associations of early-type stars are evident in the arms, similar to those in M33 and NGC 300.

The brightest stars may resolve starting about 0.5 mag fainter than the brightest stars in NGC 55, NGC 247, and NGC 300, also in the South Polar Group. From the characteristics of the Group set out in Table 2 in the introduction to the RSA2, NGC 7793 and NGC 253 are said to be more distant than NGC 55, NGC 247, and NGC 300. The **redshift** of NGC 7793 is  $v_0 = 241$  km s<sup>-1</sup>. The  $v_0$  redshifts of NGC 55, NGC 247, NGC 253, and NGC 300 are 115 km s<sup>-1</sup>, 227 km s<sup>-1</sup>, 293 km s<sup>-1</sup>, and 128 km s<sup>-1</sup>, respectively. The **order** of the luminosity level of resolution **into** stars in these galaxies is the same as the order of the redshifts, showing the extreme quietness of the local expansion velocity field and the extension of the South Polar Group in the line of sight. The velocity dispersion about an ideal linear velocity flow is at a level of only a few tens of km s<sup>-1</sup> in this region immediately beyond the Local Group. The same conclusion, based on other data for galaxies extending more than halfway to the Virgo Cluster, has been discussed elsewhere (Sandage 1986a).



PANEL  
321

PANEL  
322





*Sd and SBd Classification Sections (continued)*

NGC 5585      Sd(s)IV      M101 Gr  
PH-76-B  
June 8/9, 1950  
103aO  
30 niin

NGC 5585 is one of the four well-resolved satellite companions to M101 at a distance modulus of  $m - M = 29.3$  ( $D = 7.2$  Mpc). The four dwarf satellites, originally discussed by Holmberg (1950), are NGC 5204 (SdIV; panel 324), NGC 5474 (ScdIV pec; panel 315), NGC 5477 (Sd:)(not in the RSA; panel 326 here), and NGC 5585 here. The redshift of NGC 5585 is  $v_o = 441 \text{ km s}^{-1}$ . A discussion of the M101 Group has been made by Sandage and Tammann (1974c).

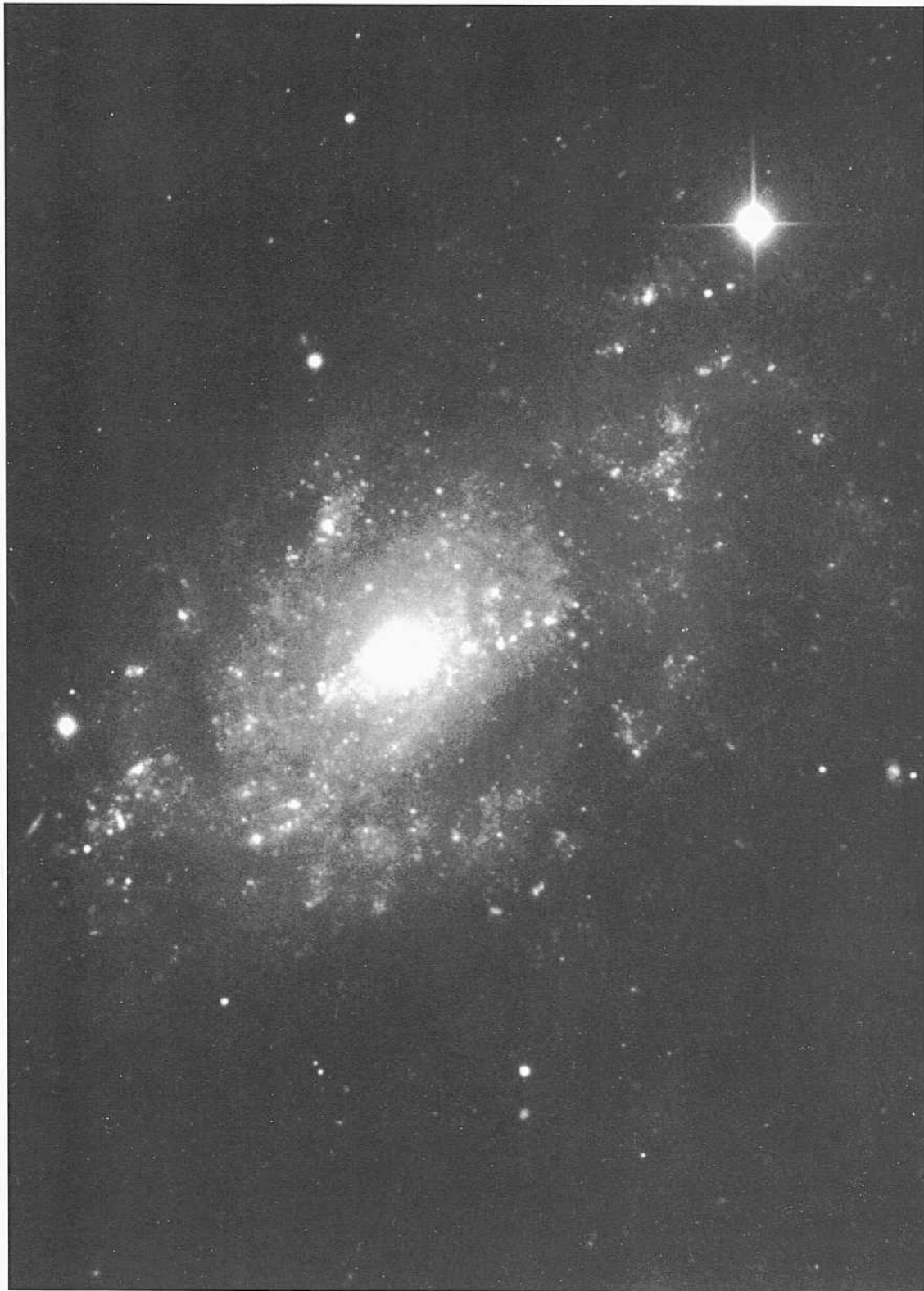
NGC 5585 is highly resolved into individual stars and HII regions. The largest HII regions resolve into disks at about the 2" level. The brightest stars are at least as bright as  $B = 20$  and may be brighter, but a study is necessary to separate the stars from the HII regions by standard methods.

IC 4710      SBd(s)IV  
CD-1472-S/Br  
May 10/11, 1980  
103aO + GG385  
45 niin

IC 4710 is similar in appearance to NGC 4242 and NGC 2552 on the preceding panel. Each is of low surface brightness. Each has a central, pointlike nucleus. Each has an ill-defined spiral pattern that is not entirely chaotic.

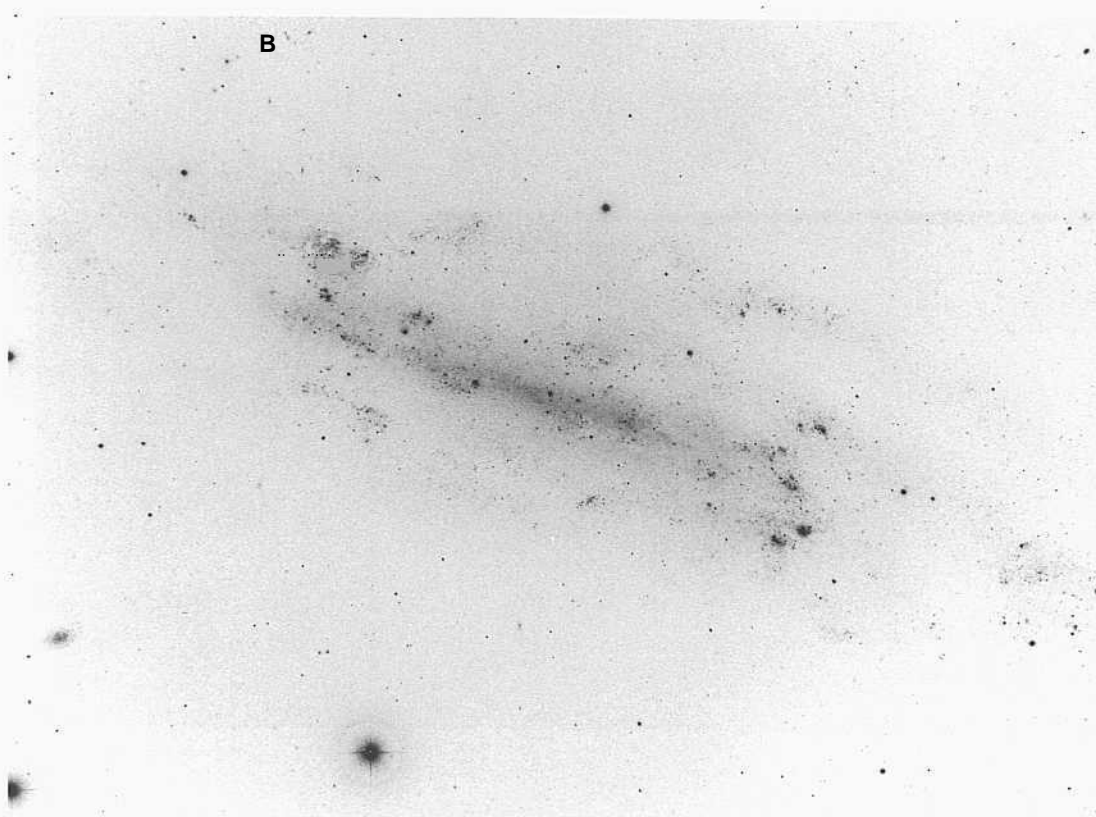
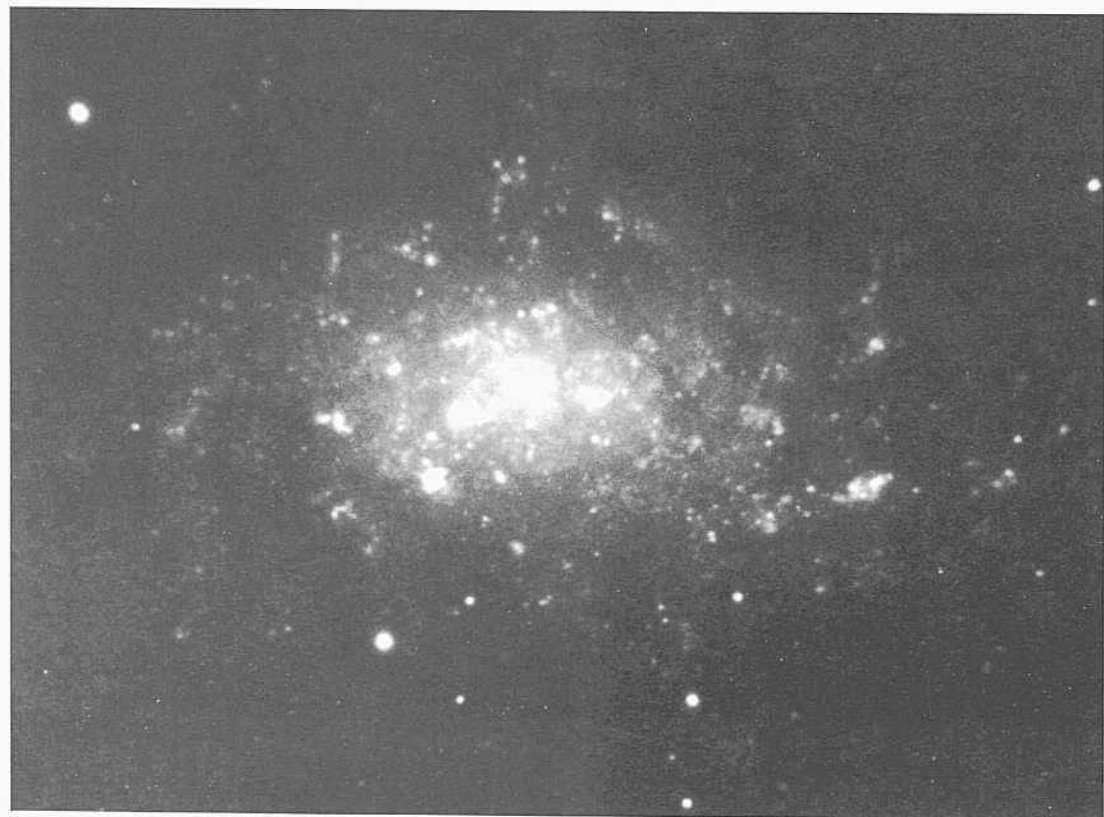
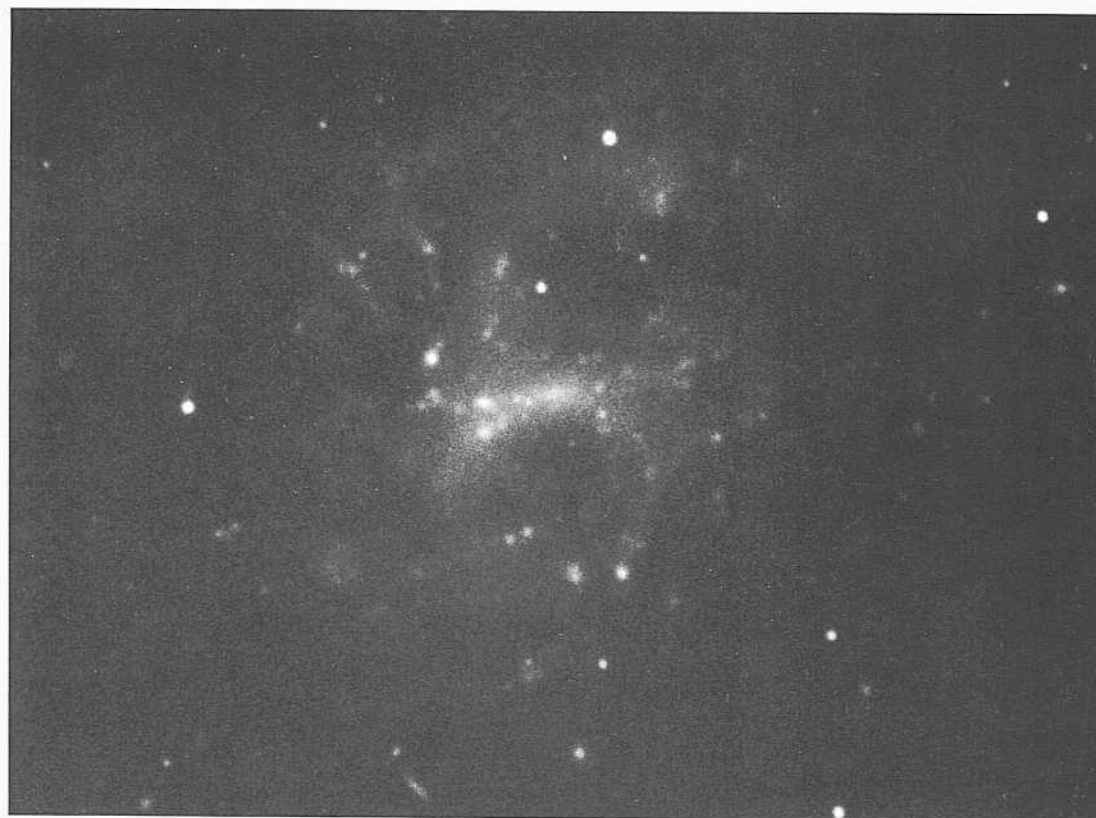
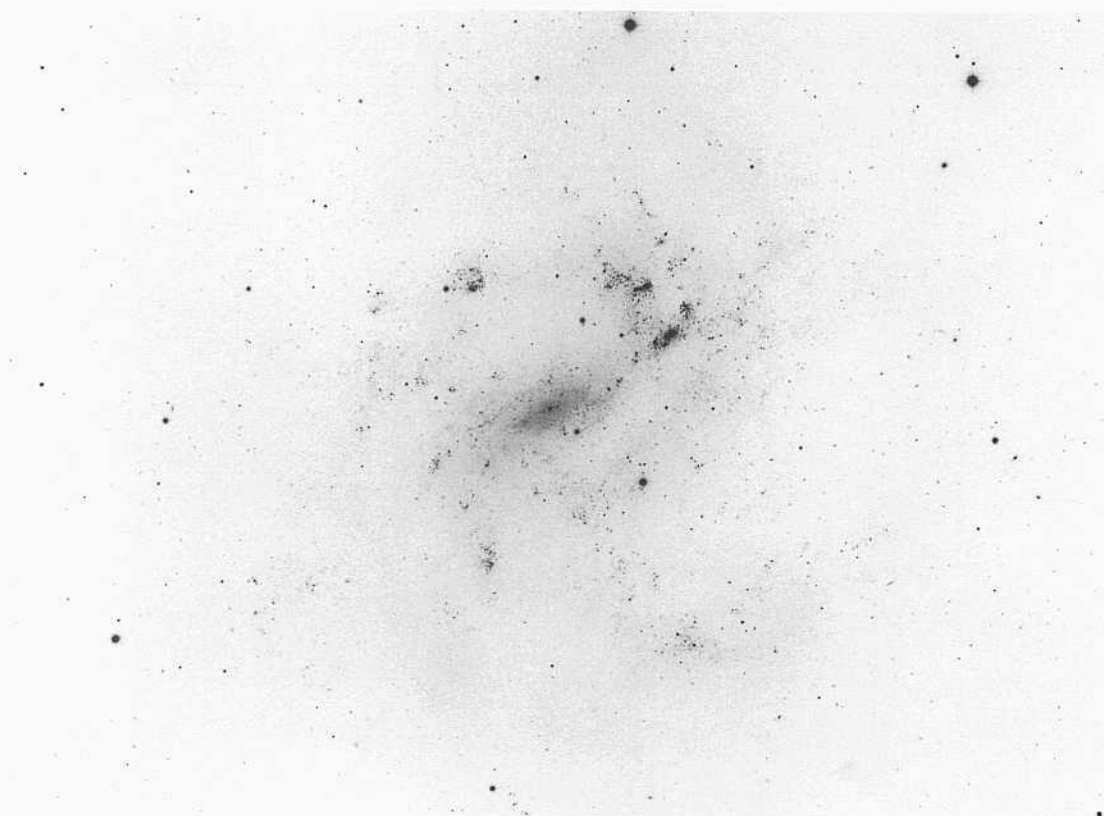
Stars begin to appear in IC 4710 at about  $11 = 21$ . The redshift of the galaxy is  $v_o = 508 \text{ km s}^{-1}$ .

A probable companion (ImIII) is separated by 4.5'. It shows about the same degree of resolution into stars and HII-region candidates as IC 4710. At a redshift distance of 10 Mpc ( $H = 50$ ) the projected linear separation from IC 4710 is small at 13 kpc.



PANEL  
323

PANEL  
324



NGC 4395      StiIII-IV      B4 Gr  
PH-7145-S      HA, p. 37  
Feb 1/2, 1976      Racine wedge  
103aD + GGII      panel S6  
45 inin

Parts of this single galaxy were catalogued separately as NGC 4395, NGC 4399, NGC 4400, and NGC 4401 in the Dreyer NGC Catalog. The moderately high surface brightness center was given one NGC number; the several separate bright associations in the loose spiral pattern were the other three. The entire complex is called NGC 4395 here.

The galaxy is in the nearby, low-redshift group in the complex Ursa Major region called Group B4 by Kraan-Korteweg and Tammann (1979) and CVn I by de Vaucouleurs (1975). The group is important for the distance scale problem because it contains NGC 4214 (SI3m; panel 330) and IC 4182 (not in the RSA or this atlas), both of which produced supernovae whose absolute magnitudes can be calibrated once precise (Cepheid) distances to these galaxies are known.

The brightest stars in NGC 4395 begin to individually resolve at about  $B = 18$ . Many associations of bright young stars exist in the several arms, similar to the pattern of the associations in NGC 300 and in M33.

The nucleus is bright ( $S$  about 16) and is starlike at 0.8" resolution.

The redshift of NGC 4395 is  $v_o = 304$ . The distance modulus is estimated to be about  $m - M = 28.5$  on the scale where  $m - M = 29.3$  for M101 and  $m - M \ll 31.7$  for the Virgo Cluster core.

The bright stars show secondary images from the Racine wedge that are 5 mag fainter than the primaries and are separated by 18".

NGC 5204      ScIV      M101 Gr  
PH-18-H      HA, p. 37  
Jan 31/Fel) 1, 1949  
103aO  
30 min

NGC 5204 is one of the four well-resolved late-type companions of M101. The others are NGC 5474 (ScdIV pec; panel 315), NCC 5477 (Sd; panel 326), and NGC 5585 (SdIV; panel 323). The M101 Group was mapped first by Hohnberg (1950). Photometry, kinematics, and illustrations of the group members are set out in Sandage and Tammann (1974c).

NGC 5204 is highly resolved into individual stars starting at about  $B = 20.5$ .

The original plate from which the reproduction here is made was one of the earliest taken with the Hale 200-inch telescope, before the Ross prime-focus corrector, which eliminates the coma aberration over a 15' field, was in place.

A description of NGC 5204 and the circumstances of the first scheduled observing run with this telescope is given by Hubble (1949). This start of the routine observing program followed more than a year of testing and adjustment of the Palomar telescope by Dr. I. S. Bowen, Director of the Mount Wilson and Palomar Observatories. Bowen's heroic effort to complete the 200-inch commissioning before astronomers had access to the telescope was highly successful but is largely unknown. The unfortunate tone of Hubble's article should be noted in that regard.

The redshift of NGC 5204 is  $v_o = 329$  km s<sup>-1</sup>.

NGC 7162A      SBod(s)III      triplet  
CD-1584-S/Br      not in RSA  
Aug 11/12, 1980  
103aO + GG385  
45 mill

NCC 7162A forms a physical triple! with NGC 7162 (She; panel 190) at a separation of 14.5'. and NGC 7166 (SO.; panel 34) at a separation of 14.9'. The redshifts are  $u_o(7162A) = 2238$  km s<sup>-1</sup>,  $u_o(7162) = 2253$  km s<sup>-1</sup>, and  $u_o(7166) = 2376$  km s<sup>-1</sup>. At the mean redshift distance of 46 Mpc ( $H \bullet 50$ ), the projected linear separations from NGC 7162A are 194 kpc for NGC 7162 and 199 kpc for NGC 7166.

NGC 4236      SBdIV      M81 Gr  
PH-4506-S      panel S10  
April 13/14, 1964  
103aO  
20 min

NGC 4236 is a highly resolved nearby galaxy that Holmberg (1950) placed just outside the border of his M81/NGC 2403 Group. The resolution into stars in NGC 4236 is at the same high level as in those members of the group agreed upon by all. Both the RSA, and Kraan-Korteweg and Tammann (1979) consider NGC 4236 to be in the group. The level of resolution into stars shows the distance to be nearly the same as that of NGC 2403, NGC 2366, IC 2574, and other members of the group at  $m - M = 27.6$  (Tammann and Sandage 1968).

The brightest stars begin to resolve at about  $B = 19$ . The largest HII regions have (halo) diameters of 14". The angular diameter of the galaxy itself is large at  $D_{25} = 19'$ .

The redshift is  $u_o = 157$  km s<sup>-1</sup>, consistent with the very high level of resolution into stars and a nearly noiseless Hubble expansion flow just beyond the Local Group (Sandage 1986a).



## *The Sm, SBm, and Im Classification Sections*

**T**he Large Magellanic Cloud is the prototype galaxy of the Sm and SBm morphological type. In galaxies of this type there is either a very weak spiral pattern or some other indication of weak regularity, rather than general chaos. Whatever regularity is present in galaxies of this type is undoubtedly associated with the observed small but finite rotational velocity. Such a kinematic field is needed to set up a shear velocity field that imparts regularity to the pattern, no matter how weak; the stronger the field, the greater the regularity.

The Sm and SBm galaxies in the RSA are illustrated on this and the next five panels. Galaxies with no indication of regularity in a coherent spiral pattern are in the final morphological box of the Im type, shown on panels 329-332.

LMC                      SBmIII                      HA, p. 38  
Bex-164-Henize  
Nov4/5, 1951  
103aE + Red Plexiglas  
**240 niin**

The print of the LMC here is made from an original Ha plate taken by Henize with the Mount Wilson 10-inch refractor. This telescope had been set up by Henize in South Africa in a cooperative arrangement between the Carnegie Institution, the University of Michigan, and the South African Science Research Council.

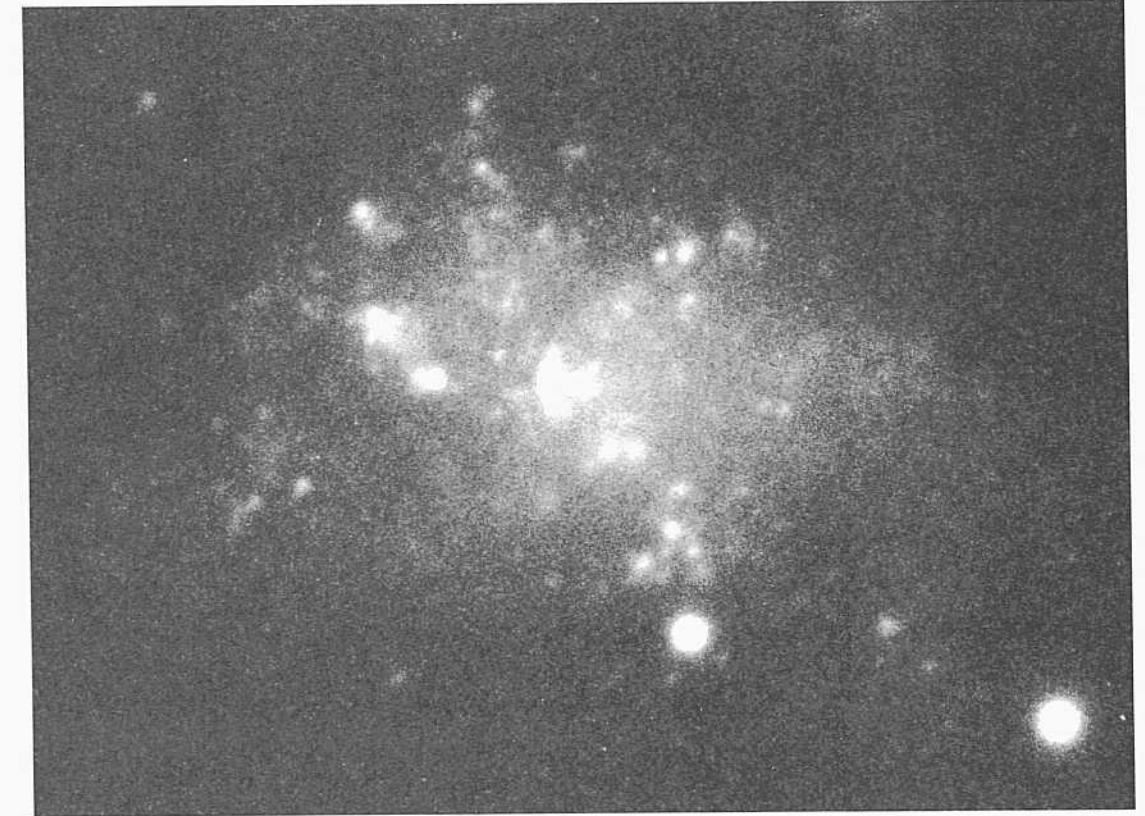
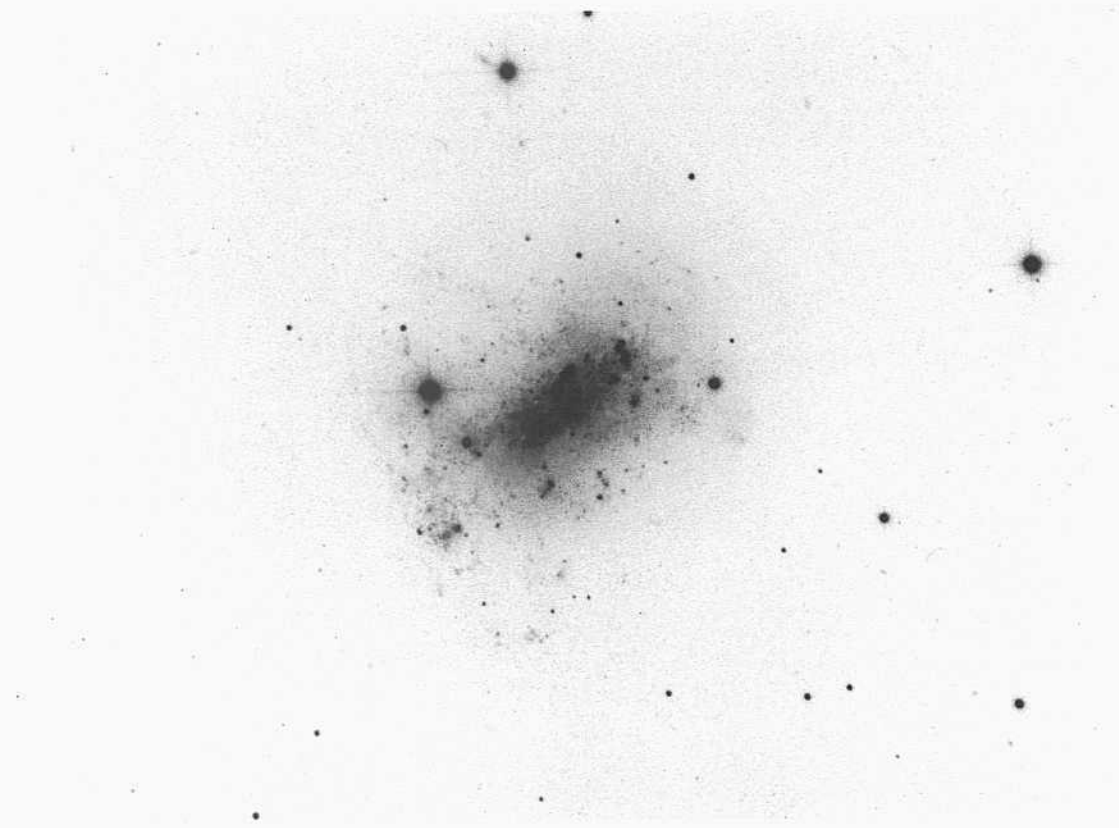
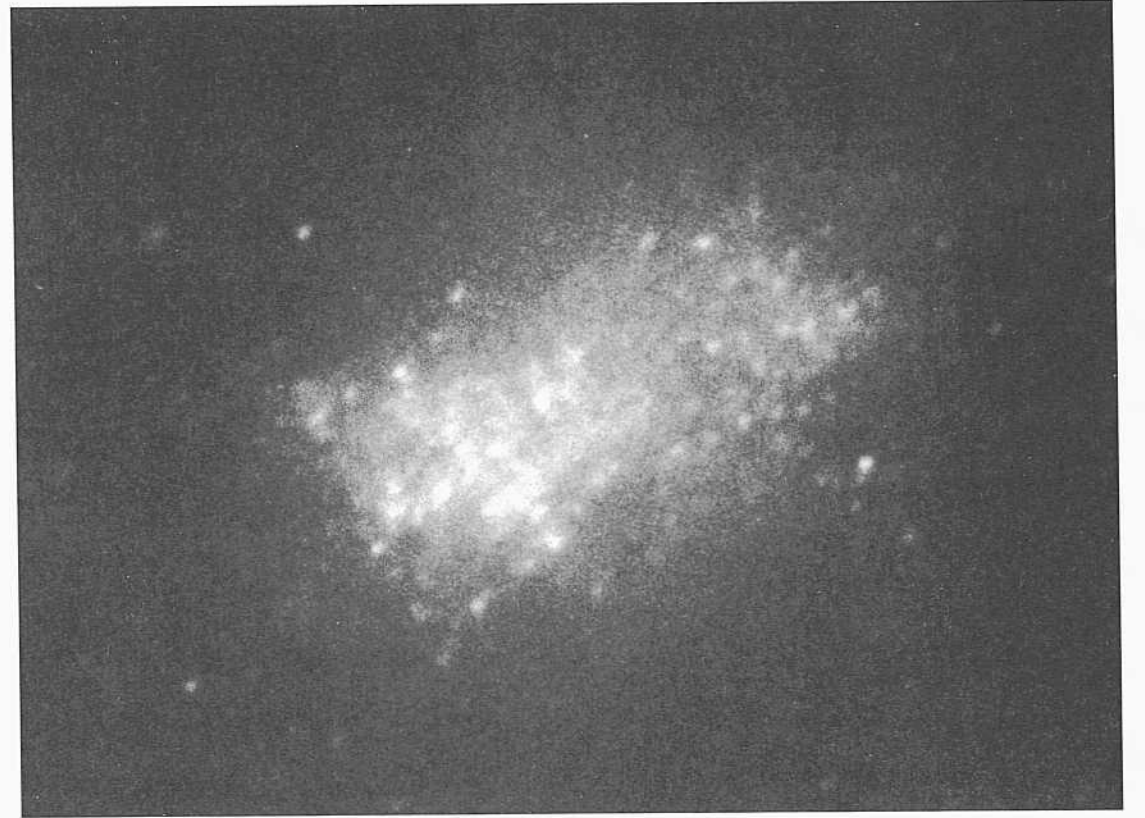
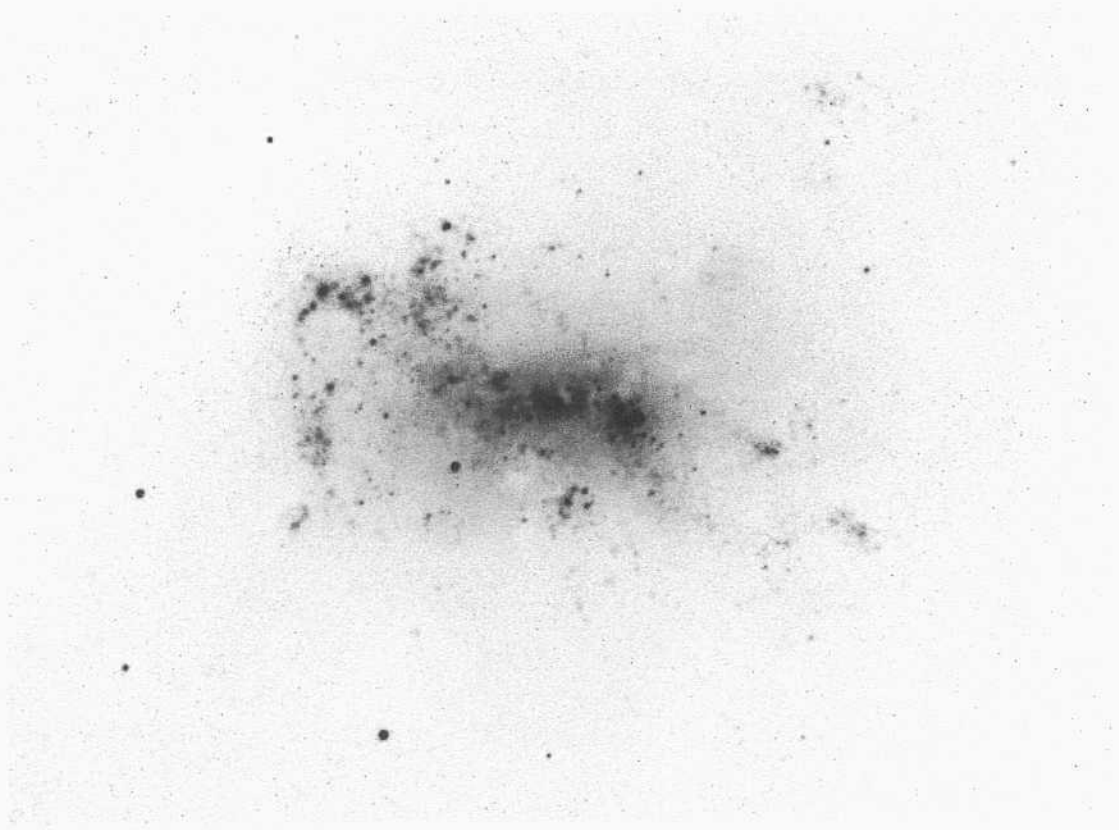
The **LMC** is a satellite of our own Galaxy at a distance modulus of  $m - M = 18.5$  ( $D = 50$  kpc), determined from **Cepheids**.

Weak spiral features exist (de **Vaucouleurs** 1955). The galaxy is also rotating with a peak velocity for young disk objects of  $40 \text{ km s}^{-1}$  (reviewed by Andrews and Evans 1972, and by Freeman, Illingworth, and **Oemler** 1983 with references to previous data). The smallness of the rotational **velocity is** presumed to be the reason that the spiral **pattern is so** poorly developed (compare **Kennicutt 1981**).



PANEL  
325

PANEL  
326





*Sm, SBin, and Im Classification Sections (continued)*

NGC 4656/4657 Im pair  
 H-3633-S HA, p. 40  
 Feb 18/19, 1963 panel S6  
 103aO + GG13  
 27 niini

The complex system of NGC 4656/4657 is listed as two galaxies in the Dreyer NGC Catalog. It may be a single galaxy in the process of (or having just completed) a close encounter with NGC 4631 (Sc on edge; panel 290), which is 31' distant. NGC 4631 is obviously at the same distance, shown by the near equality of the redshifts and the nearly identical levels of resolution into individual brightest stars. The redshifts are  $v_0 = 606 \text{ km s}^{-1}$  for NGC 4631 and  $v_0 = 624 \text{ km s}^{-1}$  for NGC 4656/4657. The galaxies resolve well into brightest stars beginning at about  $B = 19$ .

The largest HII region in NGC 4656/4657 is complex and has an angular diameter (halo) of 1". At an assumed distance of 5 Mpc (Sandage and Tammann 1974a) the linear diameter of this HII complex is about 270 psc. At this distance the projected linear separation of the NGC 4656/4631 pair is small, at 44 kpc. The 2.1-cm content of the pair has been measured by Wellichew, Sancisi, and Guélin (1978). A model of the tidal interaction is discussed by Combes (1978).

The resolution into individual stars is so pronounced in part of NGC 4656/4657 as to make this galaxy a prime candidate for detailed study of its stellar content.

NGC 4532 SmIII VCC 1554  
 CD-2111-S  
 March 19/20, 1982  
 103aO + GG385  
 50 niini

NGC 4532 is listed as a cluster member in the Virgo Cluster Catalog. It is located about 1.5° south of the center of subcluster B centered on NGC 4472. It is illustrated on the same enlargement scale as other galaxies in the Virgo region in the Atlas of Virgo Cluster Spirals (Sandage, Binggeli, and Tammann 1985a, panel 11).

The surface brightness of the nearly edge on disk is very high, making reconnaissance of the stellar content difficult. Robust star formation is evidently occurring. One particularly bright region with a complex of candidate HII regions has an apparent diameter (halo) of 8". Individual stars are not seen, but the surface brightness is so high on the available plate material as to overwhelm the image here.

The redshift is  $v_0 = 1858 \text{ km s}^{-1}$  but redshifts of individual Virgo Cluster galaxies are dominated by large virial velocities rather than by cosmological expansion velocities.

NGC 4861 SBmIH  
 PH-8033-S  
 Feb 3/4, 1981  
 103aO  
 12 niini

NGC 4861 is similar to NGC 2366 below. It is highly resolved into individual stars beginning at about  $B = 21$ . The most unusual feature of the stellar content is the enormous HII-region complex (similar to that in NGC 2366, but much larger here) at one end of the image. Its angular diameter (halo) is about 12".

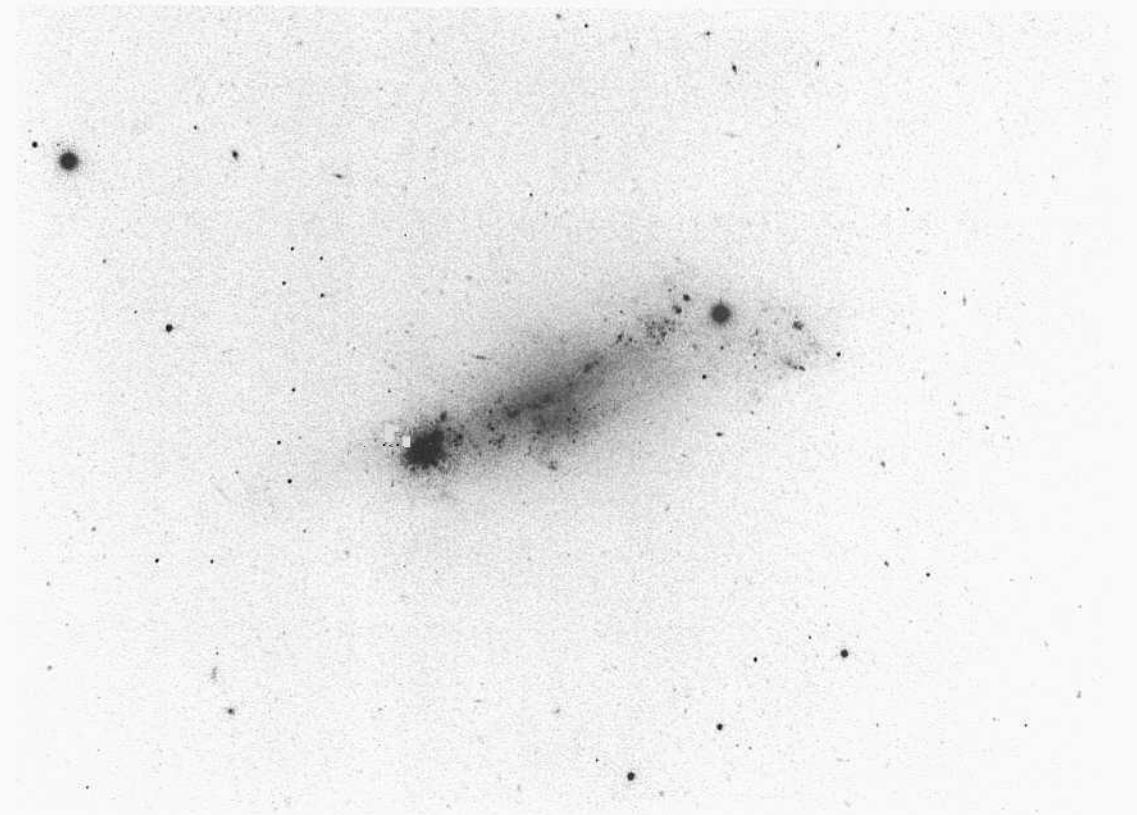
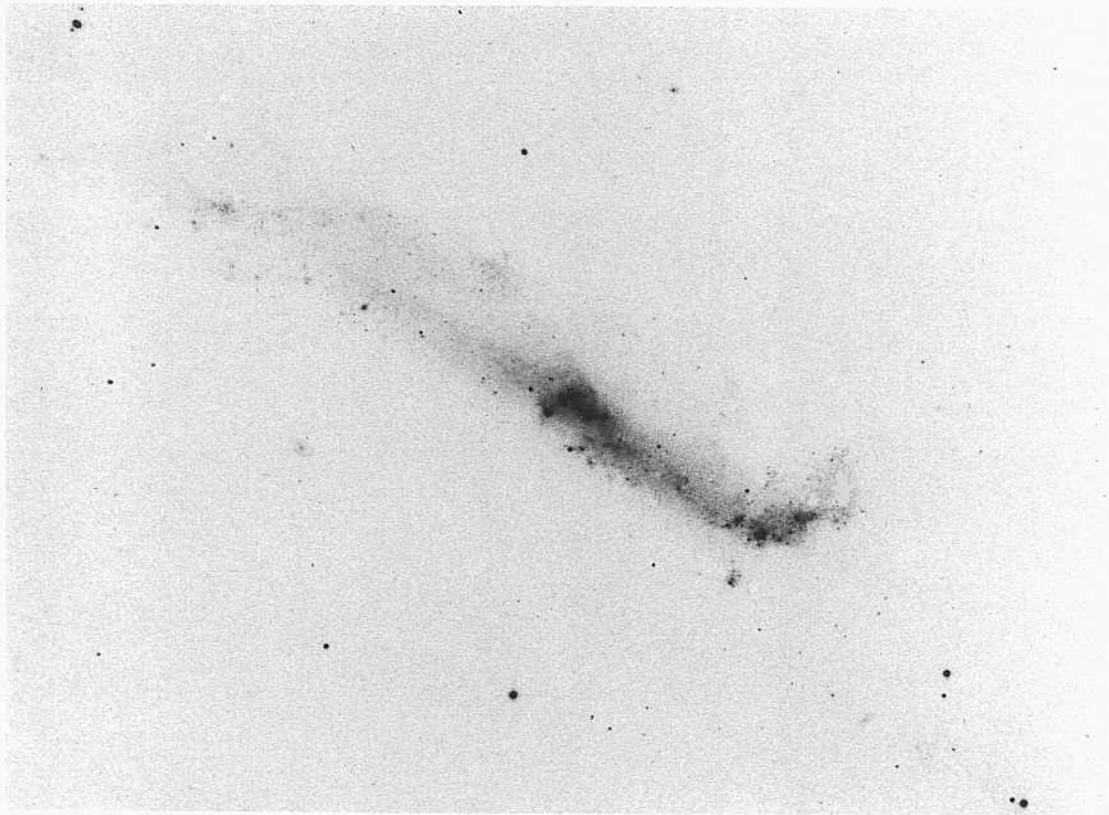
The redshift is  $v_0 = 836 \text{ km s}^{-1}$ . At the redshift distance of 17 Mpc the linear diameter of this complex is large, at 1000 psc. It is one of the largest HII-region complexes known.

NGC 2366 SBmIV-V HA, p. 39  
 PH-555-B M81/NGC 2403 Gr  
 Oct 31/Nov 1, 1951  
 103aO + GG1  
 30 niini

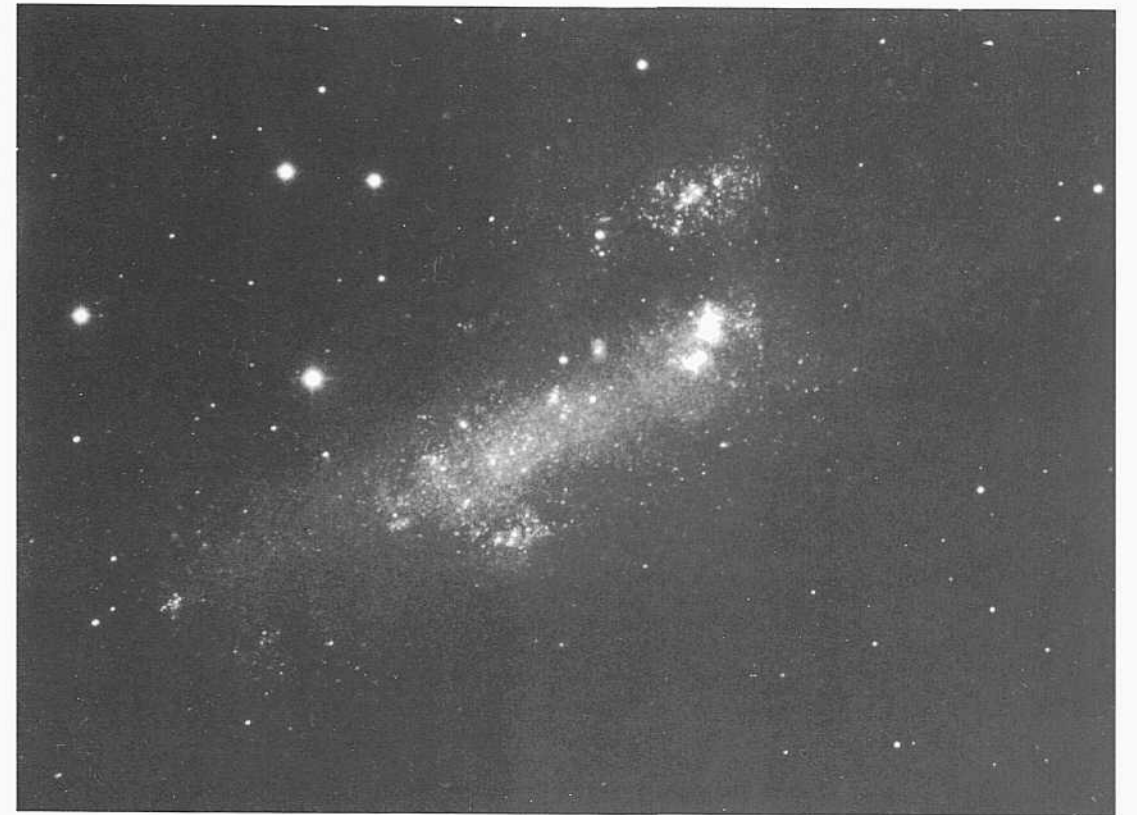
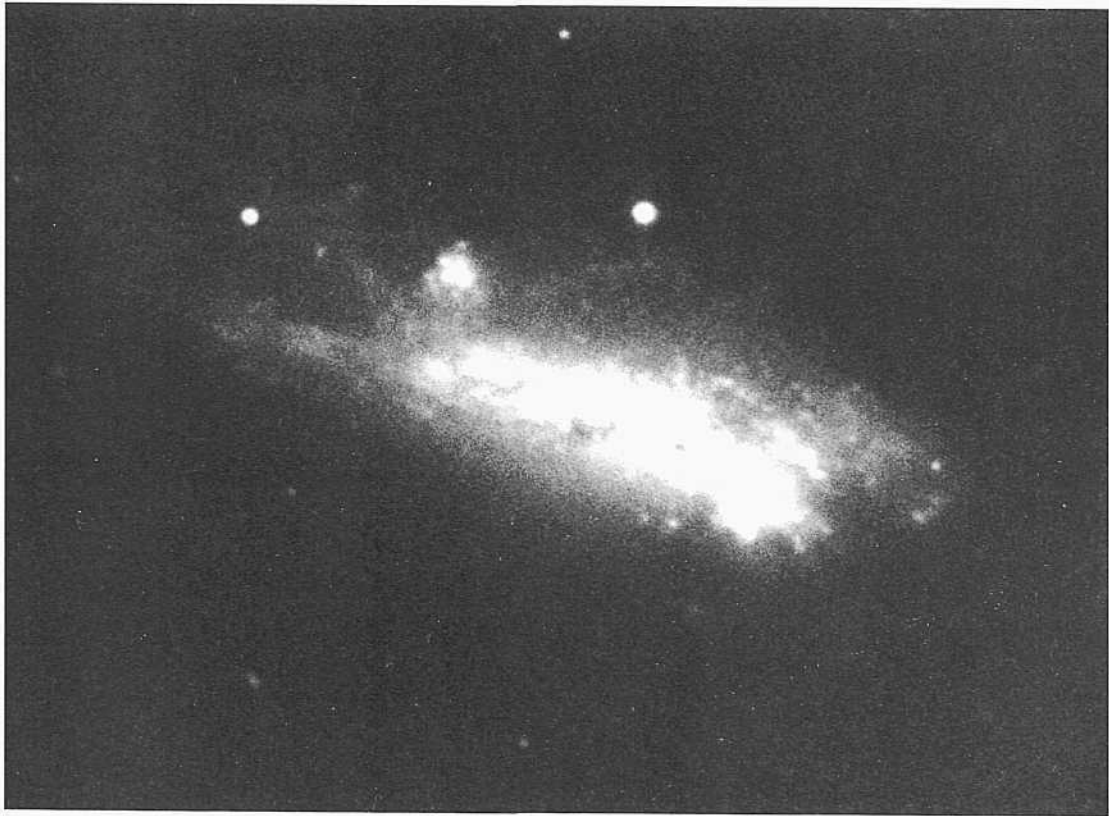
NGC 2366 is a member of the M81/NGC 2403 Group, as originally defined and catalogued by Holmberg (1950). It resolves into stars as easily as other members of the group, such as NGC 2403, M81, IC 2574, Hoi, HoII, and NGC 4236. The brightest stars begin to resolve at about  $B = 19$ . The distance modulus of the group is  $m - M = 27.6$  (Tammann and Sandage 1968). The value has been confirmed (Freedman and Madore 1988).

The largest of the HII regions at one end of the major axis has a diameter of about 12" for its high-surface-brightness main body. The extent of its outer associated filaments is 18". These angular diameters correspond to linear diameters of 190 psc and 290 psc, respectively, at a distance of 3.3 Mpc (Tammann and Sandage 1968).

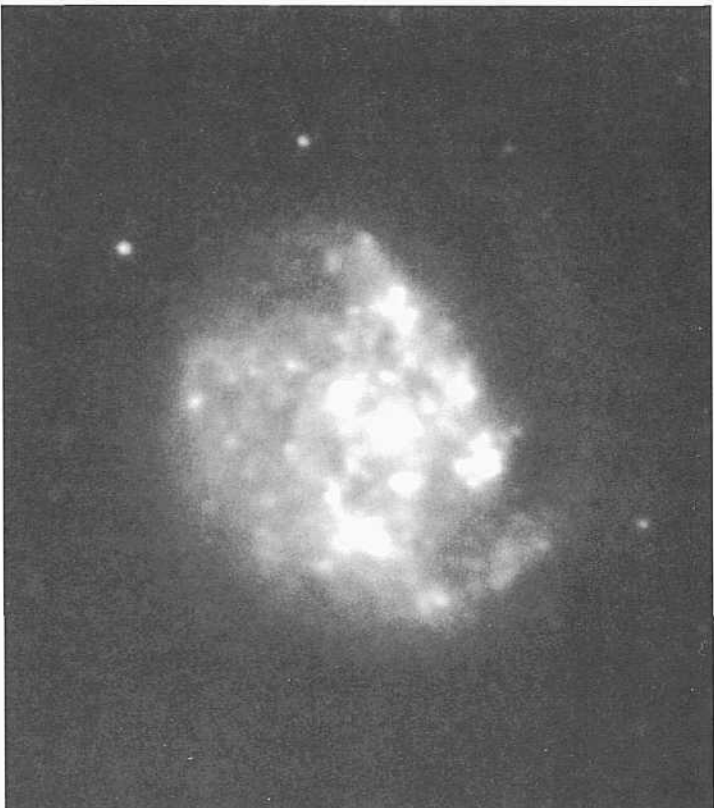
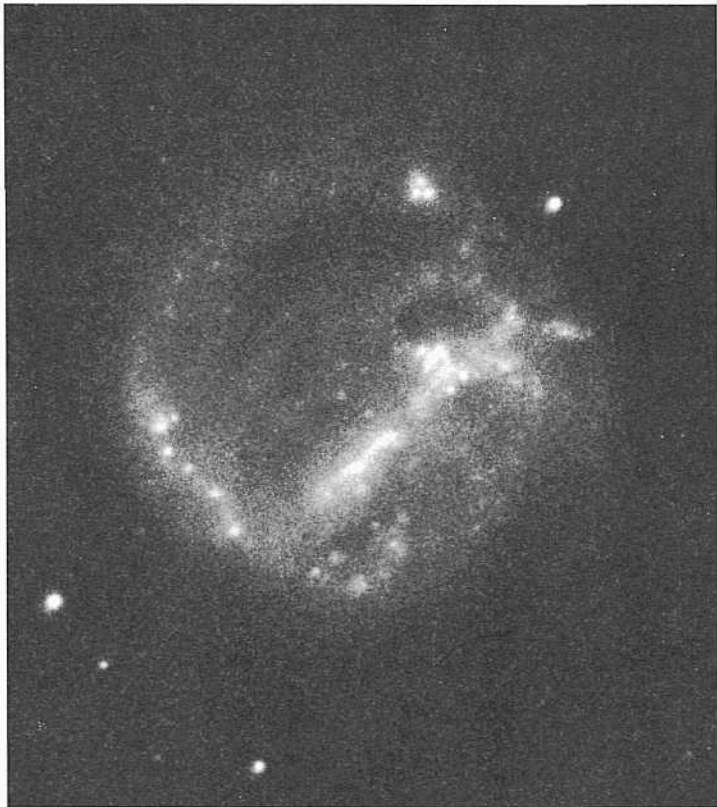
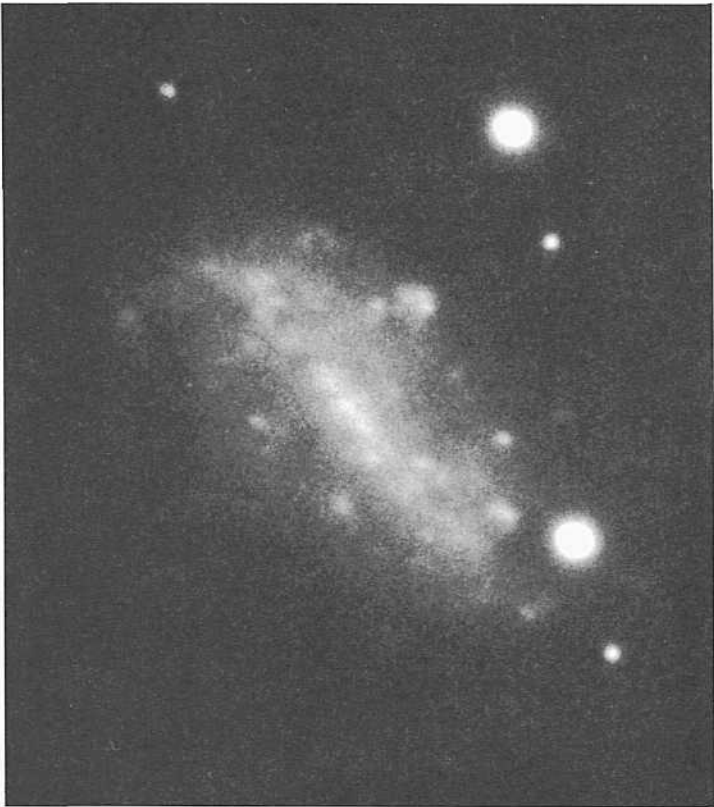
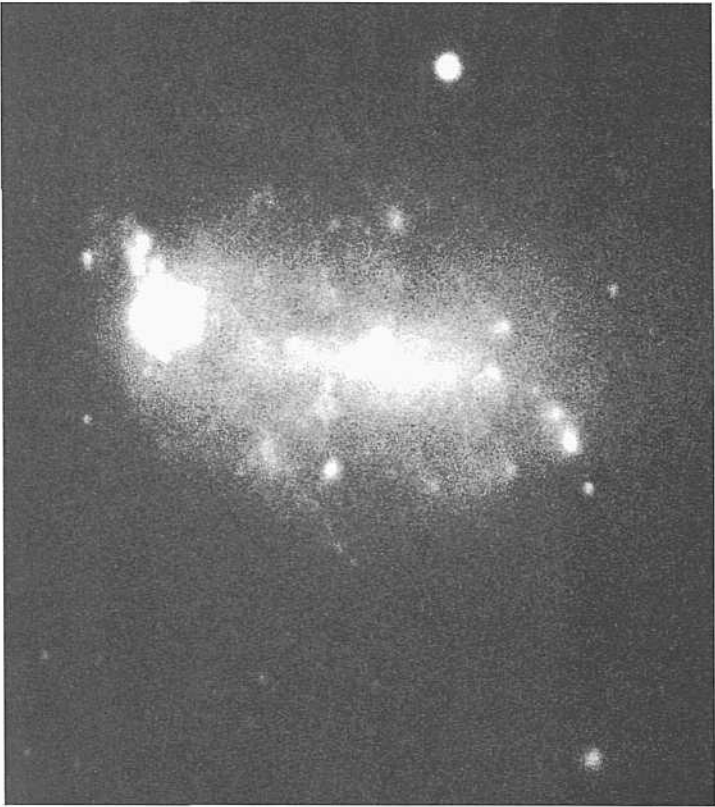
The redshift is  $v_{vir} = 281 \text{ km s}^{-1}$ .



PANEL  
327



PANEL  
328



NGC 1602 SBm pair  
 CD-676-Br not ill RSA  
 Jan 25/26, 1979 panel 51  
 IlaO + GG385  
 180 niin

NGC 1602 is the highly resolved companion to the SO(7) galaxy NGC 1596 (panel 51). The redshifts are  $V_o(1596) = 1324 \text{ km s}^{-1}$  and  $u_o(1602) = 1382 \text{ km s}^{-1}$ . The near-equality of the redshifts and the proximity of the components at an angular separation of 3.1', suggest a binary pair. At the mean redshift distance of 27 Mpc, the projected linear separation of the pair would be small at 24 kpc.

NGC 1602 is resolved into many HII regions. There is a complex of six such regions (unresolved in the print here) near the end of the major axis. The envelope of this complex has an angular diameter of 10", which, at the distance of 27 Mpc, is a linear diameter of 1300 pc, similar to the diameter of the complex in NGC 4861 on the preceding panel. At higher spatial resolution, this complex would presumably appear as an association of early-type stars and HII regions.

The NGC 1596/1602 pair is of particular interest because of the large difference in morphological type. The SO and Im types span the total range of the classification sequence (see the diagram of the dwarf classification sequence in Chapter II here). Pairs with such diverse types are of obvious importance in studies of the meaning of the Hubble sequence for galaxy formation and possible evolution within the sequence. Does one morphological type change into the other with time or with the type of environment, or are the morphological types of individual galaxies stable over most of a Hubble time, as suggested by the calculations of Roberts (1963) and of Sandage (1986d)? These central points are discussed in Chapter IV here, "The Meaning of the Classification."

NGC 3738 SdHI BI Cr  
 PH-7106-S Racine wedge  
 Jim 7/8, 1976  
 103aO + GG13  
 25 niin

NGC 3738 is a member of the very nearby group containing NGC 4214, NCC 4395, IC 4182, and other highly resolved late-type galaxies just beyond the Local Group. The aggregate is called the CVn I Cloud by de Vaucouleurs (1975) and by Sandage and Tammann (1975a). It is Group B4 in Kraan-Korteweg and Tammann (1979).

NGC 3738 is small ( $D_{25} = 2.6'$ ) for its bright apparent magnitude. The surface brightness of the disk is high, making reconnaissance of its stellar content difficult. Images that are probably brightest stars appear in the outer part of the disk beginning at about  $B = 20$ , but their discrimination from HII regions by standard methods has not yet (1991) been done.

The redshift is  $v_r = 312 \text{ km s}^{-1}$ .

NGC 3782 SBcd(s)III CVn [I Cloud?  
 PH-8026-S Racine wedge  
 Feb3/4, 1981  
 103aO  
 2 niin

NGC 3782 is probably a member of the CVn II Cloud (Sandage and Tammann 1975a), which has a mean redshift of about  $\langle v_o \rangle = 750 \text{ km s}^{-1}$ . The redshift of NCC 3782 is  $v_r = 785 \text{ km s}^{-1}$ .

The III-region candidates are unresolved at the 1.5" level. Brightest stars may exist starting at about  $B = 21$  but they have not yet been distinguished from the III-region confusion by the standard methods.

NGC 4299 Sd(s)III VCC 491  
 CD-1318-S/Br Karachentsev 330  
 March 12/13, 1980  
 103aO  
 75 niin

The spiral pattern in NGC 4299 is better formed than in other galaxies on this and several of the preceding panels: hence, the classification of NGC 4299 is Sd rather than Sm.

The galaxy is listed as a cluster member in the Virgo Cluster Catalog. It is illustrated in the Atlas of Virgo Cluster Spirals (Sandage, Binggeli, and Tammann 1985a, panel 15) on a common scale with other Virgo Cluster spirals.

NGC 4299 forms an apparent pair with NGC 4294 (SBcII-III) at the separation of 5.5'. Small angular separations in the Virgo Cluster region do not always mean a physical pair because of the depth effect of the cluster. However, the near-equality of the redshifts and their abnormally low value make the case for a binary pair strong here. The redshifts listed in the RSA are  $i_{>0}(4294) = 232 \text{ km s}^{-1}$  and  $i_{>0}(4299) = 107 \text{ km s}^{-1}$ . At a common distance of 21.9 Mpc ( $m - M = 31.7$  for the Virgo Cluster) the projected linear separation of the pair would be small at 35 kpc.

NGC 366-1 SBmIII pair  
 CD-1858-HB  
 April 6/7, 1981  
 103aO + GG385  
 15 ...in

Many III-region candidates exist in the bar of the disturbed morphology of NGC 3664. A smaller companion (NGC 3664A; type Slim) with the same disturbed morphology and the same high degree of resolution into III-region candidates exists at a separation of 6.3'. The redshift of NGC 3661 is  $v_r = 1231 \text{ km s}^{-1}$ . It seems likely, the two galaxies form a pair at the same redshift distance of 25 Mpc, their projected linear separation is small at 16 kpc. This, and their disturbed morphology, suggest that a close encounter may have occurred.

None of the many III-region candidates are resolved at the 1" level.

NGC 5464 SBmIII  
 CD-1355-S/Br  
 March 15/16, 1980  
 103aO + GG385  
 5 niin

NGC 5464 and NGC 178, below, are similar. Both have small angular diameters, high surface brightness, HH-region candidates, spiral patterns that are difficult to track, and bright absolute magnitudes for the SBm morphology.

The redshift of NGC 5464 is  $v_o = 2455 \text{ km s}^{-1}$ . The largest III-region candidate appears to resolve at the 2" level, corresponding to a linear diameter of about 475 pc. The absolute magnitude, corresponding to the apparent magnitude of  $B_T = 13.2$ , is bright, at  $M_B = -20.6$ .

NGC 178 SBmIII  
 CD-1567-S/Br  
 Aug9/10, 1980  
 103aO + GG385  
 8 niin

The redshift of NGC 178 is  $v_r = 1599 \text{ km s}^{-1}$ . The largest of the III-region candidates in the narrow plume away from the main body may resolve at about the 1.5" level. The high surface brightness of the main body and the bright knots it contains show that a robust star-formation rate is occurring.

The absolute magnitude of NGC 178, based on  $B_T = 13.1$ , is bright for SBm types, at  $M_j = -19.9$ .



The remaining late-type RSA galaxies in the regular sequence of the classification, shown in the next four panels, are mostly of type Im. (A few are still of the slightly earlier SBm type.) Im types have no discernible spiral pattern. They are dwarfs (mostly fainter than absolute magnitude  $M_j = -17$  where  $H = 50$ ).

The Im dwarfs listed in the RSA, where the apparent magnitude limit is  $m_{pg} = 13$ , must be very nearby. Because of their closeness, the galaxies on the next four panels are highly resolved into individual stars. They are prime candidates for studies of stellar content.

**IC4662**                      **ImIII**  
**CD-2198-S**  
**March 30/31, 1982**  
**103aO + GG385**  
**35 min**

IC 4662 is highly resolved into individual stars beginning at about  $B = 19$ . Because the galaxy is at low galactic latitude ( $b = -18^\circ$ ), contamination of the faint stellar content of IC 4662 with foreground stars is appreciable.

The redshift of IC 4662 is  $v_0 = 240 \text{ km a}^{-1}$ . The angular diameter is small at  $D_{25} = 2.2'$ . Assuming a distance of 5 Mpc, the absolute magnitude is  $M_g = -17.2$  and the linear diameter is 3.2 kpc.

**IC5152**                      **SdmlV-V**  
**CD-57-D**  
**Aug 19/20, 1977**  
**103aO + GG385**  
**75 min**

From kinematic arguments alone, IC 5152 is a member of the Local Group (Sandage 1986a). Its measured heliocentric redshift is  $v_{sun} = 119 \text{ km s}^{-1}$ . It is well known that the direction of the solar motion relative to the Local Group is toward Galactic coordinates of approximately  $l = 97^\circ$ ,  $b = -5^\circ$ , with an amplitude of approximately  $295 \text{ km s}^{-1}$  (Yahil, Tammann, and Sandage 1977; Sandage 1986a). Subtracting this vector of the solar motion from the heliocentric redshift of IC 5152 gives a negligible cosmological redshift vector for IC 5152 of  $v_0 = 47 \text{ km s}^{-1}$ ; hence, IC 5152 is at rest relative to the Local Group to within the errors of the determination (compare Fig. 9 of Sandage 1986a).

Local Group membership is consistent with the proximity required by the profound resolution of IC 5152 into stars beginning at about  $B = 17$ . Cepheid variables have been found (Sandage and Carlson, unpublished 1988), but a precise distance based on them is not yet available (c. 1991). The estimated distance modulus is  $m - M = 26$  ( $D = 1.6 \text{ Mpc}$ ).

NGC 3377A = UGC 5889      **Im**      Leo Gr  
**PH-711-B**  
**Jail 19/20, 1953**  
**103aO + GG1**  
**30 min**

This dwarf companion to NGC 3377 (E6; panel 19) is separated from the principal galaxy by  $6.8'$ . The 1950 coordinates of this dwarf are RA =  $10^h 44.73^m$ , Dec =  $14^\circ 20.2'$ . Its angular diameter is **Large** at  $D_{95} = 2.0'$ . Its surface brightness is low, at about  $24 \text{ B mag sec}^{-2}$ .

A pointlike knot exists close to the center. This may be a nucleus similar to the bright nuclei in dE.N galaxies. Other starlike images exist over the face, similar to the prototype large Im galaxy IC 3475 in the Virgo Cluster, illustrated in the Atlas of Virgo Cluster Dwarfs (Sandage and Binggeli 1984).

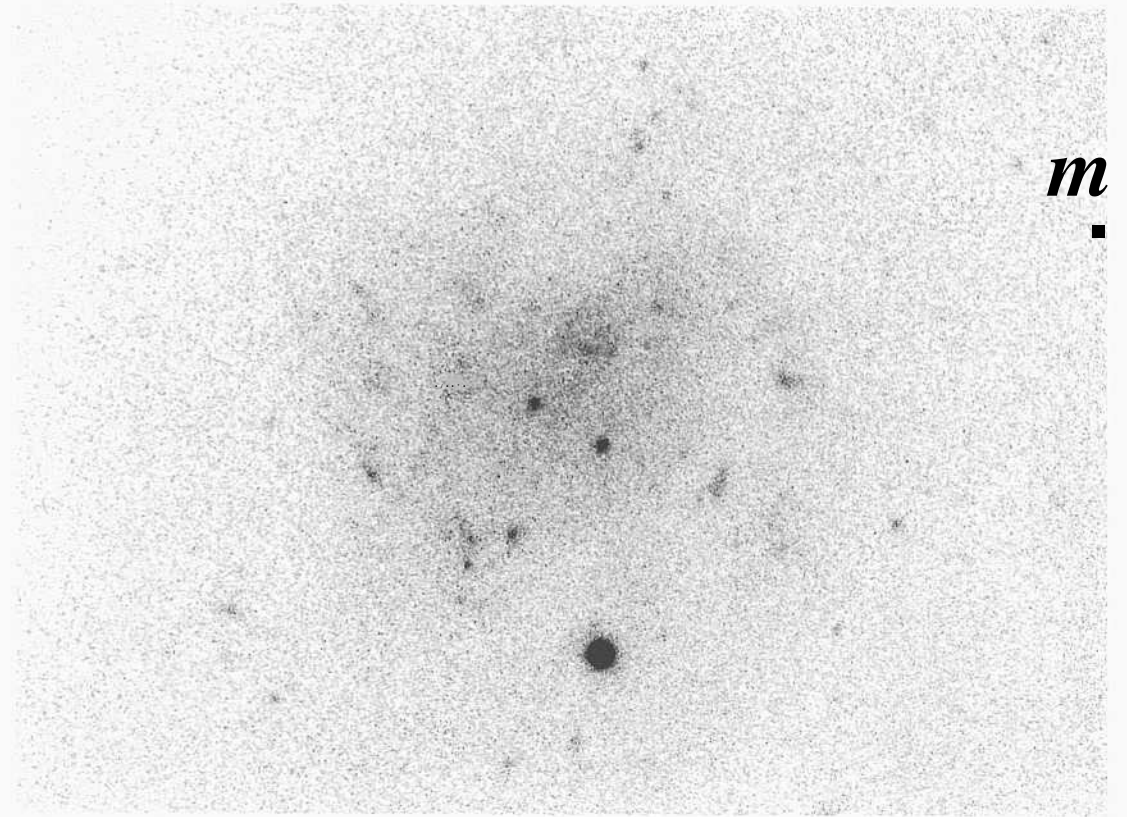
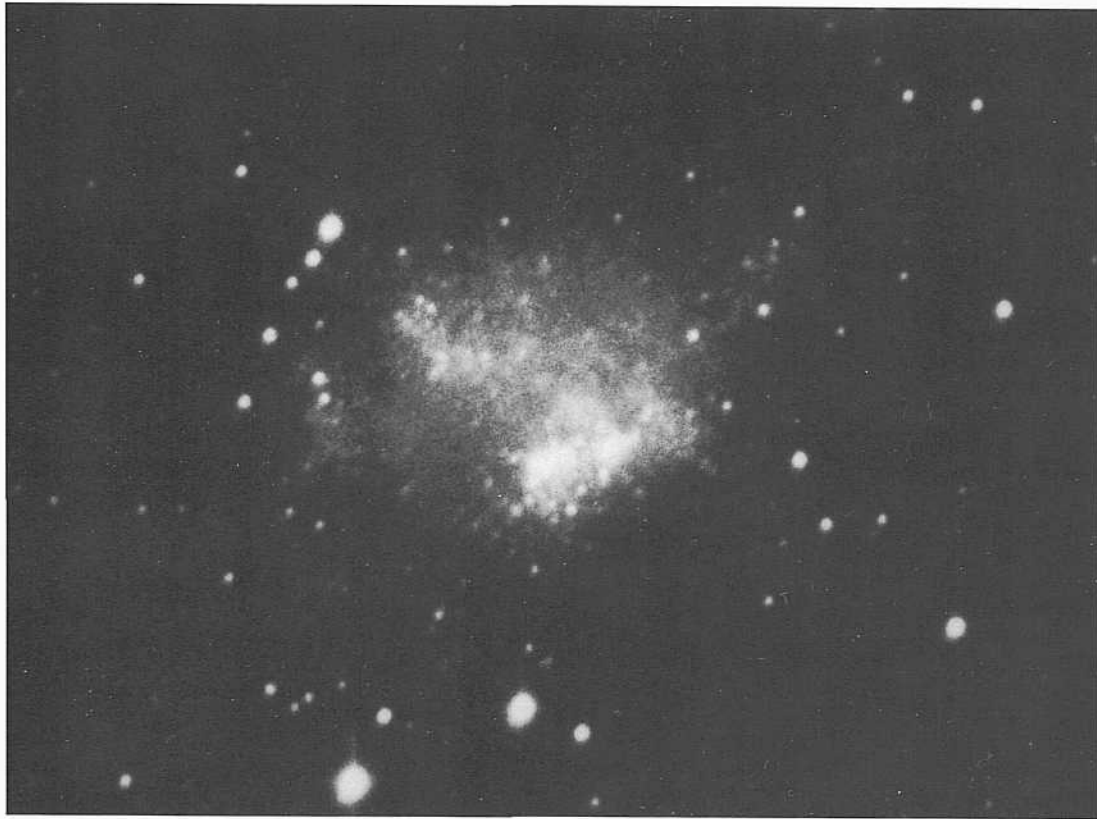
HI 21-cm radiation has been detected in NGC 3377A at a redshift (corrected to the centroid of the Local Group) of  $v_0 = 446 \text{ km s}^{-1}$  (Lewis 1987). The redshift of NGC 3377 is  $v_0 = 591 \text{ km s}^{-1}$ , suggesting that NGC 3377 and NGC 3377A form a binary pair. At the redshift distance of 10 Mpc, the linear diameter of NGC 3377A would be very large at 5.8 kpc, and the projected linear separation from NGC 3377 would be small at 20 kpc. If the distance were larger at 18 Mpc as assumed by Ferguson and Sandage (1990) for members of the Leo Group, the diameter would be 10.4 kpc and the separation from NGC 3377 would be 36 kpc.

In either case, the linear diameter of NGC 3377A is huge, as in the class of huge dE and/or Im dwarfs that exist in the Virgo Cluster (Binggeli, Sandage, and Tammann 1985, Table XIV; Sandage and Binggeli 1984, panels 6, 18, and 19).

A case has been made (Sandage and Hoffman 1991) that NGC 3377A is in a state of transition between a gas-rich Im dwarf and a gas-poor dE.N by self-transformation caused by gas sweeping from stellar winds. The winds are generated by super star clusters similar to those observed in NGC 625 (panel 336), NGC 1569 (panel 336), and NGC 1705 (panel 335). **described** in the next section on **Amorphous galaxies**.

NGC 7764                      **SBmIII**  
**CD-1064-Br**  
**Aug 16/17, 1979**  
**103aO + GG385**  
**45 min**

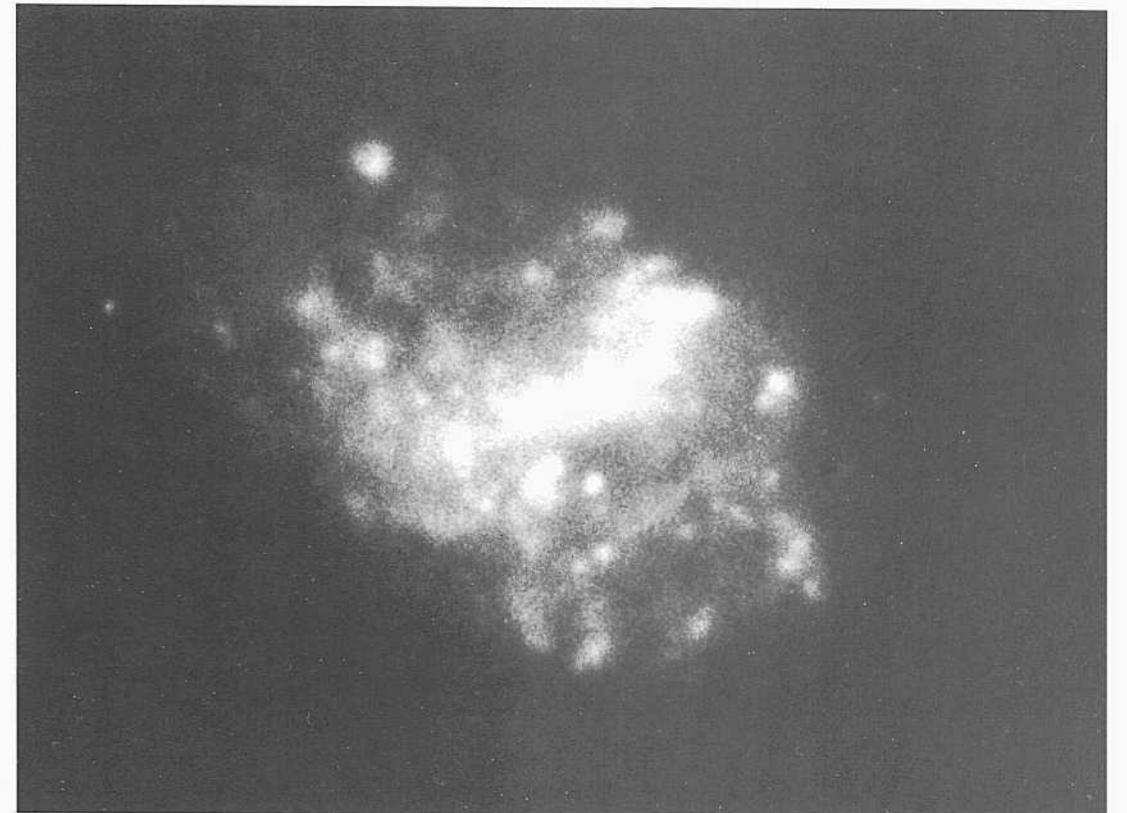
NGC 7764 has high surface brightness, many HII-region candidates, and a poorly defined spiral pattern. The redshift is  $v_0 = 1674 \text{ km s}^{-1}$ . The absolute magnitude of this SBm galaxy is bright at  $iW_n = -20.1$ . The absolute magnitude of the LMC, which is the prototype galaxy of the SBm class, is five times fainter at  $M_B = -18.4$ .



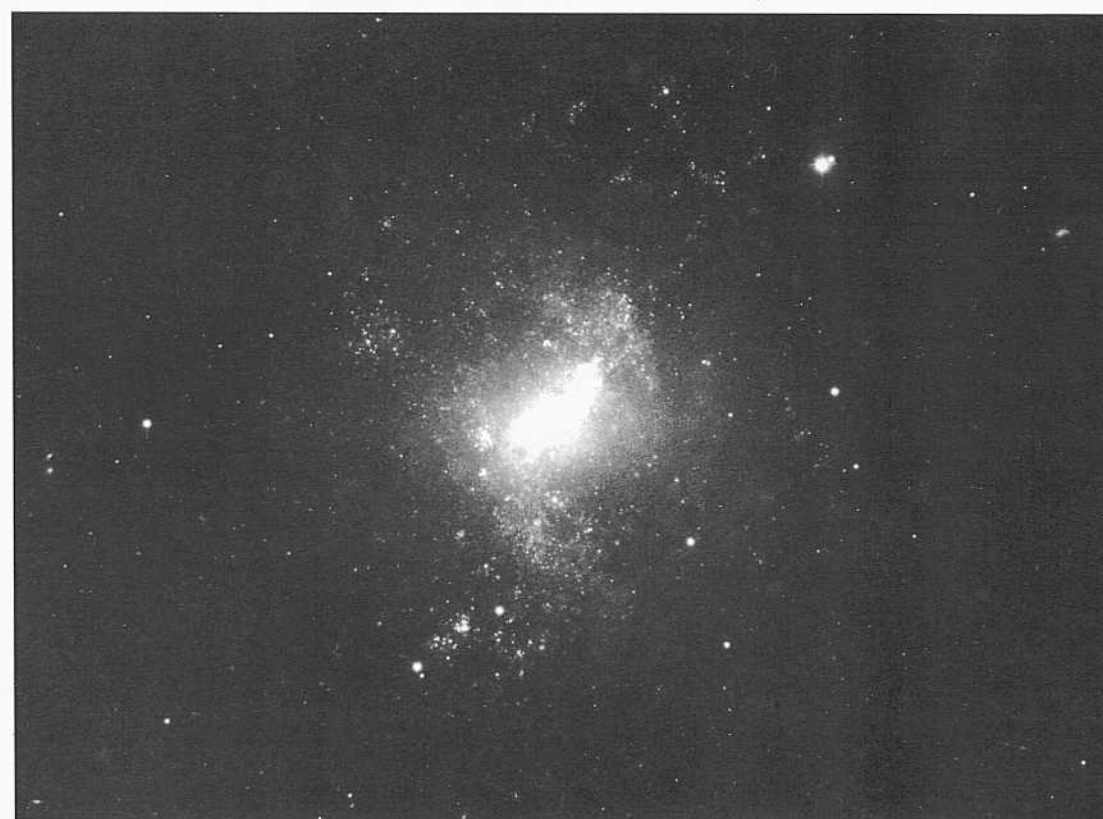
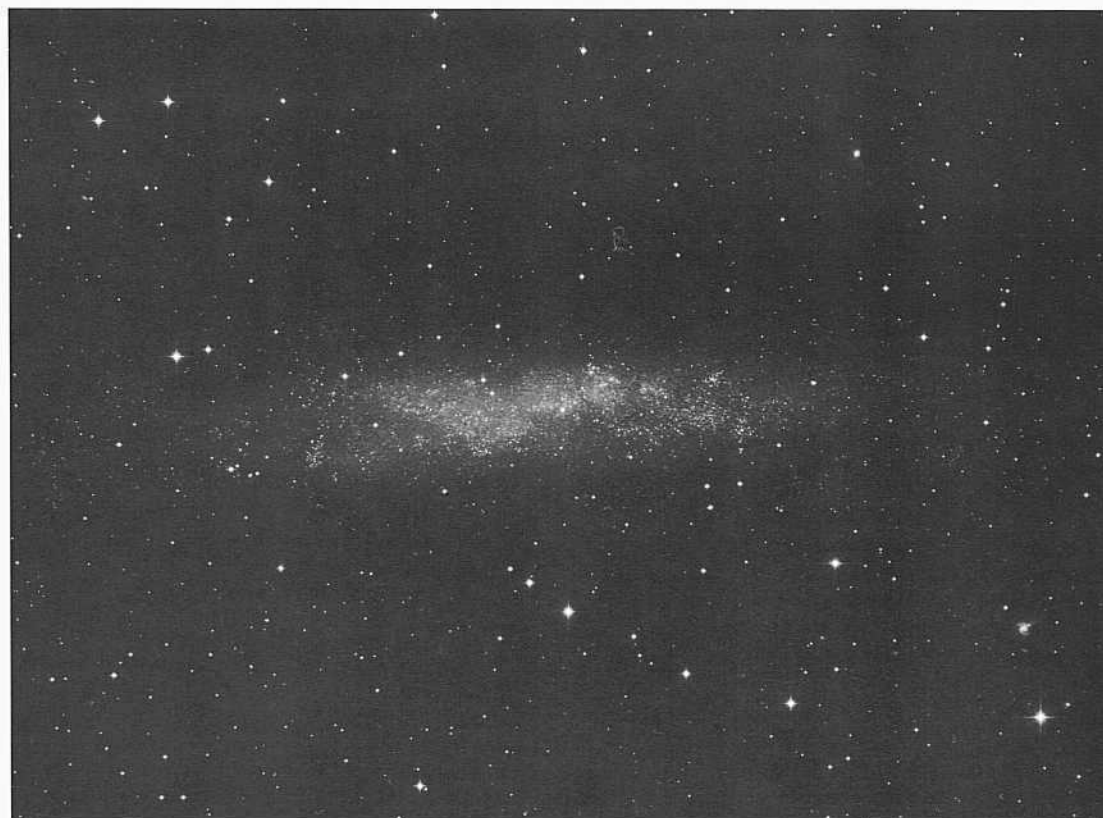
*m*



PANEL  
329



PANEL  
330



NGC 6822            ImlV-V            Local Gr

PH-103-S

Aug 19/20, 1952

103aO + GG1

30 min

NGC 6822 is the first external galaxy for which **Hubble** (1925) published details of the discovery and photometry of Cepheid variables. This **low-surface-brightness** Im dwarf shows no evidence of a spiral pattern. It is in the **Local Group** at a distance modulus of  $(m - M)_0 = 23.95$ , corresponding to a distance of 61.6 kpc (Kayser 1967).

The brightest stars resolve at  $B = 17$  (Kayser 1967, Fig. 3). Large resolved III regions exist; the largest has an angular diameter of  $50''$ , corresponding to a lineal-diameter of 150 pc.

SMC                    ImlV-V            Local Gr

W10-Bex-115-Henize

The Small **Magellanic** Cloud is a satellite of our Galaxy in the Local Group at a mean distance modulus of  $m - M = 18.85$  determined from Cepheids. However, the galaxy is **extended** in the line of sight due to its tidal disruption in a recent close encounter with the LMC (**Murai and Fujimoto** 1980). The extension in the sight line, determined by Mathewson, Ford, and Visvanathan (1986, 1988) is from a near distance of 43 kpc to a far distance of 75 kpc. The main concentration of the SMC is at a distance of 59 kpc from the Sun.

The brightest blue stars begin to resolve at  $B = 10.2$ . The brightest red supergiants resolve individually at  $V = 11.8$  at a color of  $li - V = 1.7$ .

NGC 3109            SmlV                HA, p. 39

CD-1S5-S

Feh 3/1, 1978

103aO + GG385

60 min

NGC 3109 is a highly resolve,! nearby galaxy **immediately** outside the **Local Group**, It has a **redshift, corrected to the centroid of the Local Group**, of  $v_0 = 122 \text{ km s}^{-1}$ . Evidently it is at ;i distance where the local expansion field has become evident, just beyond the zero velocity surface of the Local Group (**Sandage 1986a, Fig.**

**The distance modulus determined from Cepheids** is  $m - M = 26.4$ , or  $l) - 1.9 \text{ Mpc}$  (Sandage and Carlson 1988). **The brightest blue stars** begin to resolve at  $B = 18.0$ . **Tin- brightest red stars** begin to resolve at  $V = 18.8$  at a color of  $l; - v = 1.7$ .

NGC 4214            SBmlII              CVn I Cloud

PH-3563-S

April 15/16, 1960

103aO + GG13

20 min

NGC 4214 is a highly resolved Magellanic Cloud-type galaxy in the nearby CVn I Cloud (the B4 Group), which also contains NGC 1190, NGC 4395, NGC 4449, and [C 4 182, among other well-resolved very-late-type galaxies. A description of the group is in the paragraphs for NGC 4395 (panel 324). **The redshift** of NGC 4214 is  $v_r = 290 \text{ km s}^{-1}$ .

Preliminary photometry of the **brightest** resolved stars in NGC 4214 gives a distance modulus of  $m - M = 28.4$  based on  $V = 20.4$  for the brightest red supergiants. The apparent magnitude for the brightest blue supergiants is  $B = 18.8$ , also from this **preliminary** photometry.

*Sm, SBm, and Im Classification Sections (continued)*

HoII ImlV-V HA, p. 39  
 PH-1600-B M81/NGC 2403 Gr  
 Nov 30/Dec 1, 1956  
 103aO + GG1  
 25 niiii

Hull was first identified by Holmberg (1950) in his catalog and study of the M81/NGC 2403 Group. The resolution into individual stars is at the same bright level as in other members of the Group, such as NGC 2403 (Sc; panel 273), NGC 2366 (SBmlV-V; panel 327), and NGC 4236 (SBdIV; panels 324, S10).

Photometry of the brightest red and blue stars has been done by Sandage and Tammann (1974b) and by Hoessell and Danielson (1984). The blue stars begin to resolve at about  $B = 19.7$  in the photometry of Santiago and Tammann. The brightest red supergiants begin to resolve at about  $V = 20.2$ .

In the photometry of Hoessell and Danielson, the brightest blue stars resolve at  $B = 17.8$ . The identification of the brightest stars differs between the two studies. Finding charts of the individual stars are given in both. New photometry is required (c. 1991) to remove this important discrepancy.

HoII has a maximum "rotational velocity" of  $58 \text{ km s}^{-1}$ , determined from the 21-cm line profile (Huchtmeir, Seiradakis, and Materne 1981). Its heliocentric systemic velocity is  $v_{sl(0)} = 159 \text{ km s}^{-1}$ . Correction to the centroid of the Local Group gives  $v_0 = 329 \text{ km s}^{-1}$ , clearly beyond the zero velocity surface of the Local Group. HoII is, beyond doubt, in the near expansion field (see Fig. 9 of Sandage 1986a) of the very local Hubble flow.

Leo A ImV  
 PH-95-S  
 Jaii 3/4, 1952  
 103aO + WG2  
 15 min

The dwarf galaxy Leo A ( $RA_{50} = 9^h 57.55^m$ ,  $Dec_{50} = +30^\circ 59.2'$ ) was discovered by Zwicky (1942) in one of the first surveys done with the Palomar 18-inch Schmidt beginning in 1936. Photometry of the stellar content (Sandage 1986b) shows that the brightest blue stars begin to resolve at  $B = 19$  and the brightest red supergiants at  $V = 19$ . Leo A is one of the faintest dwarfs of type Im in or near the Local Group. If the distance modulus is  $m - M = 26$  (Sandage 1986b), its absolute magnitude is  $M_g = -13$ .

Leo A has a redshift relative to the centroid of the Local Group of  $v_0 = -32 \text{ km s}^{-1}$  (Sandage 1986a). It is, therefore, a Local Group member near the zero velocity surface that separates the Local Group from the cosmological expansion field. It is evident from the velocity and distance data that the kinematic radius of the Local Group in the direction of Leo A extends to a distance of about 1.6 Mpc from the Sun.

Sextans A ImlV HA, p. 39  
 CD-156-S  
 Feb 3/4, 1978  
 103aO + GG385  
 60 min

Sextans A and B are just beyond the zero velocity surface of the Local Group at a distance modulus common to both at  $m - M = 26.2$  ( $D = 1.7 \text{ Mpc}$ ), determined from Cepheids (Sandage and Carlson 1982, 1985). The redshift of Sextans A, corrected to the centroid of the Local Group, is  $v_0 = 102 \text{ km s}^{-1}$ . Hence, Sextans A is in the very nearby expansion field, immediately beyond the zero velocity surface (Sandage 1986a, Fig. 9); it is not a kinematic member of the Local Group.

Photometry of the brightest resolved stars (Sandage and Carlson 1985; Hoessell, Schommer, and Danielson 1983) shows that the brightest blue supergiants in Sextans A begin to resolve at  $B = 18.5$ ; the brightest red supergiants begin to resolve at  $V = 18.2$ .

Pegasus Dwarf ImV  
 PH-7288-S  
 Nov 20/21, 1976  
 103aO + GG13  
 30 min

The Pegasus Dwarf ( $RA_{50} = 23^h 26.05^m$ ,  $Dec_{50} = +14^\circ 29'$ ) was discovered by A.G. Wilson during the early stages of the original National Geographic-Palomar Sky Survey. Photometry of the brightest stars has been done by Hoessell and Mould (1982) and by Sandage (1986b). The photometry of Cepheid variables (Hoessell *et al.* 1990) has led to a distance modulus of  $m - M = 26.2$ .

The brightest blue stars begin to resolve at about  $B = 20$ . The brightest red supergiants begin to resolve at about  $V = 20.4$ .

The redshift, corrected to the centroid of the Local Group, is  $v_0 = 43 \text{ km s}^{-1}$  (Sandage 1986a); hence, as with Leo A, the Pegasus dwarf at a distance of 1.7 Mpc is close to the zero-velocity surface of the Local Group.

Sextans B ImlV-V  
 PH-7105-S  
 Jan 7/8, 1976  
 103aO + GG13  
 30 min

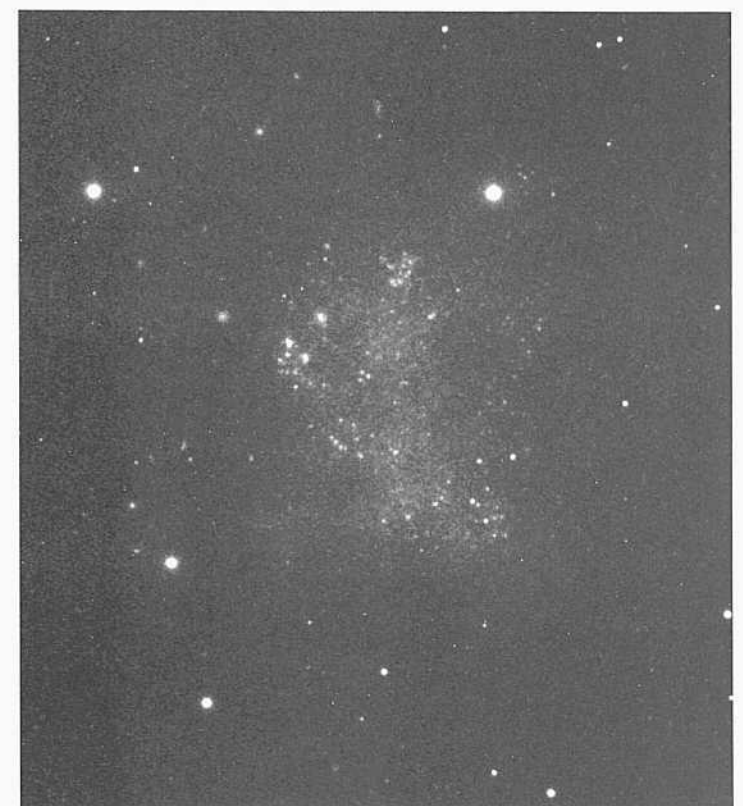
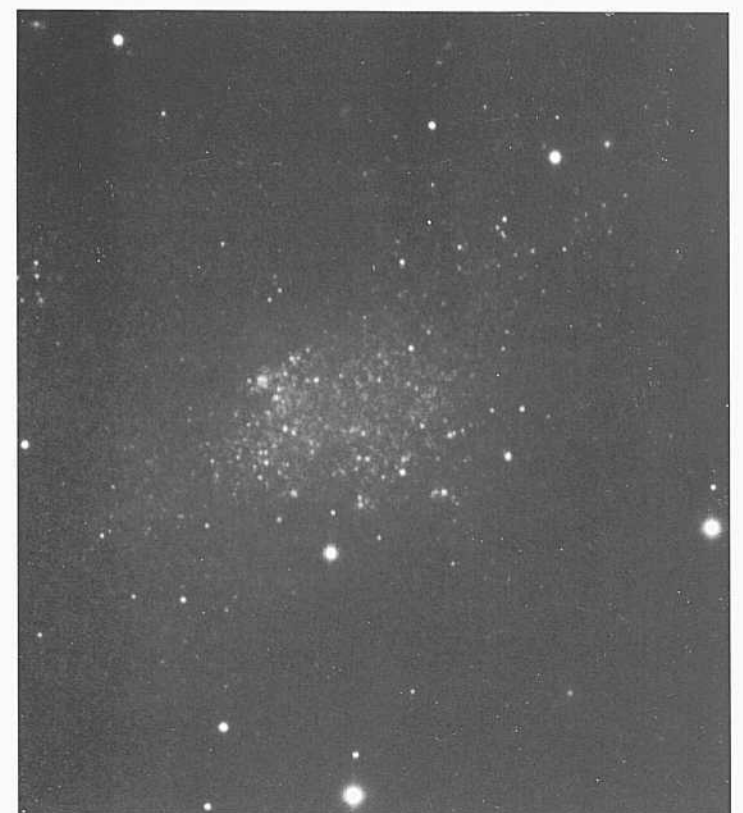
Sextans B, at the same distance as Sextans A based on a study of Cepheids in both galaxies (Sandage and Carlson 1985), has a redshift corrected to the centroid of the Local Group of  $v_0 = +114 \text{ km s}^{-1}$ . The Cepheid distance modulus is  $m - M = 26.2$ . Hence, in the direction of Sextans A and B the zero-velocity surface of the Local Group is closer to the Sun than 1.7 Mpc.

The brightest blue stars begin to resolve at  $B = 19$ ; the brightest red supergiants begin to resolve at about  $V = 19$ .

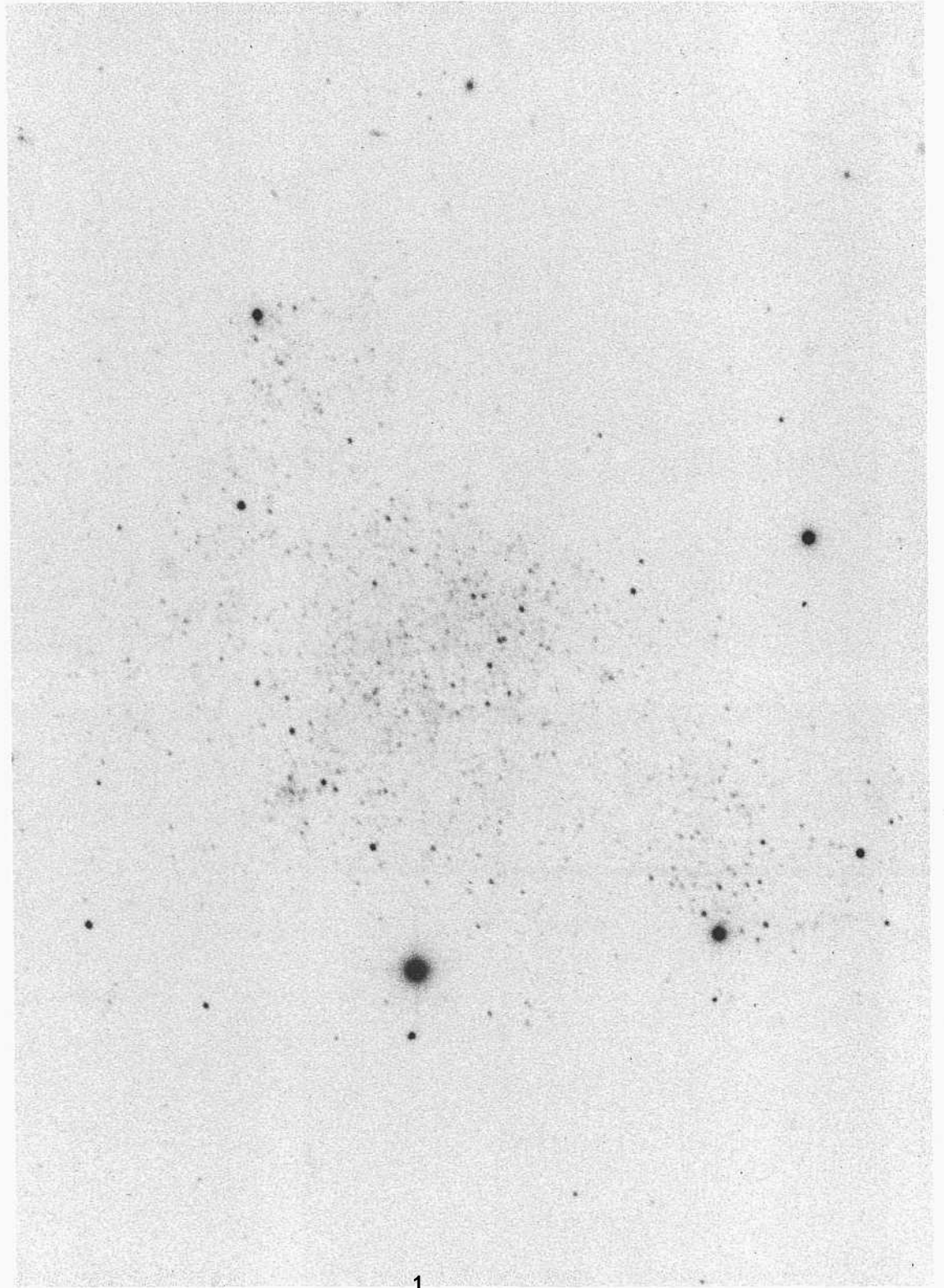
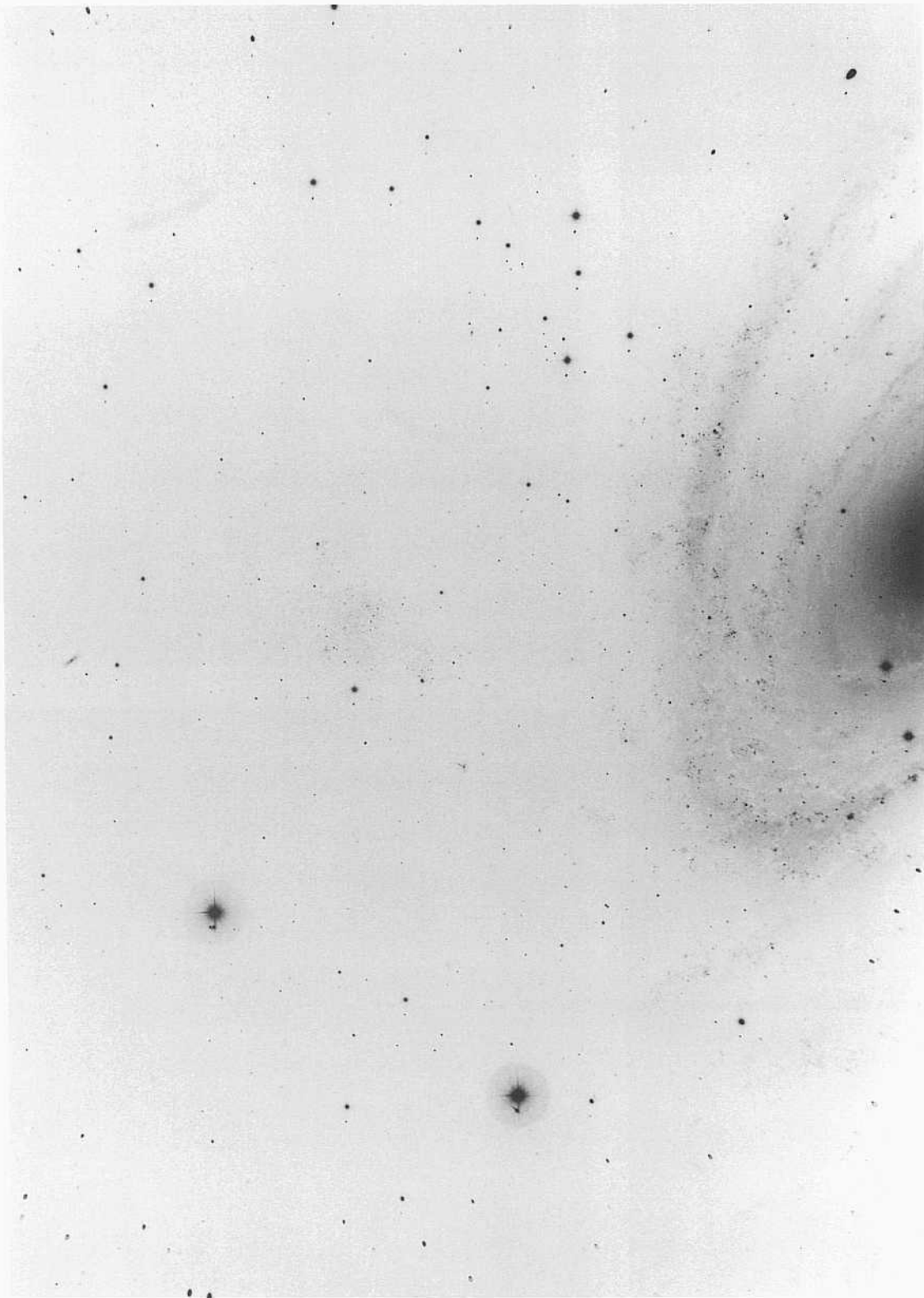
Hoi ImV M81/NGC 2403 Gr  
 PH-5740-S  
 Jan 18/19, 1971  
 103aO + GG13  
 20 min

Hoi was first catalogued by Holmberg (1950) in his study of the M81/NGC 2403 Group. The 21-cm systemic velocity of Hoi is  $v_{sun} = 140 \text{ km s}^{-1}$ . Reduction to the centroid of the Local Group gives  $v_0 = 300 \text{ km s}^{-1}$ , placing the object well beyond the zero-velocity surface of the Local Group. The distance of the M81/NGC 2403 Group, based on Cepheids in NGC 2403, is  $m - M = 27.6$  (Tammann and Sandage 1968). This distance was confirmed by Freedman and Madore (1988).

Hoi is less active in its star formation than HoII, shown at the upper left panel. From the photometry and color-magnitude diagram of Hoessell and Danielson (1984), stars of 15 solar masses are currently forming in Hoi, compared with 25-solar-mass stars in HoII.



PANEL  
332



*Sin, SBm, and Iin Classification Sections (continued)*

HoIX + NGC 303 I ImV + Sb(r)I-H HA, p. 19  
PH-7140-S panel 129

Feb 1/2, 1976

103aO + GG13

30 niin

HoIX, a dwarf companion in M8 I, has been catalogued by van den Bergh (1979, listed as DUO 66) and by Holmberg (1969). The low-surface-brightness Im dwarf is 10' nearly due east of MB I. Bertola and Maffei (1974) measured a magnitude within an isophote of 26  $I$  in  $\text{arcsec}^{-2}$  of  $\bar{I} = 1.17$ . Kraan-Korteweg and Tammann (1979) adopt a total magnitude of  $I_S = 14.6$ . The distance modulus of  $m - M = 27.6$  for M8 I (Tammann and Sandage 196B), as confirmed by Freedman and Madore (1990), gives a total absolute magnitude of  $M_I = -13.0$  for HoIX.

HoIX ImV M81/NGC 2403 Gr  
PH-7110-S

Feb 1/2, 1976

103aO + GG13

30 niin

Photometry of the stellar content (Sandage 1984a) shows that the brightest blue stars begin to resolve at about  $B = 19.5$ . The brightest red supergiants begin at about  $V = 20.5$  although there are red star candidates whose membership is unknown as bright as  $V = 19.4$ .

A 21-cm study of M81 and the region of HoIX has been made by Gottman and Weliaehew (1975) where III radiation was detected at the position of HoIX.



## The Amorphous Classification Section

Following definitions and a discussion given elsewhere (Sandage and Brucato 1979), we have classified galaxies as Amorphous based on an amorphous appearance to the unresolved light, the generally high surface brightness of the image, and the Ha filaments that often cover the disk. Examples are M82, NGC

1569, NGC 625, NGC 1705, and others shown in this section. Many of the galaxies of this new morphological type have variously been called "starburst" galaxies; the connection may be important in understanding the physical processes giving rise to the morphological form.

NGC 3034      Amorphous      HA, p. 41  
 PH-3921-S      Karachentsev 218  
 March 29/30, 1962      M81/NGC 2403 Gr  
 (103aE + Inter) - (103aD + GG11)      M82  
 60 min      panel 334

M82 is the prototype of the Amorphous class. It is a companion of M81 at a separation of 3.7'. At a distance of 3.3 Mpc determined from Cepheids, the projected linear separation of M81 and M82 is small, at 36 kpc.

The image on the left is a combination of an Ha interference filter photograph and a 103aD + GG11 yellow continuum image that has been photographically subtracted from it. The extensive series of Ha emission filaments perpendicular to the plane is emphasized in this subtraction image.

The H $\alpha$  emission is polarized to the same high degree (identical intensity and position angle) as the continuum radiation at the same locations, showing that the high filaments are due to scattered H $\alpha$  emission light from the more central regions (Visvanathan and Sandage 1972).

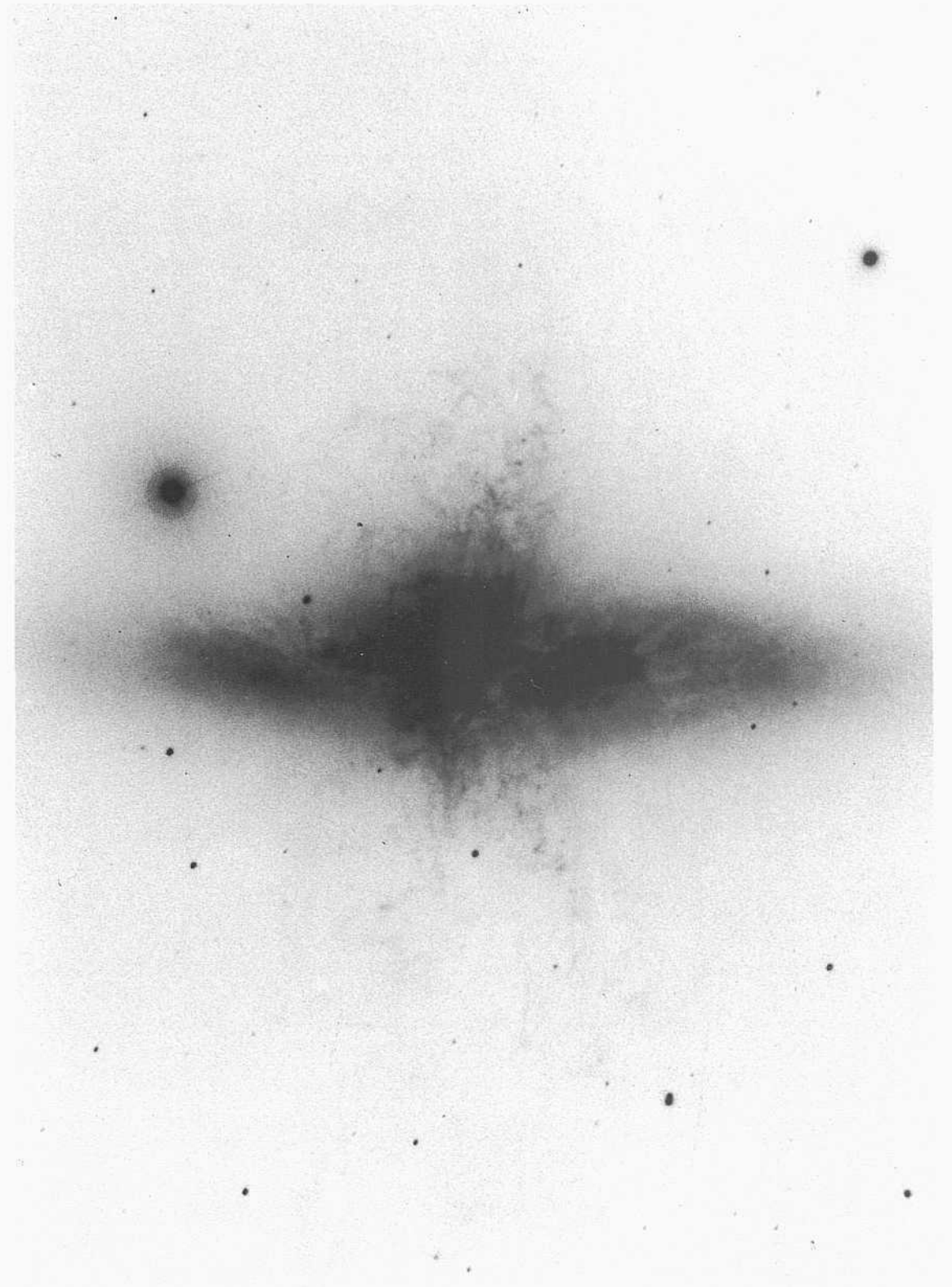
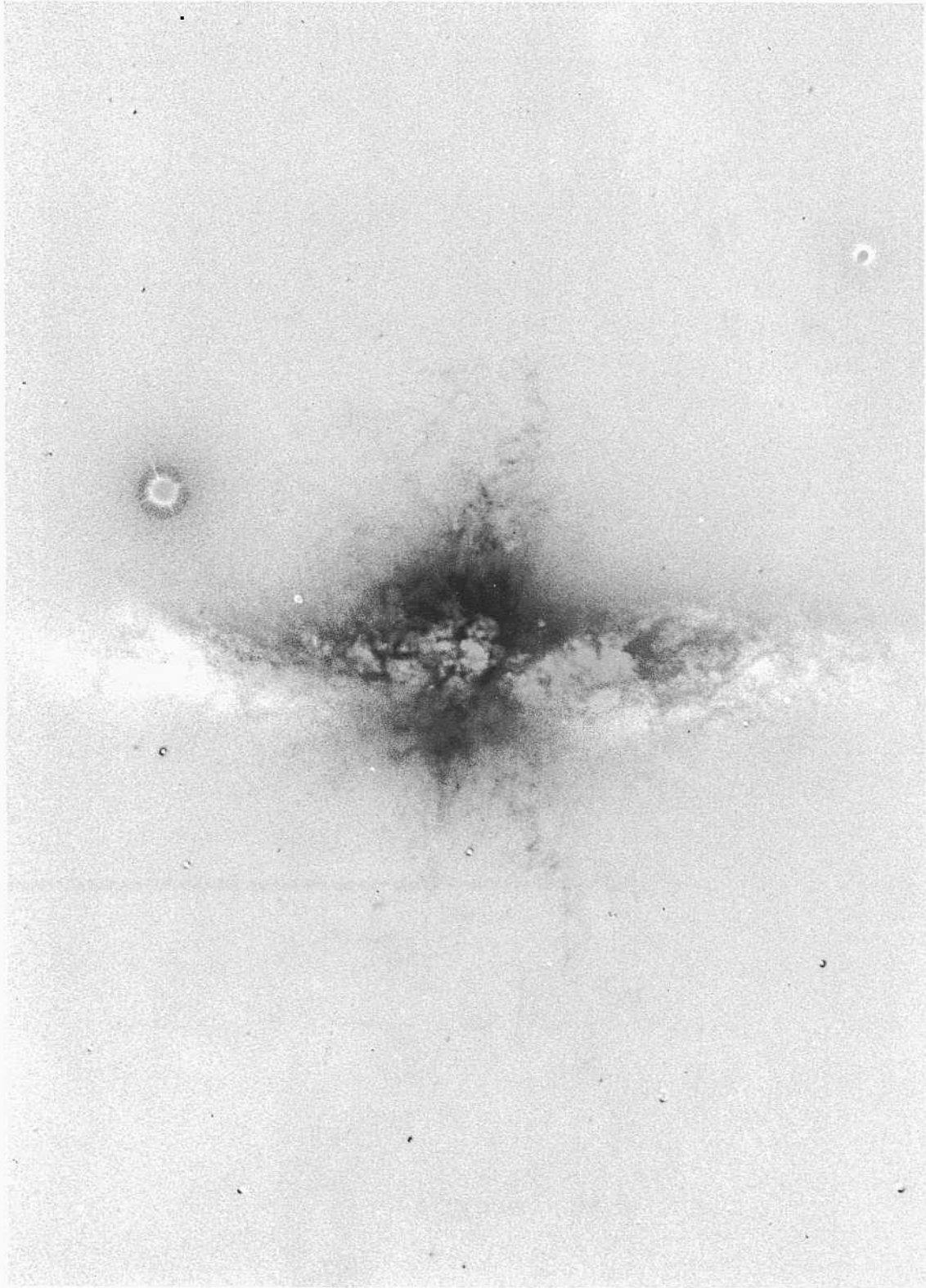
Nevertheless, there is an expansion of material from the center that is real, as shown from long-slit spectroscopy (Lynds and Sandage 1963). O'Connell and Mangano (1978) have suggested that the expulsion of material from the central regions may be due to massive star formation in the center. Extensive early discussions of the process have been made by many authors. A listing of the initial references is given by Kronberg *et al.* (1979).

The hot OB stars, and probably supernovae as well, excite and extrude the gas along the minor axis. This process is a favorite hypothesis to explain the amorphous form. Many galaxies in this class (e.g., NGC 625 and NGC 1569 later in this section) show the same features of emission filaments and explosive motions. Such galaxies, and therefore those members of the Amorphous class similar to M82, have been called starburst galaxies.

NGC 3034      Amorphous      HA, p. 41  
 Masked Ha interference      Karachentsev 218  
 PH-3921-S      M81/NGC 2403 Gr  
 March 29/30, 1962      M82  
 103aE + interference filter      panel 334  
 180min

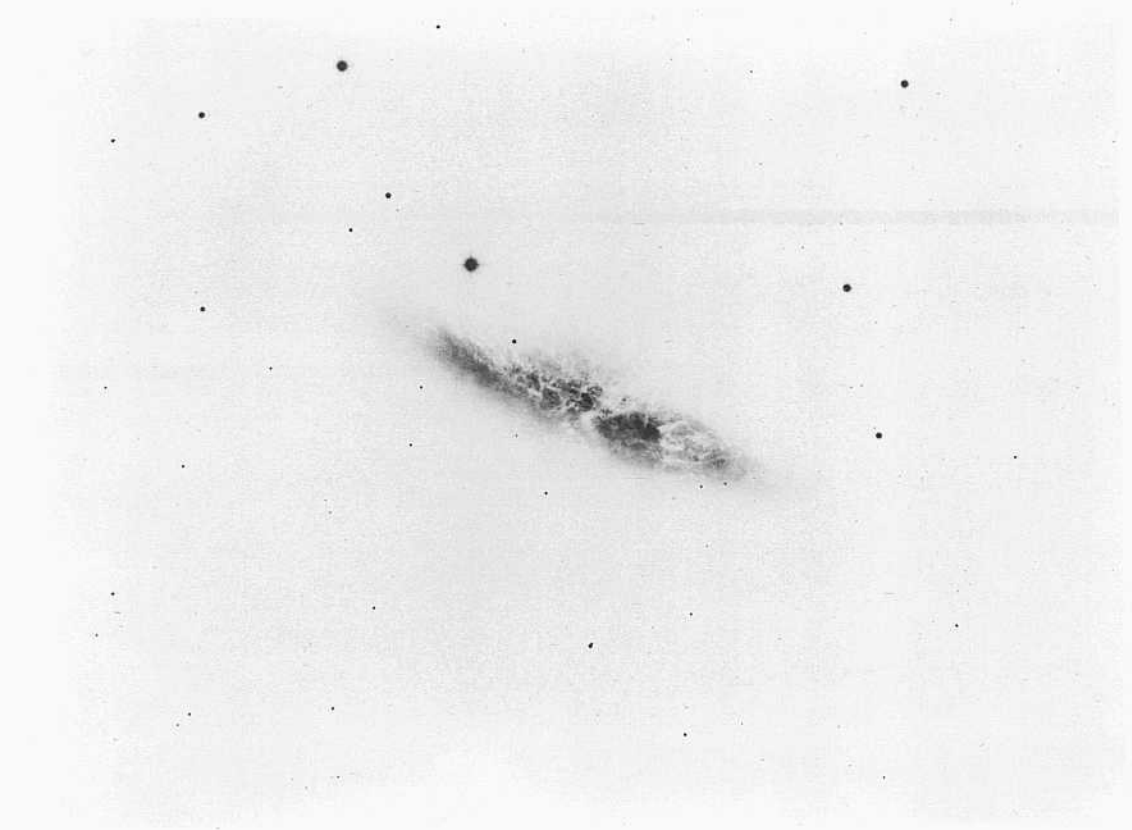
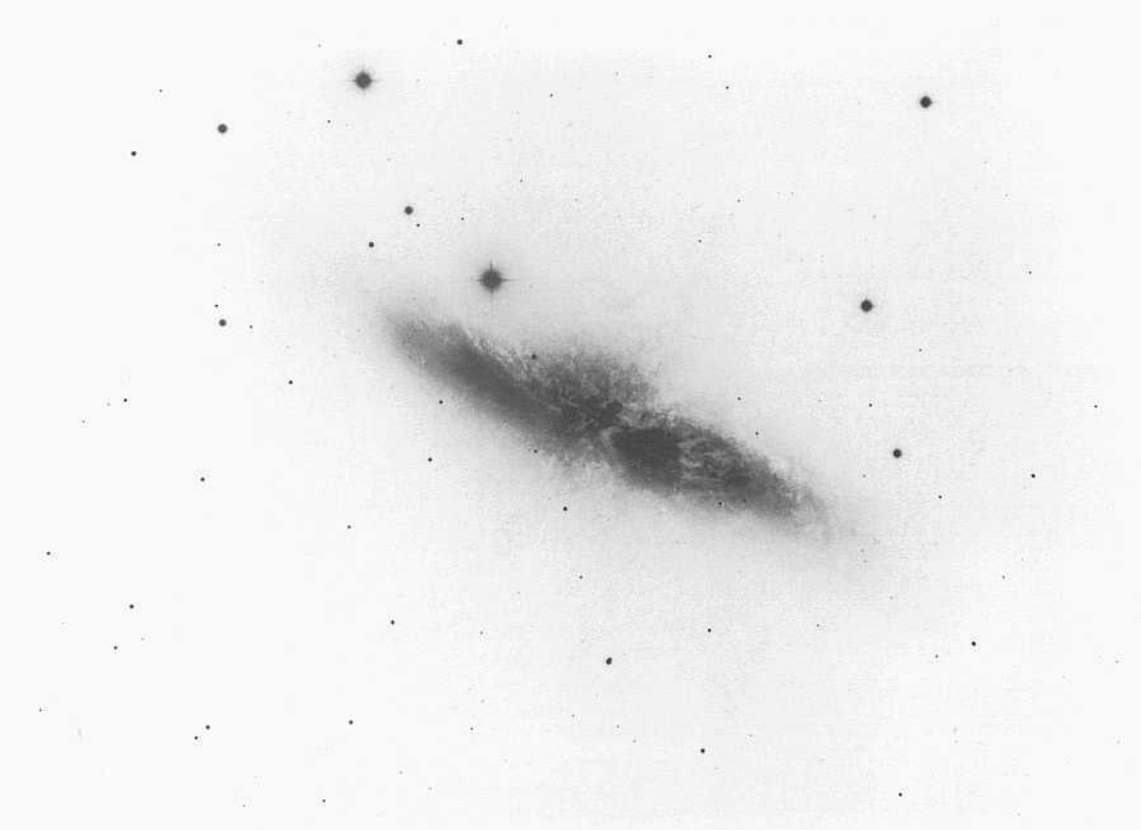
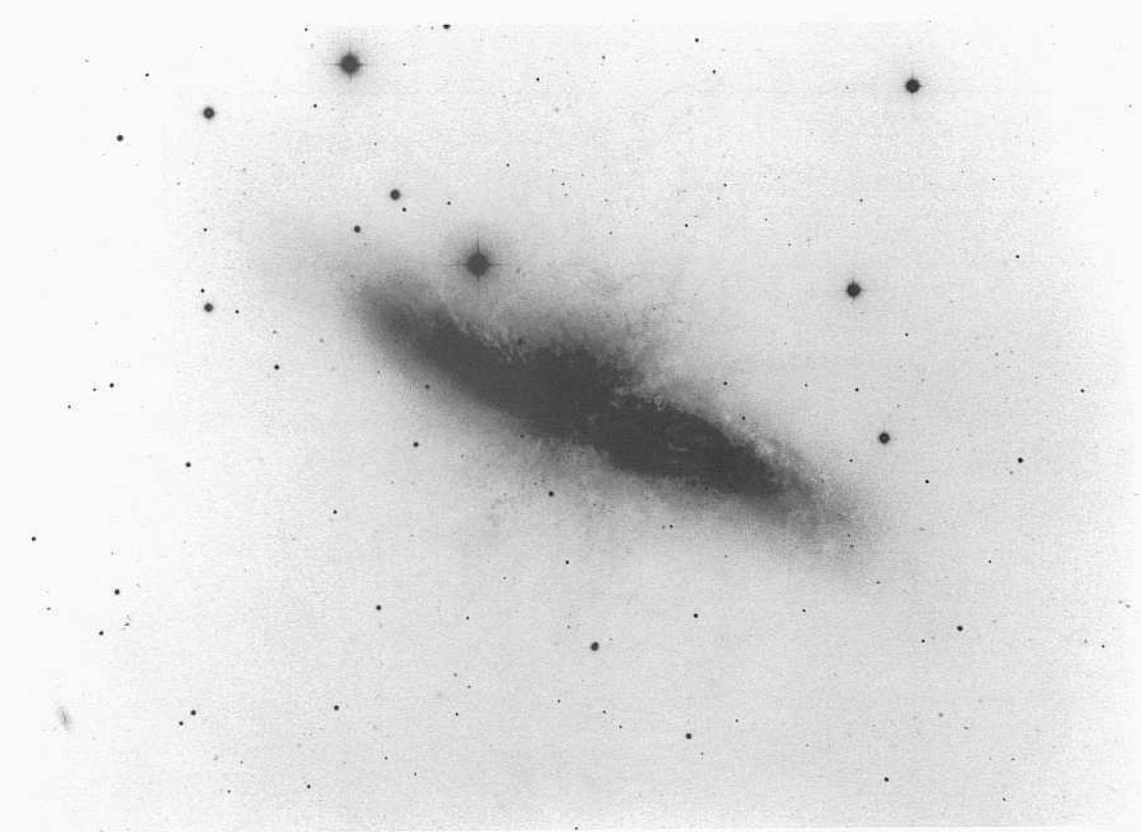
The image on the right is from an H $\alpha$  photograph taken with an interference filter of 80 Å total half-width, dodged to increase the latitude of the print. Spectra with the slit along the minor axis show that the Ha gas mass is expanding from the center on both sides of the major axis (Lynds and Sandage 1963). Confirmation, and a more detailed mapping of the expansion velocity field along the minor axis, were made by Burbidge, Burbidge, and Rubin (1964).

As mentioned in the paragraphs at the left, light from the base of the minor-axis filaments is highly polarized, as was discovered by Elvius (1962, 1967, 1969). The outer filaments are also highly polarized (Sandage and Miller 1964; Sandage and Visvanathan 1969; Visvanathan and Sandage 1972).



PANEL  
333

PANEL  
334





*Amorphous Classification Section (continued)*

NGC 3077      Amorphous      HA, p. 41  
**PH-896-S**                      M81/NGC 2403 Gr  
 Jaii 23/24, 1955  
 103aD + GG11  
 30 niin

NGC 3077 was catalogued as a member of the M81/NGC 2403 Group by Holmberg (1950) in his identification and study of the group. The original Hubble type was Irr. Holmberg's (1958) type for NGC 3077, in dividing the Irr types into two groups (by analogy with Baade's two population types), was Irr II, based on color.

The unusual feature in both M82 and NGC 3077 is that neither are well resolved into stars despite the small distance of 3.3 Mpc, based on Cepheids in NGC 2403 and in M81. The small redshifts of M82 and NGC 3077 confirm membership in the group. The redshifts are  $f_o(82) = 409 \text{ km s}^{-1}$  and  $u_o(3077) = 165 \text{ km s}^{-1}$ .

Both galaxies have high surface brightness and a smooth texture to their surface luminosity, as if there is a veiling of the stellar content. In addition, both have emission-line spectra.

The heavy print of NGC 3077 at the upper left shows the lack of resolution into individual stars. Compare this feature with the very high stellar resolution level in NGC 2403 (panel 273), M81 (panel 129), NGC 2366 (panel 327), HoII (panel 331), and NGC 4236 (panel 324), which are other members of the group. If NGC 3077 is a starburst galaxy like M82, the activity is hidden (as in M82) presumably by dust and/or by a dominating continuum luminosity that floods the image. These characteristics define the Amorphous class.

NGC 3077      Amorphous      HA, p. 41  
 PH-867-S                      M81/NGC 2403 Gr  
 Nov 3/4, 1954  
 103aO  
 20 niin

The positive print of NGC 3077 at the bottom left is from a blue plate rather than a yellow plate as in the image above it. Heavy dust absorption lanes exist throughout the image. A few knots are present near the center. These are either individual stars or are star clusters such as are known in other galaxies of this class including NGC 1705 on this panel and NGC 1569 and NGC 625 on the next.

These few individual starlike objects in NGC 3077 begin to appear at about  $B = 18$ . Three are very *viel*, appearing at about  $V = 17$ . Two of the others are moderately blue, found by comparing red and blue plates. At a distance modulus of  $m - M = 27.6$ , these apparent magnitudes translate into absolute magnitudes of about  $-10$  and  $-11$ , similar to the luminosities of super star clusters in other galaxies of this type, discussed in the remaining panels of this section.

NGC 5253      Amorphous      Centaurus Gr  
 CD-245-S  
 Feb 14/15, 1978  
 103aO + GG385  
 35 niin

NGC 5253 is a member of the nearby Centaurus Group, whose central member is NGC 5128. The mean redshift of the group is near  $\langle v_o \rangle = 280 \text{ km s}^{-1}$ . The group has a diameter of approximately  $20^\circ$  on the plane of the sky. The distance to the group is presently (1991) controversial, ranging between 3 Mpc (Tonry and Schechter 1991) and 8 Mpc (Sandage and Tamman 1975a). At a distance of 5 Mpc ( $m - M = 28.5$ ) the projected linear diameter of the group, corresponding to  $20^\circ$  angular diameter, is 1.7 Mpc, similar to the Local Group.

The heavy print at the top of the middle column shows the characteristic high-surface-brightness, smooth-structured envelope luminosity of the main body that defines part of the features of the Amorphous class. On small-scale photographs with low spatial resolution, such forms would incorrectly be classed as E or SO types because of this enveloping light. Yet we know that such galaxies are copious current producers of high-luminosity stars. The case is particularly clear in NGC 5253 because of evidence that two very bright supernovae have occurred within the past hundred years (SN 1895B = Z Cen; SN 1972E). The 1972 supernova, discovered by Kowai, probably reached  $B = 8.5$  magnitude at maximum.

NGC 5253      Amorphous      Centaurus Gr  
 CD-2123-S  
 March 20/21, 1982  
 103aO + GG385  
 5 min

The thin positive print at the bottom of the middle column is made from a different original plate than was used above. The high surface brightness of the amorphous light still dominates the central part of the image, but the individual stars in this starburst galaxy are now visible, starting at about  $B = 18.5$ . At a distance modulus of  $m - M = 28.5$ , the corresponding absolute magnitudes of these objects are  $M_j = -10$ , in agreement with the calibration made of such stars at the Eddington limit using galaxies with known Cepheid distances (Sandage and Carlson 1988).

Note that the dust lanes in NGC 5253 are similar to those in NGC 3077 but are less opaque.

The redshift of NGC 5253 is  $v_o = 147 \text{ km s}^{-1}$ .

NGC 1705      Amorphous  
 CD-140-S  
 Feb 1/2, 1978  
 103aO + GG385  
 50 min

NGC 1705 was classed as an SO pec in both the RC1 and the RC2 based on small-scale plates taken at Mount Stromlo with the 30-inch Reynolds Telescope. This classification is inappropriate; the problem is caused by the high surface brightness of the amorphous light, as described in the paragraphs on NGC 5253 in the middle column here.

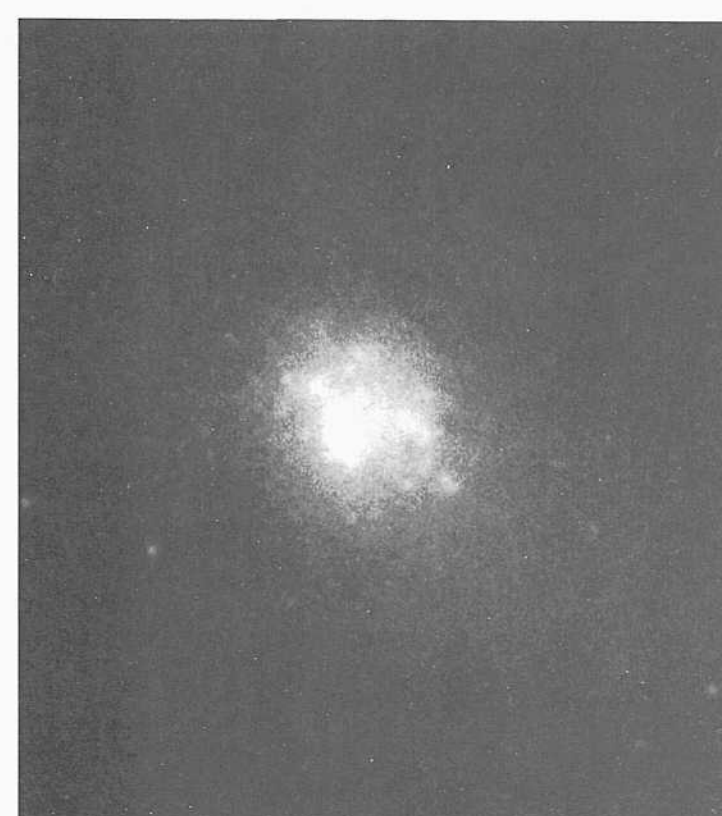
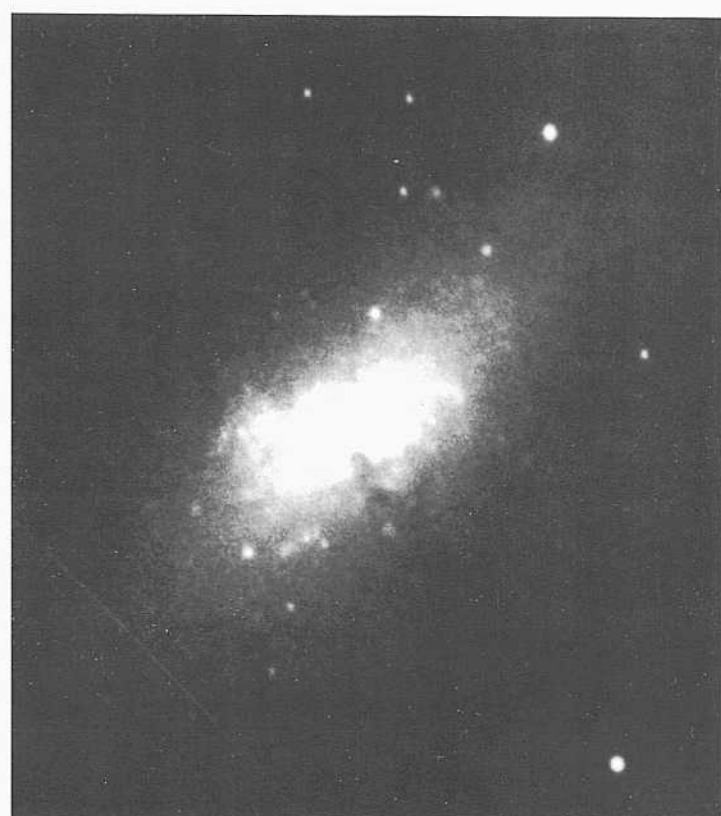
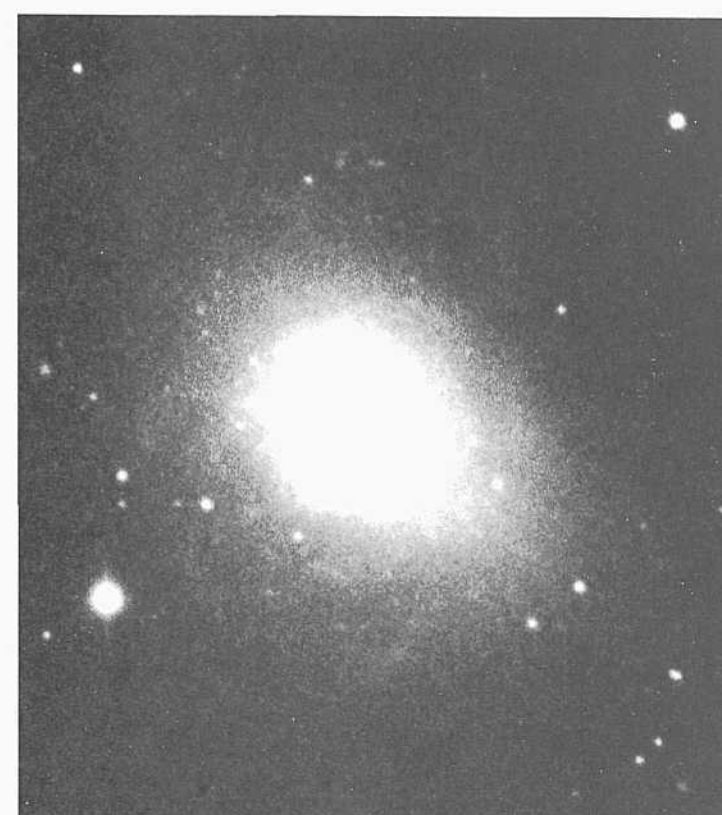
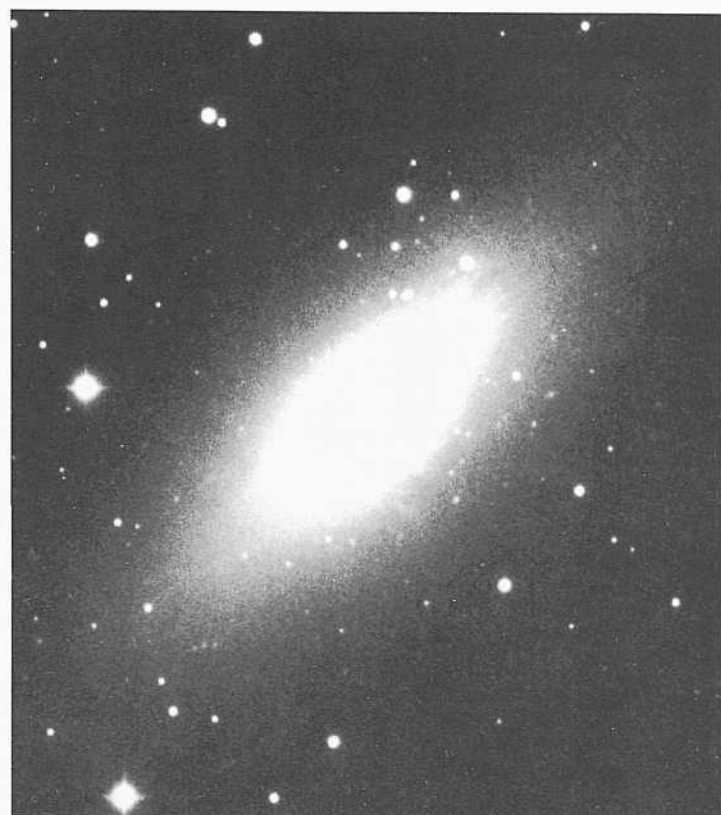
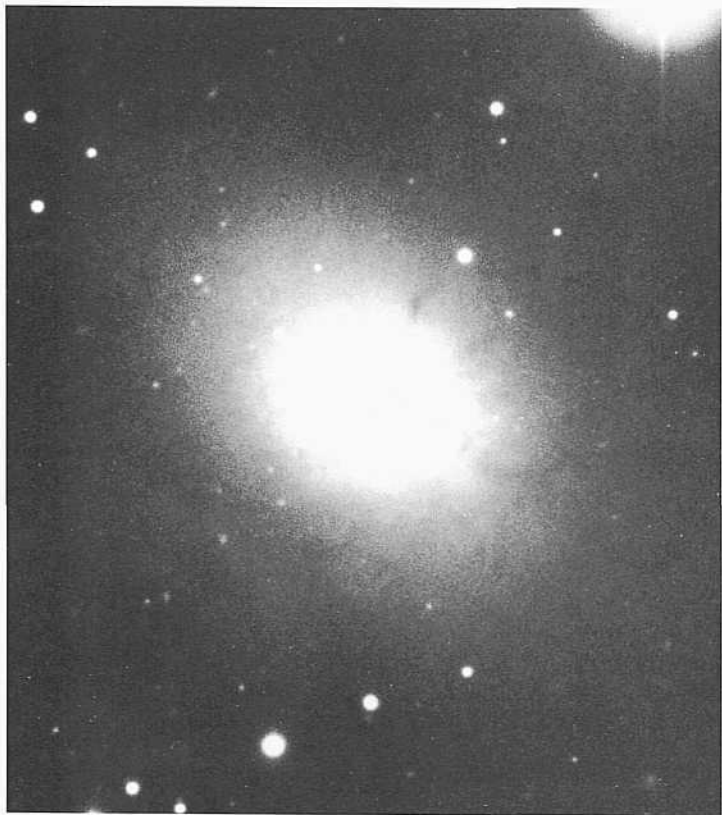
The spectrum is rich in emission lines across the entire disk (Sandage 1978). The strongest lines are Ha, H $\beta$ , and N1 and N2. Objects presumed to be stars are embedded in the intense disk light. They are numerous at  $B = 20$ , and the brightest are undoubtedly brighter than this. The color of the disk light is very blue. Robust current star formation is occurring.

NGC 1705      Amorphous  
 CD-145-S  
 Feb 2/3, 1978  
 103aO + GG385  
 20 min

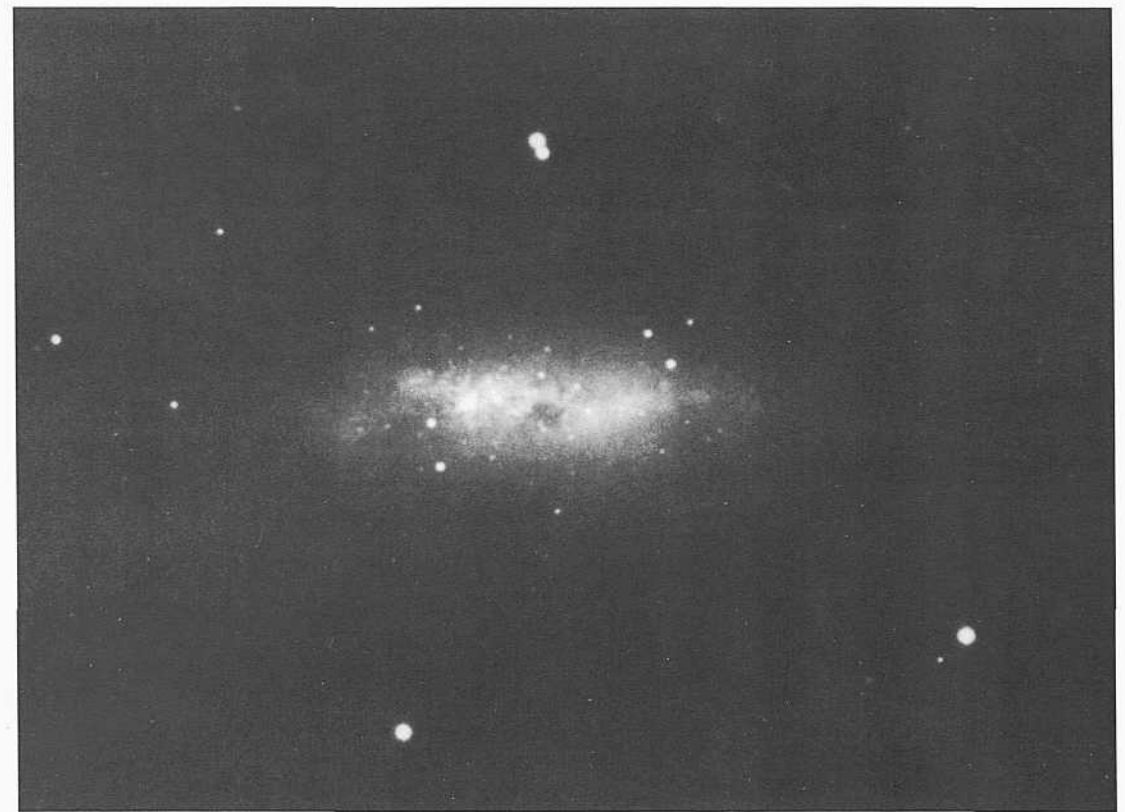
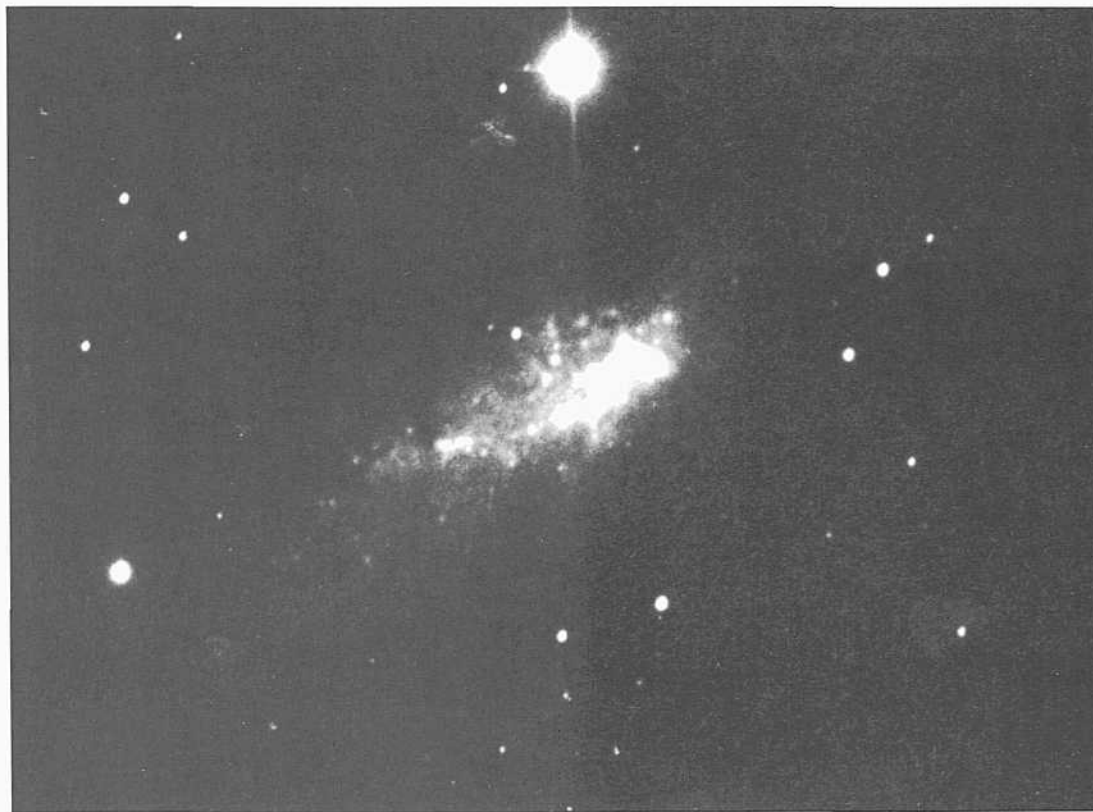
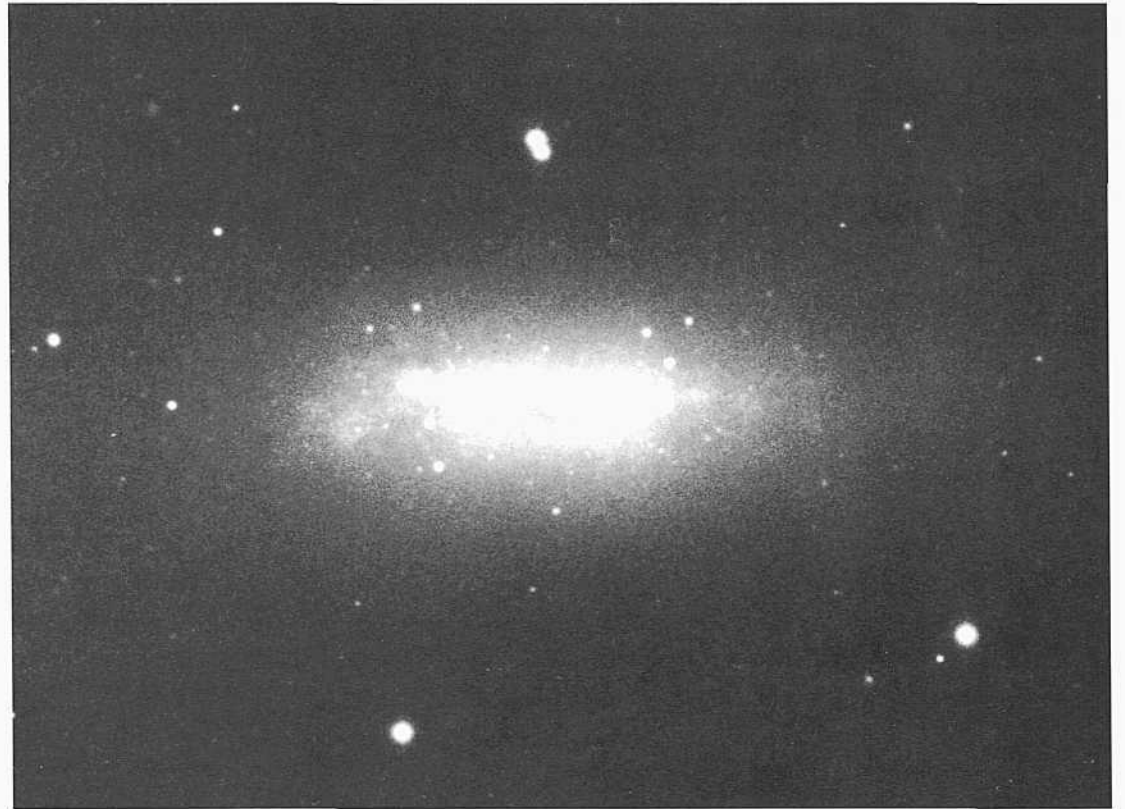
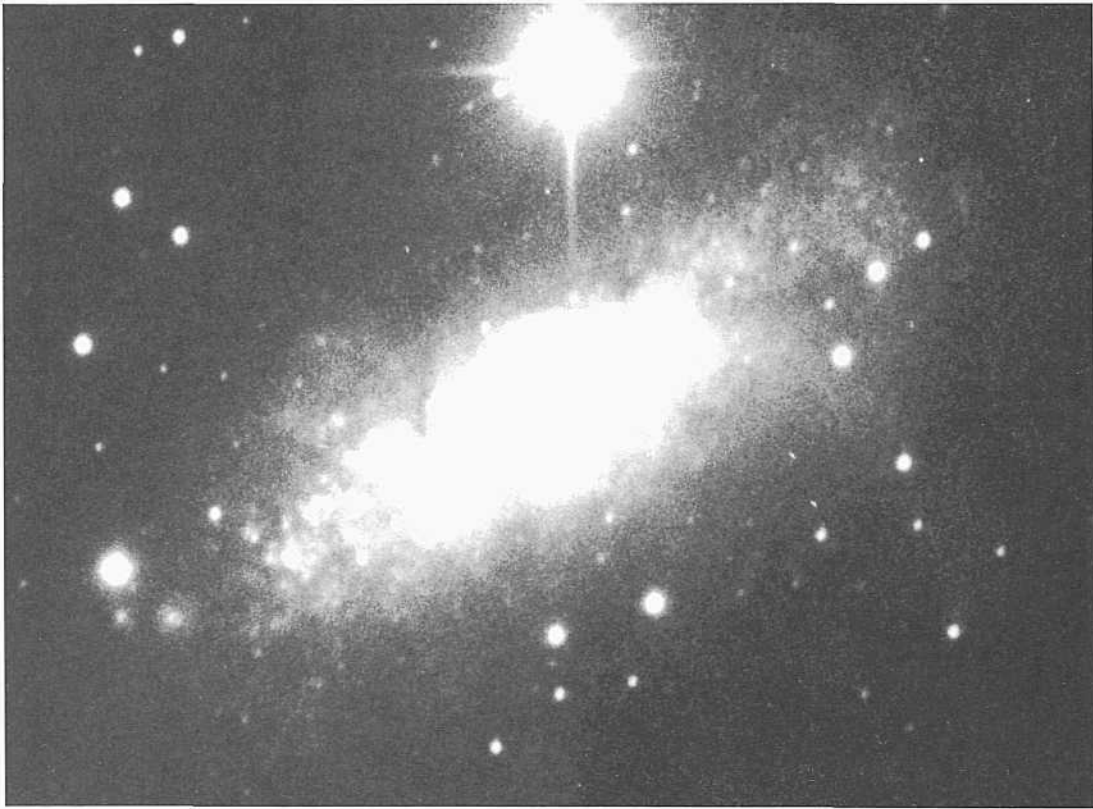
The most curious feature in the image is the presence of an intense blue object displaced from the center by about a third the disk length. The object has a hydrogen absorption spectrum showing the same velocity as the disk emission. The spectrum resembles those of the super star clusters in NGC 1569 (Arp and Sandage 1985) that have absolute magnitudes of  $M_g = -13$ .

The redshift of NGC 1705 is  $v_o = 445 \text{ km s}^{-1}$ . At the redshift distance of 9 Mpc ( $m - M = 29.8$ ) the compact blue object with an apparent magnitude of  $B = 16$  must have an absolute magnitude of  $M_B = -14$ . Such super clusters are known in NGC 625 (panel 336), NGC 1705 here, NGC 1569 (panel 336), and perhaps NGC 1140.

Spectra (Meurer *et al.* 1988, 1992) show that gas is being expelled from NGC 1705 by super-galactic winds created by the momentum transfer of the photon energy from the super star cluster to the gas. This is the characteristic process in starburst galaxies and may be a common feature throughout the Amorphous type.



PANEL  
336



NGC 1569 SmlV/Ainorplious  
PH-147-H  
Oct 13/14, 1952  
103aO  
25 mill

The distance modulus of NGC 1569 is about  $m - M \approx 29$  ( $D = 6$  Mpc) from arguments based on its stellar content (Arp and Sandage 1985). Holmberg (1958) classified the galaxy as Irr I, similar to, for example, NGC 2366. However, the image is dominated by a high-surface-brightness amorphous light over much of the central region, shown in the heavy print at the top left. The spectrum of the disk light is dominated by emission lines (Mayall 1935; de Vaucouleurs, de Vaucouleurs, and Pence 1974).

Stars begin to resolve over the image at about  $B = 20$  (Abies 1971). The redshift of NGC 1569 is  $u_B = 144 \text{ km s}^{-1}$ . The extragalactic nature of the galaxy was first recognized by Baade (1931), who made the suggestion that its type is similar to the Magellanic Clouds, one of the first of the type to be identified in the general field.

NGC 1569 SmlV  
PH-150-H  
Oct 13/14, 1952  
103aO  
5 min

The print here, from a short-exposure plate by Hubble, shows the resolution of the inner region into stars, beginning at about  $B = 20$ . However, two very bright objects of  $B = 15.7$  and  $B = 16.5$  exist in the image. These are members of the galaxy, as shown from the equality of their velocities with the emission velocities of the gas in the disk (Arp and Sandage 1985). The spectra also show that these bright objects are super star clusters, as also described in the discussion of NGC 1705 on the preceding panel. The absolute magnitude of these bright young clusters is unusually high (but matched in NGC 1705 and NGC 625) at  $B = -1.3$ .

A discussion and a series of stepped exposure prints of NGC 1569 showing these clusters is given by Arp and Sandage (1985, Fig. 10).

A discussion of the role of supergalactic winds in the self-transformation of Im and BCD galaxies into dE,N dwarf elliptical and dS0,N dwarf SO galaxies is given by Sandage and Hoffman (1991).

NGC 625 Amorphous or ImIII  
CD-526-S  
Sep 29/30, 1978  
103aO + GG385  
45 min

NGC 625 shares the Amorphous features that have been described on this and the preceding panel for NGC 5253, NGC 1705, and NGC 1569. The very-high-surface-brightness disk has an emission-line spectrum that contains the standard high excitation lines of 3727. HeII, [NeIII], HeI, H, NI, N2, [NiI], [SII], [AMI], and [AIV]. These lines are evidently excited by the high current star-formation rate of massive stars, evidenced by the resolution of these stars beginning at about  $B = 17$ .

The redshift of NGC 625 is  $v_o = 352$ . The distance modulus is about  $m - M = 21$ , judged from the stellar content.

NGC 625 Amorphous or ImIII  
CD-526-S  
Sep 29/30, 1978  
103aO + GG385  
45 min

The light print made from the same plate, above, shows some of the resolution into stars. In addition, visual inspection of the image at the Mount Stromlo 74-inch reflector showed the presence of a bright blue object displaced from the center (as in NGC 1705) at about  $ii = 15$  (Sandage 1978). This object is a super star cluster similar to those in NGC 1705 and NGC 1569, previously described on this and the preceding panel. The absolute magnitude of the super star cluster in NGC 625 is near  $M_j = -1.3$ , similar to the values in the other cases just cited.



*Amorphous Classification Section (continued)*

NGC 4691 H Amorphous pec pair:  
 CD-1873-HB HA, p. 44  
 April 10/11, 1981  
 103aO  
 75 min

NGC 4691 forms a wide apparent pair with NGC 4684 (SO2/3; panel 42) at a separation of 19'. The redshifts are  $z_{(4684)} = 1411 \text{ km s}^{-1}$  and  $z_{(4691)} = 942 \text{ km s}^{-1}$ . At the mean redshift distance of 24 Mpc ( $H = 50$ ) the projected linear separation is 135 kpc if they form a kinematic pair. However, the redshift difference of 470  $\text{km s}^{-1}$  is high and fails to establish a definite case.

The heavy print at the top left shows the external ring; of low surface brightness, interpreted by Hubble as smooth arms; hence his classification was SBa.

The classification here is based on the intricate dust pattern in the central regions, similar to the dust in NGC 3077. However, the Amorphous classification is less certain than in the prototype galaxies on the preceding four panels.

NGC 4691 R Amorphous pec pair?  
 CD-1873-HB HA, p. 44  
 April 10/11, 1981  
 103aO  
 75 min

The light print here, from the same plate used for the heavy print above, shows the dust pattern in the central regions. The dust lanes are generally perpendicular to the major axis, similar to part of the pattern in NGC 1808 (Sbc pec; panel 193), attributed in the description there to a galactic fountain activity. By analogy, this has been taken to suggest the possibility that the gas and dust of NGC 4691 might have a starburst property. Supporting evidence is the emission-line spectrum throughout the disk (Sandage 1978), composed of strong 3727, strong Balmer series emission, strong N2, and weaker N1.

NGC 2968 Amorphous or SO3 pec panel 49  
 PH-7603-S Karachentsev 210  
 April 3/4, 1979  
 H&J + GG385  
 30 min

NGC 2968 is also illustrated and described in the SO section on panel 49. H forms a triplet with NGC 2964 (Sc; panels 240, 251) at a separation of 6.3' and with NGC 2970 (SO<sub>3</sub>; not in the RSA) at a separation of 5.0'. The redshifts are  $z_{(2968)} = 1551 \text{ km s}^{-1}$ ,  $z_{(2970)} = 1629 \text{ km s}^{-1}$ , and  $z_{(2964)} = 1292 \text{ km s}^{-1}$ . At the mean redshift distance of 30 Mpc ( $H = 50$ ) the projected linear separation of NGC 2964 from NGC 2968 is 55 kpc and the separation of NGC 2970 from NGC 2968 is 44 kpc. A physical association between NGC 2968 and NGC 2970 is assured by the circumstance that a supernova occurred (SN 1970L, discovered by Wild) on the luminous bridge connecting NGC 2968 and NGC 2970. A photograph of the configuration is in Tammann (1973).

The Amorphous classification of NGC 2968 is based on the character of the dust (similar to that in M82 and NGC 3077).

NGC 4383 Amorphous? (not SO) VCC 801  
 CD-1854-HB  
 April 4/5, 1981  
 103aO  
 75 min

NGC 4383 is listed as a member of the Virgo Cluster in the Virgo Cluster Catalog. Its redshift is small at  $z_0 = 284 \text{ km s}^{-1}$ , but its distance is much larger than would be implied by this small value, consistent with cluster membership and the high virial velocities of cluster members. Resolution into stars and HII-region candidates does not occur, indicating a distance that must be similar to that of the Virgo Cluster core.

The classification of NGC 4383 as Amorphous is indicated by the high surface brightness of the image and the character of the dust lanes.

NGC 1531 Amorphous group  
 CD-1669-S panel 197  
 Dec 31/Jan 1, 1980/1981  
 103aO + GG385  
 4-5 min

NGC 1531, here, is a close companion of NGC 1532 (Sbc; panel 197); the pair is presently in a close encounter.

The enlargement of this print is great enough to exclude any part of NGC 1532 (panel 197) which is at an angular separation greater than 1.8'. A description of the pair and the peculiar morphology of NGC 1532 is on panel 197.

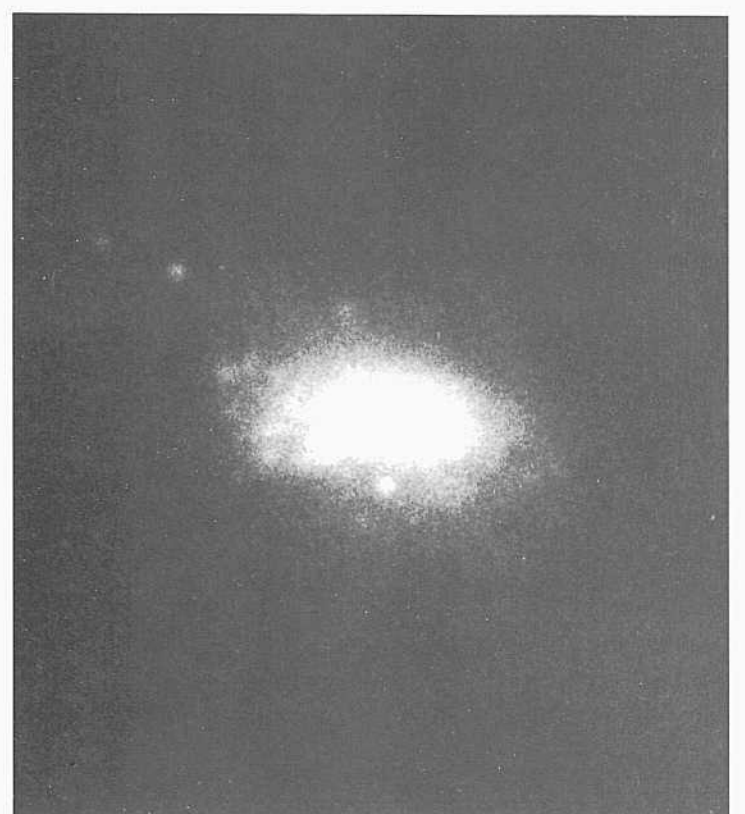
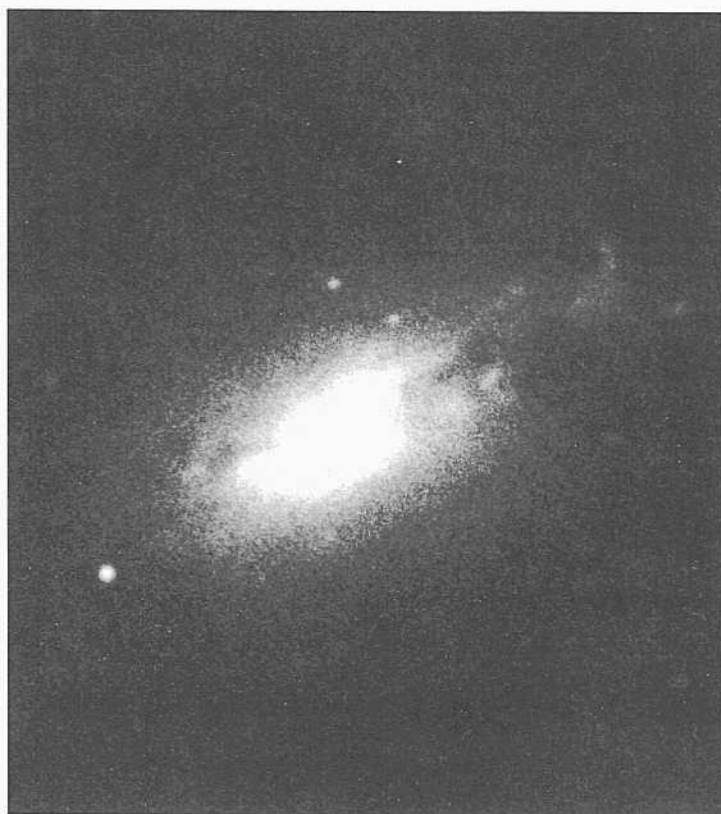
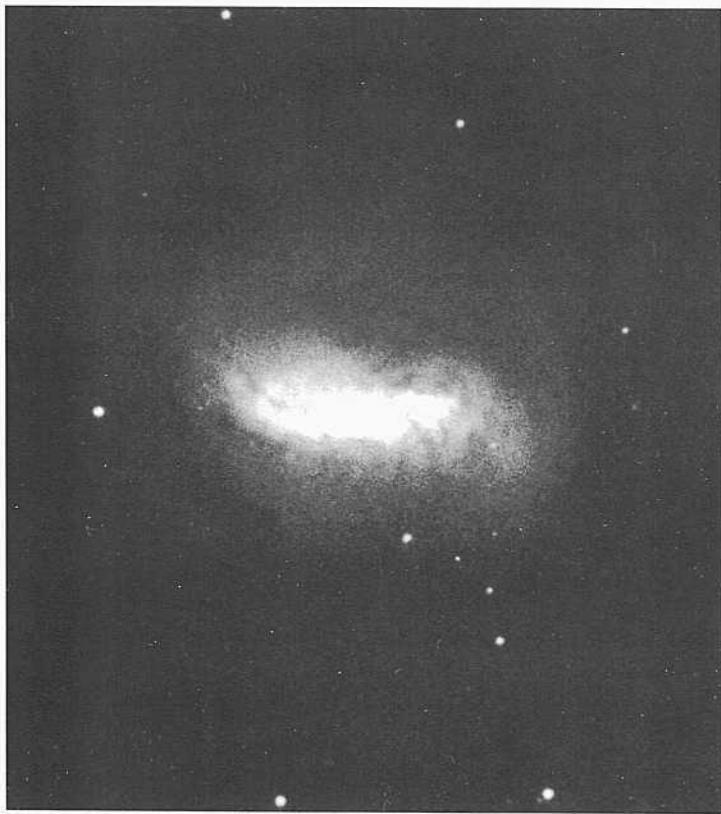
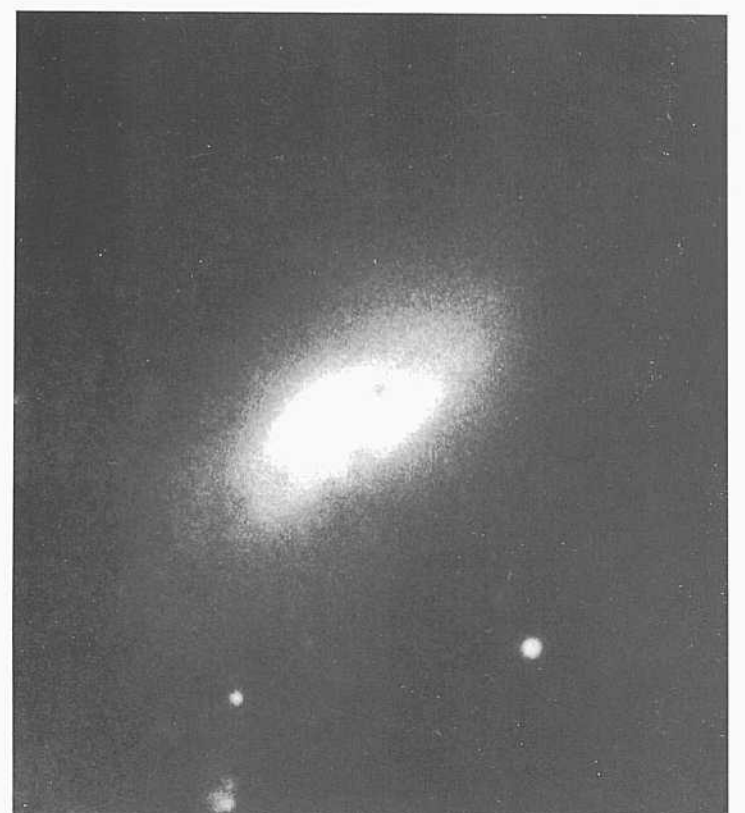
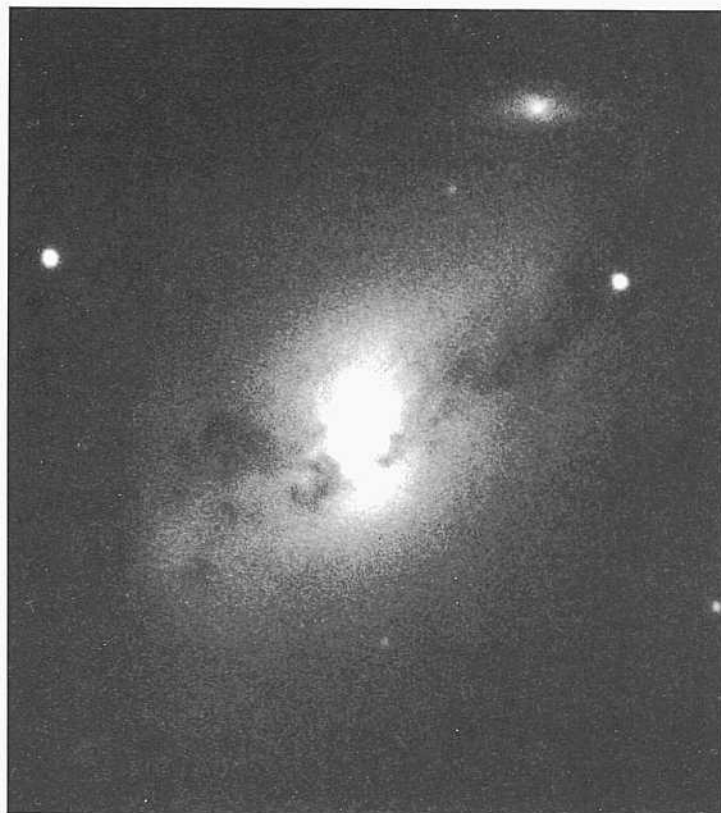
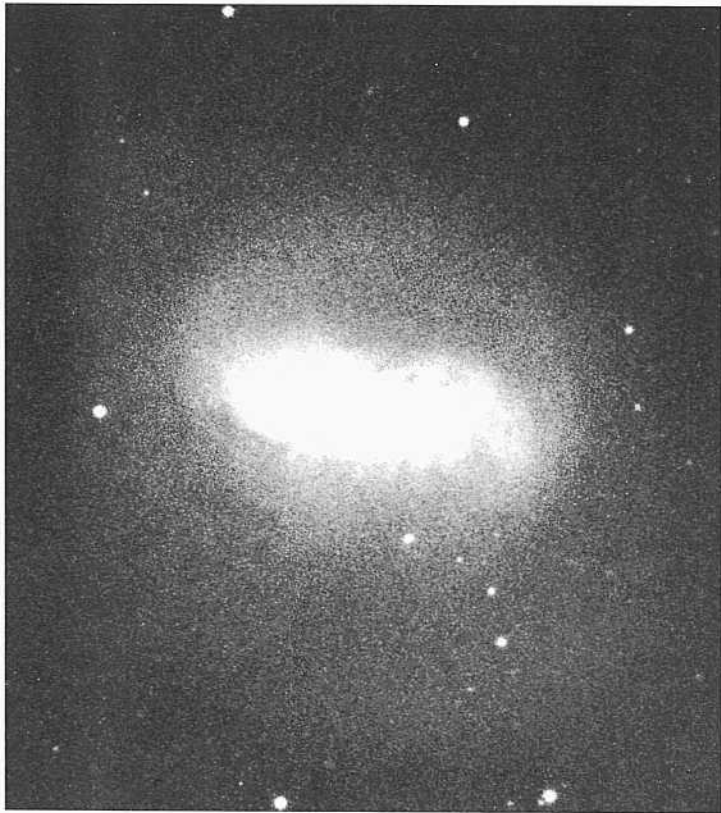
NGC 1531 has an amorphous texture to its luminosity distribution; there is evidence of dust in the image.

NGC 4765 Amorphous?  
 CD-2165-S  
 March 27/28, 1982  
 103aO + GG385  
 45 min

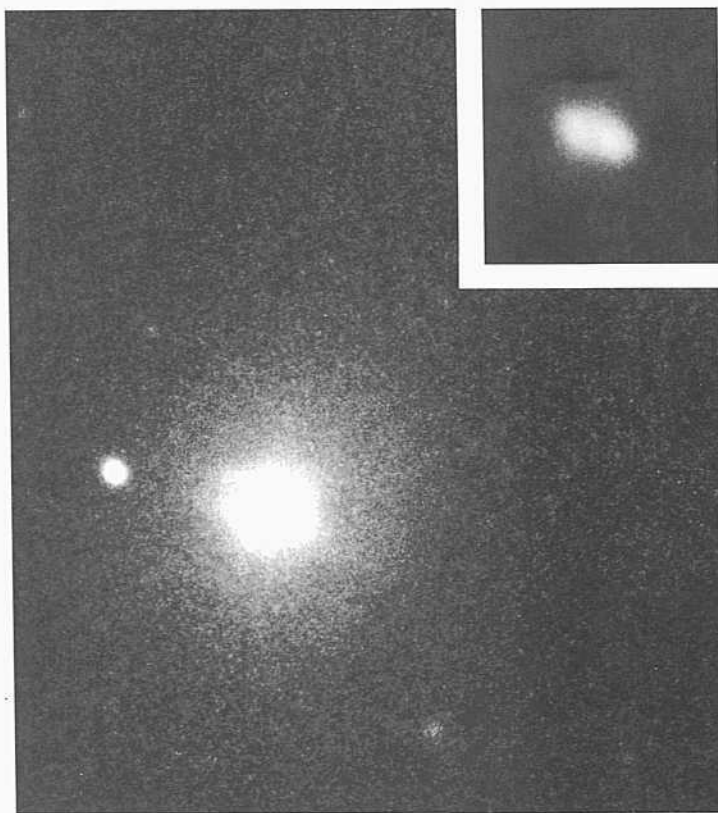
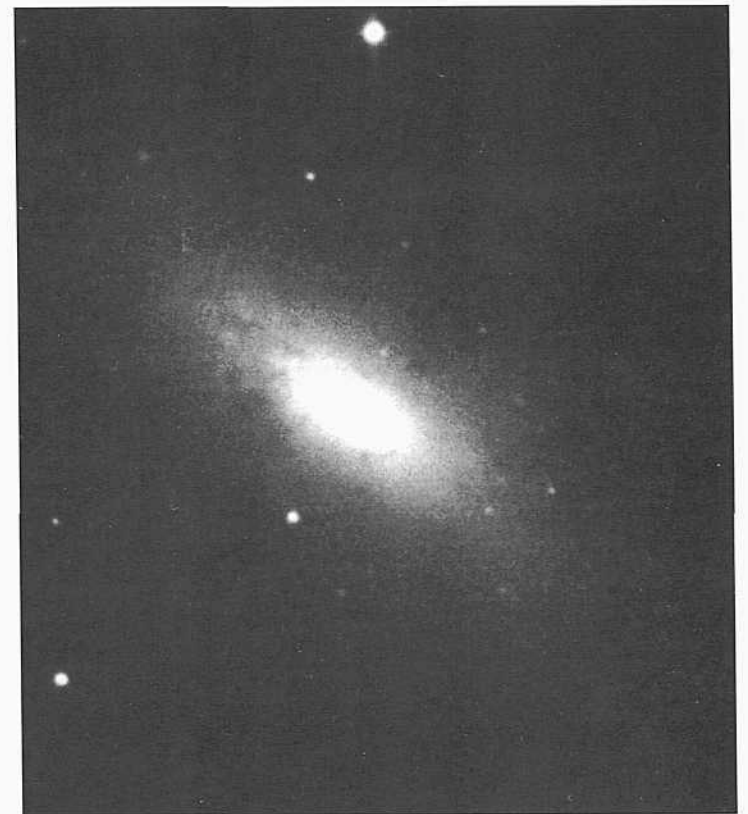
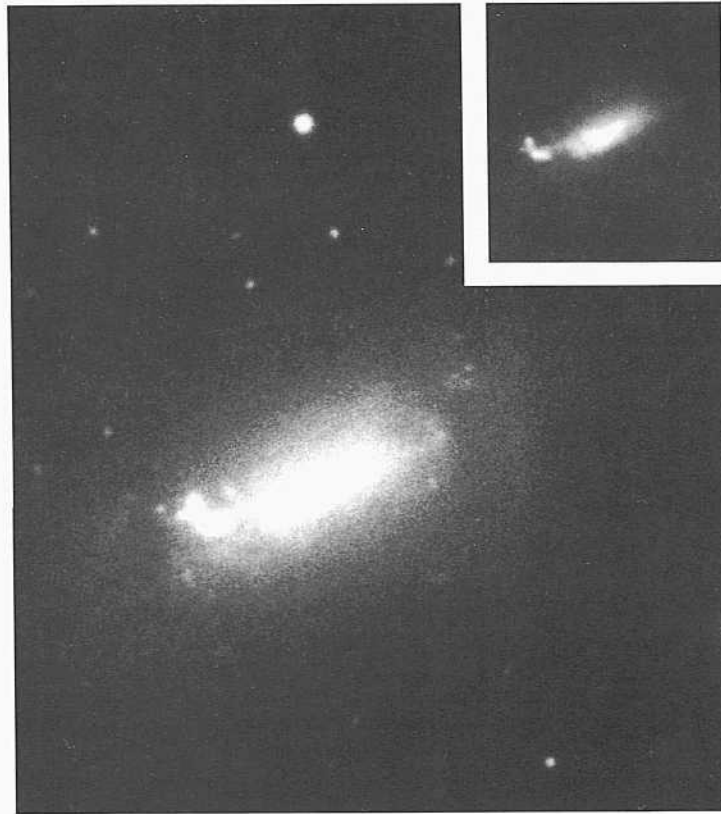
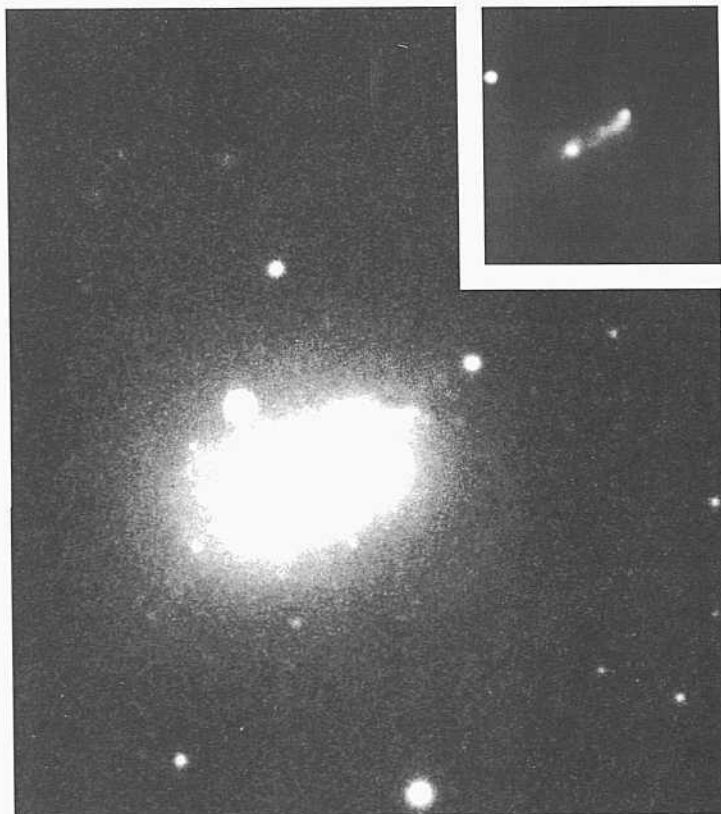
NGC 4765 is just outside the boundary of the Virgo Cluster survey region (Binggeli, Sandage, and Tammann 1985). The region is complex; it is near the supergalactic ridge-line in a confused kinematic area where redshifts do not indicate distance.

The redshift is  $z_0 = 626 \text{ km s}^{-1}$ . Resolution into knots is visible at the periphery of the disk. It is probable that such resolution is present throughout the disk but is hidden by the high surface brightness.

The morphological classification is uncertain.



PANEL  
338



NGC 3125 Amorphous  
 CD-721-S  
 Feb 1/2, 1979  
 103aO + GG385  
 15 mill

NGC 3125 has an outer envelope morphology similar to those in NGC 625, NGC 1705, and NGC 5253. The disk is of high surface brightness. There is a hint of resolution into individual objects (stars?) in the outer envelope. The most telling feature suggesting the Amorphous classification is the two very bright objects near the center (seen in the insert), of magnitude  $B = 17$ .

The redshift is  $v_o = 827 \text{ km s}^{-1}$ . At the redshift distance of 16 Mpc ( $m - M = 31$ ) the absolute magnitudes of the knots are  $M_g = -14$ , similar to the luminosities of the four super star clusters in NGC 625, NGC 1705, and NGC 1569, described on the preceding panels.

The spectrum of the disk of NGC 3125 shows extremely hard, high-excitation emission lines including H $\delta$  at 4686 (Penston, Fosbury, Ward, and Wilson 1977). The three amorphous galaxies just mentioned also have high excitation emission spectra.

The presence of the super star clusters, the hard emission radiation, and the amorphous light of the envelope are the reasons for assigning the Amorphous classification.

NGC 3773 Amorphous; pec jet  
 CD-2184-S  
 March 29/30, 1982  
 103aO + GG385  
 30 mill

NGC 3773 insert  
 CD-2183-S  
 March 29/30, 1982  
 103aO + GG385  
 5 min

The morphology of NGC 3773 is similar to that of NGC 3125, above. The surface brightness of the smooth disk light is very high. The spectrum of the disk shows a strong ultraviolet continuum and intense emission lines of 3727, hydrogen Balmer  $\epsilon$ , N1, and N2 (Sandage 1978).

The two very bright objects at the center each have an apparent magnitude of about  $B = 16$ . These show in the insert print as a merged pair. The redshift of NGC 3773 is  $v_o = 851 \text{ km s}^{-1}$ . At the redshift distance of 17 Mpc ( $m - M = 31$ ), the absolute magnitude of each of the objects is  $M_g = -15$ , similar to the bright objects in NGC 3125 and other galaxies of this class.

The insert print is made from a different original plate than is used in the heavy main print, but is not of short-enough exposure to separate the images of the pair of central objects that still overlap here.

NGC 1800 Amorphous  
 CD-527-S  
 Sep 29/30, 1978  
 103aO + GG385  
 45 min

NGC 1800 insert  
 CD-1345-S/Br  
 March 15/16, 1980  
 103aO + GG385  
 10 min

The optical morphology of NGC 1800 is similar to that of NGC 625. The surface brightness is high. The light is amorphous. Individual stars resolve in the outer regions of the disk, outside the high-surface-brightness area (and very likely inside as well). Bright knots exist that may be superluminous star clusters. The spectrum of the disk light shows high excitation conditions; moderately strong 3727, H $\beta$ , N1, N2, and [Ni] emissions are present. The radiation is hard, judged by the greater intensity of the N2 line than that of H $\beta$  (Sandage 1978).

The redshift is  $v_o = 586 \text{ km s}^{-1}$ .

The bright knots in the outer regions show in the insert print. The surface brightness in the center is still too high to see the center where other possible superluminous star clusters may exist.

NGC 3353 Amorphous? Ursa Major Cluster  
 PH-7978-S  
 Feb 1/2, 1981  
 103aO  
 12 min

NGC 3353 insert  
 PH-7979-S  
 Feb 1/2, 1981  
 103aO  
 2 min

The optical morphology of NGC 3353 is similar to that of other galaxies on this and the preceding panels. The surface brightness of the amorphous light is high. The optical spectrum of the disk shows intense high-excitation emission lines and many lines of the Balmer series, also in emission (Sandage 1978).

The redshift is  $v_o = 1089 \text{ km s}^{-1}$ .

A bright knot exists close to the center, embedded in the high-surface-brightness image and not seen in this insert print. On the available plate material the object is not circular. (It may be double, similar to the double "cluster" in NGC 3773, at the left). The apparent brightness is  $B = 15$  (or if double,  $B = 16$  for a single image).

At a distance modulus of  $m - M = 31.7$  ( $H = 50$ ) the absolute magnitude of the object(s) would be  $M_g = -16$ . Hence, the objects are candidates for super star clusters, similar to such objects in other galaxies of this class.

The six galaxies on this page do not fit into the morphological boxes of the standard classification system. Each, at the resolution available on the existing plate material, has certain features common to the Amorphous galaxies shown on the preceding five panels. Therefore these galaxies have been put at the end of this section.

Most have intense emission spectra. Several (NGC 3125, NGC 3773, etc.) have possible superluminous star clusters at absolute magnitudes of about  $M_g = -15$ .

NGC 4694 Amorphous VCC. 2066  
 CD-802-S  
 Feb 24/25, 1979  
 103aO + Wr2c  
 45 min

NGC 4694 is at the eastern edge of the Virgo Cluster survey field (Binggeli, Sandage, and Tamman 1985). It is listed as a cluster member in the cluster catalog. Its redshift is  $v_o = 1059 \text{ km s}^{-1}$ .

The spectrum shows a strong UV continuum and a pronounced hydrogen absorption spectrum in the center. Several features, all similar to the various characteristics of other Amorphous galaxies in this section such as M82 and NGC 3077, are (1) the early-type absorption spectrum, indicating recent star formation, (2) the character of the amorphous light in the image, and (3) the nature of the evident dust patches.

NGC 3043 S pec  
 PH-7956-S  
 Nov 8/9, 1980  
 103aO  
 12 mill

The classification of NGC 3043 is uncertain because of the high inclination and poor spatial resolution. The surface brightness is low. Emission lines of 3727 and H $\alpha$  extend across the image (Sandage 1978). The galaxy is shown here for completeness.

*Amorphous Classification Section (continued)*

NGC 3418      Amorphous      pair  
PII-8049-S      Arp 205  
Feb 4/5, 1981      Racine wedge  
103aO  
12 min

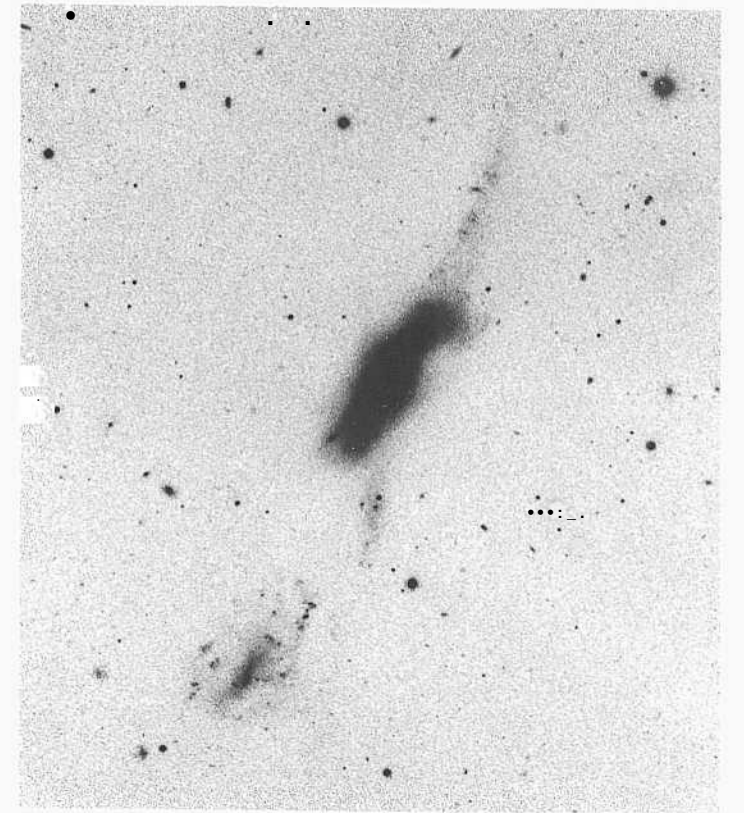
NGC 3448 is the brightest member of a pair that is evidently in a close encounter. What appears to be a tidal plume exists on one side of the main body (toward the upper-right corner of the prints on the right).

A close companion exists on the other side, at a separation of 3.9' (near the lower-left corner of the two). This anonymous galaxy of very low surface brightness is of morphological type Scd with some suggestion of a tidal perturbation in one of its arms. There is also a shred (tidal debris?) between the main body of NGC 3448 and the companion.

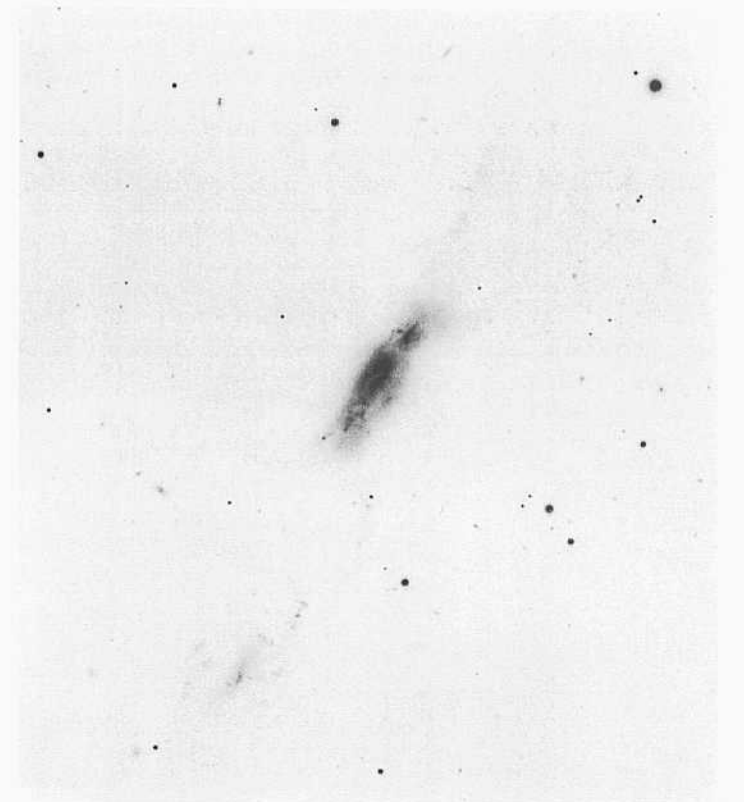
The  $v_0$  redshifts for each segment of the configuration listed by Palumbo, Tanzella-Nitti, and Vettolani (1983) are about 1440 km s<sup>-1</sup> for the main body of NGC 3448 itself, 1325 km s<sup>-1</sup> for the Scd companion, and 1494 km s<sup>-1</sup> for the tidal plume of NGC 3448 on the opposite side of the image from the companion. At the mean redshift distance of 2.8 Mpc ( $H = 50$ ) the projected linear separation of the Scd companion from NGC 3448 is small at 32 kpc.

The three prints here have been made from the same original Palomar plate, printed to different contrast and scale.

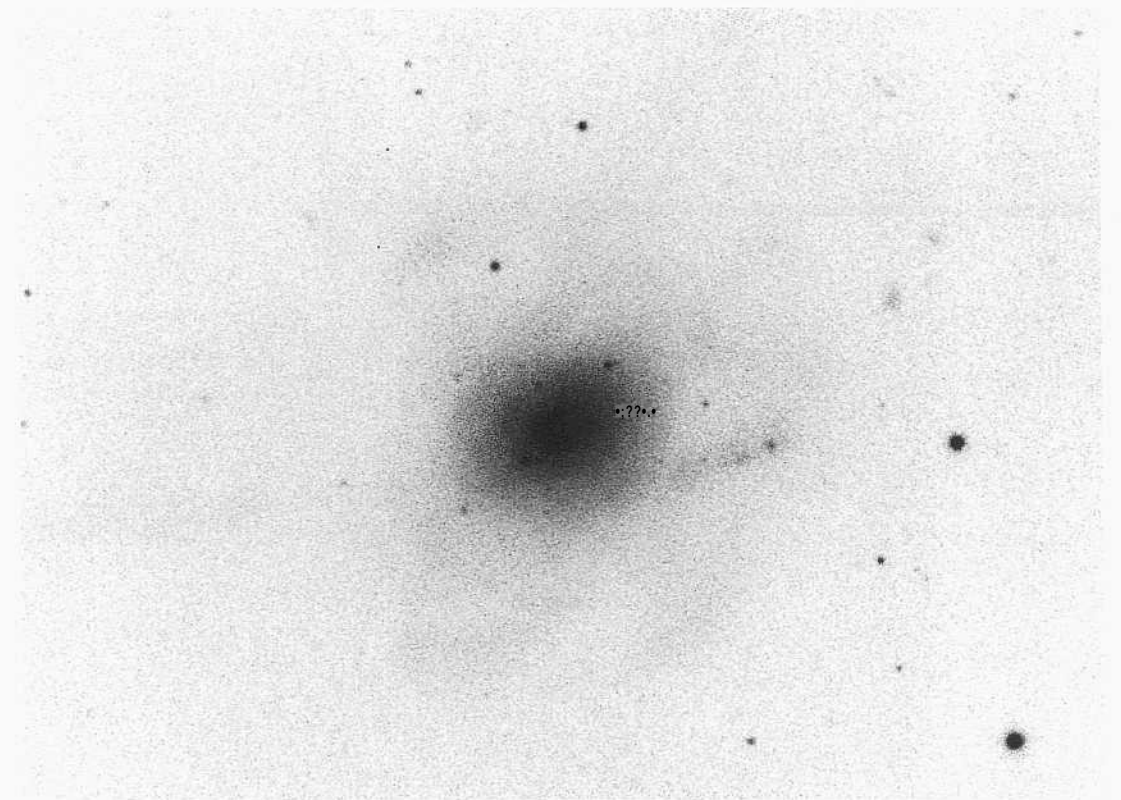
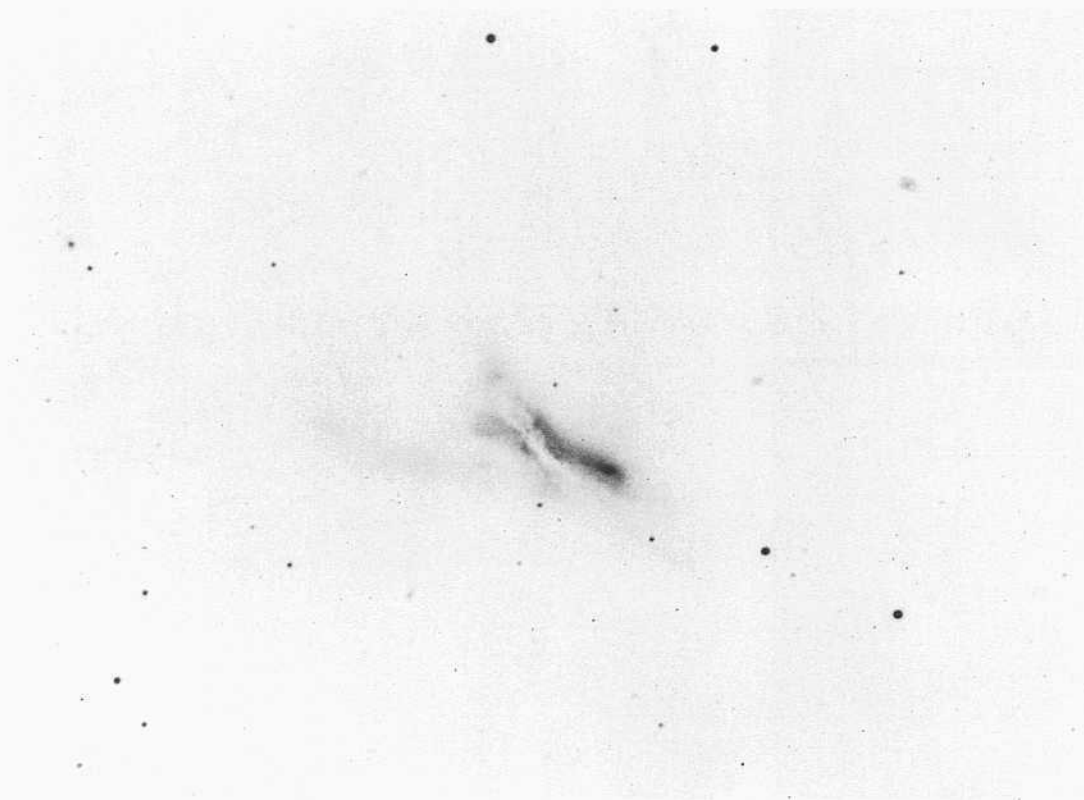
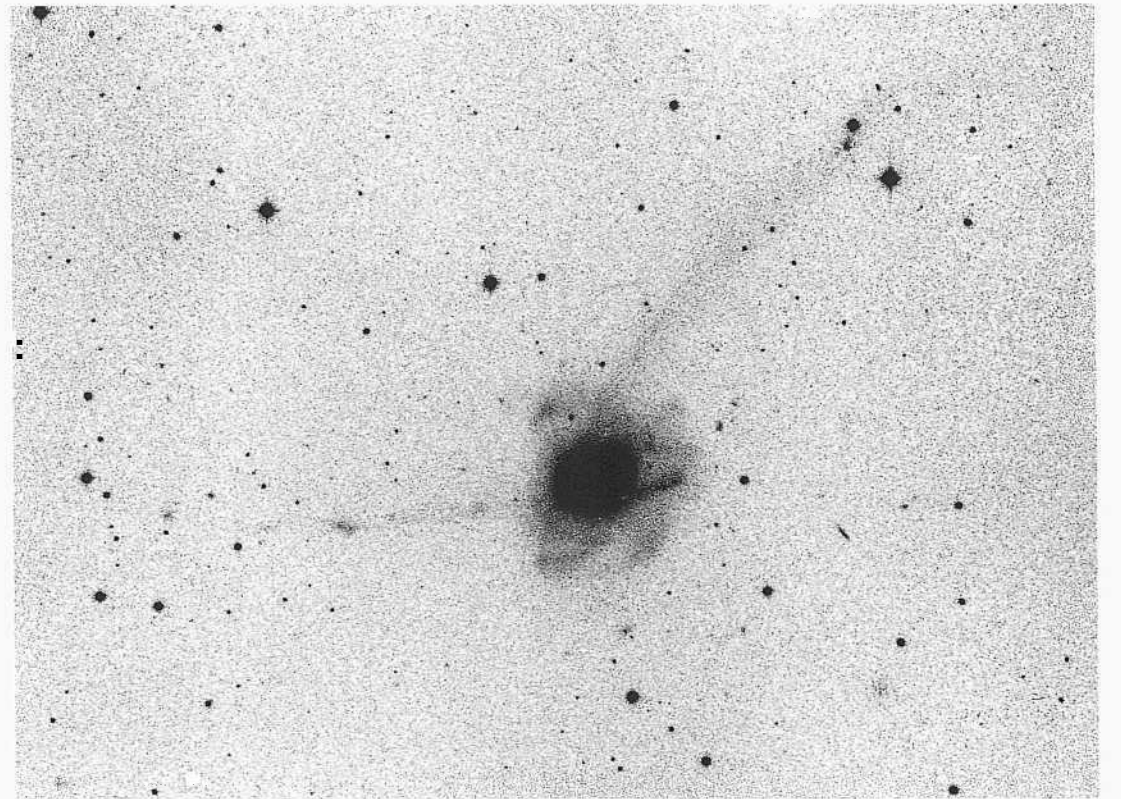
The plate was taken with a Racine wedge in the optical path. The bright stars have secondary images 5 mag fainter than the primary and are separated by 1.8" in a direction south and slightly east of the primary.



PANEL  
339



PANEL  
340



NGC 520      Amorphous      HA, p. 41  
 PH-176-H  
 Sep 3/4, 1953  
 103aD + GG11  
 40 min

The morphology of NGC 520 has always been described as unusual, not fitting into any of the morphological boxes of the standard classification sequence. Hubble (as reported by Pettit 1954) classified NGC 520 as Irr. Holmberg (1958) placed NGC 520 into his new Irr II class, based on the amorphous appearance of its luminous image, the absence of resolved stars, and its red color. These are the same features, along with the dust pattern similar to that in M82 (panels 333, 334) and NGC 3077 (panel 335), used in classifying the galaxy Amorphous here.

However, the faint plumes on opposite sides of the center suggest either tidal interaction or, following Toomre and Toomre (1972), the result of a merger, as in NGC 4038/4039 (panel 280).

Images of what may be individual stars appear in the main plume beginning at about  $B = 22.5$ . The redshift is  $v_o = 2350 \text{ km s}^{-1}$ . At the redshift distance of 47 Mpc ( $H = 50$ ,  $m - M = 33.4$ ), the absolute magnitude of such objects is bright, at  $M_B = -11$ .

NGC 520      Amorphous      HA, p. 41  
 H-1674-H  
 Nov 28/29, 1935  
 Imp. Eel.  
 60 min

The light print of NGC 520 made from a plate taken with the Mount Wilson Hooker 100-inch telescope shows no evidence for the double nucleus that might be expected from a recent merger, although some theories suggest that none need be expected. Based simply on the morphology of the image, the idea that a merger has occurred remains an unproved hypothesis.

NGC 7252      Merger or SO, pec  
 CD-1564-S/Br  
 Aug 9/10, 1980  
 103aO + GG385  
 4.5 min

NGC 7252, with its two principal long, thin plumes and its many shorter plumes near the main body, was originally suggested by Toomre and Toomre (1972) to be the product of a merger. Schweizer (1982, 1983) argued the case for a merger of two disk galaxies using data on surface brightness, spectroscopy, and internal kinematic structure. Dynamical interaction simulations by Borne and Richstone (1982, 1991) support this interpretation.

The heavy exposure in the top print with a wide view shows the principal plumes. These features are shown particularly well in the series of images by Schweizer (1982). Star formation (HH-region candidates) in each of the outer plumes is also suggested there.

NGC 7252      Merger or SOi pec  
 CD-1564-S/Br  
 Aug 9/10, 1980  
 103aO + GG385  
 4.5 min

This light print is made from the same original plate used for the heavy print above. The inner image shows an SO-like luminosity distribution, and the central core is clearly SO; there is an apparent break in the gradient of the profile two-thirds the way out the disk, giving the two-zone look characteristic of the SO class often discussed in the SO section.





## REFERENCES

- Abell, G. O. 1958, *Ap. J. Suppl.* 3, 211.
- Abies, H. D. 1971, *Pub. U. S. Naval Obs.* 20, part IV, 60.
- Andrews, P. J., and Evans, L. T. 1972, *M. N. R. A. S.* 759, 445.
- Arp, H. C. 1966, *Atlas of Peculiar Galaxies, Ap. J. Suppl.* 14, 1.
- Arp, H. C., and Sandage, A. 1985, *A. J.* 90, 1163.
- Athanassoula, E. 1984, *Phys. Reports* 114, 319.
- Baade, W. 1931, *Astron. Nachr.* 243, 303.
- Baade, W. 1944a, *Ap. J.* 100, 137.
- Baade, W. 1944b, *Ap. J.* 100, 147.
- Baade, W. 1951, *Publ. Univ. Michigan Obs.* 10, 7.
- Baade, W. 1963, in *Evolution of Stars and Galaxies* (Harvard Univ. Press), p. 15.
- Baade, W., and Minkowski, R. 1954, *Ap. J.* 119, 215.
- Baade, W., and Swope, H. H. 1963, *A. J.* 68, 435.
- Bacon, F. 1620, *Novuni Organum*, many editions.
- Baura, W. A. 1955, *Publ. A. S. P.* 67, 328.
- Bertola, F., and Galletta, G. 1978, *Ap. J. Lett.* 226, L115.
- Bertola, F., Galletta, G., and Zeilinger, W. W. 1985, *Ap. J. Lett.* 292, L51.
- Bertola, F., and Mallei, P. 1974, *Astron. Astrophys.* 32, 117.
- Binggeli, B., Sandage, A., and Tammann, G. A. 1985, *A. J.* 90, 1681.
- Binggeli, B., Sandage, A., and Tarengbi, M. 1984, *A. J.* 89, 64.
- Binggeli, B., Tammann, G. A., and Sandage, A. 1987, *A. J.* 94, 251.
- Binney, J. 1978, *M. N. R. A. S.* 183, 501.
- Blanco, V. M., Graham, T. A., Lasker, B. M., and Osmer, P. S. 1975, *Ap. J. Lett.* 198, L63.
- Borne, K. D., and Richstone, D. O. 1982, *Bull. A. A. S.* 14, 972.
- Borne, K. D., and Richstone, D. O. 1991, *Ap. J.* 369, 111.
- Börngen, F., Karachentseva, V. E., et al. 1982, *Astron. Nachr.* 303, 287.
- Börngen, F., and Karachentseva, V. E. 1982, *Astron. Nachr.* 303, 189.
- Börngen, F., Karachentseva, V. E., and Karachentsev, I. D. 1984, *Astron. Nachr.* 305, 53.
- Boroson, T. 1980, Ph.D. Thesis, Univ. of Arizona.
- Brosch, N. 1985, *Astron. Astrophys.* 153, 199.
- Burbidge, E. M., and Burbidge, G. R. 1959a, *Ap. J.* 129, 271.
- Burbidge, E. M., and Burbidge, G. R. 1959b, *Ap. J.* 130, 20.
- Burbidge, E. M., and Burbidge, G. R. 1960, *Ap. J.* 131, 224.
- Burbidge, E. M., and Burbidge, G. R. 1965, *Ap. J.* 142, 351.
- Burbidge, E. M., Burbidge, G. R., and Prendergast, K. H. 1961, *Ap. J.* 134, 236.
- Burbidge, E. M., Burbidge, G., and Rubin, V. C. 1964, *Ap. J.* 140, 942.
- Burbidge, G. R., Burbidge, E. M., and Sandage, A. 1963, *Rev. Mod. Phys.* 35, 947.
- Burkhead, M. S. 1980, in *Photometry, Kinematics, and Dynamics of Galaxies*, ed. D. S. Evans (Univ. of Texas Press, Austin), p. 143.
- Caldwell, N., and Bothun, G. D. 1987, *I. J.* 94, 1126.
- Campbell, W. V., and Paddock, J. F. 1911, *Publ. A. S. P.* 30, 68.
- Capaccioli, M. 1986, in *IAU Symposium 127. Structure and Dynamics of Elliptical Galaxies*, ed. T. de Zeeuw (Reidel, Dordrecht), p. 17.
- Chincarini, G., and Rood, H. J. 1971, *Ap. J.* 168, 321.
- Combes, A. 1978, *Astron. Astrophys.* 65, 17.
- Curtis, H. D. 1918, *Publ. Lick Obs.* 13, 29.
- de Vaucouleurs, G. 1950, *Ann. Astrophys.* 13, 362.
- de Vaucouleurs, G. 1955, *A. J.* 60, 126.
- de Vaucouleurs, G. 1956a, *Mem. of the Commonwealth Obs. (Mount Stromlo)*, 13.
- de Vaucouleurs, G. 1956b, in *Vistas in Astronomy*, vol. 2, ed. A. Beer (Pergamon Press), p. 1584.
- de Vaucouleurs, G. 1958, *Ap. J.* 127, 487.
- de Vaucouleurs, G. 1959a, *Ap. J.* 230, 718.
- de Vaucouleurs, G. 1959b, *Handbuch tier Physik* (Springer-Verlag, Berlin), p. 275.
- de Vaucouleurs, G. 1963, *Mem. R. A. S.* 611, I 1.
- de Vaucouleurs, G. 1975, in *Stars and Stellar Systems*, vol. 9, chap. 14, eds. A. Sandage, M. Sandage, and J. Kristian (Univ. of Chicago Press, Chicago), p. 557.
- de Vaucouleurs, G., de Vaucouleurs, A., and Niello, J. L. 1979, *A. J.* 84, 1811.
- de Vaucouleurs, G., de Vaucouleurs, A., and Pence, W. 1974, *Ap. J. Lett.* 191, L19.
- Dickens, R. (Currie, M. J.), and Lucey, J. R. 1986, *M. N. R. A. S.* 220, 679.
- Doyle, A. (1887, in *Beeton's Christmas An-nuitil* (Ward, Lock & Co., London, New York, Melbourne).
- Dressier, A. 1980, *Ap. J.* 236, 351.
- Dressier, A., and Sandage, A. 1983, *Ap. J.* 265, 664.
- Eddington, A. S. 1926, *The Internal Constitution of the Stars* (Cambridge Univ. Press, Cambridge), p. 16.
- Eggen, O. J., Lynden-Bell, D., and Sandage, A. 1962, *Ap. J.* 236, 748.
- Elmegreen, D. M. 1981, *Ap. J. Suppl.* 47, 229.
- Elmegreen, D. M., and Elmegreen, B. G. 1982, *M. N. R. A. S.* 201, 1021.
- Elmegreen, D. M., and Elmegreen, B. G. 1987, *Ap. J.* 314, 3.
- Elvius, A. 1962, *Lowell Obs. Bull.* 5, 281.
- Elvius, A. 1967, *A. J.* 72, 791.
- Elvius, A. 1969, *Loucll Obs. Hull.* 7, 117.
- Faber, S. M., and Gallagher, J. S. 1976, *Ap. J.* 204, 668.
- Ferguson, B. C. 1989, *A. J.* 89, 367.
- Ferguson, H. C., and Sandage, A. 1988, *A. J.* 96, 1520.
- Ferguson, H. C., and Sandage, A. 1990, *A. J.* 100, 1.
- Ferguson, H. C., and Sandage, A. 1991, *A. J.* 101, 765.
- Field, G. 1975, in *Stars and Stellar Systems*, vol. 9, chap. 10, eds. A. Sandage, M. Sandage, and J. Kristian (Univ. of Chicago Press, Chicago), p. 359.
- Ford, H. C., Jacoby, G. G., and Jenner, D. C. 1977, *Ap. J.* 223, 18.
- Freedraan, W. L. 1989, *A. J.* 98, 1285.

- Freedman, W., and Madore, B. 1988, *Ap. J. Lett.* 332, L63.
- Freeman, K. C. 1975, *IAU Symposium 69, Dynamics of Stellar Systems*, ed. A. Hayli (Reidel, Dordrecht), p. 367.
- Freeman, K. C., Illingworth, G., and Oemler, A. 1983, *Ap. J.* 272, 488.
- Gallagher, J. S., Knapp, G. R., Faber, S. M., and Balick, B. 1977, *Ap. J.* 275, 463.
- Gottesman, S. T., and Weliachew, L. 1975, *Ap. J.* 195, 23.
- Graham, J. A. 1979, *Ap. J.* 232, 60.
- Graham, J. A. 1984, *A. J.* 89, 1332.
- Hanes, D. A., and Harris, W. E. 1986, *Ap. J.* 309, 564.
- Harris, W. E. 1986, *A. J.* 91, 822.
- Harris, W. E. 1988, in *IAU Symposium 126, Globular Cluster Systems in Galaxies*, eds. J. E. Grindlay and A. G. Davis Philip (Reidel, Dordrecht), p. 237.
- Harris, W. E., and van den Bergh, S. 1981, *A. J.* 86, 1627.
- Harwarden, T. G., Elson, R. A. W., Longmore, A. J., Tritton, S. B., and Corwin, H. G. 1981, *M. N. R. A. S.* 196, 747.
- Herschel, W. 1785, *Phil. Trans.*, p. 213.
- Hoag, A. A. 1950, *A. J.* 55, 170.
- Hodge, P. W. 1963, *A. J.* 68, 691.
- Hodge, P. W., 1971, *Ann. Rev. Astron. Astrophys.* 9, 35.
- Hodge, P. W. 1973, *Ap. J.* 182, 671.
- Hodge, P. W. 1976, *A. J.* 81, 25.
- Hoessell, J. G., Abbott, M. J., Saha, A., Mossman, A. E., and Danielson, G. E. 1990, *A. J.* 100, 1151.
- Hoessell, J. G., and Danielson, G. E. 1984, *Ap. J.* 286, 159.
- Hoessell, J. G., and Mould, J. R. 1982, *Ap. J.* 254, 38.
- Hoessell, J. G., Schommer, R. A., and Danielson, G. E. 1983, *Ap. J.* 274, 577.
- Hoffman, G. L., Helou, G., Salpeter, E. E., Glosson, J., and Sandage, A. 1987, *Ap. J. Suppl.* 63, 247.
- Hoffman, G. L., Lewis, B. M., Helou, G., Salpeter, E. E., and Williams, H. L. 1989, *Ap. J. Suppl.* 69, 65.
- Hogg, D., Roberts, M. S., and Sandage, A. 1993, *A. J.* 106, in press (Sept issue).
- Hohl, F., and Zang, T. A. 1979, *A. J.* 84, 585.
- Holmberg, E. 1950, *Medd. Lunds Astron. Obs. II*, no. 128.
- Holmberg, E. 1958, *Medd. Lunds Astron. Obs. II*, no. 136.
- Holmberg, E. 1969, *Ark. Astron.* 5, 305.
- Hopp, U., and Materne, J. 1985, *Astron. Astrophys. Suppl.* 61, 93.
- Hoyle, F. 1954, *Ap. J. Suppl.* 1, 121.
- Hubble, E. 1922, *Ap. J.* 56, 162.
- Hubble, E. 1925, *Ap. J.* 62, 409.
- Hubble, E. 1926, *Ap. J.* 64, 321.
- Hubble, E. 1927, *Observatory* 50, 276.
- Hubble, E. 1929, *Proc. Nat. Acad. Sci. U. S. A.* 15, 169.
- Hubble, E. 1930, *Ap. J.* 71, 231.
- Hubble, E. 1932, *Ap. J.* 76, 44.
- Hubble, E. 1936a, *Ap. J.* 84, 158.
- Hubble, E. 1936b, *Realm of the Nebulae* (Yale Univ. Press, New Haven).
- Hubble, E. 1943, *Ap. J.* 97, 112.
- Hubble, E. 1949, *Publ. A. S. P.* 61, 121.
- Hubble, E., and Humason, M. L. 1931, *Ap. J.* 74, table 1, 43.
- Huchtmeier, W. K., and Richter, O. 1989, *A General Catalog of HI Observations of Galaxies* (Springer-Verlag, New York, Berlin).
- Huchtmeier, W. K., Seiradakis, J. H., and Materne, J. 1981, *Astron. Astrophys.* 102, 134.
- Humason, M. L. 1929, *Proc. Nat. Acad. Sci. U. S. A.* 15, 167.
- Humason, M. L., Mayall, N. U., and Sandage, A. 1956, *A. J.* 61, 97.
- Humphreys, R. M., and Sandage, A. 1980, *Ap. J. Suppl.* 44, 319.
- Huntley, J. M. 1978, *Ap. J.* 225, L101.
- Huntley, J. M. 1980, *Ap. J.* 238, 524.
- Huntley, J. M., Sanders, R. H., and Roberts, W. W. 1978, *Ap. J.* 221, 521.
- Hutchings, J. B., Neff, S. G., Stanford, S. A., Lo, E., and Unger, S. W. 1990, *A. J.* 100, 60.
- Illingworth, G. 1977, *Ap. J. Lett.* 218, L43.
- Jarvis, B. J. 1986, *A. J.* 91, 65.
- Jarvis, B. J., and Freeman, K. C. 1985, *Ap. J.* 295, 324.
- J Jeans, J. H. 1928, *Astronomy and Cosmogony* (Cambridge Univ. Press, Cambridge).
- Johnson, D. W., and Gottesman, S. T. 1983, *Ap. J.* 275, 549.
- Kahn, F. D., and Woltjer, L. 1959, *Ap. J.* 130, 705.
- Karachentsev, I. 1987, *Catalog of Binary Galaxies* (Moscow).
- Kayser, S. E. 1967, *A. J.* 72, 134.
- Kennicutt, R. C. 1981, *A. J.* 86, 1847.
- Kennicutt, R. C., and Edgar, B. K. 1986, *Ap. J.* 300, 132.
- Kinman, T. D. 1978, *A. J.* 83, 764.
- Kormendy, J. 1983, *Ap. J.* 275, 529.
- Kormendy, J. 1986, in *Nearly Normal Galaxies*, ed. S. M. Faber (Springer-Verlag, London), p. 163.
- Kormendy, J., and Illingworth, G. 1982, *Ap. J.* 256, 460.
- Kormendy, J., and Norman, C. A. 1979, *Ap. J.* 233, 539.
- Kraan-Korteweg, R. C., and Tammann, G. A. 1979, *Astron. Nachr.* 300, 181.
- Kronberg, P. P., Biermann, P., and Schwab, F. R. 1981, *Ap. J.* 246, 151.
- Kronberg, P. P., Emerson, D. T., Klein, U., and Wielebinski, R. 1979, *Ap. J. Lett.* 230, L149.
- Lewis, B. M. 1987, *Ap. J. Suppl.* 63, 515.
- Lindblad, B. 1951, *Publ. A. S. P.* 63, 133.
- Lucey, J. R., Currie, M. J., and Dickens, R. J. 1986, *M. N. R. A. S.* 222, 427.
- Lundmark, K. 1927, *Medd. Astr. Obs. Uppsala*, no. 30.
- Lynds, C. R. 1970, *Ap. J. Lett.* 159, L151.
- Lynds, C. R., and Sandage, A. 1963, *Ap. J.* 137, 1005.
- Lynds, C. R., and Toomre, A. 1976, *Ap. J.* 209, 382.
- Maia, M. A. G., da Costa, L. N., and Latham, D. W. 1989, *Ap. J. Suppl.* 69, 809.
- Malin, D. F. 1979, *Nature* 277, 279.
- Malin, D. F., and Carter, D. 1980, *Nature* 285, 643.
- Mathewson, D. S., Ford, V. L., and Visvanathan, N. 1986, *Ap. J.* 301, 664.
- Mathewson, D. S., Ford, V. L., and Visvanathan, N. 1988, *Ap. J.* 333, 617.
- Matthews, T. A., and Sandage, A. 1963, *Ap. J.* 138, 30.
- Mayall, N. U. 1935, *Publ. A. S. P.* 47, 319.
- Mayall, N. U., and Lindblad, P. O. 1970, *Astron. Astrophys.* 8, 364.
- Meurer, G. H., Freeman, K. C., and Dopita, M. A. 1988, *Astrophys. and Space Science* 156, 141.
- Meurer, G. H., Freeman, K. C., Dopita, M. A., and Cacciari, C. 1992, *A. J.* 103, 60.
- Miller, R. H., and Smith, B. F. 1979, *Ap. J.* 227, 785.
- Minkowski, R. 1957, in *IAU Symposium 4, Radio Astronomy*, ed. H. C. van de Hulst (Cambridge Univ. Press, Cambridge), p. 107.
- Mould, J., Kristian, J., and Da Costa, G. S. 1984, *Ap. J.* 278, 575.
- Murai, T., and Fujimoto, M. 1980, *Publ. Astr. Soc. Japan* 32, 581.
- Noerdlinger, P. D. 1979, *Ap. J.* 234, 802.
- O'Connell, R. W., and Mangano, J. J. 1978, *Ap. J.* 221, 62.
- O'Connell, R. W., Scargle, J. D., and Sargent, W. W. 1974, *Ap. J.* 191, 61.
- Oemler, A. 1976, *Ap. J.* 209, 693.
- Osterbrock, D. O. 1960, *Ap. J.* 132, 325.
- Palumbo, G. G. C., Tanzella-Nitti, G., and Vettolani, G. 1983, *Catalog of Radial Velocities of Galaxies* (Gordon and Breach Science Publishers).
- Pease, F. 1917, *Ap. J.* 47, 24.

- Pease, F. 1920, *Ap. J.* 51, 276.
- Penston, M. V., Fosbury, R. A. E., Ward, M. J., and Wilson, A. S. 1977, *M. N. R. A. S.* 180, 19.
- Peterson, C. J., and Huntley, J. M. 1980, *Ap. J.* 242, 913.
- Pettit, E. 1954, *Ap. J.* 120, 413.
- Poe, E. A. 1849, *Eureka*, many eds.
- Prendergast, K. 1962, in *Interstellar Matter in Galaxies*, ed. L. Woltjer (W. A. Benjamin, New York), p. 217.
- Prendergast, K. H. 1983, in *IAU Symposium 100, Internal Kinematics and Dynamics of Galaxies*, ed. E. Athanassoula (Reidel, Dordrecht), p. 215.
- Price, J. S., and Grasdalen, G. L. 1983, *Ap. J.* 275, 559.
- Quinn, P. J. 1984, *Ap. J.* 279, 596.
- Radnitzky, G. 1973, *Contemporary Schools of Metascience* (Henry Regnery Co., Chicago), p. 215.
- Reaves, G. 1956, *A. J.* 61, 69.
- Reif, K., Mebold, U., Goss, W. M., van Woerden, EL, and Siegman, B. 1982, *Astron. Astrophys. Suppl.* 50, 451.
- Reynolds, J. H. 1927a, *Observatory* 50, 185.
- Reynolds, J. H. 1927b, *Observatory* 50, 308.
- Richter, O., and Huchtmeier, W. K. 1983, *Astron. Astrophys.* 125, 187.
- Richter, O., Materne, J., and Huchtmeier, W. K. 1982, *Astron. Astrophys.* 111, 193.
- Ritchey, G. W. 1910, *Ap. J.* 32, 26.
- Roberts, M. S. 1963 *Ann. Rev. Astron. Astrophys.* 1, 149.
- Roberts, M. S. 1969, *A. J.* 74, 859.
- Roberts, M. S. 1975, in *Galaxies and the Universe*, chap. 9, eds. A. Sandage, M. Sandage, and J. Kristian (Univ. of Chicago Press, Chicago).
- Roberts, W. W., Huntley, J. M., and van Albada, G. D. 1979, *Ap. J.* 233, 67.
- Rogers, A. W. 1978, *Ap. J. Lett.* 219, L7.
- Rogstad, D. II., Wright, M. C. H., and Lockhart, I. A. 1976, *Ap. J.* 204, 703.
- Rubin, V. C., Burstein, D., Ford, W. K., and Thonnard, N. 1985, *Ap. J.* 289, 81.
- Saha, A., and Hoessel, J. G. 1987, *A. J.* 94, 1556.
- Saha, A., and Hoessel, J. G. 1990, *A. J.* 99, 97.
- Sandage, A. 1957, *Ap. J.* 125, 422.
- Sandage, A. 1961, *The Hubble Atlas of Galaxies* (Carnegie Institution of Washington, Washington, D. C.), **Publ.** 618.
- Sandage, A. 1962, *Ap. J.* 136, 319.
- Sandage, A. 1972, *Ap. J.* 178, 25.
- Sandage, A. 1975a, in *Galaxies and the Universe*, chap. 1, eds. A. Sandage, M. Sandage, and J. Kristian (Univ. of Chicago Press, Chicago).
- Sandage, A. 1975b, *Ap. J.* 202, 563.
- Sandage, A. 1976, *A. J.* 81, 954.
- Sandage, A. 1978, *A. J.* 83, 904.
- Sandage, A. 1983a, in *IAU Symposium 100, Internal Kinematics and Dynamics of Galaxies*, ed. E. Athanassoula (Reidel, Dordrecht), p. 367.
- Sandage, A. 1983b, *A. J.* 88, 1569.
- Sandage, A. 1984a, *A. J.* 89, 621.
- Sandage, A. 1984b, *A. J.* 89, 630.
- Sandage, A. 1986a, *Ap. J.* 307, 1.
- Sandage, A. 1986b, *A. J.* 91, 496.
- Sandage, A. 1986c, *Ann. Rev. Astron. Astrophys.* 24, 421.
- Sandage, A. 1986d, *Astron. Astrophys.* 161, 89.
- Sandage, A. 1990, *J. Roy. Astron. Soc. Canada* 84, 70.
- Sandage, A., and Binggeli, B. 1984, *A. J.* 89, 919.
- Sandage, A., Binggeli, B., and Tammann, G. A. 1985a, *A. J.* 90, 395.
- Sandage, A., Binggeli, B., and Tammann, G. A. 1985b, *A. J.* 90, 1759.
- Sandage, A., and Brucato, R. 1979, *A. J.* 84, 472.
- Sandage, A., and Carlson, G. 1982, *Ap. J.* 258, 439.
- Samalage, A., and Carlson, G. 1985, *A. J.* 90, 1019.
- Sandage, A., and Carlson, G. 1988, *A. J.* 96, 1599.
- Sandage, A., and Fomalont, E. 1993, *Ap. J.* 407, 14.
- Sandage, A., and Fouts, G. 1987, *A. J.* 93, 74.
- Sandage, A., Freeman, K. C., and Stokes, N. R. 1970, *Ap. J.* 760, 831.
- Sandage, A., and Hoffman, G. L. 1991, *Ap. J. Lett.* 379, L45.
- Sandage, A., and Humphreys, R. M. 1980, *Ap. J. Lett.* 236, L1.
- Sandage, A., and Miller, W. C. 1964, *Science* 144, 382.
- Sandage, A., and Perelmutler, J.-M. 1990, *Ap. J.* 361, 1.
- Sandage, A., and Tammann, G. A. 1974a, *Ap. J.* 190, 525.
- Sandage, A., and Tammann, G. A. 1974b, *Ap. J.* 191, 603.
- Sandage, A., and Tammann, G. A. 1974c, *Ap. J.* 194, 223.
- Sandage, A., and Tammann, G. A. 1974d, *Ap. J.* 194, 559.
- Sandage, A., and Tammann, G. A. 1975a, *Ap. J.* 196, 313.
- Sandage, A., and Tammann, G. A. 1975b, *Ap. J.* 197, 265.
- Sandage, A., and Tammann, G. A. 1976a, *Ap. J. Lett.* 207, L1.
- Sandage, A., and Tammann, G. A. 1976b, *Ap. J.* 210, 7.
- Sandage, A., and Tammann, G. A. 1981, *A Revised Shapley-Ames Catalog of Bright Galaxies* (Carnegie Institution of Washington, Washington, D. C.), **Publ.** 635, 1st ed.
- Sandage, A., and Tammann, G. A. 1982, *Ap. J.* 256, 339.
- Sandage, A., and Tammann, G. A. 1985, in *Supernovae as Distance Indicators*, ed. N. Bartel (Springer, Berlin), p. 1.
- Sandage, A., and Tammann, G. A. 1987, *A Revised Shapley-Ames Catalog of Bright Galaxies* (Carnegie Institution of Washington, Washington, D. C.), **Publ.** 635, 2nd ed.
- Sandage, A., and Tammann, C. A. 1990, *Ap. J.* 365, 1.
- Sandage, A., and Visvanathan, N. 1967, *Ap. J.* 157, 1065.
- Sandage, A., and Visvanathan, N. 1978a, *Ap. J.* 223, 707.
- Sandage, A., and Visvanathan, N. 1978b, *Ap. J.* 227, 742.
- Sargent, W. L. W., Kowal, S. T., Hartwick, F. D. A., and van den Bergh, S. 1977, *A. J.* 82, 947.
- Schechter, P. L., and Gunn, J. E. 1978, *A. J.* 83, 1360.
- Schwarzschild, M. 1982, *Ap. J.* 263, 599.
- Schweizer, F. 1977, in *IAU Symposium 77, Structure and Properties of Nearby Galaxies*, eds. E. M. Berkhuijsen and R. Wielebinski (Reidel, Dordrecht), p. 279.
- Schweizer, F. 1980, *Ap. J.* 237, 303.
- Schweizer, F. 1981, *Ap. J.* 246, 722.
- Schweizer, F. 1982, *Ap. J.* 252, 455.
- Schweizer, F. 1983, in *IAU Symposium 100, Internal Kinematics and Dynamics of Galaxies*, ed. E. Athanassoula (Reidel, Dordrecht), p. 319.
- Schweizer, F. 1986, *Science* 231, 193.
- Schweizer, F., Ford, W. K., Jedrzejewski, R., and Giovanelli, R. 1987, *Ap. J.* 320, 454.
- Schweizer, F. and Seitzer, P. 1988, *Ap. J.* 328, 88.
- Schweizer, F., Whitmore, B. C. and Rubin, V. C. 1983, *A. J.* 88, 909.
- Searle, L., and Zinn, R. 1978, *Ap. J.* 225, 357.
- Sersic, J. L. 1958, *Observatory* 78, 125.
- Sersic, J. L. 1967, *Zsf. Ap.* 67, 306.
- Sersic, J. L., and Pastoriza, M. 1965, *Publ. A. S. P.* 77, 287.
- Seyfert, K. 1913, *Ap. J.* 97, 28.
- Shapley, H. 1950, *Publ. Univ. Michigan Obs.* 10, 79.

- Shapley, H. and Ames, A. 1932. *Annals of the Harvard College Observatory* 88. No. 2.
- Shapley, H., and Paraskevopoulos, J. S. 1940, *Proc. Nat. Acad. Sci. U. S. A.* 26. 31.
- Shaya, E. J. 1984, *Ap. J.* 280. 470.
- Shobbrook, R. R. 1966. *M. N. R. A. S.* 131, 365.
- Silva, D. R., Boroson, T. A., and Thompson. I. B. 1989. *A. J.* 98. 131.
- Simonson, G. F. 1982, Ph.D. Thesis, Yale University-
- Smith, S. 1935, *Ap. J.* 82. 192.
- Spitzer, L., and Baade, W. 1951. *Ap. J.* 113. 413.
- Steiman-Cameron, T. Y., and Durisen. R. 11. 1982, *Ap. J. Lett.* 263. LSI.
- Steiman-Cameron, T. Y., Kormendy, J., and Durisen, R. M. 1992. *A. J.* 104. 1339.
- Tammann, G. A. 1973. in *Supernovae and Supernova Remnants*, ed. C. B. Cosmovici (Reidel, Dordrecht), p. 215.
- Tammann, G. A., and Leiundgut, B. 1990. *Astron. Astrophys.* 236. 9.
- Tammann, G. A., and Sandage, A. 1968. *Ap. J.* 151.82 5.
- Tammann, G. A., and Sandage, A. 1985, *Ap. J.* 294.81.
- ten Bruggencate, P. 1930. *Is. f. Ap.* 7.275.
- Theys, I. J. C., and Spiegel, E. A. 1976. *A. J.* 208. 650.
- Theys, I. J. C., and Spiegel, E. A. 1977. *Ap. J.* 212.616.
- Tonry, J. L., and Schechter, P. L. 1991. *A. J.* 100.1794.
- Toomre, A. 1977. in *The Evolution of Galaxies and Stellar Populations*, eds. B. M. Tinsley and R. B. Larson (Yale Univ. Observatory), p. 401.
- Toomre, A., and Toomre, J. 1972, *Ap. J.* 178. 623.
- Tubbs, A. D. 1980, *Ap. J.* 241.969.
- Ulrich, M. 1975. *Publ. A. S. P.* 7. 965.
- Usher, P. 1980. *The Astronomy Quarterly* 3. 115.
- van Albada, T. S., Kotanyi, C. G., and Schwarzschild, M. 1982, *M. N. R.A.S.* 198. 303.
- van den Bergh, S. 1959. *Publ. David Dunlop Obs. II*, 147.
- van den Bergh, S. 1960a, *Publ. David Dunlop Obs. II*. no. 6.
- van den Bergh, S. 1960b, *Ap. J.* 131. 215.
- van den Bergh, S. 1960c, *Ap. J.* 131. 558.
- van den Bergh, S. 1976a. *Ap. J.* 206. 883.
- van den Bergh, S. 1976b. *Ap. J.* 208. 673.
- van den Bergh, S. 1989. *Publ. A. S. P.* 101, 1072.
- van der Kruit, P. 1986, *Astron. Astrophys.* 157. 230.
- van der Kruit, P. C and Searle, L. 1981, *Astron. Astrophys.* 95. 116.
- van der Kruit, P., and Searle, L. 1982, *Astron. Astrophys.* 110.19.
- van Houten, C. J. 1961. *Bull. Astr. Inst. Netherlands* 16.1.
- Varnas, S. R., Bertola, F., Galletta, G. F., Freeman, K. C., and Carter, D. 1987, *Ap. J.* 313.69.
- Visvanathan, N., and Sandage, A. 1972. *Ap. J.* 176.57.
- Vorontsov-Velyaminov, B. A., Krasnogorskaja, A., and Arkipova, V. 1962, 1963, 1964, 1968, *Morphological Catalog of Galaxies*.
- Vorontsov-Velyaminov, B. A. 1977, *Astron. Astrophys. Suppl.* 28. 1.
- Vorontsov-Velyaminov, B. A. 1987, *Extragalactic Astronomy*, trans. R. B. Rodman (Harwood Academic Publishers).
- Welch, G. A., Chincarini, G., and Rood. H. J. 1975. *A. J.* 80. 77.
- Weliachew, L., Sancisi, R., and Guélin, M. 1978. *Astron. Astrophys.* 65. 37.
- Whitmore, B. C., and Bell, M. 1988, *Ap. J.* 324. 741.
- Woltjer, L. 1959. *Ap. J.* 130. 38.
- Wolf, M. 1908, *Publ. Ap. Inst. König. Heidelberg*, vol. 3, no. 5.
- Yahil, A., Tammann, G. A., and Sandage, A. 1977, *Ap. J.* 227. 903.
- Zinnecker, H., and Cannon, R. D. 1985, in *Star Forming Dwarf Galaxies*, eds. D. Kunth, T. X. Thuan, and J. Trail Thanh Van (Frontières, Paris), p. 164.
- Zwicky, F. 1942, *Phys. Rev.* 61. 489.
- Zwicky, F. 1955, *Publ. A. S. P.* 67. 232.



NAME	PANEL	TYPE	NAME	PANEL	TYPE	NAME	PANEL	TYPE	NAME	PANEL	TYPE
NGC 108 7	2 79	Sc(s)III.3	NGC 1400	43	S0 <sub>3</sub> (1)	NGC 1800	3 38	Amorph	NGC 2681	62, 87	Sa
NGC 1090	2 96	SBc(s)I.8	NGC 1404	5	E2	NGC 1808	193	She pec	NGC 2683	1 49	SI(nearly on edge)
NGC 109 7	201	RSBbc(s)I-n	NGC 1406	291	Sc	NGC 1832	160	SBb(r)I	NGC 2685	45	SO3(7) pec
NGC 1 156	326	SmIV	NGC 1411	40	SO2(4)	NGC 1947	45	SO 3(0) pec	NGC 2693	22	E2
NGC 1 169	96.106.S9	<b>SBa(r)</b>	NGC 1415	77	Sa/SBa(ate)	NGC 1961	137	Sb(rs)II pec	NGC 2701	271	Sc(s)II-III
NGC 1 172	31	SO i (0.3)	NGC 1417	128	Sb(s)I.3	NGC 1964	131	Sb(s)I-II	NGC 2712	165	SBb(s)I-II
NGC 1175	40	S0 <sub>2</sub> (8)	NGC 1421	291	Sc	NGC2082	270	Sc(s)II-III	NGC 2713	174	Sbc(s)I
NGC 1179	2 95	SBc(r)II.2	NGC 1425	139	Sb(r)II	NGC 2090	250, 257	Sc(s)II	NGC 2715	246	Sc(s)II
NGC 1 187	182	Sbc(s)II	NGC 1433	158.169.1 70	SBb(s)I-II	NGC 2139	312	SBc	NGC2732	36	S0i(8)
NGC 1199	22	E2	NGC 1437	254	Sc(s)II	NGC 2146	146	SbII pec	NGC 2742	250	Sc(rs)II
NGC 1201	3 3	SO!(6)	NGC 1440	5 7	SBOj/2/a	NGC2179	64	Sa	NGC 2748	288	Sc(s)II
NGC 1209	13	E6	NGC 1448	287	Sc(s)II	NGC 2188	3 19	Scd/SBcd	NGC 2749	8	E3
NGC 1232	2 1 6. S13	Sc(rs)I	NGC 1452	97.107	SBa(r)	NGC 2196	111	Sab(s)I	NGC 2763	243	Sc(s)II
NGC 1232A2	16	SBmIII	NGC 1453	2	E0	NGC 2207	214	Sc(s)I.2	NGC2764	145.195	Amorph or Sli pec
NGC 1241	2 06	SBbc(rs)I.2	NGC 1461	40	S0i/2(7)	NGC 2217	101, 104, 107	SBa(s)	NGC 2768	38, 53	S0i/2(6)
NGC 1249	3 11	SBc	NGC 1493	308	SBc	NGC 222 3	2 05	<b>SBbc(r)I.3</b>	NGC2775	78.87, S12	Sa(r)
NGC 125 5	250	Sc(s)II	NGC 1494	315	Scd/SBcd	NGC 2268	188	Sbc(s)II	NGC 2776	221	Sc(rs)I
NGC 1275	24	E pec	NGC 1507	318	Scd/SBcd	NGC 227 6	2 63	Sc(r)II-III	NGC 2781	67	Sa(r)
NGC 12 88	134	Sb(r)I-II	NGC 1511	292	Sc pec or Amorph?	NGC 2280	22 1	Sc(s)I.2	NGC 2782	82	Sa(s) pec
NGC 1291	100.102.S8	SBa	NGC 1512	161	SBb(rs)I pec	NGC 2300	6	E3	NGC 2784	32	S0i(0,4)
NGC 1292	249	<b>Sc(s)II</b>	NGC 1515	139	<b>Sb(s)II</b>	NGC 2310	42	S0 <sub>2/3</sub> (8)	NGC 2787	57, 95	SBO/a
NGC 129 7	42	S0 <sub>2/3</sub> (0)	NGC 1518	272	ScIII	NGC 2314	8	E3	NGC 2793	252	Sell pec
NGC 1300	154.S8	SBb(s)I.2	NGC 1521	8	E3	NGC 232 5	9	E	NGC 2798	105	SBa(s) tides
NGC 1302	70	Sa	NGC 1527	40	S0 <sub>2</sub> (6)	NGC 232 5	10	E4	NGC 281 1	6 5	Sa
NGC 1309	255	Sc(s)II	NGC 1531	197,337	Amorph	NGC 233 6	204, S13	<b>SBbc(r)I</b>	NGC 2815	131	Sb(s)I-II
NGC 1313	3 09	SBc	NGC 1532	197	Sbc(s)(tides?)	NGC 2339	299	SBc(s)II	NGC 2832	22	E3 (tides)
NGC 1316	7 3	Sa pec (ripples)	NGC 1533	90	SB0 <sub>2</sub> (2)/SBa	NGC 2347	186	Sbc(r)I-II	NGC 2835	2 96	SBc(rs)I.2
NGC 1317	62.S12	Sals)	NGC 1536	313	SBc	NGC 2366	327	SBmIV-V	NGC 2841	142.S4.S12	Sb
NGC 1325	141	Sb(s)II	NGC 1537	13	E6	NGC 2369	178	Sbc(s)I pec	NGC 2844	77	Sa(r)
NGC 1326	100	RSBa	NGC 1543	100.102	RSB0 <sub>2/3</sub> (0)/a)	NGC 2397	279	Sc(s)III	NGC 2848	2 44	Sc(s)II
NGC 1332	34	S0i(6)	NGC 1546	273	Sc(s)III	NGC 2403	273	Sc(s)III	NGC 2851	43	SO <sub>3</sub> /Sa
NGC 133 7	231	Sc(s)I-II	NGC 1549	5, S1	E2	NGC 242 7	269	Sc(s)II-III	NGC 2855	73, 74	Sa(r)
NGC 1339	10	E4	NGC 1553	39	SO i/2(5) pec	NGC 2434	1	E0	NGC 2859	58, S7	RSB0 <sub>2</sub> (3)
NGC 1341	304	SBc(s)II-III	NGC 1559	299	SBc(s)II.2	NGC 2441	227	Sc(r)I-II	NGC 2865	10	E4 (SO?)
NGC 1344	28	E5/S0](5)	NGC 1566	171,S5	Sbc(s)I.2	NGC 2442	207	SBbc(rs)II	NGC 2880	54	SBOi
NGC 1350	71, 88, S3	Sa(r)	NGC 1569	3 36	SmIV/Amorph	NGC 2460	111, 145, S3	Sab(s)	NGC 2888	6	E2 (SO?)
NGC 1351	28	E6/S0](6)	NGC 1574	56, S7	SB0 <sub>2</sub> (3)	NGC 2500	262	Sc(s)II.8	NGC 2889	135	Sb(r)II
NGC 1353	190	Sbc(r)II	NGC 1596	51	S0i(7)	NGC2523	160	SBb(r)I	NGC 2902	30	S0i(0)
NGC 135 7	68	Sa	NGC 1602	51,328	SBm	NGC 252 5	298, S10	SBc(s)II	NGC 2903	226	Sc(s)I-II
NGC 1358	100.107.S8	SBa(s)I	NGC 1617	79, 87	Sa(s)	NGC 253 7	275	ScIII pec	NGC 2907	48	SO3(6) pec
NGC 1359	271	<b>Sc(s)II-III</b>	NGC 1625	186	Sbc(s)I-II	NGC 2541	2 64	Sc(s)III	NGC 2911	49	SO3(2) or SO pec
NGC 1365	199.S8	SBbc(s)I	NGC 1637	3 06	SBc(s)II.3	NGC 2545	203	SBbc(r)I-II	NGC 2924	21	E0
NGC 1366	28	S0!(7)/E7	NGC 1638	7 3	Sa	NGC 2549	40	S0 <sub>1/2</sub> (7)	NGC2935	155	SBb(s)I.2
NGC 1371	<b>64, 80.88.S3</b>	Sa(s)	NGC 1640	206	SBbc(r)I-II	NGC 2551	134	Sb(r)I-II	NGC 2942	214	Sc(s)I.3
NGC 1376	221	Sc(s)I	NGC 1659	2 63	Sc(s)II-III	NGC 2552	322	Sd/SBd	NGC 2950	5 7	RSB02/3
NGC 13 79	2	E0	NGC 1667	234	Sc(r)I-II	NGC 2608	183	Sbc(s)II	NGC 295 5	215	Sc(s)I
NGC 1380	61	S03(7)/Sa	NGC 1672	136	Sb(rs)II	NGC 2613	139, S4	<b>Sb(s)II</b>	NGC 2962	93	RSB0 <sub>2</sub> /Sa
NGC 138 1	3 7.50	S0 <sub>x</sub> (8)	NGC 1688	299	SBc(s)II	NGC 2633	155	SBb(s)I.3	NGC 2964	240,251	Sc(s)If.2
NGC 138 5	308	SBc	NGC 1700	8	E3	NGC 2639	77	Sa	NGC 2967	230	Sc(rs)I-II
NGC 1386	76, S14	Sa	NGC 1705	3 35	Amorph	NGC 2642	163	<b>SBb(rs)I-II</b>	NGC 2968	49,337	Amorph or SO3
NGC 138 7	5 6	SB0 <sub>2</sub> pec	NGC 1726	27	E4/S0 <sub>2</sub> (4)	NGC 2646	5 6	SB0 <sub>2</sub>	NCC 2974	9	E4
NGC 1389	3 5	S0i(5)/SB0!	NGC 1744	3 16	Scd/SBcd	NGC 2654	114	Sab:	NGC 2976	317	Scd/SBcd
NGC 1395	5	E2	NGC 1784	210	SBbc(r)II	NGC 265 5	62	Sa pec	NGC 2983	9 5	SBa
NGC 1398	12 0.121	SBab (r)I	NGC 1792	2 55	Sc(s)II	NGC 2672	22	E2 (tides)	NGC 2985	111	Sab(s)
NGC 1399	19	E1	NGC 1796	313	SBc	NGC 2673	22	E0 (tides)	NGC 2986	5	E2



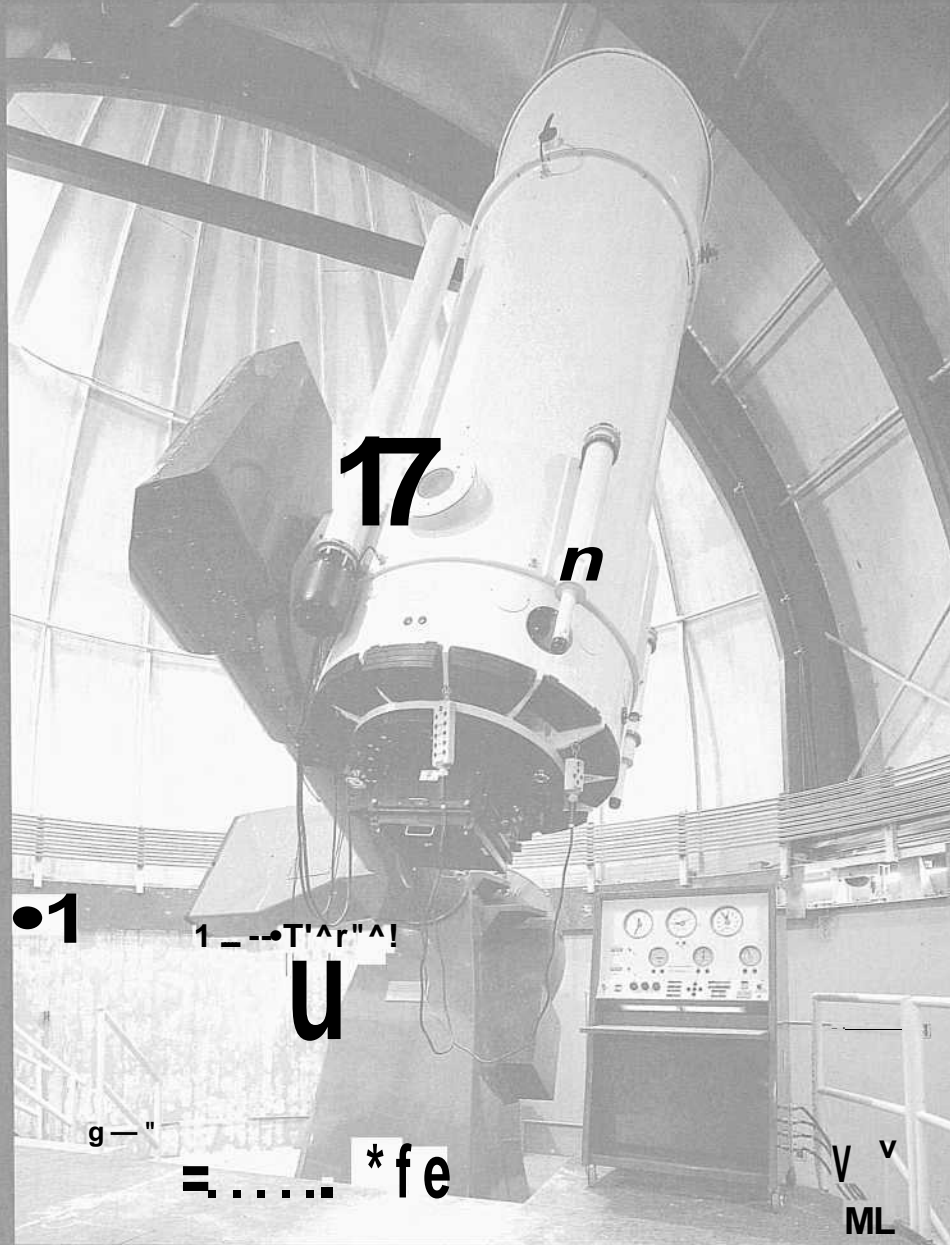


NAME	PANEL	TYPE	NAME	PANEL	TYPE	NAME	PANEL	TYPE	NAME	PANEL	TYPE
NGC 4008	33	SO i(5)	NGC 4234	3 10	SBc	NGC4395	324 . S6	ScIII-IV	NGC 4559	247	Sc(s)II
NGC4013	19-1	SL:-:	NGC4235	76	Sa	NGC 4406	27	SOi(3)/E3	NGC 4564	13. S1	E6
NGC. 4024	31	SOi(2.5.2.1	NGC 4236	324. S10	SBdIV	NGC 4412	201	SBbc(s)I-II pec	NGC 4567	281	Sc(s)II-III
NGC 4026	50	SOi/2(9)	NGC 4237	246	Sc(r)II.2	NCC 4414	254	Sc(sr)II.2	NGC 4568	281	Sc(s)II-III
NGC4027	252	Sc(s)II.2	NGC 4242	322	Sd/SBd	NCC 4417	47	SOx(7)	NGC4569	109	Sab(s)I-H
NGC. 4033	35	SO i(fi)	NCC 4244	3 19	Scd/SBcd	NGC4419	86. 114	Sa(dust only)	NGC 4570	29	SO,(7)/E7
NGC 4036	60	SO3(8)/Sa	NGC 4245	95	SBa(s)	NGC 4420	274	Sc(s)III	NGC 4571	260	Sc(s)II-III
NGC 4038	280	Sc(tid.-<)	NGC 4251	36. S2	SOi(8)	NGC 4424	60	S(a?) pec	NGC 4578	38	SO]2(4)
NGC 4039	280	Sc(tides)	NGC 4254	224	Sc(s)1.3	NGC 4425	57. 60	SBO pec or Sa	NGC 4579	108	Sab(s)II
NGC 4041	268	Sc(s)II-III	NGC 4256	150	Sb(s)	NGC 4428	265	Se(s)11.3	NGC 4580	86.276	Sc(s)/Sa
NGC 4047	232	Sc(s)I-I]	NGC4258	135	Sb(s)II	NGC 4429	60. S2	SO3(6)/Sa	NGC 4580	276	Sc
NGC 4050	131	SL<.-)I-I]	NGC 4260	94	SBa(s)	NCC 4433	194	SbcIII	NGC 4586	76	Sa
NGC 4051	180	S1,c(t)II	NGC4261	6	E3	NGC 4435	56. 153	SB0](7)	NGC 4589	6	E2
NGC 4062	265	S.-sIII-III	NGC4262	56	SBOi	NGC 4438	56. 153	Sli(tides)	NGC 4592	319	Scd/SBcd
NGC 4064	313	SBc	NGC4267	54	SB01	NGC 4442	55	SBO 1(6)	NGC 4593	165	SBb(rs)I-II
NGC 4073	12	E5	NGC 4270	35	SO!(6)	NGC 4448	69	Sa(late)	NGC 4594	113.S11	Sa+/Sb"
NGC 4085	291	ScIII:	NCC 4273	3 10	SBc	NCC 4449	326. S6	SmIV	NGC 4595	265	Se(s)II-III
NGC 4088	271	Sc(s)II-III/SBc	NGC 4274	66.88	Sa(sr)	NGC 4450	110. S14	Sal, pec	NGC4596	101	SBa(very early)
NGC 4094	189	Sbc(s)I]	NGC4278	20	E1	NGC 4452	36	SOjI(O)	NGC 4597	304	SBc(r)III:
NGC 4096	287	SO3(s)H	NCC4281	44	SO3(6)	NGC 4454	67	Sa	NCC 4602	229	Sc(i-)-1-11
NGC 4100	229	Sc(s)I-II	NGC4283	2	EO	NGC 4457	138	RSb(s)II	NGC 4603	176	Sbc(s)I-II
NGC 4102	140	Sb(r)1.....<	NGC 4283	20	EO	NGC 4459	43	SO3(3)	NGC 4605	292	Sc(s)III
NGC 4105	56. 105	SOi/2(3)	NGC4286	20	dE.N/Im	NGC 4460	36	SO/Sc:	NGC 4608	97	SBO3/a
NGC4106	56.105	SBO/a(tides)	NGC 4293	59	Sa	NGC 4461	61	Sa	NGC4612	57	RSBO1/2
NGC -1111	47. 53	SO2(91	NGC 4294	310	SBc	NGC 4462	123	SBab(s)I-II	NGC 4618	212	SBI)c(rs)II.2
NGC 4116	306	SBc(r)II-III	NGC 4298	279.289	Sc(s)III	NGC 4469	114	Sab(on edge)	NCC 4621	12. 32	E5
NGC 4123	201.S8	SBbc(rs)I.8	NCC 4299	328	SdU)III	NGC 4472	18. 26	E1/SOj d)	NCC 4623	13. S1	E7
NGC 4121	44	802(1-116)	NGC 4302	289	Sc(on edge)	NGC 4473	11	E5	NCC 4625	275	Sc(s)II-II] pec
NGC4 125	28	E6/SO 1/2(6)	NGC 4303	213	Sc(s)1.2	NGC 4474	37	SO1(8)	NGC 4627	290	dE5.N
NGC 4128	35	SOi(6)	NGC4304	208	SBbc(s)II	NGC 4476	11.12	E5 pec(dust);SO3(5)	NGC 4630	275	Sc(s)III
NGC 4129	291	Sc(s)II	NGC 4307	150	SD)	NGC 4477	90	SBOi/2/SBa	NGC4631	290	Se(on edge)
NGC 4136	230	Sc(r)I-II	NCC 4314	95. 106	SBa(rs) pec	NGC 4478	6	E2	NCC4632	288	Sc(s)IL3
NGC 4138	74	Sa(r)	NGC 4321	213	Sc(s)I	NGC 4483	54	SBO, (5)	NGC 4636	26	E0/SO](6)
NGC 4143	59	SO](5)/Sa	NGC4324	66	Sa(i-) ring	NGC 4485	317	Scd/SBcd	NCC 4639	164	SBb(r)IJ
NGC 4144	319	Scd/SBcd	NCC 4339	38	SOi/2(0)	NGC 4486	17	EO	NGC 4643	97. 107	SB03/SBa
NGC 4145	235	Si-Ii-III	NGC 4340	57. S7	RSBO2	NGC 4487	250	Se(s)II.2	NGC 4645	12	E5
NGC 4150	72	SOj(4)/Sa	NGC 4342	23	E7(SO!)	NGC 4490	317	Scd/SBcd	NGC4647	51. 278. S14	Sc(-.s)III
NGC 4151	119	Sab	NGC4346	55	SB0i(8)	NGC 4494	4	E1	NGC 4649	51	SO 1(2)
NGC4152	233	Sc(r)1.4	NGC 4350	35	SOi(8)	NGC 4496	308	SBc	NGC4651	233	Sc(r)I-II
NGC 4162	231	Sc(-I-I-II	NGC 4365	7. 18. S1	E3	NGC4501	187	Sbc(*)II	NGC 4653	230	Sc(rs)1.3
NGC 4178	311	SBc	NGC 4369	275	Sc(s)III-IV	NGC 4503	61	Sa	NGC 4654	302	SBe(i-s)II-III
NGC -1179	36. S2	SOi(91	NGC 4371	57	SB02/3(r)(3)	NCC 4504	247	Sc(s)II	NGC 4656	327. S6	Im
NGC 4183	320	Scd/SBcd	NGC 4373	23	E4	NGC4507	123	SBab(rs)I	NGC 4657	327. S6	Im
NGC 4189	244	SBe(sr)I]	NCC 4374	4	E1	NGC4519	304	SBe(rs)II.2	NGC 4660	11.19	E5 (E/SO)
NGC 4190	326	SmIV	NGC 4377	52	SO](3)	NGC 4522	194. 291	Sc/SL:-:	NGC 4666	194	SbcII.3
NGC -1192	135	SLII:	NCC 4378	70	Sa(s)	NGC 4526	44	SO3(6)	NCC 4668	313	SBc
NGC -1203	41	SO]2(11	NGC4379	31	SO1(2)	NGC 4527	141	Sb(<)II	NCC 4679	141	Sb(s)I-I]
NGC 4212	278	Sc(s)II-III	NGC 4380	117	Sab(s)	NGC4532	327	SmIII	NGC 4682	192	Sbc(rs)II
NGC 1211	330	SBmIII	NGC 4382	41	SO2(3)pec	NGC4535	297	SBc(s)I.3	NGC 4684	42	SO](7)
NGC 4215	47	SO]191	NGC 4383	337	Amorph?(not SO)	NGC4536	174	Sbc(s)I-II	NGC 4689	277	Sc(s)II.3
NGC -1216	119	Sb(s)	NCC4385	211	SBbc(s)II	NGC 4540	275	Sc(s)III	NGC4691	337	R Amorph pet:
NGC -1219	190	Sbc(s)II-III	NGC 4386	34	SO 1(5)	NCC 4546	89	SBOi/Su	NGC 4694	338	Amorph
NGC -1220	77	Sa(r)	NCC 4388	111	Sal,	NGC4548	169.170	SBb(rs)I-II	NCC4696	43	SO3(0)
NGC -1224	76	Sa	NGC -1389	313	SBc	NGC 4550	29	E7/SO](7)	NGC 4697	13. 19	E6
NGC 4233	77	SB0i(6)	NGC 4394	165	SBb(sr)I-II	NGC4552	30	SO](0)	NGC 4698	78.79.87	S11



NAME	PANEL	TYPE			
NGC 5970	211	SBbc(r)I	NGC 6935	67	Sa(r)
NGC 5982	22	E3	NGC 6942	92.106	SBa(s)
NGC 5981	320	Scd/SBcd	NGC 6943	140	Sb(rs)I]
NGC 5985	160	SBb(r)]	NGC 6946	239	Sc(s)II
NGC 6015	265	Sc(s)II-II]	NGC 6951	155	Sb/SBb(rs)I.3
NCC 6070	229	Sc(s)I-H	NGC 6958	30	SO (3)
NGC 6106	264	Sc(rs)II.3	NGC 6970	253	Sc(s)II
NGC 6118	229	Sc(s)I.3	NGC 6981	183	Sbc(r)I.8
NGC 6181	240	Sc(s)II	NGC 7007	59	SO 2/3/a
NGC 6207	274	Sell!	NGC 7014	23	E5
NGC 6215	251	Sc(s)I]	NGC 7020	70	RS02(5)/RSa
NGC 6217	209	RSBbc(s)I]	NGC 7029	32	SO, (5)
NGC 6221	189	Sbc(s)II-III	NGC 7038	175	Sbc(s)I.8
NGC 6239	310	Sbc	NCC 7041	29	SO
NGC 6300	168	SBb(s)II pec	NGC 7049	59.74	SO <sub>3</sub> (4)/Sa
NGC 6340	62	Sa(r)I	NGC 7059	249	Sc(r)I]
NGC 6384	12 7.S4	Sb(r)I.2	NGC 7064	320	Scd/SBcd
NGC 6412	304	SBc(s)/Sc(s)I-I]	NGC 7070	306	Sbc:
NGC 6482	6	E2	NGC 7079	97	Sba
NGC 6503	288	Sc-(s)II.8	NGC 7083	130	Sb(s)I-II
NGC 6574	219	Sc(s)II	NGC 7090	195	Amorph. ir SBc:(on edge)
NGC 6643	216.217	Sc(s)II	NGC 7096	68.88.S3	Sa(r)I
NGC 6684	97	SBa(s)	NGC 7097	9	E4
NGC 6699	184	Slc(s)I.2	NGC 7107	316	Scd/SBcd
NGC 6721	3	E1	NGC 7119	282	Sc(s)II
NGC 6744	188	Sbc(r)II/SBbc(r)II	NGC 7124	174	Sbc(rs)I-II
NGC 6753	125	Sb(r)I	NGC 7125	225	Sc(rs)I-II/SBc(s)I-I]
NGC 6754	192	Sbc(s)II-m	NGC 7126	111	Sab(s)I
NGC 6758	5	E2	NGC 7135	51	SO i per (merger)
NGC 6769	153	Sb(r)n	NGC 7137	266	Sc(rs)II.8
NGC 6770	153	SBb(tides)	NGC 7144	1	E0
NGC 6776	3	E1 pec (ripple)	NGC 7145	1	E0
NGC 6780	177	Sbc(rs)I-II	NGC 7155	56	SBO
NGC 6782	122	SBab(s)	NGC 7162	190	Sbc(rs)I]
NGC 6808	258	Sc(s)II	NCC 7162 A324		Sl/SBrl
NGC 6810	145	SD	NGC 7166	34	SO i(6)
NGC 6814	175	Sbc(rs)I-II	NGC 7168	7	E3
NGC 6822	330	imlV-V	NGC 7171	176	Sbc(r)I-II
NGC 6835	195	Amorph?	NCC 7177	118	Sab(r)II.2
NGC 6851	10	E4	NGC 7184	141	Sb(r)II
NGC 6854	21	E0 + E1	NGC 7192	40	SO <sub>2</sub> (0)
NGC 6861	13	SO <sub>2</sub> (6)	NGC 7196	27	E3/SO <sub>3</sub> (3)
NGC 6868	26	E3/SO 2/3 (3)	NGC 7205	144	Sb(r)II.8
NGC 6870	26	E/SO	NGC 7213	75.S14	Sa(rs)
NGC 6875	59	SO/a (ripples)	NGC 7217	143	Sb(r)II-III
NGC 6876	22	E3	NGC 7218	271	Sc(s)II.8
NGC 6878	228	Sc(r)I.3	NGC 7232	51	SO3(7) in- Sb
NGC 6887	133	Sl(s)I-II	NGC 7233	51	Sa(late)
NGC 6890	144	Sb(s)II-II]	NGC 7252	340	Merger or SO i pec
NGC 6893	113	SO 3(4)	NCC 7300	228	Sc(s)I-E
NGC 6902	69	Sa(r)	NGC 7302	32	SO](4)
NGC 6907	208	Sl?!x(s)II	NGC 7307	311	Sbc
NGC 6909	11	E5 (E/SO)	NGC 7309	228	Sr(rs)I-I]
NGC 6923	208	SBbc(s)II	NGC 7314	278	S^sJIII
NGC 6925	185	SD(-r)I-II	NGC 7329	163	SBb(r)I-II
NGC 7331	133	Sb(rs)I-U	NGC 7332	42	SO <sub>2</sub> /3(8)
NGC 7332	42	SO <sub>2</sub> /3(8)	NGC 7361	288	Sc(s)II-III
NGC 7371	96, 106.S12	SBa(r)II	NGC 7377	75.SI 4	SO <sub>2</sub> /3/Sa pec
NGC 7392	186	Slic(s)I-II	NGC 7410	96	SBa or Sa
NGC 7410	96	SBa or Sa	NGC 7412	227	Sc(s)I-II
NGC 7418	238	Sc(rs)I.8	NGC 7421	210	SBbc(rs)II-III
NGC 7424	295.S9	Sc(rs)II.3/SBc(s)II.3	NGC 7424	295.S9	Sc(rs)II.3/SBc(s)II.3
NGC 7448	251	Se(r)II.2	NGC 7448	251	Se(r)II.2
NGC 7456	264	Se(s)II-III	NGC 7456	264	Se(s)II-III
NGC 7457	33	SOi (5)	NGC 7457	33	SOi (5)
NGC 7462	311	Sbc	NGC 7462	311	Sbc
NGC 7479	200.S8	SBbc(s)I-II	NGC 7479	200.S8	SBbc(s)I-II
NGC 7496	303.S10	SBc(s)II.8	NGC 7496	303.S10	SBc(s)II.8
NCC 7507	1	E0	NCC 7507	1	E0
NGC 7531	175	Slie(r)I-II	NGC 7531	175	Slie(r)I-II
NGC 7537	282	Sc(s)	NGC 7537	282	Sc(s)
NGC 7541	255.282	Sc(s)II	NGC 7541	255.282	Sc(s)II
NCC 7552	156	SBb(s)I-II	NCC 7552	156	SBb(s)I-II
NGC 7582	122	SBab(rs)	NGC 7582	122	SBab(rs)
NCC 7585	84	SOi(3)/Sa	NCC 7585	84	SOi(3)/Sa
NGC 7600	33	SOi(5)	NGC 7600	33	SOi(5)
NGC 7606	127.S13	Sb(r)I	NGC 7606	127.S13	Sb(r)I
NGC 7619	7	E3	NGC 7619	7	E3
NGC 7623	23	E5	NGC 7623	23	E5
NGC 7626	3	E1	NGC 7626	3	E1
NGC 7640	311	Sbc	NGC 7640	311	Sbc
NGC 7678	201	SBbc(s)I-II	NGC 7678	201	SBbc(s)I-II
NGC 7679	86, 292	Se(s)/Sa(tides?)	NGC 7679	86, 292	Se(s)/Sa(tides?)
NGC 7689	241	Sc(sr)II	NGC 7689	241	Sc(sr)II
NGC 7690	118	Sab(s)	NGC 7690	118	Sab(s)
NGC 7702	66	RSa(r)	NGC 7702	66	RSa(r)
NGC 7713	267	Sc(s)II-III	NGC 7713	267	Sc(s)II-III
NGC 7716	111	Sab(r)I	NGC 7716	111	Sab(r)I
NGC 7721	176	Sbc(s)II.2	NGC 7721	176	Sbc(s)II.2
NGC 7723	163	SBI(rs)I-II	NGC 7723	163	SBI(rs)I-II
NGC 7727	83	Sa pec	NGC 7727	83	Sa pec
NGC 7741	297.S10	SBc(s)H.2	NGC 7741	297.S10	SBc(s)H.2
NGC 7742	66	Sa(r)!	NGC 7742	66	Sa(r)!
NGC 7743	91.106	SBa	NGC 7743	91.106	SBa
NGC 7744	56	SBO!(3)	NGC 7744	56	SBO!(3)
NGC 7755	203	SBbc(r)/Sbc(r)I-II	NGC 7755	203	SBbc(r)/Sbc(r)I-II
NGC 7764	329	SBmIII	NGC 7764	329	SBmIII
NGC 7769	81.198	Sbc(s)(tides?)	NGC 7769	81.198	Sbc(s)(tides?)
NCC 7770	81.198	Sa pec	NCC 7770	81.198	Sa pec
NGC 7771	81.198	SBab pec	NGC 7771	81.198	SBab pec
NGC 7779	65.133	Sa	NGC 7779	65.133	Sa
NGC 7782	133.S13	Sb(s)I-II	NGC 7782	133.S13	Sb(s)I-II
NCC 7785	27	SO!(5)/E5	NCC 7785	27	SO!(5)/E5
NGC 7793	321.S6	Sd(s)IV	NGC 7793	321.S6	Sd(s)IV
NGC 7796	3	E1	NGC 7796	3	E1
NGC 7814	112.S11	S(ab)	NGC 7814	112.S11	S(ab)





ETS Ref-Atlas  
J



FEB 28 2007

